SANDIA REPORT
SAND2009-3055
Unlimited Release
Printed June 2009

Conceptual and Computational Basis for the Quantification of Margins and Uncertainty

Jon C. Helton

Prepared by
Sandia National Laboratories
Albuquerque, New Mexico 87185 and Livermore, California 94550

Sandia is a multiprogram laboratory operated by Sandia Corporation, a Lockheed Martin Company, for the United States Department of Energy's National Nuclear Security Administration under Contract DE-AC04-94AL85000.

Approved for public release; further dissemination unlimited.

Sandia National Laboratories

Issued by Sandia National Laboratories, operated for the United States Department of Energy by Sandia Corporation.

NOTICE: This report was prepared as an account of work sponsored by an agency of the United States Government. Neither the United States Government, nor any agency thereof, nor any of their employees, nor any of their contractors, subcontractors, or their employees, make any warranty, express or implied, or assume any legal liability or responsibility for the accuracy, completeness, or usefulness of any information, apparatus, product, or process disclosed, or represent that its use would not infringe privately owned rights. Reference herein to any specific commercial product, process, or service by trade name, trademark, manufacturer, or otherwise, does not necessarily constitute or imply its endorsement, recommendation, or favoring by the United States Government, any agency thereof, or any of their contractors or subcontractors. The views and opinions expressed herein do not necessarily state or reflect those of the United States Government, any agency thereof, or any of their contractors.

Printed in the United States of America. This report has been reproduced directly from the best available copy.

Available to DOE and DOE contractors from
U.S. Department of Energy
Office of Scientific and Technical Information
P.O. Box 62
Oak Ridge, TN 37831

Telephone: (865)576-8401
Facsimile: (865)576-5728
E-Mail: reports@adonis.osti.gov
Online ordering: http://www.doc.gov/bridge

Available to the public from
U.S. Department of Commerce
National Technical Information Service
5285 Port Royal Rd.
Springfield, VA 22161

Telephone: (800)553-6847
Facsimile: (703)605-6900
E-Mail: orders@ntis.fedworld.gov
Online ordering: http://www.ntis.gov/ordering.htm

SAND2009-3055
Unlimited Release
Printed June 2009

Conceptual and Computational Basis for the Quantification of Margins and Uncertainty

Jon C. Helton[a]
[a]Department of Mathematics and Statistics, Arizona State University, Tempe, AZ 85287-1804 USA

Abstract

In 2001, the National Nuclear Security Administration of the U.S. Department of Energy in conjunction with the national security laboratories (i.e, Los Alamos National Laboratory, Lawrence Livermore National Laboratory and Sandia National Laboratories) initiated development of a process designated Quantification of Margins and Uncertainty (QMU) for the use of risk assessment methodologies in the certification of the reliability and safety of the nation's nuclear weapons stockpile. This presentation discusses and illustrates the conceptual and computational basis of QMU in analyses that use computational models to predict the behavior of complex systems. Topics considered include (i) the role of aleatory and epistemic uncertainty in QMU, (ii) the representation of uncertainty with probability, (iii) the probabilistic representation of uncertainty in QMU analyses involving only epistemic uncertainty, (iv) the probabilistic representation of uncertainty in QMU analyses involving aleatory and epistemic uncertainty, (v) procedures for sampling-based uncertainty and sensitivity analysis, (vi) the representation of uncertainty with alternatives to probability such as interval analysis, possibility theory and evidence theory, (vii) the representation of uncertainty with alternatives to probability in QMU analyses involving only epistemic uncertainty, and (viii) the representation of uncertainty with alternatives to probability in QMU analyses involving aleatory and epistemic uncertainty. Concepts and computational procedures are illustrated with both notional examples and examples from reactor safety and radioactive waste disposal.

Key Words: Aleatory uncertainty, Epistemic uncertainty, Performance assessment, Quantification of margins and uncertainty, Risk assessment, Sensitivity analysis, Uncertainty analysis

Acknowledgments

Work performed at Sandia National Laboratories (SNL), which is a multiprogram laboratory operated by Sandia Corporation, a Lockheed Martin Company, for the U.S. Department of Energy's National Nuclear Security Administration under Contract No. DE-AC04-94AL85000. Review provided by L.P. Swiler and T.G. Trucano at SNL and by K. Sentz at Los Alamos National Laboratory. Technical support on graphics provided by J.D. Johnson at ProStat and C.J. Sallaberry at SNL. Editorial support provided by F. Puffer and J. Ripple of Tech Reps, a division of Ktech Corporation. This presentation is an independent product of the author and does not necessarily reflect views held by either SNL or the U.S. Department of Energy.

Contents

Acronyms 13

1 Introduction 15

2 Types of Uncertainty 19

3 Representation of Uncertainty with Probability 21
3.1 Probability Spaces, Cumulative Distribution Functions and Complementary Cumulative Distribution Functions 21
3.2 Basic Entities Underlying an Analysis 23
3.3 Analysis in the Presence of Only Epistemic Uncertainty 25
3.4 Example Analysis in the Presence of Only Epistemic Uncertainty 26
3.5 Analysis in the Presence of Aleatory and Epistemic Uncertainty 30
3.6 Example Analysis in the Presence of Aleatory and Epistemic Uncertainty 33
3.7 Kaplan-Garrick Ordered Triple Representation for Risk 37
3.8 Verification and Validation 38
3.9 An Admonition 38

4 QMU with Epistemic Uncertainty: Characterization with Probability 39
4.1 Epistemic Uncertainty with a Specified Bound 39
4.2 Epistemic Uncertainty with a Specified Bounding Interval 45
4.3 Epistemic Uncertainty with a Specified Bounding Interval over Time 48
4.4 Epistemic Uncertainty with an Uncertain Bound 52
4.5 Information Loss in a “Margin/ Uncertainty” Ratio 55

5 QMU with Aleatory and Epistemic Uncertainty: Characterization with Probability 59
5.1 Epistemic Uncertainty with a Specified Bound on a Quantile 60
5.2 Epistemic Uncertainty with a Specified Bound on an Expected Value 63

6 Example QMU Analyses 67
6.1 Nuclear Reactor Accident Safety Goals 67
6.2 Regulatory Requirements for Waste Isolation Pilot Plant (WIPP) 79
6.3 Regulatory Requirements for Yucca Mountain Repository 84

7 Uncertainty and Sensitivity Analysis for Models of Complex Systems 91
7.1 Characterization of Uncertainty 91
7.2 Generation of Sample 92
7.3 Propagation of Sample Through the Analysis 93
7.4 Presentation of Uncertainty Analysis Results 94
7.5 Determination of Sensitivity Analysis Results 95

8 Alternative Representations of Uncertainty 103
8.1 Interval Analysis 103
8.2 Possibility Theory 104
8.3 Evidence Theory 106
8.4 Probability Theory 108
8.5 Sampling-Based Uncertainty Propagation 110

9 QMU with Epistemic Uncertainty: Characterization with Alternative Uncertainty Representations 113
9.1 Electrical Circuit Used for Illustration 113
9.2 Epistemic Uncertainty without a Specified Bound 115
9.3 Epistemic Uncertainty with a Specified Bound 117
9.4 Epistemic Uncertainty with a Specified Bounding Interval 119

9.5 Epistemic Uncertainty with a Specified Bounding Interval Over Time 122
9.6 Epistemic Uncertainty with an Uncertain Bound 124

10 QMU with Aleatory and Epistemic Uncertainty: Characterization with Alternative Uncertainty Representations 127
10.1 Randomly Perturbed System Used for Illustration 127
10.2 Epistemic Uncertainty Without a Specified Bound 127
10.3 Epistemic Uncertainty with a Specified Bound on a Quantile 128
10.4 Epistemic Uncertainty with a Specified Bound on an Expected Value 129

11 Summary Discussion 133
11.1 Margins in QMU 133
11.2 Uncertainty in QMU 134
11.3 Quantification in QMU 137
11.4 Presentation of QMU Results 139

12 References 141

Appendix A: Rechard RP. Historical Relationship Between Performance Assessment for Radioactive Waste Disposal and Other Types of Risk Assessment. *Risk Analysis* 1999;19(5):763-807

Appendix B: Helton JC, Johnson JD, Sallaberry CJ, Storlie CB. Survey of Sampling-Based Methods for Uncertainty and Sensitivity Analysis. *Reliability Engineering and System Safety* 2006;91(10-11):1175-1209

Appendix C: Helton JC, Breeding RJ. Calculation of Reactor Accident Safety Goals. *Reliability Engineering and System Safety* 1993;39(2):129-158

Appendix D: Helton JC, Anderson DR, Jow H-N, Marietta MG, Basabilvazo G. Performance Assessment in Support of the 1996 Compliance Certification Application for the Waste Isolation Pilot Plant. *Risk Analysis* 1999;19(5):959 – 986

Appendix E, Part 1: Helton JC, Hansen CW, Sallaberry CJ. Yucca Mountain 2008 Performance Assessment: Conceptual Structure and Computational Implementation. In. *Proceedings of the International High-Level Radioactive Waste Management Conference, September 7-11, 2008*: American Nuclear Society, 2008: 524–532;

Appendix E, Part 2: Sallaberry CJ, Aragon A, Bier A, Chen Y, Groves JW, Hansen CW, Helton JC, Mehta S, Miller SP, Min J, Vo P. Yucca Mountain 2008 Performance Assessment: Uncertainty and Sensitivity Analysis for Physical Processes. In. *Proceedings of the 2008 International High-Level Radioactive Waste Management Conference, September 7-11, 2008*: American Nuclear Society, 2008: 559–566;

Appendix E, Part 3: Hansen CW, Brooks K, Groves JW, Helton JC, Lee PL, Sallaberry CJ, Stathum W, Thom C. Yucca Mountain 2008 Performance Assessment: Uncertainty and Sensitivity Analysis for Expected Dose. In. *Proceedings of the 2008 International High-Level Radioactive Waste Management Conference, September 7-11, 2008*: American Nuclear Society, 2008: 567–574

List of Figures

Fig. 3.1. Example CDF and CCDF for variable x with (i) a loguniform distribution on [2, 10] and (ii) $p_X(\tilde{x} \leq x)$ and $p_X(x < \tilde{x})$ used as mnemonics for the probabilities $p_X(\mathcal{U}_x)$ and $p_X(\mathcal{U}_x^c)$ defined in conjunction with Eq. (3.2). 22

Fig. 3.2. Example CDF and CCDF for $y = f(\mathbf{x}) = x_1^2 + 2x_1x_2 + x_2^2$ generated with (i) a random sample $\mathbf{x}_i = [x_{i1}, x_{i2}]$, $i = 1, 2, \ldots, 100$, from uniform distributions on [0, 2] for x_1 and x_2 and (ii) $\hat{p}_X[f(\mathbf{x}) \leq y]$ and $\hat{p}_X[y < f(\mathbf{x})]$ used as mnemonics for the estimated probabilities $\hat{p}_Y(\mathcal{U}_y)$ and $\hat{p}_Y(\mathcal{U}_y^c)$ defined in conjunction with Eq. (3.10) to emphasize the dependence of $p_Y(\mathcal{U}_y)$ and $p_Y(\mathcal{U}_y^c)$ on the probability space $(\mathcal{X}, \mathbb{X}, p_X)$. 23

Fig. 3.3. Solution $Q(t)$ shown in Eq. (3.31) to differential equation in Eq. (3.29) obtained with $L = 1$ henry, $R = 100$ ohms, $C = 10^{-4}$ farads, $E_0 = 1000$ volts, and $\lambda = 0.1$ s^{-1}. 27

Fig. 3.4. Illustration of sets $\mathcal{E}_{i1}$, $\mathcal{E}_{i2}$, $\mathcal{E}_{i3}$ and $\mathcal{E}_{i4}$ defined in Eqs. (3.38) – (3.41) with the interval $[a, b]$ normalized to the interval [0, 8] for representational simplicity. 28

Fig. 3.5. Solutions $Q(t|\mathbf{a}, \mathbf{e}_{Mi})$ to differential equation in Eq. (3.29) obtained with the first 50 elements of the LHS in Eq. (3.44) (i.e., with $\mathbf{e}_{Mi}$ for $i = 1, 2, \ldots, 50$). 29

Fig. 3.6. Estimated CDF and CCDF for $Q(0.1|\mathbf{a}, \mathbf{e}_{Mi})$ (i) obtained with the LHS of size 200 in Eq. (3.44) generated from $\mathcal{EM}$ in consistency with the defining density functions for the probability space $(\mathcal{EM}, \mathbb{EM}, p_{EM})$ and (ii) presented with $\hat{p}_{EM}[Q(0.1|\mathbf{a}, \mathbf{e}_M) \leq Q]$ and $\hat{p}_{EM}[Q < Q(0.1|\mathbf{a}, \mathbf{e}_M)]$ used as mnemonics for estimated probabilities of the form $\hat{p}_{EM}[\mathcal{U}y(0.1|\mathbf{a})]$ and $\hat{p}_{EM}[\mathcal{U}_y^c(0.1|\mathbf{a})]$ defined in conjunction with Eq. (3.25). 29

Fig. 3.7. Estimated time-dependent expected value and quantile curves for $Q(t|\mathbf{a}, \mathbf{e}_M)$ obtained with the LHS of size 200 in Eq. (3.44) generated from $\mathcal{EM}$ in consistency with the defining density functions for the probability space $(\mathcal{EM}, \mathbb{EM}, p_{EM})$. 30

Fig. 3.8. Estimated CDF and CCDF for amplitude $A(10|\mathbf{a}, 0.7)$ with $\mathbf{e}_A = [1.0, 1.5, 3.0, 4.5]$ and $\mathbf{e}_M = [0.7]$ (i) determined with a sample of size $nSA = 10{,}000$ from the set $\mathcal{A}$ of possible values for $\mathbf{a}$ conditional on $\mathbf{e} = [\mathbf{e}_A, \mathbf{e}_M] = [1.0, 1.5, 3.0, 4.5, 0.7]$ and (ii) presented with $\hat{p}_A[A(10|\mathbf{a}, 0.7) \leq A|\mathbf{e}_A]$ and $\hat{p}_A[A < A(10|\mathbf{a}, 0.7)|\mathbf{e}_A]$ used as mnemonics for estimated probabilities of the form $\hat{p}_A[\mathcal{U}_y(10|\mathbf{e})|\mathbf{e}_A]$ and $\hat{p}_A[\mathcal{U}_y^c(10|\mathbf{e})|\mathbf{e}_A]$ defined in conjunction with Eq. (3.47). 34

Fig. 3.9. Illustration of time-dependent amplitudes $A(t|\mathbf{a}_j, 0.7)$ used in generation of CDF and CCDF in Fig. 3.8 for aleatory uncertainty in amplitude at $t = 10$ s conditional on $\mathbf{e} = [1.0, 1.5, 3.0, 4.5, 0.7]$: (a) $A(t|\mathbf{a}_j, 0.7)$ for $j = 1$, and (b) $A(t|\mathbf{a}_j, 0.7)$ for $j = 1, 2, \ldots, 5$. 35

Fig. 3.10. Estimated expected value and quantile curves for aleatory uncertainty in amplitude $A(t|\mathbf{a}, 0.7)$ as a function of time conditional on $\mathbf{e} = [1.0, 1.5, 3.0, 4.5, 0.7]$. 35

Fig. 3.11. Estimated CDFs and CCDFs for amplitude $A(10|\mathbf{a}, r)$ obtained for the first 50 elements of the LHS in Eq. (3.67) and estimated with the random samples of size $nSA = 10{,}000$ in Eq. (3.68) from the corresponding sets $\mathcal{A}$ of possible values for $\mathbf{a}$: (a) CDFs, and (b) CCDFs. 36

Fig. 3.12. Estimated CCDFs plotted with log-transformed exceedance probabilities for amplitude $A(10|\mathbf{a}, r)$ obtained for individual elements of the LHS in Eq. (3.67) and estimated with the random samples of size $nSA = 10{,}000$ in Eq.(3.68) from the corresponding sets $\mathcal{A}$ of possible values for $\mathbf{a}$: (a) individual CCDFs for 50 elements in the LHS , and (b) summary statistics for the distribution of CCDFs. 36

Fig. 3.13. Estimated CDF and CCDF (i) for expected values $E_A[A(10|\mathbf{a}, r_i)|\mathbf{e}_{Ai}]$, $i = 1, 2, \ldots, nSE = 200$, associated with CDFs and CCDFs in Figs. 3.11 and 3.12 and (ii) with $\hat{p}_E\{E_A[A(10|\mathbf{a}, r)|\mathbf{e}_A] \leq \bar{A}\}$ and $\hat{p}_E\{\bar{A} < {}_{EA}[A(10|\mathbf{a}, r)|\mathbf{e}_A]\}$ used as mnemonics for estimated probabilities of the form $\hat{p}_E[\mathcal{U}_{\bar{y}}(10)]$ and $\hat{p}_E[\mathcal{U}_{\bar{y}}^c(10)]$ defined in conjunction with Eq. (3.53). 37

Fig. 4.1. Example bounds on $Q(0.1|\mathbf{a}, \mathbf{e}_M)$: (a) Lower bounds $Q_{b1} = 0.075$ and $Q_{b2} = 0.09$ and estimated CDF for $Q(0.1|\mathbf{a}, \mathbf{e}_M)$, and (b) Upper bounds $Q_{b3} = 0.105$ and $Q_{b4} = 0.125$ and estimated CCDF for $Q(0.1|\mathbf{a}, \mathbf{e}_M)$. 40

Fig. 4.2. Estimated CDFs for margins $Q_{mk}(0.1|\mathbf{a}, \mathbf{e}_M)$ associated with bounds Q_{bk} for k = 1, 2, 3, 4: (a) $Q_{m1}(0.1|\mathbf{a}, \mathbf{e}_M)$ for Q_{b1} = 0.075, (b) $Q_{m2}(0.1|\mathbf{a}, \mathbf{e}_M)$ for Q_{b2} = 0.09, (c) $Q_{m3}(0.1|\mathbf{a}, \mathbf{e}_M)$ for Q_{b3} = 0.105, and (d) $Q_{m4}(0.1|\mathbf{a}, \mathbf{e}_M)$ for Q_{b4} = 0.125. 41
Fig. 4.3. Estimated CDFs for normalized margins $Q_{nk}(0.1|\mathbf{a}, \mathbf{e}_M)$ associated with bounds Q_{bk} for k = 1, 2, 3, 4: (a) $Q_{n1}(0.1|\mathbf{a}, \mathbf{e}_M)$ for Q_{b1} = 0.075, (b) $Q_{n2}(0.1|\mathbf{a}, \mathbf{e}_M)$ for Q_{b2} = 0.09, (c) $Q_{n3}(0.1|\mathbf{a}, \mathbf{e}_M)$ for Q_{b3} = 0.105, and (d) $Q_{n4}(0.1|\mathbf{a}, \mathbf{e}_M)$ for Q_{b4} = 0.125. 42
Fig. 4.4. Scatterplots for $Q(0.1|\mathbf{a}, \mathbf{e}_M)$: (a) $[E_{0i}, Q(0.1|\mathbf{a}, \mathbf{e}_{Mi})]$, i = 1,2, …, nSE = 200, and (b) $[C_i, Q(0.1|\mathbf{a}, \mathbf{e}_{Mi})]$, i = 1,2, …, nSE = 200. 45
Fig. 4.5. Example bounding interval $[\underline{Q}_b, \overline{Q}_b]$ = [0.08, 0.12] for $Q(0.1|\mathbf{a}, \mathbf{e}_M)$. 46
Fig. 4.6. Estimated CDF summarizing uncertainty in margin $Q_m(0.1|\mathbf{a}, \mathbf{e}_M)$ defined in Eq. (4.29)for bounding interval $[\underline{Q}_b, \overline{Q}_b]$ = [0.08, 0.12]. 46
Fig. 4.7. Estimated CDF summarizing uncertainty in normalized margin $Q_n(0.1|\mathbf{a}, \mathbf{e}_M)$ defined in Eq. (4.30) for bounding interval $[\underline{Q}_b, \overline{Q}_b]$ = [0.08, 0.12]. 47
Fig. 4.8. Scatterplots for margin $Q_m(0.1|\mathbf{a}, \mathbf{e}_M)$ defined in Eq. (4.29): (a) $[E_{0i}, Q_m(0.1|\mathbf{a}, \mathbf{e}_{Mi})]$, i = 1,2, …, nSE = 200, and (b) $[C_i, Q_m(0.1|\mathbf{a}, \mathbf{e}_{Mi})]$, i = 1,2, …, nSE = 200. 48
Fig. 4.9. Example bounding interval $[\underline{Q}_b, \overline{Q}_b]$ = [0.07, 0.14] over the time interval $[t_{mn}, t_{mx}]$ = [0.02, 0.18 s] for $Q(t|\mathbf{a}, \mathbf{e}_M)$. 49
Fig. 4.10. Estimated CDF summarizing uncertainty in margin $Q_m(t|\mathbf{a}, \mathbf{e}_M, [t_{mn}, t_{mx}])$ defined in Eq. (4.40) for bounding interval $[\underline{Q}_b, \overline{Q}_b]$ = [0.07, 0.14] and time interval $[t_{mn}, t_{mx}]$ = [0.02, 0.18 s]. 49
Fig. 4.11. Estimated CDF summarizing uncertainty in normalized margin $Q_n(t|\mathbf{a}, \mathbf{e}_M, [t_{mn}, t_{mx}])$ defined in Eq. (4.41) for bounding interval $[\underline{Q}_b, \overline{Q}_b]$ = [0.07, 0.14] and time interval $[t_{mn}, t_{mx}]$ = [0.02, 0.18 s]. 50
Fig. 4.12. Sensitivity analysis for $Q(t|\mathbf{a}, \mathbf{e}_M)$ for 0 < t < 0.2 s with PCCs (left column) and SRCs (right column). 52
Fig. 4.13. Scatterplots for margin $Q_m(t|\mathbf{a}, \mathbf{e}_M, [t_{mn}, t_{mx}])$ defined in Eq. (4.40): (a) $[R_i, Q_m(t|\mathbf{a}, \mathbf{e}_{Mi}, [t_{mn}, t_{mx}])$, i = 1,2, …, nSE = 200, (b) $[E_{0i}, Q_m(t|\mathbf{a}, \mathbf{e}_{Mi}, [t_{mn}, t_{mx}])$, i = 1,2, …, nSE = 200, (c) $[C_i, Q_m(t|\mathbf{a}, \mathbf{e}_{Mi}, [t_{mn}, t_{mx}])$, i = 1,2, …, nSE = 200, and (d) $[L_i, Q_m(t|\mathbf{a}, \mathbf{e}_{Mi}, [t_{mn}, t_{mx}])$, i = 1,2, …, nSE = 200. 53
Fig. 4.14. Example uncertain bounding interval $[\underline{Q}_b, \overline{Q}_b]$ with 0.06 ≤ $\underline{Q}_b$ ≤ 0.08 and 0.14 ≤ $\overline{Q}_b$ ≤ 0.16 over the time interval $[t_{mn}, t_{mx}]$ = [0.02, 0.18 s] for $Q(t|\mathbf{a}, \mathbf{e}_M)$. 54
Fig. 4.15. Estimated CDF summarizing uncertainty in margin $Q_m(t|\mathbf{a}, \mathbf{e}_M, [t_{mn}, t_{mx}])$ defined in Eq. (4.40) for time interval $[t_{mn}, t_{mx}]$ = [0.02, 0.18 s] and uncertain bounding interval $[\underline{Q}_b, \overline{Q}_b]$ with 0.06 ≤ $\underline{Q}_b$ ≤ 0.08 and 0.14 ≤ $\overline{Q}_b$ ≤ 0.16. 55
Fig. 4.16. Estimated CDF summarizing uncertainty in normalized margin $Q_n(t|\mathbf{a}, \mathbf{e}_M, [t_{mn}, t_{mx}])$ defined in Eq. (4.41) for time interval $[t_{mn}, t_{mx}]$ = [0.02, 0.18 s] and uncertain bounding interval $[\underline{Q}_b, \overline{Q}_b]$ with 0.06 ≤ $\underline{Q}_b$ ≤ 0.08 and 0.14 ≤ $\overline{Q}_b$ ≤ 0.16. 55
Fig. 4.17. Scatterplots for margin $Q_m(t|\mathbf{a}, \mathbf{e}_M, [t_{mn}, t_{mx}])$ defined in Eq. (4.40) for time interval $[t_{mn}, t_{mx}]$ = [0.02, 0.18 s] and uncertain bounding interval $[\underline{Q}_b, \overline{Q}_b]$ with 0.06 ≤ $\underline{Q}_b$ ≤ 0.08 and 0.14 ≤ $\overline{Q}_b$ ≤ 0.16: (a) $[R_i, Q_m(t|\mathbf{a}, \mathbf{e}_{Mi}, [t_{mn}, t_{mx}])$, i = 1,2, …, nSE = 200, (b) $[\underline{Q}_{bi}, Q_m(t|\mathbf{a}, \mathbf{e}_{Mi}, [t_{mn}, t_{mx}])$, i = 1,2, …, nSE = 200, and (c) $[\overline{Q}_{bi}, Q_m(t|\mathbf{a}, \mathbf{e}_{Mi}, [t_{mn}, t_{mx}])$, i = 1,2, …, nSE = 200. 56
Fig. 4.18. Relationship of best estimate margin m_b and lower estimate margin m_l to "margin/uncertainty" ratio k defined by $k = m_b/(m_b - m_l)$. 57
Fig. 5.1. Summary results for $A(10|\mathbf{a}, r)$: (a) CCDFs for $A(10|\mathbf{a}, r)$ obtained with the first 50 elements of the LHS in Eq. (5.3) shown with a vertical line indicating exceedance probabilities $p_A[20 < A(10|\mathbf{a}, r)|\mathbf{e}_A]$, and (b) Estimated CCDF for $p_A[20 < A(10|\mathbf{a}, r)|\mathbf{e}_A]$. 60
Fig. 5.2. Estimated CDFs for margins $p_{mk}(10|\mathbf{e})$ associated with bounds p_{bk} for k = 1, 2: (a) $p_{m1}(10|\mathbf{e})$ for p_{b1} = 0.05, and (b) $p_{m2}(10|\mathbf{e})$ for p_{b2} = 0.1. 61
Fig. 5.3. Estimated CDFs for normalized margins $p_{nk}(10|\mathbf{e})$ associated with bounds p_{bk} for k = 1, 2: (a) $p_{n1}(10|\mathbf{e})$ for p_{b1} = 0.05, and (b) $p_{n2}(10|\mathbf{e})$ for p_{b2} = 0.1 62
Fig. 5.4. Scatterplots for exceedance probability $p_A[20 < A(10|\mathbf{a}, r)|\mathbf{e}_A]$: (a) $(r_i, p_A[20 < A(10|\mathbf{a}, r_i)|\mathbf{e}_{Ai}])$, i = 1,2, …, nSE = 200, and (b) $(\lambda_i, p_A[20 < A(10|\mathbf{a}, r_i)|\mathbf{e}_{Ai}])$, i = 1,2, …, nSE = 200. 63

Fig. 5.5. Example bound $\bar{A}_b$ = 13 on $E_A[A(10|\mathbf{a}, r)|\mathbf{e}_A]$. 63
Fig. 5.6. Margins and normalized margins for $E_A[A(10|\mathbf{a}, r)|\mathbf{e}_A]$: (a) $\bar{A}_m(10\,|\,\mathbf{e})$, and (b) $\bar{A}_n(10\,|\,\mathbf{e})$ 64
Fig. 5.7. Scatterplots for $E_A[A(10|\mathbf{a}, r)|\mathbf{e}_A]$: (a) ($r_i$, $E_A[A(10|\mathbf{a}, r_i)|\mathbf{e}_{Ai}]$), i = 1,2, …, nSE = 200, and (b) (λ_i, $E_A[A(10|\mathbf{a}, r_i)|\mathbf{e}_{Ai})]$), i = 1,2, …, nSE = 200. 65
Fig. 6.1. Exceedance frequency curves for individual early fatality probability within 1609.3 m (1 mi) of the site boundary due to accidents resulting from internal initiators at Surry (Ref. [117], Fig. D.5). 71
Fig. 6.2. Estimated CCDF for annual individual early fatality risk within 1 mile of the site boundary due to accidents resulting from internal initiators at Surry. 71
Fig. 6.3. Estimated CDFs for margins associated with safety goal SG1 for annual individual early fatality risk within 1 mile of the site boundary due to accidents resulting from internal initiators at Surry: (a) margin $mSG1$ (see Eq. (6.14)), and (b) normalized margin $nSG1$ (see Eq. (6.15)). 72
Fig. 6.4. Exceedance frequency curves for individual latent cancer fatality probability within 10 mi = 16, 903 m of the site boundary due to accidents resulting from internal initiators at Surry (Ref. [117], Fig. D.6) 73
Fig. 6.5. Estimated CCDF for annual individual latent cancer fatality risk within 10 miles of the site boundary due to accidents resulting from internal initiators at Surry. 73
Fig. 6.6. Estimated CDFs for margins associated with safety goal SG2 for individual latent cancer fatality risk within 10 miles of the site boundary due to accidents resulting from internal initiators at Surry: (a) margin $mSG2$ (see Eq. (6.24)) and (b) normalized margin $nSG2$ (see Eq. (6.25)). 74
Fig. 6.7. Estimated CCDF for annual severe accident frequency due to accidents resulting from internal initiators at Surry. 74
Fig. 6.8. Estimated CDFs for margins associated with quantitative risk goal QRG1 for accidents resulting from internal initiators at Surry: (a) margin $mQRG1$ (see Eq. (6.26)), and (b) normalized margin $nQRG1$ (see Eq. (6.27)). 75
Fig. 6.9. Estimated CCDFs for conditional probability of containment failure given a severe accident resulting from internal initiators at Surry (see Eqs. (6.39) and (6.40)). 76
Fig. 6.10. Estimated CDFs for margins associated with quantitative risk goal QRG2 for accidents resulting from internal initiators at Surry: (a) margins $mQRG2_k$, k = 1, 2, 3 (see Eq. (6.41)), and (b) normalized margins $nQRG2_k$, k = 1, 2, 3 (see Eq.(6.42)). 77
Fig. 6.11. Estimated CCDFs for conditional probability of containment failure given a severe accident with vessel breach resulting from internal initiators at Surry (see Eq. (6.43)). 77
Fig. 6.12. Estimated CDFs for margins associated with quantitative risk goal QRG2 conditional on vessel breach for accidents resulting from internal initiators at Surry: (a) margins $mQRG2_k$, k = 1, 2, 3 (see Eq. (6.41) with $pQRG2_k(\mathbf{e})$ defined in Eq. (6.43)), and (b) normalized margins $nQRG2_k$, k = 1, 2, 3 (see Eq. (6.42) with $pQRG2_k(\mathbf{e})$ defined in Eq. (6.43)). 78
Fig. 6.13. Exceedance frequency curves for early fatalities due to accidents resulting from internal initiators at Surry (Ref. [117], Fig. D.1). Each curve corresponds to one sample element. 78
Fig. 6.14. Estimated CCDFs of large release frequency for accidents resulting from internal initiators at Surry. 79
Fig. 6.15. Estimated CDFs for margins associated with quantitative risk goal QRG3 for accidents resulting from internal initiators at Surry: (a) margins $mQRG3_k$, k = 1, 2, 3 (see Eq. (6.44)) and (b) normalized margins $nQRG3_k$, k = 1, 2, 3 (see Eq. (6.45)). 80
Fig. 6.16. Estimated CCDFs for normalized release over 10^4 years generated for an LHS of size $nLHS$ = 100 from nE = 57 epistemically uncertain analysis inputs and samples of size 10,000 from the sample space $\mathcal{A}$ for aleatory uncertainty. 83
Fig. 6.17. Estimated CCDFs for normalized releases associated with exceedance probabilities of 0.1 and 10^{-3} in Fig. 6.16. 83
Fig. 6.18. Estimated CDFs for margins associated with normalized releases with exceedance probabilities of 0.1 and 10^{-3} in Fig. 6.16: (a) CDF for margin $mRL1(\mathbf{e})$ for exceedance probability of 0.1, and (b) CDF for margin $mRL2(\mathbf{e})$ for exceedance probability of 10^{-3} 84

Fig. 6.19. Expected dose curves [τ, $\bar{D}(\tau|\mathbf{e}_i)$], $0 \le \tau \le 2 \times 10^4$ yr, and associated mean and quantile curves obtained with an LHS of size 300 from the sample space $\mathcal{E}$ associated with epistemic uncertainty.....88
Fig. 6.20. Estimated CCDF for maximum expected dose $\bar{D}_{mx}(\mathbf{e})$ (see Eq.(6.77)). 88
Fig. 6.21. Estimated CDFs for margin associated with maximum expected dose: (a) margin $m\bar{D}_{mx}(\mathbf{e})$ for maximum expected dose (see Eq. (6.80)), and (b) normalized margin $n\bar{D}_{mx}(\mathbf{e})$ for maximum expected dose (see Eq. (6.81)). 89
Fig. 7.1. Characterization of epistemic uncertainty: (a) Construction of CDF from specified quantile values (Fig. 4.1, Ref. [194]), and (b) Construction of mean CDF by vertical averaging of CDFs defined by individual experts with equal weight (i.e., $1/nE = 1/3$, where $nE = 3$ is the number of experts) given to each expert (Fig. 4.2, Ref. [194]).....93
Fig. 7.2. Example of Latin hypercube sampling to generate a sample of size $nS = 5$ from $\mathbf{x} = [U, V]$ with U normal on [–1, 1] (mean = 0.0; 0.01 quantile = –1; 0.99 quantile = 1) and V triangular on [0, 4] (mode = 1): (a) Upper frames illustrate sampling of values for U and V, and (b) Lower frames illustrate two different pairings of the sampled values of U and V in the construction of a Latin hypercube sample (Fig. 5.3, Ref. [194]). 94
Fig. 7.3. Examples of rank correlations of 0.00, 0.25, 0.50, 0.75, 0.90 and 0.99 imposed with the Iman/Conover restricted pairing technique for an LHS of size $nS = 1000$ (Fig. 5.1, Ref. [195]). 95
Fig. 7.4. Representation of uncertainty in scalar-valued analysis results: (a) CDFs and CCDFs (Fig. 7.2, Ref. [194]) and (b) box plots (Fig. 7.4, Ref. [194]). 96
Fig. 7.5. Representation of uncertainty in analysis results that are functions: (a, b) Pressure as a function of time (Figs. 7.5, 7.9, Ref. [194]), and (c, d) Effects of aleatory uncertainty summarized as a CCDF (Fig. 10.5, Ref. [194]). 97
Fig. 7.6. Examples of scatterplots obtained in a sampling-based uncertainty/sensitivity analysis (Figs. 8.1, 8.2, Ref. [194]). 98
Fig. 7.7. Time-dependent sensitivity analysis results for uncertain pressure curves in Fig. 7.5a: (a) SRCs as a function of time, and (b) PCCs as a function of time (Fig. 8.3, Ref. [194]). 99
Fig. 7.8. Illustration of failure of a sensitivity analysis based on rank-transformed data: (a) Pressures as a function of time and (b) PRCCs as a function of time (Fig. 8.7, Ref. [194]).....100
Fig. 7.9. Grids used to test for nonrandom patterns: (a) Partitioning of range of x_j for tests based on common means and common distributions and ranges of x_j and y_k for test based on, common medians, and common distributions (Fig. 8.8, Ref. [194]), and (b) Partitioning of ranges of x_j and y_k for tests of no influence (Fig. 8.9, Ref. [194]). 100
Fig. 8.1. Plots of CNF, CCNF, CPoF and CCPoF for possibility space ($\mathcal{X}$, r) with (i) $\mathcal{X} = \{x : 1 \le x \le 10\}$, (ii) $r(x) = i/4$ for $i \le x \le i + 1$ and $i = 1, 2, 3, 4$, and (iii) $r(x) = (10 - i)/10$ for $i \le x \le i + 1$ and $i = 5, 6, 7, 8, 9$. 105
Fig. 8.2. Plots of CBF, CCBF, CPF and CCPF for evidence space ($\mathcal{X}$, $\mathbb{X}$, m) with (i) $\mathcal{X} = \{x : 1 \le x \le 10\}$, (ii) $\mathbb{X} = \{\mathcal{U}_1, \mathcal{U}_2, \ldots, \mathcal{U}_{10}\}$ with $\mathcal{U}_i = [i, 2i]$ for $i = 1, 2, 3, 4, 5$ and $\mathcal{U}_i = [i - 1, i]$ for $i = 6, 7, 8, 9, 10$, and (iii) $m(\mathcal{U}) = 1/10$ if $\mathcal{U} \in \mathbb{X}$ and $m(\mathcal{U}) = 0$ otherwise. 107
Fig. 8.3. Plots of (a) CBF, CCBF, CPF and CCPF for evidence space ($\mathcal{X}$, $\mathbb{X}$, m) with (i) $\mathcal{X} = \{x : 1 \le x \le 10\}$, (ii) $\mathbb{X} = \{\mathcal{U}_1, \mathcal{U}_2, \ldots, \mathcal{U}_{10}\}$ with $\mathcal{U}_i = [i, 2i]$ for $i = 1, 2, 3, 4, 5$ and $\mathcal{U}_i = [i - 1, i]$ for $i = 6, 7, 8, 9, 10$, and (iii) $m(\mathcal{U}) = 1/10$ if $\mathcal{U} \in \mathbb{X}$ and $m(\mathcal{U}) = 0$ otherwise (see Fig. 8.2), and (b) CDF and CCDF for probability space ($\mathcal{X}$, $\mathbb{X}$, p) with density function d defined as indicated in Eq. (8.49). 109
Fig. 9.1. Uncertainty associated with $Q(0.1|\mathbf{a}, \mathbf{e}_M)$ characterized by (i) an interval (i.e., [inf($\mathcal{Q}$), sup($\mathcal{Q}$)]), (ii) a possibility space ($\mathcal{Q}$, r_Q) summarized with a CCPoF, CCNF, CPoF and CNF, (iii) an evidence space ($\mathcal{Q}$, $\mathbb{Q}$, m_Q) summarized with a CCPF, CCBF, CPF and CBF, and (iv) a probability space ($\mathcal{Q}$, $\mathbb{Q}$, p_A) summarized with a CCDF and CDF: (a) Cumulative results, and (b) Complementary cumulative results. 116
Fig. 9.2. Example bounds on $Q(0.1|\mathbf{a}, \mathbf{e}_M)$: (a) $Q_{b1} = 0.075$ and $Q_{b2} = 0.09$, and (b) $Q_{b3} = 0.105$ and $Q_{b4} = 0.125$. 118

Fig. 9.3. Uncertainty associated with margins $Q_{mk}(0.1|\mathbf{a}, \mathbf{e}_M)$, $k = 1, 2, 3, 4$, defined in Eq. (9.40) characterized by (i) intervals, (ii) possibility spaces summarized with CPoFs and CNFs, (iii) evidence spaces summarized with CPFs and CBFs, and (iv) probability spaces summarized with CDFs: (a) $Q_{m1}(0.1|\mathbf{a}, \mathbf{e}_M)$ for $Q_{b1} = 0.075$, (b) $Q_{m2}(0.1|\mathbf{a}, \mathbf{e}_M)$ for $Q_{b2} = 0.09$, (c) $Q_{m3}(0.1|\mathbf{a}, \mathbf{e}_M)$ for $Q_{b3} = 0.105$, and (d) $Q_{m4}(0.1|\mathbf{a}, \mathbf{e}_M)$ for $Q_{b4} = 0.125$. 119
Fig. 9.4. Uncertainty associated with normalized margins $Q_{nk}(0.1|\ \mathbf{a}, \mathbf{e}_M)$, $k = 1, 2, 3, 4$, defined in Eq. (9.41) characterized by (i) intervals, (ii) possibility spaces summarized with CPoFs and CNFs, (iii) evidence spaces summarized with CPFs and CBFs, and (iv) probability spaces summarized with CDFs: (a) $Q_{n1}(0.1|\mathbf{a}, \mathbf{e}_M)$ for $Q_{b1} = 0.075$, (b) $Q_{n2}(0.1|\mathbf{a}, \mathbf{e}_M)$ for $Q_{b2} = 0.09$, (c) $Q_{n3}(0.1|\mathbf{a}, \mathbf{e}_M)$ for $Q_{b3} = 0.105$, and (d) $Q_{n4}(0.1|\mathbf{a}, \mathbf{e}_M)$ for $Q_{b4} = 0.125$. 120
Fig. 9.5. Example bounding interval $[\underline{Q}_b, \overline{Q}_b] = 0.08, 0.12]$ for $Q(0.1|\mathbf{a}, \mathbf{e}_M)$. 121
Fig. 9.6. Uncertainty associated with margin $Q_m(0.1|\mathbf{a}, \mathbf{e}_M)$ defined in Eq. (9.52) characterized by (i) an interval, (ii) a possibility space summarized with a CPoF and a CNF, (iii) an evidence space summarized with a CPF and a CBF, and (iv) a probability space summarized with a CDF. 122
Fig. 9.7. Uncertainty associated with normalized margin $Q(0.1|\mathbf{a}, \mathbf{e}_M)$ defined in Eq. (9.53) characterized by (i) an interval, (ii) a possibility space summarized with a CPoF and a CNF, (iii) an evidence space summarized with a CPF and a CBF, and (iv) a probability space summarized with a CDF. 122
Fig. 9.8. Uncertainty associated with margin $Q_m(t|\mathbf{a}, \mathbf{e}_M, [t_{mn}, t_{mx}])$ defined in Eq. (9.64) characterized by (i) an interval, (ii) a possibility space summarized with a CPoF and a CNF, (iii) an evidence space summarized with a CPF and a CBF, and (iv) a probability space summarized with a CDF. 123
Fig. 9.9. Uncertainty associated with normalized margin $Q_n(t|\mathbf{a}, \mathbf{e}_M, [t_{mn}, t_{mx}])$ defined in Eq. (9.65) characterized by (i) an interval, (ii) a possibility space summarized with a CPoF and a CNF, (iii) an evidence space summarized with a CPF and a CBF, and (iv) a probability space summarized with a CDF. 124
Fig. 9.10. Uncertainty associated with margin $Q_m(t|\mathbf{a}, \mathbf{e}_M, [t_{mn}, t_{mx}])$ defined in Eq. (9.64) with $\mathbf{e}_M = [\underline{Q}_b, \overline{Q}_b, L, R, C, E, \lambda]$ characterized by (i) an interval, (ii) a possibility space summarized with a CPoF and a CNF, (iii) an evidence space summarized with a CPF and a CBF, and (iv) a probability space summarized with a CDF. 125
Fig. 9.11. Uncertainty associated with normalized margin $Q_n(t|\mathbf{a}, \mathbf{e}_M, [t_{mn}, t_{mx}])$ defined in Eq. (9.65) with $\mathbf{e}_M = [\underline{Q}_b, \overline{Q}_b, L, R, C, E, \lambda]$ characterized by (i) an interval, (ii) a possibility space summarized with a CPoF and a CNF, (iii) an evidence space summarized with a CPF and a CBF, and (iv) a probability space summarized with a CDF. 125
Fig. 10.1. Uncertainty associated with $p_A[20 < A(10|\mathbf{a}, r)|\mathbf{e}_A]$ characterized by (i) an interval (i.e., $[\inf(\mathcal{P}), \sup(\mathcal{P})]$), (ii) a possibility space $(\mathcal{P}, r_P)$ summarized with a CCPoF, CCNF, CPoF and CNF, (iii) an evidence space $(\mathcal{P}, \mathbb{P}, m_P)$ summarized with a CCPF, CCBF, CPF and CBF, and (iv) a probability space $(\mathcal{P}, \mathbb{P}, p_P)$ summarized with a CCDF and CDF: (a) Cumulative results, and (b) Complementary cumulative results. 128
Fig. 10.2. Uncertainty associated with $p_A[20 < A(10|\mathbf{a}, r)|\mathbf{e}_A]$ characterized by (i) an interval, (ii) a possibility space summarized with a CCPoF and CCNF, (iii) an evidence space summarized with a CCPF and CCBF, and (iv) a probability space summarized with a CCDF. 129
Fig. 10.3. Uncertainty associated with margins $p_{mk}(10|\mathbf{e})$, $k = 1, 2$, defined in Eq. (10.9) characterized by (i) intervals, (ii) possibility spaces summarized with CPoFs and CNFs, (iii) evidence spaces summarized with CPFs and CBFs and (iv) probability spaces summarized with CDFs: (a) $p_{m1}(10|\mathbf{e})$, and (b) $p_{m2}(10|\mathbf{e})$. 130
Fig. 10.4. Uncertainty associated with normalized margins $p_{nk}(10|\mathbf{e})$, $k = 1, 2$, defined in Eq. (10.10) characterized by (i) intervals, (ii) possibility spaces summarized with CPoFs and CNFs, (iii) evidence spaces summarized with CPFs and CBFs and (iv) probability spaces summarized with CDFs: (a) $p_{n1}(10|\mathbf{e})$, and (b) $p_{n2}(10|\mathbf{e})$. 130

Fig. 10.5. Uncertainty associated with $E_A[A(10|\mathbf{a}, r)|\mathbf{e}_A]$ characterized by (i) an interval, (ii) a possibility space summarized with a CCPoF and CCNF, (iii) an evidence space summarized with a CCPF and CCBF, and (iv) a probability space summarized with a CCDF. 131
Fig. 10.6. Margins and normalized margins for $E_A[A(10|\mathbf{a}, r)|\mathbf{e}_A]$ characterized by (i) intervals, (ii) possibility spaces summarized with CPoFs and CNFs, (iii) evidence spaces summarized with CPFs and CBFs and (iv) probability spaces summarized with CDFs: (a) $\bar{A}_m(10\,|\,\mathbf{e})$, and (b) $\bar{A}_n(10\,|\,\mathbf{e})$ 131

List of Tables

Table 4.1. Stepwise Regression Analysis to Identify Uncertain Variables Affecting $Q(0.1|\mathbf{a}, \mathbf{e}_M)$ 45
Table 4.2. Stepwise Regression Analysis to Identify Uncertain Variables Affecting the Margin $Q_m(0.1|\mathbf{a}, \mathbf{e}_M)$ defined in Eq. (4.29) 48
Table 4.3. Stepwise Regression Analysis to Identify Uncertain Variables Affecting Margin $Q_m(t|\mathbf{a}, \mathbf{e}_M, [t_{mn}, t_{mx}])$ Defined in Eq. (4.40) 54
Table 4.4. Stepwise Regression Analysis to Identify Uncertain Variables Affecting Margin $Q_m(t|\mathbf{a}, \mathbf{e}_M, [t_{mn}, t_{mx}])$ Defined in Eq. (4.40) for Time Interval $[t_{mn}, t_{mx}]$ = [0.02, 0.18 s] and Uncertain Bounding Interval $[\underline{Q}_b, \bar{Q}_b]$ with $0.06 \le \underline{Q}_b \le 0.08$ and $0.14 \le \bar{Q}_b \le 0.16$. 55
Table 5.1. Stepwise Regression Analysis to Identify Uncertain Variables Affecting Exceedance Probability $p_A[20 < A(10|\mathbf{a}, r)|\mathbf{e}_A]$ 63
Table 5.2. Stepwise Regression Analysis to Identify Uncertain Variables Affecting $E_A[A(10|\mathbf{a}, r)|\mathbf{e}_A]$ 64
Table 7.1. Example of Stepwise Regression Analysis to Identify Uncertain Variables Affecting the Uncertainty in Pressure at 10,000 yr in Fig. 7.5a (Table 8.6, Ref. [194]) 98
Table 7.2 Comparison of Stepwise Regression Analyses with Raw and Rank-Transformed Data for Variable *BRAALIC* in Fig. 7.4b (Table 8.8, Ref. [194]) 99

Acronyms

AAR	annual assessment report
CBF	cumulative belief function
CCA	Compliance Certification Application
CCBF	complementary cumulative belief function
CCDF	complementary cumulative distribution function
CCNF	complementary cumulative necessity function
CCPF	complementary cumulative plausibility function
CCPoF	complementary cumulative possibility function
CDF	cumulative distribution function
CNF	cumulative necessity function
CPF	cumulative plausibility function
CPoF	cumulative possibility function
DOE	U.S. Department of Energy
DS	drip shield
EPA	U.S. Environmental Protection Agency
LHS	Latin hypercube sample
NAS/NRC	National Academy of Science/National Research Council
NNSA	National Nuclear Security Administration
NRC	Nuclear Regulatory Commission
PA	performance assessment
PCC	partial correlation coefficient
PRA	probabilistic risk assessment
PRCC	partial rank correlation coefficient
QMU	Quantification of Margins and Uncertainty
QRG	quantitative risk goal
RMEI	reasonably maximally exposed individual
SG	safety goal
SNL	Sandia National Laboratories
SRC	standardized regression coefficient
TRU	transuranic
WIPP	Waste Isolation Pilot Plant
WP	waste package
YM	Yucca Mountain

This page intentionally left blank

1 Introduction

In 2001, the National Nuclear Security Administration (NNSA) of the U.S. Department of Energy (DOE) in conjunction with the national security laboratories (i.e, Los Alamos National Laboratory, Lawrence Livermore National Laboratory and Sandia National Laboratories) initiated development of a process designated Quantification of Margins and Uncertainty (QMU) for the use of risk assessment methodologies in the certification of the reliability and safety of the nation's nuclear weapons stockpile [1-6]. Specifically, the following requirements have been proposed [7]:

> Design agency assessments shall incorporate QMU methodologies as an essential part of the framework necessary for the evaluation of the performance of warhead and warhead components. QMU can be used as one of the tools for identification and prioritization of actions required for a component or system. Issues that require immediate attention must be raised to the NNSA Office of Stockpile Assessments and Certification. The design agency laboratories shall develop site-appropriate QMU implementation plans. (NNSA-1)

> Certification, qualification, and significant finding investigations closure plans shall include QMU methodologies where applicable. Results of assessments using QMU shall be included in warhead certification documents, component qualification documents, annual assessment reports (AARs) and Significant Finding Investigation (SFI) closure documentation. (NNSA-2)

As indicated by the preceding statements, the NNSA intends for QMU to be an integral component of the assessment process for the nation's nuclear weapons stockpile. However, the preceding statements give no indication of what the NNSA envisions as the conceptual and computational basis for QMU. In this regard, some additional information with respect to the NNSA's intent for QMU is provided by the following definitions supplied in conjunction with the preceding statements [7]:

> Quantification of Margins and Uncertainties is a scientific methodology that identifies relevant nuclear-warhead parameters and quantifies, using available experimental and computational tools, the margin of that parameter relative to its failure point and the uncertainties associated with the parameter and the failure point. An assessment of the relationship between the margin and uncertainties facilitates stockpile management decisions, resource allocation prioritization, and informed judgments on the safety, reliability and performance of nuclear warheads. (NNSA-3)

> Uncertainty is a best estimate of the range of a particular metric which may derive from one or two broad sources. Uncertainties that reflect a lack of knowledge about the appropriate value to use for a quantity that is assumed to have (missing modifier: *a fixed?*) value in the context of a particular analysis are termed epistemic. Uncertainties that arise from an inherent randomness in the behavior of the system under study are termed aleatoric. (NNSA-4)

Although designated as definitions, the statements in Quotes (NNSA-3) and (NNSA-4) are at a high level and lack specifics. For example, QMU is defined in Quote (NNSA-3) as a "scientific methodology" but no details are given with respect to what the conceptual basis and resultant computational implementation of this methodology should be. This lack of specificity is consistent with the requirement in Quote (NNSA-1) that "site-appropriate QMU implementation plans" should be developed and has the advantage of allowing QMU to be developed and implemented in manners appropriate for specific analysis contexts. However, this lack of specificity does not exempt individual analyses from a requirement to clearly define their conceptual basis and associated computational implementation. Such definitions are essential if a specific use of QMU is to be considered a "scientific methodology."

What is unambiguous from Quote (NNSA-3) is that the appropriate treatment of uncertainty is to be an integral part of any implementation of QMU. The nature of uncertainty and the division of uncertainty into epistemic and aleatory components is elaborated on in Quote (NNSA-4). This is an important distinction that can have significant effects on the conceptual basis and computational design of an analysis and also on the interpretation of the results of the analysis.

When viewed at a high level, the application of QMU can be divided into two distinct cases: (i) comparison of experimental results against a requirement without the use of a mathematical model to transform the experimental results, and (ii) comparison of predic-

tions from a mathematical model against a requirement. This presentation is restricted to the second case, and as a result, the presented concepts, computational procedures and discussions should be viewed in the context of comparing model (i.e., computer) predictions with a requirement. In particular, the strictly statistical issues associated with the direct comparison of experimental results with a requirement are not considered.

Although the descriptor "risk assessment" does not appear in Quotes (NNSA-1) – (NNSA-4), the QMU process being described in these quotes is clearly a form of risk assessment in that it involves the determination of consequences (i.e., analysis outcomes and associated margins), likelihoods (i.e., the effects of aleatory uncertainties), and state of knowledge uncertainties (i.e., epistemic uncertainties). Such determinations are the essence of a risk assessment. As a result, the NNSA's mandate for QMU is a continuation of the extensive and ongoing use of risk assessment in many different areas. As indicated in the following three paragraphs, there is an extensive body of prior studies and techniques that are relevant to the NNSA's mandated use of QMU.

Risk assessment for complex systems has a long history and many examples relevant to QMU exist, including (i) early studies of missile reliability (Ref. [8], Sect. 3.2), (ii) the U.S. Nuclear Regulatory Commission's (NRC's) assessment of the risk from commercial nuclear power plants, which is known as WASH-1400 after a report number [9], (iii) the NRC's reassessment of the risk from commercial nuclear power plants, which is known as NUREG-1150 after a report number [10; 11], (iv) the NRC's study of margins in reactor safety [12-18], (v) the NRC's analysis of the LaSalle Nuclear Power Station as part of its Risk Methods Investigation and Evaluation Program [19], (vi) the DOE's performance assessment for the Waste Isolation Pilot Plant (WIPP) in support of a successful Compliance Certification Application to the U.S. Environmental Protection Agency (EPA) [20; 21], and (vii) the DOE's performance assessment for the proposed repository for high level radioactive waste at Yucca Mountain, Nevada, carried out in support of a licensing application to the NRC [22].

The NRC's WASH-1400 analysis is rightfully considered to be the seminal study in the analysis of complex systems. After its completion, the NRC commissioned a review of the WASH-1400 analysis known as the Lewis Committee Report after the chairman of the review committee [23]. This review was highly complimentary with respect to the overall WASH-1400 analysis but noted that the analysis had inadequately represented the (epistemic) uncertainty in its results. This led to an extensive interest in the appropriate incorporation of epistemic uncertainty into analyses for complex systems and significantly influenced the NRC's program to develop a risk assessment methodology to assess the geologic disposal of high-level radioactive waste [24-26], the NRC's development of the MELCOR code system for the analysis of nuclear reactor accidents [27-29], and the design and implementation of the analyses indicated in (iii) – (vii) above. Similarly to the analyses in (iii) – (vii), NNSA's mandate for QMU is effectively one more descendent of the WASH-1400 analyses and the associated Lewis Committee Report.

Additional information on the development of risk assessment methods for complex systems is available in the excellent review by Rechard [8], which is reproduced in App. A. The recent review by Zio is also a valuable source of background and perspectives on risk and reliability analysis for complex systems [30]. Further, the book by Bernstein is highly recommended for a broader perspective on the evolution of the ideas underlying the assessment of risk [31].

The QMU process also quite naturally falls into a broad area of study known as uncertainty and sensitivity analysis, where uncertainty analysis refers to the determination of the uncertainty in analysis results that derives from uncertainty in analysis inputs and sensitivity analysis refers to the determination of the contributions of the uncertainty in individual analysis inputs to the uncertainty in analysis results. The uncertainty being referred to in the preceding sentence is usually of an epistemic nature. Clearly, uncertainty analysis is a fundamental component of QMU; indeed, when viewed broadly, QMU is simply a call for uncertainty analyses focused on margins (i.e., differences between required performance and obtainable performance) associated with the assessment of nuclear weapon reliability and performance. However, sensitivity analysis is also a fundamental part of QMU as indicated by reference to "identification and prioritization of actions" in Quote (NNSA-1) and "assessment of the relationship between margin and uncertainties" in Quote (NNSA-3). Specifically, the indicated actions require a sensitivity analysis to determine the effects of the uncertainty in individual analysis inputs on the uncertainty in analysis results of interest (e.g., margins).

As a result of its fundamental importance in analyses of complex systems, a number of approaches to uncertainty and sensitivity analysis have been devel-

oped, including differential analysis [32-37], response surface methodology [38-44], Monte Carlo analysis [29; 45-56], and variance decomposition procedures [57-61]. Overviews of these approaches are available in several reviews [62-71]. Of the indicated approaches to uncertainty and sensitivity analysis, sampling-based (i.e., Monte Carlo) approaches are likely to be the most generally useful in QMU analyses. As an introduction to analyses of this type, the review by Helton et al. [56] is reproduced in App. B. This review provides background and additional references on many of the ideas introduced in this presentation.

A number of presentations discussing the QMU process are available [2; 72-77]. Of particular importance is the recently published National Academy of Science/National Research Council (NAS/NRC) report, which provides an overview of, and a broad perspective on, QMU at the national security laboratories [77]. However, these presentations tend to be written at a high level and, as a result, lack detail on the conceptual basis and computational organization that must underlie a real QMU analysis if that analysis is to be a manifestation of a "scientific methodology" as indicated in Quote (NNSA-3).

The purpose of this presentation is to describe the conceptual basis and computational organization of QMU analyses that use models to produce results that are then compared with requirements. The basic idea is that a QMU analysis must start with a clear understanding of the conceptual (i.e., mathematical) model used to represent uncertainty. In turn, this model leads to (i) the manner in which the uncertainty in individual analysis inputs is characterized, (ii) the procedures that are used to propagate uncertainty through the analysis, (iii) the procedures that are available for sensitivity analysis, and (iv) the interpretations and representations that are available for analysis results of interest (e.g., margins). It is important to recognize that in most real analyses there will probably be many results of interest in addition to a single margin that is the outcome of comparing a single calculated result with a single requirement.

The presentation is organized as follows. First, the important concepts of aleatory and epistemic uncertainty are discussed (Sect. 2). Next, the use of probability in the representation of uncertainty is described and two example problems are introduced that will be used to illustrate different potential QMU analyses (Sect. 3). Specifically, the first example problem involves only epistemic uncertainty and is used to illustrate QMU analyses that involve only epistemic uncertainty (Sect. 4). The second example problem involves both aleatory and epistemic uncertainty and is used to illustrate QMU analyses that involve both aleatory and epistemic uncertainty (Sect. 5). For added perspective, the presence of QMU-type margin analyses in several real, complex and computationally-demanding analyses are also described (Sect. 6); further, additional details on these analyses are presented in three appendices (Apps. C, D and E). A description of uncertainty and sensitivity analysis procedures that underlie sampling-based QMU analyses is then provided (Sect. 7). Next, alternative mathematical structures for the representation of uncertainty are described (Sect. 8) and then illustrated with notional QMU analyses involving only epistemic uncertainty (Sect. 9) and both aleatory and epistemic uncertainty (Sect. 10). The presentation then ends with a summary discussion (Sect. 11).

This page intentionally left blank

2 Types of Uncertainty

In the design and implementation of analyses for complex systems, it is useful to distinguish between two types of uncertainty: aleatory uncertainty and epistemic uncertainty [78-90]. The importance of this distinction is recognized by the NNSA in Quote (NNSA-4) and also emphasized in the NAS/NRC report on QMU (Finding 1-3, pp. 22-23, Ref. [77]).

Aleatory uncertainty arises from an inherent randomness in the properties or behavior of the system under study. For example, the weather conditions at the time of a reactor accident are inherently random with respect to our ability to predict the future. Other examples include the variability in the properties of a population of weapon components and the variability in the possible future environmental conditions that a weapon component could be exposed to. Alternative designations for aleatory uncertainty include variability, stochastic, irreducible and type A.

Epistemic uncertainty derives from a lack of knowledge about the appropriate value to use for a quantity that is assumed to have a fixed value in the context of a particular analysis. For example, the pressure at which a given reactor containment would fail for a specified set of pressurization conditions is fixed but not amenable to being unambiguously defined. Other examples include minimum voltage required for the operation of a system and the maximum temperature that a system can withstand before failing. Alternative designations for epistemic uncertainty include state of knowledge, subjective, reducible and type B.

The appropriate separation of aleatory and epistemic uncertainty is an important component of the design and computational implementation of an analysis of a complex system and also of the decisions that are made on the basis of this analysis. This point can be made with a simple notional example. Suppose an analysis concludes that the probability of a particular component failing to operate correctly is 0.01. Without the specification of additional information, there are two possible interpretations to the indicated probability. The first interpretation, which is inherently aleatoric, is that 1 in every 100 components of this type will fail to operate properly; or, put another way, there is a probability of 0.99 that a randomly selected component will operate properly and a probability of 0.01 that a randomly selected component will not operate properly. The second interpretation, which is inherently epistemic, is that there is a probability of 0.99 that all components of this type will operate properly and a probability of 0.01 that no components of this type will operate properly. Clearly, the implications of the two interpretations of the indicated probability are very different, and as a consequence, any resultant decisions about the system under study can also be expected to be very different.

The analysis of a complex system typically involves answering the following three questions about the system:

What can happen? (Q1)

How likely is it to happen? (Q2)

What are the consequences if it happens? (Q3)

and one additional question about the analysis itself:

How much confidence exists in the answers to the first three questions? (Q4)

The answers to Questions (Q1) and (Q2) involve the characterization of aleatory uncertainty, and the answer to Question (Q4) involves the characterization of epistemic uncertainty. The answer to Question (Q3) typically involves numerical modeling of the system conditional on specific realizations of aleatory and epistemic uncertainty. The posing and answering of Questions (Q1) – (Q3) gives rise to what is often referred to as the Kaplan-Garrick ordered triple representation for risk [89], which is discussed in more detail in Sect. 3.7.

The use of probability to characterize both aleatory uncertainty and epistemic uncertainty is described and illustrated in Sects. 3 – 6 and can be traced back to at least the beginning of the formal development of probability theory in the late seventeenth century [31; 91; 92]. However, as discussed in Sect. 8 and illustrated in Sects. 9 and 10, several alternative mathematical structures for the representation of epistemic uncertainty have been developed in the last several decades. It is possible that some of these alternative structures may be more appropriate than probability in certain contexts for the representation of epistemic uncertainty.

This page intentionally left blank

3 Representation of Uncertainty with Probability

The following topics related to the representation of uncertainty with probability are now introduced: probability spaces, cumulative distribution functions and complementary cumulative distribution functions (Sect. 3.1), the basic entities that underlie an analysis that involves a representation of uncertainty (Sect. 3.2), analysis in the presence of only epistemic uncertainty (Sect. 3.3), an example analysis in the presence of only epistemic uncertainty (Sect. 3.4), analysis in the presence of aleatory and epistemic uncertainty (Sect. 3.5), an example analysis in the presence of aleatory and epistemic uncertainty (Sect. 3.6), the Kaplan-Garrick ordered triple representation for risk (Sect. 3.7), verification and validation (Sect. 3.8), and an admonition about the importance of a clear specification of concepts in the representation of uncertainty (Sect. 3.9).

The NAS/NRC report on QMU emphasizes the importance of formal uncertainty quantification (Finding 1-2, p. 20, Ref. [77]). The concepts and mathematical structures introduced in this section are fundamental to such quantification.

3.1 Probability Spaces, Cumulative Distribution Functions and Complementary Cumulative Distribution Functions

Probability provides the mathematical structure traditionally used to represent both aleatory uncertainty and epistemic uncertainty [78; 80; 83; 86; 87]. Formally, a probabilistic characterization of the uncertainty associated with a quantity $\mathbf{x}$ is provided by a probability space ($\mathcal{X}$, $\mathbb{X}$, p_X), where (i) $\mathcal{X}$ is the set of all possible values for $\mathbf{x}$, (ii) $\mathbb{X}$ is a suitably restricted set of subsets of $\mathcal{X}$ for which probability is defined, and (iii) p_X is a function that defines probability for individual elements of $\mathbb{X}$ (i.e., if $\mathcal{U} \in \mathbb{X}$, then $p_X(\mathcal{U})$ is the probability of $\mathcal{U}$) (Sect. IV.4, Ref. [93]). Additional discussion of probability spaces is provided in Sect. 8.4.

In practice, a probability space ($\mathcal{X}$, $\mathbb{X}$, p_X) is often represented by a density function $d_X(\mathbf{x})$, where

$$p_X\left(\mathcal{U}\right) = \int_{\mathcal{U}} d_X\left(\mathbf{x}\right) \mathrm{d}U \tag{3.1}$$

for $\mathcal{U} \in \mathbb{X}$. Integrals of the form appearing in Eq. (3.1) are usually taken to be Lebesgue integrals in formal developments of probability theory (e.g., [93; 94]). However, for the purposes of this presentation, all presented integrals can be intuitively thought of as corresponding to the Riemann integral of elementary calculus. In computational practice, high-dimensional integrals involving probability spaces are usually evaluated with sampling-based (i.e., Monte Carlo) procedures.

When $\mathbf{x}$ corresponds to a scalar x rather than a vector, a probability space ($\mathcal{X}$, $\mathbb{X}$, p_X) can be summarized with a cumulative distribution function (CDF) or a complementary cumulative distribution function (CCDF). Specifically, the CDF and CCDF for x are defined by plots of the points

$$\left[x,\, p_X\left(\mathcal{U}_x\right)\right] \text{ and } \left[x,\, p_X\left(\mathcal{U}_x^c\right)\right], \tag{3.2}$$

respectively, for $x \in \mathcal{X}$, where

$$\begin{aligned}
\mathcal{U}_x &= \left\{\tilde{x} : \tilde{x} \in \mathcal{X} \text{ and } \tilde{x} \le x\right\}, \\
p_X\left(\mathcal{U}_x\right) &= \text{probability of } \mathcal{U}_x \text{ (i.e., of a value } \tilde{x} \le x) \\
&= \int_{\mathcal{U}_x} d_X\left(\tilde{x}\right) \mathrm{d}\tilde{x} \\
&= \int_{\mathcal{X}} \underline{\delta}_x\left(\tilde{x}\right) d_X\left(\tilde{x}\right) \mathrm{d}\tilde{x}, \\
p_X\left(\mathcal{U}_x^c\right) &= \text{probability of } \mathcal{U}_x^c \text{ (i.e., of a value } \tilde{x} > x) \\
&= \int_{\mathcal{U}_x^c} d_X\left(\tilde{x}\right) \mathrm{d}\tilde{x} \\
&= \int_{\mathcal{X}} \overline{\delta}_x\left(\tilde{x}\right) d_X\left(\tilde{x}\right) \mathrm{d}\tilde{x}, \\
\underline{\delta}_x\left(\tilde{x}\right) &= \begin{cases} 1 & \text{if } \tilde{x} \le x \\ 0 & \text{otherwise} \end{cases}
\end{aligned}$$

and

$$\overline{\delta}_x\left(\tilde{x}\right) = 1 - \underline{\delta}_x\left(\tilde{x}\right) = \begin{cases} 1 & \text{if } \tilde{x} > x \\ 0 & \text{otherwise.} \end{cases}$$

Further, it is usually assumed for plotting purposes that (i) $p_X(\mathcal{U}_x) = 1$ and $p_X(\mathcal{U}_x^c) = 0$ for $x > \sup(\mathcal{X})$ and (ii) $p_X(\mathcal{U}_x) = 0$ and $p_X(\mathcal{U}_x^c) = 1$ for $x < \inf(\mathcal{X})$.

The results of risk assessments are often summarized with CCDFs because CCDFs provide an answer to the question "How likely is it to be this large or larger?", which is typically the type of question that risk assessments are intended to answer. In contrast, CDFs answer the question "How likely is it to be this small or smaller?", which is likely to be the question of primary interest in a margin analysis.

As an example, the CDF and CCDF for x with a loguniform distribution on [2, 10] is presented in Fig. 3.1. For this example,

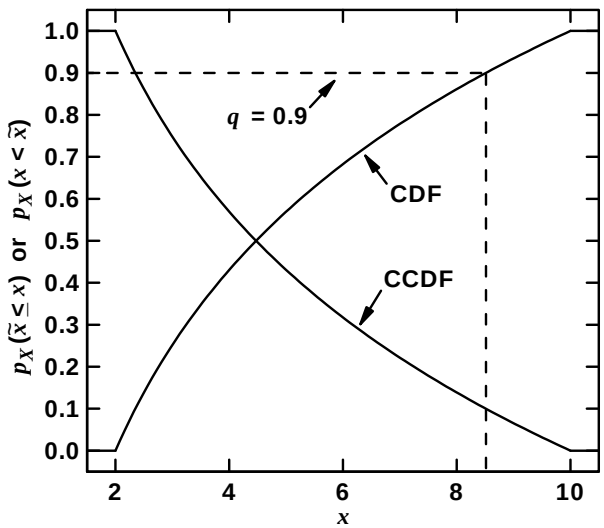

Fig. 3.1. Example CDF and CCDF for variable x with (i) a loguniform distribution on [2, 10] and (ii) $p_X(\tilde{x} \le x)$ and $p_X(x < \tilde{x})$ used as mnemonics for the probabilities $p_X(\mathcal{U}_x)$ and $p_X(\mathcal{U}_x^c)$ defined in conjunction with Eq. (3.2).

$$d_X(x) = 1/\left[x \ln(10/2)\right] = 1/\left[x \ln(5)\right],\ 2 \le x \le 10, \tag{3.3}$$

is the corresponding density function, and the probabilities $p_X(\mathcal{U}_x)$ and $p_X(\mathcal{U}_x^c)$ that define the CDF and CCDF are given by

$$p_X(\mathcal{U}_x) = \int_2^x \left\{1/\left[\tilde{x} \ln(5)\right]\right\} \mathrm{d}\tilde{x} = \ln(x/2)/\ln(5) \tag{3.4}$$

and

$$p_X\left(\mathcal{U}_x^c\right) = \int_x^{10} \left\{1/\left[\tilde{x} \ln(5)\right]\right\} \mathrm{d}\tilde{x} = \ln(10/x)/\ln(5), \tag{3.5}$$

respectively, for $2 \le x \le 10$. In practice, most probability spaces and their associated density functions are too complex to permit simple closed form representations as shown in Eqs. (3.4) and (3.5); rather, CDFs and CCDFs must be determined through the use of various numerical procedures.

Other summary measures for the distribution of x (i.e., for the probability space ($\mathcal{X}$, $\mathbb{X}$, p_E)) include the expected value $E_X(x)$ for x, the variance $V_X(x)$ for x, and the q quantile $Q_{Xq}(x)$ for x, where

$$E_X(x) = \int_{\mathcal{X}} \tilde{x}\, d_X(\tilde{x})\, \mathrm{d}\tilde{x}, \tag{3.6}$$

$$V_X(x) = \int_{\mathcal{X}} \left[\tilde{x} - E_X(x)\right]^2 d_X(\tilde{x})\, \mathrm{d}\tilde{x}, \tag{3.7}$$

and $Q_{Xq}(x)$ corresponds to the value of x for which

$$q = p_X(\mathcal{U}_x) = \int_{\mathcal{X}} \underline{\delta}_x(\tilde{x})\, d_X(\tilde{x})\, \mathrm{d}\tilde{x}. \tag{3.8}$$

Conceptually, the q quantile $Q_{Xq}(x)$ corresponds to the value of x obtained by (i) starting at q on the ordinate of the CDF for x, (ii) drawing a horizontal line to the CDF, and (iii) then drawing a vertical line down to the abscissa. The value for x at the point where the indicated vertical line intersects the abscissa corresponds to the q quantile $Q_{Xq}(x)$ for x (Fig. 3.1).

In most analyses, the result of interest is a function

$$\mathbf{y} = f(\mathbf{x}) \tag{3.9}$$

of uncertain analysis inputs. If $\mathbf{x}$ is uncertain as quantified by a probability space ($\mathcal{X}$, $\mathbb{X}$, p_X), then $\mathbf{y}$ is also uncertain, with this uncertainty quantified by a probability space ($\mathcal{Y}$, $\mathbb{Y}$, p_Y) that derives from the function $f(\mathbf{x})$ and the probability space ($\mathcal{X}$, $\mathbb{X}$, p_X) for $\mathbf{x}$. In concept, it is possible to derive the probability space ($\mathcal{Y}$, $\mathbb{Y}$, p_Y). In practice, ($\mathcal{Y}$, $\mathbb{Y}$, p_Y) is usually approximated with sampling-based procedures (see Sects. 7.2 – 7.4 and additional discussion in Refs. [55; 56]).

If $\mathbf{y}$ corresponds to a scalar y or y is a component of the vector $\mathbf{y}$, then the uncertainty in y that derives from the uncertainty in $\mathbf{x}$ is usually represented by a CDF or a CCDF that summarizes the corresponding probability space ($\mathcal{Y}$, $\mathbb{Y}$, p_Y) for y. Specifically, the CDF and CCDF for y are defined by plots of the points

$$\left[y,\ p_Y(\mathcal{U}_y)\right] \text{ and } \left[y,\ p_Y\left(\mathcal{U}_y^c\right)\right], \tag{3.10}$$

respectively, for $y \in \mathcal{Y}$, where

$$\begin{aligned}
\mathcal{U}_y &= \left\{\tilde{y} : \tilde{y} \in \mathcal{Y} \text{ and } \tilde{y} \le y\right\}, \\
p_Y(\mathcal{U}_y) &= \text{probability of } \mathcal{U}_y \text{ (i.e., of a value } \tilde{y} \le y) \\
&= \int_{\mathcal{X}} \underline{\delta}_y\left[f(\mathbf{x})\right] d_X(\mathbf{x})\, \mathrm{d}X \\
&\cong \sum_{i=1}^{nSX} \underline{\delta}_y\left[f(\mathbf{x}_i)\right]/nSX \\
&= \hat{p}_Y(\mathcal{U}_y), \\
p_Y\left(\mathcal{U}_y^c\right) &= \text{probability of } \mathcal{U}_y^c \text{ (i.e., of a value } \tilde{y} > y) \\
&= \int_{\mathcal{X}} \overline{\delta}_y\left[f(\mathbf{x})\right] d_X(\mathbf{x})\, \mathrm{d}X
\end{aligned}$$

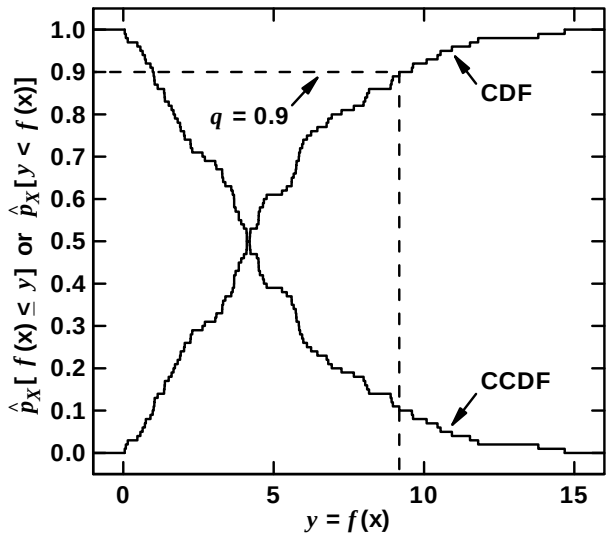

Fig. 3.2. Example CDF and CCDF for $y = f(\mathbf{x}) = x_1^2 + 2x_1x_2 + x_2^2$ generated with (i) a random sample $\mathbf{x}_i = [x_{i1}, x_{i2}]$, $i = 1, 2, \ldots, 100$, from uniform distributions on [0, 2] for x_1 and x_2 and (ii) $\hat{p}_X\,[f(\mathbf{x}) \le y]$ and $\hat{p}_X\,[y < f(\mathbf{x})]$ used as mnemonics for the estimated probabilities $\hat{p}_Y(\mathcal{U}_y)$ and $\hat{p}_Y(\mathcal{U}_y^c)$ defined in conjunction with Eq. (3.10) to emphasize the dependence of $p_Y(\mathcal{U}_y)$ and $p_Y(\mathcal{U}_y^c)$ on the probability space $(\mathcal{X}, \mathbb{X}, p_X)$.

$$\cong \sum_{i=1}^{nSX} \bar{\delta}_y\left[f\left(\mathbf{x}_i\right)\right]/nSX$$
$$= \hat{p}_Y\left(\mathcal{U}_y^c\right),$$

$\underline{\delta}_y$ and $\bar{\delta}_y$ are defined analogously to $\underline{\delta}_x$ and $\bar{\delta}_x$ in conjunction with Eq. (3.2), and $\mathbf{x}_i$, $i = 1, 2, \ldots, nSX$, is a sample from $\mathcal{X}$ generated in a manner consistent with the probability space $(\mathcal{X}, \mathbb{X}, p_X)$. The sampling-based (i.e., Monte Carlo) approximations to $p_Y(\mathcal{U}_y)$ and $p_Y(\mathcal{U}_y^c)$ are introduced because, in general, the defining integrals for $p_Y(\mathcal{U}_y)$ and $p_Y(\mathcal{U}_y^c)$ will be high-dimensional and thus too complex for a closed-form or quadrature-based evaluation.

As an example, approximations to the CDF and CCDF for

$$y = f\left(\mathbf{x}\right) = x_1^2 + 2x_1x_2 + x_2^2 \tag{3.11}$$

generated with a random sample

$$\mathbf{x}_i = \left[x_{i1}, x_{i2}\right], i = 1, 2, \ldots, nSX = 100, \tag{3.12}$$

from uniform distributions on [0, 2] for x_1 and x_2 are shown in Fig. 3.2.

Similarly to the summary measures for x in Eqs. (3.6) – (3.8), additional summary measures for the distribution of $y = f(\mathbf{x})$ (i.e., for the probability space $(\mathcal{Y}, \mathbb{Y}, p_Y)$ include the expected value $E_Y(y)$ for y, the variance $V_Y(y)$ for y,and the q quantile $Q_{Yq}(y)$ for y, where

$$\begin{aligned} E_Y\left(y\right) &= E_X\left[f\left(\mathbf{x}\right)\right] \\ &= \int_{\mathcal{X}} f\left(\tilde{\mathbf{x}}\right) d_X\left(\tilde{\mathbf{x}}\right) \mathrm{d}X, \end{aligned} \tag{3.13}$$

$$\begin{aligned} V_Y\left(y\right) &= V_X\left[f\left(\mathbf{x}\right)\right] \\ &= \int_{\mathcal{X}} \left\{f\left(\tilde{\mathbf{x}}\right) - E_X\left[f\left(\mathbf{x}\right)\right]\right\}^2 d_X\left(\tilde{\mathbf{x}}\right) \mathrm{d}X, \end{aligned} \tag{3.14}$$

and $Q_{Yq}(y) = Q_{Xq}[f(\mathbf{x})]$ corresponds to the value of y for which

$$q = p_Y\left(\mathcal{U}_y\right) = \int_{\mathcal{X}} \underline{\delta}_y\left[f\left(\tilde{\mathbf{x}}\right)\right] d_X\left(\tilde{\mathbf{x}}\right) \mathrm{d}X. \tag{3.15}$$

In practice, $Q_{Yq}(y)$ is usually approximated by the value y such that

$$q = p_Y\left(\mathcal{U}_y\right) \cong \sum_{i=1}^{nSX} \underline{\delta}_y\left[f\left(\mathbf{x}_i\right)\right]/nSX, \tag{3.16}$$

where $\mathbf{x}_i$, $i = 1, 2, \ldots, nSX$, is a sample from $\mathcal{X}$ generated in a manner consistent with the probability space $(\mathcal{X}, \mathbb{X}, p_X)$ as illustrated in Fig. 3.2. Further, $E_Y(y)$ and $V_Y(y)$ can be approximated in a similar manner with the indicated sample.

3.2 Basic Entities Underlying an Analysis

The posing and answering of Questions (Q1) – (Q4) introduced in Sect. 2 gives rise to an analysis predicated on three basic entities [95; 96]:

A probabilistic characterization of aleatory uncertainty, (EN1)

A model that predicts system behavior, (EN2)

and

A probabilistic characterization of epistemic uncertainty. (EN3)

Formally, (EN1) corresponds to a probability space $(\mathcal{A}, \mathbb{A}, p_A)$ for aleatory uncertainty and provides the an-

swers to Questions (Q1) and (Q2): "What can happen?" and "How likely is it to happen?"; (EN2) corresponds to a function f (e.g., the solution of a system of differential or partial differential equations) that determines analysis outcomes of interest and provides the answer to Question (Q3): "What are the consequences if it does happen?"; and (EN3) corresponds to a probability space ($\mathcal{E}$, $\mathbb{E}$, p_E) for epistemic uncertainty and provides the basis for answering Question (Q4): "How much confidence exists in the answers to the first three questions?"

The sample space $\mathcal{A}$ for the probability space ($\mathcal{A}$, $\mathbb{A}$, p_A) for aleatory uncertainty is a set of the form

$$\mathcal{A} = \left\{ \mathbf{a} : \mathbf{a} = \left[a_1, a_2, \ldots, a_{nA} \right] \right\}, \tag{3.17}$$

where each vector $\mathbf{a}$ contains the defining properties (e.g., time, size, location, …) for a single random occurrence associated with the system under study. In practice, ($\mathcal{A}$, $\mathbb{A}$, p_A) is usually defined by specifying probability distributions that characterize the occurrence of the individual components of $\mathbf{a}$ and hence the occurrence of the individual elements of $\mathcal{A}$. Further, the value of nA (i.e., the dimension of $\mathbf{a}$) may change for different elements of $\mathcal{A}$. For example, the elements of $\mathcal{A}$ might be of the form

$$\mathbf{a} = \left[n, t_1, \mathbf{p}_1, t_2, \mathbf{p}_2, \ldots, t_n, \mathbf{p}_n \right], \tag{3.18}$$

where n is the number of occurrences of a Poisson process over a specified period of time, t_i is the time of the ith occurrence, and $\mathbf{p}_i$ is a vector of properties associated with the ith occurrence. When needed, the density function associated with the probability space ($\mathcal{A}$, $\mathbb{A}$, p_A) is represented by $d_A(\mathbf{a})$.

Similarly, the sample space $\mathcal{E}$ for the probability space ($\mathcal{E}$, $\mathbb{E}$, p_E) for epistemic uncertainty is a set of the form

$$\mathcal{E} = \left\{ \mathbf{e} : \mathbf{e} = \left[e_1, e_2, \ldots, e_{nE} \right] \right\}, \tag{3.19}$$

where each vector $\mathbf{e}$ contains possible values for the nE epistemically uncertain variables under consideration. When needed, the density function associated with the probability space ($\mathcal{E}$, $\mathbb{E}$, p_E) is represented by $d_E(\mathbf{e})$.

In practice, ($\mathcal{E}$, $\mathbb{E}$, p_E) is usually defined by specifying probability distributions that characterize the epistemic uncertainty associated with the individual components of $\mathbf{e}$. Specifically, the distributions for the elements of $\mathbf{e}$ are providing a quantitative characterization of degrees of belief based on all available information with respect to where appropriate values of these elements are located for use in the analysis under consideration. The development of these distributions often involves an extensive expert review process [97-103]. The importance of expert review and judgment in the characterization of epistemic uncertainty is specifically recognized in the NAS/NRC report on QMU (Finding 1-5, p. 30, Ref. [77]).

In many analyses, $\mathbf{e}$ has the form

$$\mathbf{e} = \left[\mathbf{e}_A, \mathbf{e}_M \right], \tag{3.20}$$

where

$$\mathbf{e}_A = \left[\mathbf{e}_{A1}, \mathbf{e}_{A2}, \ldots, \mathbf{e}_{A,nEA} \right]$$

is a vector of nEA epistemically uncertain quantities used in the characterization of aleatory uncertainty (e.g., an imprecisely known rate λ that defines a Poisson process) and

$$\mathbf{e}_M = \left[\mathbf{e}_{M1}, \mathbf{e}_{M2}, \ldots, \mathbf{e}_{M,nEM} \right]$$

is a vector of nEM epistemically uncertain quantities used in the modeling of one or more physical processes (e.g., an imprecisely known thermal conductivity).

In some situations involving margin analyses, it may be appropriate to further decompose $\mathbf{e}_M$ into

$$\mathbf{e}_M = \left[\mathbf{e}_R, \mathbf{e}_P \right], \tag{3.21}$$

where $\mathbf{e}_R$ is a vector of epistemically uncertain quantities used in the definition of the requirements that underlie the margins under consideration and $\mathbf{e}_P$ is a vector of epistemically uncertain quantities that correspond to model parameters. The possible presence of epistemic uncertainty in the definition of requirements is specifically recognized by the NNSA is Quote (NNSA-3). Also, the NAS/NRC report on QMU recognizes the possibility of epistemic uncertainty in a requirement in a notional example involving the determination of a margin (pp. 25-26, Ref. [77]).

When $\mathbf{e}$ has the form $\mathbf{e} = [\mathbf{e}_A, \mathbf{e}_M]$ indicated in Eq. (3.20), the analysis in effect has two probability spaces for epistemic uncertainty: a probability space ($\mathcal{EA}$, $\mathbb{EA}$, p_{EA}) that characterizes the uncertainty in $\mathbf{e}_A$, and a

probability space ($\mathcal{EM}$, $\mathbb{EM}$, p_{EM}) that characterizes the uncertainty in $\mathbf{e}_M$. In turn,

$$\mathcal{E} = \mathcal{EA} \times \mathcal{EM} \tag{3.22}$$

is the sample space for the probability space ($\mathcal{E}$, $\mathbb{E}$, p_E). In practice, the probability spaces ($\mathcal{EA}$, $\mathbb{EA}$, p_{EA}) and ($\mathcal{EM}$, $\mathbb{EM}$, p_{EM}) are defined by assigning distributions to the components of $\mathbf{e}_A$ and $\mathbf{e}_M$, respectively, which in effect also defines the probability space ($\mathcal{E}$, $\mathbb{E}$, p_E). Although the probability spaces ($\mathcal{EA}$, $\mathbb{EA}$, p_{EA}) and ($\mathcal{EM}$, $\mathbb{EM}$, p_{EM}) are incorporated into the probability space ($\mathcal{E}$, $\mathbb{E}$, p_E), it is often convenient to maintain their separate identities for conceptual and notational purposes. When needed, the density functions associated with ($\mathcal{EA}$, $\mathbb{EA}$, p_{EA}) and ($\mathcal{EM}$, $\mathbb{EM}$, p_{EM}) are represented by $d_{EA}(\mathbf{e}_A)$ and $d_{EM}(\mathbf{e}_M)$, respectively. As a reminder, a different probability space ($\mathcal{A}$, $\mathbb{A}$, p_A) for aleatory uncertainty with corresponding density function $d_A(\mathbf{a}|\mathbf{e}_A)$ results for each element $\mathbf{e}_A$ of $\mathcal{EA}$.

As previously indicated, the probability spaces ($\mathcal{A}$, $\mathbb{A}$, p_A) and ($\mathcal{E}$, $\mathbb{E}$, p_E) correspond to the Entities (EN1) and (EN3). In turn, Entity (EN2) corresponds to a function of the form

$$\begin{aligned}\mathbf{y}\left(t\middle|\mathbf{a}, \mathbf{e}_M\right) &= \left[y_1\left(t\middle|\mathbf{a}, \mathbf{e}_M\right), y_2\left(t\middle|\mathbf{a}, \mathbf{e}_M\right), \ldots, y_{nY}\left(t\middle|\mathbf{a}, \mathbf{e}_M\right)\right] \\ &= \mathbf{f}\left(t\middle|\mathbf{a}, \mathbf{e}_M\right),\end{aligned} \tag{3.23}$$

where $\mathbf{a} \in \mathcal{A}$, $\mathcal{E} = \mathcal{EA} \times \mathcal{EM}$ as indicated in Eq. (3.22), $\mathbf{e}_M \in \mathcal{EM}$, t corresponds to time with the assumption that time-dependent results are under consideration, and the vertical line in $\mathbf{y}(t|\mathbf{a}, \mathbf{e}_M)$ is used to indicate the concept of "conditional on". Further, in a QMU analysis, one or more elements of $\mathbf{y}(t|\mathbf{a}, \mathbf{e}_M)$ will either be margins or analysis results used in the definition of margins. In most real analyses, the number of results under consideration (i.e., nY) is likely to be very large. However, for notational simplicity, a real-valued result

$$y\left(t\middle|\mathbf{a}, \mathbf{e}_M\right) = f\left(t\middle|\mathbf{a}, \mathbf{a}_M\right) \tag{3.24}$$

is assumed to be under consideration.

The uncertainty associated with $y(t|\mathbf{a}, \mathbf{e}_M)$ is often studied in one of two contexts. In the first context, $\mathbf{a}$ is assumed to be fixed, and the uncertainty in $y(t|\mathbf{a}, \mathbf{e}_M)$ that derives from the epistemic uncertainty associated with $\mathbf{e}_M$ is analyzed. In essence, this context involves only the Entity (EN2) corresponding to the function $y(t|\mathbf{a}, \mathbf{e}_M)$ and the Entity (EN3) corresponding to the probability space ($\mathcal{EM}$, $\mathbb{EM}$, p_{EM}) that characterizes the epistemic uncertainty associated with $\mathbf{e}_M$. The Entity (EN1) corresponding to the probability space ($\mathcal{A}$, $\mathbb{A}$, p_A) that characterizes the aleatory uncertainty associated with $\mathbf{a}$ does not enter into the analysis as a result of fixing $\mathbf{a}$ at a specific value.

In the second context, $\mathbf{a}$ is not assumed to be fixed, and the distributions of $y(t|\mathbf{a}, \mathbf{e}_M)$ that derive from the aleatory uncertainty associated with $\mathbf{a}$ characterized by probability spaces ($\mathcal{A}$, $\mathbb{A}$, p_A) conditional on specific values for $\mathbf{e} = [\mathbf{e}_A, \mathbf{e}_M]$ are central to the analysis. In this context, all three entities are present, with the analysis involving distributions that derive from epistemic uncertainty for (i) CDFs and CCDFs that derive from aleatory uncertainty or (ii) summary quantities (e.g., expected values, quantiles) for CDFs and CCDFs that derive from aleatory uncertainty. Specifically, each CDF and each CCDF indicated in the preceding sentence derives from aleatory uncertainty conditional on a specific value for $\mathbf{e} = [\mathbf{e}_A, \mathbf{e}_M]$; in turn, the epistemic uncertainty associated with $\mathbf{e}$ and characterized by the probability space ($\mathcal{E}$, $\mathbb{E}$, p_E) results in distributions of these CDFs and CCDFs and also in distributions of quantities such as means and variances that summarize these CDFs and CCDFs. The preceding distributions that derive from epistemic uncertainty are the focus of study in this second analysis context.

The two indicated analysis contexts are discussed in the next four sections (Sects. 3.3 – 3.6). However, most large analyses that involve both aleatory uncertainty and epistemic uncertainty will have various subanalyses that involve each of these analysis contexts. Specifically, some subanalyses will be carried out conditional on specific realizations of aleatory uncertainty (i.e., analyses in the sense of the first context as discussed in Sects. 3.3 and 3.4) and some subanalyses will be carried out that address the epistemic uncertainty associated with results that derive from aleatory uncertainty (i.e., analyses in the sense of the second context as discussed in Sects. 3.5 and 3.6).

3.3 Analysis in the Presence of Only Epistemic Uncertainty

This section presents a formal description of the representation of uncertainty in an analysis that involves only epistemic uncertainty. The following section (Sect. 3.4) then presents a simple example illustrating the formal concepts presented in the present section. If desired, Sect. 3.4 can be read before Sect. 3.3, with

Sect. 3.3 being referred to only when a more technical description of the results in Sect. 3.4 is desired. The importance of the quantification of the epistemic uncertainty in analysis results that derives from epistemic uncertainty in analysis inputs is emphasized in the NAS/NRC report on QMU (Recommendation 1-2, p. 22, Ref. [77]).

The CDF and CCDF introduced in the first analysis context at the end of the preceding section and conditional on specific values for t and $\mathbf{a}$ are defined as indicated in Eq. (3.10). Specifically, the CDF and CCDF for $y(t|\mathbf{a}, \mathbf{e}_M)$ that derive from the different possible values for $\mathbf{e}_M$ are defined by plots of the points

$$\left\{y,\ p_{EM}\left[\mathcal{U}_y\left(t|\mathbf{a}\right)\right]\right\} \text{ and } \left\{y,\ p_{EM}\left[\mathcal{U}_y^c\left(t|\mathbf{a}\right)\right]\right\}, \quad (3.25)$$

respectively, for $y \in \mathcal{Y}(t|\mathbf{a})$, where

$$\mathcal{Y}\left(t|\mathbf{a}\right) = \left\{y : y = y\left(t|\mathbf{a}, \mathbf{e}_M\right) \text{ for } \mathbf{e}_M \in \mathcal{EM}\right\},$$

$$\mathcal{U}_y\left(t|\mathbf{a}\right) = \left\{\tilde{y} : \tilde{y} \in \mathcal{Y}\left(t|\mathbf{a}\right) \text{ and } \tilde{y} \le y\right\},$$

$$p_{EM}\left[\mathcal{U}_y\left(t|\mathbf{a}\right)\right] = \text{ probability of } \mathcal{U}_y\left(t|\mathbf{a}\right) \text{ (i.e., of a value } \tilde{y} \le y\text{)}$$

$$= \int_{\mathcal{EM}} \underline{\delta}_y\left[y\left(t|\mathbf{a}, \mathbf{e}_M\right)\right] d_{EM}\left(\mathbf{e}_M\right) \mathrm{d}EM$$
$$\cong \sum_{i=1}^{nSE} \underline{\delta}_y\left[y\left(t|\mathbf{a}, \mathbf{e}_{Mi}\right)\right] \Big/ nSE$$
$$= \hat{p}_{EM}\left[\mathcal{U}_y\left(t|\mathbf{a}\right)\right],$$

$$p_{EM}\left[\mathcal{U}_y^c\left(t|\mathbf{a}\right)\right] = \text{ probability of } \mathcal{U}_y^c\left(t, \mathbf{a}\right) \text{ (i.e., of a value } \tilde{y} > y\text{)}$$

$$= \int_{\mathcal{EM}} \overline{\delta}_y\left[y\left(t|\mathbf{a}, \mathbf{e}_M\right)\right] d_{EM}\left(\mathbf{e}_M\right) \mathrm{d}EM$$
$$\cong \sum_{i=1}^{nSE} \overline{\delta}_y\left[y\left(t|\mathbf{a}, \mathbf{e}_{Mi}\right)\right] \Big/ nSE$$
$$= \hat{p}_{EM}\left[\mathcal{U}_y^c\left(t|\mathbf{a}\right)\right],$$

$\underline{\delta}_y$ and $\overline{\delta}_y$ are defined analogously to $\underline{\delta}_x$ and $\overline{\delta}_x$ in conjunction with Eq. (3.2), and $\mathbf{e}_{Mi}$, $i = 1, 2, \ldots, nSE$, is a sample from $\mathcal{EM}$ generated in a manner consistent with the probability space ($\mathcal{EM}$, $\mathbb{EM}$, p_{EM}) and its associated density function $d_{EM}(\mathbf{e}_M)$. The result is a CDF and CCDF of the form shown in Fig. 3.2 that summarize the epistemic uncertainty in $\mathbf{y}(t|\mathbf{a}, \mathbf{e}_M)$ that derives from the epistemic uncertainty in $\mathbf{e}_M$ characterized by the probability space ($\mathcal{EM}$, $\mathbb{EM}$, p_{EM}).

The CDF and CCDF defined in Eq. (3.25) can also be summarized with various real-valued quantities, including an expected value $E_{EM}[y(t|\mathbf{a}, \mathbf{e}_M)]$, a variance $V_{EM}[y(t|\mathbf{a}, \mathbf{e}_M)]$, and selected quantiles $Q_{EMq}[y(t|\mathbf{a}, \mathbf{e}_M)]$. As described in Eqs. (3.13) – (3.16),

$$E_{EM}\left[y\left(t|\mathbf{a}, \mathbf{e}_M\right)\right] = \int_{\mathcal{EM}} y\left(t|\mathbf{a}, \mathbf{e}_M\right) d_{EM}\left(\mathbf{e}_M\right) \mathrm{d}EM$$
$$\cong \sum_{i=1}^{nSE} y\left(t|\mathbf{a}, \mathbf{e}_{Mi}\right) \Big/ nSE$$
$$= \hat{E}_{EM}\left[y\left(t|\mathbf{a}, \mathbf{e}_M\right)\right], \quad (3.26)$$

$$V_{EM}\left[y\left(t|\mathbf{a}, \mathbf{e}_M\right)\right]$$
$$= \int_{\mathcal{EM}} \left\{y\left(t|\mathbf{a}, \mathbf{e}_M\right) - E_{EM}\left[y\left(t|\mathbf{a}, \mathbf{e}_M\right)\right]\right\}^2 d_{EM}\left(\mathbf{e}_M\right) \mathrm{d}EM$$
$$\cong \sum_{i=1}^{nSE} \left\{y\left(t|\mathbf{a}, \mathbf{e}_{Mi}\right) - \hat{E}_{EM}\left[y\left(t|\mathbf{a}, \mathbf{e}_M\right)\right]\right\}^2 \Big/ nSE$$
$$= \hat{V}_{EM}\left[y\left(t|\mathbf{a}, \mathbf{e}_M\right)\right], \quad (3.27)$$

and $Q_{EMq}[y(t|\mathbf{a}, \mathbf{e}_M)$ corresponds to the value y such that

$$q = p_{EM}\left[\mathcal{U}_y\left(t|\mathbf{a}\right)\right]$$
$$= \int_{\mathcal{EM}} \underline{\delta}_y\left[y\left(t|\mathbf{a}, \mathbf{e}_M\right)\right] d_{EM}\left(\mathbf{e}_M\right) \mathrm{d}EM \quad (3.28)$$
$$\cong \sum_{i=1}^{nSE} \underline{\delta}_y\left[y\left(t|\mathbf{a}, \mathbf{e}_{Mi}\right)\right] \Big/ nSE,$$

where $\mathbf{e}_{Mi}$, $i = 1, 2, \ldots, nSE$, is the sample indicated in conjunction with Eq. (3.25).

As discussed in Sect. 7 and in greater detail in Ref. [56], the sample $\mathbf{e}_{Mi}$, $i = 1, 2, \ldots, nSE$, also provides the basis for the implementation of a variety of sensitivity analysis procedures. The use of such procedures is a natural and important part of any sampling-based uncertainty analysis. The importance and usefulness of appropriate sensitivity analyses is emphasized in the NAS/NRC report on QMU (pp. 14-15, Ref. [77]).

3.4 Example Analysis in the Presence of Only Epistemic Uncertainty

A simple example is now presented to illustrate the concepts introduced in Sect.3.3. This example will also

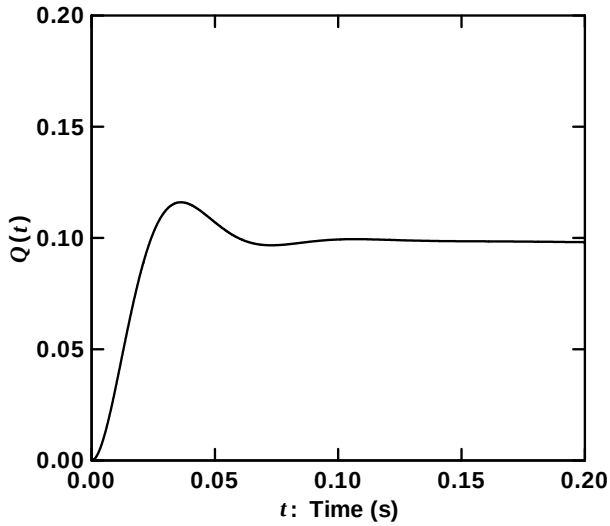

Fig. 3.3. Solution $Q(t)$ shown in Eq. (3.31) to differential equation in Eq. (3.29) obtained with L = 1 henry, R = 100 ohms, $C = 10^{-4}$ farads, E_0 = 1000 volts, and $\lambda = 0.1\ \mathrm{s}^{-1}$.

be used in Sects. 4 and 9 to illustrate potential QMU analyses involving only epistemic uncertainty.

The example is based on a closed electrical circuit that is under consideration for some unstated realization **a** of aleatory uncertainty. For example, **a** might simply correspond to nominal (i.e., unperturbed) conditions for the system under study. Specifically, the behavior of this circuit is described by a differential equation

$$\begin{aligned} &L\,\mathrm{d}^2 Q\big/\mathrm{d}t^2 + R\,\mathrm{d}Q\big/\mathrm{d}t + Q\big/C = E_0 \exp\left(-\lambda t\right) \\ &\quad Q\left(0\right) = 0,\ \mathrm{d}Q\left(0\right)\big/\mathrm{d}t = 0, \end{aligned} \tag{3.29}$$

where

$Q(t)$ = electrical charge (coulombs) at time t (s),
L = inductance (henrys),
R = resistance (ohms),
C = capacitance (farads),
$E_0\exp(-\lambda t)$ = electromotive force (volts),
$\mathrm{d}Q/\mathrm{d}t$ = current (amperes).

For this example, it is also assumed that R, L and C have values such that the inequality

$$R^2 - 4L/C < 0 \tag{3.30}$$

holds.

The significance of the preceding inequality is that it results in $Q(t)$ displaying a damped, oscillatory behavior. In particular, the closed form solution to Eq. (3.29) when the inequality in Eq. (3.30) holds is

$$\begin{aligned} Q\left(t\right) = \exp\left[\left(-R/2L\right)t\right]&\left\{c_1 \cos\left[\left(\sqrt{\left|R^2 - 4L/C\right|}\Big/2L\right)t\right]\right. \\ &\left. + c_2 \sin\left[\left(\sqrt{\left|R^2 - 4L/C\right|}\Big/2L\right)t\right]\right\} \\ &- c_1 \exp\left(-\lambda t\right) \end{aligned} \tag{3.31}$$

with

$$c_1 = -CE_0\Big/\left(CL\lambda^2 - CR\lambda + 1\right)$$

$$c_2 = \frac{2L}{\sqrt{\left|R^2 - 4L/C\right|}} \times \left[\frac{\lambda CE_0}{CL\lambda^2 - CR\lambda + 1} - \frac{RCE_0}{2L\left(CL\lambda^2 - CR\lambda + 1\right)}\right].$$

As an example, $Q(t)$ is illustrated in Fig. 3.3 with L = 1 henry, R = 100 ohms, $C = 10^{-4}$ farads, E_0 = 1000 volts, and $\lambda = 0.1\ \mathrm{s}^{-1}$.

For the examples of this section, the vector $\mathbf{e}_M$ of epistemically uncertain analysis inputs for the model defined in Eqs. (3.29) – (3.31) is

$$\mathbf{e}_M = \left[e_{M1}, e_{M2}, e_{M3}, e_{M4}, e_{M5}\right] = \left[L, R, C, E_0, \lambda\right], \tag{3.32}$$

with e_{M1}, e_{M2}, …, e_{M5} used in place of L, R, …, λ to represent the elements of **e** when notationally convenient. Incorporation of **a** and $\mathbf{e}_M$ into the notation for $Q(t)$ results in the representation $Q(t|\mathbf{a}, \mathbf{e}_M)$, with $Q(t|\mathbf{a}, \mathbf{e}_M)$ corresponding to the generic representation $y(t|\mathbf{a}, \mathbf{e}_M)$ in Eq. (3.24).

The appropriate values for L, R, C, E_0 and λ are assumed to be contained in the intervals

$$\begin{aligned} \mathcal{EM}_1 &= \left\{L : L_{mn} \le L \le L_{mx}\right\} \\ &= \left\{L : 0.8 \le L \le 1.2 \text{ henrys}\right\}, \end{aligned} \tag{3.33}$$

$$\begin{aligned} \mathcal{EM}_2 &= \left\{R : R_{mn} \le R \le R_{mx}\right\} \\ &= \left\{R : 50 \le R \le 100 \text{ ohms}\right\}, \end{aligned} \tag{3.34}$$

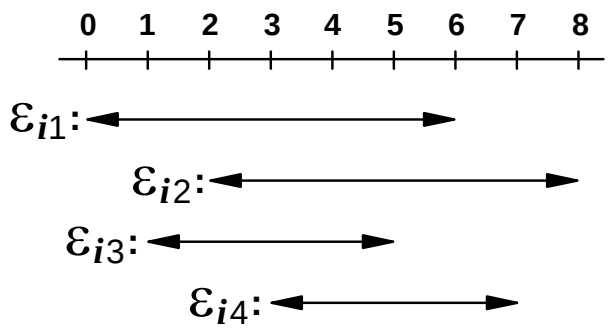

Fig. 3.4. Illustration of sets $\mathcal{E}_{i1}$, $\mathcal{E}_{i2}$, $\mathcal{E}_{i3}$ and $\mathcal{E}_{i4}$ defined in Eqs. (3.38) – (3.41) with the interval [a, b] normalized to the interval [0, 8] for representational simplicity.

$$\begin{aligned}\mathcal{EM}_3 &= \{C : C_{mn} \le C \le C_{mx}\} \\ &= \left\{C : 0.9\times10^{-4} \le C \le 1.1\times10^{-4} \text{ farads}\right\},\end{aligned} \tag{3.35}$$

$$\begin{aligned}\mathcal{EM}_4 &= \{E_0 : E_{mn} \le E_0 \le E_{mx}\} \\ &= \{E_0 : 900 \le E_0 \le 1100 \text{ volts}\},\end{aligned} \tag{3.36}$$

and

$$\begin{aligned}\mathcal{EM}_5 &= \{\lambda : \lambda_{mn} \le \lambda \le \lambda_{mx}\} \\ &= \left\{\lambda : 0.4 \le \lambda \le 0.8 \text{ s}^{-1}\right\},\end{aligned} \tag{3.37}$$

respectively.

A probabilistic characterization of the epistemic uncertainty associated with L, R, …, λ is provided by a probability distribution defined on each of the preceding intervals. Specifically, four subintervals are considered for each of the intervals $\mathcal{EM}_i$, i = 1, 2, …, 5, defined in Eqs. (3.33) – (3.37):

$$\mathcal{E}_{i1} = \left[a, b-(b-a)/4\right], \tag{3.38}$$

$$\mathcal{E}_{i2} = \left[a+(b-a)/4, b\right], \tag{3.39}$$

$$\mathcal{E}_{i3} = \left[a+(b-a)/8, b-3(b-a)/8\right], \tag{3.40}$$

$$\mathcal{E}_{i4} = \left[a+3(b-a)/8, b-(b-a)/8\right], \tag{3.41}$$

where [a, b] corresponds to [L_{mn}, L_{mx}], [R_{mn}, R_{mx}], [C_{mn}, C_{mx}], [E_{mn}, E_{mx}] and [λ_{mn}, λ_{mx}] for i = 1, 2, 3, 4 and 5, respectively (Fig. 3.4). For example and for a given element e_{Mi} of $\mathbf{e}_M$, each of the preceding intevals could have been indicated by a different source as containing the correct value to use for e_{Mi} in the analysis under consideration.

In turn, the corresponding density function $d_i(e_{Mi})$ for the set $\mathcal{EM}_i$ is given by

$$d_i\left(e_{Mi}\right) = \sum_{j=1}^{4} \delta_{ij}\left(e_{Mi}\right)/4\left[\max\left(\mathcal{E}_{ij}\right) - \min\left(\mathcal{E}_{ij}\right)\right] \tag{3.42}$$

under the assumption that the four sources that provided the intervals in Eqs. (3.38) – (3.41) for an element e_{Mi} of $\mathbf{e}_M$ are equally credible, where

$$\delta_{ij}\left(e_{Mi}\right) = \begin{cases} 1 & \text{if } e_{Mi} \in \mathcal{E}_{ij} \\ 0 & \text{otherwise.} \end{cases}$$

The preceding specification for $d_i(e_{Mi})$ corresponds to defining a uniform distribution on each interval $\mathcal{E}_{ij}$ and then weighting each distribution equally. The equal weighting derives from an assumption of equal credibilty for the four sources of the intervals in Eqs. (3.38) – (3.41). The definition of the density functions $d_i(e_{Mi})$ in Eq. (3.42) results in the assignment of more probability where the inervals supplied by the four sources overlap and less probability where the intervals do not overlap. The density functions $d_i(e_{Mi})$ in essence define probability spaces ($\mathcal{EM}_i$, $\mathbb{EM}_i$, $p_{EM,i}$) for the variables e_{Mi} , i = 1, 2, …, 5.

The set $\mathcal{EM}$ of possible values for $\mathbf{e}_M$ is given by

$$\mathcal{EM} = \mathcal{EM}_1 \times \mathcal{EM}_2 \times \mathcal{EM}_3 \times \mathcal{EM}_4 \times \mathcal{EM}_5, \tag{3.43}$$

where $\mathcal{EM}_1$, $\mathcal{EM}_2$, ..., $\mathcal{EM}_5$ are defined in Eqs. (3.33) – (3.37). In turn, $\mathcal{EM}$ has a probabilistic structure that derives from the distributions characterizing the uncertainty in e_{Mi}, e_{M2}, …, e_{M5}. Formally, this structure corresponds to a probability space ($\mathcal{EM}$, $\mathbb{EM}$, p_{EM}) that, in effect, is defined by the density functions introduced in Eq. (3.42).

The epistemic uncertainty associated with $Q(t|\mathbf{a}, \mathbf{e}_M)$ that derives from the probability space ($\mathcal{EM}$, $\mathbb{EM}$, p_{EM}) is now considered. As indicated in Eqs. (3.25) – (3.28), this uncertainty can be characterized by various quantities defined by integrals over $\mathcal{EM}$. However, such integrals are difficult to determine in closed form (i.e., by use of antiderivatives in conjunction with the Fundamental Theorem of Calculus) because of the high dimensionality of $\mathbf{e}_M$ and the complexity of the func tion being integrated. Instead, sampling-based methods are used in most analyses to determine these quantities.

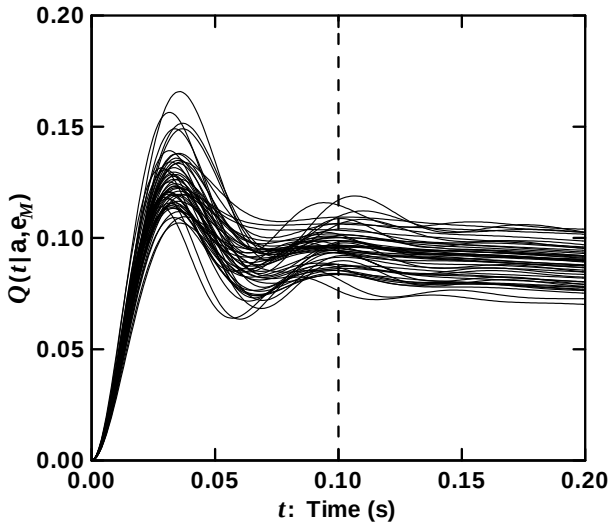

Fig. 3.5. Solutions $Q(t|\mathbf{a}, \mathbf{e}_{Mi})$ to differential equation in Eq. (3.29) obtained with the first 50 elements of the LHS in Eq. (3.44) (i.e., with $\mathbf{e}_{Mi}$ for i = 1, 2, …, 50).

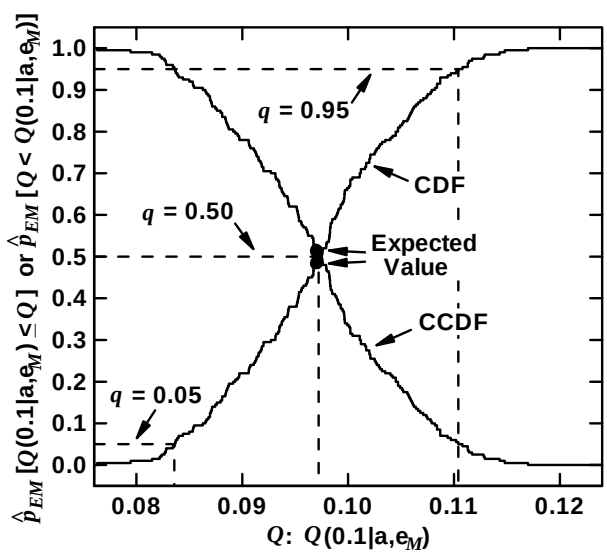

Fig. 3.6. Estimated CDF and CCDF for $Q(0.1|\mathbf{a}, \mathbf{e}_{Mi})$ (i) obtained with the LHS of size 200 in Eq. (3.44) generated from $\mathcal{EM}$ in consistency with the defining density functions for the probability space ($\mathcal{EM}$, $\mathbb{EM}$, p_{EM}) and (ii) presented with $\hat{p}_{EM}[Q(0.1|\mathbf{a}, \mathbf{e}_M) \le Q]$ and $\hat{p}_{EM}[Q < Q(0.1|\mathbf{a}, \mathbf{e}_M)]$ used as mnemonics for estimated probabilities of the form $\hat{p}_{EM}[\mathcal{U}_y(0.1|\mathbf{a})]$ and $\hat{p}_{EM}[\mathcal{U}_y^c(0.1|\mathbf{a})]$ defined in conjunction with Eq. (3.25).

Consistent with this approach, the present example uses a Latin hypercube sample (LHS)

$$\mathbf{e}_{Mi} = \left[e_{Mi1}, e_{Mi2}, \ldots, e_{Mi5}\right], i = 1, 2, \ldots, nSE, \qquad (3.44)$$

of size nSE = 200 generated from $\mathcal{EM}$ in consistency with the probability space ($\mathcal{EM}$, $\mathbb{EM}$, p_{EM}) (i.e., in consistency with the distributions associated with the density functions defined in Eq. (3.42)). As discussed in Sect. 7 and in more detail in Refs. [45; 55; 56], Latin hypercube sampling is widely used in sampling-based uncertainty and sensitivity analyses involving computationally demanding models because of its efficient stratification properties. In addition, this sampling-based approach also provides the basis for the application of a variety of sensitivity analysis procedures (see Sect. 7 and Ref. [56]).

The sample in Eq. (3.44) results in nSE = 200 time-dependent results: $Q(t|\mathbf{a}, \mathbf{e}_{Mi})$, i = 1, 2, … 200 (Fig. 3.5). The spread of the curves in Fig. 3.5 provides a nonquantitative indication of the epistemic uncertainty associated with $Q(t|\mathbf{a}, \mathbf{e}_M)$ that derives from the uncertainty in $\mathbf{e}_M$ as quantified by the probability space ($\mathcal{EM}$, $\mathbb{EM}$, p_{EM}). Only 50 of the 200 time-dependent results for $Q(t|\mathbf{a}, \mathbf{e}_{Mi})$ are presented in Fig. 3.5 as presentation of all 200 curves results in an almost solid band of overlapping curves that obscures the shape of the individual curves.

A quantitative summary of the epistemic uncertainty in $Q(t|\mathbf{a}, \mathbf{e}_M)$ that derives from the epistemic uncertainty in $\mathbf{e}_M$ is provided by the CDFs and CCDFs for $Q(t|\mathbf{a}, \mathbf{e}_M)$ at selected points in time. As an example, approximations to the CDF and CCDF at t = 0.1 s obtained with use of the sample in Eq. (3.44) are shown in Fig. 3.6. Specifically, the CDF and CCDF in Fig. 3.6 are constructed from the values for $Q(0.1|\mathbf{a}, \mathbf{e}_{Mi})$ associated with the vertical line in Fig. 3.5 as described in conjunction with Eq. (3.25). With respect to notation, the expressions $\hat{p}_{EM}[Q(0.1|\mathbf{a}, \mathbf{e}_M) \le Q]$ and $\hat{p}_{EM}[Q < Q(0.1|\mathbf{a}, \mathbf{e}_M)]$ on the ordinate of Fig. 3.6 correspond to the defining probabilities for the CDF and CCDF, respectively, for $Q(0.1|\mathbf{a}, \mathbf{e}_M)$. Specifically, $\hat{p}_{EM}[Q(0.1|\mathbf{a}, \mathbf{e}_M) \le Q]$ is the estimated probability that $Q(0.1|\mathbf{a}, \mathbf{e}_M)$ is less than or equal to a value Q on the abscissa, and $\hat{p}_{EM}[Q < Q(0.1|\mathbf{a}, \mathbf{e}_M)]$ is the estimated probability that $Q(0.1|\mathbf{a}, \mathbf{e}_M)$ is greater than a value Q on the abscissa. The indicated probabilities are characterizing epistemic uncertainty and thus are indicating degrees of belief with respect to where the correct value for $Q(0.1|\mathbf{a}, \mathbf{e}_M)$ is located. Thus, for example, there is a "degree of belief" probability of 0.9

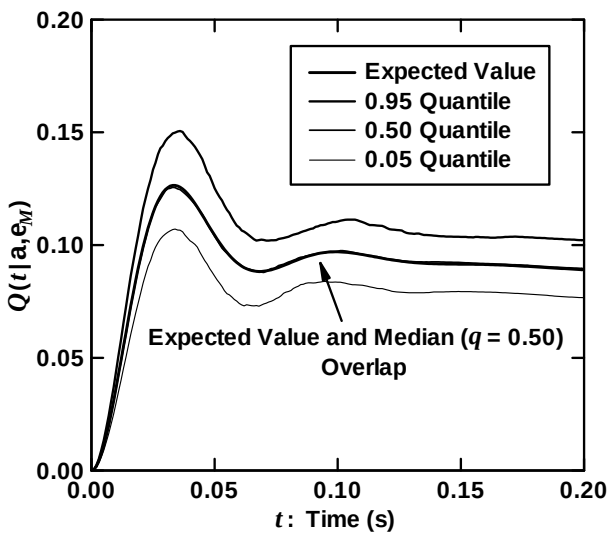

Fig. 3.7. Estimated time-dependent expected value and quantile curves for $Q(t|\mathbf{a}, \mathbf{e}_M)$ obtained with the LHS of size 200 in Eq. (3.44) generated from $\mathcal{EM}$ in consistency with the defining density functions for the probability space $(\mathcal{EM}, \mathbb{EM}, p_{EM})$.

that $Q(0.1|\mathbf{a}, \mathbf{e}_M)$ is located between the 0.05 and 0.95 quantiles in Fig. 3.6. Further, the expected value and quantile values indicated in Fig. 3.6 are obtained as described in Eqs. (3.26) and (3.28), respectively. In this example, the expected value and median value are very close together; this is often not the case in analyses that involve substantial epistemic uncertainties.

The presentation of CDFs and CCDFs of the form shown in Fig. 3.6 for multiple values of t is cumbersome. An effective alternative is to plot expected values and quantiles as functions of time (Fig. 3.7). With this presentation format, expected values and quantiles as indicated in Fig. 3.6 are determined for a sequence of values for t and then plotted above these values to obtain the expected value and quantile curves in Fig. 3.7. Specifically, the expected value curve in Fig. 3.7 is a plot of the points

$$\left(t, \hat{E}_{EM}\left[y\left(t|\mathbf{a}, \mathbf{e}_M\right)\right]\right), \; 0 \le t \le 0.20, \tag{3.45}$$

with $\hat{E}_{EM}[y(t|\mathbf{a}, \mathbf{e}_M)]$ defined as indicated in Eq. (3.26), and the quantile curves in Fig. 3.7 are plots of points

$$\left(t, \hat{Q}_{EMq}\left[y\left(t|\mathbf{a}, \mathbf{e}_M\right)\right]\right), \; 0 \le t \le 0.20, \tag{3.46}$$

for q = 0.05, 0.5 and 0.95 with $\hat{Q}_{EMq}[y(t|\mathbf{a}, \mathbf{e}_M)]$ defined as indicated in Eq. (3.28). In this example, the expected value and median value (i.e., 0.5 quantile) curves almost exactly overlap.

3.5 Analysis in the Presence of Aleatory and Epistemic Uncertainty

This section presents a formal description of the representation of uncertainty in an analysis that involves both aleatory and epistemic uncertainty. The following section (Sect. 3.6) then presents a simple example illustrating the formal concepts presented in the present section. If desired, Sect. 3.6 can be read before Sect. 3.5, with Sect. 3.5 being referred to only when a more technical description of the results in Sect. 3.6 is desired.

The analyses described in Sects. 3.5 and 3.6 involve what the NAS/NRC report on QMU refers to as the "probability of frequency approach" and recommends for use in QMU analyses (Recommendation 1-7, p. 33, and App. A, Ref. [77]). Specifically, the descriptor "probability of frequency approach" designates an analysis in which a careful distinction and separation is maintained between the effects and implications of aleatory uncertainty and the effects and implications of epistemic uncertainty.

The CDF and CCDF introduced in the second analysis context described in Sect. 3.2 and conditional on specific values for t and $\mathbf{e} = [\mathbf{e}_A, \mathbf{e}_M]$ are also defined as indicated in Eq. (3.10). Specifically, the CDF and CCDF for $y(t|\mathbf{a}, \mathbf{e}_M)$ that derive from the different possible values for $\mathbf{a}$ are defined by the plots of the points

$$\left\{y, \; p_A\left[\mathcal{U}_y\left(t|\mathbf{e}\right)\middle|\mathbf{e}_A\right]\right\} \text{ and } \left\{y, \; p_A\left[\mathcal{U}_y^c\left(t|\mathbf{e}\right)\middle|\mathbf{e}_A\right]\right\}, \tag{3.47}$$

respectively, for $y \in \mathcal{Y}(t|\mathbf{e})$, where

$$\begin{aligned}
\mathcal{Y}\left(t|\mathbf{e}\right) &= \left\{y : y = y\left(t|\mathbf{a}, \mathbf{e}_M\right) \text{ for } \mathbf{a} \in \mathcal{A}\right\}, \\
\mathcal{U}_y\left(t|\mathbf{e}\right) &= \left\{\tilde{y} : \tilde{y} \in \mathcal{Y}\left(t|\mathbf{e}\right) \text{ and } \tilde{y} \le y\right\}, \\
p_A\left[\mathcal{U}_y\left(t|\mathbf{e}\right)\middle|\mathbf{e}_A\right] &= \text{probability of } \mathcal{U}_y\left(t|\mathbf{e}\right) \text{ (i.e., of a value } \tilde{y} \le y\text{)} \\
&= \int_{\mathcal{A}} \delta_y\left[y\left(t|\mathbf{a}, \mathbf{e}_M\right)\right] d_A\left(\mathbf{a}|\mathbf{e}_A\right) \mathrm{d}A \\
&\cong \sum_{j=1}^{nSA} \delta_y\left[y\left(t|\mathbf{a}_j, \mathbf{e}_M\right)\right] \Big/ nSA \\
&= \hat{p}_A\left[\mathcal{U}_y\left(t|\mathbf{e}\right)\middle|\mathbf{e}_A\right],
\end{aligned}$$

$$p_A\left[\mathcal{U}_y^c\left(t|\mathbf{e}\right)\middle|\mathbf{e}_A\right] = \text{probability of } \mathcal{U}_y^c\left(t,\mathbf{e}\right) \text{ (i.e., of a value } \tilde{y} > y \text{)}$$
$$= \int_{\mathcal{A}} \bar{\delta}_y\left[y\left(t|\mathbf{a},\mathbf{e}_M\right)\right] d_A\left(\mathbf{a}|\mathbf{e}_A\right) \mathrm{d}A$$
$$\cong \sum_{j=1}^{nSA} \bar{\delta}_y\left[y\left(t|\mathbf{a}_j,\mathbf{e}_M\right)\right] \Big/ nSA$$
$$= \hat{p}_A\left[\mathcal{U}_y^c\left(t|\mathbf{e}\right)\middle|\mathbf{e}_A\right],$$

$\underline{\delta}_y$ and $\bar{\delta}_y$ are defined analogously to $\underline{\delta}_x$ and $\bar{\delta}_x$ in conjunction with Eq. (3.2), and $\mathbf{a}_j$, j = 1, 2, …, nSA, is a sample from $\mathcal{A}$ generated in a manner consistent with the probability space ($\mathcal{A}$, $\mathbb{A}$, p_A) and its associated density function $d_A(\mathbf{a}|\mathbf{e}_A)$. The result is a CDF and CCDF of the form shown in Fig. 3.2 that summarize the aleatory uncertainty in $y(t|\mathbf{a}, \mathbf{e}_M)$ that derives from the aleatory uncertainty in $\mathbf{a}$ characterized by the probability space ($\mathcal{A}$, $\mathbb{A}$, p_A).

In general, the set $\mathcal{A}$ could be, and often is, a function of elements of $\mathbf{e}_A$. In this case, the sets $\mathcal{A}$ and $\mathbb{A}$ would appropriately be represented by $\mathcal{A}(\mathbf{e}_A)$ and $\mathbb{A}(\mathbf{e}_A)$. Then, the representation for the probability space ($\mathcal{A}$, $\mathbb{A}$, p_A) conditional on an element $\mathbf{e} = [\mathbf{e}_A, \mathbf{e}_M]$ of $\mathcal{E}$ would be $[\mathcal{A}(\mathbf{e}_A), \mathbb{A}(\mathbf{e}_A), p_A(\mathcal{U}|\mathbf{e}_A)]$. To reduce notational clutter, this fully general representation for ($\mathcal{A}$, $\mathbb{A}$, p_A) is not used. Instead, the possible dependence of ($\mathcal{A}$, $\mathbb{A}$, p_A) on the elements of $\mathbf{e}_A$ is indicated through the use of the notations $p_A(\mathcal{U}|\mathbf{e}_A)$ and $d_A(\mathbf{a}|\mathbf{e}_A)$.

Similarly to the CDF and CCDF defined in Eq. (3.10), the CDF and CCDF defined in Eq. (3.47) can also be summarized with various real-valued quantities, including an expected value $E_A[y(t|\mathbf{a}, \mathbf{e}_M)|\mathbf{e}_A]$, a variance $V_A[y(t|\mathbf{a}, \mathbf{e}_M)|\mathbf{e}_A]$ and selected quantiles $Q_{Aq}[y(t|\mathbf{a}, \mathbf{e}_M)|\mathbf{e}_A]$. The definitions of $E_A[y(t|\mathbf{a}, \mathbf{e}_M)|\mathbf{e}_A]$, $V_A[y(t|\mathbf{a}, \mathbf{e}_M)|\mathbf{e}_A]$ and $Q_{Aq}[y(t|\mathbf{a}, \mathbf{e}_M)|\mathbf{e}_A]$ are effectively the same as the definitions for $E_{EM}[y(t|\mathbf{a}, \mathbf{e}_M)]$, $V_{EM}[y(t|\mathbf{a}, \mathbf{e}_M)]$ and $Q_{EMq}[y(t|\mathbf{a}, \mathbf{e}_M)]$ in Eqs. (3.26) – (3.28) with the only difference being that integrations are performed with respect to the probability space ($\mathcal{A}$, $\mathbb{A}$, p_A) and its associated density function $d_A(\mathbf{a}|\mathbf{e}_A)$ rather than with respect to the probability space ($\mathcal{EM}$, $\mathbb{EM}$, p_{EM}) and its associated density function $d_{EM}(\mathbf{e}_M)$. Specifically,

$$E_A\left[y\left(t|\mathbf{a},\mathbf{e}_M\right)\middle|\mathbf{e}_A\right] = \int_{\mathcal{A}} y\left(t|\mathbf{a},\mathbf{e}_M\right) d_A\left(\mathbf{a}|\mathbf{e}_A\right) \mathrm{d}A$$
$$\cong \sum_{j=1}^{nSA} y\left(t|\mathbf{a}_j,\mathbf{e}_M\right) \Big/ nSA$$
$$= \hat{E}_A\left[y\left(t|\mathbf{a},\mathbf{e}_M\right)\middle|\mathbf{e}_A\right], \qquad (3.48)$$

$$V_A\left[y\left(t|\mathbf{a},\mathbf{e}_M\right)\middle|\mathbf{e}_A\right]$$
$$= \int_{\mathcal{A}} \left\{y\left(t|\mathbf{a},\mathbf{e}_M\right) - E\left[y\left(t|\mathbf{a},\mathbf{e}_M\right)\right]\right\}^2 d_A\left(\mathbf{a}|\mathbf{e}_A\right) \mathrm{d}A$$
$$\cong \sum_{j=1}^{nSA} \left\{y\left(t|\mathbf{a}_j,\mathbf{e}_M\right) - \hat{E}_A\left[y\left(t|\mathbf{a},\mathbf{e}_M\right)\right]\right\}^2 \Big/ nSA$$
$$= \hat{V}_A\left[y\left(t|\mathbf{a},\mathbf{e}_M\right)\middle|\mathbf{e}_A\right], \qquad (3.49)$$

and $Q_{Aq}[y(t|\mathbf{a}, \mathbf{e}_M)|\mathbf{e}_A]$ and its approximation $\hat{Q}_{Aq}[y(t|\mathbf{a}, \mathbf{e}_M)|\mathbf{e}_A]$ correspond to the value y such that

$$q = p_A\left[\mathcal{U}_y\left(t|\mathbf{e}\right)\middle|\mathbf{e}_A\right]$$
$$= \int_{\mathcal{A}} \underline{\delta}_y\left[y\left(t|\mathbf{a},\mathbf{e}_M\right)\right] d_A\left(\mathbf{a}|\mathbf{e}_A\right) \mathrm{d}A$$
$$\cong \sum_{j=1}^{nSA} \underline{\delta}_y\left[y\left(t|\mathbf{a}_j,\mathbf{e}_M\right)\right] \Big/ nSA, \qquad (3.50)$$

where $\mathbf{a}_j$, j = 1, 2, …, nSA, is the sample indicated in conjunction with Eq. (3.47).

Distributions of CDFs and CCDFs result from the different possible values for $\mathbf{e} = [\mathbf{e}_A, \mathbf{e}_M]$. As indicated in conjunction with Eq. (3.47), each value for $\mathbf{e}$ results in a different CDF and associated CCDF that summarize the effects of aleatory uncertainty. In turn, these CDFs, CCDFs and their associated summary measures have distributions that characterize epistemic uncertainty and derive from the epistemic uncertainty in $\mathbf{e}$ characterized by the probability space ($\mathcal{E}$, $\mathbb{E}$, p_E).

In general, the probability space ($\mathcal{E}$, $\mathbb{E}$, p_E) will result in infinitely many CDFs and CCDFs of the form defined in conjunction with Eq. (3.47). Thus, some way of summarizing these CDFs and CCDFs is necessary. As illustrated in Sect. 3.6, this summary is provided by expected value curves and quantile curves (e.g., q = 0.05, 0.5, 0.95)

$$\left(y, E_E\left\{p_A\left[\mathcal{U}_y\left(t|\mathbf{e}\right)\middle|\mathbf{e}_A\right]\right\}\right) \text{ and } \left(y, Q_{Eq}\left\{p_A\left[\mathcal{U}_y\left(t|\mathbf{e}\right)\middle|\mathbf{e}_A\right]\right\}\right) \qquad (3.51)$$

and

$$\left(y, E_E\left\{p_A\left[\mathcal{U}_y^c\left(t|\mathbf{e}\right)\middle|\mathbf{e}_A\right]\right\}\right) \text{ and } \left(y, Q_{Eq}\left\{p_A\left[\mathcal{U}_y^c\left(t|\mathbf{e}\right)\middle|\mathbf{e}_A\right]\right\}\right) \qquad (3.52)$$

for distributions of CDFs and CCDFs, respectively, where

$$
\begin{aligned}
E_E\left\{p_A\left[\mathcal{U}_y\left(t\middle|\mathbf{e}\right)\middle|\mathbf{e}_A\right]\right\} &= \int_{\mathcal{E}} p_A\left[\mathcal{U}_y\left(t\middle|\mathbf{e}\right)\middle|\mathbf{e}_A\right] d_E\left(\mathbf{e}\right)\mathrm{d}E \\
&= \int_{\mathcal{E}}\left\{\int_{\mathcal{A}} \underline{\delta}_y\left[y\left(t\middle|\mathbf{a},\mathbf{e}_M\right)\right] d_A\left(\mathbf{a}\middle|\mathbf{e}_A\right)\mathrm{d}A\right\} d_E\left(\mathbf{e}\right)\mathrm{d}E \\
&\cong \sum_{i=1}^{nSE}\left\{\sum_{j=1}^{nSA} \underline{\delta}_y\left[y\left(t\middle|\mathbf{a}_{ij},\mathbf{e}_{Mi}\right)\right]\Big/nSA\right\}\Big/nSE \\
&= \hat{E}_E\left\{p_A\left[\mathcal{U}_y\left(t\middle|\mathbf{e}\right)\middle|\mathbf{e}_A\right]\right\},
\end{aligned}
$$

$$
\begin{aligned}
E_E\left\{p_A\left[\mathcal{U}_y^c\left(t\middle|\mathbf{e}\right)\middle|\mathbf{e}_A\right]\right\} &= \int_{\mathcal{E}} p_A\left[\mathcal{U}_y^c\left(t\middle|\mathbf{e}\right)\middle|\mathbf{e}_A\right] d_E\left(\mathbf{e}\right)\mathrm{d}E \\
&= \int_{\mathcal{E}}\left\{\int_{\mathcal{A}} \overline{\delta}_y\left[y\left(t\middle|\mathbf{a},\mathbf{e}_M\right)\right] d_A\left(\mathbf{a}\middle|\mathbf{e}_A\right)\mathrm{d}A\right\} d_E\left(\mathbf{e}\right)\mathrm{d}E \\
&\cong \sum_{i=1}^{nSE}\left\{\sum_{j=1}^{nSA} \overline{\delta}_y\left[y\left(t\middle|\mathbf{a}_{ij},\mathbf{e}_{Mi}\right)\right]\Big/nSA\right\}\Big/nSE \\
&= \hat{E}_E\left\{p_A\left[\mathcal{U}_y^c\left(t\middle|\mathbf{e}\right)\middle|\mathbf{e}_A\right]\right\},
\end{aligned}
$$

$Q_{Eq}\{p_A[\mathcal{U}_y(t|\mathbf{e})|\mathbf{e}_A]\}$ and the associated approximation $Q_{Eq}\{p_A[\mathcal{U}_y(t|\mathbf{e})|\mathbf{e}_A]\}$ correspond to the probability p such that

$$
\begin{aligned}
q &= \int_{\mathcal{E}} \underline{\delta}_p\left\{p_A\left[\mathcal{U}_y\left(t\middle|\mathbf{e}\right)\middle|\mathbf{e}_A\right]\right\} d_E\left(\mathbf{e}\right)\mathrm{d}E \\
&= \int_{\mathcal{E}} \underline{\delta}_p\left\{\int_{\mathcal{A}} \underline{\delta}_y\left[y\left(t\middle|\mathbf{a},\mathbf{e}_M\right)\right] d_A\left(\mathbf{a}\middle|\mathbf{e}_A\right)\mathrm{d}A\right\} d_E\left(\mathbf{e}\right)\mathrm{d}E \\
&\cong \sum_{i=1}^{nSE} \underline{\delta}_p\left\{\sum_{j=1}^{nSA} \underline{\delta}_y\left[y\left(t\middle|\mathbf{a}_{ij},\mathbf{e}_{Mi}\right)\right]\Big/nSA\right\}\Big/nSE,
\end{aligned}
$$

$Q_{Eq}\{p_A[\mathcal{U}_y^c(t|\mathbf{e})|\mathbf{e}_A]\}$ and the associated approximation $Q_{Eq}\{p_A[\mathcal{U}_y^c(t|\mathbf{e})|\mathbf{e}_A]\}$ correspond to the probability p such that

$$
\begin{aligned}
q &= \int_{\mathcal{E}} \underline{\delta}_p\left\{p_A\left[\mathcal{U}_y^c\left(t\middle|\mathbf{e}\right)\middle|\mathbf{e}_A\right]\right\} d_E\left(\mathbf{e}\right)\mathrm{d}E \\
&= \int_{\mathcal{E}} \underline{\delta}_p\left\{\int_{\mathcal{A}} \overline{\delta}_y\left[y\left(t\middle|\mathbf{a},\mathbf{e}_M\right)\right] d_A\left(\mathbf{a}\middle|\mathbf{e}_A\right)\mathrm{d}A\right\} d_E\left(\mathbf{e}\right)\mathrm{d}E \\
&\cong \sum_{i=1}^{nSE} \underline{\delta}_p\left\{\sum_{j=1}^{nSA} \overline{\delta}_y\left[y\left(t\middle|\mathbf{a}_{ij},\mathbf{e}_{Mi}\right)\right]\Big/nSA\right\}\Big/nSE,
\end{aligned}
$$

$\mathbf{e}_i = [\mathbf{e}_{Ai}, \mathbf{e}_{Mi}]$, i = 1, 2, …, nSE, is a sample from $\mathcal{E}$ generated in a manner consistent with the probability space ($\mathcal{E}$, $\mathbb{E}$, p_E) and its associated density function, and $\mathbf{a}_{ij}$, j = 1, 2, …, nSA, is a sample from $\mathcal{A}$ generated in a manner consistent with the probability space ($\mathcal{A}$, $\mathbb{A}$, p_A) and its associated density function $d_A(\mathbf{a}|\mathbf{e}_{Ai})$ for each $\mathbf{e}_i$. Although not incorporated into the notation in use, the sample size nSA could change for each $\mathbf{e}_i$.

An alternative summary is provided by reducing each CDF to its corresponding expected value $E_A[y|\mathbf{a}, \mathbf{e}_M)|\mathbf{e}_A]$ as indicated in Eq. (3.48) and then presenting the CDF and CCDF for $E_A[y|\mathbf{a}, \mathbf{e}_M)|\mathbf{e}_A]$that result from the epistemic uncertainty associated with $\mathbf{e} = [\mathbf{e}_A, \mathbf{e}_M]$. Similarly to the results presented in conjunction with Eq. (3.10), the CDF and CCDF for $E_A[y(t|\mathbf{a},\mathbf{e}_M)|\mathbf{e}_A]$ are defined by plots of the points

$$
\left\{\bar{y},\, p_E\left[\mathcal{U}_{\bar{y}}\left(t\right)\right]\right\} \text{ and } \left\{\bar{y},\, p_E\left[\mathcal{U}_{\bar{y}}^c\left(t\right)\right]\right\}, \tag{3.53}
$$

respectively, for $\bar{y} \in \bar{\mathcal{Y}}(t)$, where

$$
\begin{aligned}
\bar{\mathcal{Y}}\left(t\right) &= \left\{\bar{y} : \bar{y} = E_A\left[y\left(t\middle|\mathbf{a},\mathbf{e}_M\right)\middle|\mathbf{e}_A\right] \right. \\
&\qquad \left. \text{for } \mathbf{e} = \left[\mathbf{e}_A, \mathbf{e}_M\right] \in \mathcal{E}\right\}, \\
\mathcal{U}_{\bar{y}}\left(t\right) &= \left\{\tilde{\bar{y}} : \tilde{\bar{y}} \in \bar{\mathcal{Y}}\left(t\right) \text{ and } \tilde{\bar{y}} \le \bar{y}\right\}, \\
p_E\left[\mathcal{U}_{\bar{y}}\left(t\right)\right] &= \text{ probability of } \mathcal{U}_{\bar{y}}\left(t\right) \text{ (i.e., of a value } \tilde{\bar{y}} \le \bar{y}) \\
&= \int_{\mathcal{E}} \underline{\delta}_{\bar{y}}\left\{E_A\left[y\left(t\middle|\mathbf{a},\mathbf{e}_M\right)\middle|\mathbf{e}_A\right]\right\} d_E\left(\mathbf{e}\right)\mathrm{d}E \\
&\cong \sum_{i=1}^{nSE} \underline{\delta}_{\bar{y}}\left\{\sum_{j=1}^{nSA} y\left(t\middle|\mathbf{a}_{ij},\mathbf{e}_{Mi}\right)\Big/nSA\right\}\Big/nSE \\
&= \hat{p}_E\left[\mathcal{U}_{\bar{y}}\left(t\right)\right], \\
p_E\left[\mathcal{U}_{\bar{y}}^c\left(t\right)\right] &= \text{ probability of } \mathcal{U}_{\bar{y}}^c\left(t\right) \text{ (i.e., of a value } \tilde{\bar{y}} > \bar{y}) \\
&= \int_{\mathcal{E}} \overline{\delta}_{\bar{y}}\left\{E_A\left[y\left(t\middle|\mathbf{a},\mathbf{e}_M\right)\middle|\mathbf{e}_A\right]\right\} d_E\left(\mathbf{e}\right)\mathrm{d}E \\
&\cong \sum_{i=1}^{nSE} \overline{\delta}_{\bar{y}}\left\{\sum_{j=1}^{nSA} y\left(t\middle|\mathbf{a}_{ij},\mathbf{e}_{Mi}\right)\Big/nSA\right\}\Big/nSE \\
&= \hat{p}_E\left[\mathcal{U}_{\bar{y}}^c\left(t\right)\right],
\end{aligned}
$$

and the samples $\mathbf{e}_i = [\mathbf{e}_{Ai}, \mathbf{e}_{Mi}]$, i = 1, 2, …, nSE, and $\mathbf{a}_{ij}$, j = 1, 2, …, nSA, are defined the same as indicated in conjunction with Eqs. (3.51) and (3.52).

If desired, the reduction indicated in the preceding paragraph can be carried further by reducing the expected value $E_A[y(t|\mathbf{a}, \mathbf{e}_M)|\mathbf{e}_A]$ over aleatory uncertainty defined in Eq. (3.48) to an expected value $E_E\{E_A[y(t|\mathbf{a}, \mathbf{e}_M)|\mathbf{e}_A]\}$ over aleatory and epistemic uncertainty defined by

$$
\begin{aligned}
&E_E\left\{E_A\left[y\left(t\middle|\mathbf{a},\mathbf{e}_M\right)\middle|\mathbf{e}_A\right]\right\}\\
&\quad=\int_{\mathcal{E}}E_A\left[y\left(t\middle|\mathbf{a},\mathbf{e}_M\right)\middle|\mathbf{e}_A\right]d_E\left(\mathbf{e}\right)\mathrm{d}E\\
&\quad=\int_{\mathcal{E}}\left[\int_{\mathcal{A}}y\left(t\middle|\mathbf{a},\mathbf{e}_M\right)d_A\left(\mathbf{a}\middle|\mathbf{e}_A\right)\mathrm{d}A\right]d_E\left(\mathbf{e}\right)\mathrm{d}E\\
&\quad\cong\sum_{i=1}^{nSE}\left[\sum_{j=1}^{nSA}y\left(t\middle|\mathbf{a}_{ij},\mathbf{e}_{Mi}\right)\Big/nSA\right]\Big/nSE\\
&\quad=\hat{E}_E\left\{E_A\left[y\left(t\middle|\mathbf{a},\mathbf{e}_M\right)\middle|\mathbf{e}_A\right]\right\},
\end{aligned}
\tag{3.54}
$$

where the samples $\mathbf{e}_i = [\mathbf{e}_{Ai}, \mathbf{e}_{Mi}]$, $i = 1, 2, \ldots, nSE$, and $\mathbf{a}_{ij}$, $j = 1, 2, \ldots, nSA$, are again defined the same as in conjunction with Eqs. (3.51) and (3.52). The expected value $E_E\{E_A[y(t|\mathbf{a},\mathbf{e}_M)|\mathbf{e}_A]\}$ is the result of reducing all the information associated with the probability space ($\mathcal{E}$, $\mathbb{E}$, p_E) for epistemic uncertainty, the probability space ($\mathcal{A}$, $\mathbb{A}$, p_a) for aleatory uncertainty and the function $y(t|\mathbf{a}, \mathbf{e}_M)$ to a single number.

3.6 Example Analysis in the Presence of Aleatory and Epistemic Uncertainty

A simple, randomly perturbed system is now presented to illustrate the concepts introduced in Sect. 3.5. This example will also be used in Sects. 5 and 10 to illustrate potential QMU analyses involving aleatory and epistemic uncertainty. Further, the results from real analyses presented in Sect. 6 are of the form described in the present section.

The system is assumed to receive random perturbations in time whose occurrence is characterized as a stationary Poisson process with a rate λ (s^{-1}). The amplitudes (i.e., magnitudes) for the individual perturbations are assumed to vary randomly and to undergo exponential decay in a manner characterized by a rate constant r (s^{-1}). In concept, any of a large variety of systems could be under consideration, with the result that the perturbation might involve a mechanical force, an electrical impulse, a radiation impulse, a heat impulse, the injection of a material, or some additional possibility. For notational convenience, the initial perturbations will be represented by A_0 and assumed to have units of force (kg m/s^2). As a result of the indicated exponential decay,

$$A(t) = A_0 \exp\left[-r\left(t - t_0\right)\right] \tag{3.55}$$

is the amplitude at time t of a perturbation of size A_0 that occurs at time t_0. Further, the amplitudes of the individual perturbations are assumed to be characterized by a triangular distribution defined on an interval $[a, b]$ with a mode of m.

This example involves both aleatory and epistemic uncertainty. For a given time interval (e.g., [0, 10 s]), the different possible realizations of aleatory uncertainty correspond to vectors of the form

$$\mathbf{a} = \left[n, t_1, A_{01}, t_2, A_{02}, \ldots, t_n, A_{0n}\right], \tag{3.56}$$

where (i) n is the number of perturbations that occur in the time interval, (ii) $t_1 < t_2 < \ldots < t_n$ are the times at which the individual perturbations occur, and (ii) A_{01}, A_{02}, …, A_{0n} are the initial amplitudes for the individual perturbations. In turn,

$$\mathcal{A} = \left\{\mathbf{a} : \mathbf{a} = \left[n, t_1, A_{01}, t_2, A_{02}, \ldots, t_n, A_{0n}\right]\right\} \tag{3.57}$$

is the sample space for aleatory uncertainty, and the probabilistic structure required to formally complete the definition of the corresponding probability space ($\mathcal{A}$, $\mathbb{A}$, p_A) derives from λ and the probability distribution for A_0.

For a given element $\mathbf{a}$ of $\mathcal{A}$ and a given value for r, the resultant amplitude $A(t|\mathbf{a})$ at time t is given by

$$A\left(t\middle|\mathbf{a}, r\right) = \begin{cases} 0 & \text{if } t < t_1 \\ \displaystyle\sum_{k=1}^{\tilde{n}} A_{0k} \exp\left[-r\left(t - t_k\right)\right] & \text{if } t \geq t_1, \end{cases} \tag{3.58}$$

where $\tilde{n} = \max\{k : t_k \leq t\}$.

For this example, λ, a, m, b and r are assumed to be uncertain in an epistemic sense. As a result,

$$\mathbf{e} = \left[\mathbf{e}_A, \mathbf{e}_M\right] = \left[e_1, e_2, e_3, e_4, e_5\right] = \left[\lambda, a, m, b, r\right] \tag{3.59}$$

is the vector of epistemically uncertain variables under consideration, with $\mathbf{e}_A = [\lambda, a, m, b]$ and $\mathbf{e}_M = [r]$. Specifically, λ, a, m and b are involved in the definition of probability distributions that characterize aleatory uncertainty, and r relates to the physical processes involved in the decay of an initial perturbation A_0.

The appropriate values for λ, a, m, b and r are assumed to be contained in the intervals

$$
\begin{aligned}
\mathcal{EA}_1 &= \left\{\lambda : \lambda_{mn} \leq \lambda \leq \lambda_{mx}\right\}\\
&= \left\{\lambda : 0.5 \leq \lambda \leq 1.5\ \mathrm{s}^{-1}\right\}
\end{aligned}
\tag{3.60}
$$

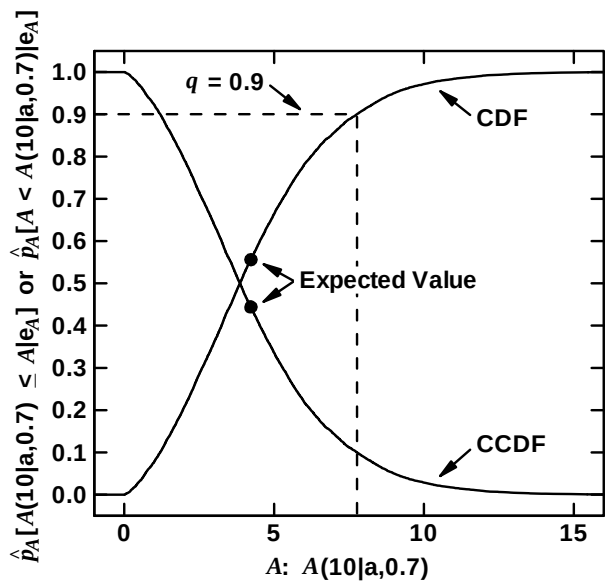

Fig. 3.8. Estimated CDF and CCDF for amplitude $A(10|\mathbf{a}, 0.7)$ with $\mathbf{e}_A$ = [1.0, 1.5, 3.0, 4.5] and $\mathbf{e}_M$ = [0.7] (i) determined with a sample of size nSA = 10,000 from the set $\mathcal{A}$ of possible values for $\mathbf{a}$ conditional on $\mathbf{e} = [\mathbf{e}_A, \mathbf{e}_M]$ = [1.0, 1.5, 3.0, 4.5, 0.7] and (ii) presented with $\hat{p}_A[A(10|\mathbf{a}, 0.7) \le A|\mathbf{e}_A]$ and $\hat{p}_A[A < A(10|\mathbf{a}, 0.7)|\mathbf{e}_A]$ used as mnemonics for estimated probabilities of the form $\hat{p}_A[\mathcal{U}_y(10|\mathbf{e})|\mathbf{e}_A]$ and $\hat{p}_A[\mathcal{U}_y^c(10|\mathbf{e})|\mathbf{e}_A]$ defined in conjunction with Eq. (3.47).

$$\begin{aligned}\mathcal{EA}_2 &= \{a : a_{mn} \le a \le a_{mx}\} \\ &= \left\{a : 1.0 \le a \le 2.0 \text{ kg m/s}^2\right\}\end{aligned} \tag{3.61}$$

$$\begin{aligned}\mathcal{EA}_3 &= \{m : m_{mn} \le m \le m_{mx}\} \\ &= \left\{m : 2.0 \le m \le 4.0 \text{ kg m/s}^2\right\}\end{aligned} \tag{3.62}$$

$$\begin{aligned}\mathcal{EA}_4 &= \{b : b_{mn} \le b \le b_{mx}\} \\ &= \left\{b : 4.0 \le b \le 5.0 \text{ kg m/s}^2\right\}\end{aligned} \tag{3.63}$$

and

$$\begin{aligned}\mathcal{EM}_1 &= \{r : r_{mn} \le r \le r_{mx}\} \\ &= \left\{r : 0.2 \le r \le 1.2 \text{ s}^{-1}\right\},\end{aligned} \tag{3.64}$$

respectively.

The resultant sample space for the vector $\mathbf{e}$ of epistemically uncertain variables is

$$\mathcal{E} = \mathcal{EA}_1 \times \mathcal{EA}_2 \times \mathcal{EA}_3 \times \mathcal{EA}_4 \times \mathcal{EM}_1 \tag{3.65}$$

with $\mathcal{EA}_1$, $\mathcal{EA}_2$, …, $\mathcal{EM}_1$ defined in Eqs. (3.60) – (3.64). Further, associated probability spaces ($\mathcal{EA}_i$, $\mathbb{EA}_i$, $p_{EA,i}$), i = 1, 2, 3, 4, and ($\mathcal{EM}_1$, $\mathbb{EM}_1$, $p_{EM,1}$) for the individual elements of $\mathbf{e}$ (i.e., λ, a, m, b and r) and also the probability space ($\mathcal{E}$, $\mathbb{E}$, p_E) for $\mathbf{e}$ are defined in the same manner as for the elements of $\mathbf{e} = [L, R, C, E_0, \lambda]$ in Eqs. (3.38) – (3.42).

For a given value for $\mathbf{e} = [\lambda, a, m, b, r]$, a distribution for $A(t|\mathbf{a}, \mathbf{e}_M) = A(t|\mathbf{a}, r)$ over the possible values for $\mathbf{a}$ results for each time t as indicated in conjunction with Eq. (3.47). As an example, the CDF and CCDF for $A(t|\mathbf{a}, r)$ at t = 10 s conditional on $\mathbf{e}$ = [1.0, 1.5, 3.0, 4.5, 0.7] (i.e., for $A(10|\mathbf{a}, 0.7)$) is illustrated in Fig. 3.8. The results in Fig. 3.8 were generated with a random sample

$$\mathbf{a}_j,\ j = 1, 2, \ldots, nSA, \tag{3.66}$$

of size nSA = 10,000 from $\mathcal{A}$ obtained in consistency with the distributions for perturbation time t and perturbation magnitude A_0 that derive from λ = 1.0 s^{-1}, a = 1.5 kg m/s^2, m = 3.0 kg m/s^2, and b = 4.5 kg m/s^2 (i.e., from $\mathbf{e}_A$ = [1.0, 1.5, 3.0, 4.5]). In addition, estimates for the expected value $E_A[A(10|\mathbf{a}, 0.7)|\mathbf{e}_A]$ and the q = 0.9 quantile $Q_{A,0.9}[A(10|\mathbf{a}, 0.7)|\mathbf{e}_A]$ for $A(10|\mathbf{a}, 0.7)$ obtained with the preceding sample as indicated in Eqs. (3.48) and (3.50) are also shown in Fig. 3.8.

A subset of the results used in the generation of Fig. 3.8 is shown in Fig. 3.9. Each of the curves in Fig. 3.9 is a plot of $A(t|\mathbf{a}_j, 0.7)$ for $0 \le t \le 20$ s and a specific element $\mathbf{a}_j$ of the sample indicated in Eq. (3.66). Specifically, a plot of $A(t|\mathbf{a}_1, 0.7)$ is shown in Fig. 3.9a, and plots of $A(t|\mathbf{a}_j, 0.7)$ for j = 1, 2, …, 5 are shown in Fig. 3.9b. The CDF and CCDF in Fig. 3.8 summarize the aleatory uncertainty (i.e., intrinsic variability) in the values for $A(10|\mathbf{a}, 0.7)$ associated with the vertical line originating at t = 10 s in Fig. 3.9 for all elements of the sample in Eq. (3.66).

The CCDF in Fig. 3.8 summarizes the aleatory uncertainty in $A(t|\mathbf{a}, 0.7)$ at t = 10 s as indicated by the vertical line in Fig. 3.9. Corresponding summaries are possible for each value of t in the interval under consideration. However, presentation of such summaries for a large number of values for t is cumbersome. A more compact summary is to present the expected value for $A(t|\mathbf{a}, 0.7)$ and selected quantiles for $A(t|\mathbf{a}, 0.7)$ (e.g., 0.05, 0.25, 0.5, 0.75, 0.95) as functions of time (Fig. 3.10). This format presents the primary uncertainty information for $A(t|\mathbf{a}, 0.7)$ as a function of time in a

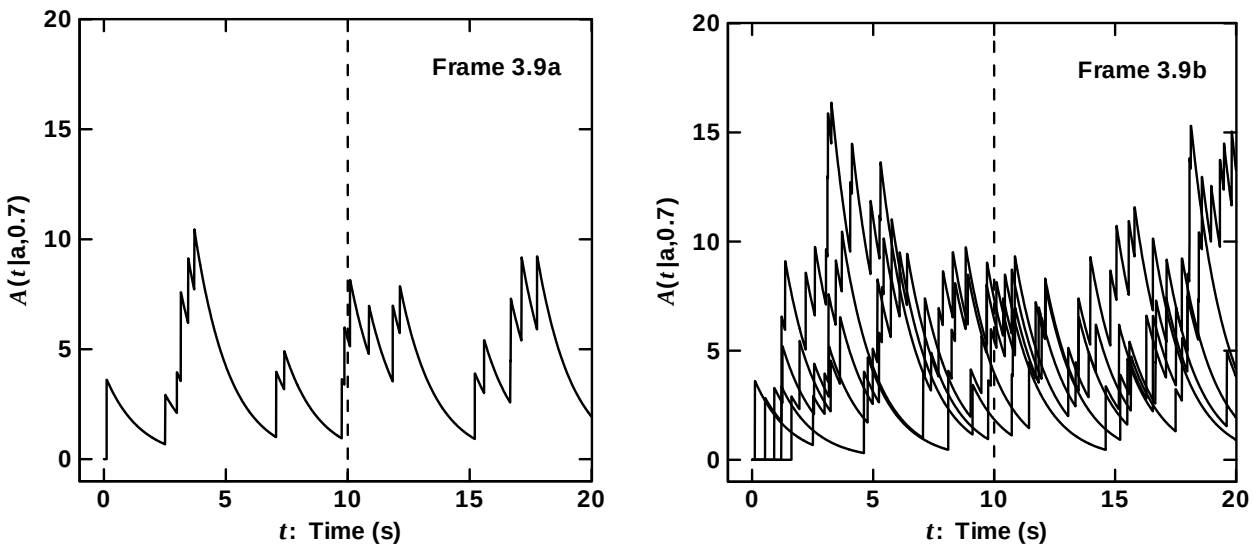

Fig. 3.9. Illustration of time-dependent amplitudes $A(t|\mathbf{a}_j, 0.7)$ used in generation of CDF and CCDF in Fig. 3.8 for aleatory uncertainty in amplitude at t = 10 s conditional on $\mathbf{e}$ = [1.0, 1.5, 3.0, 4.5, 0.7]: (a) $A(t|\mathbf{a}_j, 0.7)$ for j = 1, and (b) $A(t|\mathbf{a}_j, 0.7)$ for j = 1, 2, …, 5.

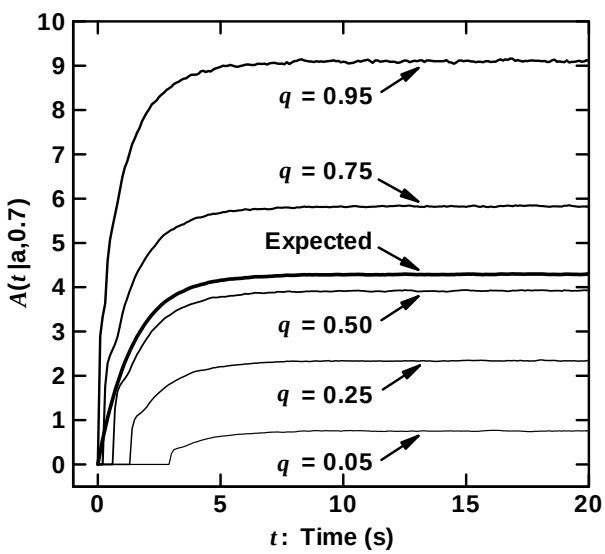

Fig. 3.10. Estimated expected value and quantile curves for aleatory uncertainty in amplitude $A(t|\mathbf{a}, 0.7)$ as a function of time conditional on $\mathbf{e}$ = [1.0, 1.5, 3.0, 4.5, 0.7].

single plot. The expected values and quantiles in Fig. 3.10 are obtained from the sample in Eq. (3.66) as described in Eqs. (3.51) and (3.52) and illustrated in Fig. 3.8.

If $\mathbf{e} = [\lambda, a, m, b, r]$ was precisely known, then results of the form shown in Figs. 3.8 and 3.10 would be the unique outcomes of the analysis. However, $\mathbf{e}$ is not precisely known and has many possible values. As a result, there are many possible values for the results in Figs. 3.8 and 3.10. For example, there are many possible values for the CDF and CCDF in Fig. 3.8 (Fig. 3.11), with each possible CDF and CCDF deriving from a different element $\mathbf{e} = [\lambda, a, m, b, r]$ of the set $\mathcal{E}$ defined in Eq. (3.65).

Specifically, the results in Fig. 3.11 were generated with an LHS

$$\begin{aligned}\mathbf{e}_i &= \left[\mathbf{e}_{Ai}, \mathbf{e}_{Mi}\right] \\ &= \left[\lambda_i, a_i, m_i, b_i, r_i\right], i = 1, 2, \ldots, nSE,\end{aligned} \tag{3.67}$$

of size nSE = 200 from the set $\mathcal{E}$ in consistency with the distributions that define the probability space ($\mathcal{E}$, $\mathbb{E}$, p_E) for epistemic uncertainty. In turn, a different CDF and associated CCDF results for each sample element $\mathbf{e}_i$. Further, the individual CDFs and CCDFs were estimated with random samples

$$\begin{aligned}\mathbf{a}_j &= \left[n_j, t_{j1}, A_{0j1}, t_{j2}, A_{0j2}, \ldots, t_{jn_j}, A_{0jn_j}\right], \\ &j = 1, 2, \ldots, nSA,\end{aligned} \tag{3.68}$$

of size nSA = 10,000 from $\mathcal{A}$ generated in consistency with $\mathbf{e}_{Ai} = [\lambda_i, a_i, m_i, b_i]$ and the corresponding probability space ($\mathcal{A}$, $\mathbb{A}$, p_A) for aleatory uncertainty and its associated density function $d_A(\mathbf{a}|\mathbf{e}_{Ai})$. Although not explicitly incorporated into the notation in use, the set $\mathcal{A}$ changes for each $\mathbf{e}_{Ai}$ as a result of the effect of the interval $[a_i, b_i]$ on the set of possible values for the size of the perturbation associated with each occurrence of the Poisson process under consideration.

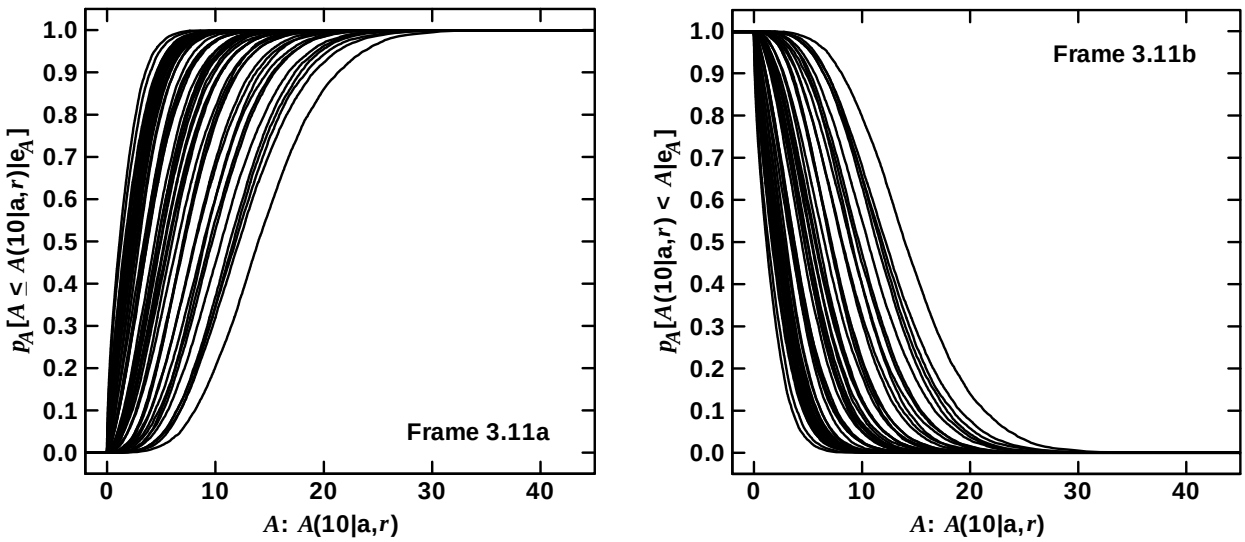

Fig. 3.11. Estimated CDFs and CCDFs for amplitude $A(10|\mathbf{a}, r)$ obtained for the first 50 elements of the LHS in Eq. (3.67) and estimated with the random samples of size nSA = 10,000 in Eq. (3.68) from the corresponding sets $\mathcal{A}$ of possible values for **a**: (a) CDFs, and (b) CCDFs.

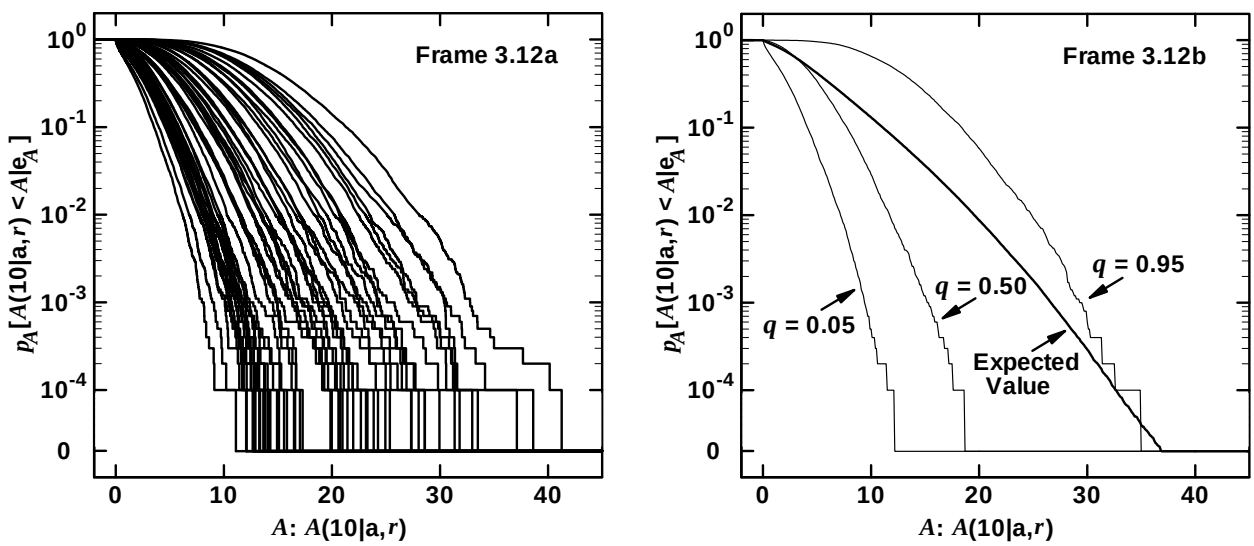

Fig. 3.12. Estimated CCDFs plotted with log-transformed exceedance probabilities for amplitude $A(10|\mathbf{a}, r)$ obtained for individual elements of the LHS in Eq. (3.67) and estimated with the random samples of size nSA = 10,000 in Eq.(3.68) from the corresponding sets $\mathcal{A}$ of possible values for **a**: (a) individual CCDFs for 50 elements in the LHS , and (b) summary statistics for the distribution of CCDFs.

When small exceedance probabilities arising from aleatory uncertainty are the analysis outcomes of interest, CCDFs are usually plotted with log-transformed values on the ordinate (Fig. 3.12a). Use of log-transformed values allows small exceedance probabilities to be displayed; in contrast, small exceedance probabilities are difficult, and sometimes impossible, to determine from plotted results when a linear scale is used on the ordinate (e.g., compare the CCDFs in Figs. 3.11b and 3.12a). In many QMU analyses, it is likely that small exceedance probabilities will be the analysis outcomes of greatest interest.

Distributions of CDFs and CCDFs can be summarized with expected value and quantile curves as indicated in conjunction with Eqs. (3.51) and (3.52). As an

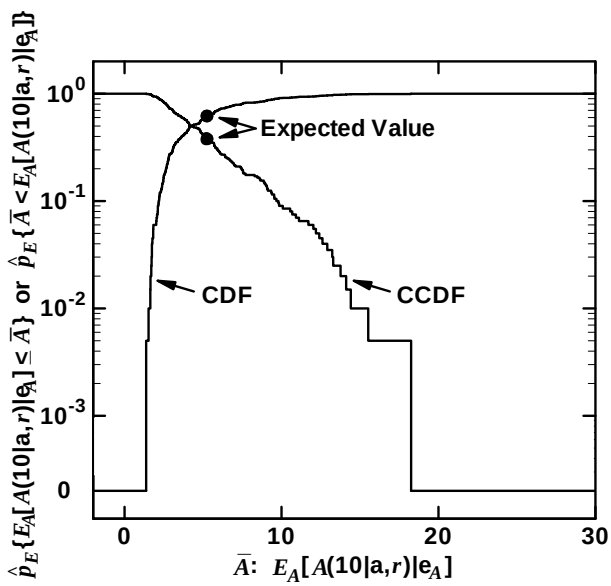

Fig. 3.13. Estimated CDF and CCDF (i) for expected values $E_A[A(10|\mathbf{a}, r_i)|\mathbf{e}_{Ai}]$, $i = 1, 2, \ldots, nSE = 200$, associated with CDFs and CCDFs in Figs. 3.11 and 3.12 and (ii) with $\hat{p}_E\{E_A[A(10|\mathbf{a}, r)|\mathbf{e}_A] \le \bar{A}\}$ and $\hat{p}_E\{\bar{A} < E_A[A(10|\mathbf{a}, r)|\mathbf{e}_A]\}$ used as mnemonics for estimated probabilities of the form $\hat{p}_E[\mathcal{U}_{\bar{y}}(10)]$ and $\hat{p}_E[\mathcal{U}_{\bar{y}}^c(10)]$ defined in conjunction with Eq. (3.53).

example, a summary of this form is presented in Fig. 3.12b for CCDFs with log-transformed exceedance probabilities.

As indicated in conjunction with Eq. (3.53), distributions of CDFs and CCDFs can also be summarized by reducing each CDF and corresponding CCDF to an expected value and then presenting the CDF and CCDF for the resultant expected values (Fig. 3.13). Specifically, Fig. 3.13 shows the CDF and CCDF for the expected values associated with the individual CDFs and CCDFs in Figs. 3.11 and 3.12. Each expected value $\hat{E}_A[A(10|\mathbf{a}, r_i)|\mathbf{e}_{Ai}]$ is calculated as indicated in Eq. (3.48), and the resultant CDF and CCDF are calculated as indicated in conjunction with Eq. (3.53). In consistency with the results in Figs. 3.11 and 3.12, the preceding calculations use the samples indicated in Eqs. (3.67) and (3.68).

The estimated expected value $\hat{E}_E\{E_A[A(10|\mathbf{a}, r)|\mathbf{e}_A]\}$ over aleatory and epistemic uncertainty is also shown in Fig. 3.13 and corresponds to the estimated expected value $\hat{E}_E\{E_A[y(t|\mathbf{a},\mathbf{e}_M)|\mathbf{e}_A]\}$ defined in Eq. (3.54). The quantity $\hat{E}_E\{E_A[A(10|\mathbf{a},r)|\mathbf{e}_A]\}$ is the outcome of reducing all the information in Figs. 3.11 and 3.12 to a single number.

3.7 Kaplan-Garrick Ordered Triple Representation for Risk

The Kaplan-Garrick ordered triple representation for risk is introduced in conjunction with Questions (Q1), (Q2) and (Q3) in Sect. 2 as a way of intuitively describing risk. More formally, this representation characterizes risk as an ordered triple of the form

$$\left(\mathcal{S}_j, pS_j, \mathbf{cS}_j\right), j = 1, 2, \ldots, nS, \tag{3.69}$$

where $\mathcal{S}_j$ is a set of similar occurrences, pS_j is the probability of the set $\mathcal{S}_j$, $\mathbf{cS}_j$ is a vector of consequences associated with $\mathcal{S}_j$, the sets $\mathcal{S}_j$ are disjoint (i.e., $\mathcal{S}_i \cap \mathcal{S}_j = \varnothing$ for $i \neq j$), and the set $\cup\mathcal{S}_j$ contains all risk significant occurrences in the particular universe under consideration.

The representation in Eq. (3.69) is simply a way to describe the components of approximations to integrals of the form appearing in Eq. (3.48) obtained with stratified sampling from the sample space $\mathcal{A}$ for aleatory uncertainty. With stratified sampling, the expected value $E_A[y(t|\mathbf{a}, \mathbf{e}_M)|\mathbf{e}_A]$ and its defining integral in Eq. (3.48) are approximated by

$$\begin{aligned} E_A\left[y\left(t|\mathbf{a}, \mathbf{e}_M\right)\middle|\mathbf{e}_A\right] &= \int_{\mathcal{A}} y\left(t|\mathbf{a}, \mathbf{e}_M\right) d_A\left(\mathbf{a}|\mathbf{e}_A\right) \mathrm{d}A \\ &\cong \sum_{j=1}^{nSA} y\left(t|\mathbf{a}_j, \mathbf{e}_M\right) p_A\left(\mathcal{A}_j\middle|\mathbf{e}_A\right), \end{aligned} \tag{3.70}$$

where the $\mathcal{A}_j$ are disjoint subsets of $\mathcal{A}$ with $\cup\mathcal{A}_j = \mathcal{A}$, $p_A(\mathcal{A}_j|\mathbf{e}_A)$ is the probability of $\mathcal{A}_j$, and $\mathbf{a}_j$ is a representative element of $\mathcal{A}_j$. With respect to the representation in Eq. (3.69), $\mathcal{A}_j$ corresponds to $\mathcal{S}_j$, $p_A(\mathcal{A}_j|\mathbf{e}_A)$ corresponds to pS_j, $y(t|\mathbf{a}_j, \mathbf{e}_M)$ corresponds to an element of $\mathbf{cS}_j$, and nSA corresponds to nS.

In turn, the defining probabilities for CDFs and CCDFs are given by

$$\begin{aligned} &p_A\left[y\left(t|\mathbf{a}, \mathbf{e}_M\right) \le y\middle|\mathbf{e}_A\right] \\ &\quad \cong \sum_{j=1}^{nSA} \underline{\delta}_y\left[y\left(t|\mathbf{a}_j, \mathbf{e}_M\right)\right] p_A\left(\mathcal{A}_j\middle|\mathbf{e}_A\right) \end{aligned} \tag{3.71}$$

and

$$p_A\left[y < y\left(t\middle|\mathbf{a}, \mathbf{e}_M\right)\middle|\mathbf{e}_A\right] \cong \sum_{j=1}^{nSA} \bar{\delta}_y\left[y\left(t\middle|\mathbf{a}_j, \mathbf{e}_M\right)\right] p_A\left(\mathcal{A}_j\middle|\mathbf{e}_A\right), \tag{3.72}$$

respectively.

In summary, the Kaplan-Garrick ordered triple representation for risk provides a simple and intuitive description of the basic components of a risk assessment. Specifically, this representation provides a display of the answers to the first three basic questions that underlie a risk assessment: (i) "What can happen?", (ii) "How likely is it to happen?", and (iii) "What are the consequences if it does happen?". However, it is important to recognize that this representation is simply a way of decomposing approximations to integrals involving aleatory uncertainty into their basic components as indicated in Eqs. (3.70) - (3.72). Use of the Kaplan-Garrick ordered triple representation for risk is suggested in App. A of the NAS/NRC report on QMU [77].

3.8 Verification and Validation

Verification and validation are two very important components of a QMU analysis that are intimately connected with the assessment and representation of uncertainty, where (i) verification is the process of determining that a model implementation accurately represents the developers' conceptual description of the model and the solution to the model, and (ii) validation is the process of determining the degree to which a model is an accurate representation of the real world from the perspective of the intended uses of the model (p. 3, [104]; [105-110]).

Sampling-based sensitivity analysis as described in Sect. 7 and illustrated in Sects. 4 and 5 is a powerful tool for checking for analysis errors and thus is an important component of analysis verification. Further, model validation is an important contributor to the insights that ultimately lead to the definition of the probability space that characterizes epistemic uncertainty.

Techniques for verification and validation are not the focus of this presentation but are necessary components of a credible QMU analysis. The importance of verification and validation is emphasized in the NAS/NRC report on QMU (p. 22, Ref. [77]).

3.9 An Admonition

As the reader has undoubtedly observed, this section essentially presents the same calculation over again and over again as different expected values and probabilities are calculated. As a reminder, the probabilities that define CDFs and CCDFs are actually themselves expected values; specifically, these probabilities are expected values for indicator functions (i.e., functions of the form $\underline{\delta}_x(\tilde{x})$ and $\bar{\delta}_x(\tilde{x})$ as defined in conjunction with Eq. (3.2)). What is changing in the calculations is the sample space under consideration (e.g., $\mathcal{EA}$, $\mathcal{EM}$, $\mathcal{E} = \mathcal{EA} \times \mathcal{EM}$, $\mathcal{A}$, …), the probability space associated with the sample space (e.g., ($\mathcal{EA}$, $\mathbb{EA}$, p_{EA}), ($\mathcal{EM}$, $\mathbb{EM}$, p_{EM}), ($\mathcal{E}$, $\mathbb{E}$, p_E), ($\mathcal{A}$, $\mathbb{A}$, p_A), …), and the function being integrated (e.g., $y(t|\mathbf{a}, \mathbf{e}_M)$, $\underline{\delta}_y[y(t|\mathbf{a}, \mathbf{e}_M)]$, $\bar{\delta}_y[y(t|\mathbf{a}, \mathbf{e}_M)]$, $E_A[y(t|\mathbf{a}, \mathbf{e}_M)|\mathbf{e}_A]$, ….). However, at a conceptual level, the basic calculation remains the same. The calculations are repeated to be explicit about the sample space, probability space and function involved rather than because of inherent conceptual differences in the probabilistic basis of the calculation.

Now for the admonition. When confronted with a probability or a calculation involving probability, the first two questions to ask are "What is the sample space?" and "What subset of the sample space is under consideration?". If you do not know the answers to these two questions, then you do not know enough to meaningfully assess the probability or calculated result under consideration. Further, if the source of the probability or calculated result cannot supply precise answers to these two questions, then there is reason to be cautious with respect to the meaning and correctness of such results. Basically, having a probability without knowing the associated sample space and the subset of that sample space for which the probability is defined is analogous to knowing the answer to a question without knowing what the question is.

For the preceding reason, this section has been very explicit in stating the sample space and the relevant subsets of that sample as different quantities have been introduced and defined. This results in some repetition at a conceptual level but has the positive effect of unambiguously defining the individual quantities under consideration.

4 QMU with Epistemic Uncertainty: Characterization with Probability

The use of probability to represent the epistemic uncertainty associated with results of the form

$$y\left(t\middle|\mathbf{a}, \mathbf{e}_M\right) = f\left(t\middle|\mathbf{a}, \mathbf{e}_M\right) \tag{4.1}$$

is extensively discussed in Sect. 3.3, where $y(t|\mathbf{a}, \mathbf{e}_M)$ is a generic real-valued quantity conditional on a specific realization $\mathbf{a}$ of aleatory uncertainty and $\mathbf{e}_M$ is a vector of epistemically uncertain analysis inputs. The result $y(t|\mathbf{a}, \mathbf{e}_M)$ is epistemically uncertain as a consequence of the epistemic uncertainty associated with the elements of $\mathbf{e}_M$. Given that the realization $\mathbf{a}$ of aleatory uncertainty is fixed, analyses related to $y(t|\mathbf{a}, \mathbf{e}_M)$ involve two of the three basic analysis components discussed in Sect. 3.2: (i) (EN2), a model that predicts system behavior (i.e., a function $f(t|\mathbf{a}, \mathbf{e}_M)$), and (ii) (EN3), a probabilistic characterization of epistemic uncertainty (i.e., a probability space $(\mathcal{EM}, \mathbb{EM}, p_{EM})$ that characterizes the epistemic uncertainty associated with the elements of $\mathbf{e}_M$).

Margins can be defined for $y(t|\mathbf{a}, \mathbf{e}_M)$ in a variety of ways, and in turn, the epistemic uncertainty associated with $\mathbf{e}_M$ results in uncertainty in $y(t|\mathbf{a}, \mathbf{e}_M)$ and the margins that derive from $y(t|\mathbf{a}, \mathbf{e}_M)$. At an intuitive level, a margin corresponds to a difference between a required level of performance and an estimated level of performance, with a positive margin indicating that the required level of performance is met and a negative margin indicating that the required level of performance is not met. Multiple examples of how margins could be defined are introduced in this section and in Sects. 5 and 6.

This section uses the function $Q(t|\mathbf{a}, \mathbf{e}_M)$ introduced in Sect. 3.4 to illustrate a variety of ways in which QMU analyses could arise and be carried out in the context of analyses that involve a generic result $y(t|\mathbf{a}, \mathbf{e}_M)$ of the form indicated in Eqs. (3.24) and (4.1). Further,

$$\mathbf{e}_M = \left[e_{M1}, e_{M2}, e_{M3}, e_{M4}, e_{M5}\right] = \left[L, R, C, E_0, \lambda\right] \tag{4.2}$$

has the properties defined in conjunction with Eq. (3.32), and the corresponding probability space $(\mathcal{EM}, \mathbb{EM}, p_{EM})$ that characterizes the epistemic uncertainty associated with $\mathbf{e}_M$ is defined in conjunction with Eqs. (3.33) – (3.43). The time-dependent behavior of $Q(t|\mathbf{a}, \mathbf{e}_M)$ is illustrated in Fig. 3.5.

The examples presented in this section use an LHS

$$\begin{aligned}\mathbf{e}_{Mi} &= \left[e_{Mi1}, e_{Mi2}, \ldots, e_{Mi5}\right] \\ &= \left[L_i, R_i, C_i, E_{0i}, \lambda_i\right], i = 1, 2, \ldots, nSE = 200,\end{aligned} \tag{4.3}$$

from $\mathcal{EM}$ generated in consistency with the distributions that define the probability space $(\mathcal{EM}, \mathbb{EM}, p_{EM})$. In turn, evaluation of $Q(t|\mathbf{a}, \mathbf{e}_{Mi})$ for elements of the preceding sample produces a mapping

$$\left[\mathbf{e}_{Mi}, Q\left(t\middle|\mathbf{a}, \mathbf{e}_{Mi}\right)\right], i = 1, 2, \ldots, nSE = 200, \tag{4.4}$$

from uncertain analysis inputs to analysis results that is used in the generation of the example results presented in this section.

The following topics related to QMU in the presence of only epistemic uncertainty are considered in this section: epistemic uncertainty with a specified bound (Sect. 4.1), epistemic uncertainty with a specified bounding interval (Sect. 4.2), epistemic uncertainty with a specified bounding interval over time (Sect. 4.3), epistemic uncertainty with an uncertain bound (Sect. 4.4), and information loss associated with a "margin/uncertainty" ratio (Sect. 4.5). The bounds considered in Sects. 4.1 – 4.4 correspond to the requirements that give rise to margins (i.e., the differences between required system performance and predicted system performance).

As indicated at the beginning of Sect. 3.3, the NAS/NRC report on QMU emphasizes the importance of the quantification of the epistemic uncertainty in analysis results that derives from epistemic uncertainty in analysis inputs (Recommendation 1-2, p. 22, Ref. [77]). The results presented in Sects. 4.1 – 4.2 illustrate analyses of this type.

4.1 Epistemic Uncertainty with a Specified Bound

For this example, a fixed bound is assumed to exist with respect to the value for $Q(0.1|\mathbf{a}, \mathbf{e}_M)$. Possibilities include lower bounds on $Q(0.1|\mathbf{a}, \mathbf{e}_M)$ (e.g., Q_{b1} = 0.075 and Q_{b2} = 0.09 in Fig. 4.1a) and upper bounds on $Q(0.1|\mathbf{a}, \mathbf{e}_M)$ (e.g., Q_{b3} = 0.105 and Q_{b4} = 0.125 in Fig. 4.1b). Consistent with the nature of the bounds being illustrated, the distribution of possible values for $Q(0.1|\mathbf{a}, \mathbf{e}_M)$ in Fig. 4.1a is summarized with a CDF, and the distribution of possible values for $Q(0.1|\mathbf{a}, \mathbf{e}_M)$ in Fig. 4.1b is summarized with a CCDF. Specifically, the CDF in Fig. 4.1a displays the probability of being less than a specific bound, which is the probability of

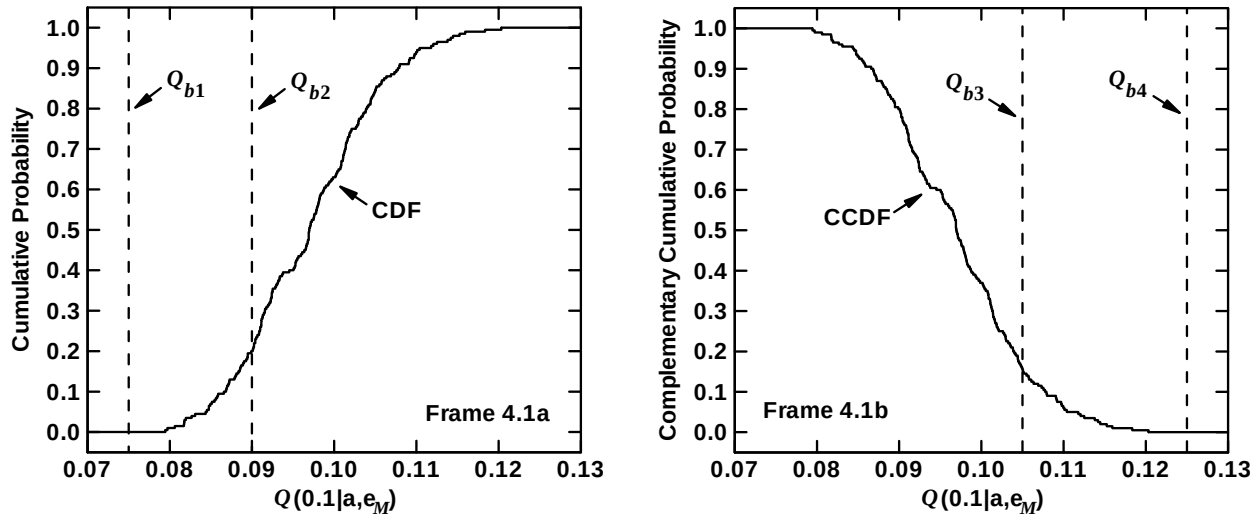

Fig. 4.1. Example bounds on $Q(0.1|\mathbf{a}, \mathbf{e}_M)$: (a) Lower bounds $Q_{b1} = 0.075$ and $Q_{b2} = 0.09$ and estimated CDF for $Q(0.1|\mathbf{a}, \mathbf{e}_M)$, and (b) Upper bounds $Q_{b3} = 0.105$ and $Q_{b4} = 0.125$ and estimated CCDF for $Q(0.1|\mathbf{a}, \mathbf{e}_M)$.

interest for the lower bounds Q_{b1} and Q_{b2}, and the CCDF in Fig. 4.1b displays the probability of being greater than a specified bound, which is the probability of interest for the upper bounds Q_{b3} and Q_{b4}. The CDF and CCDF in Fig. 4.1 were generated with the sample and associated mapping in Eqs. (4.3) and (4.4) as described in conjunction with Eq. (3.25).

For notational simplicity, the ordinates in Figs. 4.1a and 4.1b are assigned the labels "Cumulative Probability" and "Complementary Cumulative Probability" rather than the more explicit but also more complex labeling used with CDFs and CCDFs in Sect. 3. This labeling convention is also used with other similar figures.

All sampled values for $Q(0.1|\mathbf{a}, \mathbf{e}_{Mi})$ are above the bound Q_{b1}. However, this is not the case for Q_{b2}, with the CDF in Fig. 4.1a indicating that the probability of $Q(0.1|\mathbf{a}, \mathbf{e}_M)$ being below $Q_{b2} = 0.09$ is approximately 0.200.

All sampled values for $Q(0.1|\mathbf{a}, \mathbf{e}_{Mi})$ are below the bound Q_{b4}. However, this is not the case for Q_{b3}, with the CCDF in Fig. 4.1b indicating that the probability of $Q(0.1|\mathbf{a}, \mathbf{e}_M)$ being above $Q_{b3} = 0.105$ is approximately 0.155.

The margins between $Q(0.1|\mathbf{a}, \mathbf{e}_M)$ and the bounds Q_{bk}, $k = 1, 2, 3, 4$, indicated in Fig. 4.1 are defined by

$$Q_{mk}\left(0.1\middle|\mathbf{a}, \mathbf{e}_M\right) = \begin{cases} Q\left(0.1\middle|\mathbf{a}, \mathbf{e}_M\right) - Q_{bk} & \text{for } k = 1, 2 \\ Q_{bk} - Q\left(0.1\middle|\mathbf{a}, \mathbf{e}_M\right) & \text{for } k = 3, 4, \end{cases} \tag{4.5}$$

with $Q_{mk}(0.1|\mathbf{a}, \mathbf{e}_M) > 0$ indicating that a specific bound is satisfied and $Q_{mk}(0.1|\mathbf{a}, \mathbf{e}_M) < 0$ indicating that a specified bound is not satisfied (i.e., a positive margin is good and a negative margin is bad). As a result of $Q(0.1|\mathbf{a}, \mathbf{e}_M)$ being epistemically uncertain, the corresponding margins $Q_{mk}(0.1|\mathbf{a}, \mathbf{e}_M)$, $k = 1, 2, 3, 4$, are also epistemically uncertain and have an uncertainty structure that derives from the uncertainty structure assumed for $\mathbf{e}_M$ (Fig. 4.2). Representations of the form shown in Fig. 4.2 provide a complete display of the uncertainty associated with the margins $Q_{mk}(0.1|\mathbf{a}, \mathbf{e}_M)$, $k = 1, 2, 3, 4$, and thus a complete QMU representation of margin uncertainty.

An alternative format involves the use of normalized margins defined by

$$\begin{aligned} Q_{nk}\left(0.1\middle|\mathbf{a}, \mathbf{e}_M\right) &= Q_{mk}\left(0.1\middle|\mathbf{a}, \mathbf{e}_M\right) \Big/ Q_{bk} \\ &= \begin{cases} \left[Q\left(0.1\middle|\mathbf{a}, \mathbf{e}_M\right) - Q_{bk}\right] \Big/ Q_{bk} & \text{for } k = 1, 2 \\ \left[Q_{bk} - Q_{bk}\left(0.1\middle|\mathbf{a}, \mathbf{e}_M\right)\right] \Big/ Q_{bk} & \text{for } k = 3, 4, \end{cases} \end{aligned} \tag{4.6}$$

which expresses margin as a fraction of the corresponding bounding value (Fig. 4.3). This format has the advantage in that it presents margin as a multiple of the bounding value, which is a presentation format thatsome individuals prefer. However, it has the disadvan tage that it does not present the actual size of the margin.

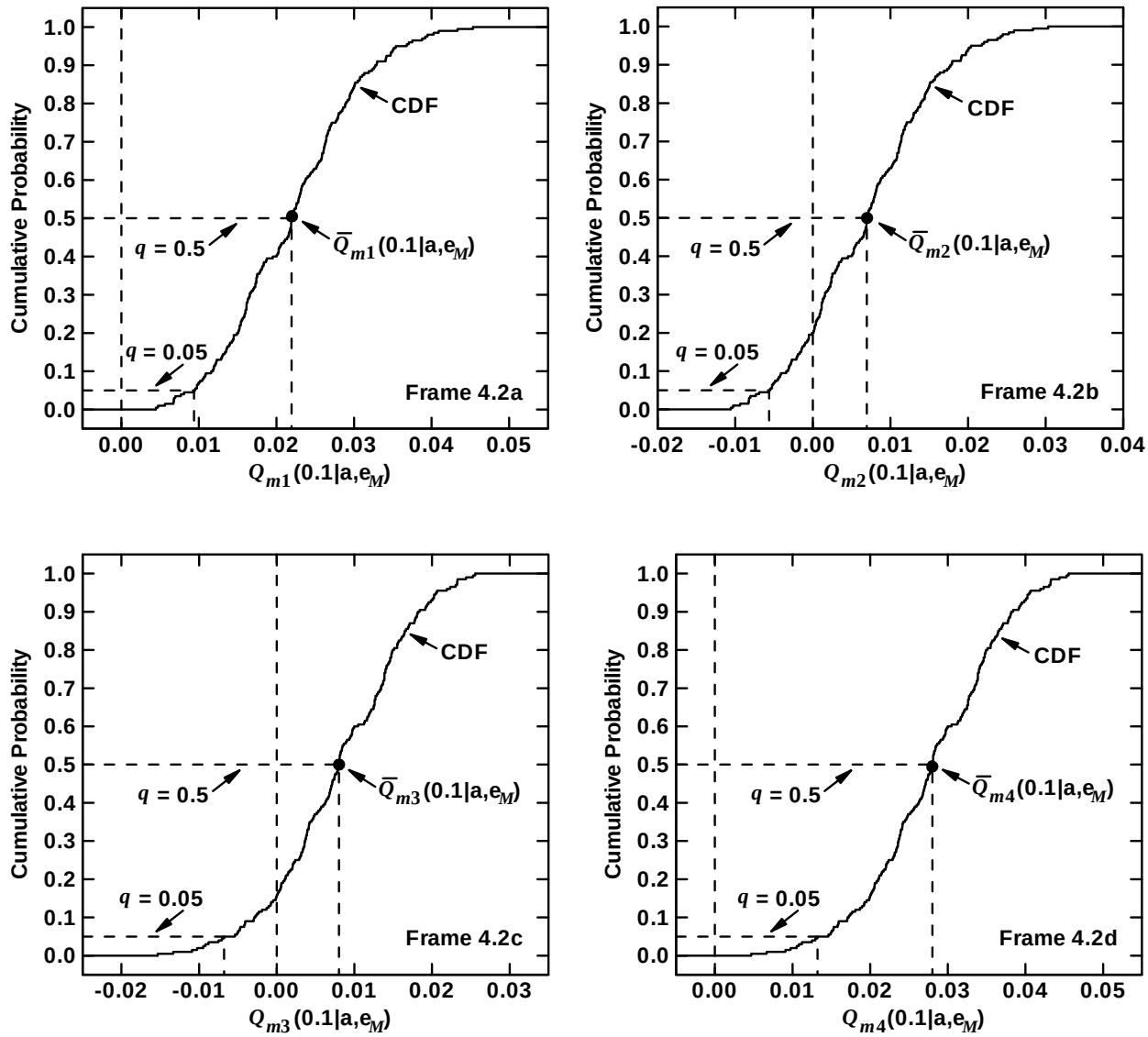

Fig. 4.2. Estimated CDFs for margins $Q_{mk}(0.1|\mathbf{a}, \mathbf{e}_M)$ associated with bounds Q_{bk} for k = 1, 2, 3, 4: (a) $Q_{m1}(0.1|\mathbf{a}, \mathbf{e}_M)$ for Q_{b1} = 0.075, (b) $Q_{m2}(0.1|\mathbf{a}, \mathbf{e}_M)$ for Q_{b2} = 0.09, (c) $Q_{m3}(0.1|\mathbf{a}, \mathbf{e}_M)$ for Q_{b3} = 0.105, and (d) $Q_{m4}(0.1|\mathbf{a}, \mathbf{e}_M)$ for Q_{b4} = 0.125.

It is sometimes stated the QMU corresponds to the determination of the ratio "margin/uncertainty." Unfortunately, it is not always apparent how this imagined concept translates into quantities that are mathematically defined and conceptually useful. In contrast, margin results of the form illustrated in Fig. 4.2 are mathematically well-defined, computationally practicable, and meaningful in a decision context as all available information about margins and their associated uncertainty is presented.

Two possible definitions of "margin/uncertainty" for an arbitrary margin $Q_m(t|\mathbf{a}, \mathbf{e}_M)$ (e.g., $Q_{mk}(0.1|\mathbf{a}, \mathbf{e}_M)$ for k = 1, 2, 3 or 4) are

$$Q_{m/u}\left(t\middle|\mathbf{a}, \mathbf{e}_M\right) = \frac{Q_{m,0.5}\left(t\middle|\mathbf{a}, \mathbf{e}_M\right)}{Q_{m,0.5}\left(t\middle|\mathbf{a}, \mathbf{e}_M\right) - Q_{m,0.05}\left(t\middle|\mathbf{a}, \mathbf{e}_M\right)} \tag{4.7}$$

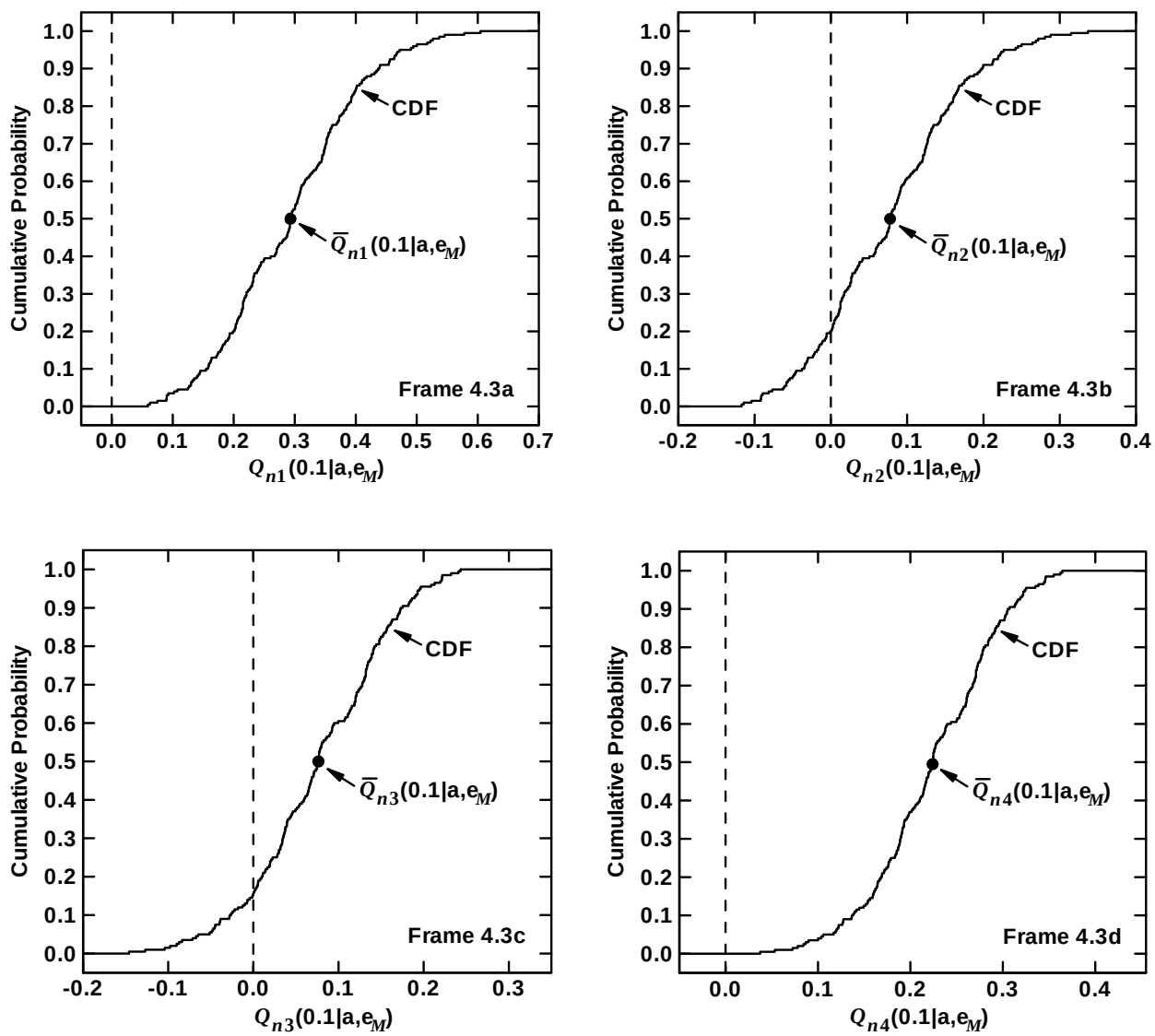

Fig. 4.3. Estimated CDFs for normalized margins $Q_{nk}(0.1|\mathbf{a}, \mathbf{e}_M)$ associated with bounds Q_{bk} for k = 1, 2, 3, 4: (a) $Q_{n1}(0.1|\mathbf{a}, \mathbf{e}_M)$ for Q_{b1} = 0.075, (b) $Q_{n2}(0.1|\mathbf{a}, \mathbf{e}_M)$ for Q_{b2} = 0.09, (c) $Q_{n3}(0.1|\mathbf{a}, \mathbf{e}_M)$ for Q_{b3} = 0.105, and (d) $Q_{n4}(0.1|\mathbf{a}, \mathbf{e}_M)$ for Q_{b4} = 0.125.

and

$$\bar{Q}_{m/u}\left(t\middle|\mathbf{a}, \mathbf{e}_M\right) = \frac{\bar{Q}_m\left(t\middle|\mathbf{a}, \mathbf{e}_M\right)}{\bar{Q}_m\left(t\middle|\mathbf{a}, \mathbf{e}_M\right) - Q_{m,0.05}\left(t\middle|\mathbf{a}, \mathbf{e}_M\right)}, \tag{4.8}$$

where

$Q_{m,0.5}\left(t\middle|\mathbf{a}, \mathbf{e}_M\right)$ = median (i.e., q = 0.5 quantile) for $Q_m(t\,|\mathbf{a}, \mathbf{e}_M)$,
$Q_{m,0.05}\left(t\middle|\mathbf{a}, \mathbf{e}_M\right)$ = 0.05 quantile for $Q_m(t|\mathbf{a}, \mathbf{e}_M)$,
$\bar{Q}_m\left(t\middle|\mathbf{a}, \mathbf{e}_M\right)$ = expected value for $Q_m(t|\mathbf{a}, \mathbf{e}_M)$.

As illustrated in Fig. 4.2, quantities such as $Q_{m,0.5}(t|\mathbf{a}, \mathbf{e}_M)$, $Q_{m,0.05}(t|\mathbf{a}, \mathbf{e}_M)$ and $\bar{Q}_m(t|\mathbf{a}, \mathbf{e}_M)$ are typically esitimated with sampling based procedures. With respect to the more detailed notation used in Sects. 3.3 and 3.4, $Q_{m,0.5}(t|\mathbf{a}, \mathbf{e}_M)$ and $Q_{m,0.05}(t|\mathbf{a}, \mathbf{e}_M)$ correspond to $Q_{EMq}[Q_m(t|\mathbf{a}, \mathbf{e}_M)]$ for q = 0.5 and 0.05, respectively, and $\bar{Q}_m(t|\mathbf{a}, \mathbf{e}_M)$ corresponds to $E_{EM}[Q_m(t|\mathbf{a}, \mathbf{e}_M)]$.

The quantities $Q_{m/u}(t|\mathbf{a}, \mathbf{e}_M)$ and $\bar{Q}_{m/u}(t|\mathbf{a}, \mathbf{e}_M)$ defined in Eqs. (4.7) and (4.8) are based on using the median and mean margins $Q_{m,0.5}(t|\mathbf{a}, \mathbf{e}_M)$ and $\bar{Q}_m(t|\mathbf{a}, \mathbf{e}_M)$ as best estimates for an uncertain margin and then defining uncertainty as the difference between this best estimate and a low quantile (e.g., q = 0.05) of the un-

certainty distribution for margin. In general, large positive margins are good and small or negative margins are bad; in turn, margins associated with small quantiles correspond to small differences between required bounds and predicted system behavior and thus are less desirable than margins associated with larger quantiles. As a result, the differences in the denominators in Eqs. (4.7) and (4.8) provides a measure of the epistemic uncertainty present in the determination of the margin under consideration.

At least notionally, values for $Q_{m/u}(t|\mathbf{a}, \mathbf{e}_M)$ and $\bar{Q}_{m/u}(t|\mathbf{a}, \mathbf{e}_M)$ significantly larger than 1 are good because this situation results when $Q_{m,0.5}(t|\mathbf{a}, \mathbf{e}_M)$ and $\bar{Q}_m(t|\mathbf{a}, \mathbf{e}_M)$ are close to $Q_{m,0.05}(t|\mathbf{a}, \mathbf{e}_M)$ in value, which in turn implies that there is little epistemic uncertainty present in the estimation of the margin under consideration. However, values for $Q_{m/u}(t|\mathbf{a}, \mathbf{e}_M)$ and $\bar{Q}_{m/u}(t|\mathbf{a}, \mathbf{e}_M)$ significantly greater than 1 do not exclude the undesirable situation in which the estimated margins are very close to 0. Values for $Q_{m/u}(t|\mathbf{a}, \mathbf{e}_M)$ and $\bar{Q}_{m/u}(t|\mathbf{a}, \mathbf{e}_M)$ equal to or only slightly larger than 1 are undesirable because this situation results when $Q_{m,0.05}(t|\mathbf{a}, \mathbf{e}_M)$ is equal to or only slightly larger than 0, and values for $Q_{m/u}(t|\mathbf{a}, \mathbf{e}_M)$ and $\bar{Q}_{m/u}(t|\mathbf{a}, \mathbf{e}_M)$ less than 1 are bad because this situation results when $Q_{m,0.05}(t|\mathbf{a}, \mathbf{e}_M)$ is negative. It is important to recognize that very different distributions for $Q_m(t|\mathbf{a}, \mathbf{e}_M)$ can result in similar values for $Q_{m/u}(t|\mathbf{a}, \mathbf{e}_M)$ and also for $\bar{Q}_{m/u}(t|\mathbf{a}, \mathbf{e}_M)$. As a result, consideration of only summary values such as $Q_{m/u}(t|\mathbf{a}, \mathbf{e}_M)$ and $\bar{Q}_{m/u}(t|\mathbf{a}, \mathbf{e}_M)$ can result in an incomplete and potentially misleading assessment of the implications of the uncertainty associated with the margin $Q_m(t|\mathbf{a}, \mathbf{e}_M)$. Additional discussion of the nature of "margin/uncertainty" results is provided in Sect. 4.5.

For the example margins under consideration in this section (Fig. 4.2) and the normalization defined in Eq. (4.7), the values for $Q_{m/u}(0.1|\mathbf{a}, \mathbf{e}_M)$ are

$$Q_{m/u,1}\left(0.1\middle|\mathbf{a}, \mathbf{e}_M\right) = 0.022/\left(0.022-0.009\right) = 1.7, \tag{4.9}$$

$$Q_{m/u,2}\left(0.1\middle|\mathbf{a}, \mathbf{e}_M\right) = 0.0070/\left[0.0070-\left(-0.0056\right)\right] = 0.56, \tag{4.10}$$

$$Q_{m/u,3}\left(0.1\middle|\mathbf{a}, \mathbf{e}_M\right) = 0.0080/\left[0.0080-\left(-0.0068\right)\right] = 0.54, \tag{4.11}$$

and

$$Q_{m/u,4}\left(0.1\middle|\mathbf{a}, \mathbf{e}_M\right) = 0.028/\left(0.028-0.013\right) = 1.9. \tag{4.12}$$

The values for $\bar{Q}_{m/u,k}(0.1|\,\mathbf{a}, \mathbf{e}_M)$ are essentially the same as the values for $Q_{m/u,k}(0.1|\mathbf{a}, \mathbf{e}_M)$ in Eqs. (4.9) – (4.12) because of the similarity of the mean and median values for $Q_m(0.1|\mathbf{a}, \mathbf{e}_M)$ (see Fig. 4.2). However, such similarity will not exist in many analyses.

As discussed in Sect. 4.5, "margin/uncertainty" ratios of the form defined in Eqs. (4.7) and (4.8) and illustrated in Eqs. (4.9) – (4.12) are in (i) the interval $[1, +\infty)$ if the best margin estimate (e.g., the mean or median) is positive and the lower margin estimate (e.g., the 0.05 quantile) is nonnegative, (ii) the interval $[0, 1)$ if the best margin estimate is nonnegative and the lower margin estimate is negative, and (iii) the interval $(-\infty, 0)$ if the best margin estimate and the lower margin estimate are both negative. With respect to the preceding statements, it is tacitly assumed that the best margin estimate is greater than the lower margin estimate. Further, the indicated ratio (i) equals 1 only when the best estimate is positive and the lower estimate is 0, (ii) equals 0 only when the best estimate is 0 and the lower estimate is negative, and (iii) is undefined when the best estimate and the lower estimate are equal. Consistent with the indicated relationships, the "margin/uncertainty" ratios $Q_{m/u,1}(0.1|\mathbf{a}, \mathbf{e}_M) = 1.7$ and $Q_{m/u,4}(0.1|\mathbf{a}, \mathbf{e}_M) = 1.9$ in Eqs. (4.9) and (4.12) are greater than 1 because both the best and lower margin estimates are nonnegative, and the "margin/uncertainty" ratios $Q_{m/u,2}(0.1|\mathbf{a}, \mathbf{e}_M) = 0.56$ and $Q_{m/u,3}(0.1|\mathbf{a}, \mathbf{e}_M) = 0.54$ in Eqs. (4.10) and (4.11) are in the interval $(0, 1)$ because the best and lower margin estimates are positive and negative, respectively.

The "margin/uncertainty" results defined in Eqs. (4.7) and (4.8) and illustrated in Eqs. (4.9) – (4.12) reduce the individual CDFs in Fig. 4.2 to single numbers. As a result, a large amount of information is lost in this reduction. Further, as discussed and illustrated in Sect. 4.5, a "margin/uncertainty" ratio provides no information on the actual values for the best and lower margin values used in the determination of this ratio. Thus, for example, there is no way to use the results in Eqs. (4.9) – (4.12) to retrieve the margin values used in the determination of these results. Simply put, all the information in Figs. 4.1 and 4.2 has been lost.

At their most extreme, $Q_{m/u}(t|\mathbf{a}, \mathbf{e}_M)$ and $\bar{Q}_{m/u}(t|\mathbf{a}, \mathbf{e}_M)$ have the forms

$$Q_{m/u}\left(t\middle|\mathbf{a},\mathbf{e}_M\right)=\frac{Q_{m,0.5}\left(t\middle|\mathbf{a},\mathbf{e}_M\right)}{Q_{m,0.5}\left(t\middle|\mathbf{a},\mathbf{e}_M\right)-Q_{m,0.00}\left(t\middle|\mathbf{a},\mathbf{e}_M\right)} \tag{4.13}$$

and

$$\bar{Q}_{m/u}\left(t\middle|\mathbf{a},\mathbf{e}_M\right)=\frac{\bar{Q}_m\left(t\middle|\mathbf{a},\mathbf{e}_M\right)}{\bar{Q}_m\left(t\middle|\mathbf{a},\mathbf{e}_M\right)-Q_{m,0.00}\left(t\middle|\mathbf{a},\mathbf{e}_M\right)}, \tag{4.14}$$

where

$$\begin{aligned} Q_{m,0.00}\left(t\middle|\mathbf{a},\mathbf{e}_M\right) &= 0.00 \text{ quantile for } Q_m\left(t\middle|\mathbf{a},\mathbf{e}_M\right) \\ &= \inf\left\{Q_m\left(t\middle|\mathbf{a},\mathbf{e}_M\right):\mathbf{e}_M\in\mathcal{E}\right\}. \end{aligned}$$

In words, $Q_{m,0.00}(t|\mathbf{a}, \mathbf{e}_M)$ is the smallest possible value for the margin $Q_m(t|\mathbf{a}, \mathbf{e}_M)$. As a result of the inequality

$$Q_{m,0.00}\left(t\middle|\mathbf{a},\mathbf{e}_M\right)\le Q_{m,0.05}\left(t\middle|\mathbf{a},\mathbf{e}_M\right), \tag{4.15}$$

use of $Q_{m,0.00}(t|\mathbf{a}, \mathbf{e}_M)$ in the definition of $Q_{m/u}(t|\mathbf{a}, \mathbf{e}_M)$ and $\bar{Q}_{m/u}(t|\mathbf{a}, \mathbf{e}_M)$ results in smaller values for these quantities than the use of $Q_{m,0.05}(t|\mathbf{a}, \mathbf{e}_M)$.

For the example margins under consideration in this section, the values for $Q_{m/u}(0.1|\mathbf{a}, \mathbf{e}_M)$ obtained with $Q_{m,0.00}(0.1|\mathbf{a}, \mathbf{e}_M)$ as indicated in Eq. (4.13) are

$$\begin{aligned} Q_{m/u,1}\left(0.1\middle|\mathbf{a},\mathbf{e}_M\right) &= 0.022/\left(0.022-0.004\right) \\ &= 1.2, \end{aligned} \tag{4.16}$$

$$\begin{aligned} Q_{m/u,2}\left(0.1\middle|\mathbf{a},\mathbf{e}_M\right) &= 0.0070/\left[0.0070-\left(-0.0106\right)\right] \\ &= 0.40, \end{aligned} \tag{4.17}$$

$$\begin{aligned} Q_{m/u,3}\left(0.1\middle|\mathbf{a},\mathbf{e}_M\right) &= 0.0080/\left[0.0080-\left(-0.0153\right)\right] \\ &= 0.34, \end{aligned} \tag{4.18}$$

and

$$\begin{aligned} Q_{m/u,4}\left(0.1\middle|\mathbf{a},\mathbf{e}_M\right) &= 0.028/\left(0.028-0.005\right) \\ &= 1.2. \end{aligned} \tag{4.19}$$

Again, the values for $\bar{Q}_{m/u,k}(0.1\,|\,\mathbf{a}, \mathbf{e}_M)$ defined in Eq. (4.14) are very similar to the values for $Q_{m/u}(0.1|\mathbf{a}, \mathbf{e}_M)$ defined in Eq. (4.13) because of the similarity of the mean and median values for $Q_m(0.1|\mathbf{a}, \mathbf{e}_M)$. As noted in conjunction with the inequality in Eq. (4.15), "margin/-uncertainty" ratios obtained with $Q_{m,0.00}(0.1|\mathbf{a}, \mathbf{e}_M)$ are smaller than the ratios obtained with $Q_{m,0.05}(0.1|\mathbf{a}, \mathbf{e}_M)$ (i.e., compare results in Eqs. (4.9) – (4.12) with results in Eqs. (4.16) – (4.19)).

The importance of sensitivity analysis is recognized in the NAS/NRC report on QMU (pp. 14-15, Ref. [77]). Indeed, sensitivity analysis should be an integral part of any QMU analysis. As an example, a sensitivity analysis for $Q(0.1|\mathbf{a}, \mathbf{e}_M)$ based on stepwise regression analysis is presented in Table 4.1. Specifically, stepwise regression analysis is used to explore the mapping

$$\left[\mathbf{e}_{Mi}, Q\left(0.1\,|\,\mathbf{a},\mathbf{e}_{Mi}\right)\right], i=1,2,\ldots,nSE=200, \tag{4.20}$$

used to generate the uncertainty results in Figs. 4.1 – 4.3. With this procedure, variable importance is indicated by the order in which variables are selected in the stepwise process, the incremental changes in R^2 values with the entry of individual variables into the regression model, and the sizes and signs of the standardized regression coefficients (SRCs) in the final regression model (see Sect. 7 and Ref. [56] for additional discussion of regression-based sensitivity analysis).

As examination of Table 4.1 shows, the dominant variables affecting the uncertainty in $Q(0.1|\mathbf{a}, \mathbf{e}_M)$ are E_0 and C. Specifically, the positive SRCs associated with E_0 and C indicate that $Q(0.1|\mathbf{a}, \mathbf{e}_M)$ tends to increase in value as each of these variables increases. In addition, small negative effects are indicated for R and λ, and a small positive effect is indicated for L.

The examination of scatterplots is also an informative part of sampling-based sensitivity analysis. For example, the scatterplots in Fig. 4.4 clearly reveal the positive effects of E_0 and C on $Q(0.1|\mathbf{a}, \mathbf{e}_M)$ and the resultant outcomes that negative or small positive margins associated with requirements Q_{b1} and Q_{b2} occur for small values of E_0 and C and that negative or small positive margins associated with requirements Q_{b3} and Q_{b4} occur for large values of E_0 and C.

Regression-based sensitivity analysis could also be carried out for the margins $Q_{mk}(0.1|\mathbf{a}, \mathbf{e}_M)$, k = 1, 2, 3, 4, defined in Eq. (4.5) and illustrated in Fig. 4.2. However, given that the margins are simply affine transformations (i.e., linear scalings plus constant shifts) of $Q(0.1|\mathbf{a}, \mathbf{e}_M)$ defined by the bounds Q_{bk}, k = 1, 2, 3, 4, the resultant regression analyses for $Q_{mk}(0.1|\mathbf{a}, \mathbf{e}_M)$, k = 1, 2, would be the same as presented in Table 4.1 as a result of the defining transformation

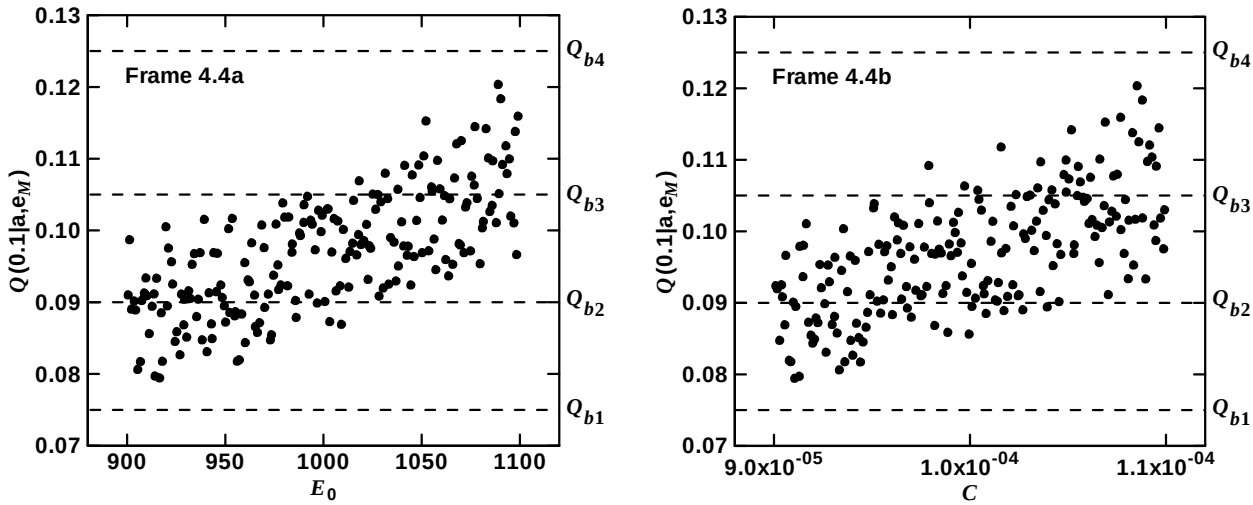

Fig. 4.4. Scatterplots for $Q(0.1|\mathbf{a}, \mathbf{e}_M)$: (a) $[E_{0i}, Q(0.1|\mathbf{a}, \mathbf{e}_{Mi})]$, $i = 1,2, \ldots, nSE = 200$, and (b) $[C_i, Q(0.1|\mathbf{a}, \mathbf{e}_{Mi})]$, $i = 1,2, \ldots, nSE = 200$.

Table 4.1. Stepwise Regression Analysis to Identify Uncertain Variables Affecting $Q(0.1|\mathbf{a}, \mathbf{e}_M)$

Step[a]	Variable[b]	SRC[c]	R^{2d}
1	E_0	0.70	0.51
2	C	0.63	0.91
3	R	–0.22	0.96
4	λ	–0.12	0.98
5	L	0.06	0.98

[a] Steps in stepwise regression analysis with an α-value of 0.01 or less required for a variable to enter a regression model.
[b] Variables listed in the order of selection in regression analysis.
[c] SRCs for variables in final regression model.
[d] Cumulative R^2 value with entry of each variable into regression model.

$$Q_{mk}\left(0.1\,|\,\mathbf{a},\mathbf{e}_M\right) = Q\left(0.1\,|\,\mathbf{a},\mathbf{e}_M\right) - Q_{bk} \tag{4.21}$$

for $k = 1, 2$, and the resultant regression analyses for $Q_{mk}(0.1|\mathbf{a}, \mathbf{e}_M)$, $k = 3, 4$, would also be the same as presented in Table 4.1 except for a reversal in the signs of the SRCs as a result of the defining transformation

$$Q_{mk}\left(0.1\,|\,\mathbf{a},\mathbf{e}_M\right) = Q_{bk} - Q\left(0.1\,|\,\mathbf{a},\mathbf{e}_M\right) \tag{4.22}$$

for $k = 3, 4$. Similarly, the scatterplots for the margins $Q_{mk}(0.1|\mathbf{a}, \mathbf{e}_M)$, $k = 1, 2, 3, 4$, would effectively convey the same information as the scatterplots for $Q(0.1|\mathbf{a}, \mathbf{e}_M)$ in Fig. 4.4.

4.2 Epistemic Uncertainty with a Specified Bounding Interval

A QMU problem involving a bounding interval rather than simply an upper or lower bound is now considered. Specifically, the problem involves a specified interval within which the quantity of interest is required to be located. For the quantity $Q(0.1|\mathbf{a}, \mathbf{e}_M)$, this involves the specification of an interval $[\underline{Q}_b, \overline{Q}_b]$ such that the inequalities

$$\underline{Q}_b \le Q\left(0.1\middle|\mathbf{a},\mathbf{e}_M\right) \le \overline{Q}_b \tag{4.23}$$

hold (Fig. 4.5). For illustration, $[\underline{Q}_b, \overline{Q}_b]$ is assumed to equal [0.08, 0.12] as indicated in Fig. 4.5. This example corresponds to consideration of what is called a "gate" in some discussions of QMU [1; 4].

There are several ways in which the epistemic uncertainty associated with compliance with the specified bounds can be represented. The easiest is simply to consider whether or not $Q(0.1|\mathbf{a}, \mathbf{e}_M)$ falls within the specified bounds. This involves consideration of the indicator function

$$\delta\left[Q\left(0.1\middle|\mathbf{a},\mathbf{e}_M\right)\right] = \begin{cases} 1 & \text{if } \underline{Q}_b \le Q\left(0.1\middle|\mathbf{a},\mathbf{e}_M\right) \le \overline{Q}_b \\ 0 & \text{otherwise} \end{cases} \tag{4.24}$$

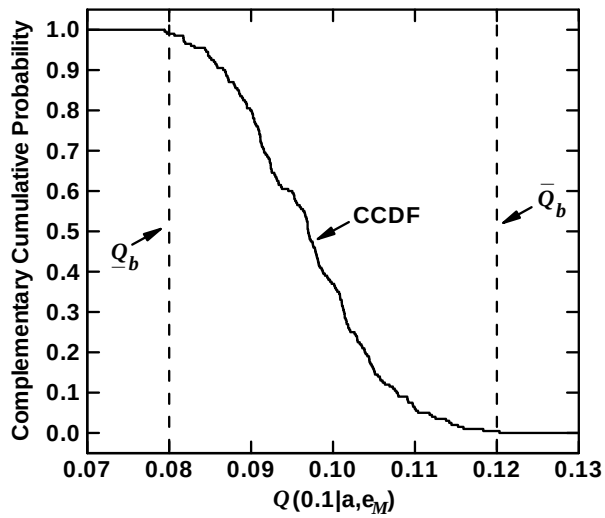

Fig. 4.5. Example bounding interval $[\underline{Q}_b, \overline{Q}_b]$ = [0.08, 0.12] for $Q(0.1|\mathbf{a}, \mathbf{e}_M)$.

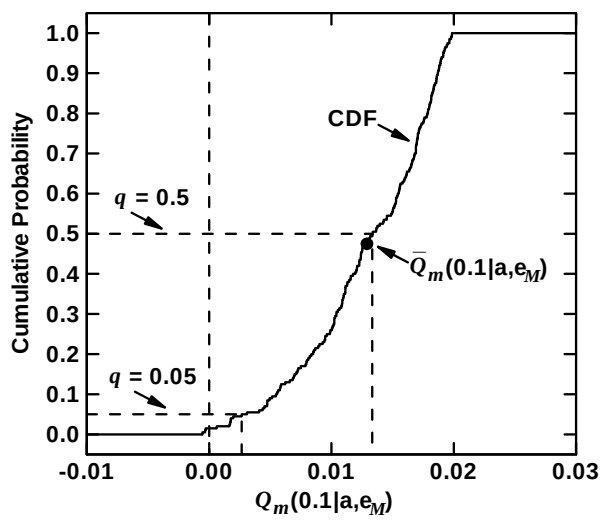

Fig. 4.6. Estimated CDF summarizing uncertainty in margin $Q_m(0.1|\mathbf{a}, \mathbf{e}_M)$ defined in Eq. (4.29) for bounding interval $[\underline{Q}_b, \overline{Q}_b]$ = [0.08, 0.12].

and the associated sets

$$\mathcal{X}^+ = \left\{ \mathbf{e}_M : \mathbf{e}_M \in \mathcal{EM} \text{ and } \delta\left[Q\left(0.1 \middle| \mathbf{a}, \mathbf{e}_M\right)\right] = 1 \right\} \tag{4.25}$$

and

$$\mathcal{X}^- = \left\{ \mathbf{e}_M : \mathbf{e}_M \in \mathcal{EM} \text{ and } \delta\left[Q\left(0.1 \middle| \mathbf{a}, \mathbf{e}_M\right)\right] = 0 \right\}. \tag{4.26}$$

Then, the probabilities of compliance and noncompliance are given by

$$p_{EM}\left(\mathcal{X}^+\right) \cong \sum_{i=1}^{nSE} \delta\left[Q\left(0.1 \middle| \mathbf{a}, \mathbf{e}_{Mi}\right)\right] \Big/ nSE = 0.985 \tag{4.27}$$

and

$$p_{EM}\left(\mathcal{X}^-\right) = 1 - p_{EM}\left(\mathcal{X}^+\right) \cong 1 - 0.985 = 0.015, \tag{4.28}$$

respectively.

The representation in the preceding paragraph summarizes the uncertainty in whether or not the specified interval bound will be satisfied. However, the uncertainty in the location of $Q(0.1|\mathbf{a}, \mathbf{e}_M)$ relative to the ends of the bounding interval $[\underline{Q}_b, \overline{Q}_b]$ is not indicated. The consideration of this uncertainty requires the determination of margins and the uncertainty associated with these margins. Specifically, a margin associated with the containment of $Q(0.1|\mathbf{a}, \mathbf{e}_M)$ in the interval $[\underline{Q}_b, \overline{Q}_b]$ can be defined by

$$Q_m\left(0.1 \middle| \mathbf{a}, \mathbf{e}_M\right) = \min \begin{cases} Q\left(0.1 \middle| \mathbf{a}, \mathbf{e}_M\right) - \underline{Q}_b \\ \overline{Q}_b - Q\left(0.1 \middle| \mathbf{a}, \mathbf{e}_M\right), \end{cases} \tag{4.29}$$

with the result that (i) $Q_m(0.1|\mathbf{a}, \mathbf{e}_M)$ is nonnegative if $Q(0.1|\mathbf{a}, \mathbf{e}_M)$ falls within the interval $[\underline{Q}_b, \overline{Q}_b]$, and (ii) $Q_m(0.1|\mathbf{a}, \mathbf{e}_M)$ is negative if $Q(0.1|\mathbf{a}, \mathbf{e}_M)$ falls outside the interval $[\underline{Q}_b, \overline{Q}_b]$. In turn, $Q_m(0.1|\mathbf{a}, \mathbf{e}_M)$ has an uncertainty structure that derives from the uncertainty structure imposed on $\mathbf{e}_M$ (Fig. 4.6). The probability $p_{EM}(\mathcal{X}^-) = 0.015$ in Eq. (4.28) corresponds to the cumulative probability associated with $Q_m(0.1|\mathbf{a}, \mathbf{e}_M) = 0$ in Fig. 4.6.

An alternate representation is to use normalized margins. Specifically, the margin $Q_m(0.1|\mathbf{a}, \mathbf{e}_M)$ defined in Eq. (4.29) can be replaced by a normalized margin $Q_n(0.1|\mathbf{a}, \mathbf{e}_M)$ defined by

$$Q_n\left(0.1 \middle| \mathbf{a}, \mathbf{e}_M\right) = \min \begin{cases} \left[Q\left(0.1 \middle| \mathbf{a}, \mathbf{e}_M\right) - \underline{Q}_b \right] \Big/ \underline{Q}_b \\ \left[\overline{Q}_b - Q\left(0.1 \middle| \mathbf{a}, \mathbf{e}_M\right) \right] \Big/ \overline{Q}_b, \end{cases} \tag{4.30}$$

which expresses margin as a fraction of the bounding value from which $Q(0.1|\mathbf{a}, \mathbf{e}_M)$ has the smallest fractional deviation (Fig. 4.7).

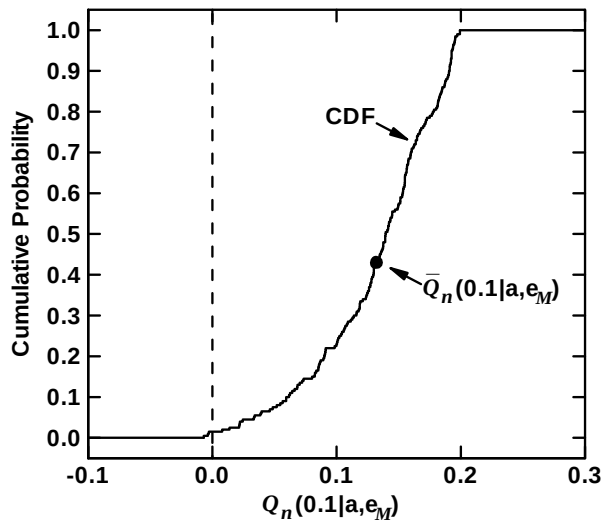

Fig. 4.7. Estimated CDF summarizing uncertainty in normalized margin $Q_n(0.1|\mathbf{a}, \mathbf{e}_M)$ defined in Eq. (4.30) for bounding interval $[\underline{Q}_b, \bar{Q}_b]$ = [0.08, 0.12].

If desired, "margin/uncertainty" summary measures of the form defined in Eqs. (4.7), (4.8), (4.13) and (4.14) can be defined for the distribution of $Q_m(0.1|\mathbf{a}, \mathbf{e}_M)$ in Fig. 4.6. Specifically,

$$Q_{m/u}\left(t|\mathbf{a}, \mathbf{e}_M\right) = \frac{Q_{m,0.5}\left(t|\mathbf{a}, \mathbf{e}_M\right)}{Q_{m,0.5}\left(t|\mathbf{a}, \mathbf{e}_M\right) - Q_{m,q}\left(t|\mathbf{a}, \mathbf{e}_M\right)} = \begin{cases} 0.013/\left(0.013-0.003\right)=1.30 \text{ for } q=0.05 \\ 0.013/\left[0.013-\left(-0.001\right)\right]=0.93 \text{ for } q=0.00 \end{cases} \tag{4.31}$$

for t = 0.1 s, and

$$\bar{Q}_{m/u}\left(t|\mathbf{a}, \mathbf{e}_M\right) = \frac{\bar{Q}_m\left(t|\mathbf{a}, \mathbf{e}_M\right)}{\bar{Q}_m\left(t|\mathbf{a}, \mathbf{e}_M\right) - Q_{m,q}\left(t|\mathbf{a}, \mathbf{e}_M\right)} \tag{4.32}$$

effectively has the same values as $Q_{m/u}(t|\mathbf{a}, \mathbf{e}_M)$ for t = 0.1 s because of the similarity of the mean and median values for $Q_m(0.1|\mathbf{a}, \mathbf{e}_M)$ (see Fig. 4.6). However, as previously discussed in Sect. 4.1, a significant amount of information is lost when the results in Figs. Fig. 4.5 and Fig. 4.6 are reduced to a single number (see Sect. 4.5 for additional discussion).

The results of a sensitivity analysis for $Q(0.1|\mathbf{a}, \mathbf{e}_M)$ are presented in Table 4.1 and Fig. 4.4. Because $Q_m(0.1|\mathbf{a}, \mathbf{e}_M)$ as defined in Eq. (4.29) for bounding interval $[\underline{Q}_b, \bar{Q}_b]$ = [0.08, 0.12] is not an affine transformation of $Q(0.1|\mathbf{a}, \mathbf{e}_M)$, these analyses do not reveal the full effects of the elements of $\mathbf{e}_M$ on $Q_m(0.1|\mathbf{a}, \mathbf{e}_M)$. To determine these effects, a stepwise regression analysis (Table 4.2) is initially performed for the mapping

$$\left[\mathbf{e}_{Mi}, Q_m\left(0.1\,|\,\mathbf{a}, \mathbf{e}_{Mi}\right)\right], i = 1, 2, ..., nSE = 200, \tag{4.33}$$

and then followed by an examination of scatterplots.

The regression analysis in Table 4.2 for $Q_m(0.1|\mathbf{a}, \mathbf{e}_M)$ is very poor, with the final regression model containing E_0 and C having an R^2 value of only 0.16. As a reminder, E_0 and C are the dominant variables affecting the uncertainty in $Q(0.1|\mathbf{a}, \mathbf{e}_M)$ (see Table 4.1 and Fig. 4.4). Given the effects of E_0 and C on $Q(0.1|\mathbf{a}, \mathbf{e}_M)$, a natural next step is to examine the scatterplots for E_0, C and $Q_m(0.1|\mathbf{a}, \mathbf{e}_M)$ (Fig. 4.8). Specifically, the scatterplots in Fig. 4.8 show that small values for $Q_m(0.1|\mathbf{a}, \mathbf{e}_M)$ are associated with both small and large values for E_0 and C. This is consistent with the monotonic effects of E_0 and C on $Q(0.1|\mathbf{a}, \mathbf{e}_M)$ shown in the scatterplots in Fig. 4.4 and the dependence of the margin $Q_m(0.1|\mathbf{a}, \mathbf{e}_M)$ on both small and large values for $Q(0.1|\mathbf{a}, \mathbf{e}_M)$ (see definition of $Q_m(0.1|\mathbf{a}, \mathbf{e}_M)$ in Eq. (4.29)). Given the monotonic effects of E_0 and C on $Q(0.1|\mathbf{a}, \mathbf{e}_M)$ and the definition of $Q_m(0.1|\mathbf{a}, \mathbf{e}_M)$, small values for $Q_m(0.1|\mathbf{a}, \mathbf{e}_M)$ will tend to occur when either (i) both E_0 and C are at the lower ends of their ranges or (ii) both E_0 and C are at the upper ends of their ranges.

The regression analysis for $Q_m(0.1|\mathbf{a}, \mathbf{e}_M)$ in Table 4.2 fails beause of the nonmonotonic relationships involving E_0, C and $Q_m(0.1|\mathbf{a}, \mathbf{e}_M)$ shown in Fig. 4.8. Given the complexity of the relationships involving E_0, C and $Q_m(0.1|\mathbf{a}, \mathbf{e}_M)$, a successful regression-based sensitivity analysis for $Q_m(0.1|\mathbf{a}, \mathbf{e}_M)$ would require the use of nonparametric regression procedures [111; 112].

As indicated by this example, sensitivity analyses associated with margins defined for bounding intervals (i.e., gates) can be challenging. This can happen for at least two reasons. First, different subranges of a variable can affect compliance with upper and lower bounds. Second, different variables can affect compliance with upper and lower bounds. The outcome of these two effects can be complex relational patterns between margins and uncertain analysis inputs whose identification requires sophisticated sensivity analysis procedures (e.g., [111; 112]).

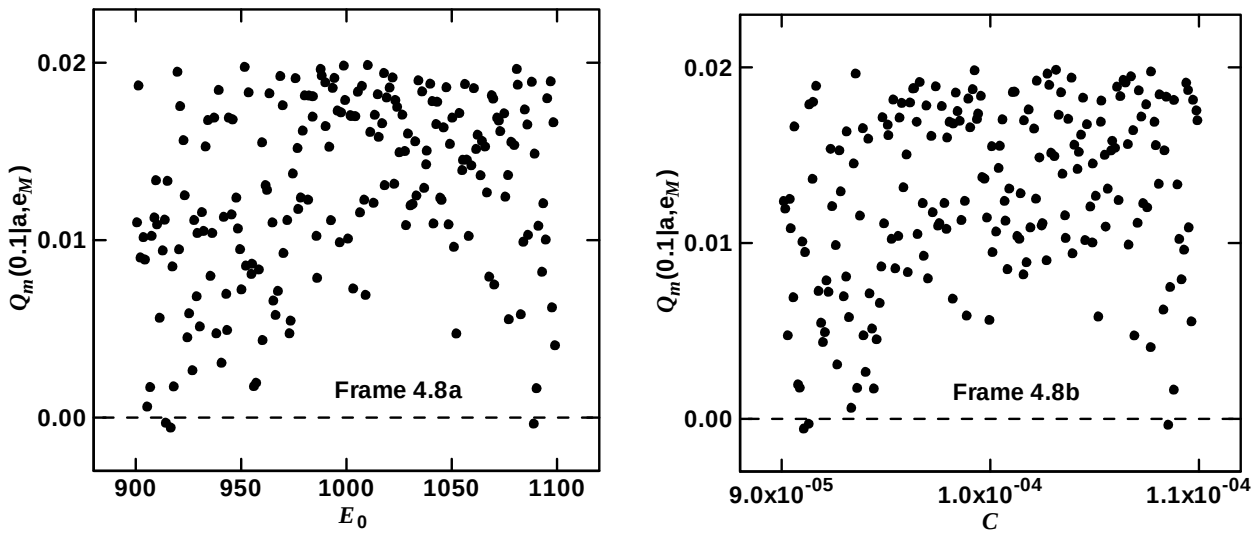

Fig. 4.8. Scatterplots for margin $Q_m(0.1|\mathbf{a}, \mathbf{e}_M)$ defined in Eq. (4.29): (a) $[E_{0i}, Q_m(0.1|\mathbf{a}, \mathbf{e}_{Mi})]$, $i = 1,2, \ldots, nSE = 200$, and (b) $[C_i, Q_m(0.1|\mathbf{a}, \mathbf{e}_{Mi})]$, $i = 1,2, \ldots, nSE = 200$.

Table 4.2. Stepwise Regression Analysis to Identify Uncertain Variables Affecting the Margin $Q_m(0.1|\mathbf{a}, \mathbf{e}_M)$ defined in Eq. (4.29)

Step[a]	Variable[b]	SRC[c]	R^{2d}
1	E_0	0.28	0.08
2	C	0.27	0.16

[a] Steps in stepwise regression analysis with an α-value of 0.01 or less required for a variable to enter a regression model.
[b] Variables listed in the order of selection in regression analysis.
[c] SRCs for variables in final regression model.
[d] Cumulative R^2 value with entry of each variable into regression model.

4.3 Epistemic Uncertainty with a Specified Bounding Interval over Time

A QMU problem involving a bounding interval at a fixed point in time is considered in Sect. 4.2. This problem is now increased in complexity by considering a situation in which a bounding interval $[\underline{Q}_b, \overline{Q}_b]$ is specified for a quantity such as $Q(t|\mathbf{a}, \mathbf{e}_M)$ that takes on values over a time interval $[t_{mn}, t_{mx}]$ (Fig. 4.9). Specifically, the requirement is that the values for $Q(t|\mathbf{a}, \mathbf{e}_M)$ stay within the bounding interval $[\underline{Q}_b, \overline{Q}_b]$ for $t_{mn} \le t \le t_{mx}$ (e.g., $[\underline{Q}_b, \overline{Q}_b] = [0.07, 0.14]$, $t_{mn} = 0.02$ s and $t_{mx} = 0.18$ s in Fig. 4.9). Formally stated, the requirement is that the inequalities

$$\underline{Q}_b \le Q\left(t\middle|\mathbf{a}, \mathbf{e}_M\right) \le \overline{Q}_b \tag{4.34}$$

be satisfied for $\mathbf{e}_M \in \mathcal{EM}$ and $t_{mn} \le t \le t_{mx}$.

Uncertainty in compliance with the indicated requirement can be represented with use of the indicator function

$$\delta\left[Q\left(t\middle|\mathbf{a}, \mathbf{e}_M\right) : t_{mn} \le t \le t_{mx}\right] = \begin{cases} 1 & \text{if } \underline{Q}_b \le Q\left(t\middle|\mathbf{a}, \mathbf{e}_M\right) \le \overline{Q}_b \text{ for } t_{mn} \le t \le t_{mx} \\ 0 & \text{otherwise} \end{cases} \tag{4.35}$$

and the associated sets

$$\mathcal{X}^+ = \left\{ \begin{array}{l} \mathbf{e}_M : \mathbf{e}_M \in \mathcal{EM} \text{ and} \\ \qquad \delta\left[Q\left(t\middle|\mathbf{a}, \mathbf{e}_M\right) : t_{mn} \le t \le t_{mx}\right] = 1 \end{array} \right\} \tag{4.36}$$

and

$$\mathcal{X}^- = \left\{ \begin{array}{l} \mathbf{e}_M : \mathbf{e}_M \in \mathcal{EM} \text{ and} \\ \qquad \delta\left[Q\left(t\middle|\mathbf{a}, \mathbf{e}_M\right) : t_{mn} \le t \le t_{mx}\right] = 0 \end{array} \right\}. \tag{4.37}$$

Then, the probabilities of compliance and noncompliance are given by

$$p_{EM}\left(\mathcal{X}^+\right) \cong \sum_{i=1}^{nSE} \delta\left[Q\left(t\middle|\mathbf{a}, \mathbf{e}_{Mi}\right) : t_{mn} \le t \le t_{mx}\right] \Big/ nSE = 0.82 \tag{4.38}$$

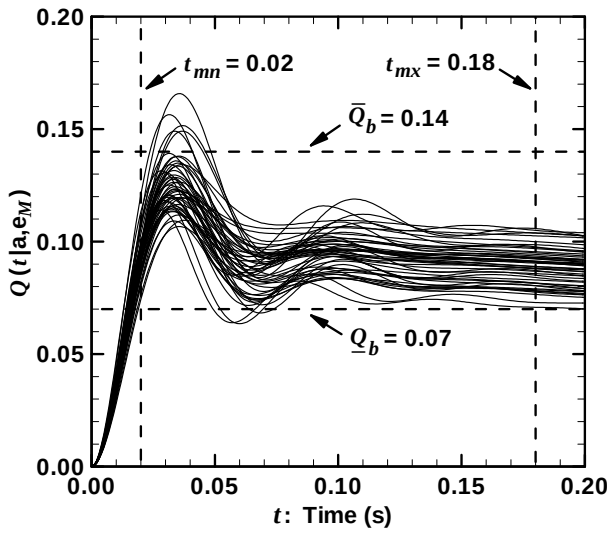

Fig. 4.9. Example bounding interval $[\underline{Q}_b, \bar{Q}_b]$ = [0.07, 0.14] over the time interval $[t_{mn}, t_{mx}]$ = [0.02, 0.18 s] for $Q(t|\mathbf{a}, \mathbf{e}_M)$.

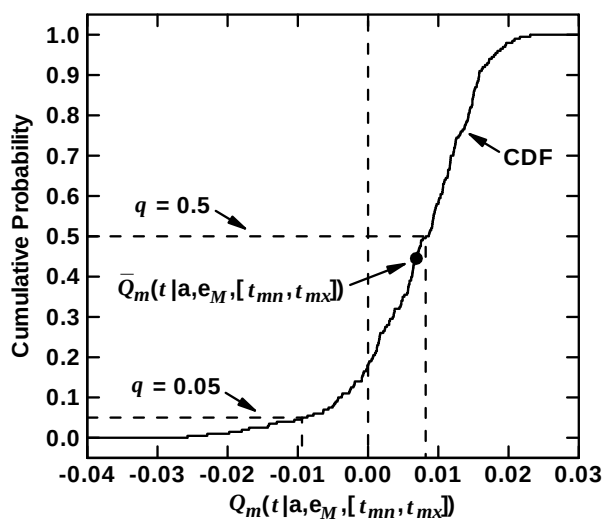

Fig. 4.10. Estimated CDF summarizing uncertainty in margin $Q_m(t|\mathbf{a}, \mathbf{e}_M, [t_{mn}, t_{mx}])$ defined in Eq. (4.40) for bounding interval $[\underline{Q}_b, \bar{Q}_b]$ = [0.07, 0.14] and time interval $[t_{mn}, t_{mx}]$ = [0.02, 0.18 s].

and

$$p_{EM}\left(\mathcal{X}^-\right) = 1 - p_{EM}\left(\mathcal{X}^+\right) \cong 1 - 0.82 = 0.18, \qquad (4.39)$$

respectively.

The preceding representation summarizes the uncertainty in whether or not compliance with the specified bounding interval over time will be satisfied. However, this representation does not display the associated margins. These margins can be defined by

$$Q_m\left(t\middle|\mathbf{a}, \mathbf{e}_M, [t_{mn}, t_{mx}]\right) = \min\begin{cases} Q_{mn}\left(t\middle|\mathbf{a}, \mathbf{e}_M, [t_{mn}, t_{mx}]\right) - \underline{Q}_b \\ \bar{Q}_b - Q_{mx}\left(t\middle|\mathbf{a}, \mathbf{e}_M, [t_{mn}, t_{mx}]\right), \end{cases} \qquad (4.40)$$

where

$$Q_{mn}\left(t\middle|\mathbf{a}, \mathbf{e}_M, [t_{mn}, t_{mx}]\right) = \min\left\{Q\left(t\middle|\mathbf{a}, \mathbf{e}_M\right) : t_{mn} \le t \le t_{mx}\right\}$$

and

$$Q_{mx}\left(t\middle|\mathbf{a}, \mathbf{e}_M, [t_{mn}, t_{mx}]\right) = \max\left\{Q\left(t\middle|\mathbf{a}, \mathbf{e}_M\right) : t_{mn} \le t \le t_{mx}\right\}.$$

In turn, $Q_m(t|\mathbf{a}, \mathbf{e}_M, [t_{mn}, t_{mx}])$ has an uncertainty structure that derives from the uncertainty structure imposed on $\mathbf{e}_M$ (Fig. 4.10). The probability $p_{EM}(\mathcal{X}^-)$ = 0.18 in Eq. (4.39) corresponds to the cumulative probability associated with $Q_m(0.1|\mathbf{a}, \mathbf{e}_M, [t_{mn}, t_{mx}])$ = 0 in Fig. 4.10.

An alternative representation is to use normalized margins. Specifically, the margin $Q_m(t|\mathbf{a}, \mathbf{e}_M, [t_{mn}, t_{mx}])$ defined in Eq. (4.40) can be replaced by a normalized margin $Q_n(t|\mathbf{a}, \mathbf{e}_M, [t_{mn}, t_{mx}])$ defined by

$$Q_n\left(t\middle|\mathbf{a}, \mathbf{e}_M, [t_{mn}, t_{mx}]\right) = \min\begin{cases} \dfrac{Q_{mn}\left(t\middle|\mathbf{a}, \mathbf{e}_M, [t_{mn}, t_{mx}]\right) - \underline{Q}_b}{\underline{Q}_b} \\ \dfrac{\bar{Q}_b - Q_{mx}\left(t\middle|\mathbf{a}, \mathbf{e}_M, [t_{mn}, t_{mx}]\right)}{\bar{Q}_b}, \end{cases} \qquad (4.41)$$

which expresses margin as a fraction of the bounding value from which $Q(t|\,\mathbf{a}, \mathbf{e}_M)$ has the smallest fractional deviation (Fig. 4.11).

If desired, "margin/uncertainty" summary measures of the form defined in Eqs. (4.7), (4.8), (4.13) and (4.14) can be defined for the distribution of $Q(0.1|\mathbf{a}, \mathbf{e}_M, [t_{mn}, t_{mx}])$ in Fig. 4.10. Specifically,

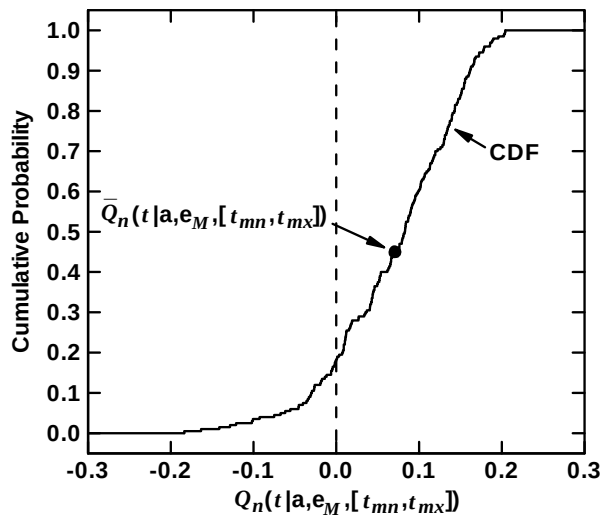

Fig. 4.11. Estimated CDF summarizing uncertainty in normalized margin $Q_n(t|\mathbf{a}, \mathbf{e}_M, [t_{mn}, t_{mx}])$ defined in Eq. (4.41) for bounding interval $[\underline{Q}_b, \bar{Q}_b] = [0.07, 0.14]$ and time interval $[t_{mn}, t_{mx}] = [0.02, 0.18$ s].

$$Q_{m/u}\left(t\middle|\mathbf{a}, \mathbf{e}_M, [t_{mn}, t_{mx}]\right) = \frac{Q_{m,0.5}\left(t\middle|\mathbf{a}, \mathbf{e}_M, [t_{mn}, t_{mx}]\right)}{Q_{m,0.5}\left(t\middle|\mathbf{a}, \mathbf{e}_M, [t_{mn}, t_{mx}]\right) - Q_{m,q}\left(t\middle|\mathbf{a}, \mathbf{e}_M, [t_{mn}, t_{mx}]\right)} = \begin{cases} 0.0082/\left[0.0082-(-0.0094)\right] = 0.47 \text{ for } q = 0.05 \\ 0.0082/\left[0.0082-(-0.0257)\right] = 0.24 \text{ for } q = 0.00 \end{cases} \tag{4.42}$$

and

$$\bar{Q}_{m/u}\left(t\middle|\mathbf{a}, \mathbf{e}_M, [t_{mn}, t_{mx}]\right) = \frac{\bar{Q}_m\left(t\middle|\mathbf{a}, \mathbf{e}_M, [t_{mn}, t_{mx}]\right)}{\bar{Q}_m\left(t\middle|\mathbf{a}, \mathbf{e}_M, [t_{mn}, t_{mx}]\right) - Q_{m,q}\left(t\middle|\mathbf{a}, \mathbf{e}_M, [t_{mn}, t_{mx}]\right)} = \begin{cases} 0.0069/\left[0.0069-(-0.0094)\right] = 0.42 \text{ for } q = 0.05 \\ 0.0069/\left[0.0069-(-0.0257)\right] = 0.21 \text{ for } q = 0.00. \end{cases} \tag{4.43}$$

However, as is always the case, a significant amount of information is lost when the results in Figs. 4.9 and 4.10 are reduced to a single number (see Sect. 4.5 for additional discussion).

Sensitivity analysis can also be performed for $Q(t|\mathbf{a}, \mathbf{e}_M)$ and the results summarized by $Q_m(t|\mathbf{a}, \mathbf{e}_M, [t_{mn}, t_{mx}])$. A natural starting point is to investigate the variables affecting $Q(t|\mathbf{a}, \mathbf{e}_M)$ over the time interval $[t_{mn}, t_{mx}]$ (Fig. 4.12). To this end, partial correlation coefficients (PCCs) and SRCs for $Q(t|\mathbf{a}, \mathbf{e}_M)$ and the elements of $\mathbf{e}_M$ are presented in Fig. 4.12.

Related, but not identical information is provided by PCCs and SRCs. Specifically, a PCC provides a measure of the strength of the linear relationship between two variables after the linear effects of all other variables have been removed, and a SRC provides a measure of the fraction of the uncertainty in a dependent variable that can be accounted for by the independent variable under consideration (see Refs. [53; 56] for additional discussion of PCCs and SRCs). Although their numeric values differ, the absolute values of PCCs and SRCs provide the same orderings of variable importance when no correlations between the independent variables (i.e., the elements of $\mathbf{e}_M$) are present. For comparison, both PCCs and SRCs are presented in Fig. 4.12. For presentation purposes, PCCs can be preferable to SRCs because PCCs tend to be more spread out in the interval [–1, 1] than SRCs, with the result that a single plot frame containing multiple time-dependent PCCs is easier to read than a single plot frame containing multiple time-dependent SRCs.

As examination of Fig. 4.12 shows, the effects of the elements of $\mathbf{e}_M$ tend to swing from positive to negative prior to approximately 0.1 s. This effect results because of the oscillatory behavior of $Q(t|\mathbf{a}, \mathbf{e}_M)$ that can be seen in Fig. 4.9 and derives from the sine and cosine terms in the closed form representation for $Q(t|\mathbf{a}, \mathbf{e}_M)$ shown in Eq. (3.31). During this early time period, all variables except λ have appreciable effects on $Q(t|\mathbf{a}, \mathbf{e}_M)$. After approximately 0.1 s, the oscillatory behavior of $Q(t|\mathbf{a}, \mathbf{e}_M)$ has significantly decayed, and the uncertainty in $Q(t|\mathbf{a}, \mathbf{e}_M)$ is dominated by C and E. As indicated by its PCCs and SRCs, λ has a strong negative partial correlation with $Q(t|\mathbf{a}, \mathbf{e}_M)$ beginning at about 0.1 s but the actual size of this effect on the uncertainty in $Q(t|\mathbf{a}, \mathbf{e}_M)$ is rather small.

In this example, the margin $Q_m(t|\mathbf{a}, \mathbf{e}_M, [t_{mn}, t_{mx}])$ is not an affine transformation of the underlying analysis result $Q(t|\mathbf{a}, \mathbf{e}_M)$. As a consequence, sensitivity analysis results for $Q(t|\mathbf{a}, \mathbf{e}_M)$ cannot be expected to be the same as sensitivity analysis results for $Q_m(t|\mathbf{a}, \mathbf{e}_M, [t_{mn}, t_{mx}])$. For this reason, a sensitivity analysis for $Q_m(t|\mathbf{a}, \mathbf{e}_M, [t_{mn}, t_{mx}])$ with stepwise regression analysis is presented in Table 4.3. This analysis indicates that R is the dominant variable affecting the uncertainty in $Q_m(t|\mathbf{a}, \mathbf{e}_M, [t_{mn}, t_{mx}])$, with $Q_m(t|\mathbf{a}, \mathbf{e}_M, [t_{mn}, t_{mx}])$ tending to increase as R increases. After R, smaller effects on $Q_m(t|\mathbf{a}, \mathbf{e}_M, [t_{mn}, t_{mx}])$ are indicated for E_0, C and L, with $Q_m(t|\mathbf{a}, \mathbf{e}_M, [t_{mn}, t_{mx}])$ tending to decrease as each of these variables increases.

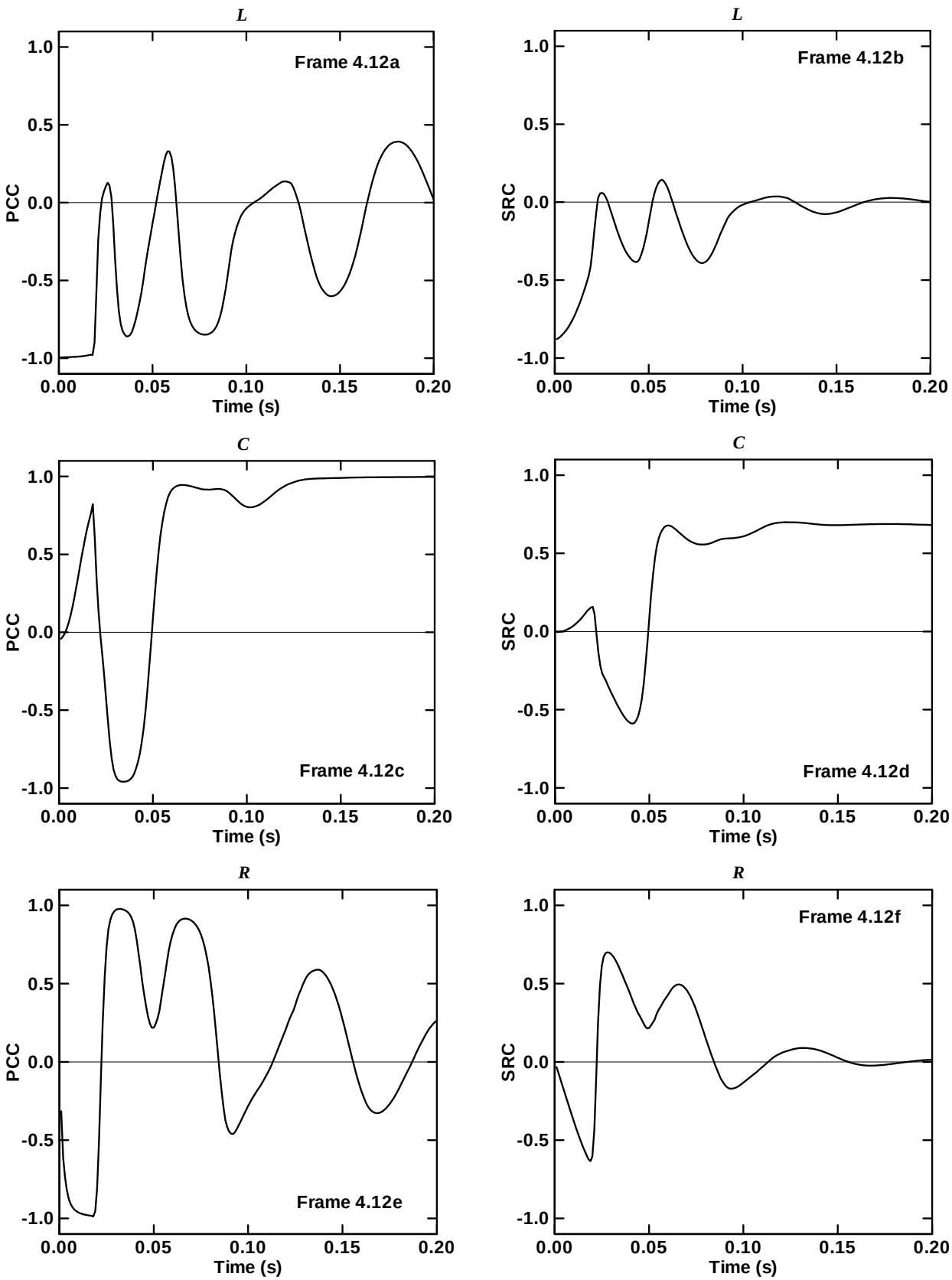
L
Frame 4.12a
PCC
Time (s)
L
Frame 4.12b
SRC
Time (s)
C
Frame 4.12c
PCC
Time (s)
C
Frame 4.12d
SRC
Time (s)
R
Frame 4.12e
PCC
Time (s)
R
Frame 4.12f
SRC
Time (s)
1.0
0.5
0.0
-0.5
-1.0
0.00
0.05
0.10
0.15
0.20

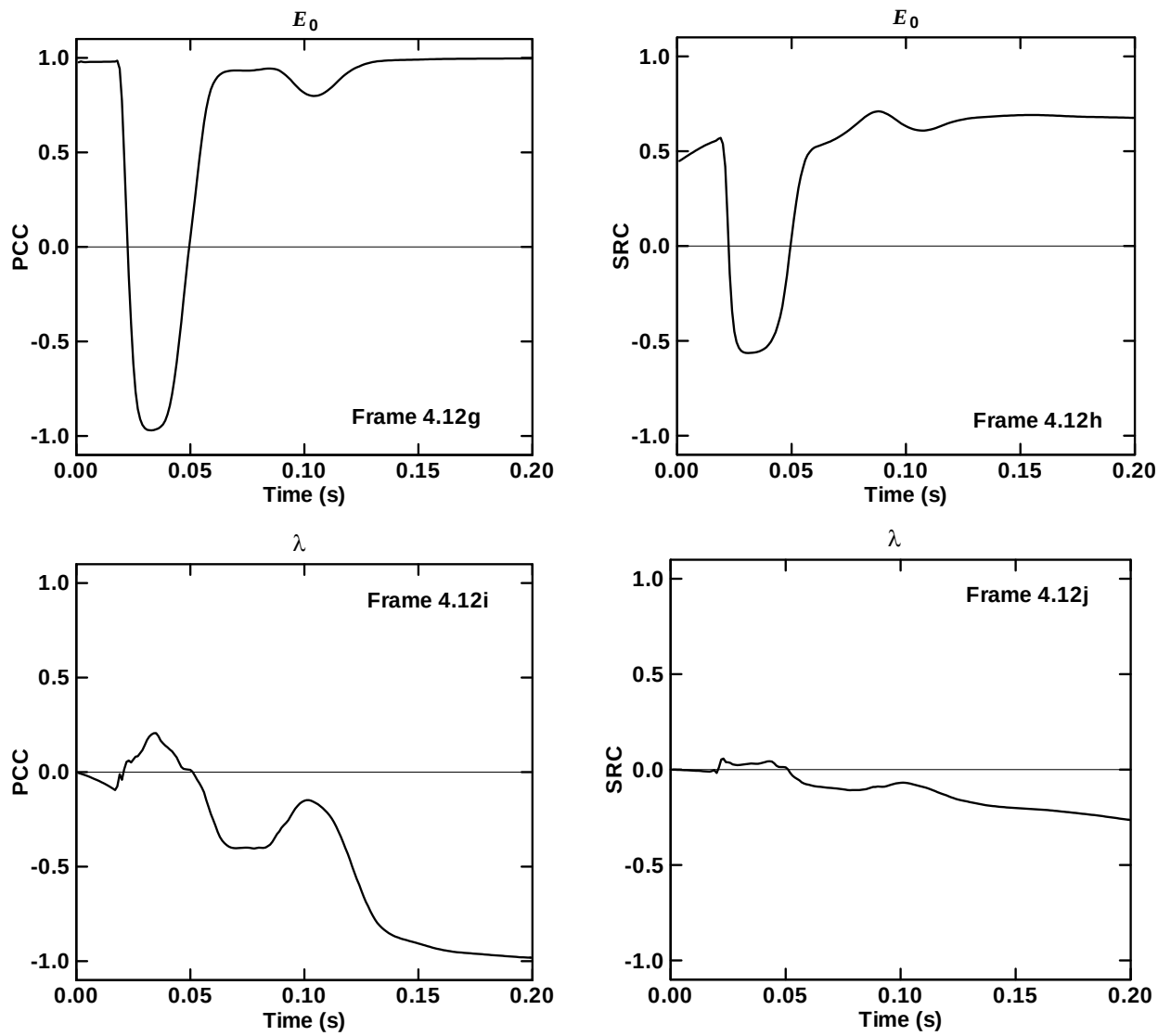

Fig. 4.12. Sensitivity analysis for $Q(t|\mathbf{a}, \mathbf{e}_M)$ for $0 < t < 0.2$ s with PCCs (left column) and SRCs (right column).

Additional insights on the effects of R, E_0, C and L on $Q_m(t|\mathbf{a}, \mathbf{e}_M, [t_{mn}, t_{mx}])$ can be obtained by examining the scatterplots involving these variables and $Q_m(t|\mathbf{a}, \mathbf{e}_M, [t_{mn}, t_{mx}])$ (Fig. 4.13). Specifically, the strong positive effect of R on $Q_m(t|\mathbf{a}, \mathbf{e}_M, [t_{mn}, t_{mx}])$ can be clearly seen, with negative values for $Q_m(t|\mathbf{a}, \mathbf{e}_M, [t_{mn}, t_{mx}])$ occurring for small values for R. Further, the negative but less strong effects of E_0, C and L on $Q_m(t|\mathbf{a}, \mathbf{e}_M, [t_{mn}, t_{mx}])$ can also be seen, with negative values for $Q_m(t|\mathbf{a}, \mathbf{e}_M, [t_{mn}, t_{mx}])$ tending to be associated with large values for E_0, C and L.

Although not particularly high, the final R^2 value of 0.62 in Table 4.3 is significantly better than the almost meaningless final R^2 value of 0.16 in Table 4.2. This difference results because the margins associated with the problem in Sect. 4.3 have relationships with the elements of $\mathbf{e}_M$ that have a monotonic character while the margins in Sect. 4.2 and their relationships with the elements of $\mathbf{e}_M$ do not have this character (i.e., compare the scatterplots in Figs. 4.8 and 4.13).

4.4 Epistemic Uncertainty with an Uncertain Bound

The QMU results presented in Sects. 4.1 – 4.3 involve uniquely specified bounds. However, it is likely that this will not always be the case in QMU analyses. For example, a requirement might be that a certain system operates but the conditions that define when the

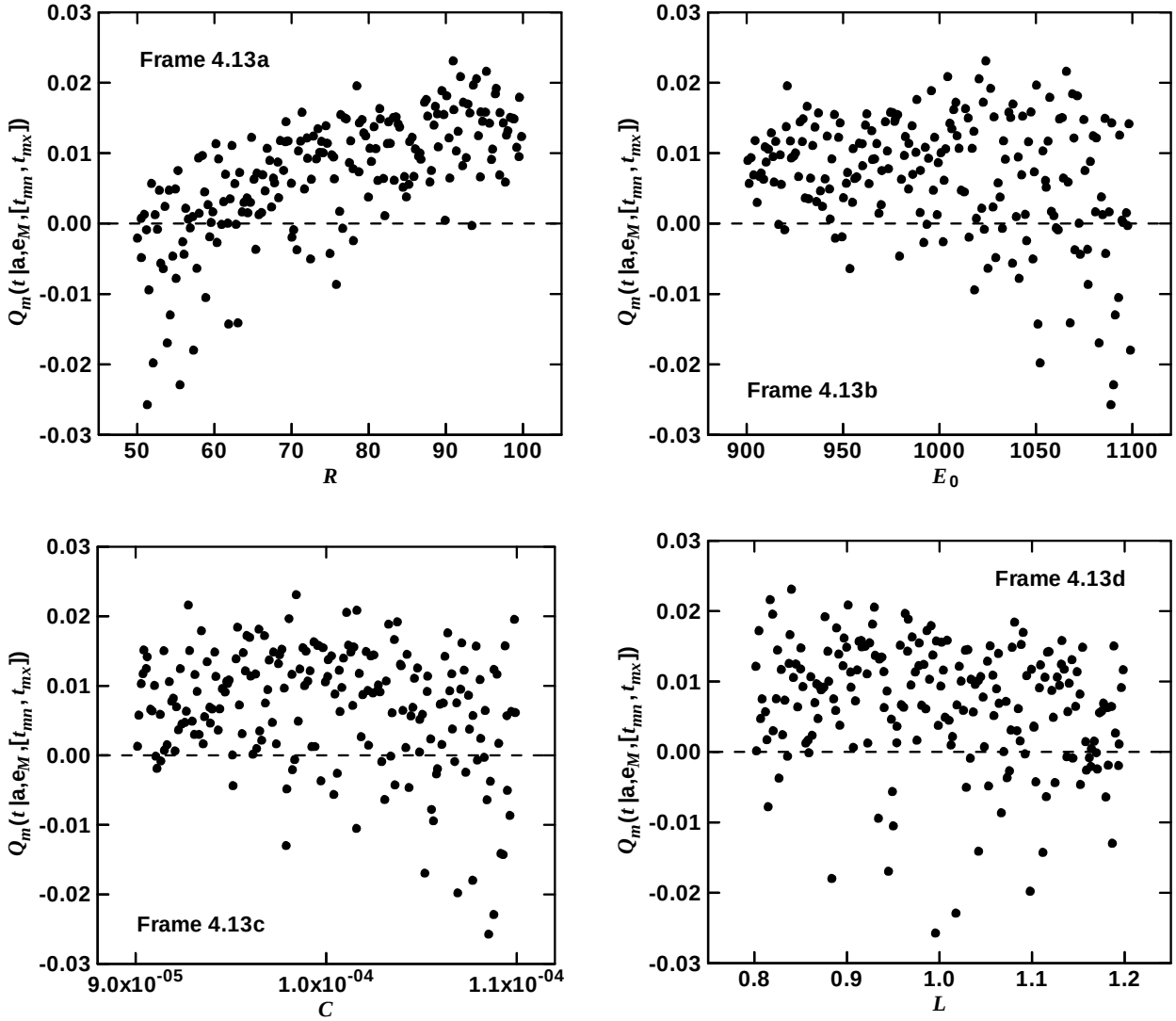

Fig. 4.13. Scatterplots for margin $Q_m(t|\mathbf{a}, \mathbf{e}_M, [t_{mn}, t_{mx}])$ defined in Eq. (4.40): (a) $[R_i, Q_m(t|\mathbf{a}, \mathbf{e}_{Mi}, [t_{mn}, t_{mx}])$, $i = 1,2, \ldots, nSE = 200$, (b) $[E_{0i}, Q_m(t|\mathbf{a}, \mathbf{e}_{Mi}, [t_{mn}, t_{mx}])$, $i = 1,2, \ldots, nSE = 200$, (c) $[C_i, Q_m(t|\mathbf{a}, \mathbf{e}_{Mi}, [t_{mn}, t_{mx}])$, $i = 1,2, \ldots, nSE = 200$, and (d) $[L_i, Q_m(t|\mathbf{a}, \mathbf{e}_{Mi}, [t_{mn}, t_{mx}])$, $i = 1,2, \ldots, nSE = 200$.

system does and does not operate appropriately may not be specified. Then, it is the responsibility of the individuals (i.e., analysts) charged with carrying out the analysis to specify the conditions under which the system operates in the manner desired. However, there may be uncertainty with respect to exactly what conditions are necessary for the appropriate operation of the system. Then, in this situation, there is epistemic uncertainty as to the conditions must be specified to define what constitutes appropriate operation of the system.

The example presented in Sect. 4.3 can be modified to illustrate this situation. As originally stated, the example in Sect. 4.3 involves a bounding interval $[\underline{Q}_b, \overline{Q}_b]$ for $Q(t|\mathbf{a}, \mathbf{e}_M)$ over the time interval $[t_{mn}, t_{mx}]$. For the example of this section, it is assumed that the specified requirement is that the system be operational over the time interval $[t_{mn}, t_{mx}]$ but the requirement does not specify what conditions are necessary for the system to be operational. For purposes of illustration, it is assumed that the analysts involved conclude that the system being operational over $[t_{mn}, t_{mx}]$ corresponds to $Q(t|\ \mathbf{a}, \mathbf{e}_M)$ being within a bounding interval $[\underline{Q}_b, \overline{Q}_b]$. However, they are uncertain with respect to the appropriate value for this bounding interval. Thus, there is epistemic uncertainty with respect to the values to use for $\underline{Q}_b$ and $\overline{Q}_b$. As a result, the vector $\mathbf{e}_M$ of epistemically uncertain inputs to the analysis now has the form

Table 4.3. Stepwise Regression Analysis to Identify Uncertain Variables Affecting Margin $Q_m(t|\mathbf{a}, \mathbf{e}_M, [t_{mn}, t_{mx}])$ Defined in Eq. (4.40)

Step[a]	Variable[b]	SRC[c]	R^{2}[d]
1	R	0.67	0.45
2	E_0	–0.26	0.53
3	C	–0.23	0.58
4	L	–0.20	0.62

[a] Steps in stepwise regression analysis with an α-value of 0.01 or less required for a variable to enter a regression model.
[b] Variables listed in the order of selection in regression analysis.
[c] SRCs for variables in final regression model.
[d] Cumulative R^2 value with entry of each variable into regression model.

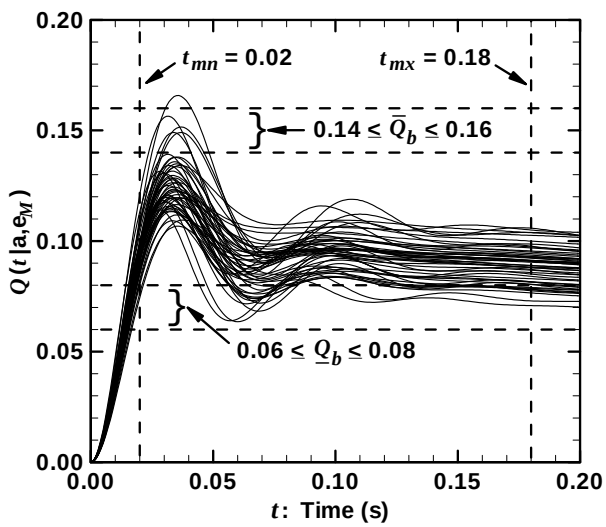

Fig. 4.14. Example uncertain bounding interval $[\underline{Q}_b, \bar{Q}_b]$ with $0.06 \le \underline{Q}_b \le 0.08$ and $0.14 \le \bar{Q}_b \le 0.16$ over the time interval $[t_{mn}, t_{mx}] = [0.02, 0.18$ s$]$ for $Q(t|\mathbf{a}, \mathbf{e}_M)$.

$$\mathbf{e}_M = [\mathbf{e}_R, \mathbf{e}_P] = \left[\underline{Q}_b, \bar{Q}_b, L, R, C, E_0, \lambda\right], \tag{4.44}$$

where $\mathbf{e}_R = [\underline{Q}_b, \bar{Q}_b]$ and $\mathrm{e}_P = [L, R, C, E_0, \lambda]$ as indicated in Eq. (3.21).

For purposes of illustration, it is assumed that the analysts conclude that (i) $\underline{Q}_b$ is contained in the interval [0.06, 0.08], (ii) $\bar{Q}_b$ is contained in the interval [0.14, 0.16], (iii) $\underline{Q}_b$ and $\bar{Q}_b$ have the same uncertainty structure specified for L, R_0, C, E and λ (see Eqs. (3.38) – (3.43) and associated discussion), and (iv) no dependency or correlation exists between $\underline{Q}_b$ and $\bar{Q}_b$ (Fig. 4.14).

This problem can now be analyzed exactly as in Sect. 4.3. The only difference is that $\mathbf{e}_M$ now contains 7 rather than 5 elements, with two of these elements being $\underline{Q}_b$ and $\bar{Q}_b$. Specifically, $\delta[Q(t|\mathbf{a}, \mathbf{e}_M): t_{mn} \le t \le t_{mx}]$, $\mathcal{X}^+$ and $\mathcal{X}^-$ are defined as indicated in Eqs. (4.35) –(4.37) with the understanding that the indicator function $\delta[\sim]$ is now a function of $\underline{Q}_b$ and $\bar{Q}_b$. Given the dependency of $\delta[\sim]$ on $\underline{Q}_b$ and $\bar{Q}_b$, a more complete but rather cumbersome notation for $\delta[\sim]$ is $\delta[\sim,(\underline{Q}_b, \bar{Q}_b)]$, which will be used below to make the dependence of $\delta[\sim]$ on $\underline{Q}_b$ and $\bar{Q}_b$ explicit. In turn, the probabilities of compliance and noncompliance are given by

$$\begin{aligned} p_{EM}\left(\mathcal{X}^+\right) &\cong \sum_{i=1}^{nSE} \frac{\delta\left[Q\left(t|a, \mathbf{e}_{Mi}\right): t_{mn} \le t \le t_{mx}, \left(\underline{Q}_{bi}, \bar{Q}_{bi}\right)\right]}{nSE} \\ &= 0.895 \end{aligned} \tag{4.45}$$

and

$$p_{EM}\left(\mathcal{X}^-\right) \cong 1 - p_{EM}\left(\mathcal{X}^+\right) = 1 - 0.895 = 0.105, \tag{4.46}$$

respectively, where

$$\mathbf{e}_{Mi} = \left[\underline{Q}_{bi}, \bar{Q}_{bi}, L_i, R_i, C_i, E_{0i}, \lambda_i\right], i = 1, 2, \ldots, nSE,$$

is now an LHS of size nSE = 200 from vectors of the form defined in Eq. (4.44).

Margin analysis results $Q_m(t|\mathbf{a}, \mathbf{e}_M, [t_{mn}, t_{mx}])$ and normalized margin analysis results $Q_n(t|\ \mathbf{a}, \mathbf{e}_M, [t_{mn}, t_{mx}])$ of the form defined in Eqs. (4.40) and (4.41), respectively, can also be obtained (Figs. 4.15 4.16).

Similarly to the results in Eqs. (4.42) and (4.43), "margin/uncertainty" ratios $Q_{m/u}(t|\mathbf{a}, \mathbf{e}_M, [t_{mn}, t_{mx}])$ and $\bar{Q}_{m/u}(t|\mathbf{a}, \mathbf{e}_M, [t_{mn}, t_{mx}])$ can be used to summarize the distribution for $Q_m(t|\mathbf{a}, \mathbf{e}_M, [t_{mn}, t_{mx}])$ in Fig. 4.15. Specifically,

$$\begin{aligned} &Q_{m/u}\left(t|\mathbf{a}, \mathbf{e}_M, \left[t_{mn}, t_{mx}\right]\right) \\ &= \begin{cases} 0.011 \big/ \left[0.011 - (-0.005)\right] = 0.69 \text{ for } q = 0.05 \\ 0.011 \big/ \left[0.011 - (-0.021)\right] = 0.34 \text{ for } q = 0.00, \end{cases} \end{aligned} \tag{4.47}$$

and similar values are obtained for $\bar{Q}_{m/u}(t|\mathbf{a}, \mathbf{e}_M, [t_{mn}, t_{mx}])$ as a consequence of the similarity of the mean and median values for $Q(t|\mathbf{a}, \mathbf{e}_M, [t_{mn}, t_{mx}])$ (see Fig. 4.15). However, as is always the case, a significant amount of information is lost when the results in Figs. 4.14 and 4.15

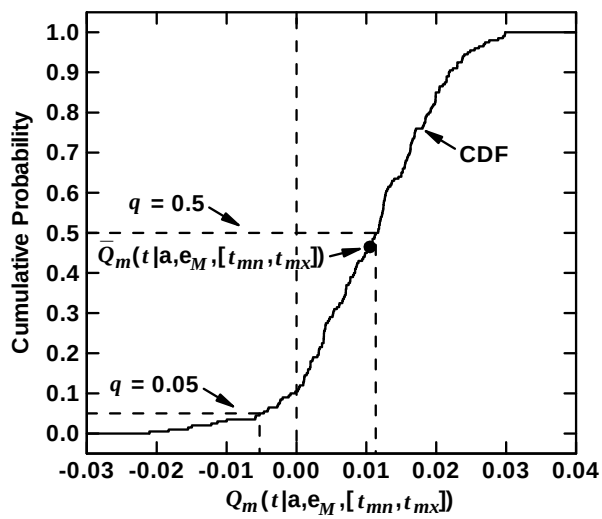

Fig. 4.15. Estimated CDF summarizing uncertainty in margin $Q_m(t|\mathbf{a}, \mathbf{e}_M, [t_{mn}, t_{mx}])$ defined in Eq. (4.40) for time interval $[t_{mn}, t_{mx}]$ = [0.02, 0.18 s] and uncertain bounding interval $[\underline{Q}_b, \bar{Q}_b]$ with $0.06 \le \underline{Q}_b \le 0.08$ and $0.14 \le \bar{Q}_b \le 0.16$.

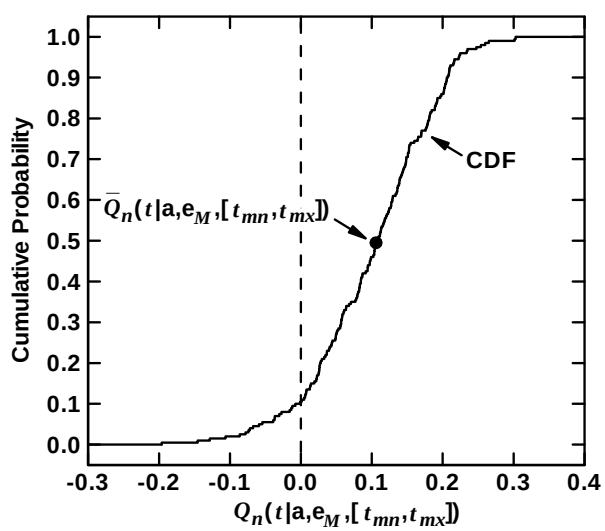

Fig. 4.16. Estimated CDF summarizing uncertainty in normalized margin $Q_n(t|\mathbf{a}, \mathbf{e}_M, [t_{mn}, t_{mx}])$ defined in Eq. (4.41) for time interval $[t_{mn}, t_{mx}]$ = [0.02, 0.18 s] and uncertain bounding interval $[\underline{Q}_b, \bar{Q}_b]$ with $0.06 \le \underline{Q}_b \le 0.08$ and $0.14 \le \bar{Q}_b \le 0.16$.

are reduced to a single number (see Sect. 4.5 for additional discussion).

A sensitivity analysis for $Q_m(t|\mathbf{a}, \mathbf{e}_M, [t_{mn}, t_{mx}])$ based on stepwise regression analysis is presented in Table 4.4. The two most important variables affecting the uncertainty in $Q_m(t|\mathbf{a}, \mathbf{e}_M, [t_{mn}, t_{mx}])$ are R and $\underline{Q}_b$, with $Q_m(t|\mathbf{a}, \mathbf{e}_M, [t_{mn}, t_{mx}])$ tending to increase as R increases and tending to decrease as $\underline{Q}_b$ increases. In addition, a negative effect is indicated for L and positive effects are indicated for $\bar{Q}_b$ and E_0.

Table 4.4. Stepwise Regression Analysis to Identify Uncertain Variables Affecting Margin $Q_m(t|\mathbf{a}, \mathbf{e}_M, [t_{mn}, t_{mx}])$ Defined in Eq. (4.40) for Time Interval $[t_{mn}, t_{mx}]$ = [0.02, 0.18 s] and Uncertain Bounding Interval $[\underline{Q}_b, \bar{Q}_b]$ with $0.06 \le \underline{Q}_b \le 0.08$ and $0.14 \le \bar{Q}_b \le 0.16$.

Step[a]	Variable[b]	SRC[c]	R^{2d}
1	R	0.53	0.28
2	$\underline{Q}_b$	–0.40	0.43
3	L	–0.32	0.54
4	$\bar{Q}_b$	0.23	0.59
5	E_0	0.13	0.61

[a] Steps in stepwise regression analysis with an α-value of 0.01 or less required for a variable to enter a regression model.
[b] Variables listed in the order of selection in regression analysis.
[c] SRCs for variables in final regression model.
[d] Cumulative R^2 value with entry of each variable into regression model.

The effects of R, $\underline{Q}_b$ and $\bar{Q}_b$ on $Q_m(t|\mathbf{a}, \mathbf{e}_M, [t_{mn}, t_{mx}])$ can be seen in the scatterplots in Fig. 4.17. In particular, negative values for $Q_m(t|\mathbf{a}, \mathbf{e}_M, [t_{mn}, t_{mx}])$ tend to be associated with small values for R that occur in conjunction with a large value for $\underline{Q}_b$ and a small value for $\bar{Q}_b$.

4.5 Information Loss in a "Margin/ Uncertainty" Ratio

As already emphasized several times, results of the form "margin/uncertainty" involve a significant loss of information. This loss is particularly acute because the actual magnitudes of the margins involved in the determination of "margin/uncertainty" are suppressed and cannot be determined from this ratio. Specifically, many different pairings of "margin" and "uncertainty" can result in the same "margin/uncertainty" ratio. In particular, it is impossible to determine from a "margin/uncertainty" ratio whether the underlying margins are large or small. Generally, large margins are preferable to small margins but insights into whether the margins underlying a "margin/uncertainty" ratio are large or small are not directly obtainable from this ratio.

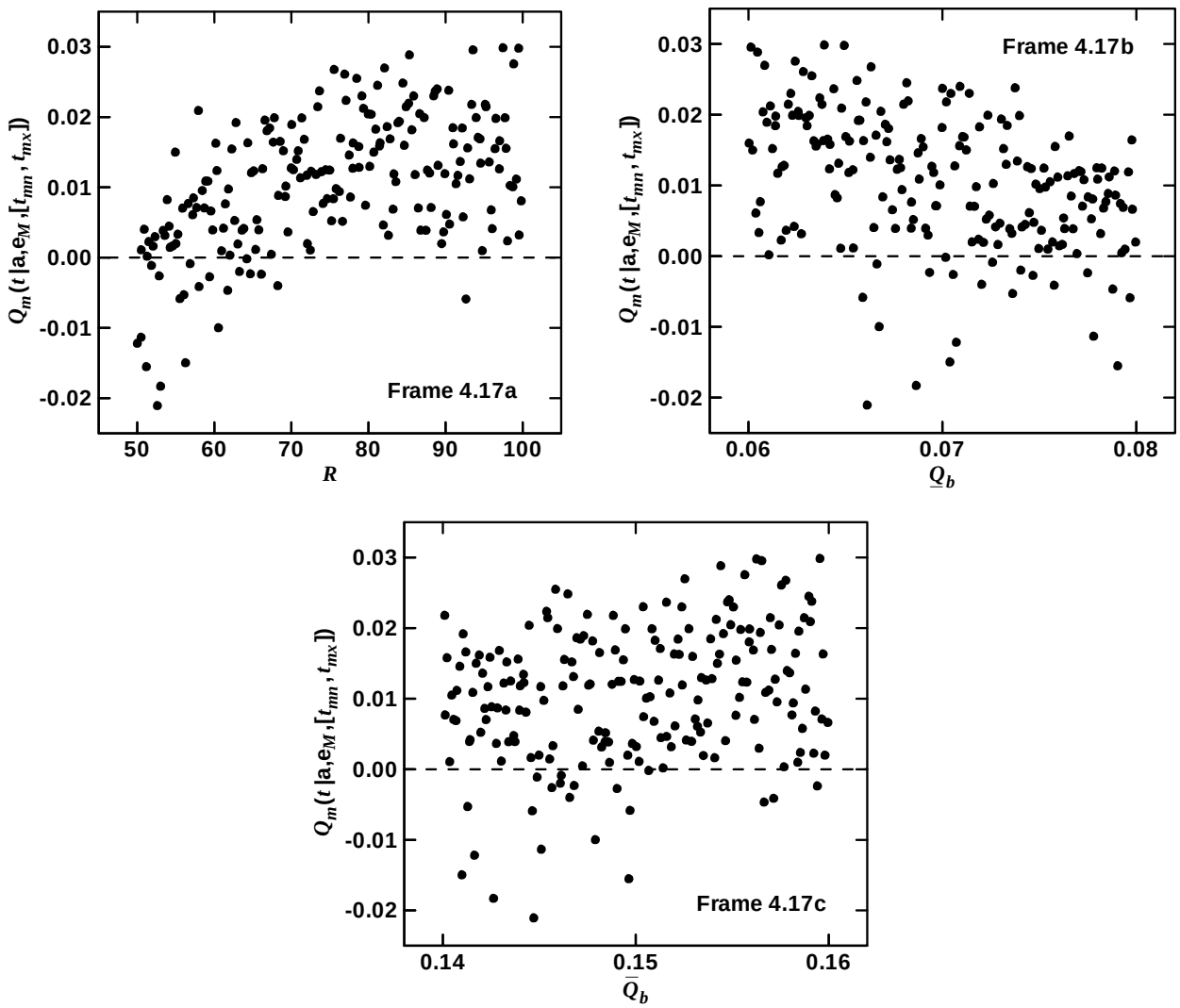

Fig. 4.17. Scatterplots for margin $Q_m(t|\mathbf{a}, \mathbf{e}_M, [t_{mn}, t_{mx}])$ defined in Eq. (4.40) for time interval $[t_{mn}, t_{mx}] = [0.02, 0.18$ s] and uncertain bounding interval $[\underline{Q}_b, \overline{Q}_b]$ with $0.06 \le \underline{Q}_b \le 0.08$ and $0.14 \le \overline{Q}_b \le 0.16$: (a) $[R_i, Q_m(t|\mathbf{a}, \mathbf{e}_{Mi}, [t_{mn}, t_{mx}])$, $i = 1,2, \ldots, nSE = 200$, (b) $[\underline{Q}_{bi}, Q_m(t|\mathbf{a}, \mathbf{e}_{Mi}, [t_{mn}, t_{mx}])$, $i = 1,2, \ldots, nSE = 200$, and (c) $[\overline{Q}_{bi}, Q_m(t|\mathbf{a}, \mathbf{e}_{Mi}, [t_{mn}, t_{mx}])$, $i = 1,2, \ldots, nSE = 200$.

The ambiguity of a "margin/uncertainty" ratio can be illustrated with a simple plot involving the ratio

$$k = m_b / \left(m_b - m_l\right), \tag{4.48}$$

where m_b is the best estimate for a margin (e.g., the mean or median of the epistemic uncertainty distribution for the margin under consideration), m_l is the lower estimate for a margin (e.g., the 0.05 or 0.00 quantile of the epistemic uncertainty distribution for the margin under consideration), and the difference $m_b - m_l$ defines the "uncertainty" in the margin under consideration. Then, as shown in Fig. 4.18, infinitely many pairs (m_b, m_l) of margin estimates result in the same "margin/uncertainty" ratio k. Specifically, each line segment in Fig. 4.18 defines pairs (m_b, m_l) of margin estimates that result in the same "margin/uncertainty" ratio k. As a consequence, knowledge of the "margin/uncertainty" ratio k provides no information on whether the underlying margins involved in the definition of k are large or small.

Some additional properties of the "margin/uncertainty" ratio k are also illustrated by Fig. 4.18. Specifically, (i) $1 \le k < \infty$ results for $0 \le m_l < m_b$ with k approaching ∞ as m_l approaches m_b and k approaching 1

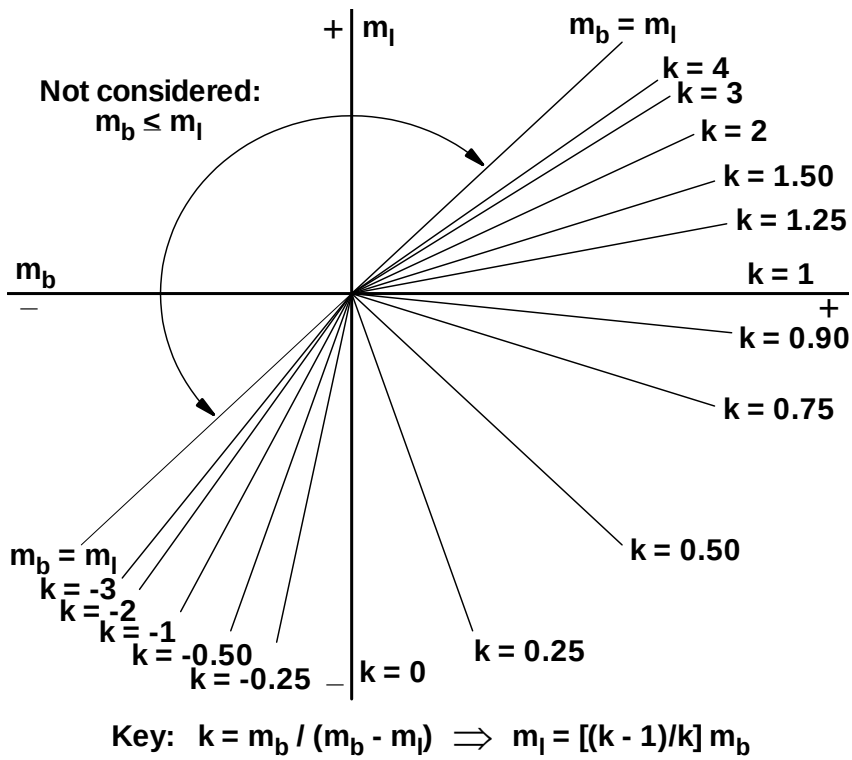

Fig. 4.18. Relationship of best estimate margin m_b and lower estimate margin m_l to "margin/uncertainty" ratio k defined by $k = m_b/(m_b - m_l)$.

as m_l approaches 0, (ii) $0 < k < 1$ results for $m_l < 0 < m_b$ with k approaching 1 as m_l approaches 0 and k approaching 0 as m_l approaches $-\infty$, and (iii) $-\infty < k < 0$ results for $m_l < m_b < 0$ with k approaching 0 as m_l approaches $-\infty$ and k approaching $-\infty$ as m_l approaches m_b. However, as already discussed, knowledge of k provides no information on the underlying margins m_b and m_l. Presumably, the half plane to the left of the line $m_b = m_l$ in Fig. 4.18 is not of interest as the pairs (m_b, m_l) in this region correspond to the best estimate margin m_b being less than the lower margin estimate m_l. Also, the "margin/uncertainty" ratio k is not defined for points on the straight line $m_b = m_l$ as this situation involves an undefined division by $m_b - m_l = 0$.

Significant reservations about the use of "uncertainty/margin" ratios are also expressed in the NAS/NRC report on QMU (e.g., Finding 1-4, p. 25, Ref. [77]).

This page intentionally left blank

5 QMU with Aleatory and Epistemic Uncertainty: Characterization with Probability

The use of probability to represent epistemic uncertainty in analyses that involve only epistemic uncertainty is discussed and illustrated in Sects. 3.3, 3.4 and 4. Specifically, the formal discussion in Sect. 3.3 involves a generic real-valued quantity

$$y\left(t|\mathbf{a}, \mathbf{e}_M\right) = f\left(t|\mathbf{a}, \mathbf{e}_M\right) \tag{5.1}$$

conditional on a specific realization $\mathbf{a}$ of aleatory uncertainty. The vector $\mathbf{e}_M$ contains epistemically uncertain analysis inputs, with the uncertainty in these inputs characterized by a probability space ($\mathcal{EM}$, $\mathbb{EM}$, p_{EM}).

As discussed in Sect. 3.5, an increase in complexity is to include the aleatory uncertainty associated with $\mathbf{a}$ in the analysis. Then, in addition to the probability space ($\mathcal{EM}$, $\mathbb{EM}$, p_{EM}) that characterizes the epistemic uncertainty associated with $\mathbf{e}_M$, there is also a probability space ($\mathcal{A}$, $\mathbb{A}$, p_A) that characterizes the aleatory uncertainty associated with $\mathbf{a}$. Further, there can be, and often is, epistemic uncertainty with respect to a vector $\mathbf{e}_A$ of quantities used in the definition of the probability space ($\mathcal{A}$, $\mathbb{A}$, p_A). As a result, there is also a probability space ($\mathcal{EA}$, $\mathbb{EA}$, p_{EA}) that characterizes the epistemic uncertainty associated with $\mathbf{e}_A$. The vector $\mathbf{e} = [\mathbf{e}_A, \mathbf{e}_M]$ then contains the epistemically uncertain inputs to the analysis, with the uncertainty in $\mathbf{e}$ characterized by a probability space ($\mathcal{E}$, $\mathbb{E}$, p_E) that derives from the probability spaces ($\mathcal{EA}$, $\mathbb{EA}$, p_{EA}) and ($\mathcal{EM}$, $\mathbb{EM}$, p_{EM}). Conceptually, the resultant analysis involves the three basic analysis components discussed in Sect. 3.2: (i) (EN1), a probabilistic characterization of aleatory uncertainty (i.e., a probability space ($\mathcal{A}$, $\mathbb{A}$, p_A) that characterizes the aleatory uncertainty associated with the elements of $\mathbf{a}$), (ii) (EN2), a model that predicts system behavior (i.e., a function $f(t|\mathbf{a}, \mathbf{e}_M)$), and (iii) (EN3), a probabilistic characterization of epistemic uncertainty (i.e., a probability space ($\mathcal{E}$, $\mathbb{E}$, p_E) that characterizes the epistemic uncertainty associated with the elements of $\mathbf{e} = [\mathbf{e}_A, \mathbf{e}_M]$).

The results of analyses involving aleatory and epistemic uncertainty are usually summarized with CDFs and CCDFs that display the effects of aleatory uncertainty conditional on specific realizations of epistemic uncertainty and also with various quantities derived from such CDFs and CCDFs (e.g., quantiles and expected values). In turn, margins can be defined in a variety of ways for CDFs, CCDFs and associated derived quantities, and the presence of epistemic uncertainty results in a corresponding epistemic uncertainty in the resulting margins.

This section uses the function $A(t|\mathbf{a}, \mathbf{e}_M)$ introduced in Sect. 3.6 to illustrate two ways in which QMU analyses could arise and be carried out in the context of analyses that involve a generic result $y(t|\mathbf{a}, \mathbf{e}_M)$ of the form indicated in Eqs. (3.24) and (5.1). Further,

$$\begin{aligned}\mathbf{e} &= \left[\mathbf{e}_A, \mathbf{e}_M\right] \\ &= \left[e_1, e_2, e_3, e_4, e_5\right] \\ &= \left[\lambda, a, m, b, r\right],\end{aligned} \tag{5.2}$$

where (i) $\mathbf{e}_A = [\lambda, a, m, b]$ and $\mathbf{e}_M = [r]$ have the properties defined in conjunction with Eq. (3.59) and (ii) the corresponding probability space ($\mathcal{E}$, $\mathbb{E}$, p_E) that characterizes the epistemic uncertainty associated with $\mathbf{e}$ is defined in conjunction with Eqs. (3.60) – (3.65).

The time-dependent behavior of $A(t|\mathbf{a}, \mathbf{e}_M) = A(t|\mathbf{a}, r)$ is illustrated in Figs. 3.9 and 3.10, and the CDFs and CCDFs for $A(10|\mathbf{a}, \mathbf{e}_M) = A(10|\mathbf{a}, r)$ that result for different values of $\mathbf{e}$ are illustrated in Figs. 3.11 and 3.12 and are defined by the probabilities $p_A[A(10|\mathbf{a}, r) \le A\ |\mathbf{e}_A]$ and $p_A[A < A(10|\mathbf{a}, r)|\mathbf{e}_A]$, respectively. As indicated by the vertical line " | ", the value of $A(t|\mathbf{a}, r)$ is conditional on $\mathbf{a}$ and r. As a result, $\mathbf{e}_A$ does not affect the value of $A(t|\mathbf{a}, r)$ but does affect the distribution of $A(t|\mathbf{a}, r)$ arising from the distribution of possible values for $\mathbf{a}$. In contrast, probabilities of the form $p_A[A(t|\mathbf{a}, r) \le A\ |\mathbf{e}_A]$ and $p_A[A < A(t|\mathbf{a}, r)|\mathbf{e}_A]$ are conditional on $\mathbf{e}_A$ and hence on the probability space ($\mathcal{A}$, $\mathbb{A}$, p_A) with associated density function $d_A(\mathbf{a}|\mathbf{e}_A)$.

The examples presented in this section use an LHS

$$\begin{aligned}\mathbf{e}_i &= \left[\mathbf{e}_{Ai}, \mathbf{e}_{Mi}\right] \\ &= \left[e_{i1}, e_{i2}, \ldots, e_{i5}\right] \\ &= \left[\lambda_i, a_i, m_i, b_i, r_i\right],\ i = 1, 2, \ldots, nSE = 200,\end{aligned} \tag{5.3}$$

from $\mathcal{E}$ generated in consistency with the distributions that define the probability space ($\mathcal{E}$, $\mathbb{E}$, p_E). Further, results conditional on individual sample elements $\mathbf{e}_i$ are generated with a random sample

$$\mathbf{a}_j,\ j = 1, 2, \ldots, nSA, = 10{,}000, \tag{5.4}$$

from $\mathcal{A}$ consistent with the probability space ($\mathcal{A}$, $\mathbb{A}$, p_A). As a result of the values associated with $\mathbf{e}_{Ai} = [\lambda_i, a_i, m_i, b_i]$, the sample space ($\mathcal{A}$, $\mathbb{A}$, p_A) underlying the generation of the sample in Eq. (5.4) changes for each

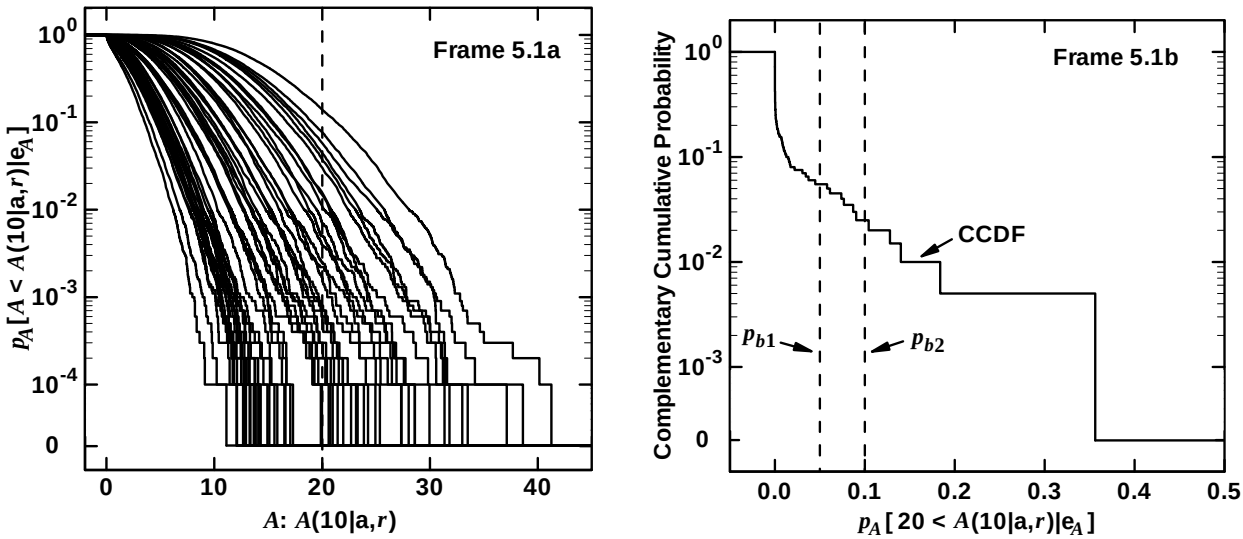

Fig. 5.1. Summary results for $A(10|\mathbf{a}, r)$: (a) CCDFs for $A(10|\mathbf{a}, r)$ obtained with the first 50 elements of the LHS in Eq. (5.3) shown with a vertical line indicating exceedance probabilities $p_A[20 < A(10|\mathbf{a}, r)|\mathbf{e}_A]$, and (b) Estimated CCDF for $p_A[20 < A(10|\mathbf{a}, r)|\mathbf{e}_A]$.

sample element $\mathbf{e}_i = [\mathbf{e}_{Ai}, \mathbf{e}_{Mi}] = [\mathbf{e}_{Ai}, r_i]$. Evaluation of $A(t|\mathbf{a}_j, r_i)$ and results such as $p_A[A < A(t|\mathbf{a}, r_i)|\mathbf{e}_A]$ for elements of the preceding samples generates mappings of the form

$$\left[r_i, A\left(t|\mathbf{a}_j, r_i\right)\right], \quad i = 1, 2, \ldots, nSE = 200,\ j = 1, 2, \ldots, nSA = 10{,}000 \tag{5.5}$$

and

$$\left\{\mathbf{e}_i, p_A\left[A < A\left(t|\mathbf{a}, r_i\right)\middle|\mathbf{e}_{Ai}\right]\right\}, \quad i = 1, 2, \ldots, nSE = 200, \tag{5.6}$$

that are used in the generation of the example results presented in this section.

The following topics related to QMU in the presence of aleatory and epistemic uncertainty are considered in this section: epistemic uncertainty in margins associated with a specified bound on a quantile deriving from aleatory uncertainty (Sect. 5.1), and epistemic uncertainty in margins associated with a specified bound on an expected value deriving from aleatory uncertainty (Sect. 5.2).

As indicated at the beginning of Sect. 3.5, the NAS/NRC report on QMU recommends the use of what it describes as the "probability of frequency approach" in QMU analyses (Recommendation 1-7, p. 33, and App. A, Ref. [77]). The examples presented in Sects. 5.1 and 5.2 involve what the NAS/NRC report describes as the "probability of frequency approach" (i.e., an analysis that involves an explicit separation of aleatory and epistemic uncertainty).

5.1 Epistemic Uncertainty with a Specified Bound on a Quantile

For this example, it is assumed that $p_A[20 < A(10|\mathbf{a}, r)|\mathbf{e}_A]$ is required to be less than a bound (e.g., the possible bounds $p_{b1} = 0.05$ and $p_{b2} = 0.1$ in Fig. 5.1b). Specifically, the values for $p_A[20 < A(10|\mathbf{a}, r)|\mathbf{e}_A]$ in Fig. 5.1b correspond to the exceedance probabilities associated with the vertical line in Fig. 5.1a, and the corresponding distribution of these probabilities and the associated bounds p_{b1} and p_{b2} are shown in Fig. 5.1b. In particular, the probabilities that $p_A[20 < A(10|\mathbf{a}, r)|\mathbf{e}_A]$ will exceed $p_{b1} = 0.05$ and $p_{b2} = 0.1$ are 0.055 and 0.025, respectively. The indicated exceedance probabilities of 0.055 and 0.025 derive from epistemic uncertainty and thus characterize degrees of belief that $p_A[20 < A(10|\mathbf{a}, r)|\mathbf{e}_A]$ will exceed p_{b1} and p_{b2}, respectively.

In turn, the margins between $p_A[20 < A(10|\mathbf{a}, r)|\mathbf{e}_A]$ and the bounds p_{bk}, $k = 1, 2$, indicated in Fig. 5.1b can be defined in the same manner as the margins in Eq. (4.5). Specifically, the margin $p_{mk}(10|\mathbf{e})$ is defined by

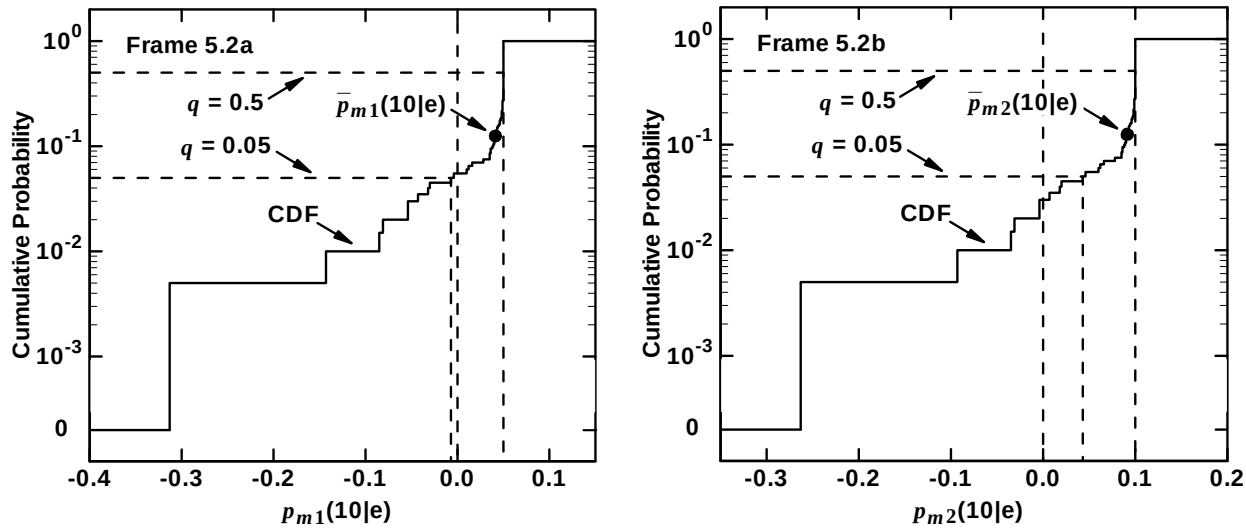

Fig. 5.2. Estimated CDFs for margins $p_{mk}(10|\mathbf{e})$ associated with bounds p_{bk} for k = 1, 2: (a) $p_{m1}(10|\mathbf{e})$ for p_{b1} = 0.05, and (b) $p_{m2}(10|\mathbf{e})$ for p_{b2} = 0.1.

$$p_{mk}\left(10\middle|\mathbf{e}\right) = p_{bk} - p_A\left[20 < A\left(10\middle|\mathbf{a}, r\right)\middle|\mathbf{e}_A\right], \tag{5.7}$$

with $p_{mk}(10|\mathbf{e}) > 0$ indicating that bound p_{bk} is satisfied and $p_{mk}(10|\mathbf{e}) < 0$ indicating that bound p_{bk} is not satisfied. As a result of $p_A[20 < A(10|\mathbf{a}, r)|\mathbf{e}_A]$ being epistemically uncertain, the corresponding margins $p_{mk}(10|\mathbf{e})$ are also epistemically uncertain and have an uncertainty structure that derives from the corresponding uncertainty structure assumed for $\mathbf{e}$ (Fig. 5.2).

As discussed in conjunction with Eq. (4.6), an alternative presentation involves the use of normalized margins. For the present example, normalized margins are defined by

$$p_{nk}\left(10\middle|\mathbf{e}\right) = p_{mk}\left(10\middle|\mathbf{e}\right)\Big/ p_{bk} \tag{5.8}$$

for k = 1, 2 and express margin as a fraction of the corresponding bounding value (Fig. 5.3).

If desired, the CDFs for margin in Fig. 5.2 can be converted into summary "margin/uncertainty" results as indicated in Eqs. (4.7) and (4.8) by the normalizations

$$p_{m/u}(10) = p_{m,0.5}(10)\Big/\left[p_{m,0.5}(10) - p_{mq}(10)\right] \tag{5.9}$$

and

$$\bar{p}_{m/u}(10) = \bar{p}_m(10)\Big/\left[\bar{p}_m(10) - p_{mq}(10)\right], \tag{5.10}$$

where $p_{mq}(10)$ is the q quantile (e.g., q = 0.0, 0.05 or 0.5) for the margin $p_m(10|\mathbf{e})$ corresponding to $p_{m1}(10|\mathbf{e})$ in Fig. 5.2a or $p_{m2}(10|\mathbf{e})$ in Fig. 5.2b and $\bar{p}_m(10)$ is the expected value for $p_m(10|\mathbf{e})$. In turn,

$$p_{m/u,1}(10) = \begin{cases} 0.050\big/\left[0.050-(-0.007)\right] = 0.88 \text{ for } q = 0.05 \\ 0.050\big/\left[0.050-(-0.313)\right] = 0.14 \text{ for } q = 0.00 \end{cases} \tag{5.11}$$

and

$$\bar{p}_{m/u,1}(10) = \begin{cases} 0.041\big/\left[0.041-(-0.007)\right] = 0.85 \text{ for } q = 0.05 \\ 0.041\big/\left[0.041-(-0.313)\right] = 0.12 \text{ for } q = 0.00 \end{cases} \tag{5.12}$$

for $p_{m1}(10|\mathbf{e})$ in Fig. 5.2a , and

$$p_{m/u,2}(10) = \begin{cases} 0.100/(0.100-0.043) = 1.75 \text{ for } q = 0.05 \\ 0.100\big/\left[0.100-(-0.263)\right] = 0.28 \text{ for } q = 0.00 \end{cases} \tag{5.13}$$

and

$$\bar{p}_{m/u,2}(10) = \begin{cases} 0.091/(0.091-0.043) = 1.90 \text{ for } q = 0.05 \\ 0.091\big/\left[0.091-(-0.263)\right] = 0.26 \text{ for } q = 0.00 \end{cases} \tag{5.14}$$

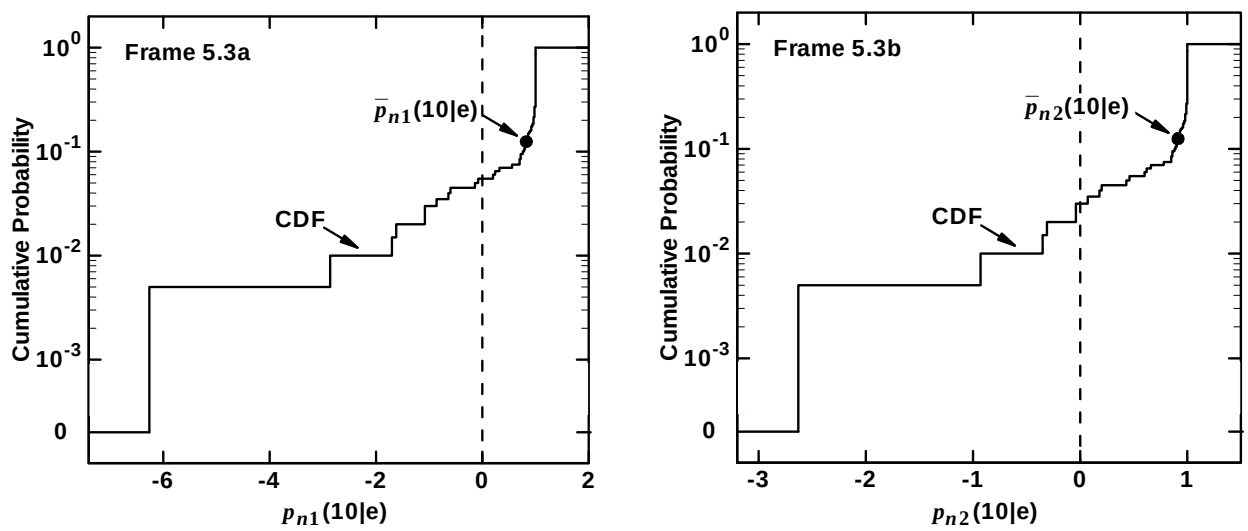

Fig. 5.3. Estimated CDFs for normalized margins $p_{nk}(10|\mathbf{e})$ associated with bounds p_{bk} for k = 1, 2: (a) $p_{n1}(10|\mathbf{e})$ for p_{b1} = 0.05, and (b) $p_{n2}(10|\mathbf{e})$ for p_{b2} = 0.1

for $p_{m1}(10|\mathbf{e})$ in Fig. 5.2b. The normalizations in Eqs. (5.11) and (5.12) are the outcomes of converting all the information in Figs. 5.1 and 5.2a into single numbers. Similarly, the normalizations in Eqs. (5.13) and (5.14)are the outcomes of converting all the information in Figs. 5.1 and 5.2b into single numbers. Because of the presence of both aleatory and epistemic uncertainty, the conversion of analysis results into a single "margin/uncertainty" ratios illustrated in this section involves a greater loss of information than is the case when only epistemic uncertainty is present (see Sect. 4.5 for additional discussion).

Additional insights with respect to the uncertainty associated with the margins $p_{m1}(10|\mathbf{e})$ and $p_{m2}(10|\mathbf{e})$ in Fig. 5.2 can be obtained by performing a sensitivity analysis on the values for $p_A[20 < A(10|\mathbf{a}, r)|\mathbf{e}_A]$ summarized in Fig. 5.1 and used in the generation of $p_{m1}(10|\mathbf{e})$ and $p_{m2}(10|\mathbf{e})$ as indicated in Eq. (5.7). Because $p_{m1}(10|\mathbf{e})$ and $p_{m2}(10|\mathbf{e})$ are obtained from an affine transformation of $p_A[20 < A(10|\mathbf{a}, r)|\mathbf{e}_A]$, the analysis of $p_A[20 < A(10|\mathbf{a}, r)|\mathbf{e}_A]$ produces effectively the same results as an analysis of $p_{m1}(10|\mathbf{e})$ and $p_{m2}(10|\mathbf{e})$. The only difference is that the effects of individual variables are reversed owing to the subtraction of $p_A[20 < A(10|\mathbf{a}, r)|\mathbf{e}_A]$ in the definition of $p_{m1}(10|\mathbf{e})$ and $p_{m2}(10|\mathbf{e})$ in Eq. (5.7).

An initial sensitivity analysis for $p_A[20 < A(10|\mathbf{a}, r)|\mathbf{e}_A]$ based on stepwise regression analysis is presented in Table 5.1. This analysis is basically a failure as it produces a regression model containing the variables r and λ that has an R^2 value of only 0.19. As a result, this regression model provides little information on the variables that are affecting the uncertainty in $p_A[20 < A(10|\mathbf{a}, r)|\mathbf{e}_A]$.

The natural next step at this point is to examine scatterplots involving $p_A[20 < A(10|\mathbf{a}, r)|\mathbf{e}_A]$ and the elements of $\mathbf{e}$ (Fig. 5.4). A clearer picture of the effects of r and λ on $p_A[20 < A(10|\mathbf{a}, r)|\mathbf{e}_A]$ emerges from an examination of these plots. Specifically, $p_A[20 < A(10|\mathbf{a}, r)|\mathbf{e}_A]$ decreases as r increases and is almost always zero when r exceeds approximately 0.75. Further, zero values for $p_A[20 < A(10|\mathbf{a}, r)|\mathbf{e}_A]$ show a strong tendency to be associated with values for λ that are less than approximately 1.0.

The failure of the regression analysis in Table 5.1 results because the large number of zero values for $p_A[20 < A(10|\mathbf{a}, r)|\mathbf{e}_A]$ results in patterns that the linear regression model in use cannot match. In such situations, there are a number of additional techniques for sampling-based sensitivity analysis that can be tried. The examination of scatterplots as illustrated is certainly the simplest of these techniques. Other possibilities include rank regression, tests for patterns based on gridding, nonparametric regression, tests for patterns based on distance measures, tree-based searches, the two-dimensional Kolmogorov-Smirnov test, and the squared differences of ranks test (see Sect. 7.5 and Refs. [53; 54; 56]).

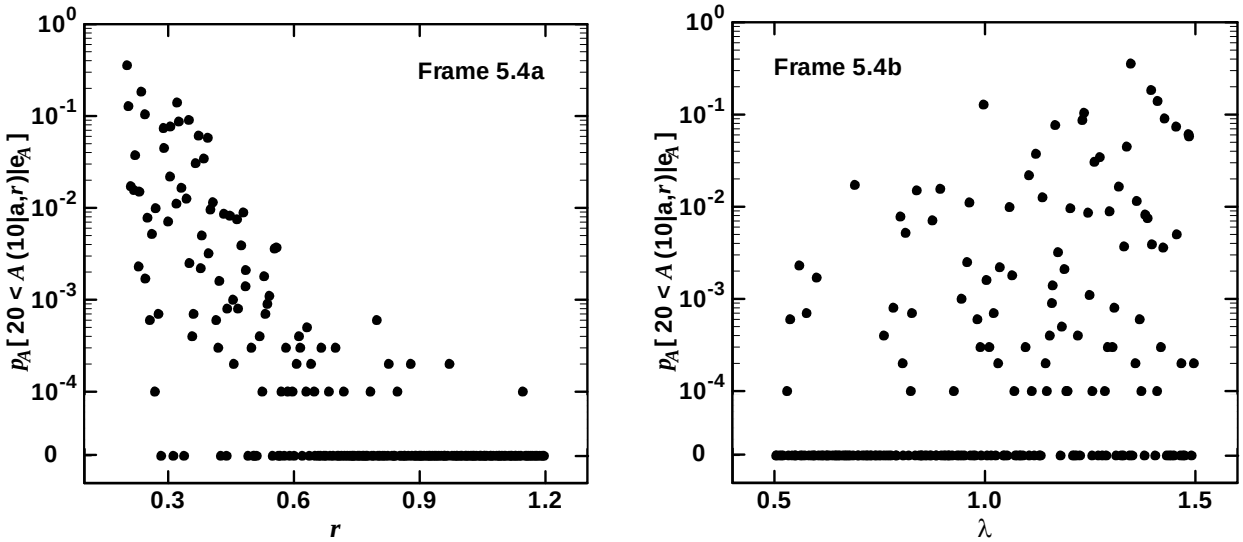

Fig. 5.4. Scatterplots for exceedance probability $p_A[20 < A(10|\mathbf{a}, r)|\mathbf{e}_A]$: (a) $(r_i, p_A[20 < A(10|\mathbf{a}, r_i)|\ \mathbf{e}_{Ai}])$, $i = 1,2, \ldots, nSE = 200$, and (b) $(\lambda_i, p_A[20 < A(10|\mathbf{a}, r_i)|\ \mathbf{e}_{Ai}])$, $i = 1,2, \ldots, nSE = 200$.

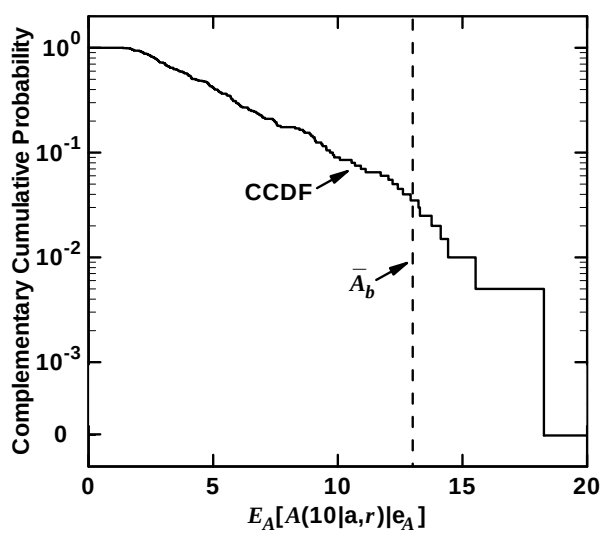

Fig. 5.5. Example bound $\bar{A}_b = 13$ on $E_A[A(10|\mathbf{a}, r)|\mathbf{e}_A]$.

Table 5.1. Stepwise Regression Analysis to Identify Uncertain Variables Affecting Exceedance Probability $p_A[20 < A(10|\mathbf{a}, r)|\mathbf{e}_A]$

Step[a]	Variable[b]	SRC[c]	R^{2d}
1	r	–0.36	0.14
2	λ	0.24	0.19

[a] Steps in stepwise regression analysis with an α-value of 0.01 or less required for a variable to enter a regression model.

[b] Variables listed in the order of selection in regression analysis.

[c] SRCs for variables in final regression model.

[d] Cumulative R^2 value with entry of each variable into regression model.

5.2 Epistemic Uncertainty with a Specified Bound on an Expected Value

For this example, it is assmed that the expected value $E_A[A(10|\mathbf{a}, r)|\mathbf{e}_A]$ summarized in Fig. 3.13 is required to be less than a bound (e.g., the bound $\bar{A}_b = 13$ in Fig. 5.5). At a conceptual level, this example is essentially the same as the example in Sect. 5.1 as the only difference is that (i) each CCDF in Sect. 5.1 is being reduced to an exceedance probability $p_A[20 < A(10|\mathbf{a}, r)|\mathbf{e}_A]$ associated with $A(10|\mathbf{a}, r) = 20$ and (ii) each CCDF in the present section is being reduced to an expected value $E_A[A(10|\mathbf{a}, r)|\mathbf{e}_A]$. In both cases, CCDFs summarizing aleatory uncertainty are being reduced to a single number. However, it is easy to envision that each of these cases could arise in QMU analyses. Specifically, the results in Sect. 5.1 involve a situation in which a bound is being placed on the likelihood of extreme outcomes arising from aleatory uncertainty, and the results in the present section involve a situation in which a bound is being placed on the expected value of outcomes arising from aleatory uncertainty.

Margins and normalized margins for $E_A[A(10|\mathbf{a}, r)|\mathbf{e}_A]$ are defined by

$$\bar{A}_m(10\,|\,\mathbf{e}) = \bar{A}_b - E_A[A(10\,|\,\mathbf{a}, r)\,|\,\mathbf{e}_A] \tag{5.15}$$

and

$$\bar{A}_n(10\,|\,\mathbf{e}) = \bar{A}_m(10\,|\,\mathbf{e}) \big/ \bar{A}_b\,, \tag{5.16}$$

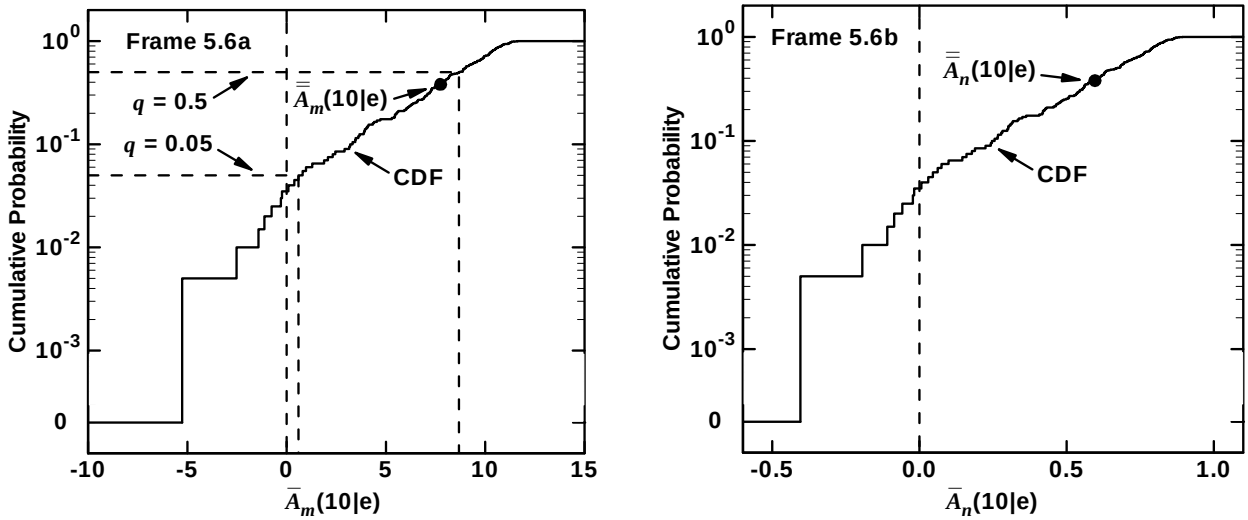

Fig. 5.6. Margins and normalized margins for $E_A[A(10|\mathbf{a}, r)|\mathbf{e}_A]$: (a) $\bar{A}_m(10\,|\,\mathbf{e})$, and (b) $\bar{A}_n(10\,|\,\mathbf{e})$.

Table 5.2. Stepwise Regression Analysis to Identify Uncertain Variables Affecting $E_A[A(10|\mathbf{a}, r)|\mathbf{e}_A]$

Step[a]	Variable[b]	SRC[c]	R^{2d}
1	r	–0.76	0.61
2	λ	0.47	0.82
3	m	0.13	0.84
4	a	0.08	0.85

[a] Steps in stepwise regression analysis with an α-value of 0.01 or less required for a variable to enter a regression model.
[b] Variables listed in the order of selection in regression analysis.
[c] SRCs for variables in final regression model.
[d] Cumulative R^2 value with entry of each variable into regression model.

respectively, and summarized in Fig. 5.6.

Similarly to the results in Eqs. (5.9) and (5.10), the CDF for margin in Fig. 5.6a can be converted into summary "margin/uncertainty" results by the normalizations

$$\bar{A}_{m/u}(10) = \bar{A}_{m,0.5}(10)\Big/\left[\bar{A}_{m,0.5}(10) - \bar{A}_{mq}(10)\right] = \begin{cases} 8.7/(8.7-0.6) = 1.1 \text{ for } q = 0.05 \\ 8.7/8.7 - [(-5.3)] = 0.6 \text{ for } q = 0.00 \end{cases} \tag{5.17}$$

and

$$\bar{\bar{A}}_{m/u}(10) = \bar{\bar{A}}_m(10)\Big/\left[\bar{\bar{A}}_m(10) - \bar{A}_{mq}(10)\right] = \begin{cases} 7.8/(7.8-0.6) = 1.1 \text{ for } q = 0.05 \\ 7.8/[7.8-(-5.3)] = 0.6 \text{ for } q = 0.00, \end{cases} \tag{5.18}$$

where $\bar{A}_{mq}(10)$ is the q quantile for the margin $\bar{A}_m(10\,|\,\mathbf{e})$ and $\bar{A}_m(10)$ is the expected value for $\bar{A}_m(10\,|\,\mathbf{e})$. The preceding normalizations are the outcomes of converting all the information in Figs. 3.11, 3.12, 5.5 and 5.6a into single numbers (see Sect. 4.5 for additional discussion).

A sensitivity analysis for $E_A[A(10|\mathbf{a}, r)|\mathbf{e}_A]$ based on stepwise regression analysis is presented in Table 5.2. As indicated, the uncertainty in $E_A[A(10|\mathbf{a}, r)|\mathbf{e}_A]$ is dominated by r and λ, with smaller effects indicated for m and a. Specifically, $E_A[A(10|\mathbf{a}, r)|\mathbf{e}_A]$ tends to decrease as r increases and tends to increase as each of λ, m and a increases. The final regression model has an R^2 value of 0.85, which indicates that most of the uncertainty in $E_A[A(10|\mathbf{a}, r)|\mathbf{e}_A]$ is being captured by the regression model. A regression-based sensitivity analysis for $\bar{A}_m(10\,|\,\mathbf{e})$ would produce the same results as shown in Table 5.2 with the exception that the signs on the SRCs would be reversed as a result of the subtraction of $E_A[A(10|\mathbf{a}, r)|\mathbf{e}_A]$ in the definition of $\bar{A}_m(10\,|\,\mathbf{e})$ in Eq. (5.15).

For perspective, the scatterplots for the two dominant variables affecting the uncertainty in $E_A[A(10|\mathbf{a}, r)|\mathbf{e}_A]$ identified in the regression analysis in Table 5.2 are shown in Fig. 5.7. Specifically, the negative effect of r and the positive effect of λ are easily seen in the two scatterplots in Fig. 5.7.

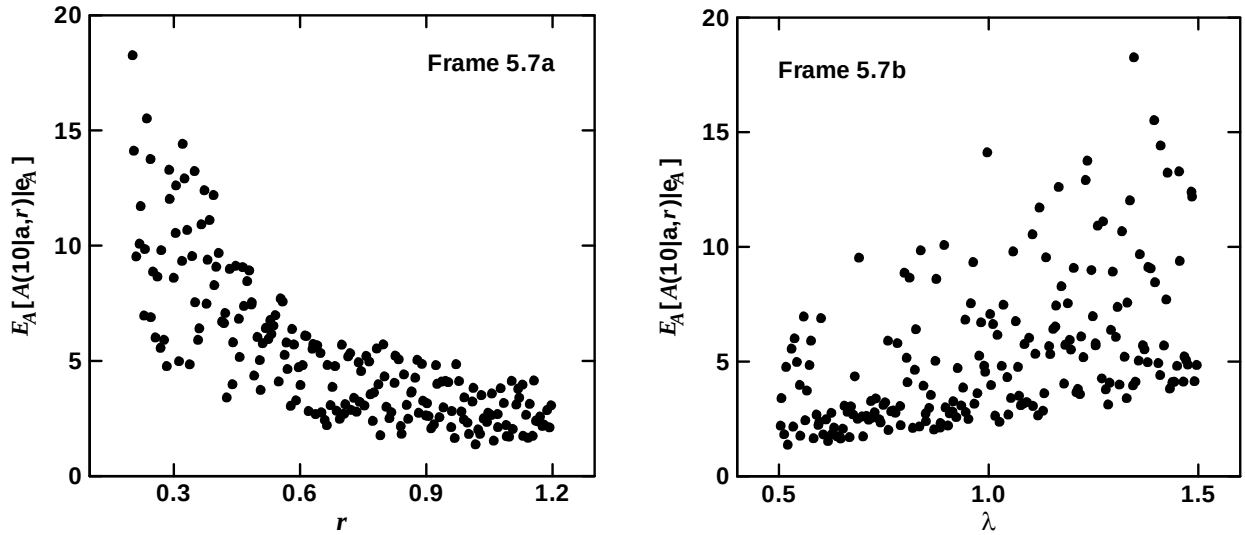

Fig. 5.7. Scatterplots for $E_A[A(10|\mathbf{a}, r)|\mathbf{e}_A]$: (a) ($r_i$, $E_A[A(10|\mathbf{a}, r_i)|\ \mathbf{e}_{Ai}]$), i = 1,2, …, nSE = 200, and (b) (λ_i, $E_A[A(10|\mathbf{a}, r_i)|\ \mathbf{e}_{Ai})]$), i = 1,2, …, nSE = 200.

This page intentionally left blank

6 Example QMU Analyses

Notional QMU analyses are presented in Sects. 4 and 5. Examples are now presented from three real analyses involving both aleatory and epistemic uncertainty in the assessment of compliance with requirements analogous to what could be encountered in real QMU analyses. Specifically, examples are presented involving compliance with the NRC's nuclear reactor accident safety goals (Sect. 6.1), the EPA's regulatory requirements for the Waste Isolation Pilot Plalnt (Sect. 6.2), and the NRC's regulatory requirements for the proposed high-level radioactive waste repository at Yucca Mountain, Nevada (Sect. 6.3).

As observed in the NAS/NRC report on QMU, past analyses of the type illustrated in this section can provide valuable insights and techniques for future QMU analyses (Finding 1-7, pp. 31-32, Ref. [77]). Consistent with this observation, the three example analyses involve (i) the "probability of frequency approach" entailing an explicit separation of aleatory and epistemic uncertainty (Finding 1-3, pp. 22-23, Recommendation 1-7, p. 33, and App. A, Ref. [77]), (ii) efficient sampling from high-dimensional input spaces (Recommendation 1-4, p. 29, Ref. [77]), (iii) extensive sensitivity analyses (pp. 14-15, Ref. [77]), (iv) extensive use of expert review and judgment (Recommendation 1-5, p. 30, Ref. [77]), and (v) a full presentation of analysis results rather than a limited number of one-dimensional summary results (Finding 1-4, p. 25, Ref. [77]).

6.1 Nuclear Reactor Accident Safety Goals

In the 1980's and into the 1990's, the NRC considered the implementation of safety goals for the operation of commercial nuclear power plants [113-116]. The proposed safety goals and their quantitative evaluation have aspects that are very similar to what might be expected in a QMU analysis of weapon system performance that involves the incorporation and representation of the implications of both aleatory and epistemic uncertainty. As a result, the proposed safety goals and analyses carried out in their support provide an excellent example of the ideas and challenges that are likely to be encountered in a nontrivial application of QMU in stockpile performance. Specifically, results from a probabilistic risk assessment (PRA) for the Surry Nuclear Power Station [117] carried out in support of the NRC's reassessment of the risk from commercial nuclear plants [10] are used to illustrate what a QMU analysis involving both aleatory and epistemic uncertainty is likely to involve.

An article summarizing this analysis [118] is reproduced in App. C and will be referred to in the following discussion as a convenient and accessible source of additional information on this analysis. Inclusion of this article in App. C makes it possible to have an accessible description of the analysis as part of this report. More detailed analysis descriptions are available in a detailed technical report [117], in a sequence of journal articles [11; 119-121], and in detailed technical reports cited in the preceding references. In addition, further discussions of the NRC's safety goals are also available [11; 122-132].

Specifically, the NRC considered two safety goals for individual fatality risk and three quantitative risk goals for accident frequency. These goals have the following form:

- *Individual early fatality risk*: The expected value for average individual early fatality risk in the region between the plant site boundary and 1609.3 m (1 mi) beyond this boundary will be less than 5×10^{-7} yr^{-1}. (SG1)

- *Individual latent cancer fatality risk*: The expected value for average individual latent cancer fatality risk in the region between the plant site boundary and 16,093 m (10 mi) beyond this boundary will be less than 2×10^{-6} yr^{-1}. (SG2)

- *Severe accident frequency*: The expected value for the frequency of a severe accident will be less than 1×10^{-4} yr^{-1}. (QRG1)

- *Conditional probability of containment failure*: The expected value for the probability of containment failure given the occurrence of a severe accident will be less than 0.1. (QRG2)

- *Large release frequency*: The expected value for the frequency of a large release will be less than 1×10^{-6} yr^{-1}. (QRG3)

The two safety goals stated in (SG1) and (SG2) and the three quantitative risk goals stated in (QRG1) – (QRG3) involve requirements and analyses similar to requirements and analyses that will be encountered in QMU applications for weapons systems. Specifically, each goal specifies a desired bound on a specific quantity. Further, the analysis for each goal involves both aleatory uncertainty and epistemic uncertainty, with aleatory uncertainty arising from the many possible accidents that could, but probably will not, occur at a

particular nuclear power plant and epistemic uncertainty arising from the many imprecisely known quantities required in a PRA for a nuclear power plant.

Because the goals in (SG1) – (QRG3) involve both aleatory uncertainty and epistemic uncertainty, their evaluation is underlain by two probability spaces: a probability space ($\mathcal{A}$, $\mathbb{A}$, p_A) for aleatory uncertainty and a probability space ($\mathcal{E}$, $\mathbb{E}$, p_E) for epistemic uncertainty.

The probability space ($\mathcal{E}$, $\mathbb{E}$, p_E) for epistemic uncertainty involves nE = 130 variables (Ref. [117], Tables 2.2-9, 2.2-10, 2.3-2 and 3.2-1). Thus, each element $\mathbf{e}$ of $\mathcal{E}$ is a vector of the form

$$\mathbf{e} = \left[e_1, e_2, \ldots, e_{nE}\right] = \left[e_1, e_2, \ldots, e_{130}\right]. \tag{6.1}$$

Examples of variables that constitute elements of $\mathbf{e}$ are presented in Table 8 of Ref. [118]. With respect to notation, the set $\mathcal{E}$ corresponds to the set Ω in Ref. [118], and the vector $\mathbf{e} = [e_1, e_2, \ldots, e_{nE}]$ corresponds to the vector $\mathbf{X} = [X_1, X_2, \ldots, X_{nV}]$ in Ref. [118].

The probability space ($\mathcal{E}$, $\mathbb{E}$, p_E) was developed through an extensive expert review process that constructed a distribution D_i, i = 1, 2, …, nE = 130, for each element e_i of $\mathbf{e}$ [97; 133-140]. The review process used to define the distributions D_1, D_2, …, D_{130} and thus the probability space ($\mathcal{E}$, $\mathbb{E}$, p_E) provides an example and model of how the characterization of epistemic uncertainty could be carried out in support of QMU.

The probability space ($\mathcal{A}$, $\mathbb{A}$, p_A) characterizes the universe of possible accidents at the nuclear power station under consideration. When viewed at a high level, each element $\mathbf{a}$ of $\mathcal{A}$ is a vector of the form

$$\mathbf{a} = \left[IE, AS, PDS, APB, STG, WT\right], \tag{6.2}$$

where

- IE = designator for initiating event (see Eq. (17), Table 1, and associated discussion in Sect. 3 of Ref. [118]),
- AS = designator for accident sequence (see Eq. (18), Table 3, and associated discussion in Sect. 3 of Ref. [118]),
- PDS = designator for plant damage state (see Eq. (33), Tables 4 and 5, and associated discussion in Sect. 4 of Ref. [118]),
- APB = designator for accident progression bin (see Eqs. (37) and (38), Table 6, and associated discussion in Sect. 4 of Ref. [118]),
- STG = designator for source term group (see Eq. (53) and associated discussion in Ref. [118]),
- WT = designator for weather type (see discussion in Sect. 6 of Ref. [118]).

The analysis reported in Ref. [118] involves (i) nIE = 11 initiating events (Table 1, Ref. [118]), (ii) nAS = 28 accident sequences (Table 3, Ref. [118]), (iii) $nPDS$ = 25 plant damage states that were then reduced to $nPDS$ = 7 plant damage states for the final analysis (Tables 4 and 5, Ref. [118]), (iv) $nAPB$ = 54 to $nAPB$ = 157 accident progression bins, with the exact number depending on values assigned to epistemically uncertain quantities and a total of 1906 unique accident progression bins considered in the entire analysis (Table 6, Ref. [118]), (v) $nSTG$ = 54 source term groups (Sect. 5, Ref. [118]), and (vi) nWT = 2560 weather types (Sect. 6, Ref. [118]). However, not all combinations of initiating event, accident sequence, plant damage state, accident progression bin, source term group, and weather type are possible.

As summarized in Ref. [118] and presented in more detail in the reports cited in Ref. [11], extensive use of fault trees, event trees, and other analysis procedures are used to arrive at the actual combinations of the elements of $\mathbf{a}$ that are meaningful and also to determine their probabilities. Formally, the analysis can be represented by a sequence of matrix multiplications but it is important to realize that a large amount of analysis and modeling underlies the determination of the transition probabilities that constitute the elements of the matrices involved in the indicated multiplications. The results presented in this section provide an example of an actual implementation of the analysis approach summarized in App. A of Ref. [77].

The analysis documentation summarized in Ref. [118] never specifically refers to a probability space for aleatory uncertainty. However, such a probability space is clearly being defined by the specification of frequencies for initiating events and then conditional probabilities for transitions from initiating events to accident sequences to plant damage states to accident progression bins to source term groups to weather conditions. In essence, these transition probabilities define probabilities for vectors of the form indicated in Eq. (6.2) and thus provide a discretized approximation to the probability space ($\mathcal{A}$, $\mathbb{A}$, p_A). Technically, the vectors in Eq. (6.2) are actually designators for sets of

similar accidents rather than descriptions for single unique accidents; this point is made because a single accident described in full and complete detail would have a probability of zero. A purist would point out that the analysis is starting with frequencies rather than probabilities for initiating events; however, the conversion from frequencies to probabilities is straightforward and, for practical purposes, there is no meaningful difference between a small annual frequency and a small annual probability.

The safety goals indicated in (SG1) – QRG3) can be represented by the vector

$$\begin{aligned}\mathbf{G} &= \left[SG1,\, SG2,\, QRG1,\, QRG2,\, QRG3\ \right] \\ &= \Big[5\times10^{-7}\ \mathrm{yr}^{-1},\, 2\times10^{-6}\ \mathrm{yr}^{-1}, \\ &\qquad 1\times10^{-4}\ \mathrm{yr}^{-1},\, 0.1,\, 1\times10^{-6}\ \mathrm{yr}^{-1}\Big].\end{aligned} \tag{6.3}$$

Similarly, the estimated performance of a nuclear power station can be represented by the vector

$$\mathbf{P} = \left[pSG1,\, pSG2,\, pQRG1,\, pQRG2,\, pQRG3\right], \tag{6.4}$$

where $pSG1$, $pSG2$, $pQRG1$, $pQRG2$ and $pQRG3$ are the performance values calculated for comparison with the corresponding elements of $\mathbf{G}$. The quantities $pSG1$, $pSG2$, $pQRG1$ and $pQRG3$ are frequencies that derive from aleatory uncertainty, and the quantity $pQRG2$ is a conditional probability that derives from aleatory uncertainty. As a result, the determination of $pSG1$, $pSG2$, $pQRG1$, $pQRG2$ and $pQRG3$ involves the evaluation of integrals involving the probability space $(\mathcal{A}, \mathbb{A}, p_A)$ for aleatory uncertainty. The evaluation of these integrals is a complex process and in most PRAs is performed with algorithms that rely heavily on fault trees, event trees, selective mechanistic modeling of physical processes, and extensive use of interpolation procedures to estimate the behavior of unmodeled physical conditions. For the Surry analysis, the process used to arrive at values for the elements of $\mathbf{P}$ is summarized in Ref. [118] and described in more detail in the technical reports cited in Ref. [11].

If the probability space $(\mathcal{A}, \mathbb{A}, p_A)$ was known precisely and all additional quantities required in the evaluation of $\mathbf{P}$ were also known precisely, then the associated vector $\mathbf{M}$ of margins would be unambiguously defined by

$$\begin{aligned}\mathbf{M} &= \mathbf{G} - \mathbf{P} \\ &= \left[mSG1,\, mSG2,\, mQRG1,\, mQRG2,\, mQRG3\right],\end{aligned} \tag{6.5}$$

where

$$\begin{aligned} mSG1 &= 5\times10^{-7}\ \mathrm{yr}^{-1} - pSG1, \\ mSG2 &= 2\times10^{-7}\ \mathrm{yr}^{-1} - pSG2, \\ mQRG1 &= 1\times10^{-4}\ \mathrm{yr}^{-1} - pQRG1, \\ mQRG2 &= 0.1 - pQRG2, \\ mQRG3 &= 1\times10^{-6}\ \mathrm{yr}^{-1} - pQRG3. \end{aligned}$$

However, $(\mathcal{A}, \mathbb{A}, p_A)$ and additional quantities required in the evaluation of $\mathbf{P}$ are not known precisely in the example under consideration nor are they likely to be known precisely in any real analysis of a complex system. Rather, $\mathbf{P}$ is actually a function

$$\begin{aligned}\mathbf{P}(\mathbf{e}) = \Big[&pSG1(\mathbf{e}),\, pSG2(\mathbf{e}),\, pQRG1(\mathbf{e}), \\ &pQRG2(\mathbf{e}),\, pQRG3(\mathbf{e})\Big]\end{aligned} \tag{6.6}$$

of vectors $\mathbf{e} \in \mathcal{E}$, where $(\mathcal{E}, \mathbb{E}, p_E)$ is the probability space for epistemic uncertainty. As a result, the vector $\mathbf{M}$ of margins has the form

$$\begin{aligned}\mathbf{M}(\mathbf{e}) &= \mathbf{G} - \mathbf{P}(\mathbf{e}) \\ &= \Big[mSG1(\mathbf{e}),\, mSG2(\mathbf{e}),\, mQRG1(\mathbf{e}), \\ &\qquad mQRG2(\mathbf{e}),\, mQRG3(\mathbf{e})\Big]\end{aligned} \tag{6.7}$$

and is thus epistemically uncertain with its elements having distributions that derive from the probability space $(\mathcal{E}, \mathbb{E}, p_E)$ for epistemic uncertainty.

As stated, the safety goals in (SG1) – (QRG3) involve comparisons with expected results, where the indicated expectations are over epistemic uncertainty. Specifically, note where the modifier "expected" appears in (SG1) – (QRG3). Thus, a literal reading of (SG1) – (QRG3) implies that

$$\begin{aligned}E_E\left\{\mathbf{P}(\mathbf{e})\right\} = \Big[&E_E\left\{pSG1(\mathbf{e})\right\},\, E_E\left\{pSG2(\mathbf{e})\right\}, \\ &E_E\left\{pQRG1(\mathbf{e})\right\},\, E_E\left\{pQRG2(\mathbf{e})\right\} \\ &E_E\left\{pQRG3(\mathbf{e})\right\}\Big]\end{aligned} \tag{6.8}$$

is to be used in comparisons with the specified goals, where

$$E_E\left\{pSG1(\mathbf{e})\right\} = \int_{\mathcal{E}} pSG1(\mathbf{e})\, d_E(\mathbf{e})\, \mathrm{d}E,$$

$d_E(\mathbf{e})$ is the density function associated with the probability space ($\mathcal{E}$, $\mathbb{E}$, p_E) for epistemic uncertainty, and the remaining elements of $E_E\{\mathbf{P}(\mathbf{e})\}$ are defined similarly to $E_E\{pSG1(\mathbf{e})\}$. In the example of Ref. [118],

$$E_E\left\{\mathbf{P}(\mathbf{e})\right\} \cong \left[1.6\times10^{-8}\ \text{yr}^{-1}, 1.7\times10^{-9}\ \text{yr}^{-1}, 4.1\times10^{-5}\ \text{yr}^{-1}, 0.19, 1.5\times10^{-7}\ \text{yr}^{-1}\right], \tag{6.9}$$

and, in turn, the resultant margins are

$$\mathbf{G} - E_E\left\{\mathbf{P}(\mathbf{e})\right\} \cong \left[4.8\times10^{-7}\ \text{yr}^{-1}, 2.0\times10^{-6}\ \text{yr}^{-1}, 5.9\times10^{-5}\ \text{yr}^{-1}, -0.09, 8.5\times10^{-7}\ \text{yr}^{-1}\right]. \tag{6.10}$$

However, this approach is not consistent with the basic premises of QMU as the epistemic uncertainty in the margins is suppressed in the calculation of expected values.

Fortunately, the analyses presented in Ref. [118] use a sampling-based approach to the propagation of epistemic uncertainty. Specifically, an LHS

$$\mathbf{e}_i = \left[e_{i1}, e_{i2}, \ldots, e_{i,nE}\right], i = 1, 2, \ldots, nLHS, \tag{6.11}$$

of size $nLHS$ = 200 from the nE = 130 uncertain variables under consideration is used in the generation of the expected results in Eq. (6.8). This procedure resulted in the estimation of

$$\mathbf{P}(\mathbf{e}_i) = \left[pSG1(\mathbf{e}_i), pSG2(\mathbf{e}_i), pQRG1(\mathbf{e}_i), pQRG2(\mathbf{e}_i), pQRG3(\mathbf{e}_i)\right] \tag{6.12}$$

for i = 1, 2, …, $nLHS$ = 200, and in turn allows estimation of the margins

$$\begin{aligned}\mathbf{M}(\mathbf{e}_i) &= \mathbf{G} - \mathbf{P}(\mathbf{e}_i) \\ &= \left[mSG1(\mathbf{e}_i), mSG2(\mathbf{e}_i), mQRG1(\mathbf{e}_i), mQRG2(\mathbf{e}_i), mQRG3(\mathbf{e}_i)\right]\end{aligned} \tag{6.13}$$

for i = 1, 2, …, $nLHS$ = 200. As a result, the information needed for a QMU-type analysis of margins is present.

A sample of size $nLHS$ = 200 from nE = 130 uncertain variables may seem too small to be effective. However, replicated sampling was used to establish that this sample size was adequate to obtain stable uncertainty and sensitivity results in the Surry analysis [141]. In general, there is a tendency to overestimate the sample size needed to obtain an adequate representation and assessment of the implications of epistemic uncertainty [54; 141-143].

The individual requirements specified in (SG1) – (QRG3) and the uncertainty in the margins associated with these goals are now considered.

Safety Goal SG1. Safety goal SG1 specifies that individual early fatality risk in the region between the plant site boundary and 1609.3 m (1 mi) beyond this boundary will be less than $SG1 = 5 \times 10^{-7}$ yr^{-1}. Individual early fatality risk is obtained by first calculating an exceedance frequency curve for early fatality probability for each of the $nLHS$ = 200 LHS elements (Fig. 6.1). In turn, each exceedance frequency curve is reduced to an estimate $pSG1(\mathbf{e}_i)$ for early fatality risk (Fig. 6.2).

Conceptually although not in direct computational implementation, the individual exceedance frequency curves in Fig. 6.1 and the early fatality risk results in Fig. 6.2 are defined by integrals involving the probability space ($\mathcal{A}$, $\mathbb{A}$, p_A) for aleatory uncertainty, with ($\mathcal{A}$, $\mathbb{A}$, p_A) and other epistemically uncertain quantities changing for each LHS element $\mathbf{e}_i$ (see Sect. 3.5). In effect, each CCDF in Fig. 6.1 is reduced to an expected value (i.e., $pSG1(\mathbf{e}_i)$), with the resultant 200 expected values and their associated epistemic uncertainty summarized in Fig. 6.2. The values for $pSG1(\mathbf{e}_i)$ in Fig. 6.2 are summarized with a CCDF rather than a CDF because use of a CCDF permits a direct reading from the ordinate of the exceedance probabilities for large values for $pSG1$, which are the results of greatest interest in comparisons with safety goal SG1.

Margins associated with safety goal SG1 are now given by

$$\begin{aligned}mSG1(\mathbf{e}_i) &= SG1 - pSG1(\mathbf{e}_i) \\ &= 5\times10^{-7}\ \text{yr}^{-1} - pSG1(\mathbf{e}_i)\end{aligned} \tag{6.14}$$

for i = 1, 2, …, $nLHS$ = 200 (Fig. 6.3a). Similarly, normalized margins for safety goal SG1 are given by

$$\begin{aligned}nSG1(\mathbf{e}_i) &= \left[SG1 - pSG1(\mathbf{e}_i)\right]/SG1 \\ &= \left[5\times10^{-7}\ \text{yr}^{-1} - pSG1(\mathbf{e}_i)\right]/5\times10^{-7}\ \text{yr}^{-1}\end{aligned} \tag{6.15}$$

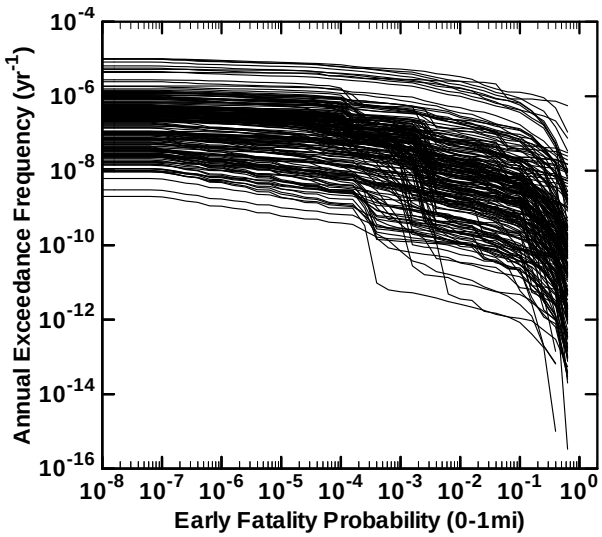

Fig. 6.1. Exceedance frequency curves for individual early fatality probability within 1609.3 m (1 mi) of the site boundary due to accidents resulting from internal initiators at Surry (Ref. [117], Fig. D.5). Each curve corresponds to one sample element.

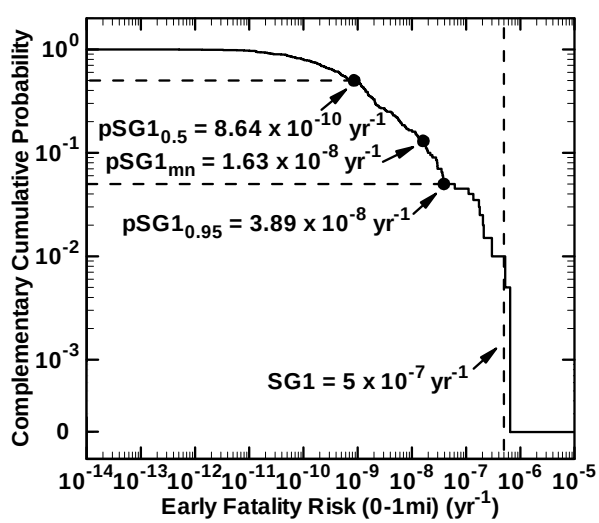

Fig. 6.2. Estimated CCDF for annual individual early fatality risk within 1 mile of the site boundary due to accidents resulting from internal initiators at Surry.

for i = 1, 2, …, $nLHS$ = 200 (Fig. 6.3b). The values for the margins in Fig. 6.3 are summarized with CDFs rather than CCDFs because use of a CDF permits a direct reading from the ordinate of the probabilities associated with small margins, which are the margin results of greater interest in comparisons with safety goal SG1.

As indicated in Eqs. (6.14) and (6.15), the margin results in Fig. 6.3 are obtained by simple translations and normalizations of the values for $pSG1(\mathbf{e}_i)$ in Fig. 6.2. Thus, Figs. 6.2 and 6.3 effectively contain the same information. Specifically, given the value for SG*1*, the results in any one of the three plot frames in Figs. 6.2 and 6.3 can be used to generate the results in the other two plot frames. The results in Fig. 6.3 provide a direct representation of the uncertainty in the margin associated with safety goal SG1. However, in the view of the author, the summary in Fig. 6.2 provides a more readily interpretable representation for the relationships involved in assessing compliance with safety goal SG1 than the margin plots in Fig. 6.3. Specifically, inspection of Fig. 6.2 provides immediate information on the uncertainty in $pSG1$, the relationship of $pSG1$ to $SG1$, and the differences (i.e., margins) between $SG1$ and pSG1. In contrast, the actual values for $SG1$ and $pSG1$ are not readily apparent in the margin results in Fig. 6.3; as a consequence, the results in Fig. 6.2 are more informative with respect to system performance than the results in Fig. 6.3.

The CDF in Fig. 6.2 provides a complete summary of the uncertainty in the margin associated with safety goal SG1 under the assumption that the analysis was performed without serious implementation or sampling errors (see discussion of verification and validation in Sect. 3.8). If desired, single number summaries of the results in Figs. 6.2 and 6.3 in the spirit of "margin/uncertainty" can be defined. Examples include

$$\begin{aligned} & mSG1_{mn} \big/ \left(mSG1_{mn} - mSG1_{0.05} \right) \\ & \quad = 4.84\times10^{-7} \Big/ \left(4.84\times10^{-7} - 4.61\times10^{-7} \right) \\ & \quad = 21.0, \end{aligned} \tag{6.16}$$

$$\begin{aligned} & mSG1_{0.5} \big/ \left(mSG1_{0.5} - mSG1_{0.05} \right) \\ & \quad = 4.99\times10^{-7} \Big/ \left(4.99\times10^{-7} - 4.61\times10^{-7} \right) \\ & \quad = 13.1, \end{aligned} \tag{6.17}$$

$$\begin{aligned} & mSG1_{mn} \big/ \left(mSG1_{mn} - mSG1_{min} \right) \\ & \quad = 4.84\times10^{-7} \Big/ \left[4.84\times10^{-7} - \left(-1.50\times10^{-7} \right) \right] \\ & \quad = 0.76, \end{aligned} \tag{6.18}$$

and

$$\begin{aligned} & mSG1_{0.5} \big/ \left(mSG1_{0.5} - mSG1_{min} \right) \\ & \quad = 4.99\times10^{-7} \Big/ \left[4.99\times10^{-7} - \left(-1.50\times10^{-7} \right) \right] \\ & \quad = 0.77, \end{aligned} \tag{6.19}$$

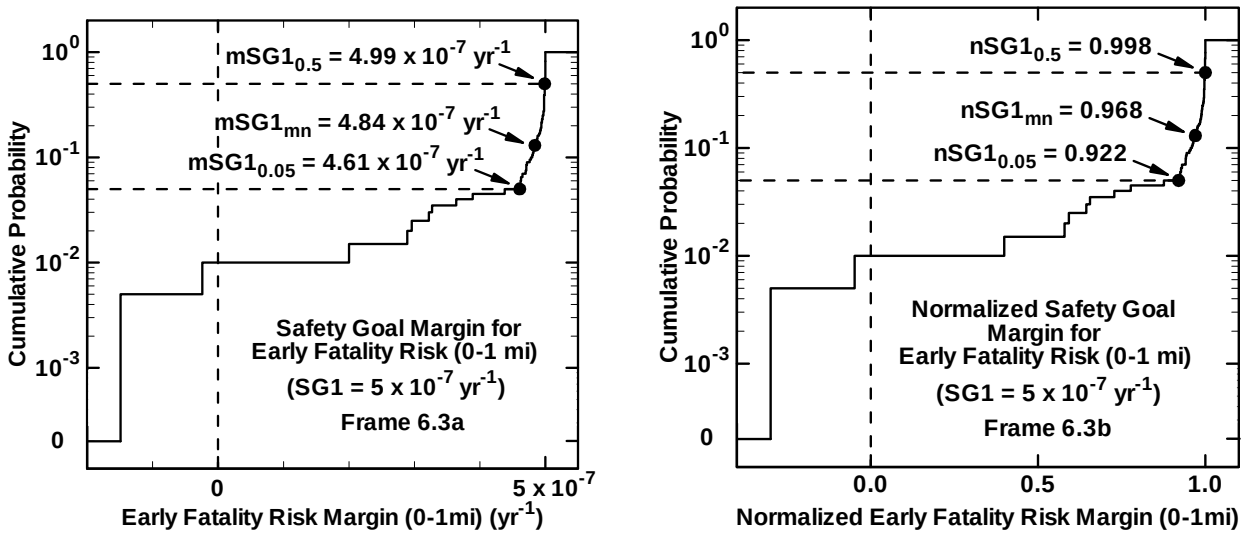

Fig. 6.3. Estimated CDFs for margins associated with safety goal SG1 for annual individual early fatality risk within 1 mile of the site boundary due to accidents resulting from internal initiators at Surry: (a) margin *mSG*1 (see Eq. (6.14)), and (b) normalized margin *nSG*1 (see Eq. (6.15)).

where

$mSG1_{mn}$ = mean value for $mSG1(\mathbf{e})$ estimated from CCDF in Fig. 6.3a,

$mSG1_q$ = quantile for q = 0.00, 0.05 and 0.5 for $mSG1(\mathbf{e})$ estimated from CDF in Fig. 6.3a,

$mSG1_{min}$ = minimum value for $mSG1(\mathbf{e})$ in Fig. 6.3a (i.e., $mSG1_q$ for q = 0.00).

However, a significant amount of information is lost in "margin/uncertainty" summaries of the form shown in Eqs. (6.16) – (6.19). Specifically, the single number summaries in Eqs. (6.16) – (6.19) are the result of reducing all the information in Fig. 6.1 to one number (see Sect. 4.5 for additional discussion).

As displayed, the "margin/uncertainty" results in Eqs. (6.16) – (6.19) are calculated directly from the margin results displayed in Fig. 6.3a. The same results can also be calculated directly from the results displayed in Fig. 6.2. Specifically,

$$\begin{aligned} & mSG1_{mn}/\left(mSG1_{mn}-mSG1_{0.05}\right) \\ &= \frac{SG1-pSG1_{mn}}{\left(SG1-pSG1_{mn}\right)-\left(SG1-pSG1_{0.95}\right)} \\ &= \left(SG1-pSG1_{mn}\right)/\left(pSG1_{0.95}-pSG1_{mn}\right) \\ &= \left(5\times10^{-7}-1.63\times10^{-8}\right)/\left(3.89\times10^{-8}-1.63\times10^{-8}\right) \\ &= 21.4, \end{aligned} \tag{6.20}$$

$$\begin{aligned} & mSG1_{0.5}/\left(mSG1_{0.5}-mSG1_{0.05}\right) \\ &= \frac{SG1-pSG1_{0.5}}{\left(SG1-pSG1_{0.5}\right)-\left(SG1-pSG1_{0.95}\right)} \\ &= \left(SG1-pSG1_{0.5}\right)/\left(pSG1_{0.95}-pSG1_{0.5}\right) \\ &= \left(5\times10^{-7}-8.64\times10^{-10}\right)/\left(3.89\times10^{-8}-8.64\times10^{-10}\right) \\ &= 13.1, \end{aligned} \tag{6.21}$$

$$\begin{aligned} & mSG1_{mn}/\left(mSG1_{mn}-mSG1_{min}\right) \\ &= \frac{SG1-pSG1_{mn}}{\left(SG1-pSG1_{mn}\right)-\left(SG1-pSG1_{mx}\right)} \\ &= \left(SG1-pSG1_{mn}\right)/\left(pSG1_{mx}-pSG1_{mn}\right) \\ &= \left(5\times10^{-7}-1.63\times10^{-8}\right)/\left(6.50\times10^{-7}-1.63\times10^{-8}\right) \\ &= 0.76, \end{aligned} \tag{6.22}$$

and

$$\begin{aligned} & mSG1_{0.5}/\left(mSG1_{0.5}-mSG1_{min}\right) \\ &= \frac{SG1-pSG1_{0.5}}{\left(SG1-pSG1_{0.5}\right)-\left(SG1-pSG1_{mx}\right)} \\ &= \left(SG1-pSG1_{0.5}\right)/\left(pSG1_{mx}-pSG1_{0.5}\right) \\ &= \left(5\times10^{-7}-8.64\times10^{-10}\right)/\left(6.50\times10^{-7}-8.64\times10^{-10}\right) \\ &= 0.77, \end{aligned} \tag{6.23}$$

where

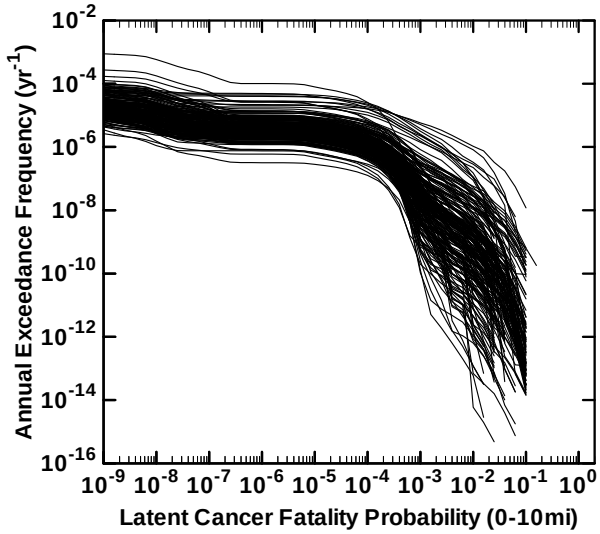

Fig. 6.4. Exceedance frequency curves for individual latent cancer fatality probability within 10 mi = 16, 903 m of the site boundary due to accidents resulting from internal initiators at Surry (Ref. [117], Fig. D.6). Each curve corresponds to one sample element.

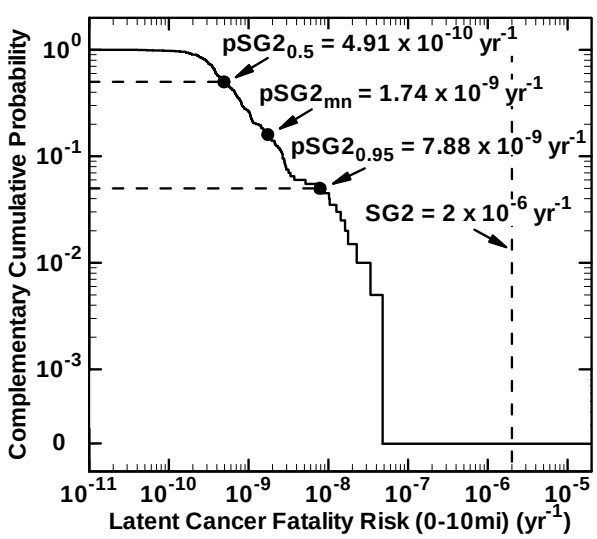

Fig. 6.5. Estimated CCDF for annual individual latent cancer fatality risk within 10 miles of the site boundary due to accidents resulting from internal initiators at Surry.

$pSG1_{mn}$ = mean value for $pSG1(\mathbf{e})$ estimated from CCDF in Fig. 6.2,

$pSG1_q$ = quantile for q = 0.5, 0.95 and 1.00 for $pSG1(\mathbf{e})$ estimated from CCDF in Fig. 6.2,

$pSG1_{mx}$ = maximum value for $pSG1(\mathbf{e})$ in Fig. 6.2 (i.e., $pSG1_q$ for q = 1.00),

and the remaining symbols in Eqs. (6.20) – (6.23) are defined the same as in conjunction with Eqs. (6.16) – (6.19). As a reminder, the quantiles $pSG1_q$ for q = 0.5, 0.95 and 1.00 correspond to exceedance probabilities of 0.5, 0.05 and 0.00 for $pSG1(\mathbf{e})$ in Fig. 6.2.

Safety Goal SG2. Safety goal SG2 specifies that individual latent cancer fatality risk in the region between the plant site boundary and 16,093 m (10 mi) beyond this boundary will be less than $SG2 = 2 \times 10^{-6}$ yr^{-1}. Similarly to individual early risk, individual latent cancer fatality risk is obtained by first calculating an exceedance frequency curve for latent cancer fatality probability for each of the $nLHS$ = 200 LHS elements (Fig. 6.4) and then reducing each exceedance frequency to an estimate $pSG2(\mathbf{e}_i)$ for latent cancer fatality risk (Fig. 6.5).

Margins and normalized margins associated with safety goal SG2 are now given by

$$\begin{aligned} mSG2(\mathbf{e}_i) &= SG2 - pSG2(\mathbf{e}_i) \\ &= 2\times10^{-6}\,\text{yr}^{-1} - pSG2(\mathbf{e}_i) \end{aligned} \tag{6.24}$$

and

$$\begin{aligned} nSG2(\mathbf{e}_i) &= \left[SG2 - pSG2(\mathbf{e}_i)\right]\Big/SG2 \\ &= \left[2\times10^{-6}\,\text{yr}^{-1} - pSG2(\mathbf{e}_i)\right]\Big/2\times10^{-6}\,\text{yr}^{-1}, \end{aligned} \tag{6.25}$$

respectively, for i = 1, 2, …, $nLHS$ = 200 (Fig. 6.6).

As discussed in conjunction with Eqs. (6.16) – (6.23), the results in Figs. 6.5 and 6.6 can be reduced to single number summaries of the "margin/uncertainty" form. As for safety goal SG1, examples include

$$\begin{aligned} &mSG2_{mn}\big/\left(mSG2_{mn} - mSG2_{0.05}\right) \\ &\quad = 1.9983\times10^{-6}\Big/\left(1.9983\times10^{-6} - 1.9921\times10^{-6}\right) \\ &\quad = 322.3, \end{aligned} \tag{6.26}$$

$$\begin{aligned} &mSG2_{0.5}\big/\left(mSG2_{0.5} - mSG2_{0.05}\right) \\ &\quad = 1.9995\times10^{-6}\Big/\left(1.9995\times10^{-6} - 1.9921\times10^{-6}\right) \\ &\quad = 270.2, \end{aligned} \tag{6.27}$$

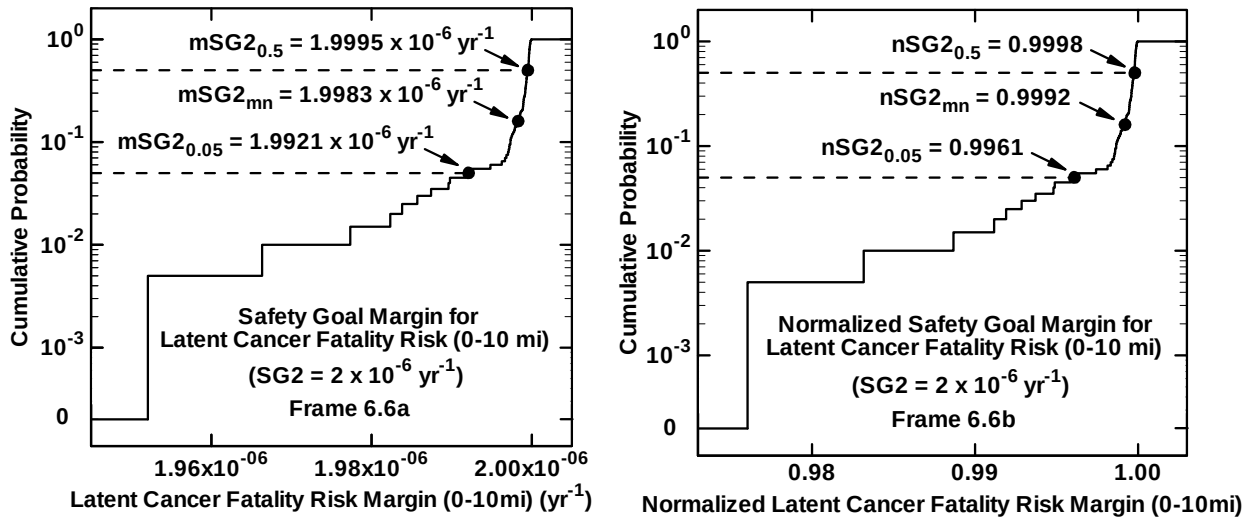

Fig. 6.6. Estimated CDFs for margins associated with safety goal SG2 for individual latent cancer fatality risk within 10 miles of the site boundary due to accidents resulting from internal initiators at Surry: (a) margin *mSG*2 (see Eq. (6.24)) and (b) normalized margin *nSG*2 (see Eq. (6.25)).

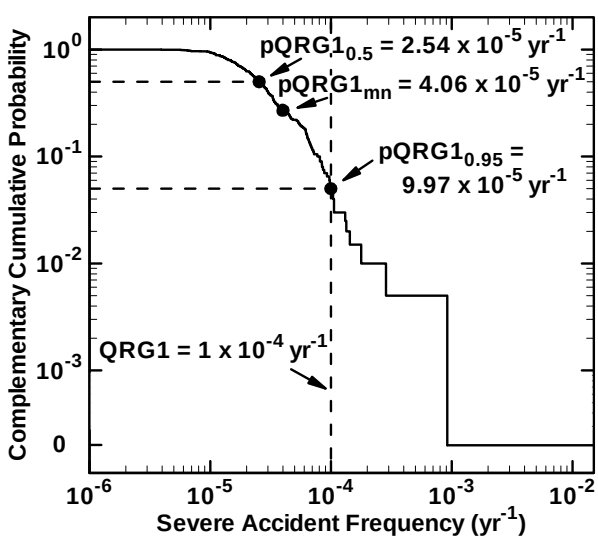

Fig. 6.7. Estimated CCDF for annual severe accident frequency due to accidents resulting from internal initiators at Surry.

$$
\begin{aligned}
&mSG2_{mn} \big/ \left(mSG2_{mn} - mSG2_{min} \right) \\
&\quad = 1.9983 \times 10^{-6} \Big/ \left(1.9983 \times 10^{-6} - 1.9521 \times 10^{-6} \right) \\
&\quad = 43.25,
\end{aligned}
\tag{6.28}
$$

and

$$
\begin{aligned}
&mSG2_{0.5} \big/ \left(mSG2_{0.5} - mSG2_{min} \right) \\
&\quad = 1.9995 \times 10^{-6} \Big/ \left(1.9995 \times 10^{-6} - 1.9521 \times 10^{-6} \right) \\
&\quad = 42.18,
\end{aligned}
\tag{6.29}
$$

with $mSG2_{mn}$, $mSG2_q$ and $mSG2_{min}$ defined similarly to $mSG1_{mn}$, $mSG1_q$ and $mSG1_{mn}$ in conjunction with Eqs. (6.16) – (6.19).

Quantitative Risk Goal QRG1. Quantitative risk goal QRG1 specifies that the frequency of a severe accident will be less than 10^{-4} yr^{-1}. For this example, a severe accident is assumed to be an accident that results in core damage. Each of the *nLHS* = 200 LHS elements results in an estimate $pQRG1(\mathbf{e}_i)$ for the frequency of a severe accident (Fig. 6.7). As for safety goals SG1 and SG2, the severe accident frequencies summarized in Fig. 6.7 are defined in concept, although not in direct computational implementation, by integrals involving the probability space ($\mathcal{A}$, $\mathbb{A}$, p_A) for aleatory uncertainty, with ($\mathcal{A}$, $\mathbb{A}$, p_A) and other epistemically uncertain quantities changing for each LHS element $\mathbf{e}_i$.

Margins and normalized margins associated with QRG1 are now given by

$$
\begin{aligned}
mQRG1(\mathbf{e}_i) &= QRG1 - pQRG1(\mathbf{e}_i) \\
&= 10^{-4}\,\text{yr}^{-1} - pQRG1(\mathbf{e}_i)
\end{aligned}
\tag{6.30}
$$

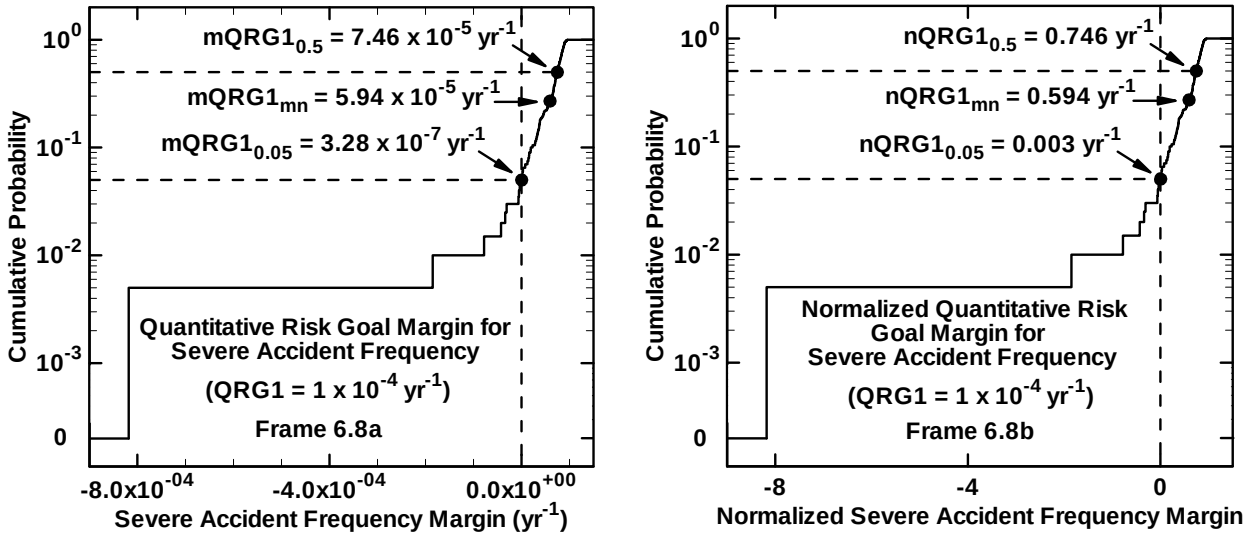

Fig. 6.8. Estimated CDFs for margins associated with quantitative risk goal QRG1 for accidents resulting from internal initiators at Surry: (a) margin *mQRG*1 (see Eq. (6.26)), and (b) normalized margin *nQRG*1 (see Eq. (6.27)).

and

$$nQRG1(\mathbf{e}_i) = \left[QRG1 - pQRG1(\mathbf{e}_i)\right] \Big/ QRG1 = \left[10^{-4}\,\mathrm{yr}^{-1} - pQRG1(\mathbf{e}_i)\right] \Big/ 10^{-4}\,\mathrm{yr}^{-1}, \tag{6.31}$$

respectively, for i = 1, 2, …, $nLHS$ = 200 (Fig. 6.8).

As discussed in conjunction with Eqs. (6.16) – (6.23), the results in Figs. 6.7 and 6.8 can be reduced to single number summaries of the "margin/uncertainty" form. As for safety goal SG1, examples include

$$mQRG1_{mn} \big/ \left(mQRG1_{mn} - mQRG1_{0.05}\right) = 5.94\times10^{-5} \Big/ \left(5.94\times10^{-5} - 3.28\times10^{-7}\right) = 1.01, \tag{6.32}$$

$$mQRG1_{0.5} \big/ \left(mQRG1_{0.5} - mQRG1_{0.05}\right) = 7.46\times10^{-5} \Big/ \left(7.46\times10^{-5} - 3.28\times10^{-7}\right) = 1.00, \tag{6.33}$$

$$mQRG1_{mn} \big/ \left(mQRG1_{mn} - mQRG1_{min}\right) = 5.94\times10^{-5} \Big/ \left[5.94\times10^{-5} - \left(-8.20\times10^{-4}\right)\right] = 0.068, \tag{6.34}$$

and

$$mQRG1_{0.5} \big/ \left(mQRG1_{0.5} - mQRG1_{min}\right) = 7.46\times10^{-5} \Big/ \left[7.46\times10^{-5} - \left(-8.20\times10^{-4}\right)\right] = 0.083, \tag{6.35}$$

with $mQRG1_{mn}$, $mQRG1_q$ and $mQRG1_{min}$ defined similary to $mSG1_{mn}$, $mSG1_q$ and $mSG1_{mn}$ in conjunction with Eqs. (6.16) – (6.19).

Quantitative Risk Goal QRG2. Quantitative risk goal QRG2 specifies that the probability of containment failure given the occurrence of a severe accident will be less than 0.1. For this risk goal, an exact definition for containment failure has not been specified. Thus, it is the responsibility of the individuals (i.e., analysts) charged with carrying out the analysis to formulate this definition. This is certainly a situation that could occur in QMU analyses for weapons systems when all aspects of a requirement have not been fully and unambiguously specified. Further, given that risk goal QRG2 places a bound on the conditional probability of an undesirable event given a particular type of accident, this goal is identical in concept to the Walske criterion [144] for accidents involving nuclear weapons (i.e., the requirement that the probability of inadvertent detonation conditional on the occurrence of a credible accident is to be less than 10^{-6}).

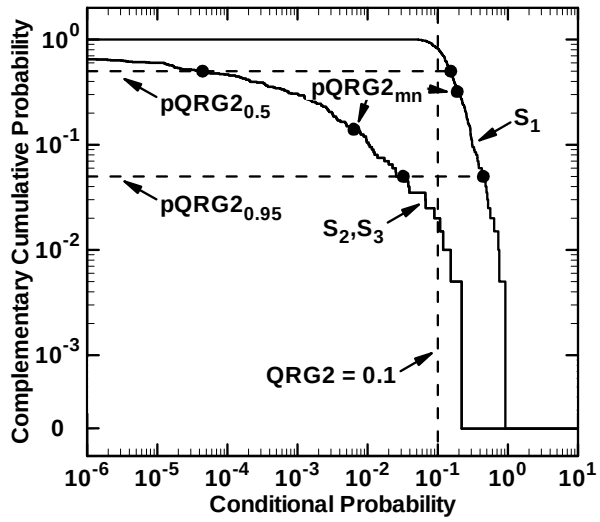

Fig. 6.9. Estimated CCDFs for conditional probability of containment failure given a severe accident resulting from internal initiators at Surry (see Eqs. (6.39) and (6.40)).

For the analyses presented in Ref. [118], three possible sets of accidents are proposed for use in the evaluation of quantitative risk goal QRG2:

$\mathcal{S}_1 = \{$**a**: **a** involves core damage and the containment fails (by a leak, rupture or catastrophic rupture) or a containment bypass occurs or a steam generator tube rupture occurs$\}$. (6.36)

$\mathcal{S}_2 = \{$**a**: **a** involves core damage and the containment fails by rupture or catastrophic rupture$\}$. (6.37)

and

$\mathcal{S}_3 = \{$**a**: **a** involves vessel failure and the containment fails by rupture or catastrophic rupture$\}$. (6.38)

The following ordering exists: $\mathcal{S}_3 \subset \mathcal{S}_2 \subset \mathcal{S}_1$. Further, in the Surry analysis in use as an example, the equality $\mathcal{S}_3 = \mathcal{S}_2$ was found to exist (i.e., rupture and catastrophic rupture of the containment only occurred in conjunction with vessel failure).

Given the preceding sets involving core damage and containment failure, possible definitions for the conditional probabilities specified in risk goal QRG2 are

$$pQRG2_k = p_A(\mathcal{S}_k)/p_A(\mathcal{S}) \tag{6.39}$$

for k = 1, 2, 3, where

$$\mathcal{S} = \{\mathbf{a} : \mathbf{a} \text{ involves core damage}\}.$$

In practice, the sets $\mathcal{S}_1$, $\mathcal{S}_2$, $\mathcal{S}_3$, $\mathcal{S}$ and also their probabilities depend on values for uncertain variables contained in **e**. As a result, the equality in Eq. (6.39) is more appropriately written as

$$pQRG2_k(\mathbf{e}) = p_A[\mathcal{S}_k(\mathbf{e})]/p_A[\mathcal{S}(\mathbf{e})] \tag{6.40}$$

to emphasize the dependence on **e**. In concept, $p_A[\mathcal{S}_k(\mathbf{e})]$ and $p_A[\mathcal{S}(\mathbf{e})]$ are defined by complex integrals involving the probability space ($\mathcal{A}$, $\mathbb{A}$, p_A) for aleatory uncertainty and a large amount of underlying analysis. In the analysis being used as example, the discretization procedure summarized in conjunction with Eq. (43) of Ref. [118] is used in the evaluation of $p_A[\mathcal{S}_k(\mathbf{e})]$ and hence $pQRG2_k(\mathbf{e})$.

Each of the $nLHS$ = 200 LHS elements results in estimates $pQRG2_k(\mathbf{e}_i)$, k = 1, 2, 3, for the conditional probability of containment failure given core damage (Fig. 6.9).

In turn, margins and normalized margins associated with QRG2 are given by

$$\begin{aligned} mQRG2_k(\mathbf{e}_i) &= QRG2 - pQRG2_k(\mathbf{e}_i) \\ &= 0.1 - pQRG2_k(\mathbf{e}_i) \end{aligned} \tag{6.41}$$

and

$$\begin{aligned} nQRG2_k(\mathbf{e}_i) &= [QRG2 - pQRG2_k(\mathbf{e}_i)]/QRG2 \\ &= [0.1 - pQRG2_k(\mathbf{e}_i)]/0.1 \end{aligned} \tag{6.42}$$

respectively, for i = 1, 2, …, $nLHS$ = 200 (Fig. 6.10).

As discussed in Ref. [118], an alternate and possibly more appropriate definition for the conditional probability associated with QRG2 is

$$pQRG2_k(\mathbf{e}) = p_A[\mathcal{SC}_k(\mathbf{e})]/p_A[\mathcal{SC}(\mathbf{e})], \tag{6.43}$$

where

$$\mathcal{SC}(\mathbf{e}) = \{\mathbf{a} : \mathbf{a} \text{ involves vessel breach}\}$$

and

$$\mathcal{SC}_k(\mathbf{e}) = \mathcal{S}_k(\mathbf{e}) \cap \mathcal{SC}(\mathbf{e})$$

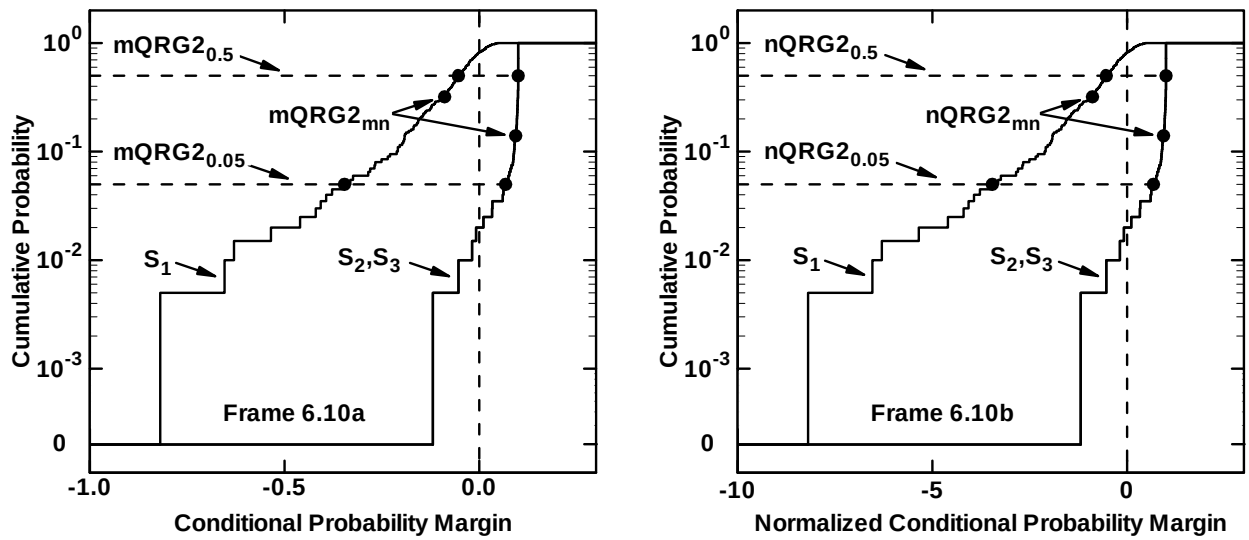

Fig. 6.10. Estimated CDFs for margins associated with quantitative risk goal QRG2 for accidents resulting from internal initiators at Surry: (a) margins $mQRG2_k$, k = 1, 2, 3 (see Eq. (6.41)), and (b) normalized margins $nQRG2_k$, k = 1, 2, 3 (see Eq.(6.42)).

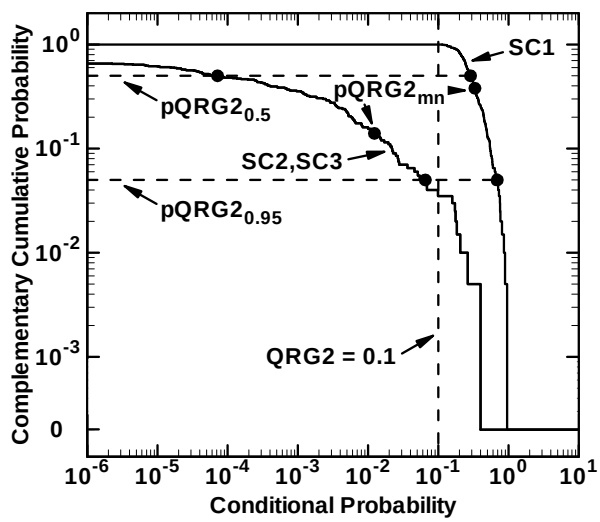

Fig. 6.11. Estimated CCDFs for conditional probability of containment failure given a severe accident with vessel breach resulting from internal initiators at Surry (see Eq. (6.43)).

for k = 1, 2, 3. This results in QRG2 being a more demanding requirement because the required probability is now conditional on a more severe accident (i.e., an accident involving vessel breach rather than core damage), which in turn tends to raise the value for this probability. In the analysis being used as an example, the discretization procedure summarized in conjunction with Eq. (48) of Ref. [118] is used in the evaluation of $p_A[\mathcal{SC}_k(\mathbf{e})]$, $p_A[\mathcal{SC}(\mathbf{e})]$ and hence $pQRG2_k(\mathbf{e})$ as defined in Eq. (6.43). The resultant conditional probabilities and margins for the $nLHS$ = 200 LHS elements are summarized in Figs. 6.11 and 6.12, respectively.

Although not presented, various results in the form of "margin/uncertainty" can also be calculated for the indicated variants of quantitative risk goal QRG2 as shown in Eqs. (6.16) – (6.23).

Note: The results in Figs. 6.9 – 6.12 were calculated from original Surry results saved in Ref. [145]. The results in Figs. 6.9 and 6.11 differ from what should be corresponding results in Figs. 6 and 7 of Ref. [118]. Checking has not revealed any errors in the generation of Figs. 6.9 and 6.11; unfortunately, the program used to generate Figs. 6 and 7 of Ref. [118] is no longer available. Given that all other figures Sect. 6.1 were also generated directly from original results contained in Ref. [145] and are the same as corresponding results contained in Ref. [118], it is felt that the results in Figs. 6.9 and 6.11 are correct.

Quantitative Risk Goal QRG3. Quantitative risk goal QRG3 specifies that the frequency of a large release will be less than 10^{-6} yr^{-1}. The guidance associated with risk goal QRG3 defines a large release as a release that has the potential to cause an early fatality, although the word "potential" is not defined. Thus, a decision must be made as to exactly what constitutes the potential to cause an early fatality. The analysis reported in Ref. [118] considers exceedance frequencies

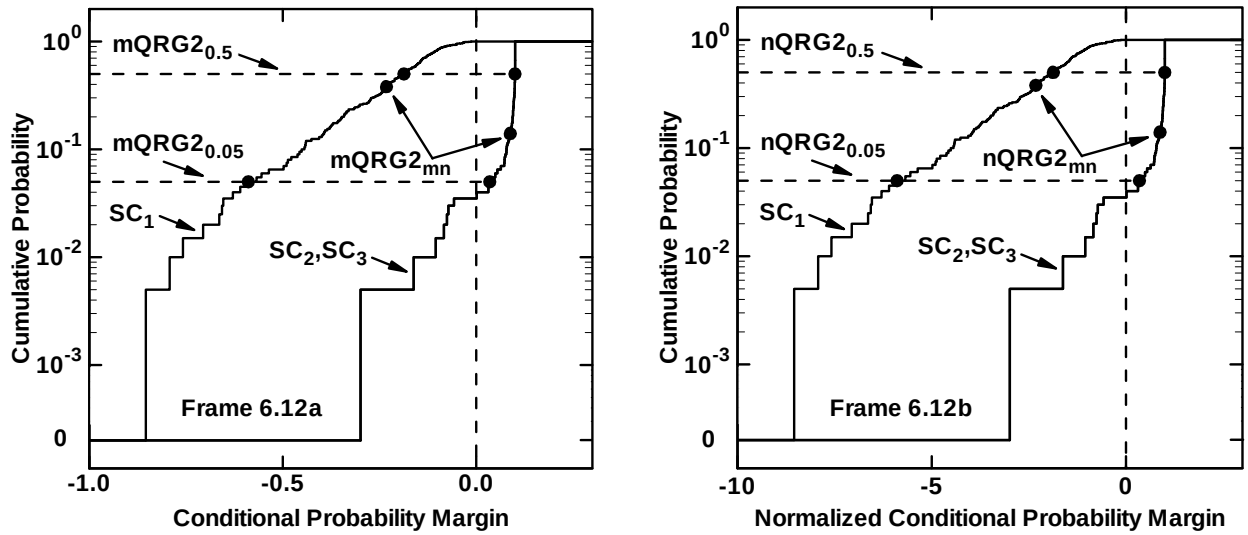

Fig. 6.12. Estimated CDFs for margins associated with quantitative risk goal QRG2 conditional on vessel breach for accidents resulting from internal initiators at Surry: (a) margins $mQRG2_k$, k = 1, 2, 3 (see Eq. (6.41) with $pQRG2_k(\mathbf{e})$ defined in Eq. (6.43)), and (b) normalized margins $nQRG2_k$, k = 1, 2, 3 (see Eq. (6.42) with $pQRG2_k(\mathbf{e})$ defined in Eq. (6.43)).

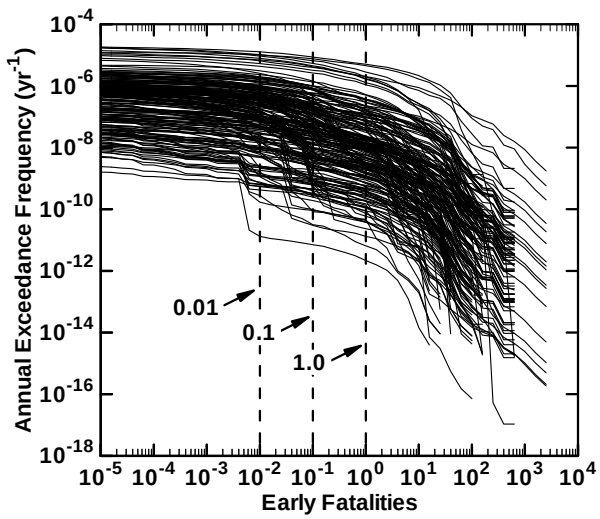

Fig. 6.13. Exceedance frequency curves for early fatalities due to accidents resulting from internal initiators at Surry (Ref. [117], Fig. D.1). Each curve corresponds to one sample element.

(i.e., annual probabilities of exceeding) for three numbers of early fatalities as possible threshold levels for "potential" to cause an early fatality. These early fatality members are 0.01, 0.1 and 1. Values less than 1 early fatality result because low levels of radiation have a probability of causing an early fatality that is considerably less than 1 and also because most of the potentially-exposed population (i.e., 99.5%) is assumed to evacuate.

The initial step in obtaining results for comparison with risk goal QRG3 is to determine the exceedance frequency curves for number of early fatalities, with one exceedance frequency curve resulting for each of the $nLHS$ = 200 LHS sample elements $\mathbf{e}_i$. The result of this calculation is summarized in Fig. 6.13. Specifically, each curve in Fig. 6.13 is conditional on the value for epistemically uncertain variables contained in an LHS element $\mathbf{e}_i$ and defines the frequencies of exceeding different numbers of early fatalities. The construction of the exceedance frequency curves in Fig. 6.13 is summarized in Ref. [118].

Early fatality levels of 0.01, 0.1 and 1 have been posited as possibly appropriate values for correspondence with "potential" to cause an early fatality. In the following, $pQRG3_1(\mathbf{e})$, $pQRG3_2(\mathbf{e})$ and $pQRG3_3(\mathbf{e})$ are used to represent the frequency (yr^{-1}) of exceeding early fatality values of 0.01, 0.1 and 1, respectively, conditional on the values for epistemically uncertain analysis inputs contained in $\mathbf{e}$. For the LHS of size $nLHS$ = 200 under consideration, each LHS element $\mathbf{e}_i$ results in values for $pQRG3_1(\mathbf{e}_i)$, $pQRG3_2(\mathbf{e}_i)$ and $pQRG3_3(\mathbf{e}_i)$. These values correspond to the exceedance frequencies on the ordinate of Fig. 6.13 associated with the vertical lines originating at 0.01, 0.1 and 1 on the abscissa. The resultant estimated CCDFs for $pQRG3_k(\mathbf{e})$, k = 1, 2, 3, are presented in Fig. 6.14.

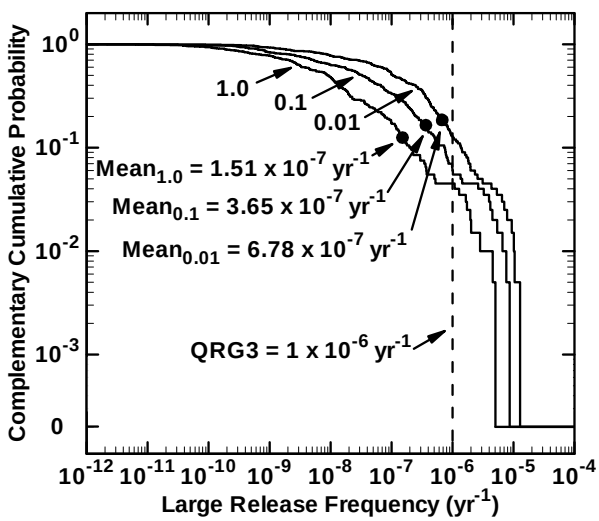

Fig. 6.14. Estimated CCDFs of large release frequency for accidents resulting from internal initiators at Surry.

In turn, margins associated with the three possible definitions of "potential" to cause an early fatality in QRG3 are given by

$$\begin{aligned} mQRG3_k\left(\mathbf{e}_i\right) &= QRG3 - pQRG3_k\left(\mathbf{e}_i\right) \\ &= 10^{-6}\ \mathrm{yr}^{-1} - pQRG3_k\left(\mathbf{e}_i\right) \end{aligned} \tag{6.44}$$

and

$$\begin{aligned} nQRG3_k\left(\mathbf{e}_i\right) &= \left[QRG3 - pQRG3_k\left(\mathbf{e}_i\right)\right] \big/ QRG3 \\ &= \left[10^{-6}\ \mathrm{yr}^{-1} - pQRG3_k\left(\mathbf{e}_i\right)\right] \big/ 10^{-6}\ \mathrm{yr}^{-1}, \end{aligned} \tag{6.45}$$

respectively, for $i = 1, 2, \ldots, nLHS = 200$ (Fig. 6.15).

Although not shown, various results in the form of "margin/uncertainty" can also be calculated for the indicated variants of risk goal QRG3 as shown in Eqs. (6.16) – (6.23).

6.2 Regulatory Requirements for Waste Isolation Pilot Plant (WIPP)

The Waste Isolation Pilot Plant (WIPP) in Southeastern New Mexico has been developed by the DOE for the geologic disposal of transuranic (TRU) waste generated at government defense installations in the United States. For the WIPP to be certified for operation, the DOE had to establish that the WIPP met regulatory standards promulgated by the EPA. Like the NRC's safety goals for nuclear power stations discussed in Sect. 6.1, the EPA's standards for the WIPP have aspects that are very similar to what might be expected in a QMU analysis that involves the incorporation and representation of the effects of aleatory and epistemic uncertainty. As a result, the EPA's standards for the WIPP provide another example of the ideas and challenges that are likely to be encountered in a nontrivial application of QMU. Specifically, results from the performance assessment (PA) that supported the successful Compliance Certification Application (CCA) for WIPP to the EPA [20] are used as another example to illustrate what a QMU analysis involving both aleatory and epistemic uncertainty is likely to involve.

An article summarizing the PA that supported the CCA for WIPP [146] is reproduced in App. D and will be referred to in the following discussion as a convenient and accessible source of additional information on this analysis. Inclusion of this article in App. D makes it possible to have a moderately detailed description of the analysis under consideration as part of this report. More detailed analysis descriptions are available in Refs. [20; 21] and in a number of additional detailed technical reports cited in the two preceding references.

The conceptual structure of the 1996 WIPP PA ultimately derives from the regulatory requirements imposed on this facility [147; 148]. The primary regulation determining this structure is the EPA's standard for the geologic disposal of radioactive waste (40 CFR 191) [148; 149], which is divided into three parts. Subpart A applies to a disposal facility prior to decommissioning and limits annual radiation doses to members of the public from waste management and storage operations. Subpart B applies after decommissioning and sets probabilistic limits on cumulative releases of radionuclides to the accessible environment for 10,000 years (40 CFR 191.13) and assurance requirements to provide confidence that 40 CFR 191.13 will be met (40 CFR 191.14). Subpart B also sets limits on radiation doses to members of the public in the accessible environment for 10,000 years of undisturbed performance (40 CFR 191.15). Subpart C limits radioactive contamination of certain sources of groundwater for 10,000 years after disposal (40 CFR 191.24). Subparts A, B and C all have requirements that could be used as illustrations of QMU-type analyses. This presentation uses the Subpart B release requirements for illustration owing to the fundamental role that these requirements played in the design and implementation of the analyses that supported the WIPP's CCA.

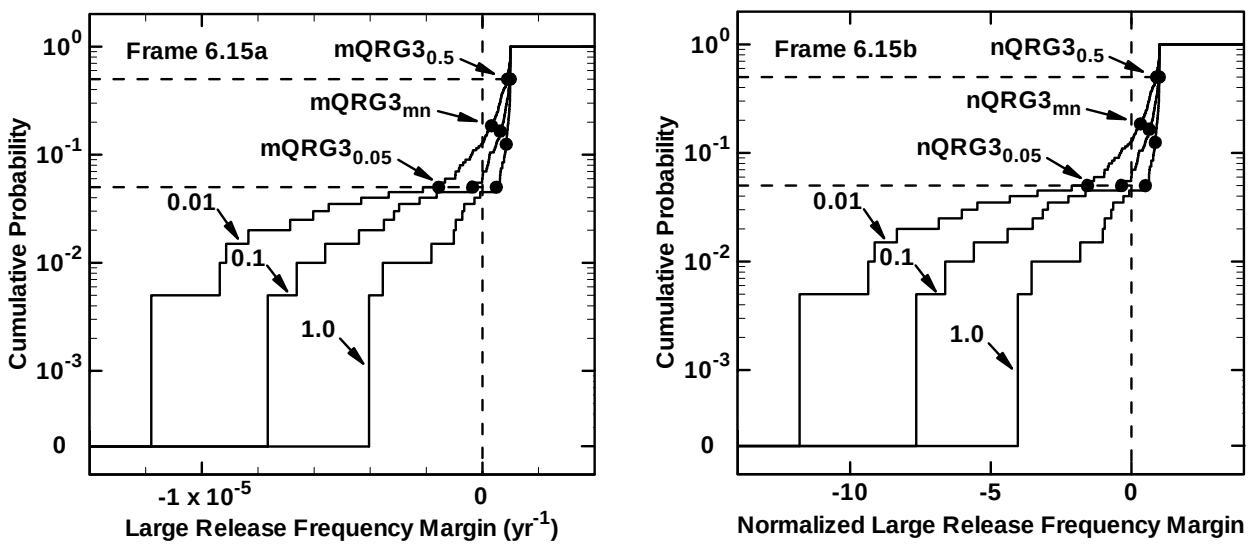

Fig. 6.15. Estimated CDFs for margins associated with quantitative risk goal QRG3 for accidents resulting from internal initiators at Surry: (a) margins $mQRG3_k$, k = 1, 2, 3 (see Eq. (6.44)) and (b) normalized margins $nQRG3_k$, k = 1, 2, 3 (see Eq. (6.45)).

The following is the central requirement in 40 CFR 191, Subpart B, and the primary determinant of the conceptual structure of the 1996 WIPP PA (Ref. [150], p. 38086):

> § 191.13 Containment requirements:
>
> (a) Disposal systems for spent nuclear fuel or high-level or transuranic radioactive wastes shall be designed to provide a reasonable expectation, based upon performance assessments, that cumulative releases of radionuclides to the accessible environment for 10,000 years after disposal from all significant processes and events that may affect the disposal system shall: (1) Have a likelihood of less than one chance in 10 of exceeding the quantities calculated according to Table 1 (Appendix A); and (2) Have a likelihood of less than one chance in 1,000 of exceeding ten times the quantities calculated according to Table 1 (Appendix A).
>
> (b) Performance assessments need not provide complete assurance that the requirements of 191.13(a) will be met. Because of the long time period involved and the nature of the events and processes of interest, there will inevitably be substantial uncertainties in projecting disposal system performance. Proof of the future performance of a disposal system is not to be had in the ordinary sense of the word in situations that deal with much shorter time frames. Instead, what is required is a reasonable expectation, on the basis of the record before the implementing agency, that compliance with 191.13(a) will be achieved.

Containment Requirement 191.13(a) refers to "quantities calculated according to Table 1 (App. A)," which means a normalized radionuclide release to the accessible environment based on the type of waste being disposed of, the initial waste inventory, and the release that takes place (Ref. [150], Appendix A). The indicated table specifies allowable releases (i.e., release limits) for individual radionuclides and is reproduced as Table I of Ref. [146]. The WIPP is intended for TRU waste, which is defined to be "waste containing more than 100 nanocuries of alpha-emitting transuranic isotopes, with half-lives greater than twenty years, per gram of waste" (Ref. [150], p. 38084). The normalized release R for transuranic waste is defined by

$$R = \sum_i \left(Q_i / L_i\right)\left(1\times 10^6 \text{ Ci}/C\right), \tag{6.46}$$

where Q_i is the cumulative release of radionuclide i to the accessible environment during the 10,000-year period following closure of the repository (Ci), L_i is the release limit for a radionuclide i given in Table I of Ref. [146] (Ci), 1×10^6 Ci is a normalization term, and C is the amount of transuranic waste emplaced in the repository (Ci). The normalized release R is unitless as a result of the release limit being scaled by the inventory of the repository; for convenience, R will be referred to as being in "EPA units." In the 1996 WIPP PA, $C = 3.44 \times 10^6$ Ci [151].

A full reading of the explanatory material associated with "Table 1 (Appendix A)" of Ref. [150] establishes that the intent of the containment requirement in 191.13(a) is that the normalized release R defined in Eq. (6.46) is to have a probability of less than 0.1 of exceeding 1 and a probability of less than 10^{-3} of exceeding 10. Specifically, this component of the regulatory requirements placed on the WIPP can be summarized as follows:

> The probability of exceeding a normalized release of size $RL1 = 1$ over 10^4 years must be less than $RP1 = 0.1$ (RL1)

> The probability of exceeding a normalized release of size $RL2 = 10$ over 10^4 years must be less than $RP2 = 10^{-3}$. (RL2)

The EPA also promulgated 40 CFR 194 [152], where the following elaboration on the intent of 40 CFR 191.13 is given (Ref. [152], pp. 5242-5243):

> *§ 194.34 Results of performance assessments.* (a) The results of performance assessments shall be assembled into "complementary, cumulative distribution functions" (CCDFs) that represent the probability of exceeding various levels of cumulative release caused by all significant processes and events. (b) Probability distributions for uncertain disposal system parameter values used in performance assessments shall be developed and documented in any compliance application. (c) Computational techniques, which draw random samples from across the entire range of the probability distributions developed pursuant to paragraph (b) of this section, shall be used in generating CCDFs and shall be documented in any compliance application. (d) The number of CCDFs generated shall be large enough such that, at cumulative releases of 1 and 10, the maximum CCDF generated exceeds the 99th percentile of the population of CCDFs with at least a 0.95 probability. (e) Any compliance application shall display the full range of CCDFs generated. (f) Any compliance application shall provide information which demonstrates that there is at least a 95 percent level of statistical confidence that the mean of the population of CCDFs meet the containment requirements of § 191.13 of this chapter.

The requirements placed on PAs for the WIPP in the quoted material from 191.13 and 194.34 clearly indicate an analysis that involves the three basic entities indicated in Sect. 3.2: EN1, a probability space ($\mathcal{A}$, $\mathbb{A}$, p_A) for aleatory uncertainty; EN2, a model for predicting system behavior; and EN3, a probability space ($\mathcal{E}$, $\mathbb{E}$, p_E) for epistemic uncertainty. The CCDFs indicated in 194.34 derive from aleatory uncertainty and define the exceedance probabilities associated with normalized releases of 1 and 10 in the containment requirements in 191.13(a). The determination of the releases themselves requires the extensive use of models for repository behavior and the movement of radionuclides away from the repository and ultimately to the accessible environment. Statements in both 191.13(b) and 194.34 indicate the importance of an adequate treatment of epistemic uncertainty. In particular, the statements in 194.34(b) – (f) all relate to various aspects of the treatment of epistemic uncertainty in a PA for the WIPP. With respect to terminology, the WIPP PA used the terms stochastic and subjective for the now more widely used terms aleatory and epistemic, respectively.

An overview of the definition of the probability space ($\mathcal{A}$, $\mathbb{A}$, p_A) for aleatory uncertainty is given in Sect. 4 of Ref. [146]. Specifically, the sample space $\mathcal{A}$ is defined by

$$\mathcal{A} = \{\mathbf{a}\text{: } \mathbf{a} \text{ is a possible 10,000 year sequence of occurrences at the WIPP}\}. \tag{6.47}$$

The development process for the WIPP PA identified drilling for natural resources as the only disruption with sufficient likelihood and consequence for inclusion in the definition of EN1 (Ref. [146], Sect. 3; Ref. [20], Appendix SCR). In addition, 40 CFR 194 specifies that the possible occurrence of mining within the land withdrawal boundary must be included in the analysis. The preceding considerations led to the elements $\mathbf{a}$ of $\mathcal{A}$ being vectors of the form

$$\begin{aligned}\mathbf{a} = \big[&\underbrace{t_1, l_1, e_1, b_1, p_1, \mathbf{a}_1,}_{\text{1st intrusion}} \quad \underbrace{t_2, l_2, e_2, b_2, p_2, \mathbf{a}_2,}_{\text{2nd intrusion}} \\ &\ldots, \underbrace{t_n, l_n, e_n, b_n, p_n, \mathbf{a}_n,}_{n\text{th intrusion}} \quad t_{min}\big],\end{aligned} \tag{6.48}$$

where n is the number of drilling intrusions, t_i is the time (years) of the ith intrusion, l_i designates the location of the ith intrusion, e_i designates the penetration of an excavated or nonexcavated area by the ith intrusion, b_i designates whether or not the ith intrusion penetrates pressurized brine in the Castile Formation, p_i designates the plugging procedure used with the ith intrusion, $\mathbf{a}_i$ designates the type of waste penetrated by the ith intrusion, and t_{min} is the time at which potash mining occurs

within the land withdrawal boundary. Additional information on the elements of **a** and their probabilistic characterization is given in Table III of Ref. [146] and in Ref. [153].

The WIPP PA used a variety of mathematical models and techniques in the determination of radionuclide releases to the accessible environment. A summary of these models and techniques is given in Sect. 5 of Ref. [146]. Additional information is available in individual articles in a special journal issue devoted to the WIPP PA in support of the CCA [21].

An overview of the definition of the probability space ($\mathcal{E}$, $\mathbb{E}$, p_E) for epistemic uncertainty is given in Sect. 6 of Ref. [146]. Specifically, the sample space $\mathcal{E}$ is defined by

$$\mathcal{E} = \{\mathbf{e}\text{: } \mathbf{e} \text{ is possibly the correct vector of parameter values to use in the WIPP PA models}\}. \tag{6.49}$$

The elements **e** of $\mathcal{E}$ are vectors of the form

$$\mathbf{e} = [e_1, e_2, \ldots, e_{nE}] = [e_1, e_2, \ldots, e_{57}], \tag{6.50}$$

where each of the $nE = 57$ elements of **e** is an epistemically uncertain input of the WIPP PA. Examples of the elements of **e** are given in Table V of Ref. [146]. A full listing of the elements of **e** and description of their probabilistic characterization is given in Ref. [154]. In the WIPP PA, all elements of **e** are quantities used in models for physical processes. Thus, technically, ($\mathcal{E}$, $\mathbb{E}$, p_E) as defined for the WIPP PA corresponds to the probability space ($\mathcal{EM}$, $\mathbb{EM}$, p_{EM}) introduced in Sect. 3.2.

The regulatory requirements summarized in (RL1) and (RL2) can be represented by the vector

$$\mathbf{R} = [RL1, RL2] = [1, 10], \tag{6.51}$$

where $RL1$ and $RL2$ are the maximum acceptable normalized releases over 10^4 years with exceedance probabilities of 0.1 and 10^{-3}, respectively. Similarly, the estimated performance of the WIPP can be represented by the vector

$$\mathbf{P} = [pRL1, pRL2], \tag{6.52}$$

where $pRL1$ and $pRL2$ are the performance values calculated for comparison with the corresponding elements of **R**. The quantities $pRL1$ and $pRL2$ are quantile values that derive from aleatory uncertainty. Specifically, $pRL1$ is the normalized release associated with an exceedance probability of 0.1 and thus corresponds to the 0.9 quantile of the distribution of normalized releases, and $pRL2$ is the normalized release associated with an exceedance probability of 10^{-3} and thus corresponds to the 0.999 quantile of the distribution of normalized releases. The determination of $pRL1$ and $pRL2$ in effect requires the solution of integral equations to determine quantiles (see Sect. 3.5). As summarized in Sect. 9 of Ref. [146] and described in more detail in Refs. [96; 153; 155-157], the WIPP PA uses a Monte Carlo procedure to construct the CCDF for normalized release and thus, in effect, solve the integral equations that define $pRL1$ and $pRL2$.

If the probability space ($\mathcal{A}$, $\mathbb{A}$, p_A) was known precisely and all additional quantities required in the evaluation of **P** were also known precisely, then the vector **M** of margins would be unambiguously defined by

$$\mathbf{M} = [mRL1, mRL2], \tag{6.53}$$

where

$$mRL1 = RL1 - pRL1 = 1 - pRL1$$

$$mRL2 = RL2 - pRL2 = 10 - pRL2.$$

The WIPP PA did not consider any uncertainty in the definition of the probability space ($\mathcal{A}$, $\mathbb{A}$, p_A) for aleatory uncertainty but did consider the uncertainty associated with the modeling physical process in the determination of $pRL1$ and $pRL2$ (see Eq. (6.50)). As a result, **P** is actually a function

$$\mathbf{P}(\mathbf{e}) = [pRL1(\mathbf{e}), pRL2(\mathbf{e})] \tag{6.54}$$

of vectors $\mathbf{e} \in \mathcal{E}$, where ($\mathcal{E}$, $\mathbb{E}$, p_E) is the probability space for epistemic uncertainty. As a result the vector **M** of margins has the form

$$\begin{aligned}\mathbf{M}(\mathbf{e}) &= \mathbf{R} - \mathbf{P}(\mathbf{e}) \\ &= [1 - pRL1(\mathbf{e}), 10 - pRL2(\mathbf{e})] \\ &= [mRL1(\mathbf{e}), mRL2(\mathbf{e})]\end{aligned} \tag{6.55}$$

and is thus epistemically uncertain with $mRL1(\mathbf{e})$ and $mRL2(\mathbf{e})$ having distributions that derive from the probability space ($\mathcal{E}$, $\mathbb{E}$, p_E) for epistemic uncertainty.

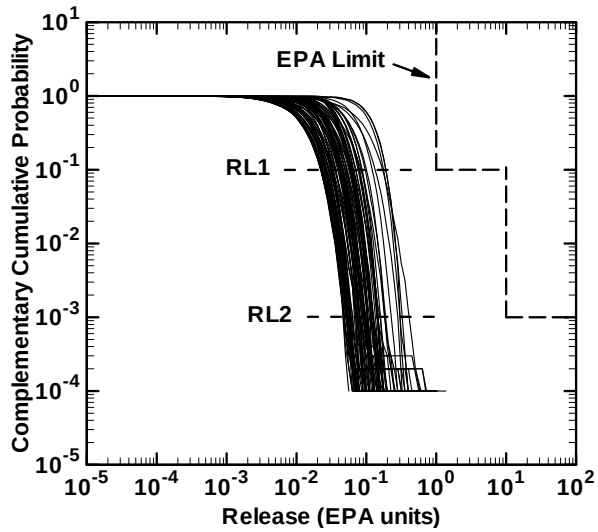

Fig. 6.16. Estimated CCDFs for normalized release over 10^4 years generated for an LHS of size *nLHS* = 100 from *nE* = 57 epistemically uncertain analysis inputs and samples of size 10,000 from the sample space $\mathcal{A}$ for aleatory uncertainty.

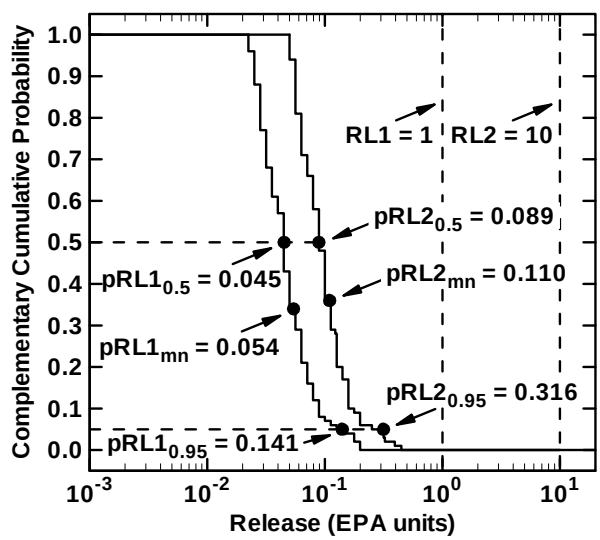

Fig. 6.17. Estimated CCDFs for normalized releases associated with exceedance probabilities of 0.1 and 10^{-3} in Fig. 6.16.

The WIPP PA used a sampling-based approach to the propagation of epistemic uncertainty. Specifically, an LHS

$$\mathbf{e}_i = \left[e_{i1}, e_{i2}, \ldots, e_{i,57}\right], i = 1, 2, \ldots, nLHS, \tag{6.56}$$

of size *nLHS* = 100 from the *nE* = 57 uncertain variables under consideration was used in the generation of CCDFs for normalized release. Further, the CCDF for each sample element $\mathbf{e}_i$ was generated with a random sample of size 10,000 from the sample space $\mathcal{A}$ for aleatory uncertainty. The result is the 100 CCDFs for normalized release in Fig. 6.16.

To establish compliance with all the conditions specified in 194.34, the WIPP PA actually used three replicated (i.e., independently generated) LHSs of size *nLHS* = 100, which resulted in a total sample size of 300 (see [158] and Sects. 6 and 7 of Ref. [154] for discussion). The indicated replicated samples were used to establish the adequacy of an LHS of size 100 for the generation of uncertainty and sensitivity analysis results in the WIPP PA. The results used for illustration in this presentation are for the first of the three replicated samples (i.e., the replicate designated *R*1 in the WIPP PA).

The normalized releases $pRL1(\mathbf{e}_i)$ and $pRL2(\mathbf{e}_i)$ that result for the LHS in Eq. (6.56) correspond to the normalized releases on the abscissa of Fig. 6.16 associated with the locations where the individual CCDFs are crossed by the two indicated horizontal lines (Fig. 6.17).

In turn, the corresponding margins $mRL1(\mathbf{e}_i)$ and $mRL2(\mathbf{e}_i)$ are defined as indicated in Eq. (6.55) (Fig. 6.18). Normalized margins of the form

$$nRL1(\mathbf{e}_i) = mRL1(\mathbf{e}_i)/RL1 = mRL1(\mathbf{e}_i)/1 \tag{6.57}$$

and

$$nRL2(\mathbf{e}_i) = mRL2(\mathbf{e}_i)/RL2 = mRL2(\mathbf{e}_i)/10 \tag{6.58}$$

can also be defined but effectively replicate the results in Fig. 6.18 as $nRL1(\mathbf{e}_i) = mRL1(\mathbf{e}_i)$ and $nRL2(\mathbf{e}_i) = mRL1(\mathbf{e}_i)/10$.

The estimated CCDFs and CDFs in Figs. 6.17 and 6.18 summarize all available information about the uncertainty in margins associated with compliance with the release requirements RL1 and RL2. Various results in the form of "margin/uncertainty" can also be calculated for requirements RL1 and RL2 as indicated in Eqs. (6.16) – (6.23). For example, the following results can be calculated for requirement RL1:

$$\begin{aligned} &mRL1_{mn}/(mRL1_{mn} - mRL1_{0.05}) \\ &\quad = 0.9458/(0.9458 - 0.8741) \\ &\quad = 13.2, \end{aligned} \tag{6.59}$$

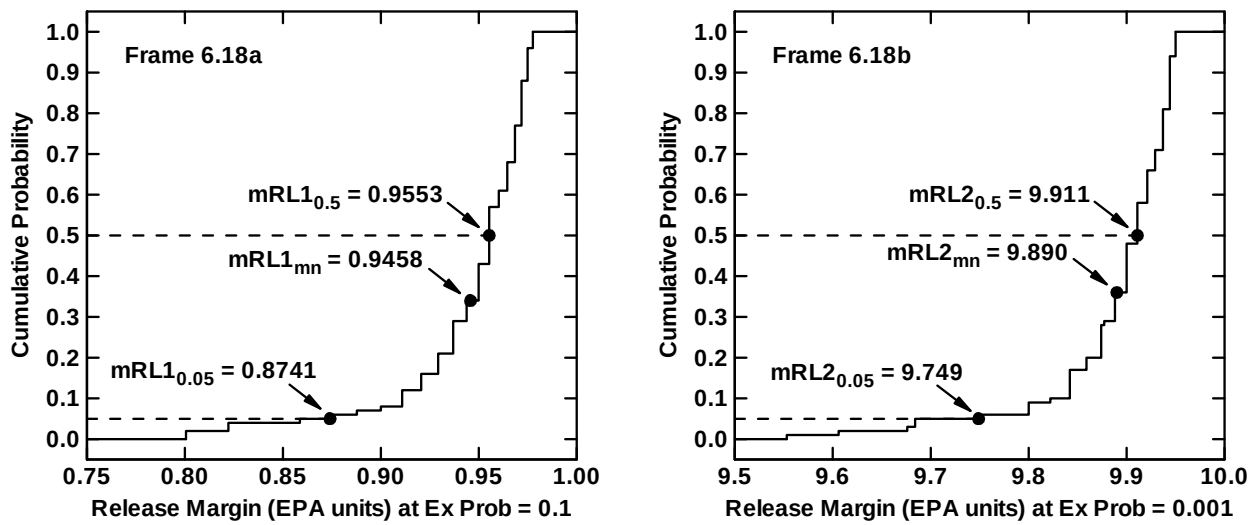

Fig. 6.18. Estimated CDFs for margins associated with normalized releases with exceedance probabilities of 0.1 and 10^{-3} in Fig. 6.16: (a) CDF for margin $mRL1(\mathbf{e})$ for exceedance probability of 0.1, and (b) CDF for margin $mRL2(\mathbf{e})$ for exceedance probability of 10^{-3}.

$$\begin{aligned} & mRL1_{0.5} / \left(mRL1_{0.5} - mRL1_{0.05} \right) \\ & \quad = 0.9553 / \left(0.9553 - 0.8741 \right) \\ & \quad = 11.8, \end{aligned} \tag{6.60}$$

$$\begin{aligned} & mRL1_{mn} / \left(mRL1_{mn} - mRL1_{min} \right) \\ & \quad = 0.9458 / \left(0.9458 - 0.8005 \right) \\ & \quad = 6.5, \end{aligned} \tag{6.61}$$

and

$$\begin{aligned} & mRL1_{0.5} / \left(mRL1_{0.5} - mRL1_{min} \right) \\ & \quad = 0.9553 / \left(0.9553 - 0.8005 \right) \\ & \quad = 6.2. \end{aligned} \tag{6.62}$$

Similar results can also be obtained for requirement RL2. However, information is lost in calculations of this type as they in effect reduce all the information in Fig. 6.16 to single numbers (see Sect. 4.5 for additional discussion).

If desired, the regulatory requirements RL1 and RL2 can also be represented by the vector

$$\mathbf{R} = \left[RP1,\ RP2 \right] = \left[0.1, 10^{-3} \right], \tag{6.63}$$

where $RP1$ and $RP2$ are the maximum acceptable probabilities for exceeding normalized releases of size 1 and 10, respectively. Similarly, the corresponding performance of the WIPP would be

$$\mathbf{P} = \left[pRP1,\ pRP2 \right], \tag{6.64}$$

where $pRP1$ and $pRP2$ are the performance values calculated for comparison with the corresponding elements of $\mathbf{R}$. Specifically $pRP1$ and $pRP2$ would be the exceedance probabilities deriving from aleatory uncertainty for normalized releases of size 1 and 10, respectively. Corresponding margins would then be defined by $\mathbf{R} - \mathbf{P}$. However, as essentially all values for $pRP1$ and $pRP2$ are zero in the present analysis as can be seen from Fig. 6.16, this formulation of margins does not result in a very interesting example.

The requirements in (RL1) and (RL2) in essence specify a boundary line beneath which the CCDF for normalized release is required to fall (Fig. 6.16). This corresponds to what is known as the Farmer limit line approach to the definition of acceptable risk [159-161]. This approach defines decreasing acceptable probabilities of occurrence for undesired consequences of increasing size. It is easy to envision that requirements of this type could be present in future QMU analyses.

6.3 Regulatory Requirements for Yucca Mountain Repository

The Yucca Mountain (YM) repository is under development by the DOE for the geologic disposal of high-level radioactive waste. For the YM repository to be licensed for operation, the DOE must establish that regulatory standards promulgated by the NRC are met. Like the NRC's safety goals for nuclear power stations discussed in Sect. 6.1 and the EPA's standards for the

WIPP discussed in Sect. 6.2, the NRC's standards for the YM repository have aspects that are very similar to what might be expected in a QMU analysis. As a result, the NRC's standards for the YM repository provide another example of the ideas and challenges that are likely to be encountered in a nontrivial application of QMU. Specifically, results from the PA that supported the 2008 license application to the NRC for the YM repository [22] are used as an additional example to illustrate a QMU analysis involving both aleatory and epistemic uncertainty.

Three articles summarizing the PA that supported the 2008 license application for the YM repository [162-164] are reproduced in App. E and will be referred to in the following discussion as convenient and accessible sources of additional information on this analysis. Inclusion of these articles in App. E makes it possible to have a moderately detailed description of the analysis under consideration as part of this report. More detailed analysis descriptions are available in Ref. [22] and in a number of additional detailed technical reports cited in this reference.

The regulations that relate to the YM repository are complex and specify a number of requirements that must be met for the repository to be licensed [165; 166]. This presentation will use one aspect of these regulations as an example: the maximum expected dose (mrem/yr) over 10^4 years to the reasonably maximally exposed individual (RMEI). The RMEI is a hypothetical individual with well-defined and time-invariant characteristics who is assumed to be exposed to potential radionuclide releases from the YM repository. For the purposes of this presentation, the indicated expected dose is assumed to be an expectation over aleatory uncertainty at individual points in time. As such, this expected dose is a surrogate for cancer risk as multiplication by an appropriate scalar converts expected dose to cancer risk.

The regulatory wording that defines the requirements with respect to expected dose to the RMEI is spread over multiple locations (e.g., see Refs. [163; 167] and a more detailed discussion in App. J of Ref. [22]). At the time of this writing, the most current NRC requiements for the YM repository are given in Ref. [168]. The following statement summarizes the requirement on expected dose to the RMEI for the initial 10^4 year period after repository closure as interpreted and implemented in the PA supporting the 2008 license application for the YM repository:

> The maximum expected dose to the RMEI over the first 10^4 years following repository closure shall be less than 15 mrem/yr. (YM1)

Further, a number of statements made by the NRC stress the importance of an appropriate representation of epistemic uncertainty in analyses supporting a license application for the YM repository (e.g., see Refs. [163; 167] and a more detailed discussion in App. J of Ref. [22]).

The NRC has specified an expected dose requirement for the time interval following the 10^4 year time period after repository closure and extending through the period of geologic stability, with the period of geologic stability assumed to end 10^6 years after repository closure [168]. This requirement can be summarized as follows:

> The maximum expected dose to the RMEI over the time interval [10^4, 10^6 yr] following repository closure shall be less than 100 mrem/yr. (YM2)

However, as noted above, the emphasis of this presentation is on the 10^4 year requirement.

As in the examples in Sects. 6.1 and 6.2, an analysis is under consideration that involves the three basic entities indicated in Sect. 3.2: EN1, a probability space ($\mathcal{A}$, $\mathbb{A}$, p_A) for aleatory uncertainty; EN2, a model for predicting dose to the RMEI; and EN3, a probability space ($\mathcal{E}$, $\mathbb{E}$, p_E) for epistemic uncertainty.

As already indicated, the expected dose to the RMEI is an expectation over aleatory uncertainty. Thus, there must be a probability space ($\mathcal{A}$, $\mathbb{A}$, p_A) for aleatory uncertainty. An overview of the definition of ($\mathcal{A}$, $\mathbb{A}$, p_A) is given in Sect. III of Ref. [163]. Conceptually, the sample space $\mathcal{A}$ for this probability space is

$$\mathcal{A} = \{\mathbf{a} : \mathbf{a} \text{ is a possible 10,000 year sequence of occurrences at the YM repository}\} \tag{6.65}$$

when occurrences over the time interval [0, 10^4 yr] are under consideration. Because of interest in results occurring both before and after 10^4 years, the sample space used in the 2008 YM PA to assess compliance with the requirement in (YM1) was defined for the time interval [0, 2×10^4 yr]; however, compliance with (YM1) was assessed for the time interval [0, 10^4 yr] as required.

After an extensive review and selection process [22], the following conditions/occurrences related to aleatory uncertainty were identified for inclusion in the 2008 YM PA: nominal (i.e., undisturbed) conditions, early waste package (WP) failure, early drip shield (DS) failure, igneous intrusive events, igneous eruptive events, seismic ground motion events, and seismic fault displacement events. Consistent with this, each aleatory future $\mathbf{a}$ can be represented by

$$\mathbf{a} = \left[nEW, nED, nII, nIE, nSG, nSF, \mathbf{a}_{EW}, \mathbf{a}_{ED}, \mathbf{a}_{II}, \mathbf{a}_{IE}, \mathbf{a}_{SG}, \mathbf{a}_{SF} \right] \tag{6.66}$$

where, for the time interval [0, 2 × 10^4 yr],

nEW = number of early WP failures,
nED = number of early DS failures,
nII = number of igneous intrusive events,
nIE = number of igneous eruptive events,
nSG = number of seismic ground motion events,
nSF = number of seismic fault displacement events,
$\mathbf{a}_{EW}$ = vector defining the nEW early WP failures,
$\mathbf{a}_{ED}$ = vector defining the nED early DS failures,
$\mathbf{a}_{II}$ = vector defining the nII igneous intrusive events,
$\mathbf{a}_{IE}$ = vector defining the nIE igneous eruptive events,
$\mathbf{a}_{SG}$ = vector defining the nSG seismic ground motion events,
$\mathbf{a}_{SF}$ = vector defining the nSF fault displacement events.

In turn, the vectors $\mathbf{a}_{EW}$, $\mathbf{a}_{ED}$, $\mathbf{a}_{II}$, $\mathbf{a}_{IE}$, $\mathbf{a}_{SG}$ and $\mathbf{a}_{SF}$ are of the form

$$\mathbf{a}_{EW} = \left[\mathbf{a}_{EW,1}, \mathbf{a}_{EW,2}, \ldots, \mathbf{a}_{EW,nEW} \right], \tag{6.67}$$

$$\mathbf{a}_{ED} = \left[\mathbf{a}_{ED,1}, \mathbf{a}_{ED,2}, \ldots, \mathbf{a}_{ED,nED} \right], \tag{6.68}$$

$$\mathbf{a}_{II} = \left[\mathbf{a}_{II,1}, \mathbf{a}_{II,2}, \ldots, \mathbf{a}_{II,nII} \right], \tag{6.69}$$

$$\mathbf{a}_{IE} = \left[\mathbf{a}_{IE,1}, \mathbf{a}_{IE,2}, \ldots, \mathbf{a}_{IE,nIE} \right], \tag{6.70}$$

$$\mathbf{a}_{SG} = \left[\mathbf{a}_{SG,1}, \mathbf{a}_{SG,2}, \ldots, \mathbf{a}_{SG,nSG} \right], \tag{6.71}$$

and

$$\mathbf{a}_{SF} = \left[\mathbf{a}_{SF,1}, \mathbf{a}_{SF,2}, \ldots, \mathbf{a}_{SF,nSF} \right], \tag{6.72}$$

where

$\mathbf{a}_{EW,j}$ = vector defining early WP failure j for j = 1, 2, …, nEW,
$\mathbf{a}_{ED,j}$ = vector defining early DS failure j for j = 1, 2, …, nED,
$\mathbf{a}_{II,j}$ = vector defining igneous intrusive event j for j = 1, 2, …, nII,
$\mathbf{a}_{IE,j}$ = vector defining igneous eruptive event j for j = 1, 2, …, nIE,
$\mathbf{a}_{SG,j}$ = vector defining seismic ground motion event j for j = 1, 2, …, nSG,
$\mathbf{a}_{SF,j}$ = vector defining seismic fault displacement event j for j = 1, 2, …, nSF.

Definitions of the vectors $\mathbf{a}_{EW,j}$, $\mathbf{a}_{ED,j}$, $\mathbf{a}_{II,j}$, $\mathbf{a}_{IE,j}$, $\mathbf{a}_{SG,j}$ and $\mathbf{a}_{SF,j}$ and their associated probabilistic characterizations are given in App. J of Ref. [22]. These definitions and probabilistic characterizations underlie the complete, though never fully stated, definition of the probability space ($\mathcal{A}$, $\mathbb{A}$, p_A) for aleatory uncertainty.

Determination of dose to the RMEI requires a function $D(\tau|\mathbf{a})$ such that

$D(\tau|\mathbf{a})$ = dose to RMEI (mrem/yr) at time τ (yr) conditional on the occurrence of the future represented by the element $\mathbf{a}$ of $\mathcal{A}$. (6.73)

Technically, $D(\tau|\mathbf{a})$ is the committed 50-yr dose to the RMEI that results from radiation exposure incurred in a single year. The function $D(\tau|\mathbf{a})$ is the result of combining mathematical models for a number of complex processes, including fluid flow, heat flow, waste package degradation, chemical reactions, radionuclide transport by flowing groundwater in dual porosity mediums, radionuclide transport in the surface environment, and human exposure to radionuclides as a result of a variety of transport processes and exposure modes. A careful description of $D(\tau|\mathbf{a})$ is outside the intended scope of this presentation. Overviews of the individual models that are assembled to produce $D(\tau|\mathbf{a})$ are provided in Refs. [169-171]. A more detailed description of these models and a source of additional references is Chapt. 6 of Ref. [22].

It is also important to recognize that $D(\tau|\mathbf{a})$ corresponds to only one of hundreds of time-dependent results produced in the 2008 YM PA. This is typical of large system analyses where many individual results are produced. Results such as $D(\tau|\mathbf{a})$ are the final outcomes of a long and involved sequence of calculations.

To understand a result such as $D(\tau|\mathbf{a})$ and also to check its correctness, it is necessary to examine the intermediate results that underlie its production. A subset of the results that underlie the determination of $D(\tau|\mathbf{a})$ are presented in Refs. [162; 164]. More extensive presentation and discussion of results that underlie $D(\tau|\mathbf{a})$ are given in Apps. J and K of Ref. [22].

The probability space ($\mathcal{E}$, $\mathbb{E}$, p_E) for epistemic uncertainty involves nE = 392 variables (Ref. [22], Tables K3-1, K3-2 and K3-3). Specifically, each element $\mathbf{e}$ of $\mathcal{E}$ is a vector of the form

$$\begin{aligned}\mathbf{e} &= \left[\mathbf{e}_A, \mathbf{e}_M\right] \\ &= \left[e_{A1}, e_{A2}, \ldots, e_{A,nEA}, e_{M1}, e_{M2}, \ldots, e_{m,nEM}\right] \\ &= \left[e_1, e_2, \ldots, e_{nE}\right] \\ &= \left[e_1, e_2, \ldots, e_{392}\right],\end{aligned} \tag{6.74}$$

where

$$\mathbf{e}_A = \left[e_{A1}, e_{A2}, \ldots, e_{A,nEA}\right]$$

is a vector of epistemically uncertain variables used in the definition of the probability space ($\mathcal{A}$, $\mathbb{A}$, p_A),

$$\mathbf{e}_M = \left[e_{M1}, e_{M2}, \ldots, e_{M,nEM}\right]$$

is a vector of epistemically uncertain variables required in the evaluation of $D(\tau|\mathbf{a})$, and

$nE = nEA + nEM = 392.$

The probability space ($\mathcal{E}$, $\mathbb{E}$, p_E) was defined by developing a distribution D_i for each element e_i of $\mathbf{e}$. These distributions provide a probabilistic characterization of the available knowledge with respect to where the appropriate value to use for each variable is located. Extensive references describing the nature of each variable e_i in $\mathbf{e}$ and the development of its distribution D_i are given in Table K3-3 of Ref. [22].

With the introduction of the probability space ($\mathcal{E}$, $\mathbb{E}$, p_E) for epistemic uncertainty and the associated elements $\mathbf{e} = [\mathbf{e}_A, \mathbf{e}_M]$ of $\mathcal{E}$, the dose function $D(\tau|\mathbf{a})$ is now more appropriately represented by $D(\tau|\mathbf{a}, \mathbf{e}_M)$ to explicitly indicate the dependence of dose on the values for epistemically uncertain analysis inputs contained in $\mathbf{e}_M$. Further, the epistemic uncertainty associated with the definition of the probability space ($\mathcal{A}$, $\mathbb{A}$, p_A) for aleatory uncertainty can be formally recognized by using $d_A(\mathbf{a}|\mathbf{e}_A)$ to represent the density function associated with ($\mathcal{A}$, $\mathbb{A}$, p_A) that derives from $\mathbf{e}_A$.

The expected dose specified in (YM1) is formally defined by

$$\bar{D}\left(\tau|\mathbf{e}\right) = \int_{\mathcal{A}} D\left(\tau|\mathbf{a}, \mathbf{e}_M\right) d_A\left(\mathbf{a}|\mathbf{e}_A\right) \mathrm{d}A. \tag{6.75}$$

In words, $\bar{D}(\tau|\mathbf{e})$ is the expected value for dose to the RMEI at time τ conditional on the values for epistemically uncertain analysis inputs contained in $\mathbf{e} = [\mathbf{e}_A, \mathbf{e}_M]$. As indicated in Ref. [163] and described in detail in App. J of Ref. [22], a complex sequence of calculations is involved in the evaluation of the integral that defines $\bar{D}(\tau|\mathbf{e})$.

The regulatory requirement summarized in (YM1) requires that the inequality

$$\bar{D}_{mx}\left(\mathbf{e}\right) \le \bar{D}_b = 15 \text{ mrem/yr} \tag{6.76}$$

hold, where

$$\bar{D}_{mx}\left(\mathbf{e}\right) = \max\left\{\bar{D}\left(\tau|\mathbf{e}\right) : 0 \le \tau \le 10^4 \text{ yr}\right\} \tag{6.77}$$

is the maximum value for $\bar{D}(\tau|\mathbf{e})$ over the time interval [0, 10^4 yr] and $\bar{D}_b$ = 15 mrem/yr is the bound specified in (YM1). In turn, the associated margin $m\bar{D}_{MX}(\mathbf{e})$ is defined by

$$\begin{aligned} m\bar{D}_{mx}\left(\mathbf{e}\right) &= \bar{D}_b - \bar{D}_{mx}\left(\mathbf{e}\right) \\ &= 15 \text{ mrem/yr} - \bar{D}_{mx}\left(\mathbf{e}\right). \end{aligned} \tag{6.78}$$

If $\mathbf{e}$ was known with certainty, then $\bar{D}_{mx}(\mathbf{e})$ and $m\bar{D}_{mx}(\mathbf{e})$ would also be known with certainty. However, both $\bar{D}_{mx}(\mathbf{e})$ and $m\bar{D}_{mx}(\mathbf{e})$ are uncertain because of the epistemic uncertainty associated with $\mathbf{e}$ and characterized by the probability space ($\mathcal{E}$, $\mathbb{E}$, p_E).

In the 2008 YM PA, an LHS

$$\begin{aligned}\mathbf{e} &= \left[\mathbf{e}_{Ai}, \mathbf{e}_{Mi}\right] \\ &= \left[e_{i1}, e_{i2}, \ldots, e_{i,nE}\right], i = 1, 2, \ldots, nLHS,\end{aligned} \tag{6.79}$$

of size $nLHS$ = 300 from the nE = 392 uncertain variables under consideration is used in the propagation of epistemic uncertainty. The adequacy of this sample size was established with replicated sampling (see App. J, Ref. [22]).

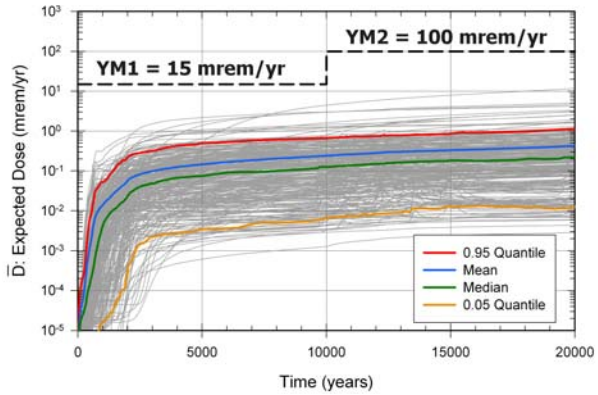

Fig. 6.19. Expected dose curves $[\tau, \bar{D}(\tau|\mathbf{e}_i)]$, $0 \le \tau \le 2 \times 10^4$ yr, and associated mean and quantile curves obtained with an LHS of size 300 from the sample space $\mathcal{E}$ associated with epistemic uncertainty.

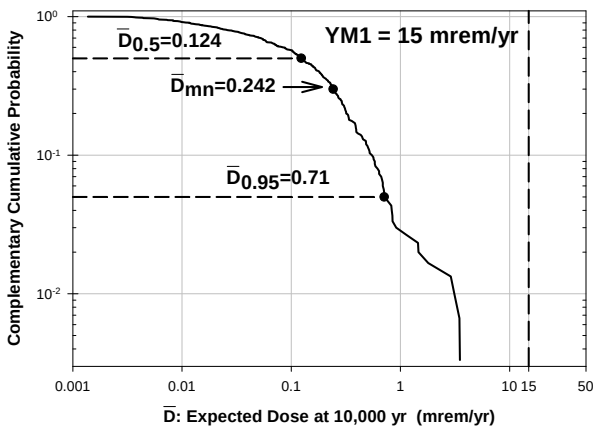

Fig. 6.20. Estimated CCDF for maximum expected dose $\bar{D}_{mx}(\mathbf{e})$ (see Eq.(6.77)).

The indicated sample results in 300 expected dose curves $[\tau, \bar{D}(\tau|\mathbf{e}_i)]$ (Fig. 6.19). In addition to the individual curves corresponding to $[\tau, \bar{D}(\tau|\mathbf{e}_i)]$, Fig. 6.19 also shows mean and quantile results that derive from epistemic uncertainty; specifically, these results correspond to quantities of the form defined in Eqs. (3.26) and (3.28) and discussed in conjunction with Fig. 1 of Ref. [163].

Corresponding to each dose curve $[\tau, \bar{D}(\tau|\mathbf{e}_i)]$ in Fig. 6.19 is a maximum dose $\bar{D}_{mx}(\mathbf{e}_i)$ for the time interval $[0, 10^4$ yr$]$ defined as indicated in conjunction with Eq. (6.77). Specifically, 300 values for $\bar{D}_{mx}(\mathbf{e}_i)$ are obtained and provide the basis for an estimated CCDF that summarizes the epistemic uncertainty associated with $\bar{D}_{mx}(\mathbf{e})$ (Fig. 6.20). Because the individual expected dose curves $[\tau, \bar{D}(\tau|\mathbf{e}_i)]$ in Fig. 6.19 are effectively monotonically increasing, the equality $\bar{D}_{mx}(\mathbf{e}_i) = \bar{D}(10^4|\mathbf{e}_i)$ is assumed to hold.

In turn, 300 values for the margin

$$\begin{aligned} m\bar{D}_{mx}(\mathbf{e}_i) &= \bar{D}_b - \bar{D}_{mx}(\mathbf{e}_i) \\ &= 15 \text{ mrem/yr} - \bar{D}_{mx}(\mathbf{e}_i) \end{aligned} \tag{6.80}$$

and also for the corresponding normalized margin

$$\begin{aligned} n\bar{D}_{mx}(\mathbf{e}_i) &= \left[\bar{D}_b - \bar{D}_{mx}(\mathbf{e}_i)\right] / \bar{D}_b \\ &= \left[15 \text{ mrem/yr} - \bar{D}_{mx}(\mathbf{e}_i)\right] / 15 \text{ mrem/yr} \end{aligned} \tag{6.81}$$

are obtained and provide the basis for estimated CDFs that summarize the epistemic uncertainty associated with $m\bar{D}_{mx}(\mathbf{e})$ and $n\bar{D}_{mx}(\mathbf{e})$ (Fig. 6.21).

As discussed in conjunction with Eqs. (6.16) – (6.23), the results in Figs. 6.20 and 6.21 can be reduced to single-valued "margin/uncertainty" summary statistics by the following calculations:

$$\begin{aligned} m\bar{D}_{mn} / \left(m\bar{D}_{mn} - m\bar{D}_{0.05}\right) &= 14.76 / (14.76 - 14.29) \\ &= 31.40, \end{aligned} \tag{6.82}$$

$$\begin{aligned} m\bar{D}_{0.5} / \left(m\bar{D}_{0.5} - m\bar{D}_{0.05}\right) &= 14.88 / (14.88 - 14.29) \\ &= 25.22, \end{aligned} \tag{6.83}$$

$$\begin{aligned} m\bar{D}_{mn} / \left(m\bar{D}_{mn} - m\bar{D}_{min}\right) &= 14.76 / (14.76 - 11.49) \\ &= 4.51, \end{aligned} \tag{6.84}$$

and

$$\begin{aligned} m\bar{D}_{0.5} / \left(m\bar{D}_{0.5} - m\bar{D}_{min}\right) &= 14.88 / (14.88 - 11.49) \\ &= 4.39, \end{aligned} \tag{6.85}$$

where

$$m\bar{D}_{mn} = \sum_{i=1}^{nLHS} m\bar{D}_{mx}(\mathbf{e}_i) / nLHS$$

is an approximation to the expected value of $m\bar{D}_{mx}(\mathbf{e})$ over epistemic uncertainty, $m\bar{D}_q$ is the estimated q-quantile for $m\bar{D}_{mx}(\mathbf{e})$, and $m\bar{D}_{min} = m\bar{D}_{0.00}$. However, as previously discussed, significant information is lost in the preceding reductions of the information in Figs. 6.20 and 6.21a and ultimately Fig. 6.19 to single numbers (see Sect. 4.5 for additional discussion).

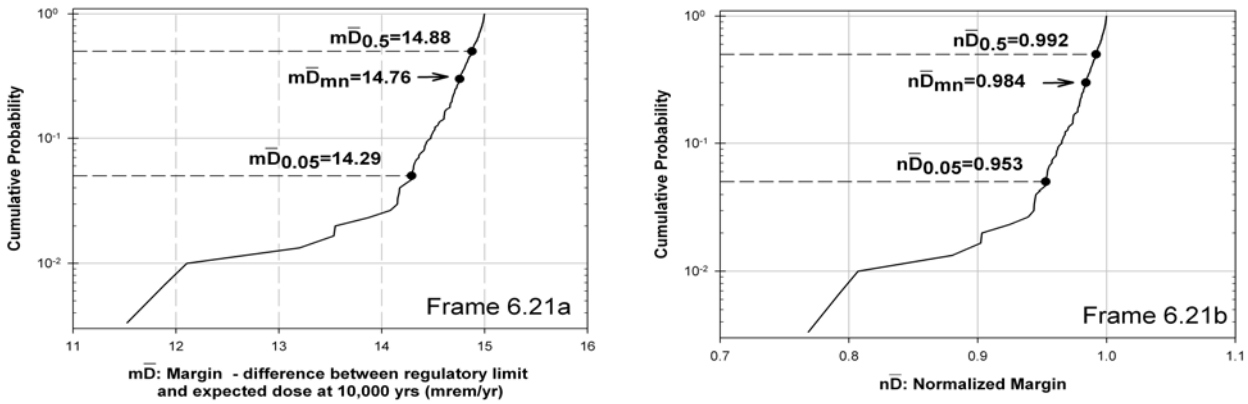

Fig. 6.21. Estimated CDFs for margin associated with maximum expected dose: (a) margin $m\bar{D}_{mx}(\mathbf{e})$ for maximum expected dose (see Eq. (6.80)), and (b) normalized margin $n\bar{D}_{mx}(\mathbf{e})$ for maximum expected dose (see Eq. (6.81)).

Note: In its regulations, the NRC implies, but never explicitly states, that the bounds in (YM1) and (YM2) are to apply to results of the form

$$\begin{aligned}\bar{D}_{mn} &= \max\left\{\int_{\mathcal{E}} \bar{D}(\tau \mid \mathbf{e})\, d_E(\mathbf{e})\, \mathrm{d}E : a \le \tau \le b\right\} \\ &\cong \max\left\{\sum_{i=1}^{nLHS} \bar{D}(\tau \mid \mathbf{e}_i)/nLHS : a \le \tau \le b\right\}\end{aligned} \tag{6.86}$$

with

$$\bar{D}(\tau \mid \mathbf{e}) = \int_{\mathcal{A}} D(\tau \mid \mathbf{a}, \mathbf{e}_M)\, d_A(\mathbf{a} \mid \mathbf{e}_A)\, \mathrm{d}A$$

and [a, b] equal to [0, 10^4 yr] and [10^4, 10^6 yr], respectively. In effect, this places the bounds of 15 mrem/yr and 100 mrem/yr in (YM1) and (YM2) on quantities defined on the basis of expected values over both aleatory and epistemic uncertainty (i.e., on the curve labeled "mean" in Fig. 6.19). Because of the expectations over both aleatory and epistemic uncertainty, there is no uncertainty in the central regulatory quantity $\bar{D}_{mn}$ once the probability spaces ($\mathcal{A}$, $\mathbb{A}$, p_A) and ($\mathcal{E}$, $\mathbb{E}$, p_E) and the dose function $D(\tau|\mathbf{a}, \mathbf{e}_M)$ have been specified. However, the NRC is also very explicit in stating that the uncertainty in results used in assessing compliance with the requirements in (YM1) and (YM2) is to be shown (see discussion in Ref. [167]). In the 2008 YM PA, this potentially contradictory situation was handled by first calculating $\bar{D}(\tau|\mathbf{e}_i)$ conditional on individual LHS elements $\mathbf{e}_i$ and then calculating $\bar{D}_{mn}$ from the expectations $\bar{D}(\tau|\mathbf{e}_i)$ over aleatory uncertainty. Specifically, the individual expected dose curves [τ, $\bar{D}(\tau|\mathbf{e}_i)$] in Fig. 6.19 provide both the desired representation of the epistemic uncertainty in the estimation of expected dose and the basis for estimatimng the central regulatory quantity $\bar{D}_{mn}$. This provides an example of a situation that also underlies the examples presented in Sects. 6.1 and 6.2 and is likely to be encountered in QMU analyses. Namely, a situation in which the descriptions of required results are not complete or possibly fully consistent and thus require some level of interpretation and/or elaboration by the analysts involved in actually defining, planning, and implementing the calculations necessary to assess compliance with an incompletely specified requirement. At the core of this process is the determination of how to convert what maybe less than fully precise verbal and numeric specifications into a well-defined mathematical structure that facilitates the planning, implementation and documentation of the analysis to be performed.

This page intentionally left blank.

7 Uncertainty and Sensitivity Analysis for Models of Complex Systems

Uncertainty analysis and sensitivity analysis are essential parts of analyses for complex systems [2; 172-182]. Specifically, uncertainty analysis refers to the determination of the uncertainty in analysis results that derives from uncertainty in analysis inputs, and sensitivity analysis refers to the determination of the contributions of individual uncertain analysis inputs to the uncertainty in analysis results. The uncertainty under consideration here is often referred to as epistemic uncertainty as previously discussed in Sect. 2; alternate designations for this form of uncertainty include state of knowledge, subjective, reducible, and type B [78-81; 83; 85-89]. Epistemic uncertainty derives from a lack of knowledge about the appropriate value to use for a quantity that is assumed to have a fixed value in the context of a particular analysis. In the conceptual and computational organization of an analysis, epistemic uncertainty is generally considered to be distinct from aleatory uncertainty, which arises from an inherent randomness in the behavior of the system under study [78-81; 83; 85-89]. Alternative designations for aleatory uncertainty include variability, stochastic, irreducible, and type A. The importnance of uncertainty and sensitivity analysis is specifically recognized in the NAS/NRC report on QMU (pp. 14-15, Ref. [77]).

A number of approaches to uncertainty and sensitivity analysis have been developed, including differential analysis [32-37], response surface methodology [38-44], Monte Carlo analysis [29; 45-56], and variance decomposition procedures[57-61]. Overviews of these approaches are available in several reviews [62-70].

The focus of this section is on Monte Carlo (i.e., sampling-based) approaches to uncertainty and sensitivity analysis. Sampling-based approaches to uncertainty and sensitivity analysis are both effective and widely used [29; 51; 53; 55; 56; 64; 65]. Analyses of this type involve the generation and exploration of a mapping from uncertain analysis inputs to uncertain analysis results. The underlying idea is that analysis results $\mathbf{y}(\mathbf{x}) = [y_1(\mathbf{x}), y_2(\mathbf{x}), \ldots, y_{nY}(\mathbf{x})]$ are functions of uncertain analysis inputs $\mathbf{x} = [x_1, x_2, \ldots, x_{nX}]$. In turn, uncertainty in $\mathbf{x}$ results in a corresponding uncertainty in $\mathbf{y}(\mathbf{x})$. This leads to two questions: (i) What is the uncertainty in $\mathbf{y}(\mathbf{x})$ given the uncertainty in $\mathbf{x}$?, and (ii) How important are the individual elements of $\mathbf{x}$ with respect to the uncertainty in $\mathbf{y}(\mathbf{x})$? The goal of uncertainty analysis is to answer the first question, and the goal of sensitivity analysis is to answer the second question. In practice, the implementation of an uncertainty analysis and the implementation of a sensitivity analysis are closely connected on both a conceptual and a computational level.

The following sections summarize the five basic components that underlie the implementation of a sampling-based uncertainty and sensitivity analysis: (i) Definition of distributions $D_1, D_2, \ldots, D_{nX}$ that characterize the epistemic uncertainty in the components $x_1, x_2, \ldots, x_{nX}$ of $\mathbf{x}$ (Sect. 7.1), (ii) Generation of a sample $\mathbf{x}_1, \mathbf{x}_2, \ldots, \mathbf{x}_{nS}$ from the $\mathbf{x}$'s in consistency with the distributions $D_1, D_2, \ldots, D_{nX}$ (Sect. 7.2), (iii) Propagation of the sample through the analysis to produce a mapping $[\mathbf{x}_i, \mathbf{y}(\mathbf{x}_i)]$, $i = 1, 2, \ldots, nS$, from analysis inputs to analysis results (Sect. 7.3), (iv) Presentation of uncertainty analysis results (i.e., approximations to the distributions of the elements of $\mathbf{y}$ constructed from the corresponding elements of $\mathbf{y}(\mathbf{x}_i)$, $i = 1, 2, \ldots, nS$) (Sect. 7.4), and (v) Determination of sensitivity analysis results (i.e., exploration of the mapping $[\mathbf{x}_i, \mathbf{y}(\mathbf{x}_i)]$, $i = 1, 2, \ldots, nS$) (Sect. 7.5).

Space limitations in this presentation preclude the presentation of detailed examples of the indicated analysis components; however, extensive examples can be found in the published descriptions of uncertainty and sensitivity analyses carried out for the Waste Isolation Pilot Plant (e.g., Refs. [21; 146; 183]) and the proposed Yucca Mountain repository for high-level radioactive waste (e.g., Refs. [162-164] and Apps. J and K of Ref. [22]). These two analyses have been previously introduced in Sects. 6.2 and 6.3.

Only probabilistic characterizations of uncertainty are considered in this presentation. Alternative uncertainty representations (e.g., interval analysis, possibility theory, evidence theory) are an active area of research [184-190] and are discussed in Sects. 8 – 10.

This presentation is a lightly edited version of two prior workshop presentations [191; 192] and is intended to introduce the reader to sampling-based procedures for uncertainty and sensitivity analysis. More extensive information on these procedures is available in five technical reports [193-197] and a number of additional presentations derived from these reports [52-55; 111; 112].

7.1 Characterization of Uncertainty

Definition of the distributions $D_1, D_2, \ldots, D_{nX}$ that characterize the epistemic uncertainty in the components $x_1, x_2, \ldots, x_{nX}$ of $\mathbf{x}$ is the most important part of a sampling-based uncertainty and sensitivity analysis as these distributions determine both the uncertainty in $\mathbf{y}$ and the sensitivity of the elements of $\mathbf{y}$ to the elements

of **x**. To the extent possible, the indicated distributions should be defined on the basis of results obtained from relevant and appropriately designed experimants. Unfortunately, such experimental results do not always exist. As a result, the distributions D_1, D_2, …, D_{nX} often need to be developed, at least in part, through an expert review process [97-103]. Further, this development can constitute a major analysis cost.

It is important to recognize that the purpose of the indicated expert review process for a given element of **x** is not to replace experimental results with personnel opinion. Rather, the purpose is to assess information from what could potentially be a variety of sources of different levels of relevance and credibility and then to summarize this information with a probability distribution. In turn, the development of the indicated distributions allows the assessed epistemic uncertainty in analysis inputs to used in determining the epistemic uncertainty in analysis results.

A possible analysis strategy is to perform an initial exploratory analysis with rather crude definitions for D_1, D_2, …, D_{nX} and use sensitivity analysis to identify the most important analysis inputs; then, resources can be concentrated on characterizing the uncertainty in these inputs and a second presentation or decision-aiding analysis can be carried out with these improved uncertainty characterizations. For example, additional experimental work might be performed to reduce the epistemic uncertainty present with respect to the correct values for the variables whose uncertainty most influences the uncertainty in analysis results of interest. This strategy is particularly appropriate for analyses that involve a large number of epistemically uncertain inputs.

The scope of an expert review process can vary widely depending on the purpose of the analysis, the size of the analysis, and the resources available to carry out the analysis. At one extreme is a relatively small study in which a single analyst both develops the uncertainty characterizations (e.g., on the basis of personal knowledge or a cursory literature review). At the other extreme, is a large analysis on which important decisions will be based and for which uncertainty characterizations are carried out for a large number of variables by teams of outside experts who support the analysts actually performing the analysis.

Appropriate documentation of the information considered and how this information was used in developing distributions to characterize epistemic uncertainty is an essential part of an expert review process. Without such documentation, distributions developed through an expert review process will hve little credibility.

Given the breadth of analysis possibilities, it is beyond the scope of this presentation to provide an exhaustive review of how the distributions D_1, D_2, …, D_{nX} might be developed. However, as general guidance, it is best to avoid trying to obtain these distributions by specifying the defining parameters (e.g., mean and standard deviation) for a particular distribution type. Rather, distributions can be defined by specifying selected quantiles (e.g., 0.0, 0.1, 0.25, …, 0.9, 1.0) of the corresponding cumulative distribution function (CDF), which should keep the individual supplying the information in closer contact with the original sources of information or insight than is the case when a particular named distribution is specified (Fig. 7.1a). Distributions from multiple experts can be aggregated by averaging (Fig. 7.1b).

7.2 Generation of Sample

Several sampling strategies are available, including random sampling, importance sampling, and Latin hypercube sampling [45; 55]. Latin hypercube sampling is very popular for use with computationally demanding models because its efficient stratification properties allow for the extraction of a large amount of uncertainty and sensitivity information with a relatively small sample size [141-143].

Latin hypercube sampling operates in the following manner to generate a sample of size nS from the distributions D_1, D_2, …, D_{nX} associated with the elements of $\mathbf{x} = [x_1, x_2, \ldots, x_{nX}]$. The range of each x_j is exhaustively divided into nS disjoint intervals of equal probability and one value x_{ij} is randomly selected from each interval. The nS values for x_1 are randomly paired without replacement with the nS values for x_2 to produce nS pairs. These pairs are then randomly combined without replacement with the nS values for x_3 to produce nS triples. This process is continued until a set of nS nX-tuples $\mathbf{x}_i = [x_{i1}, x_{i2}, \ldots, x_{i,nX}]$, $i = 1, 2, \ldots, nS$, is obtained, with this set constituting the Latin hypercube sample (LHS) (Fig. 7.2).

Latin hypercube sampling is a good choice for a sampling procedure when computationally demanding models are being studied. The popularity of Latin hypercube sampling recently led to the original article being designated a Technometrics classic in experimental design [198]. When the model is not computationally demanding, many model evaluations can be performed and random sampling works as well as Latin hypercube sampling.

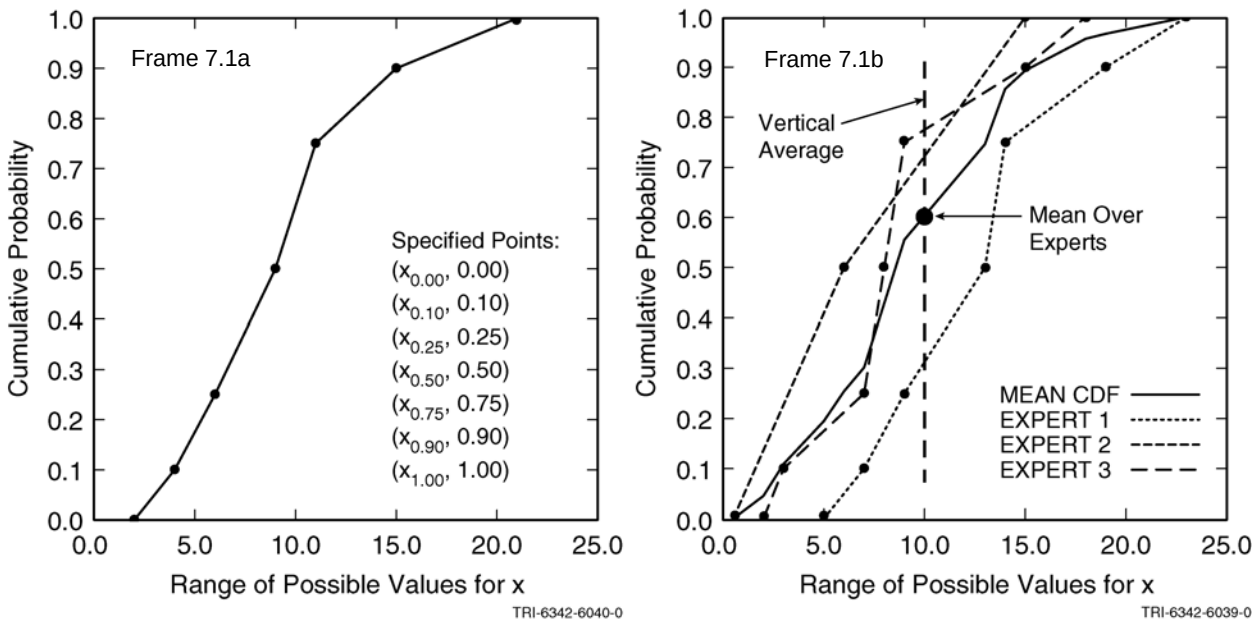

Fig. 7.1. Characterization of epistemic uncertainty: (a) Construction of CDF from specified quantile values (Fig. 4.1, Ref. [194]), and (b) Construction of mean CDF by vertical averaging of CDFs defined by individual experts with equal weight (i.e., $1/nE = 1/3$, where $nE = 3$ is the number of experts) given to each expert (Fig. 4.2, Ref. [194]).

Control of correlations is an important aspect of sample generation. Specifically, correlated variables should have correlations close to their specified values, and uncorrelated variables should have correlations close to zero. In general, the imposition of complex correlation structures is not easy. However, Iman and Conover have developed a broadly applicable procedure to impose rank correlations on sampled values that (i) is distribution free (i.e., does not depend on the assumed marginal distributions for the sampled variables), (ii) can impose complex correlation structures involving multiple variables, (iii) works with both random and Latin hypercube sampling, and (iv) preserves the intervals used in Latin hypercube sampling [199; 200]. Details on the implementation of the procedure are available in the original reference [199]; illustrative results are provided in Fig. 7.3.

Unlike simple random sampling, the size of an LHS cannot be increased by simply adding one sample element at a time. However, recently developed techniques provide a means to retain the elements of an initial LHS in an expanded LHS [201; 202]. This can be important in a computationally demanding analysis in which it is desired both to increase the size of an LHS and also to retain already performed calculations in the analysis. Further, the stability of results obtained with Latin hypercube sampling for a given sample size can be assessed with a replicated sampling technique developed by R.L. Iman [154; 203].

7.3 Propagation of Sample Through the Analysis

Propagation of the sample through the analysis to produce the mapping $[\mathbf{x}_i, \mathbf{y}(\mathbf{x}_i))]$, $i = 1, 2, \ldots, nS$, from analysis inputs to analysis results is often the most computationally demanding part of a sampling-based uncertainty and sensitivity analysis. The details of this propagation are analysis specific and can range from very simple for analyses that involve a single model to very complicated for large analyses that involve complex systems of linked models [11; 21].

When a single model is under consideration, this part of the analysis can involve little more than putting a DO loop around the model that (i) supplies the sampled input to the model, (ii) runs the model, and (iii) stores model results for later analysis. When more complex analyses with multiple models are involved, considerable sophistication may be required in this part of the analysis. Implementation of such analyses can involve (i) development of simplified models to approximate more complex models, (ii) clustering of results at model interfaces (i.e., at analysis pinchpoints), (iii) reuse of model results through interpolation or linearity properties, and (iv) complex procedures for the storage and retrieval of analysis results.

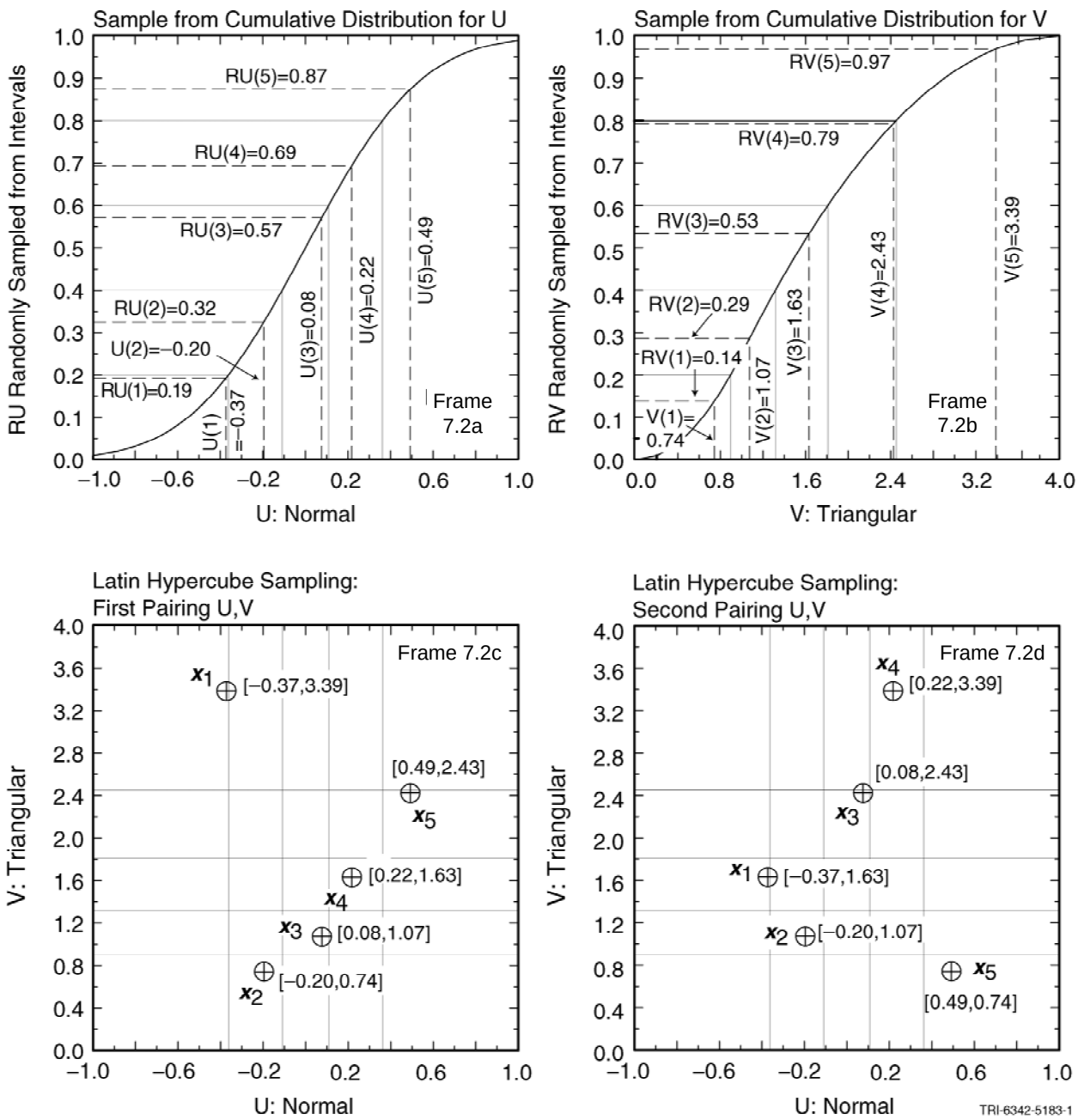

Fig. 7.2. Example of Latin hypercube sampling to generate a sample of size $nS = 5$ from $\mathbf{x} = [U, V]$ with U normal on [–1, 1] (mean = 0.0; 0.01 quantile = –1; 0.99 quantile = 1) and V triangular on [0, 4] (mode = 1): (a) Upper frames illustrate sampling of values for U and V, and (b) Lower frames illustrate two different pairings of the sampled values of U and V in the construction of a Latin hypercube sample (Fig. 5.3, Ref. [194]).

7.4 Presentation of Uncertainty Analysis Results

Presentation of uncertainty analysis results is generally straightforward and involves little more than displaying the results associated with the already calculated mapping $[\mathbf{x}_i, \mathbf{y}(\mathbf{x}_i)]$, $i = 1, 2, \ldots, nS$. Presentation possibilities include means and standard deviations, density functions, cumulative distribution function (CDFs), complementary cumulative distribution functions (CCDFs), and box plots [55; 64]. Presentation formats such as CDFs (Fig. 7.4a), CCDFs (Fig. 7.4a) and box plots (Fig. 7.4b) are preferable to means and standard deviations because of the large amount of uncertainty information that is lost in the calculation of

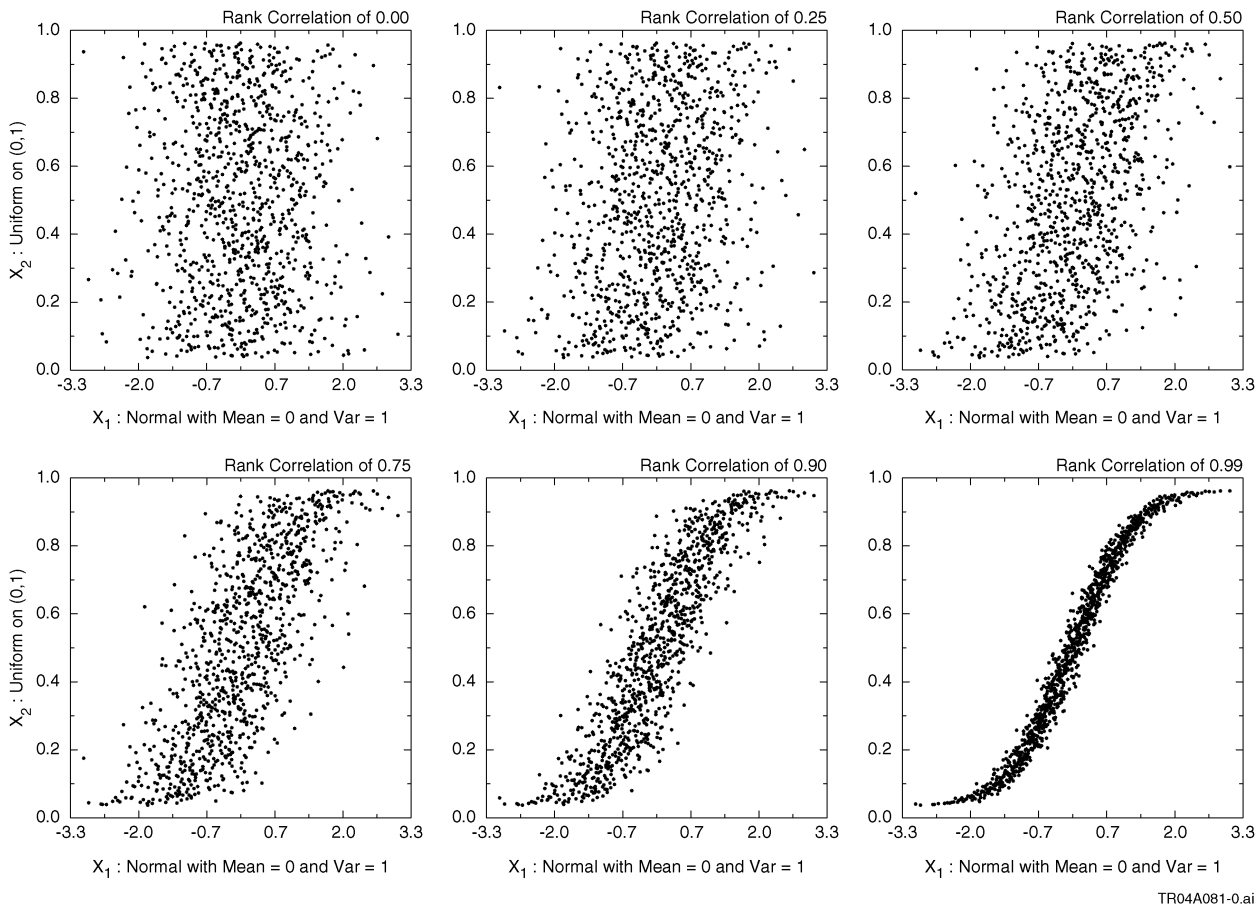

Fig. 7.3. Examples of rank correlations of 0.00, 0.25, 0.50, 0.75, 0.90 and 0.99 imposed with the Iman/Conover restricted pairing technique for an LHS of size nS = 1000 (Fig. 5.1, Ref. [195]).

means and standard deviations. For this reason, analysis summaries based on presenting only means and standard deviations should be avoided. Owing to their flattened shape, box plots are particularly useful when it is desired to the display and compare the uncertainty in a number of related variables.

The representational challenge is more complex when the analysis outcome of interest is a function rather than a scalar. For example, a system property that is a function of time is a common analysis outcome. As another example, a CCDF that summarizes the effects of aleatory uncertainty is a standard analysis outcome in risk assessments. An effective display format for such analysis outcomes is to use two plot frames, with the first frame displaying the analysis results for the individual sample elements and the second frame displaying summary results for the outcomes in the first frame (e.g., quantiles and means) (Fig. 7.5).

7.5 Determination of Sensitivity Analysis Results

Determination of sensitivity analysis results is usually more demanding than the presentation of uncertainty analysis results due to the need to actually explore the mapping $[\mathbf{x}_i, \mathbf{y}(\mathbf{x}_i)]$, $i = 1, 2, \ldots, nS$, to assess the effects of individual components of $\mathbf{x}$ on the components of $\mathbf{y}$. A number of approaches to sensitivity analysis that can be used in conjunction with a sampling-based uncertainty analysis are listed and briefly summarized below. In this summary, (i) x_j is an element of $\mathbf{x} = [x_1, x_2, \ldots, x_{nX}]$, (ii) y_k is an element of $\mathbf{y}(\mathbf{x}) = [y_1(\mathbf{x}), y_2(\mathbf{x}), \ldots, y_{nY}(\mathbf{x})]$, (iii) $\mathbf{x}_i = [x_{i1}, x_{i2}, \ldots, x_{i,nX}]$, $i = 1, 2, \ldots, nS$, is a random or Latin hypercube sample from the possible values for $\mathbf{x}$ generated in consistency with the joint distribution assigned to the x_j, (iv) $\mathbf{y}_i = \mathbf{y}(\mathbf{x}_i)$ for $i = 1, 2, \ldots, nS$, and (v) x_{ij} and y_{ik} are elements of $\mathbf{x}_i$ and $\mathbf{y}_i$, respectively.

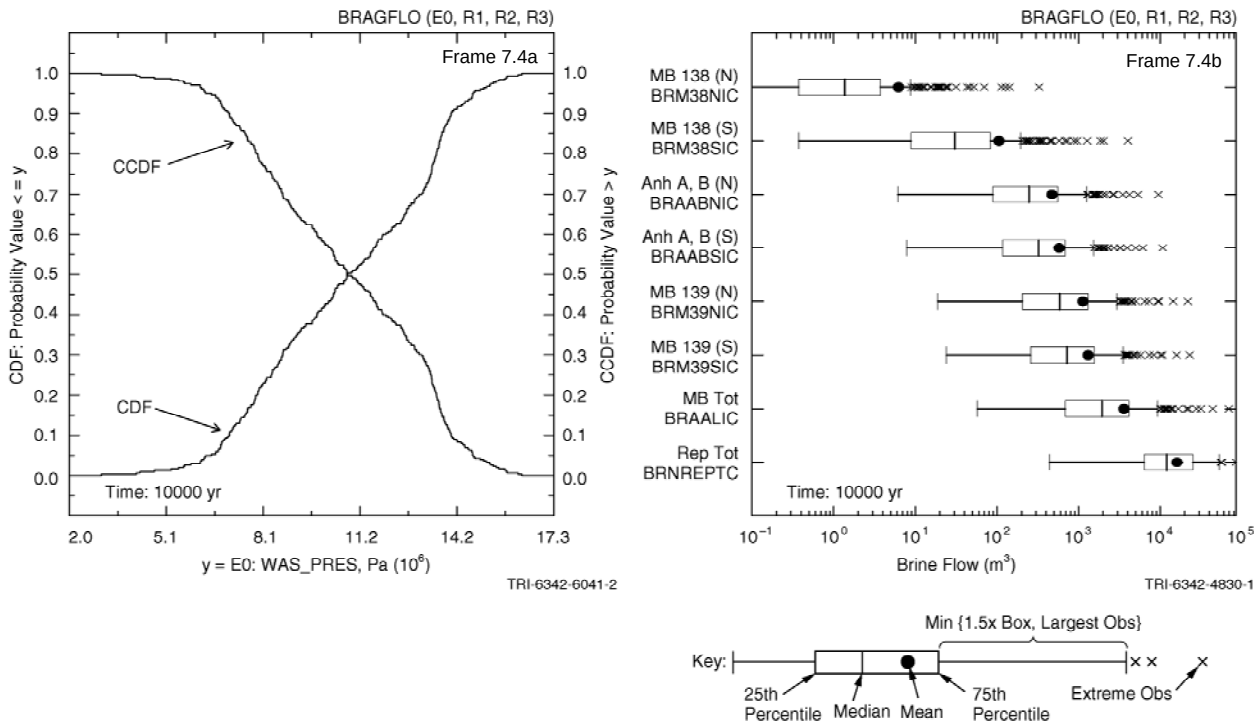

Fig. 7.4. Representation of uncertainty in scalar-valued analysis results: (a) CDFs and CCDFs (Fig. 7.2, Ref. [194]) and (b) box plots (Fig. 7.4, Ref. [194]).

Scatterplots. Scatterplots are plots of the points $[x_{ij}, y_{ik}]$ for $i = 1, 2, \ldots, nS$ and can reveal nonlinear or other unexpected relationships (Fig. 7.6). In many analyses, scatterplots provide all the information that is needed to identify the sensitivity of analysis results to the uncertainty in analysis inputs. Further, scatterplots constitute a natural starting point in a complex analysis that can help in the development of a sensitivity analysis strategy using one or more additional techniques. Additional information: Sect. 6.6.1, Ref. [53]; Sect. 6.1, Ref. [56].

Cobweb Plots. Cobweb plots are plots of the points $[\mathbf{x}_i, y_{ik}] = [x_{i1}, x_{i2}, \ldots, x_{i,nX}, y_{ik}]$ for $i = 1, 2, \ldots, nS$ and provide a two-dimensional representation for $[\mathbf{x}_i, y_{ik}]$, which is a $nX + 1$ dimensional quantity. Specifically, values for the y_{ik} and also for the elements $\mathbf{x}_{ij}$ of $\mathbf{x}_i$ appear on the ordinate of a cobweb plot and the variables themselves are designated by fixed locations on the abscissa. Then, the values y_{ik}, $i = 1, 2, .., nS$, for y_k and the values x_{ij}, $i = 1, 2, \ldots, nS$, for each x_j are plotted above the locations for y_k and x_j on the abscissa and each $nX + 1$ dimensional point $[\mathbf{x}_i, y_{ik}]$ is represented by a line connecting the values for the individual components of $[\mathbf{x}_i, y_{ik}]$. Cobweb plots provide more information in a single plot frame than a scatterplot but are harder to read. Additional information: Sect. 11.7, Ref. [204].

Correlation. A correlation coefficient (CC) provides a measure of the strength of the linear relationship between x_j and y_k. The CC between x_j and y_k has a value in the interval [–1, 1], with (i) a positive value indicating that x_j and y_k tend to increase and decrease together, (ii) a negative value indicating that x_j and y_k tend to increase and decrease in opposite directions, and (iii) the absolute value of the CC indicating the strength of the linear relationship between x_j and y_k. The CC between x_j and y_k is equal to the standardized regression coefficient (SRC) in a linear regression relating y_k to x_j and is also equal in absolute value to the square root of the R^2 value associated with the indicated regression. When calculated with raw (i.e., untransformed) data, the CC is often referred to as the Pearson CC. Additional information: Sect. 6.6.4, Ref. [53]; Sect. 6.2, Ref. [56].

Regression Analysis. Regression analysis provides an algebraic representation of the relationships between y_k and one or more x_j's. Regression analysis is usually performed in a stepwise fashion, with initial inclusion of the most important x_j, then the two most important x_j's, and so on until no more x_j's that significantly affect y_k can be identified. Variable importance is indicated by order of selection in the stepwise process, changes in R^2 values as additional variables are

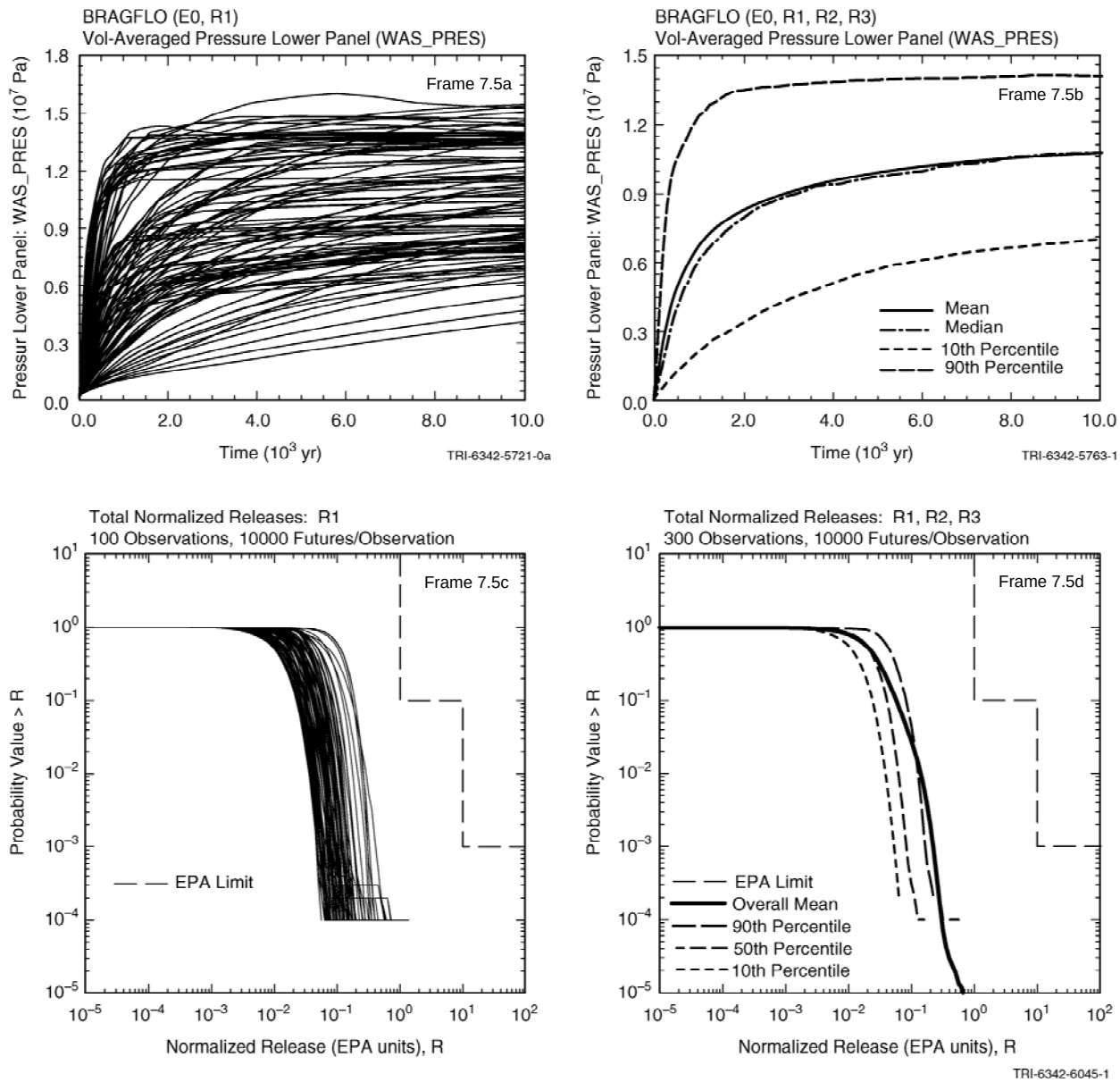

Fig. 7.5. Representation of uncertainty in analysis results that are functions: (a, b) Pressure as a function of time (Figs. 7.5, 7.9, Ref. [194]), and (c, d) Effects of aleatory uncertainty summarized as a CCDF (Fig. 10.5, Ref. [194]).

added to the regression model, and SRCs for the x_j's in the final regression model (Table 7.1). A display of regression results in the form shown in Table 7.1 is very unwieldy when results at a sequence of times are under consideration. In this situation, a more compact display of regression results is provided by plotting time-dependent SRCs (Fig. 7.7a). Additional information: Sects. 6.6.2, 6.6.3, 6.6.5, Ref. [53]; Sect. 6.3, Ref. [56].

Partial Correlation. A partial correlation coefficient (PCC) provides a measure of the strength of the linear relationship between y_k and x_j after the linear effects of all other elements of $\mathbf{x}$ have been removed. Similarly to SRCs, PCCs can be determined as a function of time for time-dependent analysis results (Fig. 7.7b). Additional information: Sect. 6.6.4, Ref. [53]; Sect. 6.4, Ref. [56].

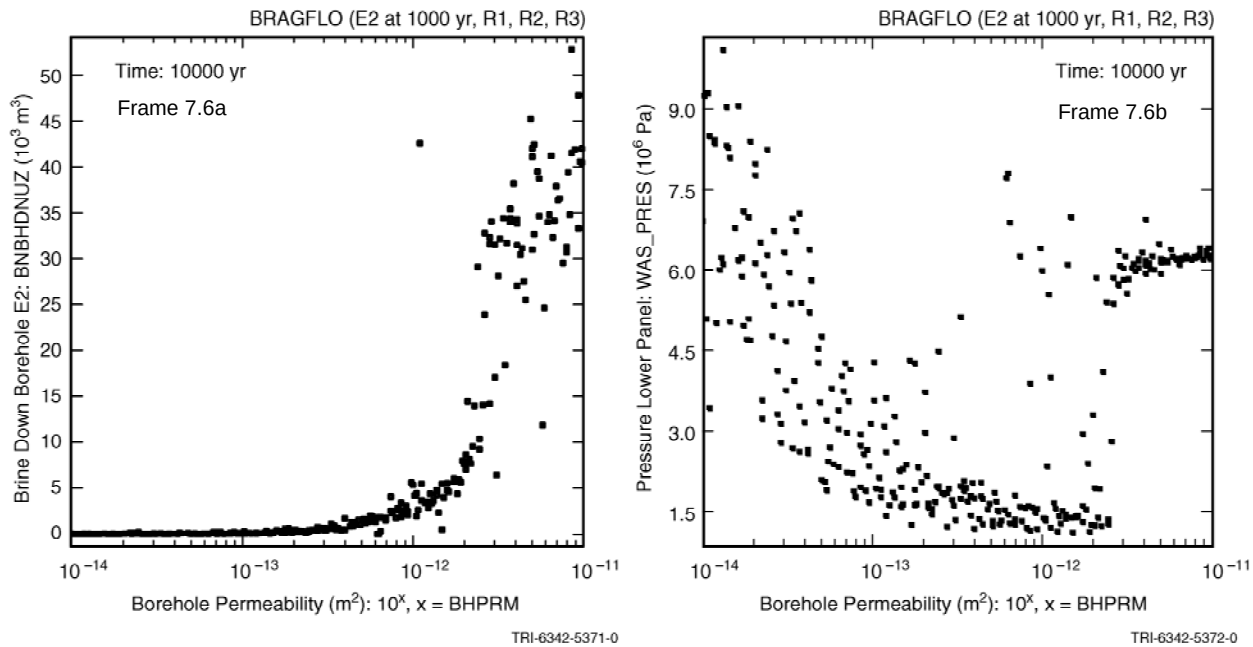

Fig. 7.6. Examples of scatterplots obtained in a sampling-based uncertainty/sensitivity analysis (Figs. 8.1, 8.2, Ref. [194]).

Table 7.1. Example of Stepwise Regression Analysis to Identify Uncertain Variables Affecting the Uncertainty in Pressure at 10,000 yr in Fig. 7.5a (Table 8.6, Ref. [194])

Step[a]	**Variable**[b]	**SRC**[c]	R^{2d}
1	*WMICDFLG*	0.718	0.508
2	*HALPOR*	0.466	0.732
3	*WGRCOR*	0.246	0.792
4	*ANHPRM*	0.129	0.809
5	*SHRGSSAT*	0.070	0.814
6	*SALPRES*	0.063	0.818

[a] Steps in stepwise regression analysis.
[b] Variables listed in the order of selection in regression analysis.
[c] SRCs for variables in final regression model.
[d] Cumulative R^2 value with entry of each variable into regression model.

Rank Transformations. A rank transformation replaces values for y_k and x_j with their corresponding ranks. Specifically, the smallest value for a variable is assigned a rank of 1; next largest value is assigned a rank of 2; tied values are assigned their average rank; and so on up to the largest value, which is assigned a rank of *nS*. Use of the rank transformation converts a nonlinear but monotonic relationship between y_k and x_j to a linear relationship and produces rank (i.e., Spearman) correlations, rank regressions, standardized rank regression coefficients (SRRCs) and partial rank correlation coefficients (PRCCs). In the presence of nonlinear but monotonic relationships between the x_j and y_k, the use of the rank transform can substantially improve the resolution of sensitivity analysis results (Table 7.2). Additional information: Sect. 6.6.6, Ref. [53]; Sect. 6.6, Ref. [56]; Ref. [205].

Tests for Patterns Based on Gridding. Analyses on raw and rank-transformed data can fail when the underlying relationships between the x_j and y_k are nonlinear and nonmonotonic (Fig. 7.8). The scatterplot in Fig. 7.6b is for the pressure at 10,000 yr in Fig. 7.8a versus the uncertain variable *BHPRM*. The analyses with PRCCs summarized in Fig. 7.8b fail at later times because the pattern appearing in Fig. 7.6b is too complex to be captured with a regression analysis based on raw or rank-transformed data. An alternative analysis strategy for situations of this type is to place grids on the scatterplot for y_k and x_j and then perform various statistical tests to determine if the distribution of points across the grid cells appears to be nonrandom. Appearance of a nonrandom pattern indicates that x_j has an effect on y_k. Possibilities include (i) tests for common means and common distributions for values of y_k based on partitioning the range of x_j (Fig. 7.9a) and (ii) tests for common medians and no influence based on partitioning the ranges of x_j and y_k (Figs. 7.9a,b). Additional information: Ref. [52]; Sects. 6.6.8 and 6.6.9, Ref. [53]; Sects. 6.6 and 6.7, Ref. [56].

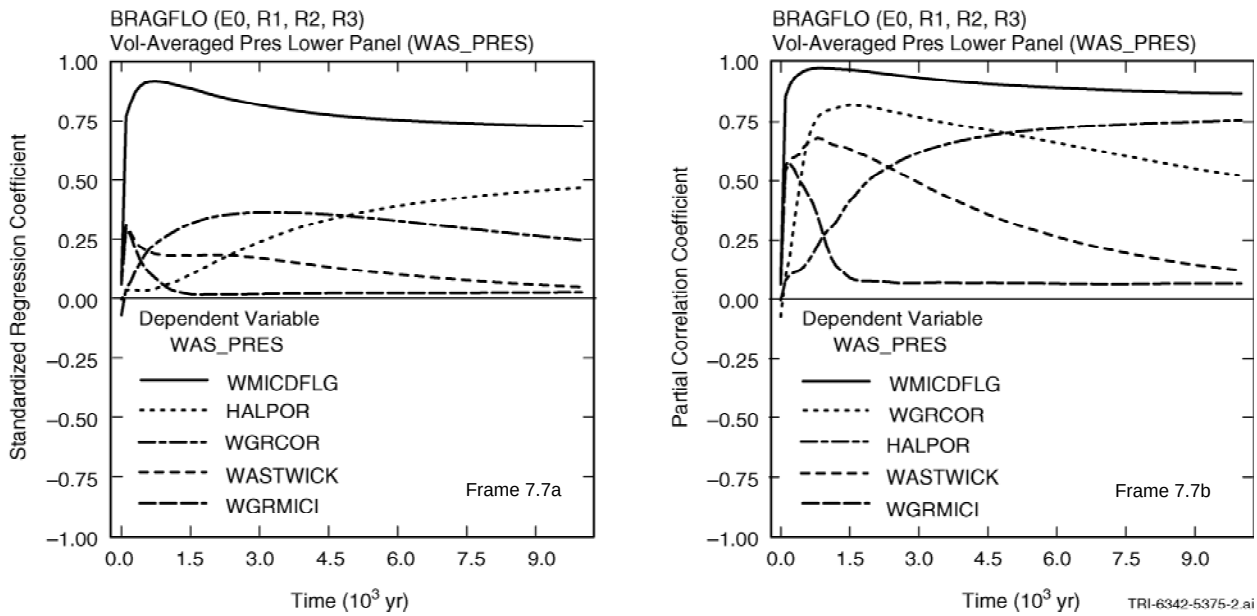

Fig. 7.7. Time-dependent sensitivity analysis results for uncertain pressure curves in Fig. 7.5a: (a) SRCs as a function of time, and (b) PCCs as a function of time (Fig. 8.3, Ref. [194]).

Table 7.2 Comparison of Stepwise Regression Analyses with Raw and Rank-Transformed Data for Variable *BRAALIC* in Fig. 7.4b (Table 8.8, Ref. [194])

Step[a]	Raw Data			Rank-Transformed Data		
	Variable[b]	SRC[c]	R^{2d}	Variable[b]	SRRC[e]	R^{2d}
1	*ANHPRM*	0.562	0.320	*WMICDFLG*	–0.656	0.425
2	*WMICDFLG*	–0.309	0.423	*ANHPRM*	0.593	0.766
3	*WGRCOR*	–0.164	0.449	*HALPOR*	–0.155	0.802
4	*WASTWICK*	–0.145	0.471	*WGRCOR*	–0.152	0.824
5	*ANHBCEXP*	–0.120	0.486	*HALPRM*	0.143	0.845
6	*HALPOR*	–0.101	0.496	*SALPRES*	0.120	0.860
7				*WASTWICK*	–0.010	0.869

[a] Steps in stepwise regression analysis.
[b] Variables listed in order of selection in regression analysis.
[c] SRCs for variables in final regression model.
[d] Cumulative R^2 value with entry of each variable into regression model.
[e] SRRCs for variables in final regression model.

Nonparametric Regression. Nonparametric regression seeks more general models than those obtained by least squares regression and can succeed in situations such as the one illustrated in Fig. 7.8 where regression and correlation analysis based on raw and rank-transformed data fail. Nonparametric regression attempts to find models that are local in the approximation to the relationship between y_k and multiple x_j's, and, as a result, are better at capturing complex nonlinear relationships than models obtained with traditional regression or rank regression. Nonparametric regression models can be constructed in a stepwise manner with incremental changes in R^2 values with the addition of successive variables to the model providing an indication of variable importance. Additional information: Sect. 6.8, Ref. [56]; Refs. [111; 112; 197; 206-208].

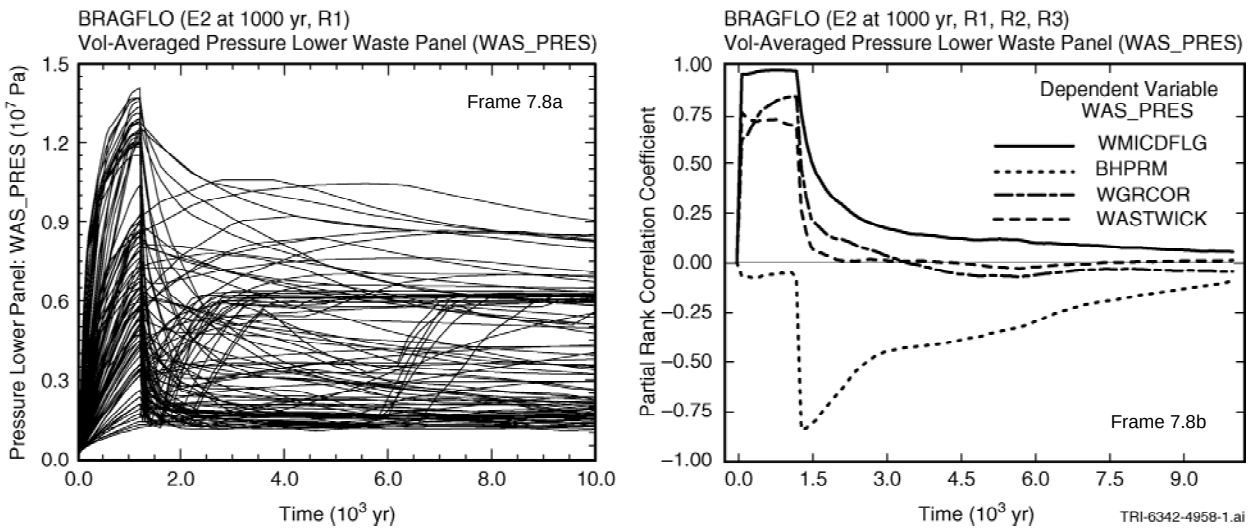

Fig. 7.8. Illustration of failure of a sensitivity analysis based on rank-transformed data: (a) Pressures as a function of time and (b) PRCCs as a function of time (Fig. 8.7, Ref. [194]).

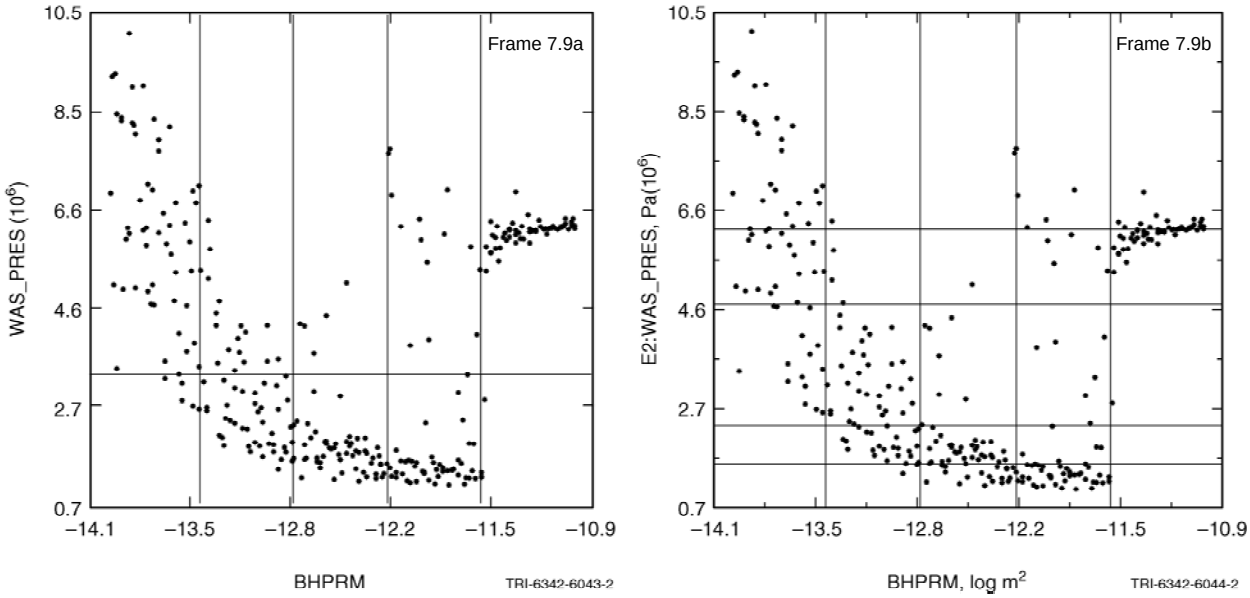

Fig. 7.9. Grids used to test for nonrandom patterns: (a) Partitioning of range of x_j for tests based on common means and common distributions and ranges of x_j and y_k for test based on, common medians, and common distributions (Fig. 8.8, Ref. [194]), and (b) Partitioning of ranges of x_j and y_k for tests of no influence (Fig. 8.9, Ref. [194]).

Tests for Patterns Based on Distance Measures. Tests based on distance measures consider relationships within the scatterplot for y_k and x_j such as the distribution of distances between nearest neighbors and provide a way to identify nonrandom relationships between y_k and x_j. A positive feature of these tests is the avoidance of the problem of defining an appropriate grid as is the case with grid-based methods. Additional information: Sect. 6.11, Ref. [56]; Refs. [209-212].

Trees. Tree-based sensitivity analyses search for relationships between y_k and multiple x_j's by successively subdividing the sample elements $\mathbf{x}_i$ on the basis of observed effects of individual x_j's on y_k. Additional information: Refs. [213; 214].

Two-Dimensional Kolmogorov-Smirnov Test. The two-dimensional Kolmogorov-Smirnov test provides a way to test for nonrandom patterns in the scatterplot for y_k and x_j that does not require the imposition

of a grid. Additional information: Sect. 6.10, Ref. [56]; Refs. [215-217].

Squared Differences of Ranks. The squared difference of ranks procedure seeks to identify the presence of nonlinear relationship between y_k and x_j and is based on squared differences of consecutive ranks of y_k when the values of y_k have been ordered by the corresponding values of x_j. Additional information: Sect. 6.9, Ref. [56]; Ref. [218].

Top-Down Concordance with Replicated Samples. This procedure uses the top-down coefficient of concordance and replicated (i.e., independently generated) samples. Sensitivity analysis with some appropriate technique to rank variable importance for each sample. The top-down coefficient is then used to identify important variables by seeking variables with similar rankings across all replicates. Additional information: Sect. 6.12, Ref. [56]; Refs. [143; 219].

Variance Decomposition. The variance decomposition procedure proposed by Sobol' and others is formally defined by high-dimensional integrals involving the x_j and $y_k(\mathbf{x})$. This procedure provides a decomposition of the variance $V(y_k)$ of y_k in terms of the contributions V_j of individual x_j's to $V(y_k)$ and also the contributions of various interactions between the x_j to $V(y_k)$. In practice, the indicated decomposition is obtained with sampling-based methods. Two samples from $\mathbf{x}$ of size nS are required to estimate all V_j; $nX + 2$ samples of size nS are required to estimate all V_j and also the contributions of each of the x_j's and its interactions with other elements of $\mathbf{x}$ to $V(y_k)$. This procedure is very appealing but can be computationally demanding as more samples and probably larger samples are required than with other sampling-based approaches to sensitivity analysis. Software for sampling-based variance decomposition is available as part of the SIMLAB package [220]. Additional information: Sect. 6.13, Ref. [56]; Refs. [57-61; 220].

This page intentionally left blank

8 Alternative Representations of Uncertainty

This section provides a brief overview of the following mathematical structures that can be used in the representation of uncertainty: interval analysis (Sect. 8.1), possibility theory (Sect. 8.2), evidence theory (Sect. 8.3), and probability theory (Sect. 8.4). For each structure, the following topics are considered: (i) the representation of uncertainty in a single variable x_i, (ii) the representation of uncertainty in a vector $\mathbf{x} = [x_1, x_2, \ldots, x_{nX}]$ of uncertain variables, and (iii) the representation of the uncertainty in a variable y defined by

$$y = F(\mathbf{x}), \mathbf{x} = [x_1, x_2, \ldots, x_{nX}], \tag{8.1}$$

where F is a function of the vector $\mathbf{x}$ of uncertain variables $x_1, x_2, \ldots, x_{nX}$. For this overview, no distinction is made between aleatory uncertainty and epistemic uncertainty. Then, the section concludes with a discussion of the use of sampling-based (i.e., Monte Carlo) procedures in the propagation of different structures for the representation of uncertainty (Sect. 8.5). The content of this section is a lightly edited adaptation of the material contained in Sect. 2 of Ref. [221].

A brief rationale for the use of each uncertainty representation is given. Of these representations, interval analysis and probability theory are the most widely used. The introduction of other uncertainty representations such as possibility theory and evidence theory has been accompanied by an extensive discussion of their potential use as alternatives to probability theory for the characterization of uncertainty, with some individuals maintaining that the use of these alternative representations is essential to an adequate representation of uncertainty in situations involving limited information and other individuals maintaining that probability provides the only appropriate structure for the representation of uncertainty [222-230]. For perspective, several comparative discussions of these different approaches to the representation of uncertainty are available [184; 188; 189; 231-236]. The view of the author is that interval analysis and probability theory will remain the dominant structures used in the representation of uncertainty but there will be analysis situations involving limited information where other representations for uncertainty, especially evidence theory, could be appropriate and beneficial.

It is important to recognize that, at least at an intuitive level, the need for alternatives to probability theory for the representation of epistemic uncertainty has already been introduced into the discussion of QMU. In particular, the following statement appears on p. 47 of Ref. [2]: "we require *positive evidence* that a nuclear weapon will work; *absence of evidence* that it will not work is not sufficient.". The preceding quote is an informal expression of the uncertainty information that evidence theory is intended to formally capture and communicate. As discussed in Sect. 8.3, evidence theory provides two measures of uncertainty: belief and plausibility. In the context of the preceding quote, belief provides a measure of the amount of "*positive evidence*" that supports the truth of a proposition, and plausibility provides a measure of the "*absence of evidence*" that refutes the truth of a proposition. Related concepts of necessity and possibility are present in possibility theory as discussed in Sect. 8.2. Thus, it should not be assumed that probability provides the only possible mathematical structure for the representation of uncertainty in QMU analyses. The possible use of alternatives to probability for the characterization of epistemic uncertainty is recognized in the NAS/NRC report on QMU (p. 29, Ref. [77]).

8.1 Interval Analysis

Interval analysis [237-242] is based on the assumption that a set $\mathcal{X}_i$ of possible values for a variable x_i is known but with no specified uncertainty structure within the set $\mathcal{X}_i$. Thus, all that is assumed to be known about x_i is that its value is contained within the set $\mathcal{X}_i$. Usually, but not necessarily, $\mathcal{X}_i$ is defined by

$$\mathcal{X}_i = \{x_i : a_i \le x_i \le b_i\}, \tag{8.2}$$

where $[a_i, b_i]$ is an interval that contains the possible values for x_i.

For a vector $\mathbf{x} = [x_1, x_2, \ldots, x_{nX}]$ of variables known only to be contained in the sets $\mathcal{X}_1, \mathcal{X}_2, \ldots, \mathcal{X}_{nX}$, the set $\mathcal{X}$ of possible values for $\mathbf{x}$ is given by

$$\mathcal{X} = \mathcal{X}_1 \times \mathcal{X}_2 \times \ldots \times \mathcal{X}_{nX}. \tag{8.3}$$

Given that there is no specified uncertainty structure for the sets $\mathcal{X}_1, \mathcal{X}_2, \ldots, \mathcal{X}_{nX}$, there is also no uncertainty structure for the set $\mathcal{X}$ of possible values for $\mathbf{x}$. Further, the preceding representation for $\mathcal{X}$ is predicated on the assumption that no restrictions exist that preclude specific combinations of values for the individual variables contained in $\mathbf{x}$.

Propagation of the individual values of $\mathbf{x}$ contained in $\mathcal{X}$ through the function F results in the set

$$\mathcal{Y} = \left\{ y : \mathbf{x} \in \mathcal{X} \text{ and } y = F\left(\mathbf{x}\right) \right\} \tag{8.4}$$

of possible values for y. Given that there is no uncertainty structure for the set $\mathcal{X}$, there is also no uncertainty structure for the set $\mathcal{Y}$.

In most applications, the indicated propagation to produce the set $\mathcal{Y}$ is based on using algebraic procedures implemented with appropriate software. However, an interval analysis can also be thought of as an optimization process in which it is desired to find the minimum and maximum of the function F on the set $\mathcal{X}$. Alternatively, the uncertainty propagation associated with an interval analysis can be approximated with a sampling-based (i.e., Monte Carlo) procedure (see Sect. 8.5).

8.2 Possibility Theory

Possibility theory [243-247] provides a representation for uncertainty that permits the specification of more structure than interval analysis and is based on the specification of a pair ($\mathcal{X}_i$, r_i) for a variable x_i, where (i) $\mathcal{X}_i$ is the set of possible values for x_i and (ii) r_i is a function defined on $\mathcal{X}_i$ such that $0 \le r_i(x_i) \le 1$ for $x_i \in \mathcal{X}_i$ and $\sup\{r(x_i) : x_i \in \mathcal{X}_i\} = 1$. The function r_i provides a measure of the amount of "likelihood" or "confidence" that is assigned to each element of $\mathcal{X}_i$ and is referred to as the possibility distribution function for x_i. The pair ($\mathcal{X}_i$, r_i) defines a possibility space for the variable x_i.

A value of $r(x_i) = 1$ indicates that there is no known information that refutes the "occurrence" or "appropriateness" of a specific value x_i contained in $\mathcal{X}_i$, and a value of $r(x_i) = 0$ indicates that known information completely refutes the "occurrence" or "appropriateness" of x_i. Further, increasing values for $r(x_i)$ between 0 and 1 indicate an increasing absence of information that refutes the "occurrence" or "appropriateness" of x_i. Intuitively, $r(x_i) = 1$ signifies that x_i is entirely possible in the sense that nothing is known that contradicts the possibility of x_i; $0 < r(x_i) < 1$ signifies that x_i is possible but with the amount of information indicating that x_i is not possible increasing as $r(x_i)$ approaches 0; and $r(x_i) = 0$ signifies that x_i is known to be impossible.

Possibility theory provides two measures of likelihood for subsets of $\mathcal{X}_i$: possibility and necessity. Specifically, possibility and necessity for a subset $\mathcal{U}$ of $\mathcal{X}_i$ are defined by

$$Pos_i\left(\mathcal{U}\right) = \sup\left\{ r_i\left(x_i\right) : x_i \in \mathcal{U}_i \right\} \tag{8.5}$$

and

$$Nec_i\left(\mathcal{U}\right) = 1 - Pos_i\left(\mathcal{U}^c\right) = 1 - \sup\left\{ r_i\left(x_i\right) : x_i \in \mathcal{U}^c \right\}, \tag{8.6}$$

respectively. In consistency with the properties of the possibility distribution function r_i, $Pos_i(\mathcal{U})$ provides a measure of the amount of information that does not contradict the proposition that $\mathcal{U}$ contains the appropriate value for x_i, and $Nec_i(\mathcal{U})$ provides a measure of the amount of uncontradicted information that supports the proposition that $\mathcal{U}$ contains the appropriate value for x_i.

Relationships satisfied by possibility and necessity for the possibility space ($\mathcal{X}_i$, r_i) include

$$1 = Nec_i\left(\mathcal{U}\right) + Pos_i\left(\mathcal{U}^c\right), \tag{8.7}$$

$$Nec_i\left(\mathcal{U}\right) \le Pos_i\left(\mathcal{U}\right), \tag{8.8}$$

$$1 \le Pos_i\left(\mathcal{U}\right) + Pos_i\left(\mathcal{U}^c\right), \tag{8.9}$$

$$1 \ge Nec_i\left(\mathcal{U}\right) + Nec_i\left(\mathcal{U}^c\right), \tag{8.10}$$

$$1 = \max\left\{ Pos_i\left(\mathcal{U}\right), Pos_i\left(\mathcal{U}^c\right) \right\}, \tag{8.11}$$

$$0 = \min\left\{ Nec_i\left(\mathcal{U}\right), Nec_i\left(\mathcal{U}^c\right) \right\}, \tag{8.12}$$

$$Pos_i\left(\mathcal{U}\right) < 1 \Rightarrow Nec_i\left(\mathcal{U}\right) = 0, \tag{8.13}$$

and

$$Nec_i\left(\mathcal{U}\right) > 0 \Rightarrow Pos_i\left(\mathcal{U}\right) = 1 \tag{8.14}$$

for subsets $\mathcal{U}$ of $\mathcal{X}_i$ (see Ref. [190], p. 34).

Convenient graphical summaries of possibility spaces are provided by cumulative necessity functions (CNFs), complementary cumulative necessity functions (CCNFs), cumulative possibility functions (CPoFs), and complementary cumulative possibility functions (CCPoFs), which are analogs of CDFs and CCDFs previously introduced as summaries for probability distributions (Sect. 3.1). Specifically, the CNF, CCNF, CPoF and CCPoF for the possibility space ($\mathcal{X}_i$, r_i) are defined by the sets

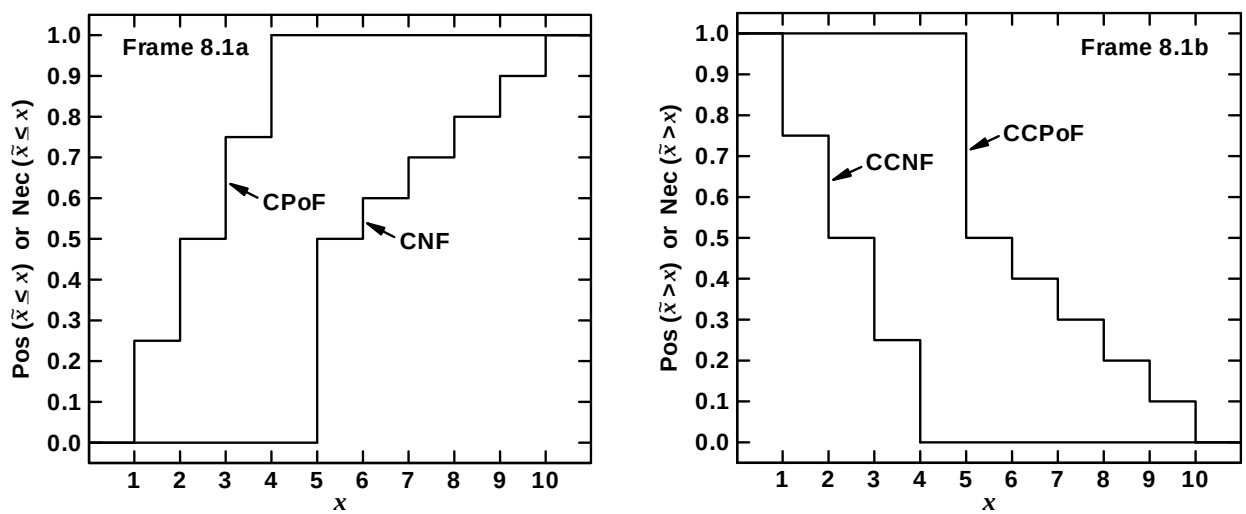

Fig. 8.1. Plots of CNF, CCNF, CPoF and CCPoF for possibility space ($\mathcal{X}$, r) with (i) $\mathcal{X} = \{x : 1 \le x \le 10\}$, (ii) $r(x) = i/4$ for $i \le x \le i + 1$ and $i = 1, 2, 3, 4$, and (iii) $r(x) = (10 - i)/10$ for $i \le x \le i + 1$ and $i = 5, 6, 7, 8, 9$.

$$\mathcal{CNF}_i = \left\{\left[x, Nec_i\left(\mathcal{U}_x\right)\right] : x \in \mathcal{X}_i\right\}, \tag{8.15}$$

$$\mathcal{CCNF}_i = \left\{\left[x, Nec_i\left(\mathcal{U}_x^c\right)\right] : x \in \mathcal{X}_i\right\}, \tag{8.16}$$

$$\mathcal{CPOF}_i = \left\{\left[x, Pos_i\left(\mathcal{U}_x\right)\right] : x \in \mathcal{X}_i\right\}, \tag{8.17}$$

$$\mathcal{CCPOF}_i = \left\{\left[x, Pos_i\left(\mathcal{U}_x^c\right)\right] : x \in \mathcal{X}_i\right\}, \tag{8.18}$$

where

$$\mathcal{U}_x = \left\{\tilde{x} : \tilde{x} \in \mathcal{X}_i \text{ and } \tilde{x} \le x\right\}.$$

Plots of the curves defined by the points associated with $\mathcal{CNF}_i$, $\mathcal{CCNF}_i$, $\mathcal{CPOF}_i$ and $\mathcal{CCPOF}_i$ yield the CNF, CCNF, CPoF, and CCPoF for the possibility space ($\mathcal{X}_i$, r_i) (Fig. 8.1).

If the variables $x_1, x_2, \ldots, x_{nX}$ have associated possibility spaces ($\mathcal{X}_1$, r_1), ($\mathcal{X}_2$, r_2), …, ($\mathcal{X}_{nX}$, r_{nX}), then the vector $\mathbf{x} = [x_1, x_2, \ldots, x_{nX}]$ also has an associated possibility space ($\mathcal{X}$, r_X), where $\mathcal{X}$ is defined the same as in Eq. (8.3) and

$$r_X\left(\mathbf{x}\right) = \min\left\{r_1\left(x_1\right), r_2\left(x_2\right), \ldots, r_{nX}\left(x_{nX}\right)\right\}. \tag{8.19}$$

The indicated definitions for $\mathcal{X}$ and r_X are predicated on the assumption that no restrictions involving possible combinations of values for the x_i's exist. If such restrictions exist, then the definition of r_X is more complex.

Once the possibility space ($\mathcal{X}$, r_X) for $\mathbf{x}$ is defined, possibility $Pos_X(\mathcal{U})$ and necessity $Nec_X(\mathcal{U})$ for subsets $\mathcal{U}$ of $\mathcal{X}$ are defined as indicated in Eqs. (8.5) and (8.6). Further, the relationships indicated in Eqs. (8.7) – (8.14) also hold.

Propagation of the individual values of $\mathbf{x}$ contained in $\mathcal{X}$ through the function F indicated in Eq. (8.1) results in a set $\mathcal{Y}$ of possible values for y of the form shown in Eq. (8.4). Given that a possibility space ($\mathcal{X}$, r_X) exists for $\mathbf{x}$, a resultant possibility space ($\mathcal{Y}$, r_Y) also exists for the values of y. Specifically, the possibility distribution function r_Y is defined by

$$\begin{aligned} r_Y\left(y\right) &= \sup\left\{r\left(\mathbf{x}\right) : \mathbf{x} \in \mathcal{X} \text{ and } y = F\left(\mathbf{x}\right)\right\} \\ &= Pos_X\left\{F^{-1}\left(y\right)\right\} \end{aligned} \tag{8.20}$$

for $y \in \mathcal{Y}$, where $F^{-1}(y)$ represents the set

$$F^{-1}\left(y\right) = \left\{\mathbf{x} : \mathbf{x} \in \mathcal{X} \text{ and } y = F\left(\mathbf{x}\right)\right\}.$$

In turn, the possibility $Pos_Y(\mathcal{U})$ and necessity $Nec_Y(\mathcal{U})$ for subsets $\mathcal{U}$ of $\mathcal{Y}$ can be defined as indicated in Eqs. (8.5) and (8.6); further, the relationships indicated in Eqs. (8.7) – (8.14) also hold.

Provided y is real valued, the possibility space ($\mathcal{Y}$, r_Y) can be summarized by presentation of the corresponding CNF, CCNF, CPoF and CCPoF as discussed in conjunction with Eqs. (8.15) – (8.18). Specifically, the CNF, CCNF, CPoF and CCPoF for y are defined by the sets

$$\mathcal{CNF} = \left\{ \left[y, Nec_Y\left(\mathcal{U}_y\right) \right] : y \in \mathcal{Y} \right\} = \left\{ \left[y, Nec_X\left(F^{-1}\left[\mathcal{U}_y\right]\right) \right] : y \in \mathcal{Y} \right\}, \tag{8.21}$$

$$\mathcal{CCNF} = \left\{ \left[y, Nec_Y\left(\mathcal{U}_y^c\right) \right] : y \in \mathcal{Y} \right\} = \left\{ \left[y, Nec_X\left(F^{-1}\left[\mathcal{U}_y^c\right]\right) \right] : y \in \mathcal{Y} \right\}, \tag{8.22}$$

$$\mathcal{CPOF} = \left\{ \left[y, Pos_Y\left(\mathcal{U}_y\right) \right] : y \in \mathcal{Y} \right\} = \left\{ \left[y, Pos_X\left(F^{-1}\left[\mathcal{U}_y\right]\right) \right] : y \in \mathcal{Y} \right\}, \tag{8.23}$$

$$\mathcal{CCPOF} = \left\{ \left[y, Pos_Y\left(\mathcal{U}_y^c\right) \right] : y \in \mathcal{Y} \right\} = \left\{ \left[y, Pos_X\left(F^{-1}\left[\mathcal{U}_y^c\right]\right) \right] : y \in \mathcal{Y} \right\}, \tag{8.24}$$

where

$$\mathcal{U}_y = \left\{ \tilde{y} : \tilde{y} \in \mathcal{Y} \text{ and } \tilde{y} \le y \right\}.$$

Plots of the curves defined by $\mathcal{CNF}$, $\mathcal{CCNF}$, $\mathcal{CPOF}$ and $\mathcal{CCPOF}$ produce a figure identical in concept to Fig. 8.1 and provide a visual representation of the uncertainty associated with y in terms of necessity and possibility.

8.3 Evidence Theory

Evidence theory [248-255], which is also known as Dempster-Shafer theory in recognition of the initial work done by these two individuals, provides a representation for uncertainty that permits the specification of more structure than possibility theory. Evidence theory is based on the specification of a triple ($\mathcal{X}_i$, $\mathbb{X}_i$, m_i) for a variable x_i, where (i) $\mathcal{X}_i$ is the set of possible values for x_i, (ii) $\mathbb{X}_i$ is a countable collection of subsets of $\mathcal{X}_i$, and (iii) m_i is a function defined for subsets $\mathcal{U}$ of $\mathcal{X}_i$ such that $m_i(\mathcal{U}) > 0$ if $\mathcal{U} \in \mathbb{X}_i$, $m_i(\mathcal{U}) = 0$ if $\mathcal{U} \notin \mathbb{X}_i$, and

$$\sum_{\mathcal{U} \in \mathbb{X}_i} m_i\left(\mathcal{U}\right) = 1. \tag{8.25}$$

In the terminology of evidence theory, (i) $\mathcal{X}_i$ is the sample space or universal set, (ii) $\mathbb{X}_i$ is the set of focal elements for $\mathcal{X}_i$ and m_i, and (iii) $m_i(\mathcal{U})$ is the basic probability assignment associated with a subset $\mathcal{U}$ of $\mathcal{X}_i$. In concept, the basic probability assignment $m_i(\mathcal{U})$ provides a measure of the amount of information (or credibility or probability) that can be associated with a subset $\mathcal{U}$ of $\mathcal{X}_i$ but which cannot be further decomposed over subsets of $\mathcal{U}$.

Evidence theory provides two measures of likelihood for subsets of $\mathcal{X}_i$: plausibility and belief. Specifically, the plausibility and belief for a subset $\mathcal{U}$ of $\mathcal{X}_i$ are defined by

$$Pl_i\left(\mathcal{U}\right) = \sum_{\mathcal{V} \cap \mathcal{U} \neq \varnothing} m_i\left(\mathcal{V}\right) \tag{8.26}$$

and

$$Bel_i\left(\mathcal{U}\right) = \sum_{\mathcal{V} \subset \mathcal{U}} m_i\left(\mathcal{V}\right), \tag{8.27}$$

respectively. As a result of the intersection requirement (i.e., $\mathcal{V} \cap \mathcal{U} \neq \varnothing$ in Eq. (8.26)), $Pl_i(\mathcal{U})$ provides a measure of the amount of information that could possibly be associated with $\mathcal{U}$. Similarly as a result of the subset requirement (i.e., $\mathcal{V} \subset \mathcal{U}$ in Eq. (8.27)), $Bel_i(\mathcal{U})$ provides a measure of the amount of information that is known to be associated with $\mathcal{U}$. In the context of the quote from Ref. [2] given at the beginning of Sect. 8, $Pl_i(\mathcal{U})$ is a measure of the "*absence of evidence*" that refutes the membership of x_i in $\mathcal{U}$, and $Bel_i(\mathcal{U})$ is a measure of the "*positive evidence*" that supports the membership of x_i in $\mathcal{U}$.

Relationships satisfied by plausibility and belief for the evidence space ($\mathcal{X}_i$, $\mathbb{X}_i$, m_i) include

$$Bel_i\left(\mathcal{U}\right) + Pl_i\left(\mathcal{U}^c\right) = 1, \tag{8.28}$$

$$Bel_i\left(\mathcal{U}\right) \le Pl_i\left(\mathcal{U}\right), \tag{8.29}$$

$$Pl_i\left(\mathcal{U}\right) + Pl_i\left(\mathcal{U}^c\right) \ge 1 \tag{8.30}$$

and

$$Bel_i\left(\mathcal{U}\right) + Bel_i\left(\mathcal{U}^c\right) \le 1 \tag{8.31}$$

for subsets $\mathcal{U}$ of $\mathcal{X}_i$.

Convenient graphical summaries of evidence spaces are provided by cumulative belief functions (CBFs), complementary cumulative belief functions (CCBFs), cumulative plausibility functions (CPFs), and complementary cumulative plausibility functions (CCPFs). Specifically, the CBF, CCBF, CPF and CCPF for the evidence space ($\mathcal{X}_i$, $\mathbb{X}_i$, m_i) are defined by the sets

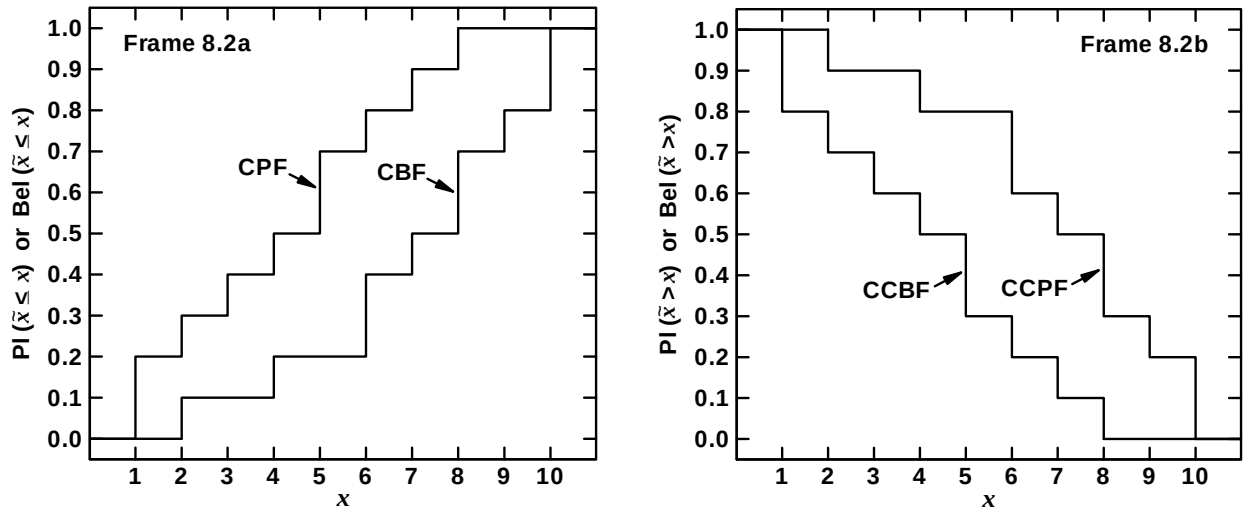

Fig. 8.2. Plots of CBF, CCBF, CPF and CCPF for evidence space ($\mathcal{X}$, $\mathbb{X}$, m) with (i) $\mathcal{X} = \{x : 1 \le x \le 10\}$, (ii) $\mathbb{X} = \{\mathcal{U}_1, \mathcal{U}_2, \ldots, \mathcal{U}_{10}\}$ with $\mathcal{U}_i = [i, 2i]$ for i = 1, 2, 3, 4, 5 and $\mathcal{U}_i = [i - 1, i]$ for i = 6, 7, 8, 9, 10, and (iii) $m(\mathcal{U})$ = 1/10 if $\mathcal{U} \in \mathbb{X}$ and $m(\mathcal{U})$ = 0 otherwise.

$$\mathcal{CBF}_i = \left\{\left[x, Bel_i\left(\mathcal{U}_x\right)\right] : x \in \mathcal{X}_i\right\}, \tag{8.32}$$

$$\mathcal{CCBF}_i = \left\{\left[x, Bel_i\left(\mathcal{U}_x^c\right)\right] : x \in \mathcal{X}_i\right\}, \tag{8.33}$$

$$\mathcal{CPF}_i = \left\{\left[x, Pl_i\left(\mathcal{U}_x\right)\right] : x \in \mathcal{X}_i\right\}, \tag{8.34}$$

and

$$\mathcal{CCPF}_i = \left\{\left[x, Pl_i\left(\mathcal{U}_x^c\right)\right] : x \in \mathcal{X}_i\right\}, \tag{8.35}$$

where $\mathcal{U}_x$ is defined the same as in conjunction with Eqs. (8.15) – (8.18). Plots of the curves defined by the points associated with $\mathcal{CBF}_i$, $\mathcal{CCBF}_i$, $\mathcal{CPF}_i$ and $\mathcal{CCPF}_i$ yield the CBF, CCBF, CPF and CCPF for the evidence space ($\mathcal{X}_i$, $\mathbb{X}_i$, m_i) (Fig. 8.2).

If the variables $x_1, x_2, \ldots, x_{nX}$ have associated evidence spaces ($\mathcal{X}_1$, $\mathbb{X}_1$, m_1), ($\mathcal{X}_2$, $\mathbb{X}_2$, m_2), …, ($\mathcal{X}_{nX}$, $\mathbb{X}_{nX}$, m_{nX}), then the vector $\mathbf{x} = [x_1, x_2, \ldots, x_{nX}]$ also has an associated evidence space ($\mathcal{X}$, $\mathbb{X}$, m_X), where (i) $\mathcal{X}$ is defined the same as in Eq. (8.3), (ii) $\mathcal{U} \in \mathbb{X}$ if, and only if,

$$\mathcal{U} = \mathcal{U}_1 \times \mathcal{U}_2 \times \ldots \times \mathcal{U}_{nX} \tag{8.36}$$

with $\mathcal{U}_i \in \mathbb{X}_i$ for i = 1, 2, …, nX, and (iii)

$$m_X\left(\mathcal{U}\right) = \prod_{i=1}^{nX} m_i\left(\mathcal{U}_i\right) \tag{8.37}$$

if $\mathcal{U} = \mathcal{U}_1 \times \mathcal{U}_2 \times \ldots \times \mathcal{U}_{nX} \in \mathbb{X}$ and $m_X(\mathcal{U})$ = 0 otherwise. The preceding definition for ($\mathcal{X}$, $\mathbb{X}$, m_X) is predicated on the assumption that no restrictions involving possible combinations of values for the x_i exist. If such restrictions exist, then the definition of ($\mathcal{X}$, $\mathbb{X}$, m_X) is more complex.

Once the evidence space ($\mathcal{X}$, $\mathbb{X}$, m_X) for $\mathbf{x}$ is defined, the plausibility $Pl_X(\mathcal{U})$ and belief $Bel_X(\mathcal{U})$ for subsets $\mathcal{U}$ of $\mathcal{X}$ are defined as indicated in Eqs. (8.26) and (8.27). Further, the relationships indicated in Eqs. (8.28) – (8.31) also hold.

Propagation of the individual values of $\mathbf{x}$ contained in $\mathcal{X}$ through the function F indicated in Eq. (8.1) results in a set $\mathcal{Y}$ of possible values for y of the form shown in Eq. (8.4). Given that an evidence space ($\mathcal{X}$, $\mathbb{X}$, m_X) exists for $\mathbf{x}$, a resultant evidence space ($\mathcal{Y}$, $\mathbb{Y}$, m_Y) also exists for the value of y. Specifically, (i)

$$\mathbb{Y} = \left\{F\left(\mathcal{V}_1\right), \quad F\left(\mathcal{V}_2\right), \ldots\right\} \tag{8.38}$$

where $\mathcal{V}_1$, $\mathcal{V}_2$, … correspond to the elements of $\mathbb{X}$, (ii)

$$m_Y\left(\mathcal{U}\right) = \sum_{k \in \mathcal{I}(\mathcal{U})} m\left(\mathcal{V}_k\right) \tag{8.39}$$

for $\mathcal{U} \in \mathbb{Y}$ with $k \in \mathcal{I}(\mathcal{U})$ if, and only if, $\mathcal{U} = F(\mathcal{V}_k)$, and (iii) $m_Y(\mathcal{U})$ = 0 if $\mathcal{U} \notin \mathbb{Y}$. The summation over k in the definition of $m_Y(\mathcal{U})$ in Eq. (8.39) is necessary to appropriately incorporate the possibility that $\mathcal{U} = F(\mathcal{V}_k)$ for

more than one element $\mathcal{V}_k$ of $\mathbb{X}$. In turn, the plausibility $Pl_Y(\mathcal{U})$ and belief $Bel_Y(\mathcal{U})$ for subsets $\mathcal{U}$ of $\mathcal{Y}$ can be defined as indicated in Eqs. (8.26) – (8.27); further, the relationships indicated in Eqs. (8.28) – (8.31) also hold.

Provided y is real valued, the evidence space ($\mathcal{Y}$, $\mathbb{Y}$, m_Y) can be summarized by presentation of the corresponding CBF, CCBF, CPF and CCPF as discussed in conjunction with Eqs. (8.32) – (8.35). Specifically, the CBF, CCBF, CPF and CCPF for y are defined by the sets

$$\begin{aligned}\mathcal{CBF} &= \left\{\left[y, Bel_Y\left(\mathcal{U}_y\right)\right] : y \in \mathcal{Y}\right\} \\ &= \left\{\left[y, Bel_X\left(F^{-1}\left[\mathcal{U}_y\right]\right)\right] : y \in \mathcal{Y}\right\},\end{aligned} \tag{8.40}$$

$$\begin{aligned}\mathcal{CCBF} &= \left\{\left[y, Bel_Y\left(\mathcal{U}_y^c\right)\right] : y \in \mathcal{Y}\right\} \\ &= \left\{\left[y, Bel_X\left(F^{-1}\left[\mathcal{U}_y^c\right]\right)\right] : y \in \mathcal{Y}\right\},\end{aligned} \tag{8.41}$$

$$\begin{aligned}\mathcal{CPF} &= \left\{\left[y, Pl_Y\left(\mathcal{U}_y\right)\right] : y \in \mathcal{Y}\right\} \\ &= \left\{\left[y, Pl_X\left(F^{-1}\left[\mathcal{U}_y\right]\right)\right] : y \in \mathcal{U}\right\},\end{aligned} \tag{8.42}$$

and

$$\begin{aligned}\mathcal{CCPF} &= \left\{\left[y, Pl_Y\left(\mathcal{U}_y^c\right)\right] : y \in \mathcal{Y}\right\} \\ &= \left\{\left[y, Pl_X\left(F^{-1}\left[\mathcal{U}_y^c\right]\right)\right] : y \in \mathcal{Y}\right\},\end{aligned} \tag{8.43}$$

where $\mathcal{U}_y$ is defined the same as in conjunction with Eqs. (8.21) – (8.24). Plots of the curves defined by the points associated with $\mathcal{CBF}$, $\mathcal{CCBF}$, $\mathcal{CPF}$ and $\mathcal{CCPF}$ produce a figure identical in concept to Fig. 8.2 and provide a visual representation of the uncertainty associated with y in terms of belief and plausibility.

Possibility theory and evidence theory differ with respect to the basic unit on which "likelihood" is characterized. In possibility theory, "likelihood" at its most basic level is defined for individual elements x of a sample space $\mathcal{X}$ by a possibility distribution function r (i.e., $r(x)$ is the amount of "likelihood" or "credence" that can be assigned to the element x of $\mathcal{X}$). In contrast, "likelihood" at its most basic level is defined in evidence theory for subsets $\mathcal{U}$ of a sample space $\mathcal{X}$ by a function m_X (i.e., $m_X(\mathcal{U})$ is the basic probability assignment for the subset $\mathcal{U}$ of $\mathcal{X}$ and corresponds to the amount of "likelihood" or "credence" that can be assigned to $\mathcal{U}$ but cannot be further partitioned over subsets of $\mathcal{U}$). Thus, possibility theory is predicated on the premise that it is both reasonable and possible to assign a measure of "likelihood" to each element of the sample space under consideration. Differently, evidence theory is predicated on the premise that, at best, it is possible to assign a nonzero measure of "likelihood" to a countable (actually, finite in most situations) collection of subsets of the sample space under consideration. As a consequence, possibility theory characterizes uncertainty at the level of individual elements of a sample space, and evidence theory characterizes uncertainty at the level of individual subsets of a sample space.

Possibility theory and evidence theory can also be viewed in the context of fuzzy set theory and probability theory, respectively. For possibility theory, the value $r(x)$ of the possibility distribution function can be thought of as characterizing the extent to which the quantity x is believed to belong to the set $\mathcal{X}$. When viewed in this manner, possibility theory is simply part of fuzzy set theory [247; 256]. For evidence theory, the basic probility assignment $m_X(\mathcal{U})$ can be viewed as the amount of probability that can be assigned to the set $\mathcal{U}$ but cannot be further partitioned over subsets of $\mathcal{U}$. When viewed in this manner, evidence theory is simply part of probability theory. Specifically, one interpretation of an evidence space ($\mathcal{X}$, $\mathbb{X}$, m_X) is that it is an incompletely defined probability space [253-255].

8.4 Probability Theory

Probability theory [83; 87; 91; 93; 94; 257-263] provides a representation for uncertainty that involves the specification of more structure than evidence theory. Similarly to evidence theory, probability theory is based on the specification of a triple ($\mathcal{X}_i$, $\mathbb{X}_i$, p_i) for a variable x_i, where (i) $\mathcal{X}_i$ is the set of possible values for x_i, (ii) $\mathbb{X}_i$ is a suitably restricted collection of subsets of $\mathcal{X}_i$ (i.e., if $\mathcal{U} \in \mathbb{X}_i$, then $\mathcal{U}^c \in \mathbb{X}_i$, and if $\mathcal{U}_1$, $\mathcal{U}_2$, … is a countable sequence of elements of $\mathbb{X}_i$, then $\cup_k \mathcal{U}_k \in \mathbb{X}_i$ and $\cap_k \mathcal{U}_k \in \mathbb{X}_i$),and (iii) and p_i defines probability for elements of $\mathcal{X}_i$ (i.e., $0 \le p_i(\mathcal{U}) \le 1$ if $\mathcal{U} \in \mathbb{X}_i$, $p_i(\mathcal{X}_i) = 1$, and $p_i\ (\cup_k \mathcal{U}_k) = \sum_k p_i(\mathcal{U}_k)$ if $\mathcal{U}_1$, $\mathcal{U}_2$, … is a countable sequence of nonintersecting elements of $\mathbb{X}_i$). However, in contrast to an evidence space ($\mathcal{X}_i$, $\mathbb{X}_i$, m_i), a probability space ($\mathcal{X}_i$, $\mathbb{X}_i$, p_i) involves the imposition of more structure on $\mathbb{X}_i$ and p_i than is the case for $\mathbb{X}_i$ and m_i for an evidence space. In the terminology of probability theory, (i) $\mathcal{X}_i$ is the sample space, (ii) the elements of $\mathbb{X}_i$ are events and collectively constitute what is known as a σ-algebra, and (iii) p_i is a probability measure (Sects. IV.3 and IV.4, Ref. [93]). For notational and computational convenience, a probability space ($\mathcal{X}_i$, $\mathbb{X}_i$, p_i) is often summarized with a density function d_i, where

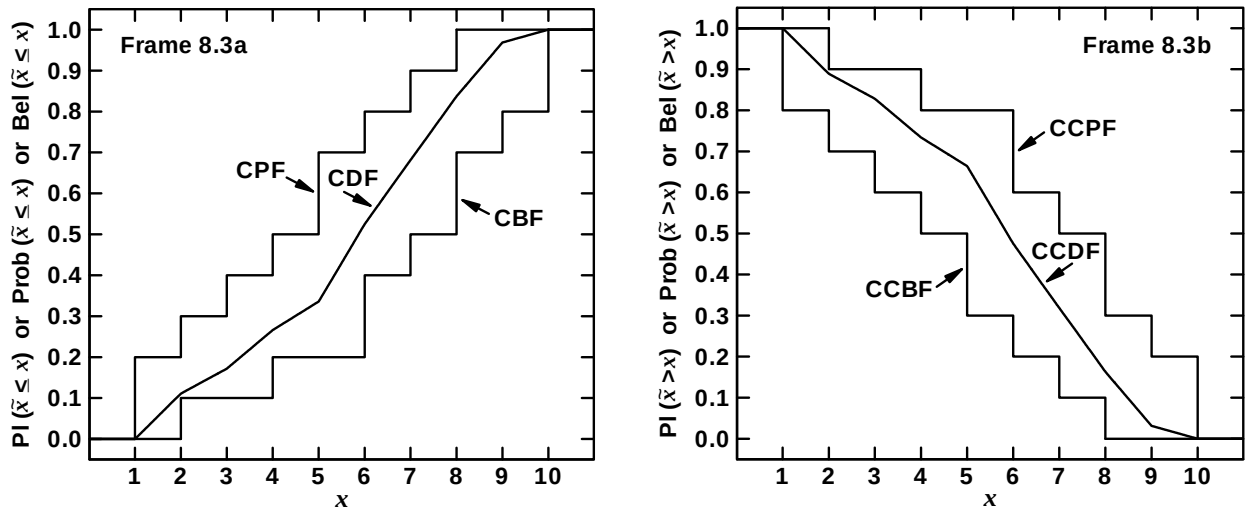

Fig. 8.3. Plots of (a) CBF, CCBF, CPF and CCPF for evidence space ($\mathcal{X}$, $\mathbb{X}$, m) with (i) $\mathcal{X} = \{x : 1 \le x \le 10\}$, (ii) $\mathbb{X} = \{\mathcal{U}_1, \mathcal{U}_2, \ldots, \mathcal{U}_{10}\}$ with $\mathcal{U}_i = [i, 2i]$ for i = 1, 2, 3, 4, 5 and $\mathcal{U}_i = [i - 1, i]$ for i = 6, 7, 8, 9, 10, and (iii) $m(\mathcal{U}) = 1/10$ if $\mathcal{U} \in \mathbb{X}$ and $m(\mathcal{U}) = 0$ otherwise (see Fig. 8.2), and (b) CDF and CCDF for probability space ($\mathcal{X}$, $\mathbb{X}$, p) with density function d defined as indicated in Eq. (8.49).

$$p_i(\mathcal{U}) = \int_{\mathcal{U}} d_i(x_i)\,\mathrm{d}x_i \tag{8.44}$$

for $\mathcal{U} \in \mathbb{X}_i$.

Unlike possibility theory and evidence theory, which provide two measures of likelihood (i.e., possibility and necessity in possibility theory and plausibility and belief in evidence theory), probability theory provides only one measure of likelihood: probability. The probabilities of a set and its complement are related by

$$p_i(\mathcal{U}) + p_i\left(\mathcal{U}^c\right) = 1 \tag{8.45}$$

for $\mathcal{U} \in \mathbb{X}_i$, which is a more restrictive requirement than shown in Eqs. (8.9) and (8.10) for possibility and necessity and in Eqs. (8.30) and (8.31) for plausibility and belief.

Convenient graphical summaries of probability spaces are provided by cumulative distribution functions (CDFs) and complementary cumulative distribution functions (CCDFs). Specifically, the CDF and CCDF for the probability space ($\mathcal{X}_i$, $\mathbb{X}_i$, p_i) with the corresponding density function d_i are defined by the sets

$$\begin{aligned}\mathcal{CDF}_i &= \left\{\left[x,\ p_i\left(\mathcal{U}_x\right)\right] : x \in \mathcal{X}_i\right\} \\ &= \left\{\left[x,\ \int_{\mathcal{U}_x} d_i(x)\,\mathrm{d}x\right] : x \in \mathcal{X}_i\right\}\end{aligned} \tag{8.46}$$

and

$$\begin{aligned}\mathcal{CCDF}_i &= \left\{\left[x,\ p_i\left(\mathcal{U}_x^c\right)\right] : x \in \mathcal{X}_i\right\} \\ &= \left\{\left[x,\ \int_{\mathcal{U}_x^c} d_i(x)\,\mathrm{d}x\right] : x \in \mathcal{X}_i\right\},\end{aligned} \tag{8.47}$$

where $\mathcal{U}_x$ is defined the same as in conjunction with Eqs. (8.15) – (8.18). Plots of the curves defined by the points associated with $\mathcal{CDF}_i$ and $\mathcal{CCDF}_i$ yield the CDF and CCDF for the probability space ($\mathcal{X}_i$, $\mathbb{X}_i$, p_i) (Fig. 8.3).

One interpretation of an evidence space ($\mathcal{X}$, $\mathbb{X}$, m) is that it is a characterization of a partially defined probability space. In general, there are many possible probability spaces ($\mathcal{X}$, $\mathbb{X}$, p) that are consistent with a given evidence space ($\mathcal{X}$, $\mathbb{X}$, m) in the sense that, if $\mathcal{U} \subset \mathcal{X}$ (i.e., technically, an element of the set $\mathbb{X}$ associated with ($\mathcal{X}$, $\mathbb{X}$, p)), then

$$Bel(\mathcal{U}) \le p(\mathcal{U}) \le Pl(\mathcal{U}). \tag{8.48}$$

As a result of the preceding inequality, if a probability space ($\mathcal{X}$, $\mathbb{X}$, p) is consistent with an evidence space ($\mathcal{X}$, $\mathbb{X}$, m), then the CDF associated with ($\mathcal{X}$, $\mathbb{X}$, p) falls between the CBF and CPF associated with ($\mathcal{X}$, $\mathbb{X}$, m) and similarly the CCDF falls between the CCBF and CCPF.

For example, if $\mathcal{X}$ corresponds to a bounded interval $\mathcal{I} = [a, b]$ and each focal element $\mathcal{U}_k$ associated with

the evidence space ($\mathcal{X}$, $\mathbb{X}$, m) is a subinterval $\mathcal{I}_k = [a_k, b_k]$ of $\mathcal{I}$, then a probability space ($\mathcal{X}$, $\mathbb{X}$, p) consistent with the evidence space ($\mathcal{X}$, $\mathbb{X}$, m) is defined by the density function

$$d(x) = \sum_k \delta_k(x) m(\mathcal{U}_k) / (b_k - a_k), \tag{8.49}$$

where

$$\delta_k(x) = \begin{cases} 1 & \text{if } x \in \mathcal{U}_k \\ 0 & \text{otherwise.} \end{cases}$$

As a result, the CDF for ($\mathcal{X}$, $\mathbb{X}$, p) falls between the CBF and CPF for ($\mathcal{X}$, $\mathbb{X}$, m), and similarly, the CCDF for ($\mathcal{X}$, $\mathbb{X}$, p) falls between the CCBF and CCPF for ($\mathcal{X}$, $\mathbb{X}$, m) (Fig. 8.3).

If the variables x_1, x_2, …, x_{nX} have associated probability spaces ($\mathcal{X}_1$, $\mathbb{X}_1$, p_1), ($\mathcal{X}_2$, $\mathbb{X}_2$, p_2), …, ($\mathcal{X}_{nX}$, $\mathbb{X}_{nX}$, p_{nX}), then the vector $\mathbf{x} = [x_1, x_2, \ldots, x_{nX}]$ also has an associated probability space ($\mathcal{X}$, $\mathbb{X}$, p_X), where (i) $\mathcal{X}$ is defined the same as in Eq. (8.3), (ii) $\mathbb{X}$ is developed from the sets contained in

$$\mathbb{C} = \{\mathcal{U} : \mathcal{U} = \mathcal{U}_1 \times \mathcal{U}_2 \times \cdots \times \mathcal{U}_{nX} \in \mathbb{X}_1 \times \mathbb{X}_2 \times \ldots \times \mathbb{X}_{nX}\} \tag{8.50}$$

(see Sect. IV.6, Ref. [93], and Sect. 2.6, Ref. [94]), and (iii) p_X is developed from the properties of p_1, p_2, …, p_{nX}. Specifically, if the x_i are independent (i.e., if the occurrence of one x_i has no implications for the occurrence of the remaining x_j, $j \neq i$), then

$$p_X(\mathcal{U}) = \prod_{i=1}^{nX} p_i[\mathcal{U}_i] \tag{8.51}$$

for $\mathcal{U} = \mathcal{U}_1 \times \mathcal{U}_2 \times \ldots \times \mathcal{U}_{nX} \in \mathbb{C}$ and, more generally,

$$p_X(\mathcal{U}) = \int_{\mathcal{U}} d_X(\mathbf{x}) \mathrm{d}X \tag{8.52}$$

for $\mathcal{U} \in \mathbb{X}$, where

$$d_X(\mathbf{x}) = \prod_{i=i}^{nX} d_i(x_i)$$

is the density function associated with ($\mathcal{X}$, $\mathbb{X}$, p_X) and d_i is the density function associated with ($\mathcal{X}_i$, $\mathbb{X}_i$, p_i) for i = 1, 2, …, nX. The definition of p_X and d_X are more complex when the x_i are not independent and will not be considered here.

Propagation of the individual values of $\mathbf{x}$ contained in $\mathcal{X}$ through the function F indicated in Eq. (8.1) results in a set $\mathcal{Y}$ of possible values for y of the form shown in Eq. (8.4). Given that a probability space ($\mathcal{X}$, $\mathbb{X}$, p_X) exists for $\mathbf{x}$, a resultant probability space ($\mathcal{Y}$, $\mathbb{Y}$, p_Y) also exists for y. In concept, the probability $p_Y(\mathcal{U})$ for a subset $\mathcal{U}$ of $\mathcal{Y}$ is given by

$$p_Y(\mathcal{U}) = p_X\left[F^{-1}(\mathcal{U})\right]. \tag{8.53}$$

A formal development of $\mathbb{Y}$ and p_Y would focus on the properties that F must possess to actually produce the probability space ($\mathcal{Y}$, $\mathbb{Y}$, p_Y) (see Sect. IV.4, Ref. [93], and Sects. 4.6 and 4.7, Ref. [94]); such details are outside the scope of this presentation.

Provided y is real valued, the probability space ($\mathcal{Y}$, $\mathbb{Y}$, p_Y) can be summarized by the presentation of the corresponding CDF and CCDF. Specifically, the CDF and CCDF for y are defined by the sets

$$\begin{aligned} \mathcal{CDF} &= \left\{\left[y,\ p_Y(\mathcal{U}_y)\right] : y \in \mathcal{Y}\right\} \\ &= \left\{\left[y,\ p_X\left(F^{-1}\left[\mathcal{U}_y\right]\right)\right] : y \in \mathcal{Y}\right\} \end{aligned} \tag{8.54}$$

and

$$\begin{aligned} \mathcal{CCDF} &= \left\{\left[y,\ p_Y\left(\mathcal{U}_y^c\right)\right] : y \in \mathcal{Y}\right\} \\ &= \left\{\left[y,\ p_X\left(F^{-1}\left[\mathcal{U}_y^c\right]\right)\right] : y \in \mathcal{Y}\right\}, \end{aligned} \tag{8.55}$$

where $\mathcal{U}_y$ is defined the same as in conjunction with Eqs. (8.21) – (8.24). Plots of the curves defined by the points associated with $\mathcal{CDF}$ and $\mathcal{CCDF}$ produce a CDF and CCDF identical in concept to the CDF and CCDF in Fig. 8.3 and provide a visual representation of a probabilistic characterization of the uncertainty associated with y.

8.5 Sampling-Based Uncertainty Propagation

An analysis outcome $y = F(\mathbf{x})$ of the form indicated in Eq. (8.1) will have an uncertainty structure that derives from the uncertainty structure associated with $\mathbf{x}$. In particular, the uncertainty associated with y will have an interval representation, a possibility theory representation, an evidence theory representation or a probabilistic representation in consistency with an interval representation (Sect. 8.1), a possibility theory representa-

tion (Sect. 8.2), an evidence theory representation (Sect. 8.3) or a probabilistic representation (Sect. 8.4) for the uncertainty associated with $\mathbf{x}$. For reasons of numerical difficulty, an exact determination of the uncertainty structure associated with y that results from the uncertianty structure associated with $\mathbf{x}$ is usually not possible in a real analysis. However, the indicated uncertainty structures for y can be approximated with sampling-based procedures.

As indicated by the name, sampling-based (Monte Carlo) procedures involve the use of a sample

$$\mathbf{x}_i = \left[x_{i1}, x_{i2}, \ldots, x_{i,nX} \right], i = 1, 2, \ldots, nS, \tag{8.56}$$

from the set $\mathcal{X}$ of possible values of $\mathbf{x}$ in the estimation of the uncertainty structure associated with $y = F(\mathbf{x})$ that derives from the uncertainty structure associated with $\mathbf{x}$ [29; 45; 55; 264-268]. For uncertainty propagations involving interval analysis, possibility theory and evidence theory, it is important that the sample provide an "adequate" coverage of $\mathcal{X}$ but there are no requirements for a specific structure for this sample. Of course, what constitutes adequate coverage of $\mathcal{X}$ depends on properties of $\mathcal{X}$ and the function $F(\mathbf{x})$. In the case of an evidence theory representation of the uncertainty associated with $\mathbf{x}$, adequate coverage of $\mathbf{x}$ corresponds to a sample that provides a reasonable estimate of the minimum and maximum value of $F(\mathbf{x})$ for each focal element in the evidence space defined for $\mathcal{X}$. However, for a probabilistic representation of the uncertainty associated with $\mathbf{x}$, the sample in Eq. (8.56) must be generated in consistency with the probability distribution defined for $\mathbf{x}$.

Once an appropriate sample of the form indicated in Eq. (8.56) is generated, an interval representation for the uncertainty associated with y is given by

$$\begin{aligned} \left[y_{mn}, y_{mx} \right] &= \left[\inf\left(\mathcal{Y}\right), \sup\left(\mathcal{Y}\right) \right] \\ &\cong \left[\min\left\{ y_i : i = 1, 2, \ldots, nS \right\}, \right. \\ &\qquad \left. \max\left\{ y_i : i = 1, 2, \ldots, nS \right\} \right], \end{aligned} \tag{8.57}$$

where $\mathcal{Y}$ is the set of possible values for y defined in Eq. (8.4) and $y_i = y(\mathbf{x}_i)$ for $i = 1, 2, \ldots, nS$. The preceding procedure will not be the most computationally efficient method for estimating $[y_{mn}, y_{mx}]$ in many analyses. However, it is presented here for consistency with the sampling-based procedures described below for use in conjunction with possibility theory, evidence theory and probability theory representations of the epistemic uncertainty in $\mathbf{x}$ and hence in y.

If the epistemic uncertainty associated with $\mathbf{x}$ is characterized by a possibility space $(\mathcal{X}, r_X)$, then the corresponding possibility space $(\mathcal{Y}, r_Y)$ for y can be summarized by its associated CNF, CCNF, CPoF and CCPoF (see Eqs. (8.21) – (8.24)). Specifically, the CNF, CCNF, CPoF and CCPoF associated with $(\mathcal{Y}, r_Y)$ can be approximated with use of the sample in Eq. (8.56) through the relationships

$$\begin{aligned} \mathcal{CNF} &= \left\{ \left[y, Nec_Y\left(\mathcal{U}_y\right) \right] : y \in \mathcal{Y} \right\} \\ &= \left\{ \left[y, 1 - Pos_Y\left(\mathcal{U}_y^c\right) \right] : y \in \mathcal{Y} \right\} \\ &\cong \left\{ \left[y, 1 - Pos_X\left(\left\{ \mathbf{x}_i : 1 \le i \le nS \text{ and } y_i > y \right\} \right) \right] : y \in \mathcal{Y} \right\}, \end{aligned} \tag{8.58}$$

$$\begin{aligned} \mathcal{CCNF} &= \left\{ \left[y, Nec_Y\left(\mathcal{U}_y^c\right) \right] : y \in \mathcal{Y} \right\} \\ &= \left\{ \left[y, 1 - Pos_Y\left(\mathcal{U}_y\right) \right] : y \in \mathcal{Y} \right\} \\ &\cong \left\{ \left[y, 1 - Pos_X\left(\left\{ \mathbf{x}_i : 1 \le i \le nS \text{ and } y_i \le y \right\} \right) \right] : y \in \mathcal{Y} \right\}, \end{aligned} \tag{8.59}$$

$$\begin{aligned} \mathcal{CPOF} &= \left\{ \left[y, Pos_Y\left(\mathcal{U}_y\right) \right] : y \in \mathcal{Y} \right\} \\ &\cong \left\{ \left[y, Pos_X\left(\left\{ \mathbf{x}_i : 1 \le i \le nS \text{ and } y_i \le y \right\} \right) \right] : y \in \mathcal{Y} \right\}, \end{aligned} \tag{8.60}$$

and

$$\begin{aligned} \mathcal{CCPOF} &= \left\{ \left[y, Pos_Y\left(\mathcal{U}_y^c\right) \right] : y \in \mathcal{Y} \right\} \\ &\cong \left\{ \left[y, Pos_X\left(\left\{ \mathbf{x}_i : 1 \le i \le nS \text{ and } y_i > y \right\} \right) \right] : y \in \mathcal{Y} \right\} \end{aligned} \tag{8.61}$$

as indicated in conjunction with Table 2 of Ref. [188], where $\mathcal{U}_y$ denotes a subset of $\mathcal{Y}$ of the form defined in conjunction with Eqs. (8.21) – (8.24). As the sample values for $\mathbf{x}$ become increasingly dense in $\mathcal{X}$, the approximations in Eqs. (8.58) – (8.61) will approach the CNF, CCNF, CPoF and CCPoF for y.

If the epistemic uncertainty associated with $\mathbf{x}$ is characterized by an evidence space $(\mathcal{X}, \mathbb{X}, m_X)$, then the corresponding evidence space $(\mathcal{Y}, \mathbb{Y}, m_Y)$ for y can be summarized by its associated CBF, CCBF, CPF and CCPF (see Eqs. (8.32) – (8.35)). Specifically, the CBF, CCBF, CPF and CCPF associated with $(\mathcal{Y}, \mathbb{Y}, m_Y)$ can be approximated with use of the sample in Eq. (8.56) through the relationships

$$\begin{aligned}\mathcal{CBF} &= \left\{\left[y,\, Bel_Y\left(\mathcal{U}_y\right)\right] : y \in \mathcal{Y}\right\} \\ &= \left\{\left[y, 1 - Pl_Y\left(\mathcal{U}_y^c\right)\right] : y \in \mathcal{Y}\right\} \\ &\cong \left\{\left[y, 1 - Pl_X\left(\left\{\mathbf{x}_i : 1 \le i \le nS \text{ and } y_i > y\right\}\right)\right] : y \in \mathcal{Y}\right\},\end{aligned} \tag{8.62}$$

$$\begin{aligned}\mathcal{CCBF} &= \left\{\left[y,\, Bel_Y\left(\mathcal{U}_y^c\right)\right] : y \in \mathcal{Y}\right\} \\ &= \left\{\left[y, 1 - Pl_Y\left(\mathcal{U}_y\right)\right] : y \in \mathcal{Y}\right\} \\ &\cong \left\{\left[y, 1 - Pl_X\left(\left\{\mathbf{x}_i : 1 \le i \le nS \text{ and } y_i < y\right\}\right)\right] : y \in \mathcal{Y}\right\},\end{aligned} \tag{8.63}$$

$$\begin{aligned}\mathcal{CPF} &= \left\{\left[y,\, Pl_Y\left(\mathcal{U}_y\right)\right] : y \in \mathcal{Y}\right\} \\ &\cong \left\{\left[y,\, Pl_X\left(\left\{\mathbf{x}_i : 1 \le i \le nS \text{ and } y_i \le y\right\}\right)\right] : y \in \mathcal{Y}\right\},\end{aligned} \tag{8.64}$$

and

$$\begin{aligned}\mathcal{CCPF} &= \left\{\left[y,\, Pl\left(\mathcal{U}_y^c\right)\right] : y \in \mathcal{Y}\right\} \\ &\cong \left\{\left[y,\, Pl_X\left(\left\{\mathbf{x}_i : 1 \le i \le nS \text{ and } y_i > y\right\}\right)\right] : y \in \mathcal{Y}\right\}\end{aligned} \tag{8.65}$$

as indicated in conjunction with Table 1 of Ref. [188], where $\mathcal{U}_y$ is defined the same as in Eqs. (8.58) – (8.61). As the sample values for $\mathbf{x}$ become increasingly dense in $\mathcal{X}$ and, in particular, approach the values at which F has its minimum and maximum values for the individual focal elements in $\mathbb{X}$, the approximations in Eq. (8.62) – (8.65) will approach the CBF, CCBF, CPF and CCPF for y.

If the epistemic uncertainty associated with $\mathbf{x}$ is characterized by a probability space ($\mathcal{X}$, $\mathbb{X}$, p_X), then the corresponding probability space ($\mathcal{Y}$, $\mathbb{Y}$, p_Y) for y can be summarized by its associated CDF and CCDF (see Eqs. (8.54) – (8.55)). If the sample in Eq. (8.56) is generated in consistency with the distribution for $\mathbf{x}$ defined by the probability space ($\mathcal{X}$, $\mathbb{X}$, p_X), then the CCDF and CDF associated with ($\mathcal{Y}$, $\mathbb{Y}$, p_Y) can be approximated through the standard sampling-based relationships

$$\begin{aligned}\mathcal{CDF} &= \left\{\left[y,\, p_Y\left(\mathcal{U}_y\right)\right] : y \in \mathcal{Y}\right\} \\ &\cong \left\{\left[y, C\left(\left\{y_i : 1 \le i \le nS \text{ and } y_i \le y\right\}\right)/nS\right] : y \in \mathcal{Y}\right\} \\ &= \left\{\left[y, \sum_{i=1}^{nS} \underline{\delta}_y\left(y_i\right)/nS\right] : y \in \mathcal{Y}\right\},\end{aligned} \tag{8.66}$$

and

$$\begin{aligned}\mathcal{CCDF} &= \left\{\left[y,\, p_Y\left(\mathcal{U}_y^c\right)\right] : y \in \mathcal{Y}\right\} \\ &\cong \left\{\left[y, C\left(\left\{y_i : 1 \le i \le nS \text{ and } y_i > y\right\}\right)/nS\right] : y \in \mathcal{Y}\right\} \\ &= \left\{\left[y, \sum_{i=1}^{nS} \overline{\delta}_y\left(y_i\right)/nS\right] : y \in \mathcal{Y}\right\},\end{aligned} \tag{8.67}$$

where (i) $\mathcal{U}_y$ is defined the same as in Eqs. (8.58) – (8.61), (ii) C designates set cardinality (i.e., the number of elements in a set), and (iii) the indicator functions $\underline{\delta}_y$ and $\overline{\delta}_y$ are defined by

$$\underline{\delta}_y\left(\tilde{y}\right) = \begin{cases} 1 & \text{if } \tilde{y} \le y \\ 0 & \text{otherwise} \end{cases} \text{ and } \overline{\delta}_y\left(\tilde{y}\right) = \begin{cases} 1 & \text{if } y < \tilde{y} \\ 0 & \text{otherwise,} \end{cases}$$

respectively. As the sample size increases, the approximations in Eqs. (8.66) and (8.67) will approach the CDF and CCDF for y.

9 QMU with Epistemic Uncertainty: Characterization with Alternative Uncertainty Representations

Examples illustrating the use of the alternative uncertainty representations introduced in Sect. 8 are now presented for QMU problems involving only epistemic uncertainty. Specifically, the example problem in Sect. 3.4 is expanded to include the alternative uncertainty representations in Sect. 8 (Sect. 9.1). Then, the following topics are considered: epistemic uncertainty without a specified bound (Sect. 9.2), epistemic uncertainty with a specified bound (Sect. 9.3), epistemic uncertainty with a specified bounding interval (Sect. 9.4), epistemic uncertainty with a specified bounding interval over time (Sect. 9.5), and epistemic uncertainty with an uncertain bound (Sect. 9.6).

9.1 Electrical Circuit Used for Illustration

As an example, this section uses the closed electrical circuit defined in Eqs. (3.29) – (3.31) and previously used in the illustration of QMU analyses with probability-based representations of epistemic uncertainty in Sect. 4. As defined in Eq. (3.32) and previously used in Sect. 4, the vector $\mathbf{e}_M$ of epistemically uncertain analysis inputs is

$$\begin{aligned}\mathbf{e}_M &= \left[e_{M1}, e_{M2}, e_{M3}, e_{M4}, e_{M5}\right] \\ &= \left[L, R, C, E_0, \lambda\right],\end{aligned} \tag{9.1}$$

with e_{M1}, e_{M2}, …, e_{M5} used instead of L, R, …, λ to represent the elements of $\mathbf{e}_M$ when notationally convenient. Definitions for L, R, C, E_0 and λ are given in conjunction with Eq. (3.29).

To provide the examples presented in this section, uncertainty structures are specified for L, R, C, E_0 and λ based on interval analysis, possibility theory, evidence theory and probability theory. Then, the resultant uncertainty structures for Q and related quantities are presented.

For interval analysis, the appropriate values for L, R, C, E_0 and λ are assumed to be contained in the intervals

$$\begin{aligned}\mathcal{EM}_1 &= \left\{L : L_{mn} \le L \le L_{mx}\right\} \\ &= \left\{L : 0.8 \le L \le 1.2 \text{ henrys}\right\}\end{aligned} \tag{9.2}$$

$$\begin{aligned}\mathcal{EM}_2 &= \left\{R : R_{mn} \le R \le R_{mx}\right\} \\ &= \left\{R : 50 \le R \le 100 \text{ ohms}\right\}\end{aligned} \tag{9.3}$$

$$\begin{aligned}\mathcal{EM}_3 &= \left\{C : C_{mn} \le C \le C_{mx}\right\} \\ &= \left\{C : 0.9\times10^{-4} \le C \le 1.1\times10^{-4} \text{ farads}\right\}\end{aligned} \tag{9.4}$$

$$\begin{aligned}\mathcal{EM}_4 &= \left\{E_0 : E_{mn} \le E_0 \le E_{mx}\right\} \\ &= \left\{E_0 : 900 \le E_0 \le 1100 \text{ volts}\right\}\end{aligned} \tag{9.5}$$

and

$$\begin{aligned}\mathcal{EM}_5 &= \left\{\lambda : \lambda_{mn} \le \lambda \le \lambda_{mx}\right\} \\ &= \left\{\lambda : 0.4 \le \lambda \le 0.8 \text{ s}^{-1}\right\},\end{aligned} \tag{9.6}$$

respectively. No additional information about the location of the appropriate values for L, R, C, E and λ is assumed to be known. These are the same intervals defined in Eqs. (3.33) – (3.37).

For possibility theory, four subintervals are considered for each of the intervals $\mathcal{EM}_i$, i = 1, 2, …, 5, defined in Eqs. (9.2) – (9.6):

$$\mathcal{E}_{i1} = \left[a, b-(b-a)/4\right], \tag{9.7}$$

$$\mathcal{E}_{i2} = \left[a+(b-a)/4, b\right], \tag{9.8}$$

$$\mathcal{E}_{i3} = \left[a+(b-a)/8, b-3(b-a)/8\right], \tag{9.9}$$

and

$$\mathcal{E}_{i4} = \left[a+3(b-a)/8, b-(b-a)/8\right], \tag{9.10}$$

where [a, b] corresponds to [L_{mn}, L_{mx}], [R_{mn}, R_{mx}], [C_{mn}, C_{mx}], [E_{mn}, E_{mx}] and [λ_{mn}, λ_{mx}] for i equal 1, 2, 3, 4 and 5, respectively (Fig. 3.4). The preceding intervals are the same intervals defined in Eqs. (3.38) – (3.41). In turn, the corresponding possibility distribution function $r_{EM,i}(e_{Mi})$ for the set $\mathcal{E}_i$ is given by

$$r_{EM,i}\left(e_{Mi}\right) = \sum_{j=1}^{4} \delta_{ij}\left(e_{Mi}\right)/4, \tag{9.11}$$

where

$$\delta_{ij}\left(e_{Mi}\right)=\begin{cases}1 & \text{if } e_{Mi}\in\mathcal{E}_{ij}\\ 0 & \text{otherwise.}\end{cases}$$

For example, if each of the intervals $\mathcal{E}_{i1}$, $\mathcal{E}_{i2}$, $\mathcal{E}_{i3}$ and $\mathcal{E}_{i4}$ of possible values for e_{Mi} was obtained from a different source, then $r_{EM,i}(e_{Mi})$ is the fraction of sources that provided an interval that contains e_{Mi}. The result is a possibility distribution ($\mathcal{EM}_i$, $r_{EM,i}$) for each element e_{Mi} of $\mathbf{e}_M$.

The same sets $\mathcal{EM}_i$, i = 1, 2, …, 5, and subsets $\mathcal{E}_{ij}$, j = 1, 2, 3, 4, considered for possibility theory can also be used to obtain an evidence theory representation ($\mathcal{EM}_i$, $\mathbb{EM}_i$, $m_{EM,i}$) for each e_{Mi}. Specifically, the set $\mathbb{EM}_i$ of focal elements is given by

$$\mathbb{EM}_i=\left\{\mathcal{E}_{i1},\mathcal{E}_{i2},\mathcal{E}_{i3},\mathcal{E}_{i4}\right\} \tag{9.12}$$

and the BPA $m_{EM,i}$ is given by

$$m_{EM,i}\left(\mathcal{U}\right)=\begin{cases}1/4 & \text{if } \mathcal{U}=\mathcal{E}_{i1},\mathcal{E}_{i2},\mathcal{E}_{i3} \text{ or } \mathcal{E}_{i4}\\ 0 & \text{otherwise.}\end{cases} \tag{9.13}$$

The preceding corresponds to defining the basic probability assignment for a subset $\mathcal{U}$ of $\mathcal{EM}_i$ to be the fraction of sources that indicated $\mathcal{U}$ contained the appropriate, but unknown, value for e_{Mi}.

By use of the Laplacian concept of insufficient reason (pp. 52-55, Ref. [258]), the sets $\mathcal{EM}_i$, i = 1, 2, …, 5, and subsets $\mathcal{E}_{ij}$, j = 1, 2, 3, 4 can also be used to obtain a probability theory representation ($\mathcal{EM}_i$, $\mathbb{EM}_i$, $p_{EM,i}$) for each e_{Mi}. In this example, as is usually the case, it is easier and more useful to obtain the corresponding density function $d_{EM,i}(e_{Mi})$ for e_{Mi} rather than to develop the σ-algebra $\mathbb{EM}_i$ of subsets of $\mathcal{EM}_i$ and the associated probability measure $p_{EM,i}$. Specifically,

$$d_{EM,i}\left(e_{Mi}\right)=\sum_{j=1}^{4}\delta_{ij}\left(e_{Mi}\right)/4\left[\max\left(\mathcal{E}_{ij}\right)-\min\left(\mathcal{E}_{ij}\right)\right], \tag{9.14}$$

where $\delta_{ij}(e_{Mi})$ is defined in conjunction with Eq. (9.11). The preceding specification for $d_{EM,i}(e_{Mi})$ corresponds to defining a uniform distribution on each interval $\mathcal{E}_{ij}$ and then weighting each distribution by the fraction of sources that indicated the corresponding interval contained the appropriate, but unknown, value to use for e_{Mi}. The preceding definition for $d_{EM,i}(e_{Mi})$ is the same as given in Eq. (3.42), with the result that the probabilistic uncertainty characterization used for $\mathbf{e}_M$ in the examples of this section is the same as used for $\mathbf{e}_M$ in the examples of Sect. 4.

The set $\mathcal{EM}$ of possible values for $\mathbf{e}_M$ is given by

$$\mathcal{EM}=\mathcal{EM}_1\times\mathcal{EM}_2\times\mathcal{EM}_3\times\mathcal{EM}_4\times\mathcal{EM}_5, \tag{9.15}$$

where $\mathcal{EM}_1$, $\mathcal{EM}_2$, ..., $\mathcal{EM}_5$ are defined in Eqs. (9.2) – (9.6). From an interval analysis perspective, all that is known about $\mathbf{e}_M$ is that its appropriate value is contained somewhere in $\mathcal{EM}$. In turn, the uncertainty structures defined by the possibility spaces ($\mathcal{EM}_i$, $r_{EM,i}$), i = 1, 2, …, 5, the evidence spaces ($\mathcal{EM}_i$, $\mathbb{EM}_i$, $m_{EM,i}$), i = 1, 2, …, 5, and the probability spaces ($\mathcal{EM}_i$, $\mathbb{EM}_i$, $p_{EM,i}$), i = 1, 2, …, 5, imply increasing levels of resolution with respect to where the appropriate value for $\mathbf{e}_M$ is located in $\mathcal{EM}$. As discussed in Sect. 8, the indicated possibility spaces lead to a possibility space ($\mathcal{EM}$, r_{EM}) for $\mathbf{e}_M$; the indicated evidence spaces lead to an evidence space ($\mathcal{EM}$, $\mathbb{EM}$, m_{EM}) for $\mathbf{e}_M$; and the indicated probability spaces lead to a probability space ($\mathcal{EM}$, $\mathbb{EM}$, p_{EM}) for $\mathbf{e}_M$. The set of possible values for the solution $Q(t)$ of the differential equation in Eq. (3.29) is the same for all four uncertainty structures defined on $\mathcal{EM}$ (Fig. 3.5). However, the properties of the uncertainty structure existing for these solutions are different for each of the uncertainty structures assumed for $\mathcal{EM}$.

The results presented in this section are constructed as described in Sect. 8.5. Specifically, a random sample

$$\begin{aligned}\mathbf{e}_{Mi}&=\left[e_{M1,i},e_{M2,i},\ldots,e_{M5,i}\right]\\&=\left[L_i,R_i,C_i,E_{0i},\lambda_i\right],\ i=1,2,\ldots,nSE=10^5,\end{aligned} \tag{9.16}$$

from $\mathcal{EM}$ generated in consistency with the distributions that define the probability space ($\mathcal{EM}$, $\mathbb{EM}$, p_{EM}) is used. Evaluation of $Q(t|\mathbf{a}, \mathbf{e}_{Mi})$ for the elements of the preceding sample results in the mapping

$$\left[\mathbf{e}_{Mi},Q\left(t\middle|\mathbf{a},\mathbf{e}_{Mi}\right)\right],\ i=1,2,\ldots,nSE=10^5, \tag{9.17}$$

that is used in the generation of the example results presented in this section.

The use of a large sample (i.e., $nSE = 10^5$) is possible in this example analysis because the function $Q(t|\mathbf{a}, \mathbf{e}_M)$ is inexpensive to evaluate. When computationally demanding models are under consideration, the analysis must be planned very carefully to hold computational costs to an acceptable level. Often, this will involve the use of an initial sampling to construct a surrogate mod-

el, which is then used in a subsequent and larger sampling to produce uncertainty results.

Techniques for sensitivity analysis in conjunction with alternative representations for epistemic uncertainty are not as well developed as is the case for probabilistic representations for epistemic uncertainty. However, possible techniques for sensitivity analysis in conjunction with evidence theory representations for epistemic uncertainty are presented in Refs. [269; 270].

9.2 Epistemic Uncertainty without a Specified Bound

As an example, the uncertainty in the possible values for $Q(0.1|\mathbf{a}, \mathbf{e}_M)$ is considered. These are the values associated with the vertical line in Fig. 3.5. More formally, the set

$$\mathcal{Q} = \left\{ Q\left(0.1 \middle| \mathbf{a}, \mathbf{e}_M\right) : \mathbf{e}_M = \left[L, R, C, E_0, \lambda\right] \in \mathcal{EM} \right\} \tag{9.18}$$

is under consideration, where $\mathbf{a}$ is a fixed but unspecified realization of aleatory uncertainty. In turn, $\mathcal{Q}$ has an uncertainty structure that derives from the uncertainty structure imposed on $\mathcal{EM}$. Thus, the uncertainty associated with $Q(0.1|\mathbf{a}, \mathbf{e}_M)$ is characterized by an interval (i.e., $[\inf(\mathcal{Q}), \sup(\mathcal{Q})]$, a possibility space $(\mathcal{Q}, r_Q)$, an evidence space $(\mathcal{Q}, \mathbb{Q}, m_Q)$ or a probability space $(\mathcal{Q}, \mathbb{Q}, p_Q)$ depending on which characterization is assumed for $\mathcal{X}$ (Fig. 9.1).

The CPoF, CNF, CCPoF and CCNF for $Q(0.1|\mathbf{a}, \mathbf{e}_M)$ in Fig. 9.1 have step sizes of 0.25 because the underlying possibility distribution function for $Q(0.1|\mathbf{a}, \mathbf{e}_M)$ assumes only the values of $k/4$ for $k = 1,2,3,4$ as a result of constructing the possibility space associated with the set $\mathcal{EM}$ by assigning these same possibility distribution values to the potential values for the elements e_{Mi} of $\mathbf{e}_M$ (see Eqs. (9.11) and (8.19)). In concept, the CPF, CBF, CCPF and CCBF for $Q(0.1|\mathbf{a}, \mathbf{e}_M)$ in Fig. 9.1 have step sizes of approximately $1/4^5 = 1/1024$, which results from constructing the evidence space associated with $\mathcal{EM}$ from 5 variables each of which has 4 focal elements with basic probability assignments of 1/4 (see Eqs. (9.13) and (8.37)). There is some variation from this small step size in Fig. 9.1 because of approximation and plotting effects. In concept, the CDF and CCDF for $Q(0.1|\mathbf{a}, \mathbf{e}_M)$ in Fig. 9.1 should be continuous as a result of defining the probability space associated with $\mathcal{E}$ from 5 variables each of which has a piecewise constant density function (see Eqs. (9.14) and (8.52)). Because of the use of a sample of size 10^5 from the distributions that define the probability space associated with $\mathcal{EM}$ (see Eq. (9.16)), the CDF and CCDF for $Q(0.1|\mathbf{a}, \mathbf{e}_M)$ are approximated with a step size of 10^{-5}, which is below the resolution at which Fig. 9.1 is plotted.

The potential value of 0.09 for $Q(0.1|\mathbf{a}, \mathbf{e}_M)$ is used as an example (see vertical lines in Figs. 9.1a and 9.1b). In the context of the interval analysis results, all that is known about 0.09 is that it is a potential value for $Q(0.1|\mathbf{a}, \mathbf{e}_M)$ (i.e., 0.09 is contained in the interval $[inf(\mathcal{Q}), sup(\mathcal{Q})] = [0.077, 0.121]$, which corresponds to the set $\mathcal{Q}$), with nothing else known about 0.09 or levels of credence that can be given to other potential values for $Q(0.1|\mathbf{a}, \mathbf{e}_M)$ on the basis of their location relative to 0.09. For example, no information is provided on whether more credence should be given to the possibility that the inequality $Q(0.1|\mathbf{a}, \mathbf{e}_M) \le 0.09$ is true or to the possibility that the inequality $Q(0.1|\mathbf{a}, \mathbf{e}_M) > 0.09$ is true.

The additional information about the potential value of 0.09 for $Q(0.1|\mathbf{a}, \mathbf{e}_M)$ available in the context of possibility theory, evidence theory and probability theory is now considered. Initially, measures of the credence that exist for potential values of $Q(0.1|\mathbf{a}, \mathbf{e}_M)$ that are less than or equal to 0.09 are considered. Specifically, measures of credence that exist for the set

$$\mathcal{Q}_{0.09} = \left\{ \tilde{Q} : \tilde{Q} \in \mathcal{Q} \text{ and } \tilde{Q} \le 0.09 \right\} \tag{9.19}$$

are under consideration (see analogous definition of $\mathcal{U}_y$ in conjunction with Eqs. (8.21) – (8.24)). These measures are given by

$$\left[Nec_Q\left(\mathcal{Q}_{0.09}\right), Pos_Q\left(\mathcal{Q}_{0.09}\right) \right] = \left[0.0, 0.75\right], \tag{9.20}$$

$$\left[Bel_Q\left(\mathcal{Q}_{0.09}\right), Pl_Q\left(\mathcal{Q}_{0.09}\right) \right] = \left[0.0, 0.959\right] \tag{9.21}$$

and

$$p_Q\left(\mathcal{Q}_{0.09}\right) = 0.133 \tag{9.22}$$

for possibility theory, evidence theory and probability theory, respectively, and correspond to the locations where the vertical line in Fig. 9.1a crosses for the CNF, CPoF, CBF, CPF and CDF for $Nec_Q(\mathcal{Q}_{0.09})$, $Pos_Q(\mathcal{Q}_{0.09})$, $Bel_Q(\mathcal{Q}_{0.09})$, $Pl_Q(\mathcal{Q}_{0.09})$ and $p_Q(\mathcal{Q}_{0.09})$, respectively.

As shown, possibility theory provides two measures, $Nec_Q(\mathcal{Q}_{0.09})$ and $Pos_Q(\mathcal{Q}_{0.09})$, of the amount of credence associated with the set $\mathcal{Q}_{0.09}$ with

$$0.0 = Nec_Q\left(\mathcal{Q}_{0.09}\right) < Pos_Q\left(\mathcal{Q}_{0.09}\right) = 0.75. \tag{9.23}$$

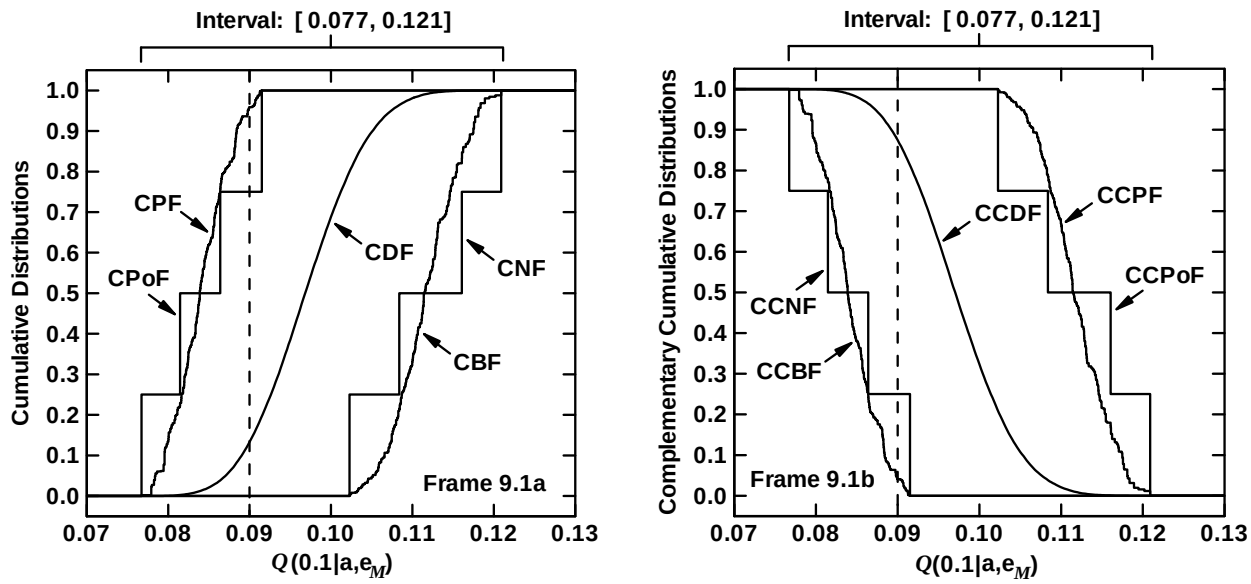

Fig. 9.1. Uncertainty associated with $Q(0.1|\mathbf{a}, \mathbf{e}_M)$ characterized by (i) an interval (i.e., [inf($\mathcal{Q}$), sup($\mathcal{Q}$)]), (ii) a possibility space ($\mathcal{Q}$, r_Q) summarized with a CCPoF, CCNF, CPoF and CNF, (iii) an evidence space ($\mathcal{Q}$, $\mathbb{Q}$, m_Q) summarized with a CCPF, CCBF, CPF and CBF, and (iv) a probability space ($\mathcal{Q}$, $\mathbb{Q}$, p_A) summarized with a CCDF and CDF: (a) Cumulative results, and (b) Complementary cumulative results.

Specifically, and in the context of the possibility theory formulation of this example, $Nec_Q(\mathcal{Q}_{0.09})$ provides a measure of the amount of uncontradicted information that supports the proposition that the appropriate value for $Q(0.1|\mathbf{a}, \mathbf{e}_M)$ is contained in $\mathcal{Q}_{0.09}$, and $Pos_Q(\mathcal{Q}_{0.09})$ provides a measure of the amount of information that does not refute the proposition that the appropriate value for $Q(0.1|\mathbf{a}, \mathbf{e}_M)$ is contained in $\mathcal{Q}_{0.09}$. Similarly, evidence theory provides two measures, $Bel_Q(\mathcal{Q}_{0.09})$ and $Pl_Q(\mathcal{Q}_{0.09})$, of the amount of credence associated with the set $\mathcal{Q}_{0.09}$ with

$$0.0 = Bel_Q\left(\mathcal{Q}_{0.09}\right) < Pl_Q\left(\mathcal{Q}_{0.09}\right) = 0.959. \tag{9.24}$$

Specifically, and in the context of the evidence theory formulation of this example, $Bel_Q(\mathcal{Q}_{0.09})$ provides a measure of the amount of uncontradicted information that supports the proposition that the appropriate value for $Q(0.1)$ is contained in $\mathcal{Q}_{0.09}$, and $Pl_Q(\mathcal{Q}_{0.09})$ provides a measure of the amount of information that does not refute the proposition that the appropriate value for $Q(0.1|\mathbf{a}, \mathbf{e}_M)$ is contained in $\mathcal{Q}_{0.09}$. In contrast, probability theory provides only one measure, $p_Q(\mathcal{Q}_{0.09})$ = 0.126, of the amount of credence associated with the set $\mathcal{Q}_{0.09}$.

Measures of the credence that exist for potential values for $Q(0.1|\mathbf{a}, \mathbf{e}_M)$ that are greater than 0.09 are now considered. Specifically, measures of credence for the set

$$\mathcal{Q}_{0.09}^c = \left\{\tilde{Q} : \tilde{Q} \in \mathcal{Q} \text{ and } 0.09 < \tilde{Q}\right\} \tag{9.25}$$

are now considered. These measures are given by

$$\left[Nec_Q\left(\mathcal{Q}_{0.09}^c\right), Pos_Q\left(\mathcal{Q}_{0.09}^c\right)\right] = \left[0.25, 1.0\right] \tag{9.26}$$

$$\left[Bel_Q\left(\mathcal{Q}_{0.09}^c\right), Pl_Q\left(\mathcal{Q}_{0.09}^c\right)\right] = \left[0.041, 1.0\right] \tag{9.27}$$

and

$$p_Q\left(\mathcal{Q}_{0.09}^c\right) = 0.874 \tag{9.28}$$

for possibility theory, evidence theory and probability theory, respectively, and correspond to the locations where the vertical line in Fig. 9.1b crosses the CCNF, CCPoF, CCBF, CCPF and CCDF for $Nec_Q(\mathcal{Q}_{0.09}^c)$, $Pos_Q(\mathcal{Q}_{0.09}^c)$, $Bel_Q(\mathcal{Q}_{0.09}^c)$, $Pl_Q(\mathcal{Q}_{0.09}^c)$ and $p_Q(\mathcal{Q}_{0.09}^c)$, respectively.

As previously discussed for the measures of credence associated with $\mathcal{Q}_{0.09}$, the quantities $Nec_Q(\mathcal{Q}_{0.09}^c)$

= 0.25 and $Bel_Q(\mathcal{Q}_{0.09}^c)$ = 0.041 provide measures in the context of possibility theory and evidence theory, respectively, of the amount of uncontradicted information that supports the proposition that the appropriate value for $Q(0.1|\mathbf{a}, \mathbf{e}_M)$ is contained in $\mathcal{Q}_{0.09}^c$. Similarly, $Pos_Q(\mathcal{Q}_{0.09}^c)$ = 1.0 and $Pl_Q(\mathcal{Q}_{0.09}^c)$ = 1.0 provide measures in the context of possibility theory and evidence theory, respectively, of the amount of information that does not refute the proposition that the appropriate value for $Q(0.1|\mathbf{a}, \mathbf{e}_M)$ is contained in $\mathcal{Q}_{0.09}^c$. In contrast, probability theory provides a single measure, $p_Q(\mathcal{Q}_{0.09}^c)$ = 0.874, of the amount of credence associated with the set $Q_{0.09}^c$.

The equalities

$$1 = Nec_Q\left(\mathcal{Q}_{0.09}\right) + Pos_Q\left(\mathcal{Q}_{0.09}^c\right) = 0.0 + 1.0 \tag{9.29}$$

$$1 = Nec_Q\left(\mathcal{Q}_{0.09}^c\right) + Pos_Q\left(\mathcal{Q}_{0.09}\right) = 0.25 + 0.75 \tag{9.30}$$

$$1 = Bel_Q\left(\mathcal{Q}_{0.09}\right) + Pl_Q\left(\mathcal{Q}_{0.09}^c\right) = 0.0 + 1.0 \tag{9.31}$$

$$1 = Bel_Q\left(\mathcal{Q}_{0.09}^c\right) + Pl_Q\left(\mathcal{Q}_{0.09}\right) = 0.041 + 0.959 \tag{9.32}$$

and

$$1 = p_Q\left(\mathcal{Q}_{0.09}\right) + p_Q\left(\mathcal{Q}_{0.09}^c\right) = 0.126 + 0.874 \tag{9.33}$$

hold as indicated in Eqs. (8.7), (8.28) and (8.45) and indicate the relationships that exist between a measure of the credence for a potential result and a measure of the credence for its complement.

Additional relationships also hold for possibility theory and evidence theory as indicated in Eqs. (8.8) – (8.14) and (8.29) – (8.31). Overall, possibility theory and evidence theory allow a more nuanced representation of epistemic uncertainty than is possible with probability theory because they permit a distinction between information that supports a proposition and information that does not refute a proposition.

Thus far, measures of credence have been considered for the proposition that $Q(0.1|\mathbf{a}, \mathbf{e}_M)$ is less than or equal to 0.09 (i.e., for the set $\mathcal{Q}_{0.09}$) and the proposition that $Q(0.1|\mathbf{a}, \mathbf{e}_M)$ is greater than 0.09 (i.e., for the set $\mathcal{Q}_{0.09}^c$). It is also possible to consider the proposition that $Q(0.1|\mathbf{a}, \mathbf{e}_M) = 0.09$. In this case,

$$\left[Nec_Q\left(\{0.09\}\right), Pos_Q\left(\{0.09\}^c\right)\right] = \left[0.0, 1.0\right] \tag{9.34}$$

$$\left[Nec_Q\left(\{0.09\}^c\right), Pos_Q\left(\{0.09\}\right)\right] = \left[0.25, 0.75\right] \tag{9.35}$$

$$\left[Bel_Q\left(\{0.09\}\right), Pl_Q\left(\{0.09\}^c\right)\right] = \left[0.0, 1.0\right] \tag{9.36}$$

$$\left[Bel_Q\left(\{0.09\}^c\right), Pl_Q\left(\{0.09\}\right)\right] = \left[0.041, 0.959\right] \tag{9.37}$$

and

$$\left[p_Q\left(\{0.09\}\right), p_Q\left(\{0.09\}^c\right)\right] = \left[0.0, 1.0\right], \tag{9.38}$$

where $\{0.09\}$ denotes the subset of $\mathcal{Q}$ that contains 0.09 as its only element.

The results in Fig. 9.1 and other similar results presented in this section are approximations obtained with the sampling-based procedures described in Sect. 8.5 and the sample in Eq. (9.16). The results in Eqs. (9.35) and (9.37) require the estimation of $Pos_Q(\{0.09\})$ and $Pl_Q(\{0.09\})$ for a set that contains a single number (i.e., the set $\{0.09\}$). Because $\mathcal{EM}$ has an uncountably infinite number of elements, $Pos_Q(\{0.09\})$ and $Pl_Q(\{0.09\})$ cannot be estimated directly with sampling-based methods as the chance of sampling values for $\mathbf{e}_M$ that result in the equality $Q(0.1|\mathbf{a}, \mathbf{e}_M) = 0.09$ is effectively nonexistent. Therefore, $Pos_Q(\{0.09\})$ and $Pl_Q(\{0.09\})$ were estimated by $Pos_Q(\{0.09\}) \cong Pos_Q(\mathcal{U})$ and $Pl_Q(\{0.09\}) \cong Pl_Q(\mathcal{U})$, where

$$\begin{aligned}\mathcal{U} = \big\{ & Q : Q = Q\left(0.1 \mid \mathbf{a}, \mathbf{e}_M\right), \mathbf{e}_M \in \mathcal{EM}, \text{ and} \\ & 0.08999999 \le Q\left(0.1 \mid \mathbf{a}, \mathbf{e}_M\right) \le 0.09000001 \big\}\end{aligned} \tag{9.39}$$

is a very small interval containing 0.09. The values for $Pos_Q(\mathcal{U})$ and $Pl_Q(\mathcal{U})$ were estimated with a random sample of size 10^8 from $\mathcal{EM}$, which resulted in 412 values for $Q(0.1|\mathbf{a}, \mathbf{e}_M)$ that satisfied the defining inequalities for the set $\mathcal{U}$. The similarity of the results in Eqs. (9.29) – (9.32) with the results in Eqs. (9.34) – (9.37) is a property of this analysis and does not hold in general.

9.3 Epistemic Uncertainty with a Specified Bound

A QMU problem is now considered. Specifically, a fixed bound is assumed to exist with respect to the value for $Q(0.1|\mathbf{a}, \mathbf{e}_M)$. Possibilities include bounds

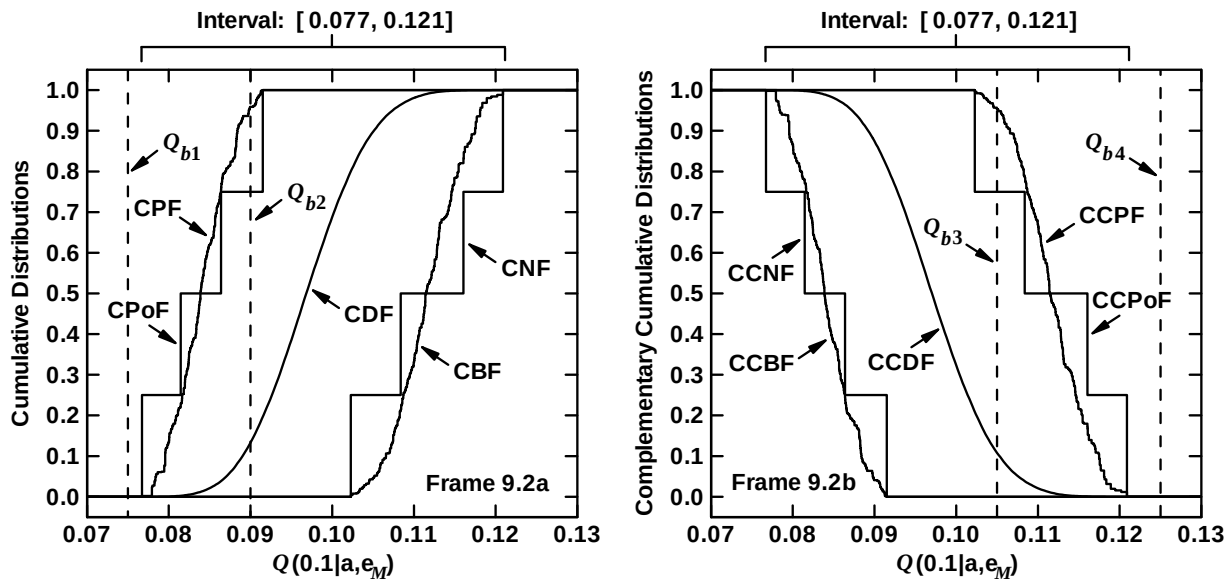

Fig. 9.2. Example bounds on $Q(0.1|\mathbf{a}, \mathbf{e}_M)$: (a) Q_{b1} = 0.075 and Q_{b2} = 0.09, and (b) Q_{b3} = 0.105 and Q_{b4} = 0.125.

that bound $Q(0.1|\mathbf{a}, \mathbf{e}_M)$ from below (e.g., Q_{b1} = 0.075 and Q_{b2} = 0.09 in Fig. 9.2a) and bounds that bound $Q(0.1|\mathbf{a}, \mathbf{e}_M)$ from above (e.g., Q_{b3} = 0.105 and Q_{b4} = 0.125 in Fig. 9.2b).

All values for $Q(0.1|\mathbf{a}, \mathbf{e}_M)$ are above the bound Q_{b1}. However, this is not the case for the bound Q_{b2}. In particular, the possibility and necessity of falling below Q_{b2} are 0.75 and 0, respectively; the plausibility and belief of falling below Q_{b2} are 0.959 and 0, respectively; and the probability of falling below Q_{b2} is 0.126.

Similarly, all values for $Q(0.1|\mathbf{a}, \mathbf{e}_M)$ are below the bound Q_{b4}. However, this is not the case for the bound Q_{b3}. In particular, the possibility and necessity of exceeding Q_{b3} are 0.75 and 0, respectively; the plausibility and belief of exceeding Q_{b3} are 0.953 and 0, respectively; and the probability of exceeding Q_{b3} is 0.108.

As previously presented in Eq. (4.5), the margins between $Q(0.1|\mathbf{a}, \mathbf{e}_M)$ and the bounds Q_{bk}, k = 1, 2, 3, 4, indicated in Fig. 9.2 are defined by

$$Q_{mk}\left(0.1|\mathbf{a}, \mathbf{e}_M\right) = \begin{cases} Q_{bk} - Q\left(0.1|\mathbf{a}, \mathbf{e}_M\right) & \text{for } k = 1,2 \\ Q\left(0.1|\mathbf{a}, \mathbf{e}_M\right) - Q_{bk} & \text{for } k = 3,4, \end{cases} \tag{9.40}$$

with $Q_{mk}(0.1|\mathbf{a}, \mathbf{e}_M) > 0$ indicating that a specified bound is satisfied and $Q_{mk}(0.1|\mathbf{a}, \mathbf{e}_M) < 0$ indicating that a specified bound is not satisfied (i.e., a positive margin is good and a negative margin is bad). As a result of $Q(0.1|\mathbf{a}, \mathbf{e}_M)$ being uncertain, the corresponding margins $Q_{mk}(0.1|\mathbf{a}, \mathbf{e}_M)$, k = 1, 2, 3, 4, are also uncertain and have an uncertainty structure that derives from the uncertainty structure assumed for $\mathbf{e}_M$ (Fig. 9.3). Representations of the form shown in Fig. 9.3 provide a complete representation of the uncertainty associated with the margins $Q_{mk}(0.1|\mathbf{a}, \mathbf{e}_M)$, k = 1, 2, 3, 4, and thus a complete QMU representation.

An alternative presentation format previously introduced in Eq. (4.6) involves the use of normalized margins defined by

$$\begin{aligned} Q_{nk}\left(0.1|\mathbf{a}, \mathbf{e}_M\right) &= Q_{mk}\left(0.1|\mathbf{a}, \mathbf{e}_M\right)/Q_{bi} \\ &= \begin{cases} \left[Q\left(0.1|\mathbf{a}, \mathbf{e}_M\right) - Q_{bk}\right]/Q_{bk} & \text{for } k = 1,2 \\ \left[Q_{bk} - Q\left(0.1|\mathbf{a}, \mathbf{e}_M\right)\right]/Q_{bk} & \text{for } k = 3,4, \end{cases} \end{aligned} \tag{9.41}$$

which expresses margin as a fraction of the corresponding bounding value (Fig. 9.4). This format has the advantage in that it presents margin as a multiple of the bounding value, which is a presentation format that some individuals like. It has the disadvantage that it does not present the actual size of the margin.

It is sometimes stated that QMU corresponds to the determination of the ratio "margin/uncertainty." Possible definitions of "margin/uncertainty" are indicated in Eqs. (4.7) and (4.8) that can be used with probability-based representations for epistemic uncertainty. The appropriate definition of corresponding quantities for analyses based on interval analysis, possibility theory or evidence theory is not apparent. However, a significant

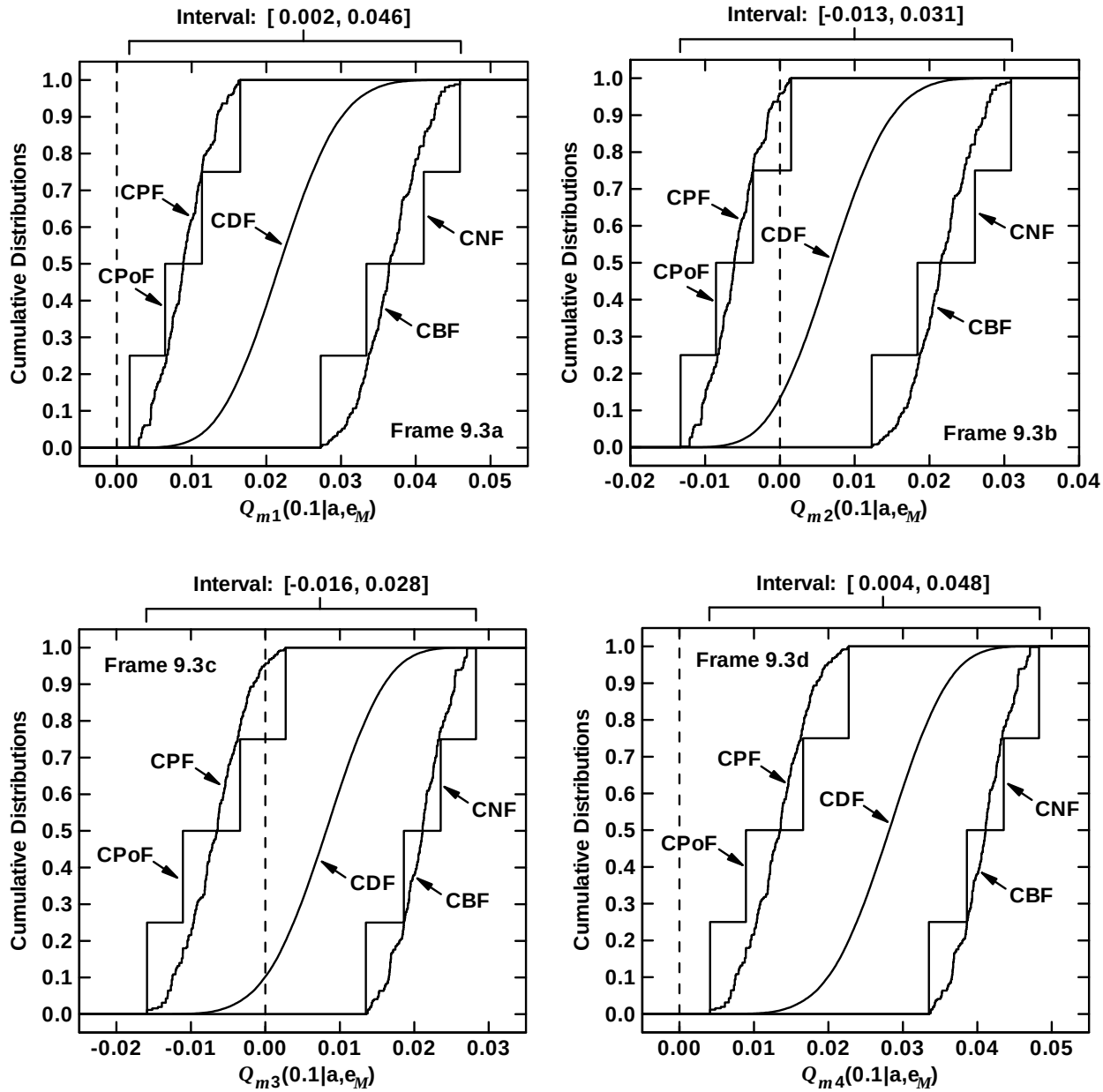

Fig. 9.3. Uncertainty associated with margins $Q_{mk}(0.1|\mathbf{a}, \mathbf{e}_M)$, k = 1, 2, 3, 4, defined in Eq. (9.40) characterized by (i) intervals, (ii) possibility spaces summarized with CPoFs and CNFs, (iii) evidence spaces summarized with CPFs and CBFs, and (iv) probability spaces summarized with CDFs: (a) $Q_{m1}(0.1|\mathbf{a}, \mathbf{e}_M)$ for Q_{b1} = 0.075, (b) $Q_{m2}(0.1|\mathbf{a}, \mathbf{e}_M)$ for Q_{b2} = 0.09, (c) $Q_{m3}(0.1|\mathbf{a}, \mathbf{e}_M)$ for Q_{b3} = 0.105, and (d) $Q_{m4}(0.1|\mathbf{a}, \mathbf{e}_M)$ for Q_{b4} = 0.125.

amount of important information is lost any time an attempt is made to reduce a complex analysis to a single number (see Sect. 4.5 for additional discussion).

9.4 Epistemic Uncertainty with a Specified Bounding Interval

A QMU problem involving a bounding interval rather than simply an upper or lower bound is now considered. Specifically, the problem involves a specified interval within which the quantity of interest is required to be located. For the quantity

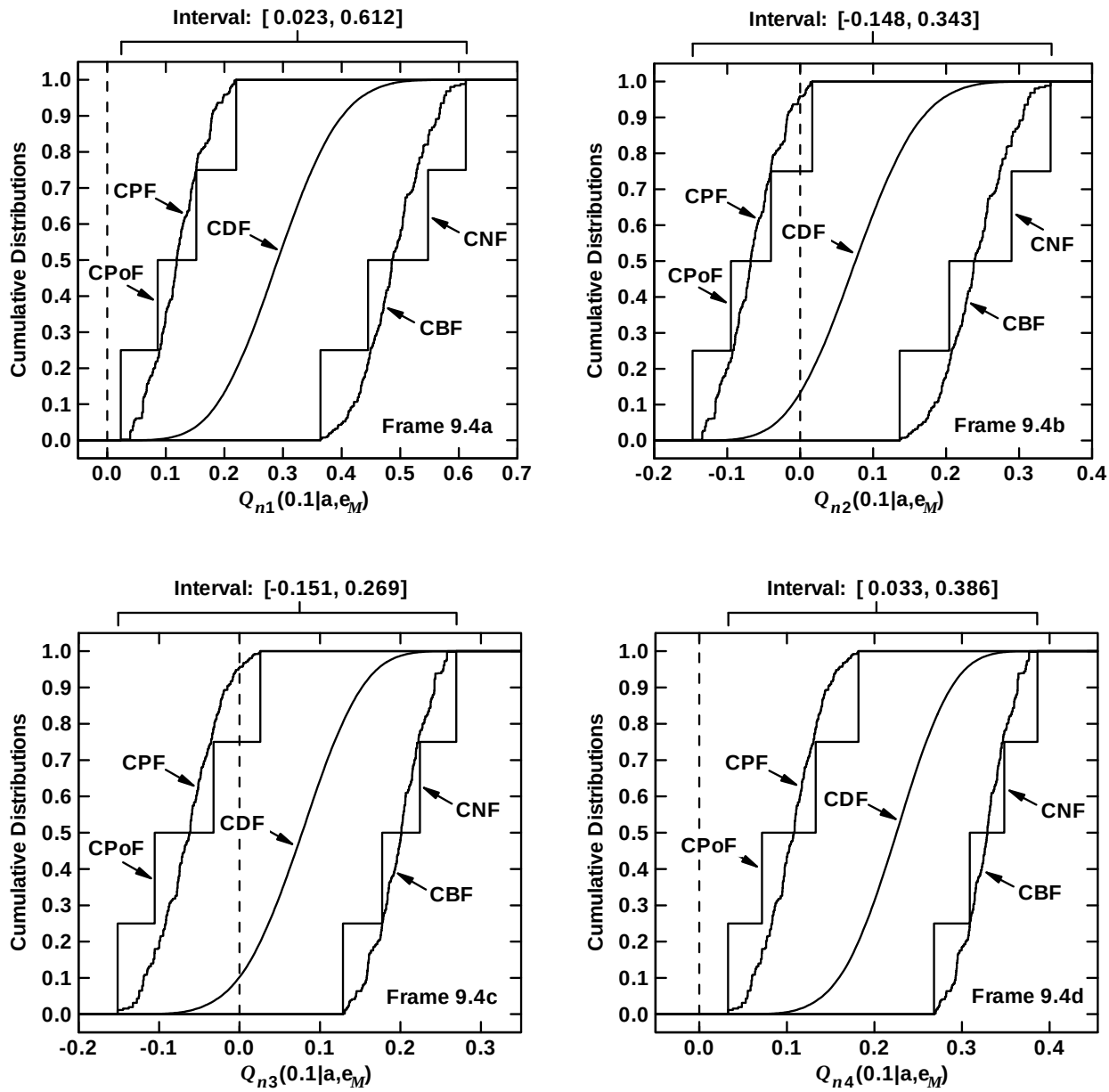

Fig. 9.4. Uncertainty associated with normalized margins $Q_{nk}(0.1|\ \mathbf{a}, \mathbf{e}_M)$, k = 1, 2, 3, 4, defined in Eq. (9.41) characterized by (i) intervals, (ii) possibility spaces summarized with CPoFs and CNFs, (iii) evidence spaces summarized with CPFs and CBFs, and (iv) probability spaces summarized with CDFs: (a) $Q_{n1}(0.1|\mathbf{a}, \mathbf{e}_M)$ for Q_{b1} = 0.075, (b) $Q_{n2}(0.1|\mathbf{a}, \mathbf{e}_M)$ for Q_{b2} = 0.09, (c) $Q_{n3}(0.1|\mathbf{a}, \mathbf{e}_M)$ for Q_{b3} = 0.105, and (d) $Q_{n4}(0.1|\mathbf{a}, \mathbf{e}_M)$ for Q_{b4} = 0.125.

$Q(0.1|\mathbf{a}, \mathbf{e}_M)$, this involves the specification of an interval $[\underline{Q}_b, \overline{Q}_b]$ such that the inequalities

$$\underline{Q}_b \le Q\left(0.1\middle|\mathbf{a}, \mathbf{e}_M\right) \le \overline{Q}_b \tag{9.42}$$

hold (Fig. 9.5). For illustration $[\underline{Q}_b, \overline{Q}_b]$ is assumed to equal [0.08, 0.12] as indicated in Fig. 9.5.

There are several ways in which the epistemic uncertainty associated with compliance with the specified bounds can be represented. The simplest is to consider whether or not $Q(0.1|\mathbf{a}, \mathbf{e}_M)$ falls within the specified bounds. This involves consideration of the indicator function

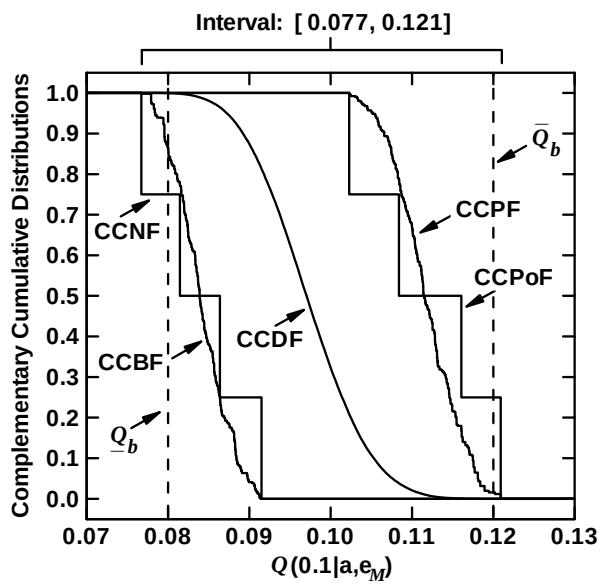

Fig. 9.5. Example bounding interval [$\underline{Q}_b$, $\overline{Q}_b$] = 0.08, 0.12] for $Q(0.1|\mathbf{a}, \mathbf{e}_M)$.

$$\delta\left[Q\left(0.1\middle|\mathbf{e}_M\right)\right] = \begin{cases} 1 & \text{if } \underline{Q}_b \le Q\left(0.1\middle|\mathbf{a}, \mathbf{e}_M\right) \le \overline{Q}_b \\ 0 & \text{otherwise} \end{cases} \tag{9.43}$$

and the associated sets

$$\mathcal{X}^+ = \left\{\mathbf{e}_M : \mathbf{e}_M \in \mathcal{EM} \text{ and } \delta\left[Q\left(0.1\middle|\mathbf{a}, \mathbf{e}_M\right)\right] = 1\right\} \tag{9.44}$$

and

$$\mathcal{X}^- = \left\{\mathbf{e}_M : \mathbf{e}_M \in \mathcal{EM} \text{ and } \delta\left[Q\left(0.1\middle|\mathbf{a}, \mathbf{e}_M\right)\right] = 0\right\} \tag{9.45}$$

as previously indicated in Eqs. (4.23) – (4.26).

For interval analysis, compliance is an "either/or" concept, with compliance with the specified bounding interval existing only if $\mathcal{X}^+ = \mathcal{EM}$ (i.e., if $Q(0.1|\mathbf{a}, \mathbf{e}_M)$ falls inside the interval [$\underline{Q}_b$, $\overline{Q}_b$] = [0.08, 0.12] for all values of $\mathbf{e}_M$), which is not the case in this example. For possibility theory, evidence theory and probability theory, the uncertainty in compliance with the specified bounds is given by

$$Nec_{EM}\left(\mathcal{X}^+\right) = 0.75, \quad Pos_{EM}\left(\mathcal{X}^+\right) = 1.00, \tag{9.46}$$

$$Bel_{EM}\left(\mathcal{X}^+\right) = 0.85, \quad Pl_{EM}\left(\mathcal{X}^+\right) = 1.00, \tag{9.47}$$

and

$$p_{EM}\left(\mathcal{X}^+\right) = 0.99945, \tag{9.48}$$

respectively. The results in Eqs. (9.46) – (9.48) were obtained with the sampling-based procedures described in Sect. 8.5.

Similarly, the uncertainty in noncompliance with the specified bounds is given by

$$Nec_{EM}\left(\mathcal{X}^-\right) = 0.00, \quad Pos_{EM}\left(\mathcal{X}^-\right) = 0.25, \tag{9.49}$$

$$Bel_{EM}\left(\mathcal{X}^-\right) = 0.00, \quad Pl_{EM}\left(\mathcal{X}^-\right) = 0.15, \tag{9.50}$$

and

$$p_{EM}\left(\mathcal{X}^-\right) = 0.00055 \tag{9.51}$$

for possibility theory, evidence theory, and probability theory, respectively.

The representations in the preceding two paragraphs summarize the uncertainty in whether or not the specified bound will be satisfied. However, these representations do not indicate the uncertainty in the location of $Q(0.1|\mathbf{a}, \mathbf{e}_M)$ relative to the ends of the bounding interval [$\underline{Q}_b$, $\overline{Q}_b$]. The consideration of this uncertainty requires the determination of margins and the uncertainty associated with these margins. Specifically, a margin associated with the containment of $Q(0.1|\mathbf{a}, \mathbf{e}_M)$ in the interval [$\underline{Q}_b$, $\overline{Q}_b$] can be defined by

$$Q_m\left(0.1\middle|\mathbf{a}, \mathbf{e}_M\right) = \min\begin{cases} Q\left(0.1\middle|\mathbf{a}, \mathbf{e}_M\right) - \underline{Q}_b \\ \overline{Q}_b - Q\left(0.1\middle|\mathbf{a}, \mathbf{e}_M\right) \end{cases} \tag{9.52}$$

as previously indicated in Eq. (4.29), with the result that (i) $Q_m(0.1|\mathbf{a}, \mathbf{e}_M)$ is nonnegative if $Q(0.1|\mathbf{a}, \mathbf{e}_M)$ falls within the interval [$\underline{Q}_b$, $\overline{Q}_b$], (ii) $Q_m(0.1|\ \mathbf{a}, \mathbf{e}_M)$ is negative if $Q(0.1|\mathbf{a}, \mathbf{e}_M)$ falls outside the interval [$\underline{Q}_b$, $\overline{Q}_b$], and (iii) $|Q_m(0.1|\mathbf{a}, \mathbf{e}_M)|$ characterizes the maximum deviation of $Q(0.1|\mathbf{a}, \mathbf{e}_M)$ from the ends of the interval [$\underline{Q}_b$, $\overline{Q}_b$]. In turn, $Q_m(0.1|\mathbf{a}, \mathbf{e}_M)$ has an uncertainty structure that derives from the uncertainty structure imposed on $\mathbf{e}_M$ (Fig. 9.6).

The compliance results in Eqs. (9.46) – (9.51) can be obtained directly from the uncertainty results for $Q_m(0.1|\mathbf{a}, \mathbf{e}_M)$ in Fig. 9.6. Specifically, the values $Nec_{EM}(\mathcal{X}^-)$, $Pos_{EM}(\mathcal{X}^-)$, $Bel_{EM}(\mathcal{X}^-)$, $Pl_{EM}(\mathcal{X}^-)$ and $p_{EM}(\mathcal{X}^-)$ associated with $\mathcal{X}^-$ in Eqs. (9.49) – (9.51) correspond to the cumulative values in Fig. 9.6

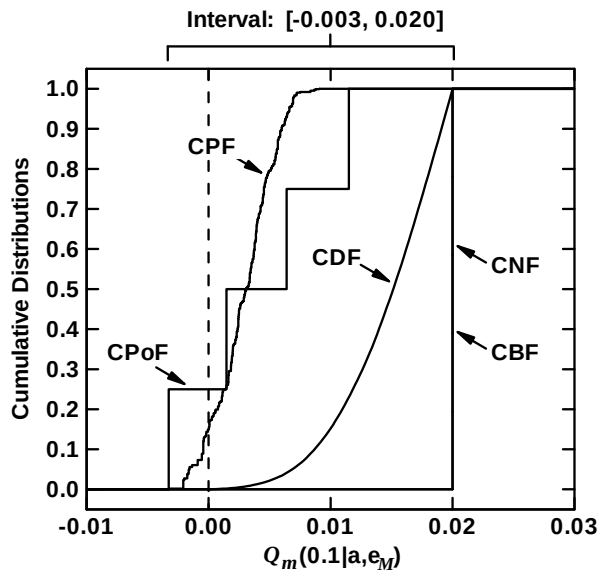

Fig. 9.6. Uncertainty associated with margin $Q_m(0.1|\mathbf{a}, \mathbf{e}_M)$ defined in Eq. (9.52) characterized by (i) an interval, (ii) a possibility space summarized with a CPoF and a CNF, (iii) an evidence space summarized with a CPF and a CBF, and (iv) a probability space summarized with a CDF.

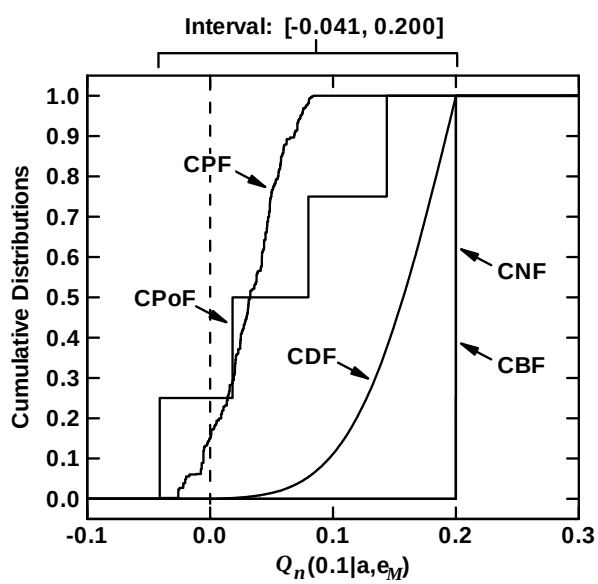

Fig. 9.7. Uncertainty associated with normalized margin $Q(0.1|\mathbf{a}, \mathbf{e}_M)$ defined in Eq. (9.53) characterized by (i) an interval, (ii) a possibility space summarized with a CPoF and a CNF, (iii) an evidence space summarized with a CPF and a CBF, and (iv) a probability space summarized with a CDF.

associated with $Q_m(0.1|\mathbf{a}, \mathbf{e}_M) = 0.00$. In turn, the values $Nec_{EM}(\mathcal{X}^+)$, $Pos_{EM}(\mathcal{X}^+)$, $Bel_{EM}(\mathcal{X}^+)$, $Pl_{EM}(\mathcal{X}^+)$ and $p_{EM}(\mathcal{X}^+)$ associated with $\mathcal{X}^+$ in Eqs. (9.46) – (9.48) can be obtained from the relationships in Eqs. (8.7), (8.28) and (8.45). Specifically, $Nec_{EM}(\mathcal{X}^+) = 1 - Pos_{EM}(\mathcal{X}^-)$, $Pos_{EM}(\mathcal{X}^+) = 1 - Nec_{EM}(\mathcal{X}^-)$, $Bel_{EM}(\mathcal{X}^+) = 1 - Pl_{EM}(\mathcal{X}^-)$, $Pl_{EM}(\mathcal{X}^+) = 1 - Bel_{EM}(\mathcal{X}^-)$, and $p_{EM}(\mathcal{X}^+) = 1 - p_{EM}(\mathcal{X}^-)$.

An alternate representation is to use normalized margins as previously indicated in Eq. (4.30). Specifically, the margin $Q_m(0.1|\mathbf{a}, \mathbf{e}_M)$ defined in Eq. (9.52) can be replaced by a normalized margin $Q_n(0.1|\mathbf{a}, \mathbf{e}_M)$ defined by

$$Q_n\left(0.1\middle|\mathbf{a}, \mathbf{e}_M\right) = \min\begin{cases}\left[Q\left(0.1\middle|\mathbf{a}, \mathbf{e}_M\right) - \underline{Q}_b\right]\Big/\underline{Q}_b \\ \left[\bar{Q}_b - Q\left(0.1\middle|\mathbf{a}, \mathbf{e}_M\right)\right]\Big/\bar{Q}_b,\end{cases} \tag{9.53}$$

which expresses margin as a fraction of the bounding value from which $Q(0.1|\mathbf{a}, \mathbf{e}_M)$ has the smallest fractional deviation (Fig. 9.7).

9.5 Epistemic Uncertainty with a Specified Bounding Interval Over Time

A QMU problem involving a bounding interval at a fixed point in time is considered in Sect. 9.4. This problem is now increased in complexity by considering a problem in which a bounding interval $[\underline{Q}_b, \bar{Q}_b]$ is specified for a quantity such as $Q(t|\mathbf{a}, \mathbf{e}_M)$ that takes on values over a time interval $[t_{mn}, t_{mx}]$ (Fig. 4.9). Specifically, the requirement is that the values for $Q(t|\mathbf{a}, \mathbf{e}_M)$ stay within the bounding interval $[\underline{Q}_b, \bar{Q}_b]$ for $t_{mn} \le t \le t_{mx}$ (e.g., $[\underline{Q}_b, \bar{Q}_b] = [0.07, 0.14\ \mathrm{C}]$, $t_{mn} = 0.02$ s and $t_{mx} = 0.18$ s in Fig. 4.9). Formally stated, the requirement is that the inequality

$$\underline{Q}_b \le Q\left(t\middle|\mathbf{a}, \mathbf{e}_M\right) \le \bar{Q}_b \tag{9.54}$$

be satisfied for $\mathbf{e}_M \in \mathcal{EM}$ and $t_{mn} \le t \le t_{mx}$.

Uncertainty in compliance with the indicated requirement can be represented with use of the indicator function

$$\delta\left[Q\left(t\middle|\mathbf{a}, \mathbf{e}_M\right): t_{mn} \le t \le t_{mx}\right] = \begin{cases}1 & \text{if } \underline{Q}_b \le Q\left(t\middle|\mathbf{a}, \mathbf{e}_M\right) \le \bar{Q}_b \text{ for } t_{mn} \le t \le t_{mx} \\ 0 & \text{otherwise}\end{cases} \tag{9.55}$$

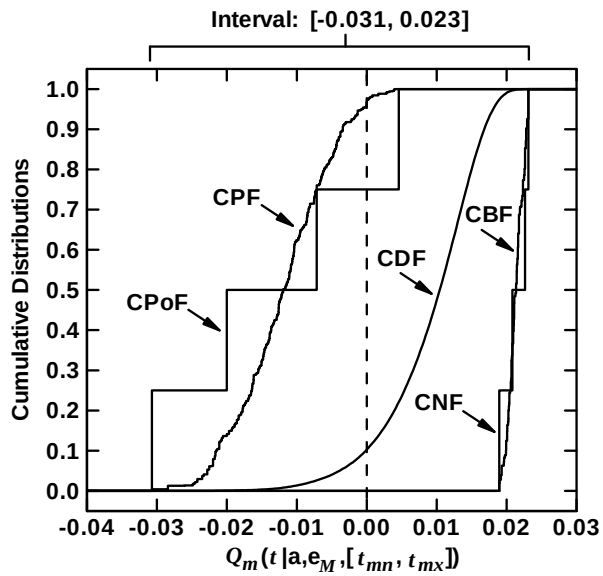

Fig. 9.8. Uncertainty associated with margin $Q_m(t|\mathbf{a}, \mathbf{e}_M, [t_{mn}, t_{mx}])$ defined in Eq. (9.64) characterized by (i) an interval, (ii) a possibility space summarized with a CPoF and a CNF, (iii) an evidence space summarized with a CPF and a CBF, and (iv) a probability space summarized with a CDF.

and the associated sets

$$\mathcal{X}^+ = \{\mathbf{e}_M : \mathbf{e}_M \in \mathcal{EM} \text{ and } \delta\left[Q\left(t\middle|\mathbf{a}, \mathbf{e}_M\right) : t_{mn} \le t \le t_{mx}\right] = 1\} \tag{9.56}$$

and

$$\mathcal{X}^- = \{\mathbf{e}_M : \mathbf{e}_M \in \mathcal{EM} \text{ and } \delta\left[Q\left(t\middle|\mathbf{a}, \mathbf{e}_M\right) : t_{mn} \le t \le t_{mx}\right] = 0\}. \tag{9.57}$$

as previously indicated in Eqs. (4.34) – (4.37).

For interval analysis, compliance with the requirement is indicated if $\mathcal{X}^+ = \mathcal{EM}$. For possibility theory, evidence theory, and probability theory, the uncertainty in compliance with the specified bounding interval over time is given by

$$Nec_{EM}\left(\mathcal{X}^+\right) = 0.25, \quad Pos_{EM}\left(\mathcal{X}^+\right) = 1.00, \tag{9.58}$$

$$Bel_{EM}\left(\mathcal{X}^+\right) = 0.034, \quad Pl_{EM}\left(\mathcal{X}^+\right) = 1.00, \tag{9.59}$$

and

$$p_{EM}\left(\mathcal{X}^+\right) = 0.897, \tag{9.60}$$

respectively.

Similarly, the uncertainty in noncompliance is given by

$$Nec_{EM}\left(\mathcal{X}^-\right) = 0.00, \quad Pos_{EM}\left(\mathcal{X}^-\right) = 0.75, \tag{9.61}$$

$$Bel_{EM}\left(\mathcal{X}^-\right) = 0.00, \quad Pl_{EM}\left(\mathcal{X}^-\right) = 0.966, \tag{9.62}$$

and

$$p_{EM}\left(\mathcal{X}^-\right) = 0.103 \tag{9.63}$$

for possibility theory, evidence theory, and probability theory, respectively.

The preceding representations summarize the uncertainty in whether or not compliance with the specified bounding interval over time will be satisfied. However, these representations do not display the associated margins. As previously indicated in Eq. (4.40), these margins can be defined by

$$Q_m\left(t\middle|\mathbf{a}, \mathbf{e}_M, [t_{mn}, t_{mx}]\right) = \min\begin{cases} Q_{mn}\left(t\middle|\mathbf{a}, \mathbf{e}_M, [t_{mn}, t_{mx}]\right) - \underline{Q}_b \\ \overline{Q}_b - Q_{mx}\left(t\middle|\mathbf{a}, \mathbf{e}_M, [t_{mn}, t_{mx}]\right), \end{cases} \tag{9.64}$$

where

$$Q_{mn}\left(t\middle|\mathbf{a}, \mathbf{e}_M, [t_{mn}, t_{mx}]\right) = \min\left\{Q\left(t\middle|\mathbf{a}, \mathbf{e}_M\right) : t_{mn} \le t \le t_{mx}\right\}$$

and

$$Q_{mx}\left(t\middle|\mathbf{a}, \mathbf{e}_M, [t_{mn}, t_{mx}]\right) = \max\left\{Q\left(t\middle|\mathbf{a}, \mathbf{e}_M\right) : t_{mn} \le t \le t_{mx}\right\}.$$

In turn, $Q_m(t|\mathbf{a}, \mathbf{e}_M, [t_{mn}, t_{mx}])$ has an uncertainty structure that derives from the uncertainty structure imposed on $\mathbf{e}_M$ (Fig. 9.8).

As discussed in conjunction with the margin results in Fig. 9.6, the compliance results in Eqs. (9.58) – (9.63) can be obtained from the cumulative results in Fig. 9.8 associated with $Q_m(t|\mathbf{a}, \mathbf{e}_M, [t_{mn}, t_{mx}]) = 0.00$.

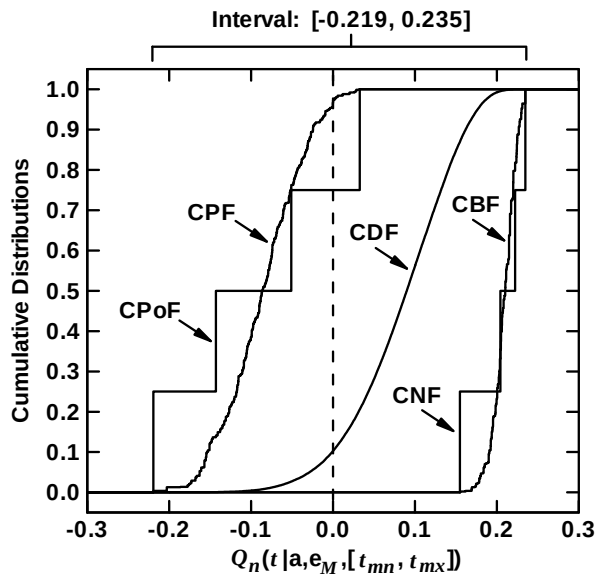

Fig. 9.9. Uncertainty associated with normalized margin $Q_n(t|\mathbf{a}, \mathbf{e}_M, [t_{mn}, t_{mx}])$ defined in Eq. (9.65) characterized by (i) an interval, (ii) a possibility space summarized with a CPoF and a CNF, (iii) an evidence space summarized with a CPF and a CBF, and (iv) a probability space summarized with a CDF.

An alternate representation is to use normalized margins as previously indicated in Eq. (4.41). Specifically, the margin $Q_m(t|\mathbf{a}, \mathbf{e}_M, [t_{mn}, t_{mx}])$ defined in Eq. (9.64) can be replaced by a normalized margin $Q_n(t|\mathbf{a}, \mathbf{e}_M, [t_{mn}, t_{mx}])$ defined by

$$Q_n\left(t\middle|\mathbf{a}, \mathbf{e}_M, [t_{mn}, t_{mx}]\right) = \min\begin{cases}\left[Q_{mn}\left(t\middle|\mathbf{a}, \mathbf{e}_M, [t_{mn}, t_{mx}]\right) - \underline{Q}_b\right]\Big/\underline{Q}_b \\ \left[\overline{Q}_b - Q_{mx}\left(t\middle|\mathbf{a}, \mathbf{e}_M, [t_{mn}, t_{mx}]\right)\right]\Big/\overline{Q}_b,\end{cases} \tag{9.65}$$

which expresses margin as a fraction of the bounding value from which $Q(t|\mathbf{a}, \mathbf{e}_M)$ has the smallest fractional deviation (Fig. 9.9).

9.6 Epistemic Uncertainty with an Uncertain Bound

The QMU results presented in Sects. 9.3 – 9.5 involve uniquely specified bounds. However, it is likely that this will not always be the case in QMU analyses. For example, a requirement might be that a certain system operates but the conditions that define when the system does and does not operate appropriately may not be specified. Then, it is the analysts' responsibility to specify the conditions under which the system operates in the manner desired. However, there may be uncertainty with respect to exactly what conditions are necessary for the appropriate operation of the system. Then, in this situation, there is epistemic uncertainty as to the conditions must be specified to define what constitutes appropriate operation of the system.

The example presented in Sect. 9.5 can be modified to illustrate this situation. As originally stated, the example in Sect. 9.5 involves a bounding interval $[\underline{Q}_b, \overline{Q}_b]$ for $Q(t|\mathbf{a}, \mathbf{e}_M)$ over the time interval $[t_{mn}, t_{mx}]$. For the example of this section, it is assumed that the specified requirement is that the system be operational over the time interval $[t_{mn}, t_{mx}]$ but the requirement does not specify what conditions are necessary for the system to be operational. For purposes of illustration, it is assumed that the analysts involved conclude that the system being operational over $[t_{mn}, t_{mx}]$ corresponds to $Q(t|\mathbf{a}, \mathbf{e}_M)$ being within a bounding interval $[\underline{Q}_b, \overline{Q}_b]$. However, they are uncertain with respect to the appropriate value for this bounding interval. Thus, there is epistemic uncertainty with respect to the values to use for $\underline{Q}_b$ and $\overline{Q}_b$. As a result, the vector $\mathbf{e}_M$ of epistemically uncertain inputs to the analysis now has the form

$$\mathbf{e}_M = \left[\underline{Q}_b, \overline{Q}_b, L, R, C, E_0, \lambda\right]. \tag{9.66}$$

For purposes of illustration, it is assumed that the analysts conclude that (i) $\underline{Q}_b$ is contained in the interval [0.06, 0.08 C], (ii) $\overline{Q}_b$ is contained in the interval [0.14, 0.16 C], (iii) $\underline{Q}_b$ and $\overline{Q}_b$ have the same uncertainty structure specified for L, R_0, C, E and λ (see Eqs. (9.7) – (9.15) and associated discussion), and (iv) no dependency or correlation exists between $\underline{Q}_b$ and $\overline{Q}_b$ (Fig. 4.14).

This problem can now be analyzed exactly as in Sect. 9.5. The only difference is that $\mathbf{e}_M$ now contains 7 rather than 5 elements, with two of these elements being $\underline{Q}_b$ and $\overline{Q}_b$. Specifically, $\delta[Q(t|\mathbf{a}, \mathbf{e}_M)$: $t_{mn} \le t \le t_{mx}]$, $\mathcal{X}^+$ and $\mathcal{X}^-$ are defined as indicated in Eqs. (9.54) – (9.57). In turn, the resultant uncertainty representations with possibility theory, evidence theory and probability theory are

$$Nec_{EM}\left(\mathcal{X}^+\right) = 0.25,\ Pos_{EM}\left(\mathcal{X}^+\right) = 1.00, \tag{9.67}$$

$$Nec_{EM}\left(\mathcal{X}^-\right) = 0.00,\ Pos_{EM}\left(\mathcal{X}^-\right) = 0.75, \tag{9.68}$$

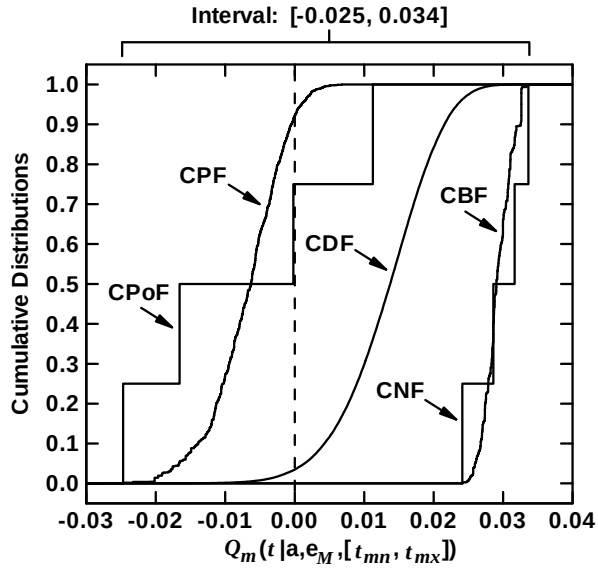

Fig. 9.10. Uncertainty associated with margin $Q_m(t|\mathbf{a}, \mathbf{e}_M, [t_{mn}, t_{mx}])$ defined in Eq. (9.64) with $\mathbf{e}_M = [\underline{Q}_b, \overline{Q}_b, L, R, C, E, \lambda]$ characterized by (i) an interval, (ii) a possibility space summarized with a CPoF and a CNF, (iii) an evidence space summarized with a CPF and a CBF, and (iv) a probability space summarized with a CDF.

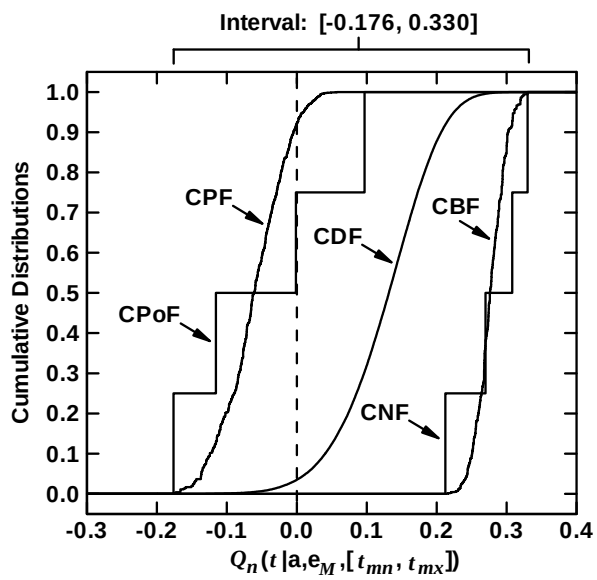

Fig. 9.11. Uncertainty associated with normalized margin $Q_n(t|\mathbf{a}, \mathbf{e}_M, [t_{mn}, t_{mx}])$ defined in Eq. (9.65) with $\mathbf{e}_M = [\underline{Q}_b, \overline{Q}_b, L, R, C, E, \lambda]$ characterized by (i) an interval, (ii) a possibility space summarized with a CPoF and a CNF, (iii) an evidence space summarized with a CPF and a CBF, and (iv) a probability space summarized with a CDF.

$$Bel_{EM}\left(\mathcal{X}^{+}\right) = 0.078,\ Pl_{EM}\left(\mathcal{X}^{+}\right) = 1.00, \tag{9.69}$$

$$Bel_{EM}\left(\mathcal{X}^{-}\right) = 0.00,\ Pl_{EM}\left(\mathcal{X}^{-}\right) = 0.922, \tag{9.70}$$

and

$$p_{EM}\left(\mathcal{X}^{+}\right) = 0.966,\ p_{EM}\left(\mathcal{X}^{-}\right) = 0.034, \tag{9.71}$$

respectively, and include the uncertainty associated with the imperfectly known values for $\underline{Q}_b$ and $\overline{Q}_b$.

Margin analysis results $Q_m(t|\mathbf{a}, \mathbf{e}_M, [t_{mn}, t_{mx}])$ and normalized margin analysis results $Q_n(t|\mathbf{a}, \mathbf{e}_M, [t_{mn}, t_{mx}])$ of the form defined in Eqs. (9.64) and (9.65), respectively, can also be obtained (Figs. 9.10 and 9.11). As discussed in conjunction with the margin results in Fig. 9.6, the compliance results in Eqs. (9.67) – (9.71) can be obtained from the cumulative results in Fig. 9.10 associated with $Q_m(t|\mathbf{a}, \mathbf{e}_M, [t_{mn}, t_{mx}]) = 0.00$.

Results analogous to those presented in this section involving uncertain bounds can also be obtained for a single bound as discussed in Sect. 9.3 and a bounding interval at a fixed point in time as discussed in Sect. 9.4.

This page intentionally left blank

10 QMU with Aleatory and Epistemic Uncertainty: Characterization with Alternative Uncertainty Representations

Examples illustrating the use of the alternative uncertainty representations introduced in Sect. 8 are now presented for QMU problems involving aleatory and epistemic uncertainty. Specifically, the example problem in Sect. 3.6 is expanded to include the alternative uncertainty representations in Sect. 8 (Sect. 10.1). Then, the following topics are considered: epistemic uncertainty in an exceedance probability deriving from aleatory uncertainty (Sect. 10.2), epistemic uncertainty in margins associated with a specified bound on a quantile deriving from aleatory uncertainty (Sect. 10.3), and epistemic uncertainty in margins associated with a specified bound on an expected value deriving from aleatory uncertainty (Sect. 10.4).

10.1 Randomly Perturbed System Used for Illustration

As an example, this section uses the randomly perturbed system defined in Eqs. (3.55) – (3.58) and previously used in Sect. 5 in the illustration of QMU analyses involving aleatory and epistemic uncertainty with probability-based representations of epistemic uncertainty. The probability space ($\mathcal{A}$, $\mathbb{A}$, p_A) characterizing aleatory associated with this example is defined in conjunction with Eqs. (3.56) and (3.57). Further, the example involves the vector

$$\begin{aligned}\mathbf{e} &= \left[\mathbf{e}_A, \mathbf{e}_M\right] \\ &= \left[e_{M1}, e_{M2}, e_{M3}, e_{M4}, e_{M5}\right] \\ &= \left[\lambda, a, m, b, r\right]\end{aligned} \tag{10.1}$$

of epistemically uncertain variables defined in conjunction with Eq. (3.59) with $\mathbf{e}_A = [\lambda, a, m, b]$ and $\mathbf{e}_M = [r]$. Specifically, λ, a, m and b are involved in the definition of probability distributions that characterize aleatory uncertainty, and r relates to the physical processes involved in the decay of an initial perturbation A_0.

For interval analysis, the appropriate values for λ, a, m, b and r are assumed to be contained in the intervals

$$\begin{aligned}\mathcal{EA}_1 &= \left\{\lambda : \lambda_{mn} \le \lambda \le \lambda_{mx}\right\} \\ &= \left\{\lambda : 0.5 \le \lambda \le 1.5\ \mathrm{s}^{-1}\right\},\end{aligned} \tag{10.2}$$

$$\begin{aligned}\mathcal{EA}_2 &= \left\{a : a_{mn} \le a \le a_{mx}\right\} \\ &= \left\{a : 1.0 \le a \le 2.0\ \mathrm{kg\ m/s^2}\right\},\end{aligned} \tag{10.3}$$

$$\begin{aligned}\mathcal{EA}_3 &= \left\{m : m_{mn} \le m \le m_{mx}\right\} \\ &= \left\{m : 2.0 \le m \le 4.0\ \mathrm{kg\ m/s^2}\right\},\end{aligned} \tag{10.4}$$

$$\begin{aligned}\mathcal{EA}_4 &= \left\{b : b_{mn} \le b \le b_{mx}\right\} \\ &= \left\{b : 4.0 \le b \le 5.0\ \mathrm{kg\ m/s^2}\right\},\end{aligned} \tag{10.5}$$

and

$$\begin{aligned}\mathcal{EM}_1 &= \left\{r : r_{mn} \le r \le r_{mx}\right\} \\ &= \left\{r : 0.2 \le r \le 1.2\ \mathrm{s}^{-1}\right\},\end{aligned} \tag{10.6}$$

respectively. No additional information about the location of the appropriate values for λ, a, m, b and r is assumed to be known. These are the same intervals defined in Eqs. (3.60) – (3.64).

For possibility theory, evidence theory and probability theory, the resultant sample space for the vector $\mathbf{e}$ of epistemically uncertain variables is

$$\mathcal{E} = \mathcal{EA}_1 \times \mathcal{EA}_2 \times \mathcal{EA}_3 \times \mathcal{EA}_4 \times \mathcal{EM}_1 \tag{10.7}$$

with $\mathcal{EA}_1$, $\mathcal{EA}_2$, …, $\mathcal{EM}_1$ defined in Eqs. (10.2) – (10.6). Further, associated possibility spaces, evidence spaces and probability spaces for the individual elements of $\mathbf{e}$ (i.e., λ, a, m, b and r) are defined in exactly the same manner as for the elements of $\mathbf{e}_M = [L, R, C, E_0, \lambda]$ in Eqs. (9.7) – (9.15). For convenience, the resultant possibility space, evidence space and probability space for $\mathbf{e}$ will be denoted ($\mathcal{E}$, r_E), ($\mathcal{E}$, $\mathbb{E}$, m_E) and ($\mathcal{E}$, $\mathbb{E}$, p_E), respectively.

The examples presented in this section are constructed from samples obtained as described in conjunction with Eqs. (5.3) – (5.6). The only difference is that a random sample of size $nSE = 10^5$ from $\mathcal{E}$ is used rather than an LHS of size $nSE = 200$ as indicated in Eq. (5.3). Specifically, the indicated random sample of size $nSE = 10^5$ is generated in consistency with the probability space ($\mathcal{E}$, $\mathbb{E}$, p_E). A large sample from $\mathcal{E}$ is needed in order to adequately cover the focal elements associated with the evidence space ($\mathcal{E}$, $\mathbb{E}$, m_E) (see Refs. [188; 270] for additional discussion).

10.2 Epistemic Uncertainty Without a Specified Bound

As an example, the uncertainty in the possible values for the probability $p_A[20 < A(10|\mathbf{a}, r)|\mathbf{e}_A]$ is considered. Specifically, the uncertainty associated with the exceedance probabilities corresponding to the vertical line in Fig. 5.1a are under consideration. In this

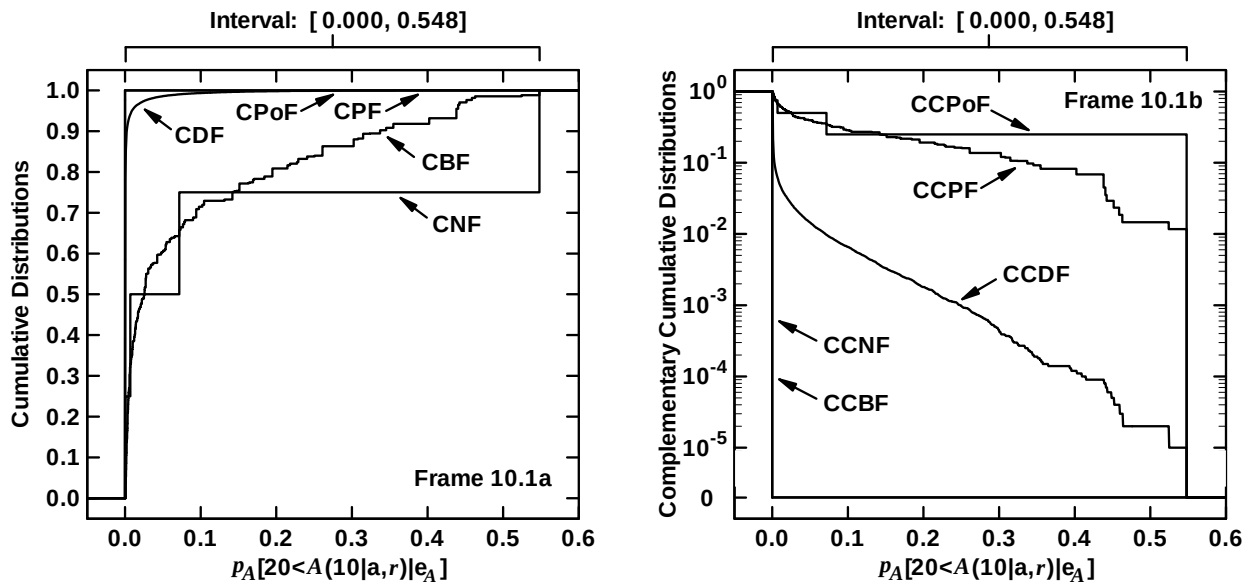

Fig. 10.1. Uncertainty associated with $p_A[20 < A(10|\mathbf{a}, r)|\mathbf{e}_A]$ characterized by (i) an interval (i.e., [inf($\mathcal{P}$), sup($\mathcal{P}$)]), (ii) a possibility space ($\mathcal{P}$, r_P) summarized with a CCPoF, CCNF, CPoF and CNF, (iii) an evidence space ($\mathcal{P}$, $\mathbb{P}$, m_P) summarized with a CCPF, CCBF, CPF and CBF, and (iv) a probability space ($\mathcal{P}$, $\mathbb{P}$, p_P) summarized with a CCDF and CDF: (a) Cumulative results, and (b) Complementary cumulative results.

example, the probabilities $p_A[20 < A(10|\mathbf{a}, r)|\mathbf{e}_A]$ derive from aleatory uncertainty (i.e., from the probability space ($\mathcal{A}$, $\mathbb{A}$, p_A)) but the uncertainty in the possible values for these probabilities derives from epistemic uncertainty (i.e., from the possible values for $\mathbf{e}$ in the set $\mathcal{E}$ and the associated spaces ($\mathcal{E}$, r_E), ($\mathcal{E}$, $\mathbb{E}$, m_E) and ($\mathcal{E}$, $\mathbb{E}$, p_E) as appropriate).

More formally, the set

$$\mathcal{P} = \left\{ p_A\left[20 < A\left(10\middle|\mathbf{a}, r\right)\middle|\mathbf{e}_A \right] : \mathbf{e} = \left[\mathbf{e}_A, \mathbf{e}_M\right] \in \mathcal{E} \right\} \tag{10.8}$$

is under consideration. In turn, $\mathcal{P}$ has an uncertainty structure that derives from the uncertainty structure imposed on $\mathcal{E}$. Thus, the uncertainty associated with $p_A[20 < A(10|\mathbf{a}, r)|\mathbf{e}_A]$ is characterized by an interval [inf($\mathcal{P}$), sup($\mathcal{P}$)], a possibility space ($\mathcal{P}$, r_P), an evidence space ($\mathcal{P}$, $\mathbb{P}$, m_P) or a probability space ($\mathcal{P}$, $\mathbb{P}$, p_P) depending on which characterization is assumed for $\mathcal{E}$ (Fig. 10.1). Specifically, cumulative and complementary results are shown in Figs. 10.1a and 10.1b, respectively.

Some individuals are uncomfortable with the concept of uncertain probabilities as illustrated in Fig. 10.1. However, in the context of epistemic uncertainty, there is no conceptual difference between the uncertainty results shown in Fig. 9.1 for electric charge and the uncertainty results shown in Fig. 10.1 for exceedance probability. In both cases, an analysis outcome is being calculated with quantities that are uncertain in an epistemic sense, with the result that the analysis outcome under consideration is also uncertain in an epistemic sense. When viewed abstractly, both cases involve a model (i.e., a function) that takes a vector $\mathbf{e}$ of inputs and produces a result. For Fig. 9.1, the model involves the solution of an ordinary differential equation and produces an electric charge; for Fig. 10.1, the model involves the evaluation of an integral and produces an exceedance probability. When viewed as "black boxes," both models are simply functions that produce a numeric result.

10.3 Epistemic Uncertainty with a Specified Bound on a Quantile

A QMU problem is now considered. For this example, it is assumed that $p_A[20 < A(10|\mathbf{a}, r)|\mathbf{e}_A]$ is required to be less than a bound (e.g., p_{b1} = 0.05 and p_{b2} = 0.1 in Fig. 10.2). In particular, the possibility and necessity of exceeding p_{b1} are 0.5 and 0.0, respectively; the plausibility and belief of exceeding p_{b1} are 0.396 and 0.0, respectively; and the probability of exceeding p_{b1} is 0.0144. The preceding uncertainty characterizations relate to epistemic uncertainty and thus provide degree of belief characterizations with different mathematical structures of the "likelihood" or "confidence" that $p_A[20 < A(10|\mathbf{a}, r)|\mathbf{e}_A]$ will be greater than p_{b1}.

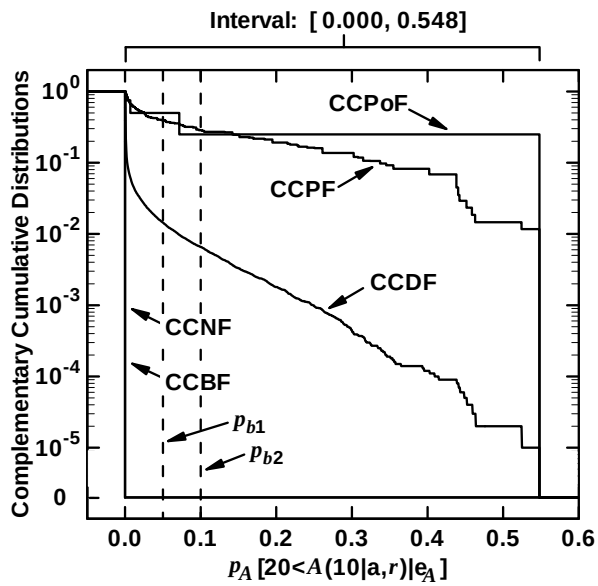

Fig. 10.2. Uncertainty associated with $p_A[20 < A(10|\mathbf{a}, r)|\mathbf{e}_A]$ characterized by (i) an interval, (ii) a possibility space summarized with a CCPoF and CCNF, (iii) an evidence space summarized with a CCPF and CCBF, and (iv) a probability space summarized with a CCDF.

Similarly, the corresponding values for p_{b2} can also be read from Fig. 10.2.

In turn, the margins between $p_A[20 < A(10|\mathbf{a}, r)|\mathbf{e}_A]$ and the bounds p_{bk}, $k = 1, 2$, indicated in Fig. 10.2 can be defined in the same manner as in the margins in Eq. (5.7). Specifically, the margin $p_{mk}(10|\mathbf{e})$ is defined by

$$p_{mk}\left(10\middle|\mathbf{e}\right) = p_{mk} - p_A\left[20 < A\left(10\middle|\mathbf{a}, r\right)\middle|\mathbf{e}_A\right], \qquad (10.9)$$

with $p_{mk}(10|\mathbf{e}) > 0$ indicating that bound p_{bk} is satisfied and $p_{mk}(10|\mathbf{e}) < 0$ indicating that bound p_{bk} is not satisfied. As a result of $p_A[20 < A(10|\mathbf{a}, r)|\mathbf{e}_A]$ being uncertain, the corresponding margins $p_{mk}(10|\mathbf{e})$ are also uncertain and have an uncertainty structure that derives from the corresponding uncertainty structure assumed for $\mathbf{e}$ (Fig. 10.3).

An alternative presentation involves the use of normalized margins. As previously presented in Eq. (5.8), normalized margins can be defined by

$$p_{nk}\left(10\middle|\mathbf{e}\right) = p_{mk}\left(10\middle|\mathbf{e}\right)\Big/p_{bk} \qquad (10.10)$$

for $k = 1, 2$ and express margin as a fraction of the corresponding bounding value (Fig. 10.4).

10.4 Epistemic Uncertainty with a Specified Bound on an Expected Value

For this example, it is assumed that the expected value $E_A[A(10|\mathbf{a}, r)|\mathbf{e}_A]$ previously summarized in Fig. 3.13 for a probabilistic representation of epistemic uncertainty is required to be less than a bound (e.g., the bound $\bar{A}_b = 13$ in Fig. 5.5). In particular, the possibility and necessity of exceeding $\bar{A}_b$ are 0.25 and 0.0, respectively; the plausibility and belief of exceeding $\bar{A}_b$ are 0.318 and 0.0, respectively; and the probability of exceeding $\bar{A}_b$ is 0.00867 (Fig. 10.5).

In turn, margins $\bar{A}_m(10\,|\,\mathbf{e})$ and normalized margins $\bar{A}_n(10\,|\,\mathbf{e})$ can be defined as indicated in Eqs. (5.15) and (5.16) (Fig. 10.6).

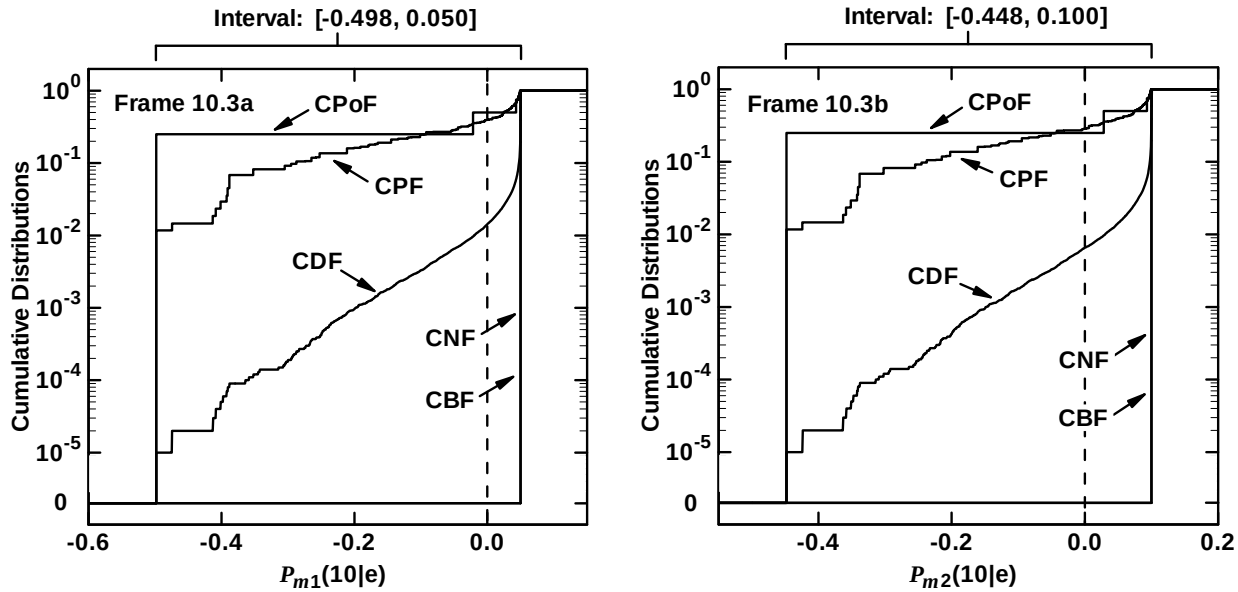

Fig. 10.3. Uncertainty associated with margins $p_{mk}(10|\mathbf{e})$, k = 1, 2, defined in Eq. (10.9) characterized by (i) intervals, (ii) possibility spaces summarized with CPoFs and CNFs, (iii) evidence spaces summarized with CPFs and CBFs and (iv) probability spaces summarized with CDFs: (a) $p_{m1}(10|\mathbf{e})$, and (b) $p_{m2}(10|\mathbf{e})$.

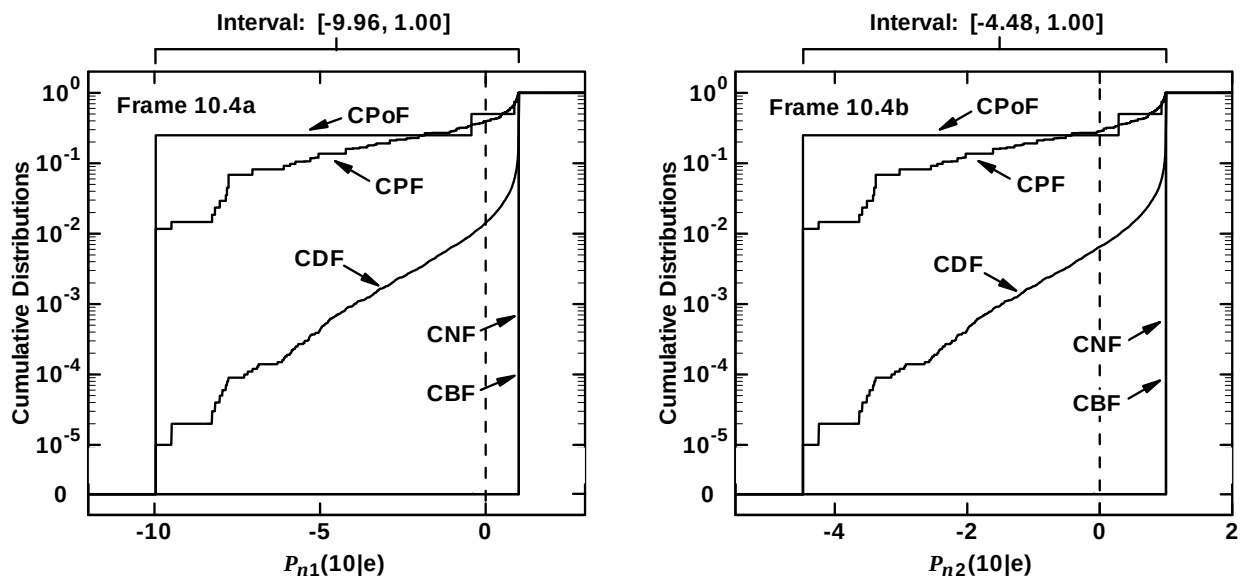

Fig. 10.4. Uncertainty associated with normalized margins $p_{nk}(10|\mathbf{e})$, k = 1, 2, defined in Eq. (10.10) characterized by (i) intervals, (ii) possibility spaces summarized with CPoFs and CNFs, (iii) evidence spaces summarized with CPFs and CBFs and (iv) probability spaces summarized with CDFs: (a) $p_{n1}(10|\mathbf{e})$, and (b) $p_{n2}(10|\mathbf{e})$.

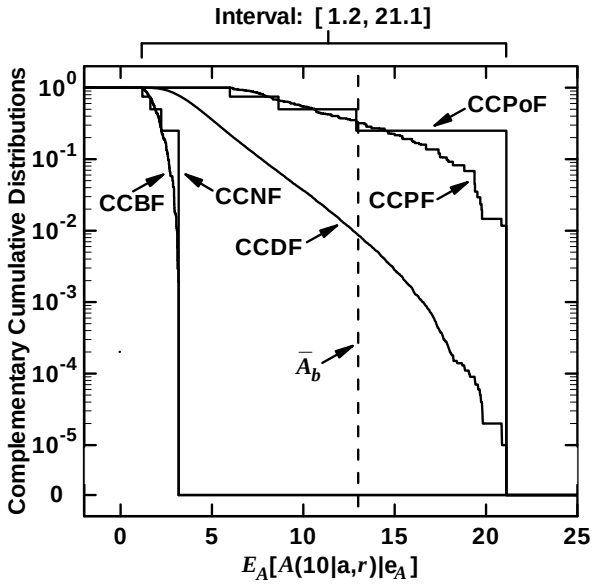

Fig. 10.5. Uncertainty associated with $E_A[A(10|\mathbf{a}, r)|\mathbf{e}_A]$ characterized by (i) an interval, (ii) a possibility space summarized with a CCPoF and CCNF, (iii) an evidence space summarized with a CCPF and CCBF, and (iv) a probability space summarized with a CCDF.

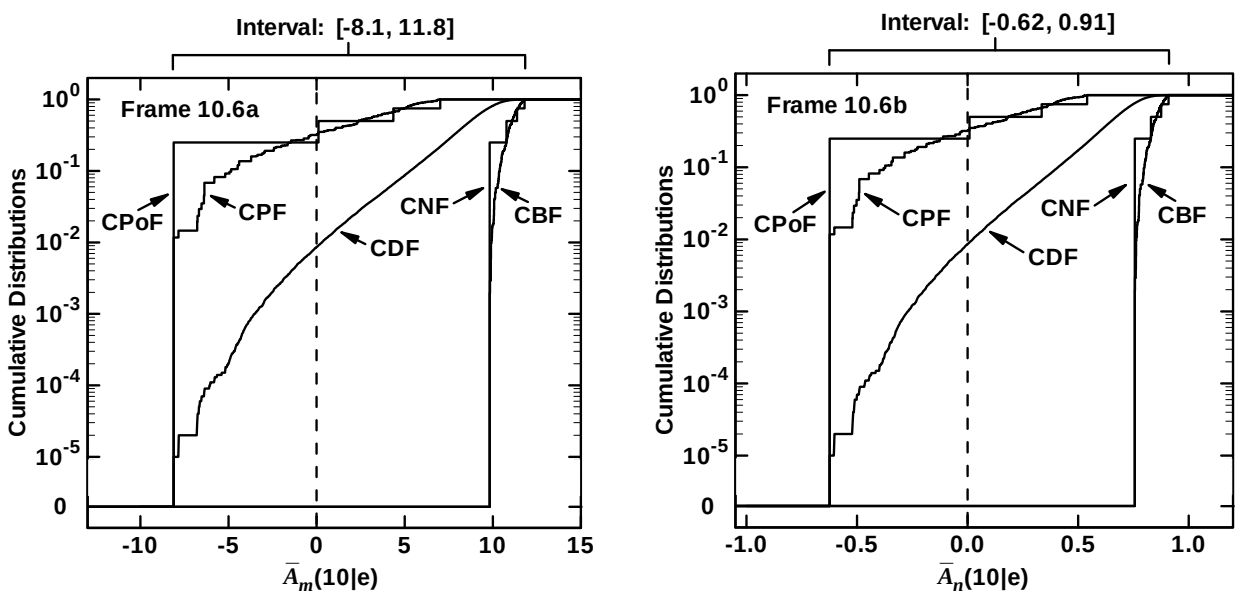

Fig. 10.6. Margins and normalized margins for $E_A[A(10|\mathbf{a}, r)|\mathbf{e}_A]$ characterized by (i) intervals, (ii) possibility spaces summarized with CPoFs and CNFs, (iii) evidence spaces summarized with CPFs and CBFs and (iv) probability spaces summarized with CDFs: (a) $\bar{A}_m(10\,|\,\mathbf{e})$, and (b) $\bar{A}_n(10\,|\,\mathbf{e})$.

This page intentionally left blank

11 Summary Discussion

As indicated by the name, QMU involves three concepts: quantification, margin and uncertainty. These concepts are discussed in the following sections: Margins (Sect. 11.1), uncertainty (Sect. 11.2), and quantification (Sect. 11.3). Then, the presentation of QMU results is discussed (Sect. 11.4).

11.1 Margins in QMU

Intuitively, a margin M is a measure of the difference between a requirement R placed on the performance of a system and the predicted performance P of the system, with $M \geq 0$ indicating that the requirement is met and $M < 0$ indicating that the requirement is not met. More explicitly, M is a function $M(R, P)$ of R and P with the properties that

$$M(R,P) \geq 0 \Rightarrow \text{ compliance of performance } P \text{ with requirement } R \tag{11.1}$$

and

$$M(R,P) < 0 \Rightarrow \text{ noncompliance of performance } P \text{ with requirement } R. \tag{11.2}$$

If R and P are single numerical values, then the definition of $M(R, P)$ could be as simple as

$$M(R,P) = R - P \tag{11.3}$$

if P is required to be less than or equal to R and

$$M(R,P) = P - R \tag{11.4}$$

if P is required to be greater than or equal to R. Margins of this type are extensively discussed and illustrated in Sects. 4, 5, 9 and 10.

In many real analyses, it is unlikely that R and P will be single numbers. Rather, greater complexity in the definition of R and P is likely to be the case. For example, R might correspond to requirements on several subsystems of a larger system, and P, in turn, would correspond to the performance of these subsystems. As another example, R and P might be functions or vectors of functions. For this reason, the requirement R and performance P are more appropriately represented as the vectors $\mathbf{R}$ and $\mathbf{P}$. The analyses presented in Sect. 6 are of this type with multiple requirements placed on system performance. Then, M is a function $M(\mathbf{R}, \mathbf{P})$ with the properties that

$$M(\mathbf{R},\mathbf{P}) \geq 0 \Rightarrow \text{ compliance of performance } \mathbf{P} \text{ with requirement } \mathbf{R} \tag{11.5}$$

and

$$M(\mathbf{R},\mathbf{P}) < 0 \Rightarrow \text{ noncompliance of performance } \mathbf{P} \text{ with requirement } \mathbf{R}. \tag{11.6}$$

In this situation, the evaluation of $M(\mathbf{R}, \mathbf{P})$ involves a more complex calculation than the simple subtractions indicated in Eqs. (11.3) and (11.4).

In practice, it is also possible for $M(\mathbf{R}, \mathbf{P})$ itself to be a vector and thus appropriately denoted by $\mathbf{M}(\mathbf{R}, \mathbf{P})$. For example, if

$$\mathbf{R} = [R_1, R_2, \ldots, R_{nR}], \tag{11.7}$$

$$\mathbf{P} = [P_1, P_2, \ldots, P_{nR}] \tag{11.8}$$

and

$$M_r(R_r, P_r) = R_r - P_r \tag{11.9}$$

is the margin associated with requirement R_r for $r = 1, 2, \ldots, nR$, then $\mathbf{M}(\mathbf{R}, \mathbf{P})$ might be defined by

$$\begin{aligned}\mathbf{M}(\mathbf{R},\mathbf{P}) &= [M_1(R_1, P_1), M_2(R_2, P_2), \ldots, M_{nR}(R_{nR}, P_{nR})] \\ &= [R_1 - P_1, R_2 - P_2, \ldots, R_{nR} - P_{nR}].\end{aligned} \tag{11.10}$$

In a situation of this type, one possibility is to consider each of the margins $M_r(R_r, P_r)$ separately, which corresponds to defining $\mathbf{M}(\mathbf{R}, \mathbf{P})$ to be the minimum of the values for $M_r(R_r, P_r)$. This is the situation illustrated in Sects. 4.2 – 4.4 and 9.4 – 9.6 and also appears to be the intent of the regulatory requirements and associated margins illustrated in Sect. 6. Another possibility is the use of some type of weighted average to reduce the margins $M_r(R_r, P_r)$ to a single number. In general, the reduction of $\mathbf{M}(\mathbf{R}, \mathbf{P})$ to a single real-valued margin

$$M(\mathbf{R},\mathbf{P}) = f[\mathbf{M}(\mathbf{R},\mathbf{P})] \tag{11.11}$$

through the application of a suitable function f is likely to be analysis specific and outside the scope of this discussion.

11.2 Uncertainty in QMU

If **R** and **P** were known with complete certainty and the function $M(\mathbf{R}, \mathbf{P})$ that defined the margin associated with **R** and **P** was unambiguously defined, then there is no uncertainty and the margin $M(\mathbf{R}, \mathbf{P})$ is uniquely defined. Unfortunately, this is unlikely to be the case in a real analysis. In the analyses of most systems, there is likely to be significant uncertainties associated with the determination of **P**, and uncertainty with respect to the appropriate definition of **R** is also possible. However, this discussion assumes there is no uncertainty in the definition of the function $M(\mathbf{R}, \mathbf{P})$ that converts **R** and **P** into a margin M. The examples in Sect. 6 illustrate analyses of real systems that involve significant uncertainties in the modeling of system performance **P**. Further, the notional analyses in Sects. 4.4 and 9.6 involve uncertainty in both **R** and **P**. The possibility of uncertainty in both **R** and **P** is recognized by the NNSA in Quote (NNSA-3).

The presence of uncertainty in the determination of $M(\mathbf{R}, \mathbf{P})$ can be acknowledged through the introduction of a vector

$$\mathbf{e}_M = \left[e_{M1}, e_{M2}, \ldots, e_{M,nEM} \right] \tag{11.12}$$

of uncertain analysis inputs required in the evaluation of $M(\mathbf{R}, \mathbf{P})$. With this introduction, $M(\mathbf{R}, \mathbf{P})$ is appropriately represented by

$M\left(\mathbf{R},\mathbf{P}\middle|\mathbf{e}_M\right) =$ margin determined with value for **P** and possibly the value for **R** conditional on the values for $e_{M1}, e_{M2}, \ldots, e_{M,nE}$ contained in $\mathbf{e}_M$. (11.13)

More specifically,

$$M\left(\mathbf{R},\mathbf{P}\middle|\mathbf{e}_M\right) = M\left[\mathbf{R},\mathbf{P}\left(\mathbf{e}_M\right)\right] \tag{11.14}$$

if only **P** depends on $\mathbf{e}_M$;

$$M\left(\mathbf{R},\mathbf{P}\middle|\mathbf{e}_M\right) = M\left[\mathbf{R}\left(\mathbf{e}_M\right), \mathbf{P}\left(\mathbf{e}_M\right)\right] \tag{11.15}$$

if **R** and **P** depend on $\mathbf{e}_M$; and

$$M\left(\mathbf{R},\mathbf{P}\middle|\mathbf{e}_M\right) = M\left[\mathbf{R}\left(\mathbf{e}_R\right), \mathbf{P}\left(\mathbf{e}_P\right)\right], \mathbf{e}_M = \left[\mathbf{e}_R, \mathbf{e}_P\right], \tag{11.16}$$

if $\mathbf{e}_M$ can be decomposed into a vector $\mathbf{e}_R$ that contains only variables affecting **R** and a vector $\mathbf{e}_P$ that contains only variables affecting **P**. Sects. 4.4 and 9.6 illustrate analyses in which $\mathbf{e}_M$ can be decomposed into a vector $\mathbf{e}_R$ and a vector $\mathbf{e}_P$; specifically, $\mathbf{e}_R$ and $\mathbf{e}_P$ correspond to $[Q_b, \bar{Q}_b]$ and $[L, R, C, E_0, \lambda]$, respectively, in these sections.

The values for the variables contained in $\mathbf{e}_M$ are assumed to be uncertain in the sense that the analysis leading to $M(\mathbf{R}, \mathbf{P})$ has been designed on the assumption that the appropriate value for $M(\mathbf{R}, \mathbf{P})$ will be obtained if the appropriate values for the elements of $\mathbf{e}_M$ are used. Unfortunately, the appropriate value to use for $\mathbf{e}_M$ is not, and cannot be in most analyses, known with certainty. Rather, there is uncertainty with respect to the appropriate value to use for each element of $\mathbf{e}_M$. Uncertainty with respect to the value of a fixed, but poorly known, quantity is usually referred to as epistemic uncertainty, which is why $\mathbf{e}_M$ is used as the designator for the vector of uncertain quantities in Eq. (11.12). Alternative descriptors used for epistemic uncertainty include subjective uncertainty, state of knowledge uncertainty, and reducible uncertainty (see Sect. 2 for additional discussion).

The epistemic uncertainty associated with the elements of $\mathbf{e}_M$ is usually characterized with probability; however, alternative mathematical structures for the characterization of epistemic uncertainty such as possibility theory and evidence theory also exist (see Sects. 8 – 10). With the use of probability to characterize epistemic uncertainty, the uncertainty associated with **e** is defined by a sequence of distributions

$$D_1, D_2, \ldots, D_{nEM}, \tag{11.17}$$

where the distribution D_r associated with element e_{Mr} of $\mathbf{e}_M$ provides a mathematical characterization of the available information with respect to where the appropriate value for e_{Mr} is located for use in evaluation $M(\mathbf{R}, \mathbf{P})$. Correlations and other restrictions involving relationships between individual elements of **e** may also be present. Distributions of the form indicated in Eq. (11.17) are often developed, at least in part, through an expert review process (see discussion in Sect. 7.1). In turn, the distribution for $\mathbf{e}_M$ that results from the distributions in Eq. (11.17) and any associated restrictions leads to a resultant distribution of values for $M(\mathbf{R}, \mathbf{P}|$

$\mathbf{e}_M$) that characterizes the (epistemic) uncertainty with respect to the appropriate value for the margin $M(\mathbf{R}, \mathbf{P})$.

The distributions $D_1, D_2, \ldots, D_{nEM}$ indicated in Eq. (11.17) are, in essence, defining a probability space ($\mathcal{EM}$, $\mathbb{EM}$, p_{EM}) for epistemic uncertainty, where $\mathcal{EM}$ is the set of possible values for $\mathbf{e}_M$, $\mathbb{EM}$ is a suitably restricted set of subsets of $\mathcal{EM}$, and p_{EM} defines the probabilities for individual sets contained in $\mathbb{EM}$. In practice, the individual distributions D_r in Eq. (11.17) are usually defined by CDFs or CCDFs that, in effect, define $\mathcal{EM}$, $\mathbb{EM}$, p_{EM} and an associated density function d_{EM} ($\mathbf{e}_M$) defined on $\mathcal{EM}$. Although $\mathcal{EM}$, $\mathbb{EM}$, p_{EM} and $d_{EM}(\mathbf{e}_M)$ are notationally useful and can be formally defined, actual calculations involving the probability space ($\mathcal{EM}$, $\mathbb{EM}$, p_{EM}) are usually carried out with direct use of the distributions $D_1, D_2, \ldots, D_{nEM}$ and any associated restrictions involving these distributions (e.g., by using random or Latin hypercube sampling to generate values for $\mathbf{e}_M$ consistent with the distributions $D_1, D_2, \ldots, D_{nEM}$).

Once the distributions $D_1, D_2, \ldots, D_{nEM}$ in Eq. (11.17) are defined, and hence the probability space ($\mathcal{EM}$, $\mathbb{EM}$, p_{EM}) is also defined, the uncertainty in the margin $M(\mathbf{R}, \mathbf{P}|\ \mathbf{e}_M)$ can be formally represented by a CDF or a CCDF. Specifically, the CDF and CCDF for $M(\mathbf{R}, \mathbf{P}|\ \mathbf{e}_M)$ are formally defined by

$$p_{EM}\left[M\left(\mathbf{R},\mathbf{P}|\mathbf{e}_M\right)\le M\right] = \int_{\mathcal{EM}} \underline{\delta}_M\left[M\left(\mathbf{R},\mathbf{P}|\mathbf{e}_M\right)\right] d_{EM}\left(\mathbf{e}_M\right)\mathrm{d}EM \tag{11.18}$$

and

$$p_{EM}\left[M < M\left(\mathbf{R},\mathbf{P}|\mathbf{e}_M\right)\right] = \int_{\mathcal{E}} \overline{\delta}_M\left[M\left(\mathbf{R},\mathbf{P}|\mathbf{e}_M\right)\right] d_{EM}\left(\mathbf{e}_M\right)\mathrm{d}EM, \tag{11.19}$$

respectively, where p_{EM} denotes epistemic probability, dEM represents an increment of volume from $\mathcal{EM}$, and the indicator functions $\underline{\delta}_M(\sim)$ and $\overline{\delta}_M(\sim)$ are defined by

$$\underline{\delta}_M\left[M\left(\mathbf{R},\mathbf{P}|\mathbf{e}_M\right)\right] = \begin{cases} 1 & \text{if } M\left(\mathbf{R},\mathbf{P}|\mathbf{e}_M\right)\le M \\ 0 & \text{otherwise} \end{cases}$$

and

$$\overline{\delta}_M\left[M\left(\mathbf{R},\mathbf{P}|\mathbf{e}_M\right)\right] = \begin{cases} 1 & \text{if } M\left(\mathbf{R},\mathbf{P}|\mathbf{e}_M\right) > M \\ 0 & \text{otherwise.} \end{cases}$$

In practice, the indicated probabilities are usually approximated by

$$p_{EM}\left[M\left(\mathbf{R},\mathbf{P}|\mathbf{e}_M\right)\le M\right] \cong \sum_{i=1}^{nS} \underline{\delta}_M\left[M\left(\mathbf{R},\mathbf{P}|\mathbf{e}_{Mi}\right)\right]\Big/nS \tag{11.20}$$

and

$$p_{EM}\left[M < M\left(\mathbf{R},\mathbf{P}|\mathbf{e}_M\right)\right] \cong \sum_{i=1}^{nS} \overline{\delta}_M\left[M\left(\mathbf{R},\mathbf{P}|\mathbf{e}_{Mi}\right)\right]\Big/nS\ , \tag{11.21}$$

where $\mathbf{e}_{Mi}$, $i = 1, 2, \ldots, nS$, is a random or Latin hypercube sample of size nS generated from $\mathcal{EM}$ in consistency with the distributions $D_1, D_2, \ldots, D_{nEM}$ and any associated restrictions. Calculations of this type are discussed in Sect. 3.3 and illustrated in Sects. 3.4, 4 and 9.

To this point, only the effects of epistemic uncertainty on the margin $M(\mathbf{R}, \mathbf{P})$ have been considered. Specifically, $M(\mathbf{R}, \mathbf{P})$ has been assumed to be a function $M(\mathbf{R}, \mathbf{P}|\ \mathbf{e}_M)$ of a vector $\mathbf{e}_M$ of epistemically uncertain analysis inputs. However, many analyses involve an additional class of uncertainty known as aleatory uncertainty (Sect. 2). Specifically, aleatory uncertainty corresponds to some form of random variability associated with the system under study. As examples, such variability might correspond to (i) variability in a population of manufactured devices, (ii) variability in the effects of aging processes, (iii) variability in the conditions associated with a particular class of accidents, or (iv) variability over time in the environmental conditions that a single device or a population of devices is subjected to. Alternative descriptors used for aleatory uncertainty include variability, stochastic uncertainty, and irreducible uncertainty.

Many analyses use probability to represent both aleatory uncertainty and epistemic uncertainty. The mathematics of probability is the same for both uncertainty representations; however, the concepts being represented are very different. The distinction between aleatory uncertainty and epistemic uncertainty is already present in the formal development of probability that began in the late sixteen hundreds. The distinction between aleatory uncertainty and epistemic uncertainty is fundamental to the design, implementation and interpretation of analyses for many complex systems.

If an analysis incorporates the effects of aleatory uncertainty, then underlying the analysis there must be

a probability space ($\mathcal{A}$, $\mathbb{A}$, p_A) for aleatory uncertainty. Each element $\mathbf{a}$ of $\mathcal{A}$ is a vector

$$\mathbf{a} = [a_1, a_2, \ldots] \tag{11.22}$$

that characterizes one possible state of the system. For example, if the failures in a population of devices over a specified time interval [u, v] are under consideration, then $\mathbf{a}$ might have the form

$$\mathbf{a} = [n, t_1, t_2, \ldots, t_n], \tag{11.23}$$

where

n = number of failed devices in time interval [u, v],
t_i = time of failure i with $u \le t_1 \le t_2 \le \ldots \le t_n \le v$.

A step up in complexity is for $\mathbf{a}$ to have the form

$$\mathbf{a} = [n, t_1, \mathbf{p}_1, t_2, \mathbf{p}_2, \ldots, t_n, \mathbf{p}_n], \tag{11.24}$$

where each $\mathbf{p}_i$ is a vector of random properties associated with the failure at time t_i. In an actual analysis for a real system, the definition of $\mathbf{a}$, and hence the associated probability space ($\mathcal{A}$, $\mathbb{A}$, p_A), can be very complicated. Notional analyses involving aleatory uncertainty are presented in Sects. 3.6, 5 and 10, and three analyses for real systems involving aleatory uncertainty are presented in Sect. 6.

Similarly to the probability space ($\mathcal{EM}$, $\mathbb{EM}$, p_{EM}) for epistemic uncertainty, the probability space ($\mathcal{A}$, $\mathbb{A}$, p_A) for aleatory uncertainty is usually defined by specifying conditions that define distributions for the elements of $\mathbf{a}$. For example, the probability space associated with vectors $\mathbf{a}$ of the form indicated in Eq. (11.23) might be arrived at through the assumption that device failures are consistent with a Poisson process defined by a rate λ (yr^{-1}). Further, the probability space associated with vectors $\mathbf{a}$ of the form indicated in Eq. (11.24) might be arrived at through the assumption again that device failures are consistent with a Poisson process defined by a rate λ and the additional specification of a joint probability distribution for the elements of the property vector $\mathbf{p}$ conditional on the occurrence of a failure at a specific time t.

In practice, the probability space ($\mathcal{A}$, $\mathbb{A}$, p_A) for aleatory uncertainty is unlikely to be precisely known. Specifically, many of the quantities employed in the definition of ($\mathcal{A}$, $\mathbb{A}$, p_A) are likely to be uncertain in an epistemic sense. For example, the occurrence of a certain type of event might be assumed to follow a Poisson process with a rate λ that is imprecisely known. This lack of knowledge about λ is epistemic uncertainty and leads to uncertainty with respect to the appropriate values for probabilities that derive from λ. The very important point being made here is that there can be, and usually is, epistemic uncertainty present in the characterization of quantities used in the definition of the probability space ($\mathcal{A}$, $\mathbb{A}$, p_A) for aleatory uncertainty. For notational purposes, these quantities can be represented by a vector $\mathbf{e}_A$ in analogy to the vectors $\mathbf{e}_R$ and $\mathbf{e}_P$ introduced in conjunction with Eq. (11.16). With the introduction of $\mathbf{e}_A$, there is now a probability space ($\mathcal{EA}$, $\mathbb{EA}$, p_{EA}) that characterizes the uncertainty in $\mathbf{e}_A$ and is developed in a manner to similar to that previously described for the probability space ($\mathcal{EM}$, $\mathbb{EM}$, p_{EM}) associated with $\mathbf{e}_M$. For notational convenience, the effects of $\mathbf{e}_A$ on ($\mathcal{A}$, $\mathbb{A}$, p_A) can be indicated by representing the density function associated with ($\mathcal{A}$, $\mathbb{A}$, p_A) by $d_A(\mathbf{a}|\mathbf{e}_A)$. In general, $\mathbf{e}_A$ can affect the definition of the sample space $\mathcal{A}$ but, for notational simplicity, this potential effect is typically not indicated

The vector of epistemically uncertain analysis inputs now has the form

$$\mathbf{e} = [\mathbf{e}_A, \mathbf{e}_R, \mathbf{e}_P] = [\mathbf{e}_A, \mathbf{e}_M], \tag{11.25}$$

and the corresponding probability space ($\mathcal{E}$, $\mathbb{E}$, p_E) derives from the properties of the probability spaces ($\mathcal{EA}$, $\mathbb{EA}$, p_{EA}) and ($\mathcal{EM}$, $\mathbb{EM}$, p_{EM}).

The consideration of the uncertainty in margins is now returned to. In concept, each possible realization $\mathbf{a}$ of aleatory uncertainty could lead to a different performance of the system under consideration. Notationally, this performance can be represented by a vector

$$\mathbf{P}_A(\mathbf{a}|\mathbf{e}_P) = [P_{A1}(\mathbf{a}|\mathbf{e}_P), P_{A2}(\mathbf{a}|\mathbf{e}_P), \ldots, P_{A,nO}(\mathbf{a}|\mathbf{e}_P)], \tag{11.26}$$

where $P_{Aj}(\mathbf{a}|\mathbf{e}_P)$, j = 1, 2, …, nO, are outcomes of an analysis given realization $\mathbf{a}$ of aleatory uncertainty (i.e., $\mathbf{a} \in \mathcal{A}$) and conditional on realization $\mathbf{e}_P$ of epistemic uncertainty (i.e., $\mathbf{e} = [\mathbf{e}_A, \mathbf{e}_R, \mathbf{e}_P] \in \mathcal{E}$). As an example from reactor risk assessment, $P_{A1}(\mathbf{a}|\mathbf{e}_P)$ could be the number of early fatalities, $P_{A2}(\mathbf{a}|\mathbf{e}_P)$ could be the number of latent cancer fatalities, and $P_{A3}(\mathbf{a}|\mathbf{e}_P)$ could be the economic cost for a reactor accident with properties defined by the vector $\mathbf{a}$ and conditional on the values for the epistemically uncertain analysis inputs contained in $\mathbf{e}_P$. In the examples of Sects. 6.1 and 6.2, nO equals 5 and 2, respectively.

In practice, performance measures used in comparisons with requirements are likely to be based on the distributions for the individual elements $P_{Aj}(\mathbf{a}|\mathbf{e}_P)$ of $\mathbf{P}_A(\mathbf{a}|\mathbf{e}_P)$ that derive from aleatory uncertainty. In this situation, the performance measures used in comparisons with requirements are defined by a functional relationship of the form

$$\begin{aligned}&\mathbf{P}\left[\mathbf{P}_A\left(\mathbf{a}|\mathbf{e}_P\right)\middle|\mathbf{e}_A\right]\\&\quad=\left[P_1\left(\mathbf{e}_P,\mathbf{e}_A\right),P_2\left(\mathbf{e}_P,\mathbf{e}_A\right),\ldots,\mathbf{P}_{nR}\left(\mathbf{e}_P,\mathbf{e}_A\right)\right],\end{aligned}\tag{11.27}$$

where the conditionality on $\mathbf{e}_A$ in $\mathbf{P}[\mathbf{P}_A(\mathbf{a}|\mathbf{e}_P)|\mathbf{e}_A]$ (i.e., "$|\mathbf{e}_A$") indicates that operations on the elements $P_{Aj}(\mathbf{a}|\mathbf{e}_P)$, j = 1, 2, …, nO, of $P_A(\mathbf{a}|\mathbf{e}_P)$ to obtain the elements $P_j(\mathbf{e}_P,\mathbf{e}_A)$, j = 1, 2, …, nR, of $\mathbf{P}[\mathbf{P}_A(\mathbf{a}|\mathbf{e}_P)|\mathbf{e}_A]$ are conditional on the probability space ($\mathcal{A}$, $\mathbb{A}$, p_A) associated with $\mathbf{e}_A$.

Three examples of possible definitions for $P_j(\mathbf{e}_P, \mathbf{e}_A)$ follow. First, $P_j(\mathbf{e}_P, \mathbf{e}_A)$ might be the expected value for $P_{Aj}(\mathbf{a}|\mathbf{e}_P)$ associated with the probability space ($\mathcal{A}$, $\mathbb{A}$, p_A) that derives from $\mathbf{e}_A$. In this case,

$$P_j\left(\mathbf{e}_P,\mathbf{e}_A\right)=\int_{\mathcal{A}}P_{Aj}\left(\mathbf{a}|\mathbf{e}_P\right)d_A\left(\mathbf{a}|\mathbf{e}_A\right)\mathrm{d}A.\tag{11.28}$$

Second, $P_j(\mathbf{e}_P, \mathbf{e}_A)$ might be the q quantile (e.g., q = 0.05, 0.5, 0.95) of the distribution of $P_{Aj}(\mathbf{a}|\mathbf{e}_P)$ associated with the probability space ($\mathcal{A}$, $\mathbb{A}$, p_A) that derives from $\mathbf{e}_A$. In this case, $P_j(\mathbf{e}_P, \mathbf{e}_A)$ is the value of P such that

$$q=\int_{\mathcal{A}}\underline{\delta}_P\left[P_{Aj}\left(\mathbf{a}|\mathbf{e}_P\right)\right]d_A\left(\mathbf{a}|\mathbf{e}_A\right)\mathrm{d}A.\tag{11.29}$$

Third, $P_j(\mathbf{e}_P, \mathbf{e}_A)$ might be the CCDF for $P_{Aj}(\mathbf{a}|\mathbf{e}_P)$ that derives from the probability space ($\mathcal{A}$, $\mathbb{A}$, p_A) associated with $\mathbf{e}_A$. In this case, $P_j(\mathbf{e}_P, \mathbf{e}_A)$ is a function defined by the points

$$\left[P,\int_{\mathcal{A}}\bar{\delta}_P\left[P_{Aj}\left(\mathbf{a}|\mathbf{e}_P\right)\right]d_A\left(\mathbf{a}|\mathbf{e}_A\right)\mathrm{d}A\right],\tag{11.30}$$

with problem specific knowledge used to limit the range of P. The expressions in Eqs. (11.28) – (11.30) may seem complicated, but expressions of this type are routinely approximated in risk assessments for complex systems (e.g., see analyses in Sect. 6). In practice, the definitions of the elements $P_j(\mathbf{e}_P, \mathbf{e}_A)$ of $\mathbf{P}[\mathbf{P}_A(\mathbf{a}|\mathbf{e}_P)|\mathbf{e}_A]$ could be more or less complex than indicated in Eqs. (11.28) – (11.30).

The determination of uncertainty in margins is now returned to. Once the determination $\mathbf{P}[\mathbf{P}_A(\mathbf{a}|\mathbf{e}_P)|\mathbf{e}_A]$ is completed, the determination and representation of the uncertainty in margins is the same as previously discussed in conjunction with Eqs. (11.13) – (11.16). Specifically, margin is defined by a function $M(\mathbf{R}, \mathbf{P}|\mathbf{e})$, which now has the form

$$\begin{aligned}M\left(\mathbf{R},\mathbf{P}|\mathbf{e}\right)&=M\left\{\mathbf{R}\left(\mathbf{e}_R\right),\mathbf{P}\left[\mathbf{P}_A\left(\mathbf{a}|\mathbf{e}_P\right)\middle|\mathbf{e}_A\right]\right\},\\\mathbf{e}&=\left[\mathbf{e}_A,\mathbf{e}_R,\mathbf{e}_P\right],\end{aligned}\tag{11.31}$$

when stated in complete generality. In turn, the uncertainty in the margin $M(\mathbf{R}, \mathbf{P}|\mathbf{e})$ is defined as indicated in Eqs. (11.18) and (11.19) and, in practice, is usually approximated as indicated in Eqs. (11.20) and (11.21). Examples of the uncertainty in margin results that derive from aleatory uncertainty are presented in Sects. 5 and 10 for notional analyses and in Sect. 6 for three real analyses.

As noted in conjunction with Eqs. (11.7) – (11.11), the meaning and analysis of margin is more complex when $M(\mathbf{R}, \mathbf{P}|\mathbf{e})$ is a vector rather than a scalar. Also, it is anticipated that $\mathbf{e}_R$ will not be present in most analyses.

11.3 Quantification in QMU

Quantification in the context of QMU is now considered. Such quantification has two distinct and important parts. The first part is the definition of the mathematical components that underlie QMU in a particular analysis. The second part is the actual performance of the necessary calculations with these components to obtain a numerical representation for the uncertainty associated with the margin or margins of interest. Two cases are considered: (i) Analyses involving only epistemic uncertainty, and (ii) Analyses involving both aleatory and epistemic uncertainty.

Case 1. The case involving only epistemic uncertainty is considered first. For full generality, the vectors $\mathbf{e}_R$ and $\mathbf{e}_P$ of epistemically uncertain quantities are assumed to be present in the analysis under consideration, although this may not be the case for a specific analysis. In particular, $\mathbf{e}_R$ is likely to be absent from many analyses, with the result that requirements placed on the system would be characterized by a single vector $\mathbf{R}$ rather than by a vector function $\mathbf{R}(\mathbf{e}_R)$.

For this case, the first part of the quantification process entails the definition (i.e., mathematical characterization) of four analysis components: (i) a function $\mathbf{R}(\mathbf{e}_R)$ that defines the requirements that are to be met

conditional on realization $\mathbf{e}_R$ of epistemic uncertainty, (ii) a function $\mathbf{P}(\mathbf{e}_P)$ that defines system performance conditional on realization $\mathbf{e}_P$ of epistemic uncertainty, (iii) a probability space ($\mathcal{EM}$, $\mathbb{EM}$, p_{EM}) that characterizes the epistemic uncertainty associated with $\mathbf{e}_M = [\mathbf{e}_R, \mathbf{e}_P]$, and (iv) a function $M(\mathbf{R}, \mathbf{P}|\mathbf{e}) = M[\mathbf{R}(\mathbf{e}_R), \mathbf{P}(\mathbf{e}_P)]$ that defines the margin associated with $\mathbf{R}(\mathbf{e}_R)$ and $\mathbf{P}(\mathbf{e}_P)$. In many analyses, $\mathbf{R}(\mathbf{e}_R)$ and $\mathbf{P}(\mathbf{e}_P)$ may be one dimensional (i.e., scalars); ($\mathcal{EM}$, $\mathbb{EM}$, p_{EM}) will probably be defined by specifying distributions for the individual elements of $\mathbf{e}_M$; and $\mathbf{P}(\mathbf{e}_P)$ is likely to be a complex mathematical structure (e.g., a system of nonlinear partial differential equations) that requires a sophisticated computer program for evaluation. If the preceding quantities are not clearly defined, then the analysis is inadequately documented and, as a consequence, it is difficult to know what any QMU results obtained from the analysis really mean.

The second part of quantification in this case involves carrying out the calculations required to obtain an approximation to the distribution of $M[\mathbf{R}(\mathbf{e}_R), \mathbf{P}(\mathbf{e}_P)]$ that results from the epistemic uncertainty associated with $\mathbf{e}_M = [\mathbf{e}_R, \mathbf{e}_P]$ and characterized by the probability space ($\mathcal{EM}$, $\mathbb{EM}$, p_{EM}). For most analyses, it is anticipated that a sampling-based approach of the form indicated in conjunction with Eqs. (11.18) – (11.21) will be used to numerically approximate the distribution that characterizes the uncertainty in the margin $M(\mathbf{R}, \mathbf{P}|\mathbf{e}) = M[\mathbf{R}(\mathbf{e}_R), \mathbf{P}(\mathbf{e}_P)]$. The major computational cost in this quantification will most likely be the numerical evaluation of $\mathbf{P}(\mathbf{e}_{Pi})$ in the sums indicated in Eqs. (11.20) and (11.21) as the evaluation of $\mathbf{R}(\mathbf{e}_{Ri})$ and $M[\mathbf{R}(\mathbf{e}_{Ri}), \mathbf{P}(\mathbf{e}_{Pi})]$ are unlikely to be numerically demanding. However, it is important to recognize that human cost rather than computational cost will dominate the cost of most analyses.

Case 2. The case involving both aleatory uncertainty and epistemic uncertainty is now considered. For full generality, the vectors $\mathbf{e}_A$, $\mathbf{e}_R$, and $\mathbf{e}_P$ of epistemically uncertain quantities are assumed to be present in the analysis under consideration, although this may not be the situation for a specific analysis. As for Case 1, $\mathbf{e}_R$ is likely to be absent from many analyses, with the result that the requirements placed on the system would be characterized by a single vector $\mathbf{R}$ rather than by a vector function $\mathbf{R}(\mathbf{e}_R)$.

For this case, the first part of the quantification process entails the definition (i.e., mathematical characterization) of six analysis components: (i) a function $\mathbf{R}(\mathbf{e}_R)$ that defines the requirements that are to be met conditional on realization $\mathbf{e}_R$ of epistemic uncertainty, (ii) a function $\mathbf{P}_A(\mathbf{a}|\mathbf{e}_P)$ the defines system performance given realization $\mathbf{a}$ of aleatory uncertainty and conditional on realization $\mathbf{e}_P$ of epistemic uncertainty (see Eq. (11.26)), (iii) a probability space ($\mathcal{A}$, $\mathbb{A}$, p_A) that characterizes aleatory uncertainty conditional on realization $\mathbf{e}_A$ of epistemic uncertainty (see Eqs. (11.22) – (11.24)), (iv) a probability space ($\mathcal{E}$, $\mathbb{E}$, p_E) that characterizes the epistemic uncertainty associated with $\mathbf{e} = [\mathbf{e}_A, \mathbf{e}_R, \mathbf{e}_P]$ (see Eq. (11.25)), (v) a function $\mathbf{P}[\mathbf{P}_A(\mathbf{a}|\mathbf{e}_P)|\mathbf{e}_A]$ that determines summary measures of system behavior that derive from aleatory uncertainty for comparison with the requirements contained in $\mathbf{R}(\mathbf{e}_R)$ conditional on realizations $\mathbf{e}_P$ and $\mathbf{e}_A$ of epistemic uncertainty (see Eqs. (11.27) – (11.30)), and (vi) a function $M\{\mathbf{R}(\mathbf{e}_R), \mathbf{P}[\mathbf{P}_A(\mathbf{a}|\mathbf{e}_P)\,|\,\mathbf{e}_A]\}$ that defines a margin based on requirement $\mathbf{R}(\mathbf{e}_R)$ and performance $\mathbf{P}[\mathbf{P}_A(\mathbf{a}|\mathbf{e}_P)|\mathbf{e}_A]$ conditional on realization $\mathbf{e} = [\mathbf{e}_A, \mathbf{e}_R, \mathbf{e}_P]$ of epistemic uncertainty (see Eq. (11.31)).

The second part of quantification for Case 2 involves carrying out the calculations required to obtain an approximation to the distribution of $M(\mathbf{R}, \mathbf{P}|\mathbf{e}) = M\{\mathbf{R}(\mathbf{e}_R), \mathbf{P}[\mathbf{P}_A(\mathbf{a}|\mathbf{e}_P)|\mathbf{e}_A]\}$ that results from the epistemic uncertainty associated with $\mathbf{e} = [\mathbf{e}_A, \mathbf{e}_R, \mathbf{e}_P]$ and characterized by the probability space ($\mathcal{E}$, $\mathbb{E}$, p_E). As for Case 1, it is anticipated that most analyses will use a sampling-based approach of the form indicated in conjunction with Eqs. (11.18) – (11.21) to numerically approximate the distribution that characterizes the uncertainty in the margin $M(\mathbf{R}, \mathbf{P}|\mathbf{e})$. Interior to this calculation for a given sample element $\mathbf{e}_i = [\mathbf{e}_{Ai}, \mathbf{e}_{Ri}, \mathbf{e}_{Pi}]$ of the form indicated in conjunction with Eqs. (11.20) and (11.21), it is necessary to estimate (i) $\mathbf{R}(\mathbf{e}_{Ri})$, (ii) $\mathbf{P}[\mathbf{P}_A(\mathbf{a}|\mathbf{e}_{Pi})|\mathbf{e}_{Ai}]$ and (iii) $M\{\mathbf{R}(\mathbf{e}_{Ri}), \mathbf{P}[\mathbf{P}_A(\mathbf{a}|\mathbf{e}_{Pi})|\mathbf{e}_{Ai}]\}$. The estimation or, most likely, exact determination of the quantities in (i) and (iii) is anticipated to be straightforward in most analyses. In contrast, the determination of $\mathbf{P}[\mathbf{P}_A(\mathbf{a}|\mathbf{e}_{Pi})|\mathbf{e}_{Ai}]$ could be a major computational challenge. This challenge exists because the determination of $\mathbf{P}[\mathbf{P}_A(\mathbf{a}|\mathbf{e}_{Pi})|\mathbf{e}_{Ai}]$ must be preceded by an estimation of the distribution of $\mathbf{P}_A(\mathbf{a}|\mathbf{e}_{Pi})$ conditional on the probability space ($\mathcal{A}$, $\mathbb{A}$, p_A) for aleatory uncertainty associated with $\mathbf{e}_{Ai}$. In most large analyses, the major computational complexity and cost is associated with the determination of the distribution of $\mathbf{P}_A(\mathbf{a}|\mathbf{e}_{Pi})$ for each pair $[\mathbf{e}_{Ai}, \mathbf{e}_{Pi}]$ of sampled values for $\mathbf{e}_P$ and $\mathbf{e}_A$. In many large analyses (e.g., probabilistic risk assessments for nuclear power plants; see Sect. 6.1), extensive use is made of fault trees and event trees in this determination. In addition, extensive modeling of physical processes is usually required.

As is the case for the example analyses in Sect. 6, a great deal of careful planning and computational or-

ganization is required to successfully carry out an analysis for a complex system that involves a separation of aleatory and epistemic uncertainty. However, without this separation, the results of the analysis are likely to provide limited and possibly misleading insights into the potential behavior of the system and extent of our knowledge with respect to this behavior.

11.4 Presentation of QMU Results

Excessive simplification in the presentation of QMU results should be avoided. For analyses that involve only epistemic uncertainty, the best presentation format is provided by cumulative or complementary cumulative summaries of the uncertainty in analysis results of interest (i.e., by CDFs or CCDFs if probability is used to characterize epistemic uncertainty) with a vertical line used to indicate the specified requirement on system performance (e.g., see Fig. 4.1 and more generally Fig. 9.2). Specifically, cumulative summaries are appropriate when system performance has a specified lower bound (Figs. 4.1a and 9.2a), and complementary cumulative summaries are appropriate when system performance has a specified upper bound (Figs. 4.1b and 9.2b). This presentation format clearly shows the actual values for the performance measure of interest, the uncertainty in this measure, the specified bound on this measure, and the implications of uncertainty with respect to compliance with the specified bound.

A less informative presentation is provided by a cumulative summary of the uncertainty in the margin for the system performance measure and associated requirement under consideration (e.g., see Figs. 4.2 and 9.3). Cumulative summaries are appropriate for margins because small margins and, in particular, negative margins are undesirable. Margin summaries (Figs. 4.2 and 9.3) are less informative than performance summaries (Figs. 4.1 and 9.2) because they obscure the actual value of the performance measure and the relationship of this measure to its associated requirement. Of course, given the numerical value of the requirement, it is mathematically possible to convert from margin values to the values for the performance measure. However, this is not as easy as simply directly looking at the summary of the actual values for the performance measure and its associated requirement as illustrated in Figs. 4.1 and 9.2. If it is desired to show margin results as illustrated in Figs. 4.2 and 9.3, it is recommended that actual performance results as illustrated in Figs. 4.1 and 9.2 also be shown as this will help the reader recognize the nature of the performance results that give rise to the presented margins.

When margins arise from complex requirements (e.g., upper and lower bounds on performance over a time interval as illustrated in Sects. 4.3 and 9.5), the display of the actual performance is more complex than simply showing a cumulative or complementary cumulative summary for a single result. However, some way of showing the actual performance of the system should be sought. For the example system and associated requirements in Sects. 4.3 and 9.5, this is accomplished by displaying the time-dependent behavior of the system with associated the required bounds on this behavior (Fig. 4.9) in addition to cumulative margin results (Figs. 4.10 and 9.8). In general, the exact form of such displays will be analysis specific.

The statement is often made that the final outcome of a QMU analysis should be a summary measure of the form “margin/uncertainty”. For purposes of illustration, summary measures of this form are extensively presented in Sects. 4, 5 and 6. However, these “margin/uncertainty” results provide a very poor representation of the outcome of a QMU analysis as too much meaningful information is lost when the results of a complex analysis are reduced to a single number. After all, the fundamental motivation for performing an uncertainty analysis derives from the recognition that it is not possible to use a single number to represent the existing knowledge about the behavior of the system. For example, the “margin/uncertainty” results in Eqs. (4.42) and (4.43) do not adequately capture the more detailed results in Figs. 4.9 and 4.10 that they are derived from and are intended to summarize. This same pattern of lost information with “margin/uncertainty” summaries for QMU analyses is repeated for all examples presented in Sects. 4, 5 and 6. Bluntly put, “margin/uncertainty” results do not contain enough information to provide a basis for appropriately informed decisions (see Sect. 4.5 for additional discussion).

For analyses that involve aleatory and epistemic uncertainty, presentations of analysis results should include displays that clearly show the separate effects of aleatory uncertainty and epistemic uncertainty. As an example, the analyses presented in Sects. 5.1 and 10.3 involve aleatory and epistemic uncertainty, with (i) the the effects of aleatory uncertainty conditional on specific realizations of epistemic uncertainty shown in Fig. 5.1a, (ii) the effects of epistemic uncertainty on the performance quantity of interest shown in Figs. 5.1b and 10.2, and (iii) the effects of epistemic uncertainty on margin shown in Figs. 5.2 and 10.3. This presentation format provides a more informative transfer of information than the “margin/uncertainty” results shown in Eqs. (5.11) – (5.14) and intended to summarize the informa-

tion contained in Figs. 5.1a and 5.1b. For complex analyses involving aleatory and epistemic uncertainty of the form illustrated in Sect. 6, single "margin/uncertainty" summaries simply cannot capture the information provided by the analysis about system behavior and the uncertainty present in our ability to predict this behavior.

In addition to uncertainty results, a QMU analysis should also present sensitivity analysis results (Sect. 7). Such results play a fundamental role in analyses of complex systems by providing (i) insights on system behavior, (ii) guidance on how to invest resources to reduce uncertainty in the assessment of system behavior, and (iii) a powerful tool for analysis verification. An uncertainty analysis without an associated sensitivity analysis is incomplete.

A fundamental part of the presentation of any QMU analysis should be quality documentation. Unfortunately, many large analyses are not well documented. This is probably due in part to a tendency to underestimate the time and resources required to produce quality documentation for a large analysis. The reality is that it can never be expected that everyone will agree with the manner in which a large analysis is conducted and consequently with the results of that analysis. However, everyone should be able to know exactly what was assumed and done in the analysis. The indicated knowledge can only result through quality documentation.

12 References

1. Goodwin BT, Juzaitus RJ. *National Certification Methdology for the Nuclear Weapon Stockpile*. Draft working paper. 2003.

2. Sharp DH, Wood-Schultz MM. QMU and Nuclear Weapons Certification: What's Under the Hood? *Los Alamos Science* 2003; 28:47-53.

3. Abeyta H, et-al. *Report on the Friendly Reviews of QMU at the NNSA Laboratories*. Defense Programs Science Council 2004.

4. Sharp DH, Wallstrom TC, Wood-Schultz MM. *Physics Package Confidence: "One" vs. "1.0"*. LA-UR-04-0496. Los Alamos, NM: Los Alamos National Laboratory 2004.

5. JASON. *Quantifications of Margins and Uncertainties (QMU)*. JSR-04-3330. McLean, VA: The Mitre Corporation 2005.

6. U.S. GAO (U.S. Government Accountability Office). *Nuclear Weapons: NNSA Needs to Refine and More Effectively Manage Its New Approach for Assessing and Certifying Nuclear Weapons*. GAO-06-261. Washington, DC: U.S. Government Accountability Office 2006.

7. NNSA (National Nuclear Security Administration). *Nuclear Weapon Assessments Using Quantification of Margins and Uncertainties Methodologies*. NNSA Policy Letter: NAP-XX, Draft 5/1/07. Washington, DC: National Nuclear Security Administration 2007.

8. Rechard RP. Historical Relationship Between Performance Assessment for Radioactive Waste Disposal and Other Types of Risk Assessment. *Risk Analysis* 1999; 19(5):763-807.

9. U.S. NRC (U.S. Nuclear Regulatory Commission). *Reactor Safety Study—An Assessment of Accident Risks in U.S. Commercial Nuclear Power Plants*. WASH-1400 (NUREG-75/014). Washington, DC: U.S. Nuclear Regulatory Commission 1975.

10. U.S. NRC (U.S. Nuclear Regulatory Commission). *Severe Accident Risks: An Assessment for Five U.S. Nuclear Power Plants*. NUREG-1150, Vols. 1-3. Washington, DC: U.S. Nuclear Regulatory Commission, Office of Nuclear Regulatory Research, Division of Systems Research 1990-1991.

11. Breeding RJ, Helton JC, Gorham ED, Harper FT. Summary Description of the Methods Used in the Probabilistic Risk Assessments for NUREG-1150. *Nuclear Engineering and Design* 1992; 135(1):1-27.

12. Boyack BE, Catton I, Duffey RB, Griffith P, Katsma KR, Lellouche GS, Levy S, Rohatgi US, Wilson GE, Wulff W, Zuber N. Quantifying Reactor Safety Margins, Part 1: An Overview of the Code Scaling, Applicability, and Uncertainty Evaluation Methodology. *Nuclear Engineering and Design* 1990; 119(1):1-15.

13. Boyack BE, Catton I, Duffey RB, Griffith P, Katsma KR, Lellouche GS, levy PS, Rohatgi US, Wulff W, Zuber N. Quantifying Reactor Safety Margins, Part 2: Characterization of Important Contributors to Uncertainty. *Nuclear Engineering and Design* 1990; 119(1):17-31.

14. Wulff W, Boyack BE, Catton I, Duffey RB, Griffith P, Katsma KR, Lellouche GS, Levy PS, Rohatgi US, Wilson GE, Zuber N. Quantifying Reactor Safety Margins, Part 3: Assessment and Ranging of Parameters. *Nuclear Engineering and Design* 1990; 119(1):33-65.

15. Lellouche GS, Levy PS, Boyack BE, Catton I, Duffey RB, Griffith P, Katsma KR, May R, Rohatgi US, Wilson C, Wulff W, Zuber N. Quantifying Reactor Safety Margins, Part 4: Uncertainty Evaluation of LBLOCA Analysis Based on TRAC-PF1/MOD 1. *Nuclear Engineering and Design* 1990; 119(1):67-95.

16. Zuber N, Wilson GE, Boyack BE, Catton I, Duffey RB, Griffith P, Katsma KR, Lellouche GS, Levy S, Rohatgi US, Wulff W. Quantifying Reactor Safety Margins, Part 5: Evaluation of Scale-Up Capabilities of Best Estimate Codes. *Nuclear Engineering and Design* 1990; 119(1):97-107.

17. Catton I, Duffey RB, Shaw RA, Boyack BE, Griffith P, Katsma KR, Lellouche GS, Levy S, Rohatgi US, Wilson GE, Wulff W, Zuber N. Quantifying Reactor Safety Margins, Part 6: A Physically Based Method of Estimating PWR Large Break Loss of Coolant Accident PCT. *Nuclear Engineering and Design* 1990; 119(1):109-117.

18. Theofanous TG, et al. Discussion on Quantifying Reactor Safety Margins. *Nuclear Engineering and Design* 1992; 132:403-447.

19. Payne AC, Jr. *Analysis of the LaSalle Unit 2 Nuclear Power Plant: Risk Methods Integration and Evaluation Program (RMIEP). Summary*. NUREG/CR-4832, SAND92-0537. Albuquerque: Sandia National Laboratories 1992.

20. U.S. DOE (U.S. Department of Energy). *Title 40 CFR Part 191 Compliance Certification Application for the Waste Isolation Pilot Plant*. DOE/CAO-1996-2184, Vols. I-XXI. Carlsbad, NM: U.S. Department of Energy, Carlsbad Area Office, Waste Isolation Pilot Plant 1996.

21. Helton JC, Marietta MG. Special Issue: The 1996 Performance Assessment for the Waste Isolation Pilot Plant. *Reliability Engineering and System Safety* 2000; 69(1-3):1-451.

22. SNL (Sandia National Laboratories). *Total System Performance Assessment Model/Analysis for the License Application*. MDL-WIS-PA-000005 Rev 00, AD 01. Las Vegas, NV: U.S. Department of Energy Office of Civilian Radioactive Waste Management 2008.

23. Lewis HW, Budnitz RJ, Kouts HJC, Loewenstein WB, W.D. Rowe, von Hippel F, Zachariasen F. *Risk Assessment Review Group Report to the U.S. Nuclear Regulatory Commission*. NUREG/CR-0400. Washington, D.C.: U.S. Nuclear Regulatory Commission 1978.

24. Iman RL, Conover WJ, Campbell JE. *Risk Methodology for Geologic Disposal of Radioactive Waste: Small Sample Sensitivity Analysis Techniques for Computer Models, with an Application to Risk Assessment*. SAND80-0020, NUREG-CR-1397. Albuquerque, NM: Sandia National Laboratories 1980.

25. Iman RL, Helton JC, Campbell JE. *Risk Methodology for Geologic Disposal of Radioactive Waste: Sensitivity Analysis Techniques*. SAND78-0912, NUREG/CR-0390. Albuquerque, NM: Sandia National Laboratories 1978.

26. Cranwell RM, Campbell JE, Helton JC, Iman RL, Longsine DE, Ortiz NR, Runkle GE, Shortencarier MJ. *Risk Methodology for Geologic Disposal of Radioactive Waste: Final Report*. SAND81-2573, NUREG/CR-2452. Albuquerque, NM: Sandia National Laboratories 1987.

27. Sprung JL, Aldrich DC, Alpert DJ, Cunningham MA, Weigand GG. Overview of the MELCOR Risk Code Development Program. In. *Proceedings of the International Meeting on Light Water Reactor Severe Accident Evaluation*. Cambridge, MA, August 28-September 1, 1983. Boston, MA: Stone and Webster Engineering Corporation, 1983:TS-10.11-11 to TS-10.11-18.

28. Iman RL, Helton JC. *A Comparison of Uncertainty and Sensitivity Analysis Techniques for Computer Models*. NUREG/CR-3904, SAND84-1461. Albuquerque, NM: Sandia National Laboratories 1985.

29. Iman RL. Uncertainty and Sensitivity Analysis for Computer Modeling Applications. In: TA Cruse, ed. *Reliability Technology - 1992, The Winter Annual Meeting of the American Society of Mechanical Engineers, Anaheim, California, November 8-13, 1992*. Vol. 28, New York, NY: American Society of Mechanical Engineers. Aerospace Division. Vol. 28, pp. 153-168. New York, NY: American Society of Mechanical Engineers, Aerospace Division, 1992.

30. Zio E. Reliability Engineering: Old Problems and New Challenges. *Reliability Engineering and System Safety* 2009; 94:125-141.

31. Bernstein PL. *Against the Gods: The Remarkable Story of Risk*. New York: John Wiley & Sons, 1996.

32. Cacuci DG. *Sensitivity and Uncertainty Analysis, Vol. 1: Theory*. Boca Raton, FL: Chapman and Hall/CRC Press, 2003.

33. Turányi T. Sensitivity Analysis of Complex Kinetic Systems. Tools and Applications. *Journal of Mathematical Chemistry* 1990; 5(3):203-248.

34. Rabitz H, Kramer M, Dacol D. Sensitivity Analysis in Chemical Kinetics. *Annual Review of Physical Chemistry* 1983; 34:419-461.

35. Lewins J, Becker M, eds. *Sensitivity and Uncertainty Analysis of Reactor Performance Parameters*. Vol. 14. New York, NY: Plenum Press, 1982.

36. Frank PM. *Introduction to System Sensitivity Theory*. New York, NY: Academic Press, 1978.

37. Tomovic R, Vukobratovic M. *General Sensitivity Theory*. New York, NY: Elsevier, 1972.

38. Myers RH. Response Surface Methodology - Current Status and Future Directions. *Journal of Quality Technology* 1999; 31(1):30-44.

39. Andres TH. Sampling Methods and Sensitivity Analysis for Large Parameter Sets. *Journal of Statistical Computation and Simulation* 1997; 57(1-4):77-110.

40. Kleijnen JPC. Sensitivity Analysis and Related Analyses: A Review of Some Statistical Techniques. *Journal of Statistical Computation and Simulation* 1997; 57(1-4):111-142.

41. Kleijnen JPC. Sensitivity Analysis of Simulation Experiments: Regression Analysis and Statistical Design. *Mathematics and Computers in Simulation* 1992; 34(3-4):297-315.

42. Morton RH. Response Surface Methodology. *Mathematical Scientist* 1983; 8:31-52.

43. Mead R, Pike DJ. A Review of Response Surface Methodology from a Biometric Viewpoint. *Biometrics* 1975; 31:803-851.

44. Myers RH. *Response Surface Methodology*. Boston, MA: Allyn and Bacon, 1971.

45. McKay MD, Beckman RJ, Conover WJ. A Comparison of Three Methods for Selecting Values of Input Variables in the Analysis of Output from a Computer Code. *Technometrics* 1979; 21(2):239-245.

46. Iman RL, Conover WJ. Small Sample Sensitivity Analysis Techniques for Computer Models, with an Application to Risk Assessment. *Communications in Statistics: Theory and Methods* 1980; A9(17):1749-1842.

47. Iman RL, Helton JC, Campbell JE. An Approach to Sensitivity Analysis of Computer Models, Part 1. Introduction, Input Variable Selection and Preliminary Variable Assessment. *Journal of Quality Technology* 1981; 13(3):174-183.

48. Iman RL, Helton JC, Campbell JE. An Approach to Sensitivity Analysis of Computer Models, Part 2. Ranking of Input Variables, Response Surface Validation, Distribution Effect and Technique Synopsis. *Journal of Quality Technology* 1981; 13(4):232-240.

49. Saltelli A, Marivoet J. Non-Parametric Statistics in Sensitivity Analysis for Model Output. A Comparison of Selected Techniques. *Reliability Engineering and System Safety* 1990; 28(2):229-253.

50. Saltelli A, Andres TH, Homma T. Sensitivity Analysis of Model Output. An Investigation of New Techniques. *Computational Statistics and Data Analysis* 1993; 15(2):445-460.

51. Blower SM, Dowlatabadi H. Sensitivity and Uncertainty Analysis of Complex Models of Disease Transmission: an HIV Model, as an Example. *International Statistical Review* 1994; 62(2):229-243.

52. Kleijnen JPC, Helton JC. Statistical Analyses of Scatterplots to Identify Important Factors in Large-Scale Simulations, 1: Review and Comparison of Techniques. *Reliability Engineering and System Safety* 1999; 65(2):147-185.

53. Helton JC, Davis FJ. Sampling-Based Methods. In: A. Saltelli, K. Chan, E.M. Scott, eds. *Sensitivity Analysis*. New York, NY: Wiley. pp. 101-153, 2000.

54. Helton JC, Davis FJ. Illustration of Sampling-Based Methods for Uncertainty and Sensitivity Analysis. *Risk Analysis* 2002; 22(3):591-622.

55. Helton JC, Davis FJ. Latin Hypercube Sampling and the Propagation of Uncertainty in Analyses of Complex Systems. *Reliability Engineering and System Safety* 2003; 81(1):23-69.

56. Helton JC, Johnson JD, Sallaberry CJ, Storlie CB. Survey of Sampling-Based Methods for Uncertainty and Sensitivity Analysis. *Reliability Engineering and System Safety* 2006; 91(10-11):1175-1209.

57. Li G, Rosenthal C, Rabitz H. High-Dimensional Model Representations. *The Journal of Physical Chemistry* 2001; 105(33):7765-7777.

58. Rabitz H, Alis OF. General Foundations of High-Dimensional Model Representations. *Journal of Mathematical Chemistry* 1999; 25(2-3):197-233.

59. Saltelli A, Tarantola S, Chan KP-S. A Quantitative Model-Independent Method for Global Sensitivity Analysis of Model Output. *Technometrics* 1999; 41(1):39-56.

60. Sobol' IM. Sensitivity Estimates for Nonlinear Mathematical Models. *Mathematical Modeling & Computational Experiment* 1993; 1(4):407-414.

61. Cukier RI, Levine HB, Shuler KE. Nonlinear Sensitivity Analysis of Multiparameter Model Systems. *Journal of Computational Physics* 1978; 26(1):1-42.

62. Iman RL, Helton JC. An Investigation of Uncertainty and Sensitivity Analysis Techniques for Computer Models. *Risk Analysis* 1988; 8(1):71-90.

63. Ronen Y. *Uncertainty Analysis.* Boca Raton, FL: CRC Press, Inc. 1988.

64. Helton JC. Uncertainty and Sensitivity Analysis Techniques for Use in Performance Assessment for Radioactive Waste Disposal. *Reliability Engineering and System Safety* 1993; 42(2-3):327-367.

65. Hamby DM. A Review of Techniques for Parameter Sensitivity Analysis of Environmental Models. *Environmental Monitoring and Assessment* 1994; 32(2):135-154.

66. Saltelli A, Chan K, E.M. Scott (eds). *Sensitivity Analysis*. New York, NY: Wiley, 2000.

67. Frey HC, Patil SR. Identification and Review of Sensitivity Analysis Methods. *Risk Analysis* 2002; 22(3):553-578.

68. Ionescu-Bujor M, Cacuci DG. A Comparative Review of Sensitivity and Uncertainty Analysis of Large-Scale Systems--I: Deterministic Methods. *Nuclear Science and Engineering* 2004; 147(3):189-2003.

69. Cacuci DG, Ionescu-Bujor M. A Comparative Review of Sensitivity and Uncertainty Analysis of Large-Scale Systems--II: Statistical Methods. *Nuclear Science and Engineering* 2004; 147(3):204-217.

70. Saltelli A, Ratto M, Tarantola S, Campolongo F. Sensitivity Analysis for Chemical Models. *Chemical Reviews* 2005; 105(7):2811-2828.

71. Saltelli A, Ratto M, Andres T, Campolongo F, Cariboni J, Gatelli D, Saisana M, Tarantolla S. *Global Sensitivity Analysis: The Primer*. New York, NY: Wiley, 2008.

72. Booker JN, Ross T, Hamada M, Reardon R, Dolin R, Faust CL, Najera L. Engineering Index: An Enginerring/Certification Metric. *Military Operations Research* 2006; 11(2):27-44.

73. Pilch M, Trucano TG, Helton JC. *Ideas Underlying the Quantification of Margins and Uncertainties (QMU): A White Paper*. SAND2006-5001. Albuqurque, NM: Sandia National Laboratories 2006.

74. Diegert K, Klenke S, Novotny G, Paulsen R, Pilch M, Trucano T. *Toward a More Rigorous Application of Margins and Uncertainties within the Nuclear Weapons Life Cycle - A Sandia Perspective*. SAND2007-6219. Albuquerque, NM: Sandia National Laboratories 2007.

75. Higdon DM, Anderson-Cook CM, Gattiker JR, Huzurbazar AP, Moore LM, Picard RR, Press WH, Williams BJ, Wallstom TC, Bornn LC, Nelson RA. *QMU for Advanced Certification: Identifying Existing Limitations with Discussion of Solution Strategies*. LA-UR-08-06887. Los Alamos, NM: Los Alamos National Laboratory 2008.

76. Wallstrom TC. *Quantification of Margins and Uncertainty: A Bayesian Approach*. LA-UR-08-4800. Los Alamos, NM: Los Alamos National Laboratory 2008.

77. NAS/NRC (National Academy of Science/National Research Council). *Evaluation of Quantification of Margins and Uncertainties for Assessing and Certifying the Reliability of the Nuclear Stockpile*. Washington, DC: National Academy Press, 2008.

78. Helton JC. Uncertainty and Sensitivity Analysis in the Presence of Stochastic and Subjective Uncertainty. *Journal of Statistical Computation and Simulation* 1997; 57(1-4):3-76.

79. Helton JC, Burmaster DE. Guest Editorial: Treatment of Aleatory and Epistemic Uncertainty in Performance Assessments for Complex Systems. *Reliability Engineering and System Safety* 1996; 54(2-3):91-94.

80. Paté-Cornell ME. Uncertainties in Risk Analysis: Six Levels of Treatment. *Reliability Engineering and System Safety* 1996; 54(2-3):95-111.

81. Winkler RL. Uncertainty in Probabilistic Risk Assessment. *Reliability Engineering and System Safety* 1996; 54(2-3):127-132.

82. Hofer E. When to Separate Uncertainties and When Not to Separate. *Reliability Engineering and System Safety* 1996; 54(2-3):113-118.

83. Parry GW, Winter PW. Characterization and Evaluation of Uncertainty in Probabilistic Risk Analysis. *Nuclear Safety* 1981; 22(1):28-42.

84. Helton JC. Probability, Conditional Probability and Complementary Cumulative Distribution Functions in Performance Assessment for Radioactive Waste Disposal. *Reliability Engineering and System Safety* 1996; 54(2-3):145-163.

85. Hoffman FO, Hammonds JS. Propagation of Uncertainty in Risk Assessments: The Need to Distinguish Between Uncertainty Due to Lack of Knowledge and Uncertainty Due to Variability. *Risk Analysis* 1994; 14(5):707-712.

86. Helton JC. Treatment of Uncertainty in Performance Assessments for Complex Systems. *Risk Analysis* 1994; 14(4):483-511.

87. Apostolakis G. The Concept of Probability in Safety Assessments of Technological Systems. *Science* 1990; 250(4986):1359-1364.

88. Haan CT. Parametric Uncertainty in Hydrologic Modeling. *Transactions of the ASAE* 1989; 32(1):137-146.

89. Kaplan S, Garrick BJ. On the Quantitative Definition of Risk. *Risk Analysis* 1981; 1(1):11-27.

90. Der Kiureghian A, Ditlevsen O. Aleatory or Epistemic? Does It Matter? *Structural Safety* 2009; 31:105-112.

91. Hacking I. *The Emergence of Probability: A Philosophical Study of Early Ideas About Probability, Induction and Statistical Inference*. London; New York: Cambridge University Press, 1975.

92. Shafer G. Non-Additive Probabilities in Work of Bernoulli and Lambert. *Archive for History of Exact Sciences* 1978; 19(4):309-370.

93. Feller W. *An Introduction to Probability Theory and Its Applications*, Vol. 2, 2nd edn. New York, NY: John Wiley & Sons, 1971.

94. Ash RB, Doléans-Dade CA. *Probability and Measure Theory*, 2nd edn. New York, NY: Harcourt/Academic Press, 2000.

95. Helton JC. Mathematical and Numerical Approaches in Performance Assessment for Radioactive Waste Disposal: Dealing with Uncertainty. In: EM Scott, ed. *Modelling Radioactivity in the Environment*. New York, NY: Elsevier Science, 2003:353-390.

96. Helton JC, Anderson DR, Jow H-N, Marietta MG, Basabilvazo G. Conceptual Structure of the 1996 Performance Assessment for the Waste Isolation Pilot Plant. *Reliability Engineering and System Safety* 2000; 69(1-3):151-165.

97. Hora SC, Iman RL. Expert Opinion in Risk Analysis: The NUREG-1150 Methodology. *Nuclear Science and Engineering* 1989; 102(4):323-331.

98. Thorne MC, Williams MMR. A Review of Expert Judgement Techniques with Reference to Nuclear Safety. *Progress in Nuclear Safety* 1992; 27(2-3):83-254.

99. Budnitz RJ, Apostolakis G, Boore DM, Cluff LS, Coppersmith KJ, Cornell CA, Morris PA. Use of Technical Expert Panels: Applications to Probabilistic Seismic Hazard Analysis. *Risk Analysis* 1998; 18(4):463-469.

100. McKay M, Meyer M. Critique of and Limitations on the Use of Expert Judgements in Accident Consequence Uncertainty Analysis. *Radiation Protection Dosimetry* 2000; 90(3):325-330.

101. Ayyub BM. *Elicitation of Expert Opinions for Uncertainty and Risks*. Boca Raton, FL: CRC Press 2001.

102. Cooke RM, Goossens LHJ. Expert Judgement Elicitation for Risk Assessment of Critical Infrastructures. *Journal of Risk Research* 2004; 7(6):643-656.

103. Garthwaite PH, Kadane JB, O'Hagan A. Statistical Methods for Eliciting Probability Distributions. *Journal of the American Statistical Association* 2005; 100(470):680-700.

104. American Institute of Aeronautics and Astronautics. *AIAA Guide for the Verification and Validation of Computational Fluid Dynamics Simulations*.

AIAA G-077-1998. Reston, VA: American Institute of Aeronautics and Astronautics 1998.

105. Roache PJ. *Verification and Validation in Computational Science and Engineering*. Albuquerque, NM: Hermosa Publishers, 1998.

106. Oberkampf WL, Trucano TG. Verification and Validation in Computational Fluid Dynamics. *Progress in Aerospace Sciences* 2002; 38(3):209-272.

107. Oberkampf WL, Trucano TG, Hirsch C. Verification, Validation, and Predictive Capability in Computational Engineering and Physics. *Applied Mechanics Review* 2004; 57(5):345-384.

108. Roache PJ. Building PDE Codes to be Verifiable and Validatable. *Computing in Science & Engineering* 2004; 6(5):30-38.

109. Babuska I, Oden JT. Verification and Validation in Computational Engineering and Science: Basic Concepts. *Computer Methods in Applied Mechanics and Engineering* 2004; 193(36-38):4057-4066.

110. Trucano TG, Swiler LP, Igusa T, Oberkampf WL, Pilch M. Calibration, Validation, and Sensitivity Analysis: What's What. *Reliability Engineering and System Safety* 2006; 91(10-11):1331-1357.

111. Storlie CB, Helton JC. Multiple Predictor Smoothing Methods for Sensitivity Analysis: Description of Techniques. *Reliability Engineering and System Safety* 2008; 93(1):28-54.

112. Storlie CB, Helton JC. Multiple Predictor Smoothing Methods for Sensitivity Analysis: Example Results. *Reliability Engineering and System Safety* 2008; 93(1):55-77.

113. U.S. NRC (U.S. Nuclear Regulatory Commission). *Implementation of Safety Goal Policy*. Letter from V. Stello to the Commissioners. Washington, D.C. 30 March 1989 1989.

114. U.S. NRC (U.S. Nuclear Regulatory Commission). Safety Goals for the Operation of Nuclear Power Plants: Policy Statement; Correction and Republication. *Federal Register* 1986; 51:30028–30033.

115. U.S. NRC (U.S. Nuclear Regulatory Commission). *Safety Goals for Nuclear Power Plant Operation*. NUREG-0880, Rev. 1. Washington, D.C. 1983.

116. U.S. NRC (U.S. Nuclear Regulatory Commission). *Safety Goals for Nuclear Power Plants: A Discussion Paper*. NUREG-0880. Washington, D.C. 1982.

117. Breeding RJ, Helton JC, Murfin WB, Smith LN. *Evaluation of Severe Accident Risks: Surry Unit 1*. NUREG/CR-4551, SAND86-1309, Vol. 3, Rev. 1. Albuquerque, NM: Sandia National Laboratories 1990.

118. Helton JC, Breeding RJ. Calculation of Reactor Accident Safety Goals. *Reliability Engineering and System Safety* 1993; 39(2):129-158.

119. Payne AC, Jr., Breeding RJ, Helton JC, Smith LN, Johnson JD, Jow H-N, Shiver AW. The NUREG-1150 Probabilistic Risk Assessment for the Peach Bottom Atomic Power Station. *Nuclear Engineering and Design* 1992; 135(1):61-94.

120. Gregory JJ, Breeding RJ, Helton JC, Murfin WB, Higgins SJ, Shiver AW. The NUREG-1150 Probabilistic Risk Assessment for the Sequoyah Nuclear Plant. *Nuclear Engineering and Design* 1992; 135(1):92-115.

121. Brown TD, Breeding RJ, Helton JC, Jow H-N, Higgins SJ, Shiver AW. The NUREG-1150 Probabilistic Risk Assessment for the Grand Gulf Nuclear Station. *Nuclear Engineering and Design* 1992; 135(1):117-137.

122. Brooks DG. Using Related Samples in Assessing Conformance to Safety Goals: A Nuclear Reactor Safety Application. *Risk Analysis* 1990; 10:229-237.

123. Niehaus F. Prospects for Use of Probabilistic Safety Criteria. *Nuclear Engineering and Design* 1989; 115:181-190.

124. Bier VM. The U.S. Nuclear Regulatory Commission Safety Goal Policy: A Critical Review. *Risk Analysis* 1988; 8:563-568.

125. Whipple C, Starr C. Nuclear Power Safety Goals in Light of the Chernobyl Accident. *Nuclear Safety* 1988; 29:20-28.

126. Cannell W. Probabilisitc Reliability Analysis, Quantitative Safety Goals, and Nuclear Licensing in the United Kingdom. *Risk Analysis* 1987; 7:311-319.

127. Okrent D. The Safety Goals of the U.S. Nuclear Regulatory Commission. *Science* 1987; 236:296-300.

128. Rathbun D, Modarres M. Development of Safety Goals for Nuclear Power Plants. *Nuclear Safety* 1987; 28:155-163.

129. Martz HF, Johnson JW. Assessing Compatibility with Reactor Safety Goals Using Uncertain Risk Analysis Results with Application to Core Melt. *Nuclear Safety* 1984; 25:305-316.

130. Kaplan S. Safety Goals and Related Questions. *Reliability Engineering* 1982; 3:267-277.

131. Griesmeyer JM, Okrent D. Risk Management and Decision Rules for Light Water Reactors. *Risk Analysis* 1981; 1:121-136.

132. Wall IB. Probabilistic Risk Assessment in Nuclear Power Plant Regulation. *Nuclear Engineering and Design* 1980; 60:11-24.

133. Ortiz NR, Wheeler TA, Breeding RJ, Hora S, Meyer MA, Keeney RL. Use of Expert Judgment in NUREG-1150. *Nuclear Engineering and Design* 1991; 126(3):313-331.

134. Harper FT, Breeding RJ, Brown TD, Gregory JJ, Payne AC, Gorham ED, Amos CN. *Evaluation of Severe Accident Risks: Quantification of Major Input Parameters, Expert Opinion Elicitation on In-Vessel Issues*. NUREG/CR-4551, SAND86-1309, Vol. 2, Part 1, Rev. 1. Albuquerque, NM: Sandia National Laboratories 1990.

135. Harper FT, Payne AC, Breeding RJ, Gorham ED, Brown TD, Rightley GS, Gregory JJ, Murfin W, Amos CN. *Evaluation of Severe Accident Risks: Quantification of Major Input Parameters, Experts' Determination of Containment Loads and Molten Core-Concrete Issues*. NUREG/CR-4551, SAND86-1309, Vol. 2, Part 2, Rev. 1. Albuquerque, NM: Sandia National Laboratories 1991.

136. Breeding RJ, Amos CN, Brown TD, Gorham ED, Gregory JJ, Harper FT, Murfin W, Payne AC. *Evaluation of Severe Accident Risks: Quantification of Major Input Parameters, Experts' Determination of Structural Response Issues*. NUREG/CR-4551, SAND86-1309, Vol. 2, Part 3, Rev. 1. Albuquerque, NM: Sandia National Laboratories 1992.

137. Harper FT, Breeding RJ, Brown TD, Gregory JJ, Jow H-N, Payne AC, Gorham ED, Amos CN, Helton JC, Boyd G. *Evaluation of Severe Accident Risks: Quantification of Major Input Parameters, Experts' Determination of Source Term Issues*. NUREG/CR-4551, SAND86-1309, Vol. 2, Part 4, Rev. 1. Albuquerque, NM: Sandia National Laboratories 1992.

138. Harper FT, et al. *Evaluation of Severe Accident Risks: Quantification of Major Input Parameters: Supporting Material*. SAND86-1309. Albuquerque: Sandia National Laboratories 1993.

139. Harper FT, Powers DA, Murata KK, Allen MD. *Evaluation of Severe Accident Risks: Quantification of Major Input Parameters: Determination of Parameter Values Not Quantified by Expert Panels*. NUREG/CR-4551, SAND86-1309. Albuquerque: Sandia National Laboratories in preparation.

140. Wheeler TA, Hora SC, Cramond WR, Unwin SD. *Analysis of Core Damage Frequency: Expert Judgment Elicitation*. NUREG/CR-4550, SAND86-2084, Vol. 2, Rev. 1. Albuquerque, NM: Sandia National Laboratories 1990.

141. Iman RL, Helton JC. The Repeatability of Uncertainty and Sensitivity Analyses for Complex Probabilistic Risk Assessments. *Risk Analysis* 1991; 11(4):591-606.

142. Helton JC, Johnson JD, McKay MD, Shiver AW, Sprung JL. Robustness of an Uncertainty and Sensitivity Analysis of Early Exposure Results with the MACCS Reactor Accident Consequence Model. *Reliability Engineering and System Safety* 1995; 48(2):129-148.

143. Helton JC, Davis FJ, Johnson JD. A Comparison of Uncertainty and Sensitivity Analysis Results Obtained with Random and Latin Hypercube Sampling. *Reliability Engineering and System Safety* 2005; 89(3):305-330.

144. Walske C. *Letter with inclosure to Brigadier General Edward B. Giller, dated March 14, 1968*. Washington, DC: Department of Defense, Military Liaison Committee the the Atomic Energy Commission 1968.

145. Isomedia. *NUREG-1150 Data Base: Surry, Vols.1 and 2*. Redmond, WA: Isomedia, Inc. 1995.

146. Helton JC, Anderson DR, Jow H-N, Marietta MG, Basabilvazo G. Performance Assessment in Support of the 1996 Compliance Certification Application for the Waste Isolation Pilot Plant. *Risk Analysis* 1999; 19(5):959 - 986.

147. Helton JC. Risk, Uncertainty in Risk, and the EPA Release Limits for Radioactive Waste Disposal. *Nuclear Technology* 1993; 101(1):18-39.

148. Helton JC, Anderson DR, Marietta MG, Rechard RP. Performance Assessment for the Waste Isolation Pilot Plant: From Regulation to Calculation for 40 CFR 191.13. *Operations Research* 1997; 45(2):157-177.

149. U.S. EPA (U.S. Environmental Protection Agency). 40 CFR Part 191: Environmental Radiation Protection Standards for the Management and Disposal of Spent Nuclear Fuel, High-Level and Transuranic Radioactive Wastes; Final Rule. *Federal Register* 1993; 58(242):66398-66416.

150. U.S. EPA (U.S. Environmental Protection Agency). 40 CFR Part 191: Environmental Standards for the Management and Disposal of Spent Nuclear Fuel, High-Level and Transuranic Radioactive Wastes; Final Rule. *Federal Register* 1985; 50(182):38066-38089.

151. Sanchez LC, Liscum-Powell J, Rath JS, Trellue HR. *WIPP PA Analysis Report for EPAUNI: Estimating Probability Distribution of EPA Unit Loading in the WIPP Repository for Performance Assessment Calculations, Version 1.01*. Albuquerque, NM: Sandia National Laboratories 1997.

152. U.S. EPA (U.S. Environmental Protection Agency). 40 CFR Part 194: Criteria for the Certification and Re-Certification of the Waste Isolation Pilot Plant's Compliance With the 40 CFR Part 191 Disposal Regulations; Final Rule. *Federal Register* 1996; 61(28):5224-5245.

153. Helton JC, Davis FJ, Johnson JD. Characterization of Stochastic Uncertainty in the 1996 Performance Assessment for the Waste Isolation Pilot Plant. *Reliability Engineering and System Safety* 2000; 69(1-3):167-189.

154. Helton JC, Martell M-A, Tierney MS. Characterization of Subjective Uncertainty in the 1996 Performance Assessment for the Waste Isolation Pilot Plant. *Reliability Engineering and System Safety* 2000; 69(1-3):191-204.

155. Stoelzel DM, O'Brien DG, Garner JW, Helton JC, Johnson JD, Smith LN. Direct Releases to the Surface and Associated Complementary Cummulative Distribution Functions in the 1996 Performance Assessment for the Waste Isolation Pilot Plant: Direct Brine Release. *Reliability Engineering and System Safety* 2000; 69(1-3):343-367.

156. Stockman CT, Garner JW, Helton JC, Johnson JD, Shinta A, Smith LN. Radionuclide Transport in the Vicinity of the Repository and Associated Complementary Cumulative Distribution Functions in the 1996 Performance Assessment for the Waste Isolation Pilot Plant. *Reliability Engineering and System Safety* 2000; 69(1-3):370-396.

157. Ramsey JL, Blaine R, Garner JW, Helton JC, Johnson JD, Smith LN, Wallace M. Radionuclide and Colloid Transport in the Culebra Dolomite and Associated Complementary Cumulative Distribution Functions in the 1996 Performance Assessment for the Waste Isolation Pilot Plant. *Reliability Engineering and System Safety* 2000; 69(1-3):397-420.

158. Iman RL. Statistical Methods for Including Uncertainties Associated with the Geologic Isolation of Radioactive Waste Which Allow for a Comparison with Licensing Criteria. In: DC Kocher, ed. *Proceedings of the Symposium on Uncertainties Associated with the Regulation of the Geologic Disposal of High-Level Radioactive Waste, Gatlinburg, TN, March 9-13, 1981*: Washington, DC: U.S. Nuclear Regulatory Commission, Directorate of Technical Information and Document Control, 1982:145-157.

159. Farmer FR. Reactor Safety and Siting: A Proposed Risk Criterion. *Nuclear Safety* 1967; 8(6):539-548.

160. Cox DC, Baybutt P. Limit Lines for Risk. *Nuclear Technology* 1982; 57(3):320-330.

161. Munera HA, Yadigaroglu G. On Farmer's Line, Probability Density Functions, and Overall Risk. *Nuclear Technology* 1986; 74(2):229-232.

162. Hansen CW, Brooks K, Groves JW, Helton JC, Lee PL, Sallaberry CJ, Stathum W, Thom C. Yucca Mountain 2008 Performance Assessment: Uncertainty and Sensitivity Analysis for Expected Dose. In. *Proceedings of the 2008 International High-*

Level Radioactive Waste Management Conference, September 7-11, 2008: American Nuclear Society, 2008:567-574.

163. Helton JC, Hansen CW, Sallaberry CJ. Yucca Mountain 2008 Performance Assessment: Conceptual Structure and Computational Implementation. In. *Proceedings of the International High-Level Radioactive Waste Management Conference, September 7-11, 2008*: American Nuclear Society, 2008:524-532.

164. Sallaberry CJ, Aragon A, Bier A, Chen Y, Groves JW, Hansen CW, Helton JC, Mehta S, Miller SP, Min J, Vo P. Yucca Mountain 2008 Performance Assessment: Uncertainty and Sensitivity Analysis for Physical Processes. In. *Proceedings of the 2008 International High-Level Radioactive Waste Management Conference, September 7-11, 2008*: American Nuclear Society, 2008:559-566.

165. U.S. NRC (U.S. Nuclear Regulatory Commission). 10 CFR Parts 2, 19, 20, etc.: Disposal of High-Level Radioactive Wastes in a Proposed Geologic Repository at Yucca Mountain, Nevada; Final Rule. *Federal Register* 2001; 66(213):55732-55816.

166. U.S. NRC (U.S. Nuclear Regualtory Commission). 10 CFR Part 63: Implementation of a Dose Standard after 10,000 Years. *Federal Register* 2005; 70(173):53313-53320.

167. Helton JC, Sallaberry CJ. Conceptual Basis for the Definition and Calculation of Expected Dose in Performance Assessments for the Proposed High Level Radioactive Waste Repository at Yucca Mountain, Nevada. *Reliability Engineering and System Safety* 2009; 94:677-698.

168. U.S. NRC (United States Nuclear Regulatory Commission). Disposal of High-Level Radioactive Wastes in a Geologic Repository at Yucca Mountain, Nevada. *Code of Federal Regulations 10 Part 63* 2008; http://www.access.gpo.gov/nara/cfr/waisidx_08/10cfr63_08.html.

169. Mackinnon RJ, Behie A, Chipman V, Chen Y, lee J, Lee PL, Mattie PD, Mehta S, Mon K, Schreiber JD, Sevougian SD, Stockman CT, Zwahlen E. Yucca Mountain 2008 Performance Assessment: Modeling the Engineered Barrier System. In. *Proceedings of the 2008 International High-Level Radioactive Waste Management Conference, September 7-11, 2008*: American Nuclear Society, 2008:542-548.

170. Mattie PD, Hadgu T, Lester B, Smith A, Wasiolek M, Zwahlen E. Yucca Mountain 2008 Performance Assessment: Modeling the Natural System. In. *Proceedings of the 2008 International High-Level Radioactive Waste Management Conference, September 7-11, 2008*: American Nuclear Society, 2008:550-558.

171. Sevougian SD, Behie A, Bullard B, Chipman V, Gross MB, Stathum W. Yucca Mountain 2008 Performance Assessment: Modeling Disruptive Events and Early Failures. In. *Proceedings of the 2008 International High-Level Radioactive Waste Management Conference, September 7-11, 2008*: American Nuclear Society, 2008:533-541.

172. Christie MA, Glimm J, Grove JW, Higdon DM, Sharp DH, Wood-Schultz MM. Error Analysis and Simulations of Complex Phenomena. *Los Alamos Science* 2005; 29:6-25.

173. Wagner RL. Science, Uncertainty and Risk: The Problem of Complex Phenomena. *APS News* 2003; 12(1):8.

174. Oberkampf WL, DeLand SM, Rutherford BM, Diegert KV, Alvin KF. Error and Uncertainty in Modeling and Simulation. *Reliability Engineering and System Safety* 2002; 75(3):333-357.

175. Risk Assessment Forum. *Guiding Principles for Monte Carlo Analysis*. EPA/630/R-97/001. Washington DC: U.S. Environmental Protection Agency 1997.

176. NCRP (National Council on Radiation Protection and Measurements). *A Guide for Uncertainty Analysis in Dose and Risk Assessments Related to Environmental Contamination*. NCRP Commentary No. 14. Bethesda, MD: National Council on Radiation Protection and Measurements 1996.

177. Draper D. Assessment and Propagation of Model Uncertainty. *Journal of the Royal Statistical Society, Series B* 1995; 57(1):45-97.

178. NRC (National Research Council). *Science and Judgment in Risk Assessment*. Washington, DC: National Academy Press 1994.

179. NRC (National Research Council). *Issues in Risk Assessment*. Washington, DC: National Academy Press, 1993.

180. U.S. EPA (U.S. Environmental Protection Agency). *An SAB Report: Multi-Media Risk Assessment for Radon, Review of Uncertainty Analysis of Risks Associated with Exposure to Radon*. EPA-SAB-RAC-93-014. Washington, DC: U.S. Environmental Protection Agency 1993.

181. IAEA (International Atomic Energy Agency). *Evaluating the Reliability of Predictions Made Using Environmental Transfer Models*. Safety Series No. 100. Vienna: International Atomic Energy Agency 1989.

182. Beck MB. Water-Quality Modeling: A Review of the Analysis of Uncertainty. *Water Resources Research* 1987; 23(8):1393-1442.

183. Helton JC. Uncertainty and Sensitivity Analysis in Performance Assessment for the Waste Isolation Pilot Plant. *Computer Physics Communications* 1999; 117(1-2):156-180.

184. Baudrit C, Dubois D. Practical Representations of Incomplete Probabilistic Knowledge. *Computational Statistics & Data Analysis* 2006; 51(1):86-108.

185. Dubois D, Prade H. Possibility Theory and Its Applications: A Retrospective and Prospective View. *CISM Courses and Lectures* 2006; 482:89-109.

186. Klir GJ. *Uncertainty and Information: Foundations of Generalized Information Theory*. New York, NY: Wiley-Interscience, 2006.

187. Ross TJ. *Fuzzy Logic with Engineering Applications*, 2nd edn. New York, NY: Wiley, 2004.

188. Helton JC, Johnson JD, Oberkampf WL. An Exploration of Alternative Approaches to the Representation of Uncertainty in Model Predictions. *Reliability Engineering and System Safety* 2004; 85(1-3):39-71.

189. Bardossy G, Fodor J. *Evaluation of Uncertainties and Risks in Geology*. New York, NY: Springer-Verlag 2004.

190. Klir GJ, Wierman MJ. *Uncertainty-Based Information*. New York, NY: Physica-Verlag 1999.

191. Helton JC. Uncertainty and Sensitivity Analysis for Models of Complex Systems. In: J.T. Fong and R. deWit, ed. *Verification & Validation of Complex Models for Design and Performance Evaluation of High-Consequence Engineering Systems*. Gaithersburg, MD: U.S. National Institute of Standards and Technology, 2004:237-263.

192. Helton JC. Uncertainty and Sensitivity Analysis for Models of Complex Systems. In: F Graziani, ed. *Granlibakken Proceedings*. New York, NY: Springer-Verlag, 2008.

193. Kleijnen JPC, Helton JC. *Statistical Analyses of Scatterplots to Identify Important Factors in Large-Scale Simulations*. SAND98-2202. Albuquerque, NM: Sandia National Laboratories 1999.

194. Helton JC, Davis FJ. *Sampling-Based Methods for Uncertainty and Sensitivity Analysis*. SAND99-2240. Albuquerque, NM: Sandia National Laboratories 2000.

195. Helton JC, Davis FJ. *Latin Hypercube Sampling and the Propagation of Uncertainty in Analyses of Complex Systems*. SAND2001-0417. Albuquerque, NM: Sandia National Laboratories 2002.

196. Helton JC, Johnson JD, Sallaberry CJ, Storlie CB. *Survey of Sampling-Based Methods for Uncertainty and Sensitivity Analysis*. SAND2006-2901. Albuquerque, NM: Sandia National Laboratories 2006.

197. Storlie CB, Helton JC. *Multiple Predictor Smoothing Methods for Sensitivity Analysis*. SAND2006-4693. Albuquerque, NM: Sandia National Laboratories 2006.

198. Morris MD. Three Technometrics Experimental Design Classics. *Technometrics* 2000; 42(1):26-27.

199. Iman RL, Conover WJ. A Distribution-Free Approach to Inducing Rank Correlation Among Input Variables. *Communications in Statistics: Simulation and Computation* 1982; B11(3):311-334.

200. Iman RL, Davenport JM. Rank Correlation Plots for Use with Correlated Input Variables. *Communications in Statistics: Simulation and Computation* 1982; B11(3):335-360.

201. Tong C. Refinement Strategies for Stratified Sampling Methods. *Reliability Engineering and System Safety* 2006; 91(10-11):1257-1265.

202. Sallaberry CJ, Helton JC, Hora SC. Extension of Latin Hypercube Samples with Correlated Variables. *Reliability Engineering and System Safety* 2008; 93:1047-1059.

203. Iman RL. Statistical Methods for Including Uncertainties Associated With the Geologic Isolation of Radioactive Waste Which Allow for a Comparison With Licensing Criteria. In: DC Kocher, ed. *Proceedings of the Symposium on Uncertainties Associated with the Regulation of the Geologic Disposal of High-Level Radioactive Waste*. Gatlinburg, TN: Washington, DC: US Nuclear Regulatory Commission, Directorate of Technical Information and Document Control, 1981:145-157.

204. Cooke RM, J.M. van Noortwijk. Graphical Methods. In: A Saltelli, K Chan, E.M. Scott, eds. *Sensitivity Analysis*. New York, NY: Wiley, 2000:pp. 245-264.

205. Iman RL, Conover WJ. The Use of the Rank Transform in Regression. *Technometrics* 1979; 21(4):499-509.

206. Hastie TJ, Tibshirani RJ. *Generalized Additive Models*. London: Chapman & Hall, 1990.

207. Simonoff JS. *Smoothing Methods in Statistics*. New York, NY: Springer-Verlag, 1996.

208. Bowman AW, Azzalini A. *Applied Smoothing Techniques for Data Analysis*. Oxford: Clarendon, 1997.

209. Ripley BD. Tests of Randomness for Spatial Point Patterns. *Journal of the Royal Statistical Society* 1979; 41(3):368-374.

210. Diggle PJ, Cox TF. Some Distance-Based Tests of Independence for Sparsely-Sampled Multivariate Spatial Point Patterns. *International Statistical Review* 1983; 51(1):11-23.

211. Zeng G, Dubes RC. A Comparison of Tests for Randomness. *Pattern Recognition* 1985; 18(2):191-198.

212. Assunçao R. Testing Spatial Randomness by Means of Angles. *Biometrics* 1994; 50:531-537.

213. Mishra S, Deeds NE, B.S. RamaRao. Application of Classification Trees in the Sensitivity Analysis of Probabilistic Model Results. *Reliability Engineering and System Safety* 2003; 79(2):123-129.

214. Breiman L, Friedman JH, Olshen RA, Stone CJ. *Classification and Regression Trees*. Belmont, CA: Wadsworth Intl, 1984.

215. Peacock JA. Two-Dimensional Goodness-Of-Fit Testing in Astronomy. *Monthly Notices of the Royal Astronomical Society* 1983; 202(2):615-627.

216. Fasano G, Franceschini A. A Multidimensional Version of the Kolmogorov-Smirnov Test. *Monthly Notices of the Royal Astronomical Society* 1987; 225(1):155-170.

217. Garvey JE, Marschall EA, Wright RA. From Star Charts to Stoneflies: Detecting Relationships in Continuous Bivariate Data. *Ecology* 1998; 79(2):442-447.

218. Hora SC, Helton JC. A Distribution-Free Test for the Relationship Between Model Input and Output when Using Latin Hypercube Sampling. *Reliability Engineering and System Safety* 2003; 79(3):333-339.

219. Iman RL, Conover WJ. A Measure of Top-Down Correlation. *Technometrics* 1987; 29(3):351-357.

220. Saltelli A, Tarantola S, Campolongo F, Ratto M. *Sensitivity Analysis in Practice*. New York, NY: Wiley, 2004.

221. Helton JC, Johnson JD, Oberkampf WL, Sallaberry CJ. *Representation of Analysis Results Involving Aleatory and Epistemic Uncertainty*. SAND2008-4379. Albuquerque, NM: Sandia National Laboratories 2008.

222. Cheeseman P. An Inquiry into Computer Understanding. *Computational Intelligence* 1988; 4(1):58-66.

223. Ferson S, Ginzburg L. Different Methods are Needed to Propagate Ignorance and Variability. *Reliability Engineering and System Safety* 1996; 54(2-3):133-144.

224. Klir GJ. Is There More to Uncertainty than Some Probability Theorists Might Have Us Believe? *International Journal of General Systems* 1989; 15:347-378.

225. Klir GJ. On the Alleged Superiority of Probability Representation of Uncertainty. *IEEE Transactions on Fuzzy Systems* 1994; 2:27-31.

226. Kosko B. Fuzziness vs. Probability. *International Journal of General Systems* 1990; 17(2-3):211-240.

227. Laviolette M, Seaman J. Evaluating Fuzzy Representations of Uncertainty. *Mathematical Science* 1992; 17:26-41.

228. Laviolette M, Seaman J, Barrett J, Woodall W. A Probabilistic and Statistical View of Fuzzy Methods. *Technometrics* 1995; 37:249-292.

229. Lindley DV. Scoring Rules and the Inevitability of Probability. *International Statistical Review* 1982; 50:1-26.

230. Lindley DV. The Probability Approach to the Treatment of Uncertainty in Artificial Intelligence and Expert Systems. *Statistical Science* 1987; 2(1):17-24.

231. Dubois D, Nguyen HT, Prade H. Possibility Theory, Probability Theory and Fuzzy Sets: Misunderstandings, Bridges and Gaps. In: D Dubois, H Prade, eds. *Fundamentals of Fuzzy Sets*. Boston, MA: Kluwer Academic Publishers, 2000:343-438.

232. Dubois D, Prade H. Fuzzy Sets, Probability and Measurement. *European Journal of Operational Research* 1989; 40:135-154.

233. Klir GJ. Measures of Uncertainty and Information. In: D Dubois, H Prade, eds. *Fundamentals of Fuzzy Sets*. Boston, MA: Kluwer Academic Publishers, 2000:439-457.

234. Ross TJ, Booker JM, W.J. Parkinson (eds.). *Fuzzy Logic and Probability Applications: Bridging the Gap*. Philadelphia, PA: Society for Industrial and Applied Mathematics, 2002.

235. Smets P. Probability, Possibility, Belief: Which and Where? In: DM Grabbay, P Smets, eds. *Handbook of Defeasible Reasoning and Uncertainty Management Systems*. Boston, MA: Kluwer Academic Publishers, 1998:1-24.

236. Wu JS, Apostolakis GE, Okrent D. Uncertainty in System Analysis: Probabilistic Versus Nonprobabilistic Theories. *Reliability Engineering and System Safety* 1990; 30:163-181.

237. Jaulin L, Kieffer M, Didrit O, Walter E. *Applied Interval Analysis*. New York, NY: Springer-Verlag, 2001.

238. Kearfott RB, Kreinovich V. *Applications of Interval Computations*. Boston, MA: Kluwer Academic Publishers 1996.

239. Hammer R, Hocks M, Kulisch U, Ratz D. *Numerical Toolbox for Verified Computing. I. Basic Numerical Problems*. New York, NY: Springer Verlag 1993.

240. Neumaier A. *Interval Methods for Systems of Equations*. Cambridge: Cambridge University Press, 1990.

241. Moore RE. *Methods and Applications of Interval Analysis*. Philadelphia, PA: Society for Industrial and Applied Mathematics 1979.

242. Moore RE. *Interval Analysis*. Englewood Cliffs, NJ: Prentice Hall 1966.

243. Dubois D, Prade H. Possibility Theory: Qualitative and Quantitative Aspects. In. *Handbook of Defeasible Reasoning and Uncertainty Management Systems*. Vol. 1. D.M. Grabbay and P. Smets (eds). Boston, MA: Kluwer Academic Publishers, 1998:169-226.

244. deCooman G. Possibility Theory Part I: Measure- and Integral-theoretic Ground-work; Part II: Conditional Possibility; Part III: Possibilistic Independence. *International Journal of General Systems* 1997; 25(4):291-371.

245. deCooman G, Ruan D, E.E. Kerre (eds). Foundations and Applications of Possibility Theory. In. *Proceedings of FAPT '95*. Ghent, Belgium, December 13-15, 1995: River Edge, NJ: World Scientific Publishing Co, 1995.

246. Dubois D, Prade H. *Possibility Theory: An Approach to Computerized Processing of Uncertainty*. New York, NY: Plenum 1988.

247. Zadeh LA. Fuzzy Sets as a Basis for a Theory of Possibility. *Fuzzy Sets and Systems* 1978; 1:3-28.

248. Halpern JY, Fagin R. Two Views of Belief: Belief as Generalized Probability and Belief as Evidence. *Artificial Intelligence* 1992; 54:275-317.

249. Guan JW, Bell DA. *Evidence Theory and Its Applications*. Vols. 1, 2. New York, NY: North-Holland 1991.

250. Wasserman LA. Belief Functions and Statistical Inference. *The Canadian Journal of Statistics* 1990; 18(3):183-196.

251. Wasserman L. *Belief Functions and Likelihood, Technical Report 420*. Pittsburgh, PA: Department of Statistics, Carnegie-Mellon University 1988.

252. Shafer G. *A Mathematical Theory of Evidence*. Princeton, NJ: Princeton Univ. Press 1976.

253. Dempster AP. A Generalization of Bayesian Inference. *Journal of The Royal Statistical Society, Series B* 1968; 30:205-247.

254. Dempster AP. Upper and Lower Probability Inferences Based on a Sample from a Finite Univariate Population. *Biometrika* 1967; 54(2-3):515-528.

255. Dempster AP. Upper and Lower Probabilities Induced by a Multivalued Mapping. *Annals of Mathematical Statistics* 1967; 38:325-339.

256. Zadeh LA. Fuzzy Sets. *Information and Control* 1965; 8(3):338-353.

257. Hacking I. *An Introduction to Probability and Inductive Logic*. Cambridge, New York: Cambridge University Press 2001.

258. Howson C, Urbach P. *Scientific Reasoning: The Bayesian Approach*, 2nd edn. Chicago, IL: Open Court, 1993.

259. Stigler SM. *The History of Statistics: The Measurement of Uncertainty Before 1900*. Cambridge, MA: Harvard University Press 1986.

260. Weatherford R. *Philosophical Foundations of Probability Theory*. London, Boston: Routledge & Kegan Paul 1982.

261. Fine TL. *Theories of Probability: An Examination of Foundations*. New York, NY: Academic Press 1973.

262. Kallenberg O. *Foundations of Modern Probability*, 2nd edn. New York, NY: Springer-Verlag, 2000.

263. Billingsley P. *Probability and Measure*, 3rd edn. New York, NY: John Wiley & Sons, 1995.

264. Joslyn C, Kreinovich V. *Convergence Properties of an Interval Probabilistic Approach to System Reliability Estimation*. LA-UR-02-6261. Los Alamos, NM: Los Alamos National Laboratory 2002.

265. Joslyn C, Helton JC. Bounds on Belief and Plausibility of Functionally Propagated Random Sets. In: J Keller, O Nasraoui, eds. *2002 Annual Meeting of the North American Fuzzy Information Processing Society Proceedings*: Piscataway, NJ: IEEE, 2002:412-417.

266. L'Ecuyer P, ed *Random Number Generation*. New York, NY: John Wiley & Sons, 1998.

267. Barry TM. Recommendations on the Testing and Use of Pseudo-Random Number Generators Used in Monte Carlo Analysis for Risk Assessment. *Risk Analysis* 1996; 16(1):93-105.

268. Fishman GS. *Monte Carlo: Concepts, Algorithms, and Applications*. New York, NY: Springer-Verlag, 1996.

269. Helton JC, Johnson JD, Oberkampf WL, Sallaberry CJ. Sensitivity Analysis in Conjunction with Evidence Theory Representations of Epistemic Uncertainty. *Reliability Engineering and System Safety* 2006; 91(10-11):1414-1434.

270. Helton JC, Johnson JD, Oberkampf WL, Storlie CB. A Sampling-Based Computational Strategy for the Representation of Epistemic Uncertainty in Model Predictions with Evidence Theory. *Computational Methods in Applied Mechanics and Engineering* 2007; 196(37-40):3980-3998.

This page intentionally left blank

Appendix A

Rechard RP. Historical Relationship Between Performance Assessment for Radioactive Waste Disposal and Other Types of Risk Assessment. *Risk Analysis* 1999;19(5):763-807.

This page intentionally left blank

Risk Analysis, Vol. 19, No. 5, 1999

Historical Relationship Between Performance Assessment for Radioactive Waste Disposal and Other Types of Risk Assessment

Rob P. Rechard[1]

This article describes the evolution of the process for assessing the hazards of a geologic disposal system for radioactive waste and, similarly, nuclear power reactors, and the relationship of this process with other assessments of risk, particularly assessments of hazards from manufactured carcinogenic chemicals during use and disposal. This perspective reviews the common history of scientific concepts for risk assessment developed until the 1950s. Computational tools and techniques developed in the late 1950s and early 1960s to analyze the reliability of nuclear weapon delivery systems were adopted in the early 1970s for probabilistic risk assessment of nuclear power reactors, a technology for which behavior was unknown. In turn, these analyses became an important foundation for performance assessment of nuclear waste disposal in the late 1970s. The evaluation of risk to human health and the environment from chemical hazards is built on methods for assessing the dose response of radionuclides in the 1950s. Despite a shared background, however, societal events, often in the form of legislation, have affected the development path for risk assessment for human health, producing dissimilarities between these risk assessments and those for nuclear facilities. An important difference is the regulator's interest in accounting for uncertainty.

KEY WORDS: Risk assessment; probabilistic risk assessment; performance assessment; policy analysis; history of technology.

1. INTRODUCTION

Fear of harm ought to be proportional not merely to the gravity of the harm, but also to the probability of the event. . . .

So wrote Antoine Arnauld and others residing in the Port Royal Monastery, France, in about 1660.[1,2] More than 300 years later, the U.S. Environmental Protection Agency (EPA) mandated an examination of the relationship between the "gravity of harm" and the "probability of the event" in the regulatory standard for disposal of radioactive wastes. This article compiles and summarizes events leading up to and following this EPA-mandated assessment in 40 CFR 191 (Title 40, Code of Federal Regulations, Part 191) that have influenced risk assessments of geologic disposal.

1.1. Selection of Historical Material

This article is intended to provide a historical context for the issues presented on disposal of radioactive waste in this special issue of *Risk Analysis* by compiling and summarizing information concerning historical events that have influenced risk assess-

[1] Performance Assessment Department (6849), Sandia National Laboratories, Albuquerque, NM 87185-0779.

0272-4332/99/1000-0763$16.00/1 © 1999 Society for Risk Analysis

ments of geologic disposal. This compendium focuses heavily on events at Sandia National Laboratories (Sandia or SNL) because of its extensive role in risk assessments for nuclear facilities, with significant international events presented in some cases. To broaden this context, however, events and their effects on other large-scale policy analyses of risk, particularly chemical carcinogens, are also presented. For example, legislation and select judicial decisions that have helped to mold risk assessments for hazardous chemicals are included. Although policy analysis in general and risk assessment in particular have received, and continue to receive, criticism, the historical aspects of the criticism are not included in this article. Ewing *et al.* (this issue) discusses current criticisms of performance assessments (PAs). Herein, risk assessment is presumed to be an important contributor to risk management decisions, but only one of several possible inputs.

The material is presented chronologically, within five sections that cover four major time periods. Section 2 of this article reviews risk management responses of ancient civilizations to hazards and the development of risk concepts (antiquity–1940; e.g., probability theory). Computational methods, along with limited application of reliability techniques, are discussed in Section 3 (1940–1970). Section 4 focuses on risk assessment for nuclear power reactors and its rudimentary application to geologic disposal systems (1970–1985); Section 5 focuses on the many differing legislative and judicial events that have influenced the use of risk assessments for hazardous chemicals (1970–present). During this period, government policy decisions based on risk assessments have been encouraged, and many diverse applications of risk assessment on different physical systems have been implemented. Section 6 serves as an introduction to this special issue by providing the historical context for the risk assessments of two prominent radioactive waste disposal programs in the United States, the Waste Isolation Pilot Plant (WIPP) for transuranic waste, and the Yucca Mountain Project (YMP), primarily for commercial spent nuclear fuel.

1.2. Risk Assessment Process

Although risk has several connotations (if not denotations) inside and outside the profession of risk analysis, *risk* is generally used in this article to express some measure that combines "the gravity of harm" to something valued by society and "the probability of the event." Frequently, within the risk profession, the measure of risk is the expected value of the consequence (e.g., probability times consequence based on average values) as used in simple annuity analysis as far back as 1660. For financial investments, where the word "risk" was used as early as 1776, the measure is often the variance of the return on investment. For situations with large uncertainty, such as disposal of radioactive wastes, the measure of risk is the entire distribution of the possible consequences as required by the EPA in 1985 in 40 CFR 191.

Similar to its use by the National Academy of Sciences (NAS) in 1983,[3] *risk management* is used to describe any means whereby an individual or society attempts to decide whether an activity is safe and, if not, how to reduce the risks of that activity, select options, and prioritize among options. It is an activity that has been performed for thousands of years. Safe is used herein as defined by Lowrance in 1976, that is, having risks that are judged acceptable by an individual or a society (through a political process in the latter case).[4,5] As used in this journal since 1980, *risk analysis* describes all facets of the risk topic such as management and risk assessment.

In the late 1970s and early 1980s, risk assessments that "quantified" risk through the use of mathematical models were called quantitative risk assessments, but the term is not often used now because modeling is so pervasive. Instead, *risk assessment* is used here to denote all systematic processes that estimate a measure of risk. Risk assessment is not a distinct branch of science.[6] Instead, it is a type of policy analysis of what can go wrong in human affairs, a "hybrid discipline,"[7] in which the current state of scientific and technological knowledge is made accessible to society as input to risk management decisions, with time and resource constraints specified by the policy decision makers (or tolerated by society). Important components of risk assessment were not performed until after the late 1950s, yet the development of ideas and tools within several branches of science before and after this time furthered risk assessment as a tool for decision making (Fig. 1).

Because of a common foundation with system analysis, the process of assessing the risk from various hazards is similar. Indeed, the founders of the Society for Risk Analysis recognized these shared ideas and brought practitioners together in 1980 to encourage and enhance the usefulness of risk concepts to society. In general, risk assessment is comprised of up to seven steps[9]: (0) identify appropriate measures of

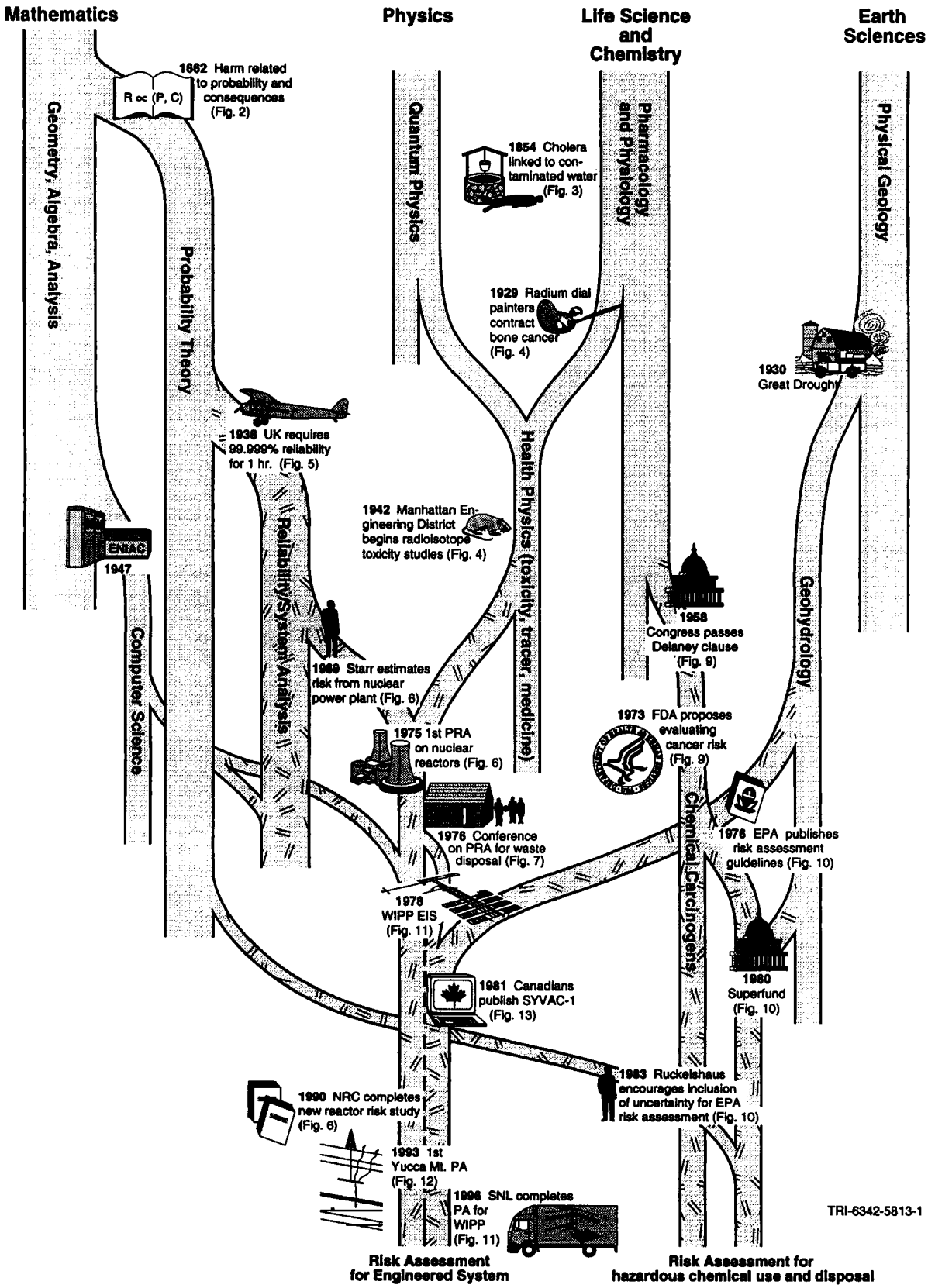

Fig. 1. Developments from various branches of science that contribute to risk assessments of nuclear facilities and hazardous chemical use and disposal.

risk and corresponding risk limits; (1) define and characterize the system and agents acting on the system; (2) identify sources of hazards and, if desired, form scenarios; (3) quantify uncertainty of factors or parameters and evaluate probability of scenarios (if formed); (4) evaluate the consequences by determining the response to exposure and, possibly, the pathway to exposure; (5) combine the evaluated consequences and probabilities and compare them with risk limits; and (6) evaluate sensitivity of results to changes in parameters to gain further understanding. As defined here, these steps include the four steps proposed by Lowrance in 1976[3,4] and refined by the NAS in 1983.[3]

The seven steps provide answers to three fundamental questions of risk assessment by Kaplan and Garrick in 1981[9-12]: What hazards can occur? What is the probability of these hazards? What are the consequences potentially caused by these hazards? As with any scientific modeling or policy process, the boundaries between steps may overlap. More important, an analyst may need to cycle through several steps[13] during an activity such as model building or defining risk goals, for example. Hence, the steps are not always truly sequential.

Although the general process of performing a risk assessment for hazards is similar, societal and legislative events during the mid-1970s produced dissimilarities in the emphasis and use of these concepts. In the assessment process, these dissimilarities are reflected in the use of specific terms used in this article. For risk assessments of nuclear facilities, two specific terms are used: probabilistic risk assessment (PRA) and performance assessment (PA).

Probabilistic risk assessment (*PRA*) denotes a risk assessment that specifically evaluates the uncertainty of knowledge from various sources in the analysis. Although not limited to such usage in this article, the term also frequently connotes (based on the use in the *Reactor Safety Study* in 1975[14]) a risk assessment of risk to health over a human lifetime from an engineered system such as a nuclear power plant, where failures are short-term events (in relation to the life of the system).

In 1991, the Nuclear Energy Agency of the European Organisation for Economic Co-Operation and Development (OECD/NEA) defined *performance assessment* (*PA*) as "an analysis to predict the performance of a system or subsystem, followed by a comparison of the results of such analysis with appropriate standards and criteria."[15] Given this definition and assuming the performance criteria are risk based and uncertainties are evaluated, PA and PRA are synonymous within the United States. (A possible exception is the implied comparison with established criteria.) However, outside the United States, PA does not always imply an evaluation of uncertainties[16]; hence, a distinction between PA and PRA is maintained. Herein, a PA is used during discussions of a risk assessment, with or without inclusion of uncertainties, to illustrate possible behavior over geologic time scales of a radioactive waste disposal system composed of both engineered and natural components and including a comparison of the results to regulatory criteria (e.g., 40 CFR 191). In such a system, the natural components evolve rather than "fail," as in a nuclear power plant.

Risk assessment is used generically during discussions of risk assessment of hazardous chemicals, despite a subtle difference between risk assessments for hazardous chemicals and those of nuclear facilities in that assessments for hazardous chemicals have a less intimate connection to systems (engineering) analysis (Fig. 1). However, a distinct and important branch of risk assessment of hazardous chemicals identified since 1976 by the EPA is carcinogenic risk assessment (Fig. 1), as noted in Volume 41 of the *Federal Register*, page 21402 (41 FR 21402). Carcinogenic risk assessment is conditional on the occurrence of external exposure to the carcinogen (i.e., the assessment omits the pathway analysis of exposure external to the human and the probability of exposure occurring). This type of assessment has also frequently omitted analysis of uncertainty in model parameters, uncertainty from alternative conceptual models, and parameter sensitivity. Because the assessment focuses on the response of the human receptor, carcinogenic risk assessment is termed a dose–response assessment herein to avoid confusion during discussion of other risk assessments for chemical disposal or ecological evaluations that encompass more steps.

2. CONTRIBUTORS TO RISK CONCEPTS

2.1. Rudimentary Hazard Identification and Risk Management

Occasional, rudimentary risk management was applied by society prior to 1600, as noted by several authors.[2,17-20] In these cases, society identified a hazard (step 2 of a risk assessment) and then pragmatically adopted risk management controls (i.e., insurance or government controls). Hazard identification,

directly followed by risk management controls, is still in use today.

An early response to a hazard was to spread risk among several social groups by issuing insurance, such as bottomry contracts in the Mediterranean in the 1600s BC. This method had been formalized by Hammurabi, King of Babylon, in 1758 BC, whereby risk of maritime loss was borne by money lenders in exchange for interest. Also, by AD 230, the Romans had rudimentary life insurance through societies (collegia) formed to pay burial expenses of its members[2,19] (Fig. 2).

Government intervention to control risk was another technique adopted by ancient civilizations. In 1758 BC, Hammurabi mandated dam maintenance with strict liability for property destroyed when the owner failed to maintain his dam.[21] The enforcement of strict liability presumably encouraged wise building practices, which have continued throughout the centuries and been reinforced by canons of ethics. For example, engineers in the 1930s and 1940s developed procedures for determining plausible upper bounds on floods (plausible maximum flood) for the emergency spillway design on dams.

In the United States, an early attempt at risk management of new technology was performed via the mandated tests and inspections by U.S. Congress to prevent deaths from boiler explosions on steamboats in 1838. Although this legislation failed to reduce explosions because no data or experience existed on necessary tests and useful inspections, a report prepared at personal expense by Guthrie, an Illinois engineer, provided the knowledge for Congress to pass a more effective law in 1852 and establish a regulatory agency, with Guthrie as its first administrator.[19]

These risk management controls were government intervention after the fact. Government intervention *before* an incident, which required the ability to recognize and differentiate among certain types of behavior or actions as hazardous and nonhazardous, and an ability to predict consequences, was not practiced until the 20th century. As described later in this article, it was employed first in the early 1900s for health hazards causing immediate harm, and then in the mid-1900s for hazards causing harm over the long term.

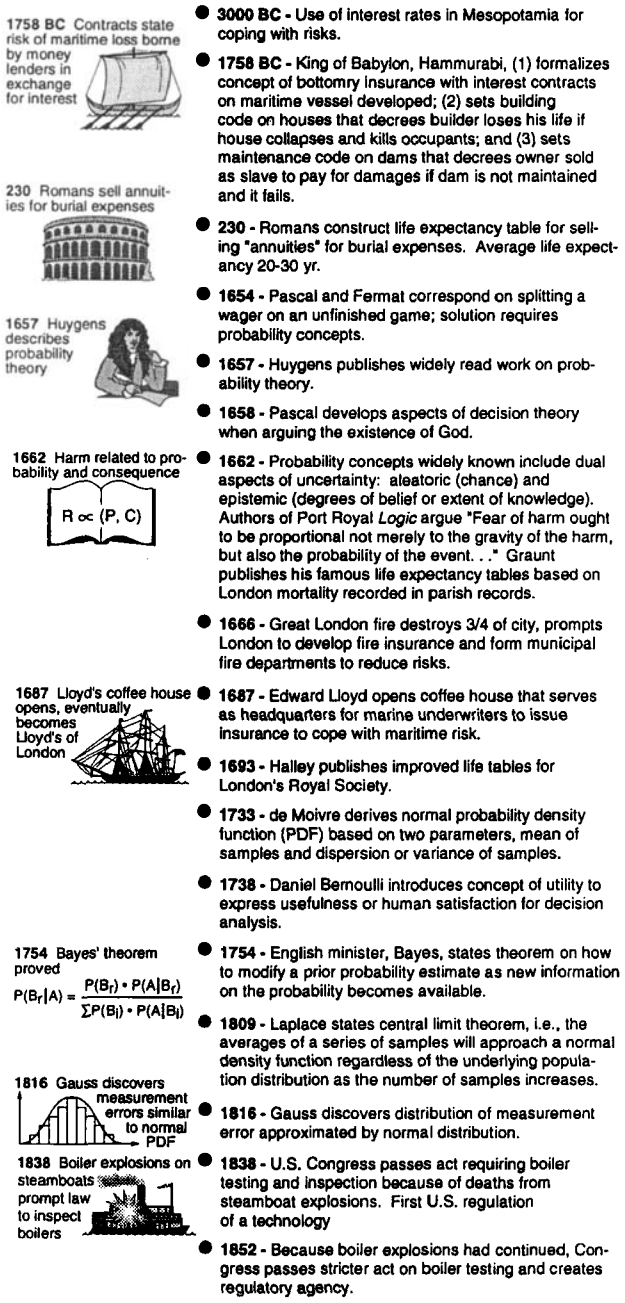

Fig. 2. Early events prompting mitigation and development of probability theory (antiquity to 1940).

2.2. Probability Foundation and Application to Annuities

Probability theory, of which a rudimentary form had emerged by 1660, spread relatively quickly as its usefulness was recognized.[1] For example, the Dutch government benefited from this theory because, unlike the Romans of early times, the Dutch often lost money when selling life annuities to finance public works. The use of probability theory, as well as tracking frequencies of disaster and death (e.g., Graunt's tables of life expectancy in 1662 for

London[22]) eventually placed life annuities on a firm foundation.[1,2]

A rudimentary application of probability theory was determining the minimum premium to charge for a death benefit in relation to the expected cost: frequency of death for a person of a certain age or older multiplied by the expected benefit (i.e., "average" cost or consequence to insurance company). Thus, the concept of risk as the expected (mean) consequence was rapidly developed and applied to insurance.[2] However, the steps for performing a formal risk assessment were far from fully developed, and determining the distribution of the consequence, as a more complete characterization of risk, would not occur until the 20th century.

2.3. Assessing Human Health

Health and Hazardous Substances

As early as 500 BC, a relationship was observed between swamps and diseases such as malaria. In his writings, Hippocrates (460–377 BC) advised that rainwater should be strained and boiled to maintain health.[25] The Romans noted health hazards from mining (beyond those incurred by a mine collapse) and metal use, as did German physicians in the 1400s at two mines in Saxony.[3] With the increased concentration of people in towns during the Industrial Revolution in the 1700s and 1800s, relationships between occupations, personal habits, living conditions, and overall health were more widely observed. Examples include observations by Dr. John Snow who, in 1854, graphically linked cholera outbreaks to contaminated water from one well by means of a map of central London (Fig. 3).[25,26]

Hazard identification followed by increased sanitation, better working conditions, and improved medical services had increased life expectancy in the United States to approximately 50 years by 1900, a doubling of the life expectancy of the Romans; however, the leading cause of death was still infectious diseases (e.g., pneumonia, influenza, tuberculosis).

Control of Health Risks

From observations about relationships between living conditions and health came efforts to protect the public from impure or untested chemicals in food and drugs. An early attempt to mitigate health risks was an English law, Assize of Bread, passed in 1263, making it unlawful to sell food "unwholesome to man's body."[17,27] The first large-scale attempt to mitigate health risks of society in the United States occurred in 1813, when Congress passed the Federal Vaccine Act (2 Stat. 806) to test the smallpox vaccine developed by E. Jenner, a British physician in 1796.[27] Prior to this time, some private doctors had inoculated individuals at their request (e.g., Thomas Jefferson in 1766) using pus from smallpox victims in the hope of causing a "light" case of smallpox. The value of this procedure, which carried a moderate probability of inducing a deadly case of smallpox, was examined by Laplace in 1792.[19] Further attempts to control health risks included the 1906 passage of the Pure Food and Drug Act (Public Law 59-384 [34 Stat. 768]), whose main impetus was widespread fraud in packaging, and the more stringent Federal Food, Drug, and Cosmetic Act in 1938 (Public Law 75-717 [52 Stat. 1040]).

By 1940, life expectancy in the United States had increased to 63 years. Knowledge of the sources of infectious diseases (Pasteur in 1864), and introduction of coagulation (1884), filtration (1892), and chlorination (1908) of water supplies,[25] had so greatly reduced incidence of deadly infections that degenerative diseases, such as heart disease and cancer, became the leading cause of death.

Dose–Response Assessment

The opinion that effects of a chemical substance could range from beneficial to harmful, based on dose, was expressed as early as 1567.[17,27] Similar observations in this century engendered the field of public health and the need to evaluate a safe level of exposure to such chemicals.[17] Initially, this was accomplished by assessing the threshold dose

[2] The close association of the word "risk" with "insurance" is possible because the word "risk" entered the English language around 1660, just as probability theory emerged, from the French word "risque," which means to expose to hazard.[23] *The Oxford English Dictionary* noted a usage apart from insurance or uncertainty, beginning in the 1900s, in relation to finances ("whether the capital owned . . . was not in risk . . .").[24]

[3] The cause of the high death rates in German mines was later discovered to be from silicosis, tuberculosis, and lung cancer caused by high concentrations of radon gas.[20]

- **500 BC ca** - Relationship between swamps and malaria noted.
- **400 BC ca** - Hippocrates admonishes that rain water should be boiled and strained to maintain health.
- **100 BC** - Romans note exposure to lead fumes injures health.
- **1263** - English pass law, Assize of Bread, making it unlawful to sell food "unwholesome for man's body."
- **1300 ca** - Edward I bans use of "sea coal" and requires use of wood in kilns around London.
- **1390 ca** - Richard II sleeks to restrict use of coal in London through taxation.
- **1472** - German booklet tells goldsmiths how to avoid poisoning by lead and mercury.
- **1500 ca** - Wood around London depleted and use of coal a necessity.
- **1556** - German mineralogist, Agricola, describes miner health problems in Saxony.

- **1567** - Physician-alchemist Paracelsus writes: "All substances are poisons. There is none which is not a poison. The right dose differentiates a poison from a remedy."
- **1661** - In London, smoke from coal fires is linked to acute and chronic respiratory problems.
- **1718** - Lady Montagu of Britain proposes inoculation with pus from victims of smallpox to get "light" case of smallpox.
- **1775** - Data suggests juvenile chimney sweeps susceptible to scrotal cancer at puberty.
- **1781** - Tobacco snuff linked to cancer of nasal passage.
- **1792** - Laplace examines the probability of death with and without small pox inoculation.
- **1796** - British physician E. Jenner inoculated 8 yr old boy with cowpox pus from hand of milk maid to vaccinate against human smallpox - human experiment successful.
- **1798** - The United States begins health service for merchant sailors.

- **1800's** - Von Bortkiewicz estimates average number of Prussian soldiers killed from horse kicks based on Poisson distribution and compares with actual deaths.

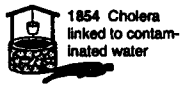

- **1813** - U.S. Congress passes Federal Vaccine Act to test smallpox vaccine.
- **1822** - Cancer linked to occupational and medicinal exposures of arsenic.
- **1842** - Chadwick reports on link between health problems and lack of nutrition and sanitation in English slums.
- **1854** - Dr. John Snow links cholera outbreaks to contaminated water.
- **1864** - Pasteur invents pasteurization and establishes link between microbes and infectious disease.
- **1870** - U.S. Congress forms Marine Hospital Service for merchant sailors.
- **1884** - Chemical-coagulation filtration patented.
- **1890** - Ohio starts regulating coal-fired industrial boilers.
- **1892** - German professor observes the value of sand filtration in protection against cholera bacteria when comparing Hamburg to Atone, Germany.
- **1894** - Physicians observe that skin cancer is only on exposed skin.

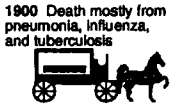

- **1900** - Life expectancy 50 yr and leading cause of death in the United States is infectious disease (pneumonia, influenza, and tuberculosis).
- **1906 - Jun:** Prompted by public concern from press reports of harmful substances in food and drugs in late 1800's, U.S. Congress passes Pure Food and Drugs Act to curb fraud.
- **1908** - Chlorination of water supply adopted at Jersey City, NJ.
- **1912** - U.S. Congress establishes public health service from Marine Hospital Service.

- **1938 - Jun:** U.S. Congress passes stronger Food, Drug, and Cosmetic Act of 1938 to replace law of 1906.
- **1940** - Life expectancy 63 yr and leading cause of death in U.S. are degenerative diseases: heart disease and cancer.
- **1954** - The U.S. Food and Drug Administration (FDA) adopts a "factor of safety of 100" for the threshold measured in the laboratory for hazardous chemicals (no observed adverse effects level [NOAEL]) – factor of 10 for variability in humans and factor of 10 for variability between species.

Fig. 3. Early observations of ill health and subsequent risk management (antiquity to 1950).

below which no ill effects could be observed (no observed adverse effects level [NOAEL]). The Food and Drug Administration (FDA)—formed through 1938 legislation (Public Law 75-717 [52 Stat. 1040])—established in 1954 a factor of safety ("uncertainty" factor[28] or factor of protection[29]) of 100 to determine the allowable daily intake (ADI). That is, the safe dose (ADI) used the estimated threshold of a chemical substance obtained from an animal study that used "small doses" over "long-times" divided by 100: a factor of 10 for variability in humans and another factor of 10 for variability between humans and the species with which the chemical response was measured (i.e., ADI = NOAEL/100).[17,28]

2.4. Radiation Health Effects and Development of Consequence Evaluation

Health Effects of Radiation

Within a year of the discovery of X rays in 1895, X-ray "burns" were reported in the medical literature. By 1910, it was known that radioactive material such as radium (discovered by the Curies in 1898) could produce similar burns.[30] Furthermore, cancers of the jaw bone reported in the 1920s in watch dial painters who used luminous paint containing radium revealed the hazard of internal ingestion of alpha-emitting radium[20] (Fig. 1). In 1927, Müller discovered that X rays could damage chromosomes in fruit

flies.[4] Consequently, in 1928, the International X-Ray and Radium Protection Commission (later named the International Commission on Radiation Protection [ICRP]) was created to set criteria to protect humans from radium and X rays. In setting up the commission, the International Congress of Radiology recommended that each nation form a national advisory commission. Furthermore, medical risks associated with radioactive elements became of interest with the availability of manufactured isotopes in the late 1920s. Hence, in 1929, the U.S. radiological societies voluntarily established the U.S. Advisory Committee on X-Ray and Radium Protection, which was the predecessor of the National Council of Radiation Protection (NCRP) chartered by Congress in 1964 (Public Law 88-376). The NCRP Advisory Committee initially recommended an occupational "tolerance dose" of ~25 rem/yr (actually expressed as 0.2 roentgen/day) for X rays and gamma rays (Fig. 4).[20] The tolerance dose was similar in concept to ADI for hazardous chemicals.

As the United States prepared for World War II, the U.S. Navy asked the NCRP to develop standards for radium to avoid the problems experienced by the young female dial painters in World War I. In May 1941, based on studies of 27 dial painters and radon exposure of numerous German miners in Saxony, a fruitful collaboration of a physicist (R. Evans), a chemist (Gettler), and physicians (Martland and Hoffman) was able to set the maximum allowable activity within the body[4] at 0.1 μCi for radium and a maximum allowable gas concentration of 10 pCi/liter in the work place for radon, the latter standard being set for the insurance industry.[20] The allowable dose was about a factor of 10 below the lowest value of 1.2 μCi residual body burden where effects had been observed. Because this low value at 1.2 μCi was residual body burden and the initial dose was between 10 and 100 times greater, the limit also had an additional factor of 10 to 100 protection.[33] In an interesting cross-over between carcinogenic and noncarcinogenic dose work, a study that compared bone sarcoma in rats that had ingested radium and surmised doses in the female dial painters of World War I was eventually used to justify 100 as a factor of protection for evaluating noncarcinogenic doses.[28,34]

[4] The concept of a maximum allowable body burden, which was adopted in 1959,[31] was modified by the ICRP in 1979[32] to a scheme weighting organ dose to obtain an effective dose equivalent.

The first atmospheric test near Alamogordo, New Mexico, in 1945, generated scientific interest and monitoring of fallout and effects on nearby cattle. Experiments were performed on effects of radiation on Columbia River fish near Hanford, Washington, and monitoring of weapons production facilities began in the late 1940s.[20] Results of the experiments and epidemiological observations in the 1950s led to the hypothesis of potential harm from chronic exposure to low levels of radiation (e.g., radiation-induced leukemia).[35] As a result of this possibility, the NCRP lowered the maximum permissible dose from ~25 rem/yr to 15 rem/yr (40% reduction) in 1948 and recommended the adoption of a policy of limiting radiation doses to as low as reasonably achievable (ALARA). (ALARA was introduced in the general Environmental Impact Statement [EIS] for light water reactors 25 years later, becoming official U.S. policy in 1975 [40 FR 19442].) In 1956, the NAS recommended a maximum dose of 10 rem/yr with 5 rem/yr be allocated to medical diagnosis procedures. In 1959, the ICRP recommended that the maximum occupational dose be lowered to 5 rem/yr (a reduction by a factor of 3) and suggested a maximum dose to the public of 0.5 rem/yr (an order of magnitude lower).[20,30] In 1960, the first Biologic Effects of Atomic Radiation (BEAR) panel was convened by the NAS to estimate the relationship of radiation dose to observed cancer. The BEAR panel reported on a notable epidemiological study of the incidence of cancer in Japanese survivors of the atomic bomb[20] in developing a model of the response of the biological organism to the input stressor.

Exposure Pathway Assessment

Several events engendered a need for developing exposure pathway model external to the receptor. In 1954, fallout from an atmospheric test on Bikini Atoll in the Pacific contaminated 43 Marshall Islanders and 14 Japanese fishermen aboard the Lucky Dragon, which prompted a public outcry to stop atmospheric tests.[20,36] In 1957, the fire in the Windscale graphite reactor in the United Kingdom released ^{131}I, and milk consumption was temporarily curtailed.[5,36] In 1961, the Atomic Energy Commission (AEC) used the bedded salt in southwestern New Mexico (Project Gnome) to evaluate the peaceful uses of nuclear explosives (Plowshare Program).[20,37] Hence, by the 1960s, Oak Ridge National Laboratory (ORNL) began predicting the movement and attendant health

- **1789** - Klaproth isolates U isolates U_2O_3 in pitchblende.
- **1841** - Peligot isolates uranium element.
- **1895** - Rutherford shows radiation from uranium looks like helium nucleus (alpha particle and beta particle).
- **1896** - French physicist Becquerel demonstrates radioactivity of uranium. Along with both Curies, he will receive Nobel Prize in physics for the discovery in 1903. "X-ray burns" reported in medical literature.
- **1898** - Marie and Pierre Curie discover polonium and radium in pitchblende (Marie receives Nobel Prize in chemistry in 1911 for study of chemical properties of radium).
- **1910** - "Burns" from radioactive material reported in medical literature (e.g., on watch dial painters using radium).
- **1917** - During WWI, young women employed to paint dial numerals on military instruments using luminous paint containing radium. After war, many clock factories employ young women for dial painting using luminous paint with radium.
- **1924** - Blum, dentist in New York, noticed an intractable case of osteomyelitis in the jaw of a girl working in a dial painting factory.

1927 X-rays widely used for diagnosis

- **1927** - Use of X-rays in diagnostic medicine widespread. Müller discovers X-rays can damage chromosomes in fruit flies.

1928 International Commission of Radiation Protection (ICRP) set up

- **1928** - International X-ray and Radium Protection Commission created at Second International Congress of Radiology in Sweden to set criteria to protect humans from radium and X-rays (name changed to International Commission of Radiation Protection [ICRP] in 1950).

1929 National Council of Radiation Protection (NCRP) recommends ~25 mrem/yr maximum dose

1929 Radium dial painters contract bone cancer

- **1929** - U.S. Radiological Society sets up U.S. Advisory committee on X-ray and radium protection (predecessor of National Council of Radiation Protection [NCRP] set up in 1948 and chartered by congress in 1964) to present viewpoints to ICRP. NCRP recommends "tolerance dose" (similar to no observed adverse effect level [NOEAL] for hazardous chemicals) of ~ 25 rem/yr for X-rays and radiation from radium. Numerous cases of jaw sarcomas in women dial painters begin to appear and linkage to radium shown. Subsequent studies of internal doses to ~800 dial painters provide solid knowledge on long-term effects of alpha emitting radium in humans.
- **1941** - **May:** Because of request by U.S. Navy, NCRP sets maximum body burden of radium at 0.1μ Ci to avoid problems that occurred in WWI to dial painters as military prepares for war; NCRP also set maximum air concentration of radiation of 10 ρ Ci/l established at request of insurance company for factories making lantern metals.

1942 Manhattan Engineering District begins radioisotope toxicity studies

- **1942** - Fermi produces first artificial nuclear chain reaction. Manhattan Engineering District begins extensive study of radioisotope toxicity-uranium first radioisotope first studied.

1945 Atomic test in NM

- **1945** - Atomic bomb test at Trinity Site near Alamogordo, New Mexico monitored. Some monitoring of radioactive fallout occurs at Trinity test in Alamogordo, New Mexico; Manhattan Engineering District asks University of Washington to start experiments on radioactive effects on Columbia River fish near Hanford.

1948 Study of radiation conservatively suggestion observable threshold and thus finite risk at low dose

- **1948** - NCRP lowers maximum permissible occupational dose to ~15 rem/yr (40% reduction) recognizing any radiation exposure might represent a health risk. Suggests adopting "as low as reasonably achievable" NCRP (ALARA) policy for radiation exposure.

1954 Nuclear fallout contacts Japanese fisherman

- **1954** - Winds at high altitude carry fallout from atmospheric tests and contaminates inhabitants of Marshall Islands and Lucky Dragon Japanese fisherman; creates need for assessments and outcry to stop tests.

1955 First Atoms for Peace conference

- **1955** - First Atoms for Peace conference in Geneva overviews hazards of radioisotopes. Atoms for Peace programs stimulate nuclear medicine.
- **1957** - Epidemiological observations of radiation-induced leukemia shows no or very low threshold dose response.
- **1958** - Second Atoms for Peace Conference.
- **1959** - NCRP and ICRP lower maximum occupational dose to 5 rem/yr (factor of 3 lower) suggests 0.5 rem/yr for general population.
- **1960** - First of series of NAS reports on biological effects of atomic radiation (BEAR reports).
- **1965** - ICRP sets permissible average dose for public to 0.17 rem/yr (max still 0.5 rem/yr); and specifies limits on occupational dose.
- **1966** - Colorado public health discovers that uranium mill tails had been used as fill dirt around new homes in Grand Junction and Durango. Because of concern of radon, Federal government pays to remove tailings.
- **1967** - Oak Ridge studies radiological hazards from nuclear explosives if used for new canal in Panama (part of Plowshare Program); results not favorable.
- **1970** - NAS forms committee on biological effects of ionizing radiation (BEIR committee) funded by EPA.
- **1972** - Light-water reactor EIS uses ALARA principle.

1975 NRC adopts ALARA policy

- **1975** - NRC adopts ALARA policy for limiting radiation exposure.

1976 EPA set ~4 mrem/yr radioisotope limit for drinking water

- **1976** - EPA sets limits on radioisotopes when implementing Safe Drinking Water Act of 1974 (SDWA) to equivalent of ~4 mrem/yr (40 times less than ICRP and NCRP suggested limits) because "single pathway". Stringent level generates lots of discussion since radium levels in several parts of country exceeded this level.
- **1977** - ICRP changes from critical organ concept to weighted whole body concept for calculation dose; equated doses to risk (5 rem/yr similar to hazardous occupations 0.5 rem/yr similar to safe industries; 0.17 rem/yr similar to 10^{-4}/lifetimes).

Fig. 4. Studies and guidance on health effects of radiation.

risks of radionuclides that might enter either the atmosphere or the groundwater: The use of different models internal and external to the receptor remains. However, the strict use of conservative assumptions for the response model of humans[5] has remained, whereas probabilistic models have since been used in PRA and PA exposure pathway models.

[5] Occasionally, average response models may be used for other receptors in ecological risk assessments (61 FR 47552; 63 FR 26846). Recent evaluations of human dose–response uncertainty are noted in Section 5.2.

3. INFLUENCE OF COMPUTATIONAL TOOLS AND RELIABILITY ANALYSIS

The lack of experience with new technologies and their mode of failure, along with the potential

for physical harm and economic loss from such failures (or "accidents"), motivated reliability and system analysis in the 20th century.

3.1. Development and Application of Reliability Analysis to Aircraft

With the development of commercial aviation in the 1930s, the ability to predict the reliability of equipment was increasingly emphasized. Although the aircraft industry primarily relied on a build-and-test learning process, it began to explore ways to improve reliability beyond those gained from direct experience. In 1939, regulations in England specified 99.999% reliability (i.e., probability of success at 0.99999) for 1 hour of flying time for commercial aircraft[38] (Fig. 1). Although the regulation was relatively lenient in that it meant that the probability of failure could be as high as 10^{-5}/hr, it is possibly the world's first probabilistic regulation. This type of regulation required that the entire aircraft system be examined, along with the influence of its components on reliability. The regulation resulted in the development of safe but slow aircraft (1 million miles for the British Handley-Page biplane without a fatality).

3.2. Application of Reliability Analysis to Missiles

During the 1940s, the advent of computers allowed new problem-solving techniques to address issues of nuclear weapon design. An important practical tool developed at this time—Monte Carlo simulation—was used by the Manhattan Project for its work on the physics of weapons, specifically diffusion of neutrons through fissile material, as first reported in 1949.[39] Computers and Monte Carlo contributed to the design of the fusion nuclear bomb, which was detonated in a 1952 atmospheric test in the Marshall Islands at the Pacific Ocean proving grounds.

Development of a fusion explosive made feasible the delivery of a nuclear weapon by missiles—its size was small enough to fit into a missile warhead, whereas the explosive energy was large enough to compensate for the missile's inaccuracy at that time. In 1957, when the Soviet Union launched Sputnik, Congress allowed the Air Force to accelerate missile development.[40] But several missile failures during fueling in 1960 prompted the military to seriously examine reliability problems. The United States adopted reliability analysis, as practiced by the Germans in World War II to improve the reliability of their V-1 rockets, and greatly expanded the use of practical tools to improve the reliability of missiles (Fig. 5).[38,40] An important starting point of determining the reliability of a missile was examining the system as a whole, which engendered the field of systems engineering.[41]

Reliability analysis used block diagrams to describe how components in a large system were connected. From these block diagrams, Watson at Bell Laboratories developed the fault-tree technique, which he applied to the Minuteman Missile launch control system, and which Boeing later adopted and also computerized.[38,42] Reliability analysis required the first three steps of risk assessment: (1) characterization of the system, (2) evaluation of potential pathways to failure (i.e., hazard identification and scenario development), and (3) evaluation of the probability of failure through the measurement of component failure rates.

3.3. Development of Related Techniques in Policy Analysis

Cost–Benefit Analysis

A noteworthy attempt at large-scale policy analysis of a government project or action *before* initiation of the project occurred in 1936, when Congress mandated that the benefits and costs of flood control projects would be assessed prior to construction (Public Law 74-738). In response, the U.S. Army Corps of Engineers developed procedures for a cost–benefit analysis, which were later required for all water resource projects and some transportation projects. Only financial costs and benefits were assessed—not health risks—but the concept of collecting and analyzing data to assist in general policy analysis was developed and accepted. Furthermore, the cost–benefit analysis grew to include sociological factors in the 1960s. In the 1980s, both ecological and sociological risks were taken into account, although they could not always be clearly defined and quantified. Prompted by the requirements of National Environment Policy Act (NEPA; Public Law 91-190 [83 Stat. 852]), federal agencies began to include health risks in their analysis, as discussed in Section 4.2. Policy analysis and, specifically, risk–cost–benefit analyses can be abused when used to substantiate a preconceived view or justify actions already taken,[43]

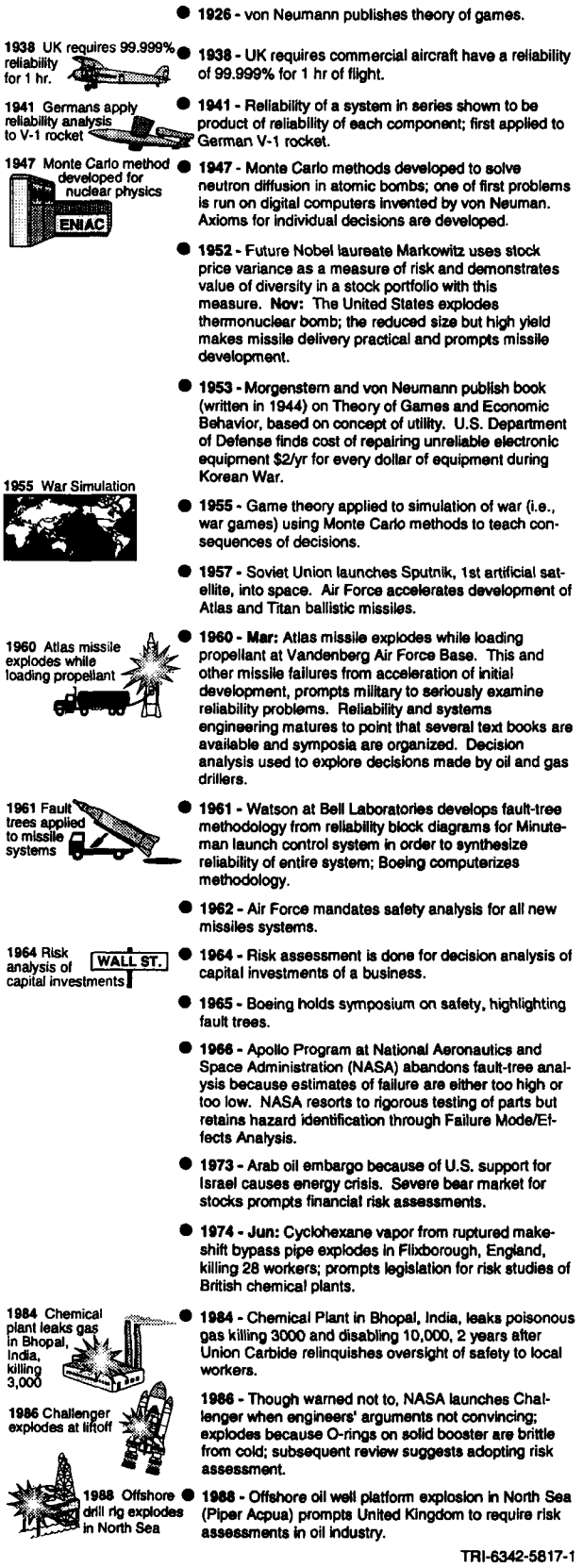

Fig. 5. Diverse applications of reliability analysis and risk assessment.

but evaluating uncertainty, peer review, full documentation, and open debate can all promote diligent and honest analysis.[13] Furthermore, in 1985, a philosophical evaluation of risk–cost–benefit analysis uncovered no fundamental ethical flaw with risk–cost–benefit analysis as input to decisions.[18]

Development of Decision Theory and Its Applications

Risk assessment, cost–benefit analysis, and decision theory share a similar early history and a similar purpose (i.e., aid in decision making). However, decision theory focuses on using the quantification of risk, along with other information, for management decisions, such as risk management. In 1738, Daniel Bernoulli introduced the concept of utility to express personal usefulness or satisfaction as an important concept of decision analysis. Other axioms for individual decisions were informally developed along with probability theory (Fig. 2). However, a more formal development occurred in the 1950s.[2] In 1953, economist Morgenstern and mathematician Von Neumann published the *Theory of Games and Economic Behavior,* which incorporated Bernoulli's utility concept.[2,22] Later, in the 1950s, decision theory benefited from Monte Carlo methods; for example, these methods appear in the game theory, especially the simulation of war, to teach the consequences of decisions.[44]

By 1964, a financial risk assessment was demonstrated to businesses for decision analysis of capital investment,[45] and textbooks were available by 1968.[46] In 1976, methods were proposed for making decisions with multiple, often conflicting, objectives,[47] and then applied a year later to determine the best location for nuclear reactors in Washington.[48] In 1986, this method was also applied to developing a portfolio of potential radioactive waste disposal sites for characterization.[49] Decision theory now includes concepts that attempt to logically resolve difficulties in making the optimal choice among options when (1) consequences of options are uncertain; (2) the decision has multiple, often conflicting, objectives; (3) multiple participants are involved in making the decision; and (4) there are intangible concerns. After the large stock market decline in 1973 and 1974, due in part to the Arab oil embargo, financial risk assessment began to gain more favor with investment firms. At that time investment firms began to seriously examine the academic work on portfolio selection (i.e.,

Markowitz's work in 1952 [Fig. 5]) to reduce investment risk, which in the investment world is associated with the second moment of the distribution of the returns or investments (variances).[6] The 1970s saw a dramatic increase in managing risk in mutual fund portfolios.[2]

4. EARLY RISK STUDIES FOR NUCLEAR FACILITIES

The application of reliability analysis to several components in nuclear facilities in the late 1960s led to large-scale, probabilistic risk studies for entire nuclear power plants in the 1970s. During this same period, the federal government began to investigate possibilities for disposal of nuclear wastes.

4.1. Adaptation of Reliability Analysis Techniques to Nuclear Power Plants

Through passage of the Atomic Energy Act of 1954 (Public Law 83-703 [68 Stat. 919]), Congress encouraged peaceful uses of atomic energy, specifically, electrical power production. An impediment to this development, however, was the inability to obtain liability insurance for public utilities, and so Congress agreed in the Price-Anderson amendments of 1957 to indemnify public utilities (Public Law 85-256). To do so, Congress and the AEC, which had been created by an earlier version of the Atomic Energy Act in 1946 (Public Law 79-585 [60 Stat. 755]), needed to know not only the reliability of a nuclear reactor but also the consequences of various types of failure. This need motivated the development of techniques for consequence evaluation, the fourth step in a risk assessment. As a result, in 1956, Pacific Northwest Laboratory (PNL) described semiquantitative effects of a major reactor accident and, in 1957, Brookhaven National Laboratory conducted a deterministic assessment of the financial risk to the federal government as part of the indemnification of the nuclear power industry[20,50] (Fig. 6).

Computational tools developed for reliability analysis were applied to assessments of nuclear reactors during the late 1960s. Specifically, in 1967, fault trees were applied to various nuclear reactor components and, in 1968, event trees were employed in the siting of those reactors.[51] Although neither fault trees nor event trees are an essential feature of risk assessment, they played an important role in improving the consistency of analyzing failure modes for nuclear reactors, similar to the block diagram's role in improving general reliability analysis. In 1969, C. Starr brought many aspects together in a risk–cost–benefit analysis to evaluate the social benefits and technological risks of nuclear power plants.[52]

4.2. Influence of National Environmental Policy Act

The National Environmental Policy Act of 1969 (NEPA; Public Law 91-190 [83 Stat. 852]) required federal agencies to consider the environmental consequences of any major action (such as decisions on development) and evaluate other options in an EIS. After passage of NEPA, the AEC prepared hearing rules for an EIS on the Calvert Cliffs reactor that limited the discussion of environmental impacts, but was quickly sued by the citizen group opposed to the reactor. In 1971, the U.S. Court of Appeals, District of Columbia Circuit, stated that environmental impacts must be given equal weight to economic and technical considerations in the EIS (449 F. 2d 1109). This and other court rulings established a large reservoir of case law that more clearly defined specific requirements based on the general policy statements in the legislation.[53] During the required hearings and written comment period, individual and special interest groups were able to express concerns with the adverse effects of large technological systems and a desire for more stringent analysis of all associated short- and long-term hazards to the physical environment and human health. These requests in turn stimulated many general and specific ecological studies and modeling advances. For the general EIS on lightwater reactors and especially for proposed nuclear facilities, NEPA indirectly stimulated the use by AEC of detailed mathematical modeling to predict the transport of radioisotopes in the environment, resulting population doses, and, ultimately, the risk consequences

[6] Variance as a measure of risk, rather than the expected value, corresponds to the oldest usage of risk noted by *The Oxford English Dictionary* (i.e., in 1776, Adam Smith in *Wealth of Nations* associated risk with financial uncertainty) (high variance that includes potential for loss) and the source of an entrepreneur's profit; safety was associated with certainty.[24] Both usages are still common.[29]

Fig. 6. Events influencing early risk studies for nuclear reactors.

- **1946** - Atomic Energy Act (AEA) of 1946:
  - creates Atomic Energy Commission
  - establishes government monopoly on atomic weapons and nuclear material (and eventually expectation to dispose of waste)
- **1948** - Construction begun on nuclear reactor for Navy.
- **1951 - Dec:** Experimental Breeder Reactor produces electricity.

- **1954 - Jan:** First nuclear submarine, Nautilus, launched. **Aug:** In AEA of 1954, Congress seeks peaceful uses of atomic energy; thus allows private but regulated atomic energy development.
- **1956** - Hanford reports on semi-quantitative effects of major reactor accident.

- **1957** - Windscale graphite reactor fire burns for 42 hr in United Kingdom (UK) and releases ^{131}I; milk consumption curtailed. Brookhaven National Laboratory (BNL) worst-case, deterministic risk assessment using expert opinion, is done to determine indemnification of nuclear industry (study similar to typical safety analysis). **Oct:** International Atomic Energy Agency (IAEA) formed to promote peaceful uses of nuclear energy. **Dec:** First large U.S. nuclear power plant operates at Shippingport, PA. To further encourage atomic energy use, Atomic Energy Damages Act ("Price-Anderson Act") sets up 2-tier insurance system for liability from accidents. First tier insurance purchased by each individual facility from private companies second tier insurance funded by premium on all facilities. (If claims exceed second tier then U.S. Congress would pay from public funds).

- **1967** - Fault trees applied to various components of nuclear reactors.

- **1968** - Event trees applied to siting of nuclear reactors. Decision analysis advances such that text books available.

- **1969** - Social benefits and technological risk of nuclear power plant estimated. Starr notes 1000-fold difference between voluntary and involuntary risks is accepted by the public and that voluntary risk is about equal to disease risk. National Environmental Policy Act (NEPA):
  - requires federal agencies to consider environmental consequences of any major action through an environmental impact statement (EIS)
  - one impetus for passage was proposed Calvert Cliffs reactor
  - requires public comment – avenue for citizen groups to push for stringent regulations for nuclear power
  - leads to citizens voicing expectation that government should protect against all long-term technological hazards (not just food and drug)
  - leads to assessing social benefits versus risks of technology
- **1971** - Appeals court requires AEC to look at *all* impacts in EIS on Calvert Cliffs reactor.

- **1972** - AEC Chairman Schlesinger asks for a probabilistic risk assessment (PRA) of severe accidents in nuclear reactors.

- **1973** - EIS for lightwater-cooled reactor is published (WASH-1258).
- **1974** - Congress splits AEC into Nuclear Regulatory Commission and Energy Research and Development Agency (ERDA). **Aug:** Draft of first major PRA published on two plants (Slurry and Peach Bottom) by 60-member team led by Rasmussen, MIT professor, for the Nuclear Regulatory Commission (NRC) *(Reactor Safety Study)*; method uses fault trees and event trees to synthesize probability of total system failure from estimates of component failure rates. American Physical Society (APS) begins review.

- **1975 - Mar:** Electrician sets cables on fire when using candle to check for air leaks below control room of Browns Ferry reactor in Alabama. **Apr:** Lewis publishes review of Reactor Safety Study draft for NRC: criticizes treatment of multiple failures, criticizes treatment of epistemic (degree of knowledge) uncertainties, but general approach applauded. **Oct:** Final of Reactor Safety Study released: probability of accidents (aleatoric uncertainty)
- **1975 (con't)** - higher than initially thought, consequences of accidents lower than initially thought, and suggests human errors could cause accident (Three Mile Island accident). APS review calls for more study of unknowns to correct potential errors in consequences and their probability and requests NRC to promulgate safety goals for reactors based on risk. **Jul:** Conover at Texas Tech develops Latin Hypercube Sampling (LHS) scheme for reactor pipe-break code at Los Alamos National Laboratory (helps make detailed modeling in stochastic simulations feasible).
- **1976** - NRC funds Sandia National Laboratories to apply event tree method to more plants (Calvert Cliffs-2, Grand Gulf-1, Sequoyan-1, and Oconee-3) but omits funding for new consequence modeling (Reactor Safety Study Method Application Program). SNL connects events from both loss-of-coolant and transient trees.
- **1977** - Decision analysis applied to siting nuclear power plants in Washington state. NRC funds SNL to evaluate risks of transporting nuclear waste — SNL develops radioactive material transportation model (RADTRAN) using event trees.

- **1979 - Mar:** Accident at Three-Mile Island Reactor occurs and partially melts fuel rods when valves fail (similar to failures in other reactors) and poorly trained operators misinterpret conditions on poorly designed readouts. In response to Three-Mile Island, NRC funds SNL to improve treatment of human actions in event trees and more detailed logic models for five plants (Crystal River-3, Browns Ferry-1, Arkansas Nuclear One-1, Calvert Cliffs-1, and Millstone-1) (Interim Reliability Evaluation Report). SNL finds support systems both contribute to and mitigate accidents. SNL issues RADTRAN II, generalized version for transportation risks of nuclear waste.
- **1980** - NRC begins to develop safety goals for nuclear power plants.
- **1981** - Zion Station probabilistic risk assessment includes external seismic and fire events, and site-specific meteorology, terrain, and evaluation routes. Kaplan and Garrick define risk using three components: scenarios, probability, and consequence ($R = \{S,P,C\}$).
- **1982** - State of New York funds PRA for Indian Point reactor.
- **1983** - NRC asks SNL to add external events, sabotage, cost/benefit analysis in PRA.

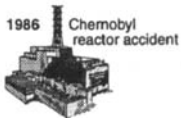

- **1986 - Apr:** Major accident at Soviet's Chernobyl reactor occurs during shut-down test; however, many emergency controls turned off by poorly trained operators. **Aug:** NRC promulgates safety goals for nuclear reactors similar to 40 CFR 191:
  - risk of prompt facilities < 0.1% of other accidents
  - risk of cancer death < 0.1% of other cancer deaths
  - suggests frequency of large release of radionuclides < 10^{-6}/yr
  - requires inclusion of uncertainty

  State of New Hampshire funds PRA for Seabrook Station. SNL issues RADTRAN III with several model changes to improve calculation of transportation risks.
- **1987** - NRC funds new study (NUREG-1150) to repeat and improve *Reactor Safety Study* "PRA".
- **1988 - Sep:** U.S. Congress amended AEA to set up Defense Nuclear Facilities Safety Board to evaluate safety of DOE defense facilities.
- **1989** - SNL issues RADTRAN IV, which uses route-specific information.

- **1990** - NRC completes new reactor risk study
  - adds detail event tree for containment
  - improves consequence analysis
  - improves analysis of uncertainties

  NRC funds SNL for LaSalle reactor PRA to get more detailed logic models and consistent treatment of uncertainties.
- **1994** - NRC funds SNL for detailed study of risks from low power/shutdown for Grand Gulf Reactor.

- **1995 - Aug:** NRC adopts use of PRA for setting policies.

of these activities, along with economic costs and benefits.

4.3. Application of Risk Assessment to Nuclear Power Plants

Reactor Safety Study

The new atmosphere created by NEPA encouraged AEC Chairman Schlesinger, a former economist at the Rand Corporation, to request, in 1972, a detailed analysis to evaluate risks from severe accidents at commercial nuclear reactors. By August 1974, a 60-member team led by N. Rasmussen, an MIT professor, drafted a report that defined hazards, estimated associated probabilities, and evaluated consequences[7] on the Surrey and Peach Bottom plants for the Nuclear Regulatory Commission[8] (NRC).[14] The *Reactor Safety Study* (or "WASH-1400" report) was significant because it was the first detailed, comprehensive, quantitative, probabilistic look at the health risks from a large, complex facility (Fig. 1). An early review of the draft in April 1975, however, did suggest that besides uncertainty in behavior of the system (i.e., uncertainty associated with event and feature conditions), which had been evaluated through event and fault trees, uncertainty associated with estimates for parameter values should be included.[54] A second review of the *Reactor Safety Study* by the American Physical Society[55] called for more study of uncertainties to correct potential errors in consequences and their probabilities and also requested that the NRC promulgate safety goals for reactors based on risk.

The final version of the *Reactor Safety Study,* released in October 1975, revealed that although the probability of accidents was higher than initially believed, the consequences of accidents were actually lower than first believed. The PRA used scenario classes rather than attempting to itemize every possible future and discovered an important scenario class for nuclear power plant operation—the potential for human error to transform a critical but controllable situation into a severe accident.[56] The *Reactor Safety Study* set a standard for risk assessments of nuclear reactors for the next 20 years. Two aspects of risk assessment for nuclear facilities were evident: (1) large multidisciplinary teams were needed to adequately explore all facets of the system and to present sufficient diversity of opinion to adequately capture uncertainty, and (2) the size of the resulting study required a dedicated multidisciplinary team of reviewers.

Because users of the PRA methodology were immediately compelled to consider uncertainties in parameters, efforts were begun to incorporate parameter uncertainty into the analysis. The Monte Carlo method was adopted for propagating uncertainty of parameters in a detailed code, and the LHS (Latin Hypercube Sampling) scheme was developed in 1975 to increase efficiency of samples.[57]

Although the move to assess probability and consequences of nuclear power plant accidents was a natural progression from the earlier analysis of system components, it also generated, and is still generating, considerable controversy, which is beyond the scope of this article. Opponents of the PRA questioned the ability of the analysis to meaningfully assess risk, much as opponents of cost–benefit analysis have challenged its capability to provide a worthwhile assessment of benefits and costs.[18]

Influence of Reactor Accident at Three Mile Island

On March 28, 1979, at 4 A.M., a clogged pipe in the second unit of the Three Mile Island Reactor initiated events that opened a pressure relief valve and inserted control rods that shut down the reactor to relieve pressure. Human errors and organizational failures compounded the problems caused by the clogged pipe, causing an accident severe enough to melt the fuel. Cleanup costs exceeded $1 billion.[5,58]

Although the exact sequence of events that caused the accident at the Three Mile Island Reactor was not in the *Reactor Safety Study,*[9] proponents of PRA emphasized that human error in combination with a loss-of-cooling event was indeed represented

[7] The 1975 *Reactor Safety Study* quantitatively defined risk as risk {consequence/time} = frequency {events/time} × magnitude {consequence/event}, from which evolved the notion within the risk profession (but not necessarily outside the profession) of risk as "probability times consequence" (i.e., expected adverse health effects per year).

[8] In 1974, the *Energy Reorganization Act* (Public Law 93-438) split the Atomic Energy Commission (AEC) into the Energy Research and Development Agency (ERDA) and the Nuclear Regulatory Commission (NRC).

[9] Those dealing with risk perceptions also like to use the various interpretations of the severe accident at the Three Mile Island Reactor as an example of how little individual perceptions change once formed and how new data are interpreted through these formed perceptions.[59,60]

in the scenario classes. Initially, the NRC had been concerned about using a PRA to support passage of regulations, but the incident at Three Mile Island eventually prompted the NRC to endorse the PRA method.[61] Specifically, in 1986, the NRC promulgated three safety goals for a nuclear reactor: (1) the probability of nuclear accidents must be less than 0.1% of all other types of accidents, (2) the annual expected value of cancer death within a 10-mile radius must be less than 0.1% of other types of cancer deaths (or $\sim 3 \times 10^{-6}$ yr^{-1} assuming normal cancer mortality of $\sim 3 \times 10^{-3}$ yr^{-1}), (3) the frequency of large release of radionuclides must be less than 10^{-6}/yr. Also, uncertainty was to be included in the estimates (51 FR 28044). Thus, 11 years after the American Physical Society had made the suggestion in its review of the *Reactor Safety Study*,[55] general safety goals based on risk were adopted. In 1990, the NRC concluded its update of the PRA for nuclear reactors[62,63] and, 4 years later, proposed extensive use of PRAs for setting policies within the NRC on all types of nuclear facilities (59 FR 63389; i.e., PRA was endorsed for policy analysis); the proposal was accepted in 1995 (60 FR 42622) and explicitly equated PRA with PA in the United States.

4.4. Other Assessments of Engineered Systems

The first applications of PRA and PA in other fields and industries were usually initiated as the result of accidents (see Fig. 5).

Assessments in Response to Accidents at Chemical Plants

In 1974, a make-shift bypass pipe ruptured in a chemical plant, killing 28 workers and releasing cyclohexane vapor into the town of Flixborough, England. The incident prompted the British to require risk analysis for chemical plants.[64] By 1980, an extensive risk analysis on the further expansion of the Canvey Island petrochemical complex near London had occurred. Eight years later, in 1988, an explosion on the Piper Acpua, an offshore oil well platform in the North Sea, prompted the British to require risk assessments in the oil exploration industry as well. Although assessments of risk at chemical plants had occurred within the United States, more extensive risk assessments within the chemical industry were encouraged as the result of a disaster in 1984 that killed 3,000 and disabled 10,000 near a Union Carbide chemical plant in Bhopal, India.[5,65]

Reevaluation of Risk Assessment After Challenger Accident

The explosion of the Challenger space shuttle in 1986 caused a reevaluation of risk assessment at the National Aeronautical and Space Administration (NASA). Similar to the missile program, NASA had adopted hazard identification through qualitative Failure Mode/Effects Analysis for the human space program in the 1960s. However, in 1966, the Apollo Program at NASA abandoned fault-tree techniques because estimates of failure were both too high and too low.[66] Thus, NASA abandoned risk analysis because of its imprecision, rather than continuing to refine estimates, but continued rigorous testing of components. As seen later with the Challenger explosion in 1986, the decision to abandon risk assessment allowed an unwarranted belief in the high reliability and safety of rockets for human space flight to evolve.[67] Consequently, when engineers intuitively sensed a dangerous situation for the Challenger during the launch at cold temperatures, their inability to quickly quantify and substantiate their intuition proved disastrous.[26] The subsequent review of the Challenger space shuttle accident suggested adopting risk assessment.[5,67,68]

4.5. Application of Probabilistic Risk Assessment to Nuclear Waste Repositories

Early History of Radioactive Waste Disposal

Initial disposal of radioactive waste by the Manhattan Engineering District in 1945 included burying solid nuclear waste in shallow trenches and augured holes at Los Alamos National Laboratory, New Mexico, and Hanford Reservation, Washington.[69,70] Although the newly formed AEC continued these practices, it tentatively explored more permanent solutions, beginning in 1955, when the AEC asked the NAS to examine the disposal issue. The 1957 NAS report[71] indicated that disposal in salt beds was the most promising method to explore, which it reaffirmed in 1961, 1966, and 1970.[70,72]

After tentatively selecting an abandoned salt mine near Lyons, Kansas, as a repository in 1970 (Fig. 7),[73] the AEC discovered the presence of drill

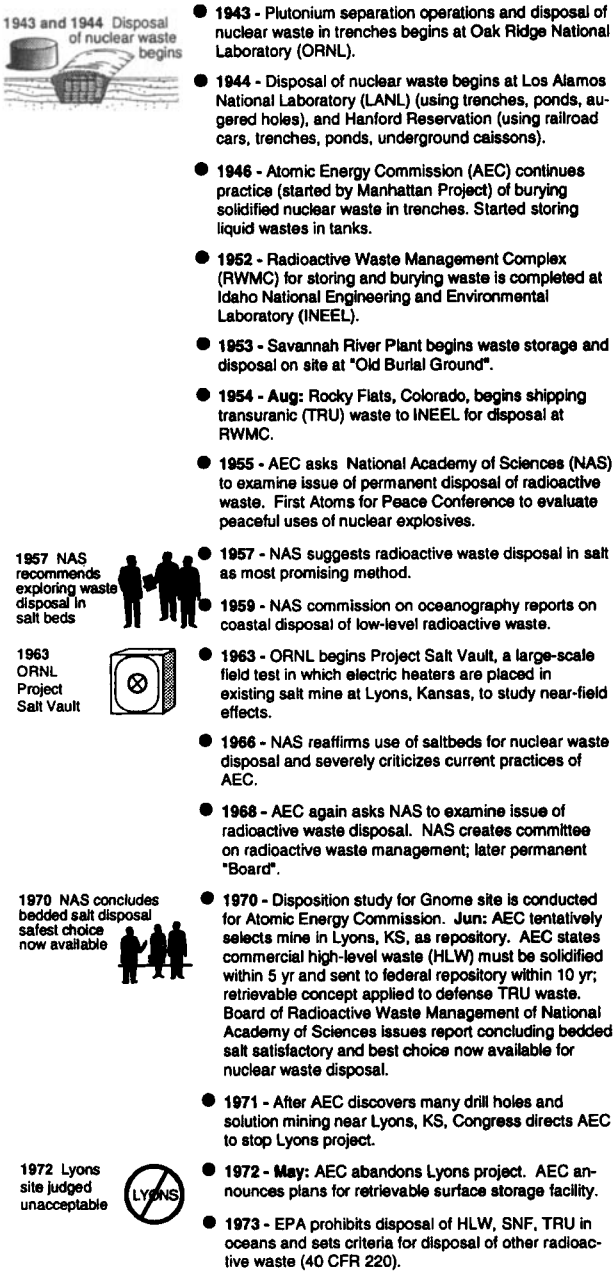

- **1943** - Plutonium separation operations and disposal of nuclear waste in trenches begins at Oak Ridge National Laboratory (ORNL).
- **1944** - Disposal of nuclear waste begins at Los Alamos National Laboratory (LANL) (using trenches, ponds, augered holes), and Hanford Reservation (using railroad cars, trenches, ponds, underground caissons).
- **1946** - Atomic Energy Commission (AEC) continues practice (started by Manhattan Project) of burying solidified nuclear waste in trenches. Started storing liquid wastes in tanks.
- **1952** - Radioactive Waste Management Complex (RWMC) for storing and burying waste is completed at Idaho National Engineering and Environmental Laboratory (INEEL).
- **1953** - Savannah River Plant begins waste storage and disposal on site at "Old Burial Ground".
- **1954 - Aug:** Rocky Flats, Colorado, begins shipping transuranic (TRU) waste to INEEL for disposal at RWMC.
- **1955** - AEC asks National Academy of Sciences (NAS) to examine issue of permanent disposal of radioactive waste. First Atoms for Peace Conference to evaluate peaceful uses of nuclear explosives.
- **1957** - NAS suggests radioactive waste disposal in salt as most promising method.
- **1959** - NAS commission on oceanography reports on coastal disposal of low-level radioactive waste.
- **1963** - ORNL begins Project Salt Vault, a large-scale field test in which electric heaters are placed in existing salt mine at Lyons, Kansas, to study near-field effects.
- **1966** - NAS reaffirms use of saltbeds for nuclear waste disposal and severely criticizes current practices of AEC.
- **1968** - AEC again asks NAS to examine issue of radioactive waste disposal. NAS creates committee on radioactive waste management; later permanent "Board".
- **1970** - Disposition study for Gnome site is conducted for Atomic Energy Commission. **Jun:** AEC tentatively selects mine in Lyons, KS, as repository. AEC states commercial high-level waste (HLW) must be solidified within 5 yr and sent to federal repository within 10 yr; retrievable concept applied to defense TRU waste. Board of Radioactive Waste Management of National Academy of Sciences issues report concluding bedded salt satisfactory and best choice now available for nuclear waste disposal.
- **1971** - After AEC discovers many drill holes and solution mining near Lyons, KS, Congress directs AEC to stop Lyons project.
- **1972 - May:** AEC abandons Lyons project. AEC announces plans for retrievable surface storage facility.
- **1973** - EPA prohibits disposal of HLW, SNF, TRU in oceans and sets criteria for disposal of other radioactive waste (40 CFR 220).
- **1976** - ERDA funds conference on modeling of geologic disposal systems to bring engineers and earth scientists together to explore predicting geological features, events, and processes. President Ford orders EPA to develop standards for permanent disposal of nuclear waste. **Oct:** Ford orders major expansion of ERDA program to demonstrate permanent disposal for nuclear waste by 1985 and orders EPA to develop standards, based on recommendations of interagency task force. **Dec:** NRC funds conference to develop generic list of potential hazards for repositories.
- **1977** - Geohydrology is important aspect of geologic isolation; hence, mathematical modeling of groundwater flow is required. **Feb:** In response to Ford's directive, EPA conducts 1st workshop to understand public concerns and technical issues of waste disposal.
- **1978** - NRC funds SNL to work on probabilistic PA and apply to hypothetical bedded salt repository (resulting method abandons fault trees and uses simple event trees). DOE funds SNL to work with Canadians, British, and other Nuclear Energy Agency (NEA) countries to analyze deep, subseabed disposal option. **Nov:** EPA publishes "Criteria for Radioactive Wastes" as guidance and seeks comments. U.S. Congress passes Uranium Mill Tailings Radiation Control Act to clean up mill tailings (90% federal funding) and control future use and disposal.
- **1980** - LHS is applied to sensitivity analysis for an assessment of the performance of a hypothetical geologic repository in bedded salt. Congress passes Low-Level Radioactive Waste Policy Act (LLRWPA) to allow states to form compacts to build several Low Level Waste (LLW) disposal sites.
- **1981** - Draft of final report to NRC on performance assessment (PA) is applied to hypothetical bedded salt repository readily available – uses a set of loosely connected codes, precursors to SWIFT_II (fluid flow code), and NEFTRAN (network transport code). **Mar:** Developing generic disposal criteria for radioactive wastes difficult, thus EPA starts developing standards for each waste type.
- **1982** - EPA drafts 40 CFR 191, defines PA, suggests use of complementary cumulative distribution function (CCDF) to show results.
- **1984 - Feb:** EPA's Science Advisory Board endorses probabilistic approach in 40 CFR 191 but states criteria too restrictive.
- **1985** - EPA promulgates 40 CFR 191 for disposal of SNF, HLW, and TRU waste:
  - probabilistic criteria indirectly based on population health risk
  - desires inclusion of all uncertainty in CCDF

  U.S. Congress amends LLRWPA to allow more time for states to form compacts and build LLW disposal sites.
- **1988** - SNL extends probabilistic PA method to hypothetical basalt repository for NRC. Subseabed team reports on use of local and regional embedded detailed models for simulating ocean currents for subseabed disposal (concept used for WIPP PA).

Fig. 7. Early risk studies for nuclear waste repositories to develop an assessment methodology.

holes and solution mining. The project was officially abandoned in 1972, and the AEC then announced plans for a Retrievable Surface Storage Facility. The EPA, formed in 1970, and antinuclear groups claimed in comments on the EIS that the retrievable storage facility was *de facto* permanent disposal, which prompted the AEC to continue to search for a suitable disposal site. Soon after, the AEC, ORNL, and U.S. Geological Survey (USGS) recommended the large salt beds of southeastern New Mexico,[70] which would eventually host the Waste Isolation Pilot Plant (WIPP) discussed in Section 6.

Development of Risk Assessment Methods for Nuclear Waste Repositories

As discussed here, the method that was conceived and accepted by the engineering community

in the United States, and by the EPA and NRC as regulators for evaluating the acceptability of a disposal system, was a probabilistic PA. In this respect, PAs in the United States remained similar to "Level 3" PRAs for nuclear reactors in which offsite health risks are evaluated.[61–63,74] The PA method was first described in a 1981 draft report submitted to the NRC (final report, 1987)[75,76] for a hypothetical bedded salt repository. The method was somewhat similar to an all-encompassing total system approach that had been proposed earlier by geoscientists at PNL.[77] What follows in this section are concepts specifically developed by the NRC at that time. Applications are discussed in Section 6 and in Helton *et al.* (this issue).

System Definition/Characterization. In 1976, the ERDA (Energy, Research, and Development Administration, a precursor to the DOE) sponsored two conferences to bring together two groups of professionals: nuclear engineers familiar with the recently developed PRA methodology for reactors and earth scientists familiar with the uncertainties of geologic investigations[78] (Fig. 1). At the time, other countries were also addressing the need for nuclear waste disposal and, in 1977, the International Atomic Energy Agency (IAEA) recommended site selection criteria.[79] The ERDA conferences provided an opportunity to exchange viewpoints among representatives from various disciplines and produced ideas about how to perform an assessment for a geologic disposal system, which were examined in the following years by the NRC.[77] In general, the proposed method sought answers in the form of system engineering analysis, rather than a conceptual analog model, by developing a mathematical model, $C(\cdot)$, and an appropriate parameter space, $\mathbf{x} = \{x_1, x_2, \ldots x_{nP}\}$, where nP is total number of parameters. Because of the inclusion of natural components (components that do not "fail" but rather evolve) and the need to evaluate the interaction of the natural component with engineered components, earth scientists pointed out that the mathematical model had to analyze basic natural phenomena over long periods.[78] The blending of the disciplines to produce a performance assessment has not been without tension. Ewing *et al.*[80] continue the dialog among various disciplines in this special issue.

Hazard Identification and Scenario Development. For hazard identification (or risk identification as it was called by Rowe[81]), an initial, generic list of features, events, and processes (FEPs) (i.e., "universe") is defined for consideration in the assessment. Although hazard identification is a part of all risk assessments, the formality with which FEPs are selected for inclusion in modeling is distinctive of PAs and PRAs.

In a companion draft report to the NRC also available in 1981 (final report published in 1990), Cranwell *et al.*[82] proposed a method to screen out unreasonable FEPs, and form a limited number of scenarios based on only discrete events and features, not processes. Other early efforts included the generation of a starting list of FEPs that was developed by a panel of scientists and engineers supporting the NRC in 1976–1977[76,82]; an international effort on hazards by the IAEA in 1981[83]; and development of scenarios for a hypothetical repository in basalt in 1983.[84] In developing scenarios, the parameter space was conceptually divided into two subsets, $\mathbf{x} = [\mathbf{x}^s, \mathbf{x}^P]$, although not described in those terms at the time. One subset included the parameters that defined certain conditions for a scenario, $S_j \subset \mathbf{x}^s$, that an analyst may want to highlight in the analysis (or because the Monte Carlo integration to evaluate the uncertainty was easy to perform separately for this subset). For example, for the WIPP, discussed in Section 6 and Helton *et al.* (this issue), S_j defined conditions for human intrusion and location of a brine reservoir, respectively.[9,85] The second subset contained the remaining parameters.

Probability Evaluation. For parameter uncertainty, ideally, a joint probability density function is defined, $D(\mathbf{x}^p)$, but $D(\mathbf{x}^p)$ is usually represented by $D_1(x_1^p) \cdot D_2(x_2^p) \ldots \cdot D_{nU}(x_{nU}^p)$, where the individual parameter density functions are assumed independent and nU is the number of uncertain parameters. To propagate parameter uncertainty through the analysis, the LHS technique was proposed in 1978.[75,76,86,87]

At first, the NRC insisted that Sandia, as contractor to the NRC, directly apply the techniques of the *Reactor Safety Study*[14] with only minor modification to calculate the probability of the scenarios, $P_r\{S_j\}$, mentioned here. However, discretization of a geologic disposal system by means of event and fault trees was not a simple task for the highly coupled system, as experienced by the WIPP Project[88] (see also Section 6). Eventually, it became clear that calculating probabilities of scenarios of a geologic system from fault trees was not practical.[89] In the late 1970s and early 1980s, an ad hoc assignment of probabilities of parameters and scenarios was used because initially only hypothetical sites were studied.

Consequence Evaluation. The consequence modeling for the hypothetical salt repository proposed in 1981[75] consisted of an exposure pathway assessment using a model comprised of loosely con-

nected series of codes (precursors to the finite-difference flow code, SWIFT II, and the network transport code, NEFTRAN[75]) specifically designed for the task. The study simulated a steady-state groundwater flow field, evaluated a particle pathway, and then calculated radioisotope transport along this pathway from a simple source. Because the implementation of a numerical solution for the partial differential equations describing radioisotope transport was difficult in practice, a single pathway or network transport code was used. A similar consequence evaluation was also completed in 1988 for a hypothetical disposal site in basalt.[90]

Sensitivity/Uncertainty Analysis. A feature that was adopted early in PAs of hypothetical repositories[75,76] was the inclusion of a sensitivity analysis. This type of analysis explored the individual parameters, x_n, and model forms (e.g., $f_\alpha(\cdot)$) that most influence the regulatory criteria discussed as follows.

Regulatory Criteria

Society's definition of acceptable risk from geologic disposal (i.e., society's "utility") was evaluated over the same period as various analysis tools for the PA process were being developed. In 1977, the EPA conducted several public meetings to develop societal consensus on regulatory criteria (41 FR 53363; 43 FR 2223). Initially, the EPA proposed generic criteria on all radioactive waste in 1978 (43 FR 53262), but after receiving generally unfavorable responses, they withdrew the proposed regulations in March 1981, and began developing standards for individual categories of radioactive waste.

In 1982, in response to a requirement in the Nuclear Waste Policy Act of 1982 (Public Law 97-425), the EPA published a draft of the nuclear waste disposal regulation in Title 40 of the Code of Federal Regulations Part 191 (40 CFR 191; 47 FR 58196), which had already undergone more than 20 revisions. The EPA did not promulgate the final version of 40 CFR 191 until 1985 (50 FR 38066), 3 years after submitting the proposed regulation, and then only after drawing a lawsuit to hasten its promulgation.[10] The 40 CFR 191 Standard established criteria for the disposal system as a whole and specified PA as the type of calculations to be used to show compliance with this regulation.[11]

The analysis conducted in support of regulatory standards for deep geologic disposal[30] convinced the EPA that the risks to society from such a disposal method were low. Furthermore, the EPA argued that very stringent requirements could be placed on the disposal system without adding substantially to the initial cost (50 FR 38066; i.e., the EPA indirectly adopted an ALARA policy). Thus, the EPA considered maintaining equity of risks and benefits between generations over a very long regulatory period (10,000 years) with regard to radioactive waste disposal, even though other potentially hazardous activities, such as disposal of hazardous chemicals or coal fly ash from utilities, could not sustain such an expensive program. Even considering the proposition of intergenerational equity, however, the EPA's Science Advisory Board (SAB) claimed in their review of the analysis that the release limits were an order of magnitude too stringent.[91] Furthermore, the regulations assumed a static society (i.e., using current technology during the 10,000-year period), which added another level of conservatism. (This is a conservative assumption provided one accepts the proposition that the waste is most hazardous to a society living under current conditions rather than one with a lesser or greater degree of technological prowess.) A compilation (Okrent, this issue) of the reviews and philosophical discussions held during the development of 40 CFR 191 gives the reader more background on the regulatory spirit of 40 CFR 191.

The need to model natural components over long time periods encouraged development of probabilistic performance criteria in 40 CFR 191 to account for uncertainty in characterization knowledge. For a mixture of radioisotopes, the EPA required the sum of all releases $C(\mathbf{x}^P)$, where each radioisotope (i) is normalized with respect to its radioisotope limit (L_i), should have less than 1 chance in 10 of exceeding 1 and less than 1 chance in 1,000 of exceeding 10 (50

[10] Changes in the 1985 final version of 40 CFR 191, primarily the Individual and Groundwater Protection Requirements, led to a lawsuit by the same group, the Natural Resources Defense Council, that had sued earlier to accelerate promulgation. The courts remanded the regulation shortly thereafter (as reported in Vol. 824 of Federal Reporter, second series [824 F.2d. 1258]), but the EPA repromulgated the standard in 1993 for the WIPP without changes to the most influential section, the Containment Requirements (58 FR 66398).

[11] Specifically, PA was defined as an "analysis that (1) identifies the processes and events that might affect the disposal system; (2) examines the effects of these processes and events on the performance of the disposal system; and (3) estimates the cumulative release of radioisotopes, considering the associated uncertainties caused by all the significant processes and events. These estimates shall be incorporated into an overall probability distribution of cumulative release to the extent practicable" (50 FR 38066).

FR 38067; 58 FR 66398; Fig. 8). The EPA specified radioisotope limits (L_i) so that only an exposure pathway assessment was needed for the consequence analysis. Adhering to tradition, the dose–response assessment performed by the EPA to determine L_i depended on bounding-type dose evaluations[30]; thus, a PA in the United States is not entirely probabilistic. Moreover, they specified an evaluation of cumulative releases of radioisotopes (Q_i), which required the EPA regulator to convert through crude calculations from dose, which depends on rate of release, to obtain the allowable L_i.[30] The EPA rejected dose as the primary requirement because its use might encourage disposal near large bodies of water to allow for dilution (47 FR 58196) or disposal in numerous small repositories. A dose criterion was also believed to encourage expensive engineered containers, a situation that has indeed occurred at the potential Yucca Mountain repository, as discussed in Section 6.2.[30,92] For comparison to limits in 40 CFR 191, uncertainty in the cumulative normalized release was displayed as a complementary cumulative distribution function (CCDF) (Fig. 8). Thus, the risk measure was not the first moment of the distribution (the expected value of the results) or the second moment of the distribution (the variance of the results, as in risk analysis of stock portfolios).[2] Instead, the entire distribution of the results was used.[12]

5. RISK ASSESSMENT FOR HAZARDOUS CHEMICAL EXPOSURE AND DISPOSAL

Assessments of health and environmental issues show great variability in their comprehensiveness and use of the general steps of a risk assessment. The desires of Congress, and its responses to several important environmental issues, have influenced the comprehensiveness of such assessments. Furthermore, the focus of many assessments is on only one of the general steps (i.e., evaluating the dose response of a receptor to a chemical agent). For example, in 1993, the National Academy of Public Administration (NAPA) reported that 7,579 risk assessments had been conducted by the EPA. Most (6,166 assessments) were small 2-day assessments to screen potential chemical carcinogens; only a few of the assessments were extensive, requiring 1 or 2 years to complete and costing more than 1 million each.[93]

With such a large and diverse population of risk assessments for health and environmental issues, this article does not attempt a direct comparison between assessment techniques, but rather, juxtaposed health and environmental issues, including chemical carcinogens in foods, air pollution, hazardous waste disposal, and pesticides, and of the varying legislative and regulatory responses with issues of nuclear facilities. In contrast to nuclear facilities, risk assessment has not been consistently accepted as valuable input to policy decisions or regulatory control for other types of hazards. Furthermore, there has been no mandate to include uncertainty in the analysis, and thus these risk assessments have evolved outside the traditions of reliability analysis (Fig. 1). Instead, these assessments have generally used plausible upper bounds for parameter values.[74]

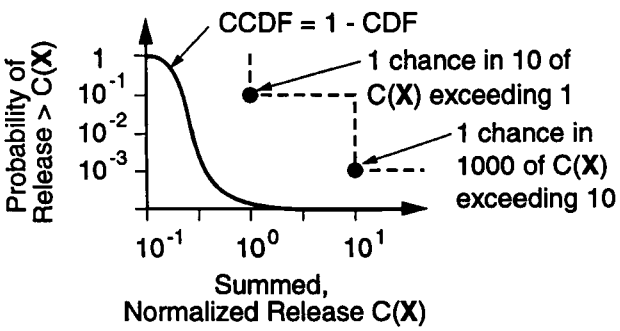

Fig. 8. In the United States, the uncertainty in a PA is expressed as a CCDF and compared with the limits in 40 CFR 191.

5.1. Dose–Response Assessments by the FDA

At about the same time as evidence accumulated about X-ray and radium exposure, some scientists hypothesized that no threshold might also apply to chemical carcinogens.[17] The FDA initially adopted safety factors of 2,000 and then 5,000, but in 1950 it banned two artificial sweeteners when animal tests demonstrated carcinogenicity.[27] Then, the FDA proposed to allow use of a carcinogenic pesticide "Aramite" (see 968 F. 2d 985). Congressional response to this chemical carcinogen hazard was the passage of the Food Additive Amendment in 1958, which contained a "Delaney Clause" that prohibited the intentional addition of additives to processed foods that induced cancer in animals or humans[3] (Public Law 85-929). A similar provision was added concerning food coloring in 1960 (Public Law 86-618; Fig. 9). In essence, Congress stated that no exposure to a carcinogen through processed food was safe, and thus only hazard identification was required. However,

1958 Congress passes Delaney clause for food additives

- **1958 - Sep:** U.S. Congress passes Food Additive Amendment containing "Delaney Clause" prohibiting human-made additives in processed food that induce cancer in animals or humans.
- **1959 - Nov:** U.S. Dept of Health and Human Services secretary, Flemming, tells people not to buy cranberries because aminotriazole pesticide residue might remain, might cause cancer, and was prohibited under "Delaney Clause." Farmers lose $40 million.
- **1960** - National Cancer Institute (NCI) begins testing of common chemicals for carcinogenicity.
- **1964** - Center for Disease Control (CDC) Surgeon General report links smoking with numerous health problems especially lung cancer.
- **1970** - Based on U.S. Food and Drug Administration (FDA) studies and World Health Organization (WHO) findings, National Academy of Sciences proposes limiting saccharin consumption to 1g/day.
- **1971** - FDA calls for gradual removal of saccharin from foods.

1973 FDA proposes risk assessment for evaluating de minimis cancer risk

- **1973** - FDA proposes risk assessment 1 chance in 100 million as de minimis for cancer risk of drugs given to food animals.
- **1974** - Israeli psychologists report on the irrational behavior of humans when managing risk and uncertainty: framing decisions as losses or gains changes risk aversion (aversion to losses); individual experience very small sample size; humans ignoring *a priori* probabilities; humans adverse to ambiguity, etc. Based on new studies, NAS reports saccharin neither highly hazardous nor entirely safe.

1976 EPA publishes risk assessment guidelines

- **1976** - EPA publishes first guidelines on carcinogenic risk assessment.

1977 FDA attempts to set 10^{-6} cancer risk as cut-off

- **1977** - Joint Canadian/U.S. study on saccharin released showing some bladder tumors in male rats. Canada bans saccharin but U.S. Congress passes moratorium on removing saccharin from foods. FDA promulgates but regulation remanded de minimis cancer risk to 1 in 1 million.
- **1978** - U.S. Department of Health and Human Services starts National Toxicology Program (NTP) to coordinate all chemical tests for carcinogenicity in animal studies.
- **1979** - FDA again proposed to use a de minimis cancer risk of 1 in 1 million and use a no threshold, linear extrapolator to develop a dose-response curve for potential carcinogens. Interagency Regulatory Liaison Group, formed by major agencies to coordinate identification of carcinogens and estimate risk, recommends procedure on risk assessments (Regan abolished before draft could be revised in response to public comments).

1980 Supreme court rules OSHA must use risk assessment, suggests between 10^{-3} to 10^{-9} bound on cut off risk

- **1980** - International Society for Risk Analysis formed. **Oct:** Supreme Court rules that the Occupational Safety and Health Administration must use risk assessment before regulating workplace hazards such as benzene; also states 10^{-3} risks of concern but 10^{-9} risk of no concern.

1983 NAS issues "red book" on chemical risk assessments

- **1983 - Mar:** NAS publishes report that endorses four steps of risk assessment and issues summary on chemical carcinogenic risk assessment for setting federal policy for FDA.

1986 EPA revises carcinogenic risk assessment guidelines

- **1986 - Sep:** EPA completes guidelines for evaluating the dose-response of carcinogens (carcinogen risk assessments) that calls for characterizing uncertainty.
- **1987** - P. Slovic has public and experts separately rank 30 activities for perceived risk. Public ranks nuclear power 1st; experts rank 20th. Both rank cars, smoking, alcohol, and handguns as risky. **Dec:** FDA promulgates rules for a risk level at 10^{-6} of straight line extrapolation when making dose assessments for potentially carcinogenic food additive for cattle, etc.
- **1989 - Feb:** NAS publishes book on ways to improve dialogue on risk.
- **1990** - Mechanistic models show carcinogens that do not interact with deoxyribonucleic acid (DNA) may have nonlinear or threshold dose response.
- **1991** - CDC studies on dioxin indicate very weak carcinogen, thus Times Beach evacuation may have been unnecessary.
- **1994** - As required by CAAA of 1990, NAS committee on air pollutants publishes summary on scientific judgment in risk assessments and concludes EPA risk assessment approach sound but uncertainty estimates not calculated. EPA releases dose-response assessment on dioxin suggesting a spectrum of possible effects, some observed in cells at low doses.

1996 EPA again revises carcinogenic risk assessment guidelines

- **1996 - Apr:** EPA proposes revisions to the guidelines for evaluating the dose-response of carcinogens ("carcinogen risk assessment") based on comments by 1994 NAS report.

Fig. 9. Events influencing evaluation of chemical carcinogens at FDA and risk communication.

the requirement specification that no potentially carcinogenic, human-produced chemical could be intentionally added to *processed* food created gross inconsistencies in policy because different legal treatment of carcinogenic and noncarcinogenic chemicals was mandated.[17]

By the 1970s, an evaluation of consequences from chemical carcinogens, in addition to identifying the potential hazard, was considered necessary in some cases, although a risk assessment could still only highlight—not correct—the discrepancy in policy. In 1976, Lowrance described four steps of risk assessment that emphasized the dose–response aspect of chemical hazards (1) define the conditions of exposure, (2) identify the adverse effects, (3) relate exposure to effect, and (4) estimate overall risk.[4][12]

In the 1980s, the use of risk assessment as a decision-making tool received Congressional support. In 1981, Congress directed the FDA to contract

[12] Lowrance also defined the concept of "safe" as used herein, "a thing is safe if its risks are judged to be acceptable." This was somewhat similar to the relationship of safety and risk introduced in the 1925 *Standard Methods for the Examination of Water and Sewage,* 7th ed., by the American Water Works Association,[25] which commented that "to state that a water supply is 'safe' does not necessarily signify that absolutely no risk is ever incurred in drinking it . . . but the total incidence of diseases has been so low that . . . the risk of infection through them is still very small compared to the ordinary hazards of everyday life."

with the NAS to study risk assessment in the federal government. The purpose of the study was to assess the merits of separating the analytical functions of risk assessment from the regulatory functions, consider the feasibility of a single agency performing all federal risk assessments, and consider the feasibility of developing uniform guidelines for all federal risk assessments. In March 1983, the NAS committee reported on its findings concerning risk assessment for cancer from toxic substances; the committee only indirectly considered risk assessment for other types of hazards. The report defined the risk assessment process using the four basic steps that the FDA (and the EPA) still use for their carcinogenic assessments[3]: (1) hazard identification, (2) dose–response assessment, (3) exposure assessment, and (4) risk characterization. Sensitivity analysis was not discussed. Interestingly, the assessment of probabilities (either of various events or parameters) was also omitted, although probability was indirectly referenced with regard to dose response for carcinogens. The NAS recommended developing uniform guidelines for risk assessments and risk management functions, making a clear distinction between the two functions. By this time, a shift in terminology had occurred. Ten years earlier, Otway (1973)[94] defined risk assessment in a manner similar to the current definition of risk analysis. In Otway's definition, a risk assessment consisted of both risk estimation (the NAS definition of risk assessment) and risk evaluation (the NAS definition of risk management).

The FDA had been struggling to define guidelines for assumptions for dose–response assessment and the meaning of significant risk in one particular area for more than a decade. In 1962, Congress amended the Food, Drug, and Cosmetic Act to allow use of potentially carcinogenic drugs in feed or injections for food animals provided no residue could be detected in the edible tissue, "the diethylstilbestrol (DES) proviso" (Public Law 87-781). Between 1962 and 1973, the FDA tested for potentially carcinogenic chemicals using a variety of analytical techniques on a case-by-case basis. However, during the 1960s, the analytical detection methods dramatically improved such that, by 1972, evidence of most drugs administered to animals could be found in edible tissue through radioactive tracer studies[27] (44 FR 17070). Hence, in July 1973, the FDA proposed using risk as a guideline rather than specifying a particular analytical technique to detect residues. The first proposed regulation used a probit-log transformation to establish a dose–response curve as a default inference that may or may not have had a threshold and defined significant risk as a chance of cancer greater than 10^{-8} over a lifetime using this curve[95] (38 FR 19226). This was the first proposed regulatory use of low-dose extrapolation, even though it had been in academic use since 1960.[27] In February 1977, the FDA promulgated this guidance but changed the risk limit to 10^{-6} over a lifetime (42 FR 10412). Because the cost of testing was a contentious point,[3] the FDA was sued by the Animal Health Institute. The regulations were remanded by the U.S. District Court in the District of Columbia in February 1978, and revoked by the FDA in May (43 FR 22675). In March 1979, the FDA proposed similar regulations; however, the FDA changed to straight-line extrapolation as the default method for developing the dose–response curve (44 FR 17070). A risk limit of 10^{-6} and straight-line extrapolation were finally adopted in December 1987 (52 FR 49586; 21 CFR 500, Subpart E).

Also during the 1970s, the FDA was confronted with two other notable carcinogens: the artificial sweetener, saccharin, and aflatoxin, found in peanut butter. In both instances, the FDA evaluated a dose–response curve and compared it with its 10^{-6} risk limit to help explain the decisions to ban saccharin in 1977 (42 FR 19996), while continuing to permit contamination of peanut products with aflatoxin in 1974 and 1978 (39 FR 42748).

5.2. Risk Assessment for Health Issues at EPA

Formation of the EPA

Congress formed the EPA in 1970, transferring to it responsibilities of research, monitoring, standard setting, permitting, and enforcement activities related to the environment (40 CFR 1). The role of standard setting somewhat differentiated the EPA from other "permitting" agencies, such as the NRC. Also, Congress greatly expanded the public's ability (later enlarged by the courts) to influence the process of setting standards. Lawsuits about EPA standards were permitted by citizens or special interest groups, with legal expenses paid by the federal government if the suit was successful, and EPA regulations were made purposely accessible to the public through numerous avenues such as comment periods. As pointed out by political scientists,[96] the increase in public participation broadened the arguments, but also accentuated the difficulty of making decisions. Hence, procedures for

setting standards became important and risk assessment, with its well-defined process, was gradually adopted for determining risks when setting standards and policy and as input for decisions.

Yet, even with these general motivating factors, the movement to use risk assessments as input to decisions was not uniform or consistent within the EPA (or across other government agencies). Although the administration of environmental law rested with one agency after 1970, Congress continued the practice of creating legislation that dealt with only one medium at a time (e.g., air, water, or soil). Hence, the EPA's management structure and programs remained fragmented, and risk assessments would often be narrowly focused without considering overall risk.[93] Furthermore, environmental laws were prescriptive, requiring a command-and-control approach,[43] so that the EPA had little flexibility in what could or could not be considered when setting environmental goals.

Controlling Pesticide Use

Congress had exercised some control of pesticide use since the 1900s (e.g., Insecticide Act of 1910; Publication 48 in U.S. Statutes, Public Law 6-152 [36 Stat. 331]), but pesticides were not used extensively in the early 1900s and so the enforcement of the law was lax.[53] The development and use of manufactured chemicals during World War II jump-started their proliferation in the late 1940s. The widespread use encouraged Congress to pass the Federal Insecticide, Fungicide, and Rodenticide Act (FIFRA) in 1947 (Public Law 104 [62 Stat. 163]) for registration and management of the chemicals, but the new law was still largely ineffective.[53]

Significant public concern for the effects of long-term chemical use occurred after the 1962 publication of *Silent Spring* by Rachel Carson,[97] which condemned pesticides such as DDT and argued for strong government control. This desire for regulation of pesticides was a major impetus in the formation of the EPA.[53,98] DDT, a pesticide with low toxicity to most mammals, had a remarkable ability (because it was both effective and inexpensive) to control mosquitoes and thereby malaria, and its synthesis in 1939 had earned its creator, Müller, a Nobel Prize in medicine. However, the discovery of biomagnification in 1960 for persistent chemicals such as DDT,[4,99] the discovery of eggshell thinning in raptors in England in 1967 from DDT, and the synthesis of other more expensive but less persistent pesticides, led EPA's first administrator, W. D. Ruckelshaus, to overturn an administration hearing's conclusion and ban DDT in the United States in 1972 (37 FR 13369). Also, in 1972, Congress rewrote FIFRA, which strengthened the EPA's control of pesticides. However, FIFRA required economic and social benefits to be considered as well as environmental and health risks. By 1975, the use of two other major pesticides, aldrin/dieldrin and chlordane/heptachlor, was suspended, based primarily on qualitative arguments of health versus social benefits. Scientific information was gathered only during adversarial hearings.[98]

Dose–Response Assessment Guidance for Carcinogens by EPA

In the summary of the administrative hearings on suspended pesticides (e.g., DDT), the attorneys for the EPA implied that only a total ban of useful but potentially carcinogenic pesticides was permissible. These "cancer principles," as they were called, were widely criticized.[3,27,98] Partly in response to the broad criticism of the cancer principles,[100] the EPA produced its first guidelines on assessments in May 1976 for evaluating the carcinogenic potential of a chemical; the EPA termed the evaluation a carcinogenic risk assessment (41 FR 21402). These guidelines were used to evaluate toxic air pollutants, toxic water pollutants, hazardous waste chemicals, and pesticides under the following acts: Clean Air Act (CAA); Federal Water Pollution Control Act (FWPCA); the FIFRA; the Resource Conservation and Recovery Act (RCRA); and the Comprehensive Environmental Response Compensation and Liability Act (CERCLA), discussed later in this article.

The 1976 guidelines proposed a two-step process: hazard identification, followed by risk management to decide whether and how to mitigate hazards. The two steps mirror the concept contained in the "Delaney Clause" that any exposure to carcinogens is unsafe. However, the guidelines stated that risk assessment was part of the second step. Hence, an important transition occurred with regard to recognizing the impracticality of enforcing zero risk from useful chemicals. Yet, by 1983, the transition was not complete nor was tension dispelled over the concept of an "ample margin of safety" (as specified in the Clean Air Act Amendments of 1970 [Public Law 91-

604], discussed in the next section) and risk assessment.[98] Furthermore, the EPA was embroiled in concerns about asbestos in schools[101] and the high rate of potential cancer deaths that had been purported in a draft epidemiology study in 1978, which indicated that 17% of all future cancer deaths would be caused by asbestos.[99] Hence, in June 1983, just 1 month after taking over as EPA administrator for a second time, W. D. Ruckelshaus strongly encouraged the EPA to increase its use of risk assessment in its policy decisions, as endorsed by the March NAS report,[3] and to include a discussion of uncertainty[7] (Fig. 1).

In 1986, the EPA extensively revised the carcinogenic risk assessment guidelines (51 FR 33992), providing guidance on default inferences to use when bridging gaps in knowledge and data for evaluating the carcinogenic potential of a chemical or estimating the dose response, as recommended by the NAS in 1983.[3] In contrast to the FDA's method, the EPA suggested a slightly more complex, linear, multistep model for extrapolating responses to low doses that had been used by the EPA since 1980.[98,102] Similar to straight-line extrapolation, the model was believed to provide a plausible upper bound to dose response in humans. In 1996, the EPA again revised the carcinogenic risk assessment procedures in response to suggestions by the NAS[103] and as mandated by the Clean Air Act Amendments of 1990. The scheme for weighting evidence indicating whether a chemical was a carcinogen was modified, descriptors for categories of potential carcinogens were changed, and the method of developing the dose–response curve was altered so that it included a simple linear extrapolation as a default option, similar to the FDA's method. Despite the EPA Administrator having encouraged an increased use of uncertainty on risk assessments in 1983,[7] the NAS committee on Hazardous Air Pollutants concluded more than 10 years later that uncertainty estimates were still not calculated routinely in EPA risk assessments.[93,103] Hence, the 1996 guidance attempted to explicitly require at least a qualitative description of uncertainty in the assessment. However, in May 1997 the EPA explicitly requires bounding estimates when evaluating human dose response.[103a] Although the report is still in draft, also in 1997, the EPA explored evaluating the uncertainty in the human dose response for radiation and radioisotopes, for which much data have been collected (see Section 2.4; 62 FR 55249; 63 FR 36677). This effort was similar to the uncertainty evaluation also done by the NCRP in 1997.

Factors of Protection for Noncarcinogens

In 1977, in a study mandated by the Safe Drinking Water Act of 1974, NAS recommended an approach for noncarcinogens similar to that adopted by the FDA in 1954, by suggesting a factor of protection of 100 when estimating ADIs for contaminants in drinking water. Furthermore, they added another factor of 10 when the contaminant threshold was estimated from short-term nonchronic animal studies. In 1980, the EPA adopted this NAS recommendation and added an additional factor between 1 and 10 when only a LOAEL (lowest observed adverse effects level) was known for setting an ADI (45 FR 79347).

In 1984, Rodericks (1984)[104] proposed a sensible but controversial approach for relating ADIs for noncarcinogens to a unit cancer risk (UCR) for carcinogens[13]; in this approach, the ADI for a noncarcinogen was assumed to represent between 10^{-5} and 10^{-6} chance of adverse effects. The approach was extended to radioisotopes and applied in an exploratory study using risk to rank chemical and radioisotope hazards at mixed waste sites at U.S. Department of Energy (DOE) facilities.[105] In general, however, studies of noncancerous chemicals are still only hazard assessments combined with a calculation of an allowable threshold dose, which is considered safe by means of standardized factors of protection, without any explicit mention of risk.

Air Pollution Laws

The earliest laws related to the environment concerned air pollution. For example, about 1300, Edward I forbade the use of "sea coal" in London. Only when wood was depleted by 1500 did coal become tolerated[106]; by 1661, ill health from smoke around London was observed (Fig. 3). In the United States, Ohio attempted to regulate air emissions from coal-fired industrial boilers as early as 1890. Much later, in 1947, California passed the first comprehensive air pollution statute.[93] Shortly thereafter, Congress encouraged more state control: the Air Pollution Control Act in 1955 (Public Law 84-150, July 14, 1955, ch. 360 [69 Stat. 322]) to fund research by the states; the Clean Air Act in 1963 (Public Law 88-

[13] In the 1980s, the EPA began using the term "reference dose" (RfD) for ADI and "carcinogenic potency factors" (CPF) for UCR.

206) to help states establish their own air pollution control agencies; and an Air Quality Act in 1967 (Public Law 90-148 [81 Stat. 485]) to set air pollution standards to be enforced by the states. Also, in 1965, Congress passed the Motor Vehicle Air Pollution Control Act (amendments to National Emissions Standards Act; Public Law 89-272), which required the federal government to set emission standards.[14] Many consumers were reluctant to support such standards when fuel efficiency dropped precipitously after the standards were first applied in 1968.[43]

In December 1970, Congress passed the Clean Air Act Amendments (Public Law 91-604), which authorized the recently formed EPA to set and enforce federal (rather than state) air quality standards, specifically, the National Ambient Air Quality Standards (NAAQS) for pollutants. Section 112 of the act also required standards be promulgated within the short time of 90 days for toxic pollutants to provide "an ample margin of safety to protect the public health." That is, human health was the sole basis of regulation and "risk" was not mentioned.[101] In response, the EPA listed arsenic, asbestos, mercury, beryllium, radioisotopes, benzene, and vinyl chloride. The EPA circumvented the impossible dictum of "ample margin of safety" for carcinogens by adopting a regulatory requirement for industry to use the "best available technology,"[101] which was more stringent than the 1972 amendments to the Federal Water Pollution Control Act that specified use of the "best practicable technology" (Public Law 89-234). In the Clean Air Act Amendments in August 1977 (Public Law 95-95), Congress mentioned risk for the first time when requiring risk assessments for setting the NAAQS for common air pollutants. The amended act also included a technology standard that required scrubbers on new coal-fired power plants, regardless of sulfur output,[93] to protect coal mining jobs in the East. This technology standard limited the risk management techniques that EPA could allow an industry to use for solving air pollution.[43]

In 1990, Congress passed the Clean Air Act Amendments (Public Law 101-549) that, besides phasing out the use of pollutants affecting stratospheric ozone, expanded the hazardous pollutants for which the EPA was required to set technological standards from 8 to 189, rather than use risk assessment (Fig. 10). However, in a limited endorsement of risk assessments, the Clean Air Act Amendments of 1990 required the NAS to evaluate the use of risk assessments (as noted previously) and the EPA to evaluate residual risks from hazardous pollutants 6 years after enactment.

Stratospheric Ozone Assessment by NAS

In 1975, the NAS studied the impact of the Supersonic Transport on stratospheric ozone. The NAS repeated the analysis of ozone depletion in 1976, this time including other sources of chemicals, such as chlorofluorocarbons (CFCs), which catalyzed the conversion of the protective layer of ozone to oxygen. The 1976 study also roughly approximated the influence of uncertainty in seven reaction rates believed to control ozone concentrations. In another iteration of the stratospheric ozone depletion analysis in 1979, under the chairmanship of statistician, John Tukey, uncertainties in parameters were formally described with probability distributions and then propagated through the models using the Monte Carlo technique to arrive at a distribution of the results. This 1979 analysis represented an early application, outside studies for nuclear facilities, of the Monte Carlo technique for evaluating the uncertainty of consequence predictions. The ozone depletion program also chose to periodically conduct the analysis as more information became available.[13]

Control of Hazardous Chemicals

In developing ways to manage chemical waste at active disposal sites, Congress has been slow to accept risk assessment. In 1976, Congress substantially amended the Solid Waste Disposal Act of 1965 (Public Law 89-272) in its passage of the Resource Conservation and Recovery Act (RCRA; Public Law 94-580), which sought to reduce or eliminate hazardous waste

[14] In the United States, similar types of laws on a similar timeline were passed to control water pollution. For example, New Mexico territory passed water pollution laws between 1860 and 1900, and Congress passed a law in 1899 requiring permits from the Army Corps of Engineers to discharge refuse in navigable rivers (March 3, 1899, ch. 425 [30 Stat. 1152]). The Federal Water Pollution Control Act (FWPCA) in 1948 (June 30, 1948, ch. 758 [62 Stat. 1155]) and 1956 (July 9, 1956, ch. 518 [70 Stat. 498]) helped states to build wastewater treatment plants; the Water Quality Act in 1965 (Public Law 89-234) required states to set their own water quality standards. In 1972, Congress completely revamped the FWPCA; in the 1977 amendment (Public Law 95-217), Congress renamed the act "the Clean Water Act" and specified 65 priority toxic pollutants that required standards to be set and were to be monitored.

- **1939** - Müller synthesizes dichlorodiphenyltrichloroethane (DDT) and discovers its value as insecticide with low toxicity to mammals.
- **1942** - Hooker Chemical Company obtains permission from the State of New York to dispose of waste in clay-lined abandoned Love Canal.
- **1947** - U.S. Congress passes the Federal Insecticide, Fungicide, Rodenticide Act (FIFRA) because WWII had stimulated use of pesticides, but statute largely ineffective. State of California passes air pollution statute.
- **1948** - Müller awarded Nobel Prize in medicine for contribution of DDT to controlling disease. DDT prices drop and DDT becomes widely used throughout world; use roughly correlates with population declines of some raptors due to eggshell thinning.
- **1952** - **Dec:** Temperature inversion traps pollution in London fog for 5 days; death rate increases 5 fold.
- **1953** - Niagara Falls Board of Education demands Love Canal land and builds school, thus disrupting clay covering disposal site; city develops neighborhood around canal.
- **1955** - **Jul:** U.S. Congress passes Air Pollution Control Act to fund research by states.
- **1960** - Discovery of biomagnification of DDD (chlorinated hydrocarbon similar to DDT) pesticide used to kill gnats occurs at Clear Lake, California, where fish concentrate pesticide and the Western Grebes birds die when consuming fish.

1962 Carson publishes *Silent Spring*

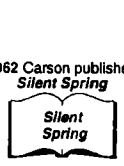

- **1962** - R. Carson publishes book **Silent Spring** that condemns use of pesticides, especially DDT and Dieldrin.
- **1963** - **Dec:** Congress passes Clean Air Act to set up state air pollution control agencies for stationary sources and allow Department of Health, Education & Welfare (HEW) to set nonmandatory federal air quality standards.
- **1965** - **Oct:** U.S. Congress passes Motor Vehicle Air Pollution Control Act to set emission standards for mobile sources.

1966 Air pollution kills 80 people in New York City

- **1966** - Air pollution trapped in temperature inversion in New York City kills 80.
- **1967** - Ratcliff discovers eggshell thinning in raptors throughout Britain and hypothesizes DDT is to blame. Congress passes Air Quality Act to set criteria to regulate air pollution by states.
- **1969** - Sweden bans DDT, but lifts in special case, when alternate pesticide is not effective against pine weevil and spruce budworm.

1970 Congress forms EPA

- **1970** - U.S. Congress forms the U.S. Environmental Protection Agency (EPA) and transfers to it responsibilities of research (conducted at 56 laboratories), monitoring, standard setting, and from 6 agencies enforcement activities related to environment; eventually becomes the agency producing or requiring the most risk assessments. U.S. Congress forms Occupational Safety and Health Administration (OSHA) to regulate work place hazards. Also, becomes agency to use risk assessments. **Dec:** Because of dissatisfaction with results from Air Quality Act, U.S. Congress passes Clean Air Amendments of 1970 authorizing EPA role in setting and enforcing air quality standards; to provide "ample margin of safety for public health" sets timetable for reducing auto emissions; makes human health sole basis of regulations does not mention "risk". Act also requires the EPA to set National Ambient Air Quality Standards (NAAQS) for pollutants within 90 days; EPA lists SO_2, CO, O_3, NOx, particulates. Act also requires standards for toxic pollutants; EPA lists As, asbestos, Hg, B, radioisotopes, benzene, and vinyl chloride. In implementing the act, EPA requires use of "best available technology". Canada restricts use of DDT.

1971 Bliss spreads PCBs and oil over Times Beach roads

- **1971** - Northeastern Pharmaceutical and Chemical Company (NEPACO) asks Bliss, a waste-oil hauler, to remove waste in tanks contaminated with dioxin from production of Agent Orange when plant owned by Hoffman Taft.
- **1971** - **(con't)** Bliss mixes waste with used oil, and sells as heating oil and dust suppressant on dirt roads and horse arenas. Horses die and 4 children severely injured when playing in stable dirt. Bliss continues to spread waste over dirt roads in Times Beach, Missouri, through 1976 and throughout Missouri until 1980.
- **1972** - **Jun:** U.S. Congress rewrites FIFRA to strengthen EPA control of pesticides, but requires EPA factor in economic and social benefits, in addition to environmental hazards. Ruckelshaus of EPA overturns administrative hearing findings and totally bans DDT in the United States.
- **1974** - CDC discovers 31,000 ppb dioxin in soil as cause of animal deaths and children's injuries in horse stables in Missouri. **Jun & Sep:** Scientists report that chlorofluorocarbons (CFCs) put chlorine into stratosphere and that catalyze conversion of ozone to oxygen.
- **1975** - National Academy of Sciences (NAS) studies impact of Super Sonic Transport (SST) on stratospheric ozone.

1976 Appeals court upholds ban on leaded gasoline based on risk assessment

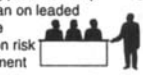

1976 Love Canal leaks

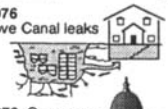

1976 Congress passes RCRA

- **1976** - U.S. Congress passes Resource Conservation and Recovery Act (RCRA), which seeks to reduce hazardous waste generation; prescriptive approach to hazards without any risk assessment beyond hazard identification, troubles with dioxin at Times Beach, Missouri, provides impetus. After 6-yr high rainfall, Love Canal overflows banks. In response to citizen complaints, New York Environmental Department investigates and finds low levels of 82 chemicals in storm sewers. U.S. Court of Appeals upholds EPA decision to reduce lead in gasoline using risk assessment based on "speculative scientific estimates." NAS continues study of thinning stratospheric ozone; reported predictions ranged between 2% (tolerable) to 20% (intolerable).
- **1977** - **Aug:** Congress amends Clean Air Act; requires risk assessment for setting NAAQS for common air pollutants, but still prohibits consideration of costs; does include technology standard requiring scrubbers regardless of sulfur output on new coal fired plants (to protect coal miner jobs in east).
- **1978** - Alar tests on rats and mice show signs of causing cancer. EPA bans CFCs as propellants in aerosol cans based on predictions of ozone destruction from models. Health Education and Welfare secretary warns of asbestos hazard in schools and cites risk that 17% of future cancer deaths would be from asbestos. Although study questioned, extreme risk management option to remove all asbestos in schools, was eventually adopted.
- **1979** - NAS continues to iterate analysis of ozone depletion more carefully, including uncertainty on the results through Monte Carlo Analysis.

1980 Congress passes Superfund

- **1980** - Congress passed Acid Precipitation Act of 1980 to create National Acid Precipitation Assessment program (NAPAP) inventory problem catalog mitigation strategies. **Dec:** U.S. Congress passes Superfund Act for emergency response to spills and remediation of inactive chemical waste sites (paid through tax on chemicals) not covered by other environmental laws. Impetus for passage provided by fires at waste sites at Chester, Pennsylvania, and Elizabeth, New York; groundwater contamination at Rocky Mt. arsenal near Denver, Colorado; EPA survey of Love Canal and thousands of abandoned waste sites.
- **1982** - NAS continues to iterate ozone depletion analysis. EPA presents use of Hazard Ranking Scheme (HRS) for listing sites on National Priorities List (NPL) under Superfund. **Dec:** Missouri Department of Health discourages Times Beach residents from returning after flooding because of 100 ppb dioxin along roads as measured by Center for Disease Control (CDC) of public health service and EPA.

Fig. 10. Events influencing environmental laws and indirectly risk assessment.

1983 Ruckelshaus encourages inclusion of uncertainty for EPA risk assessment

- **1983** - Reagan creates task force on Times Beach that recommends buying affected homes. **Jun:** Admin. Ruckelshaus announces EPA intent to use risk assessment more and include uncertainties rather than report single value. Congress passes Hazardous and Solid Waste Amendments (HSWA) (amends RCRA):
  - bans hazardous waste disposal in land fills without accepted pretreatment, unless disposal site has petitioned successfully for a "no-migration" variance.
  - prescriptive approach to hazards regardless of health risk
- **1985** - EPA promulgates 40 CFR 300 listing procedures for site cleanup under Superfund Act that includes detailed risk evaluation phase and consideration of cleanup costs. EPA decides to accelerate phasing out leaded gasoline based on assessment of lead's non-cancerous health effects. **Sep:** After reviewing EPA data and arguments of Uniroyal, EPA Scientific Advisory Board (SAB) concludes proposed ban on Alar not justified by current tests.
- **1986** - **Jan:** EPA announces it will not ban Alar, based on SAB conclusion; however, apple processors refuse to buy Alar treated apples. Prompted by Ruckelshaus initiative in 1984, EPA publishes Superfund public health evaluation manual giving carcinogenic potency factors for many chemicals. U.S. Congress reauthorizes Superfund Act (SARA); permits citizens to petition EPA for risk assessments of any site, requires revision of HRS, requires public comment period on proposed remedial plans, and starts research on radon gas.

1987 EPA ranks environmental problem based on risk

- **1987** - NAS recommends that EPA *not* apply "Delaney Clause" to carcinogenic pesticide residues in food and use risk assessment instead. EPA senior managers rank and compare environmental problems in four categories in ***Unfinished Business***. **Sep:** Based on atmospheric models, Montreal Protocol signed by 60 United Nations (UN) members to reduce use of CFCs; agreement calls for periodic review.
- **1988** - EPA adopts NAS recommendation of using risk assessment for determining allowable amounts of carcinogenic pesticide residues in or on food, limit set of 10^{-6} cancer risk. EPA publishes guidance on risk assessments for Superfund sites. **Oct:** NRDC hires Fenton Communications to publicize soon-to-be released risk assessment on Alar through television, popular magazines, etc.
- **1989** - **Feb 1:** Based on preliminary toxicity studies EPA required Uniroyal to conduct in 1986 - 1987, EPA publishes decision to stop all use of Alar on food, but allows use for 18 months because added risk from extension felt insignificant. **Feb 26:** CBS "60 Minutes" uses NRDC information and causes panic about Alar in apple juice while alleging EPA's dereliction. **Feb 27:** NRDC releases risk assessment deploring Alar residues in children's food. **Jun:** Uniroyal stops selling Alar in the United States. EPA publishes guideline on safety factors to apply in dose response assessment.
- **1990** - **Jan:** Scientists questioned need for the drastic asbestos abatement programs for schools. EPA Science Advisory Board (SAB) reviews ***Unfinished Business*** and produces own ranking of environmental ***Problems in Reducing Risk***. SAB also recommends ecological risks be assessed (a topic EPA had been exploring in various regions since 1986). **Dec:** Congress passes Clean Air Act Amendments (CAAA) of 1990 that includes phasing out use of pollutants affecting stratospheric ozone and requires EPA to set technology standards (versus risk standards) for 189 hazardous pollutants to speed up process and requires EPA to conduct risk assessments 6 yrs after enactment for "residual risks" and ambient air risks (risks must be reduced to below 10^{-6}). Act also allows utilities to buy and sell pollution credits for SO_2 pollutants. Act also requires cost benefit analysis of reducing acid rain, and sets goal of reducing SO_2 emissions by 10^7 ton from 1980 levels. "London Revision" to Montreal Protocol calls for total ban on CFCs by 2000 in developed countries and 2010 in other countries based on great concern raised by revised atmospheric models.
- **1991** - UN panel of experts concludes Alar safe for use on apples throughout world.
- **1992** - Office of Management and Budget (OMB) finds EPA spending vast sums on low risks at toxic waste sites while relatively little on high risks such as lead poisoning. After suit filed by NRDC, U.S. Court of Appeals rules that EPA must strictly apply "Delaney Clause" for carcinogenic pesticide residues and cannot use risk assessment and a *de minimis* risk policy. EPA issues Exposure Assessments Guidelines stating importance of adequately characterizing uncertainty. Montreal Protocol again amended to ban CFCs by 1996 in developed countries and 2006 in other countries.
- **1993** - Study finds that cost effectiveness of federal regulations for averting premature death varies from $\$1 \times 10^5$ to $\$5.7 \times 10^{12}$.
- **1996** - Based on exploratory studies since 1986, EPA publishes proposed guidelines for assessing risks to entire ecosystem.
- **1998** - **Apr:** EPA finalizes guidelines for ecological risk assessment stating "risk assessment explicitly evaluate uncertainty".

Fig. 10. (Continued.)

generation and control hazardous waste disposal at active sites. Its overall purpose was to minimize present and future threats to human health and the environment through control of hazardous chemicals from "cradle to grave." An important impetus for RCRA was the environmental problem that was caused by the actions of a used oil hauler, Bliss, which had been asked to remove and dispose of hazardous wastes in 1974. The wastes were from a former manufacturing plant for the herbicide, Agent Orange, often contaminated with dioxins. Bliss inappropriately mixed the waste with used oil and sold it as a heating oil and dust suppressant on dirt roads and horse arenas in Missouri through 1980, thus creating the problem at Times Beach (Fig. 10).[99]

RCRA is fairly prescriptive in its manner of controlling chemical hazards. Hazard identification is the only risk assessment component specified, and risk management practices are strictly defined. This prescriptive approach was even more pronounced in the 1984 Hazardous and Solid Waste Amendments (HWSA; Public Law 98-616) to RCRA, which banned nearly all hazardous waste disposal in landfills without pretreatment. In EPA's implementing regulations 40

CFR Parts 260 through 281, a specific technology was prescribed to treat waste before disposal, regardless of any risk assessment.

Remediation of Abandoned Chemical Disposal Sites

In December 1980, Congress passed the Comprehensive Environmental Response Compensation and Liability Act (CERCLA) or "Superfund" (Public Law 96-510) for emergency response to spills and remediation of inactive chemical waste sites not covered by other environmental laws (e.g., RCRA). The impetus for passage was provided by fires at waste sites in Pennsylvania and New York; groundwater contamination at the Rocky Mountain Arsenal near Denver, Colorado; an EPA survey of thousands of abandoned waste sites; and the well-publicized problems at Love Canal in New York.

CERCLA did not completely embrace the notion of risk assessment, but in contrast to RCRA's prescriptive approach, CERCLA did allow the EPA more latitude in determining the emergency response for an inactive chemical waste site. The EPA's 1982 Hazard Ranking Scheme (HRS) for listing sites on the National Priorities List under CERCLA lacked a sound relation either to risk assessment or the use of underlying consequence models.[105] However, the EPA chose to conduct a detailed site characterization and a feasibility study of various remediation options for those same sites in 1985, accompanied by an assessment of associated risks and cleanup costs (Fig. 10). Because the mining and smelting industry expressed concern that HRS was the real assessment and that the purpose of any risk assessment during the feasibility study would be only to justify the results of HRS (or other decisions already made), Congress asked for a reevaluation of HRS in the 1986 Superfund Amendment and Reauthorization Act (SARA; Public Law 99-499 [100 Stat. 1613]) to eliminate the potential for disparate results from HRS and later risk assessments for the feasibility study. (SARA allowed any citizen to petition for a risk assessment of a disposal site.) Unfortunately, a substantial change in HRS might have required a reevaluation of past work or already settled lawsuits under CERCLA, and thus the opportunity for change was minimal. SARA also required research on the risks of radon gas in homes, a rediscovered hazard prevalent in many areas because of better sealed and insulated homes. The impetus was the publicized problem of using uranium tailings in Grand Junction, Colorado.

5.3. Court Rulings on Use of Risk Assessment

In 1976, the U.S. Court of Appeals upheld a decision by the EPA to reduce lead in gasoline using risk assessment based on "speculative scientific estimates."[17] In 1980, the U.S. Supreme Court ruled in favor of the American Petroleum Institute and the American Industrial Health Council, and against the AFL-CIO labor union and environmental groups, when it stated that the Occupational Safety and Health Association (OSHA) must use risk assessment before regulating workplace hazards (as reported in vol. 100 of the *Supreme Court Reporter,* page 2844 [100 S. Ct. 2844]). The court also suggested that an individual's chance of hazard of 10^{-3} per year was of concern but that a chance of 10^{-9} per year was not, thus bracketing the 10^{-6} health risk cutoff that had first been proposed by the FDA in 1977[3] (42 FR 10412), as mentioned earlier. An advantage of risk assessment was its ability to provide a meaningful method to organize scientific information and document administrative decisions and thus facilitate judicial review.

Even with this important Supreme Court ruling, in 1985, Professor of Law R. Merrill noted that the "courts are schizophrenic" concerning the use of risk assessment.[107] Although the situation is somewhat different in the 1990s, in that the courts expect to see arguments posed in terms of risk, they do not always agree that risk is germane to the case. For example, this support for risk assessments did not translate into moderation with regard to the "Delaney Clause." In 1987, the NAS recommended that the EPA *not* apply the "Delaney Clause" to carcinogenic pesticide residues in food; instead, the EPA should use risk assessment.[108] One year later, the EPA adopted the NAS recommendation and set residue limits on food for four pesticides at a chance of $10^{-6}$of inducing cancer per year.[93] However, in a 1992 suit filed by several petitioners that included the National Resources Defense Council, the U.S. Court of Appeals, Ninth Circuit, ruled that the EPA must strictly apply the "Delaney Clause" and could not use risk assessment and a *de minimis* risk policy until Congress enacted such a change (968 F. 2d 985).

6. PERFORMANCE ASSESSMENT APPLICATIONS

The EPA 40 CFR 191 Standard (50 FR 38066) established criteria for radioactive waste disposal but acknowledged that "the procedures for determining compliance with subpart B have not been formulated and tested yet." These procedures were not completely formulated until they were applied to actual sites. Two applications are presented here as background for specific topics discussed in this special issue. The first application is the PA conducted for the WIPP in the late 1980s and early 1990s.[109–114] The second application conducted by the YMP has somewhat different practical details.

6.1. Application of Performance Assessment to Waste Isolation Pilot Plant

Legal Setting and Compliance Assessment

In 1979, Congress established the purpose of the WIPP as a research and development facility for storage and disposal of only transuranic waste generated by defense programs (Public Law 96-164). Yet, the actual compliance process was not defined until 1992, when Congress transferred ownership of the WIPP site to the DOE and designated the EPA as the regulator of the WIPP (Public Law 102-579). In 1996, the EPA promulgated 40 CFR 194 (61 FR 5224), a regulation to implement its 40 CFR 191 standard, which imposed several new requirements and interpretations on the modeling style for the WIPP PA. Basically, however, 40 CFR 194 adopted the risk process, as outlined here, that Sandia had implemented (Fig. 11).[11,12,109,115,116]

Site Selection and Characterization

With the tacit approval of New Mexico's governor, the AEC, the USGS, and ORNL examined and identified a potential site in the Delaware Basin in southeastern New Mexico in 1973, based on physical geologic criteria such as thick salt beds of high purity, little evidence of dissolution, tectonic stability, public support, low population density, and absence of land use conflicts. The first large-scale field test was the drilling of two wells in March 1974.[69,70] In January 1975, Sandia became the lead laboratory to draft an EIS,[117] initiate scientific studies on nuclear waste disposal in bedded salt, develop the conceptual design,[118] and select and characterize a site. The preliminary design for the repository was developed in 1977[118] and included two levels: one for TRU waste and one for other radioactive waste. The basic concept remained largely unchanged in the final design, as reported in 1986, with the exception of the removal of the level for other radioactive waste in the 1980 Final EIS[117] and some modifications to drift dimensions and storage volumes. Site characterization activities before 1989 were undertaken primarily (1) to satisfy needs for EISs in 1978 and 1989, (2) to satisfy negotiated agreements with the state of New Mexico in 1981, and (3) to develop a general understanding of selected natural phenomena associated with nuclear waste disposal. Thereafter, site characterization studies were gradually directed toward data needs for the four preliminary PAs, conducted between 1989 and 1992, and the PA for certification in 1996.

Hazard Identification and Scenario Development

In 1974, ORNL conducted the first scenario development and deterministic scoping analysis for the possible repository location.[72] For the Draft EIS in 1979, Sandia developed three scenario categories (diffusive migration of radioisotopes through salt, transport of radioisotopes to an overlying aquifer through a borehole, and direct exposure during drilling).[88] This initial work became the foundation for scenarios later used for the PAs. For preliminary PA calculations in 1989,[110, 119] features such as the presence of a brine reservoir under the repository, events such as exploratory drilling into the repository and potash mining above the repository, and processes such as climate change influencing flow in the brine aquifer overlying the repository, were included as features and events. These basic scenarios were studied in the 1990, 1991, and 1992 PAs.[69,70,111–114,120] For the final Compliance Certification Application (CCA) on the WIPP,[121] submitted to the EPA in October 1996, a formal screening process was conducted that fully documented the reasons for omitting or retaining specific features, events, and processes.[122] Although the hazard identification relied heavily on the 1980 EIS,[88,117,119,125] the screening process was similar to that initially proposed by Cranwell *et al.* (1990)[82] in the 1980s based on scenario probability, consequence, or regulatory criteria.

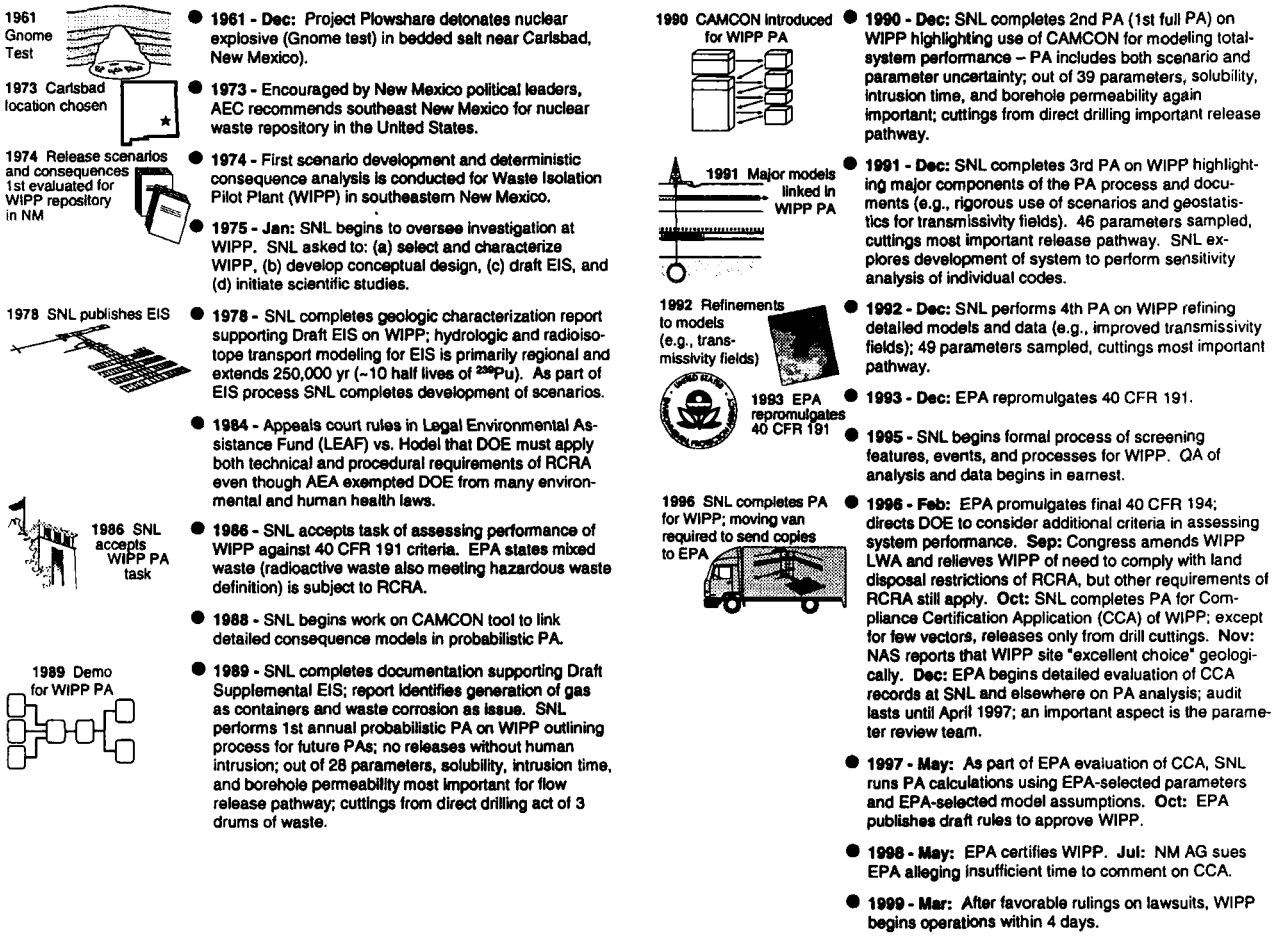

Fig. 11. Application of performance assessment at the WIPP.

Probability Evaluation

For the WIPP, as in the method proposed for the NRC in 1981,[75,76] the distribution of the results was estimated using Monte Carlo techniques. Furthermore, the Monte Carlo integration was eventually performed in two stages to facilitate flexibility. The first stage was concerned with parameter uncertainty, $\mathbf{x}^p$, and the second stage, with scenario uncertainty, $\mathbf{x}^s$. That is, the deterministic model, $C(\cdot)$, was run using nK realizations of the parameter vector, $\mathbf{x}^P$, which yielded a sequence of nK results of the form $C(\mathbf{x}_1^p)(\mathbf{x}_2^p) \ldots, (\mathbf{x}_{nK}^p)$ for each scenario, S_j, which were used to approximate the CCDF (Fig. 8).

Although the theory for probabilistic model simulation is not difficult, the practical aspects of performing the calculations are daunting for a complex system such as geologic disposal. Developing distributions for the uncertain parameters, $D_n(\mathbf{x}_n^p)$, and appropriate values for the fixed parameters in a manner sufficiently traceable for regulatory review is particularly challenging. Hence, traceable procedures for the WIPP were developed in the early 1990s,[123] which matured into an extensive quality assurance program by 1996. In addition, an important practical problem for parameter uncertainty was determining the appropriate number of uncertain parameters to propagate. Out of ~1,560 parameters, the number of uncertain parameters studied for the WIPP grew from 28 in 1989[110,111] to 57 in 1996.[69]

Consequence Evaluation

The major role of modeling in a PA made computer software fundamental to the process.[124]

Development of Computational Tools. A practical problem for a geologic disposal system is the need

to model several scales (e.g., the source term, repository, local transport, and regional fluid flow). Hence, for the WIPP PA, the exposure pathway model was a concatenation of many submodels[70] (designated by α, β, γ), $C(\cdot) = f_\alpha\{f_\beta[f_\gamma(\cdot)]\}$. Additional practical problems for analyzing a disposal system are determining the appropriate level of detail for the individual submodels so that the calculation is tractable and linking the models together, so that they are sufficiently traceable and repeatable for regulatory review.

Between 1988 and 1990, Sandia devised a scheme to link together through a controller, CAMCON, any number of complicated numerical or simple analytical codes for the WIPP.[109,120] As built, CAMCON allowed the analyst the flexibility to choose several variations of one model type (designated by α); i.e., $f_\alpha^1, f_\alpha^2, \ldots f_\alpha^{nM}$, where nM is the number of models that perform a similar function) to directly make use of the existing submodel codes and select the code with the appropriate level of detail. The latter option allowed the analysts to use CAMCON for both detailed examination of system components as well as overall disposal system performance.

Detailed Modeling Style. Sandia's contribution to the Draft EIS, issued in 1978, relied heavily on mathematical modeling using the SWIFT code to examine the potential for movement of radioisotopes by groundwater.[125] By the second iteration of the WIPP PA in 1990,[111,112,120] analysts had again chosen a modeling approach that included phenomenological detail, offered multiple dimensions in the model, and avoided conservative models and parameter values wherever possible.[123] Encouraging comments regarding detailed modeling were received from the EPA[112] on the first iteration of the WIPP PA. In addition, a detailed modeling style was generally accepted in the United States because of its earlier use in the 1975 *Reactor Safety Study*[14] and its 1990 update,[62,63] and the proposal for extensive use of PRAs in the 1995 PRA Policy Statement (60 FR 42622).

The principal advantage of a detailed modeling approach was that it incorporated a sufficient level of realism to (1) provide or demonstrate general scientific understanding, (2) explore potential sources of uncertainty, and (3) tie any lack of understanding or sources of uncertainty directly to measurable data. Note, however, that the WIPP PA continued to contain some conservative assumptions and bounding models. For example, a few conservative assumptions were built into the analysis (e.g., a stationary future and a conservative dose–response model) and others were adopted during the analysis (e.g., insufficient information was available on shear strength of corroded waste during human intrusion). Hence, the probabilistic analysis was conditional on these conservative assumptions.

Iteration of Calculations. In 1989, the WIPP PA analysts adopted the idea of conducting sequential PAs (i.e., conducting an initial PA with simple or incomplete complicated models and preliminary data), followed by other PAs with better data and more detailed computational models.[109] Sandia conducted four preliminary PAs from 1989 through 1992, with each building on the preceding PAs.[15] In October 1996, the certification PA for the CCA was completed. In May 1998, after receiving accepting comments on the proposed rule published in October 1997 (62 FR 58792), the EPA approved operation of the WIPP (63 FR 27354). Operations began in March 1999, after favorable rulings on lawsuits. Although the results are voluminous, the application of past PAs for the WIPP has been presented by Helton *et al.*, in several journal articles.[126–128] In addition, Helton *et al.* present a summary of the certification PA in this issue.[121]

Sensitivity Analysis

Sensitivity analysis was an important feature in early PAs of hypothetical repositories[75,86,87] and was quickly adopted for the WIPP evaluation. Because Monte Carlo techniques had been used to propagate uncertainty in the WIPP analysis, sensitivity of the results to changes in parameter values could be easily estimated by scatterplots, or developing a statistical regression model and comparing the size of the standardized regression coefficients.[110,112,113,126] Sensitivity analysis of alternative conceptual models was also conducted in 1989 and 1991.[111,127] Other techniques for sensitivity analysis, such as developing surrogate analytical expressions for the results ("response surface development") or differential analysis of normalized partial derivative of parameters ("adjoint procedure"), were also proposed in the 1980s.[129] However, these were never used routinely for a large-scale sensitivity analysis such as the WIPP disposal

[15] Using the terminology of the 1996 EPA ecological risk guidelines (61 FR 47552; 63 FR 26846), these repetitions were a "tiered assessment" because they were planned repetitions rather than "iterations," which EPA describes as unplanned repetitions.

system that included linked several complicated models.

Sensitivity analysis, in combination with multiple PA iterations, provided guidance to managers on how to direct experimental resources, especially after the 1992 PA. Other purposes of the sensitivity analysis[123] were to gain understanding and insight about the system, verify the correctness of the calculations, and evaluate the influence of various engineering design options. Garrick and Kaplan describe the impact that a PA can have on waste disposal decisions in this special issue.[130]

In the 1989 and 1990 WIPP PAs, the most important parameters were those associated with the scenarios for inadvertent human intrusion from exploratory drilling for oil and gas: solubility of radioisotopes, the time of intrusion into the repository, and the assumed permeability of the resulting but abandoned borehole. In the 1991 and 1992 WIPP PAs, direct release of cuttings to the surface from inadvertent human intrusion again dominated total radioisotope release. The three most important parameters were the rate constant in the Poisson model for time and number of intrusions, borehole permeability, and solubility of radioisotopes.[114] Thus, by 1992, it was evident that regulatory mandated assumptions with regard to human intrusion were dominating the results. Continued evaluation of the characteristics of the disposal system was not considered to be warranted, except for specific areas such as an evaluation of radioisotope solubilities in the repository, retardation distribution coefficients, and alternative conceptual models for transport in an overlying brine aquifer in the Culebra Dolomite.

6.2. Application of Performance Assessment for Yucca Mountain Project

Most of the issues associated with disposal of defense and commercial wastes are the same, but the congressional policy and administrative histories are different in the United States. Consequently, the approach between projects has varied for each of the risk assessment steps, as discussed here.

Legal Setting and Compliance Assessment

Three laws are significant to setting national policy on radioactive waste disposal from commercial nuclear power reactors: the Nuclear Waste Policy Act of 1982, the 1987 amendment to this act, and the Energy Policy Act of 1992 (Public Law 102-486 [106 Stat. 2776]). These laws not only establish the policy that the current generation must bear the costs of developing a permanent disposal option, but they also define steps to achieve this goal. However, each act changes the emphasis of the various steps.

The Nuclear Waste Policy Act of 1982 (Public Law 97-425) set up a mechanism to select a site and fund its selection and operation, and assigned responsibility for the construction and operation of the potential repository to a new office within the DOE, the Office of Civilian Radioactive Waste Management (OCRWM), which absorbed many of the functions for commercial waste disposal performed by the National Waste Terminal Storage Program established in 1976. The act formed a large trust, funded by utilities owning nuclear reactors, to pay for the repository; required the DOE to identify two repositories for commercial spent fuel; assigned responsibility to the DOE to select, build, and operate one repository; established a strict timetable for operating the first repository; suggested placing defense high-level waste in the commercial repository; and suggested building a monitored retrievable storage facility. The amendment of 1987 (Public Law 100-203) selected Yucca Mountain in Nevada as the first site to characterize, extended the opening date to 2010, and delayed consideration of a monitored retrievable storage facility and a second repository.

The Energy Policy Act of 1992 (Public Law 102-486) set new policy that generated substantial changes in the regulatory setting. The act required the EPA to seek advice from the NAS and to promulgate a site-specific standard for the potential nuclear waste repository at Yucca Mountain and the revision of the NRC implementing regulation, 10 CFR 60, to agree with the new EPA standard. The act strongly suggested prescribing the maximum allowable annual effective dose equivalent to individuals near the repository (possibly because of Congressional criticism of the derived limits in 40 CFR 191 when applied to gaseous release of ^{14}C along an air pathway). In 1995, NAS recommended[131] three changes from previous regulatory practice: (1) use a maximum individual risk evaluated from an annual effective dose equivalent as the criterion for protecting public health, (2) evaluate the maximum annual effective dose equivalent during a 1 million-year period, and (3) eliminate evaluating the probability of inadvertent human intrusion and instead evaluate only potential consequences of a few selected situations.

- **1972** - Winograd proposes use of unsaturated zone alluvium for HLW disposal.
- **1976** - ERDA Office of Nuclear Waste Isolation (ONWI) sets up National Waste Terminal Storage (NWTS) program to develop technology and facilities for storage and disposal of HLW and SNF from both commercial and defense sources.
- **1977 - Apr:** Carter declares United States will stop all reprocessing Spent Nuclear Fuel (SNF) from commercial reactors and dispose SNF directly.
- **1980 - Dec:** DOE search for disposal site for commercial and defense spent nuclear fuel and high-level waste; because of prior land use by federal government, basalt at Hanford and volcanic tuff at Yucca Mt. on Nevada Test Site (NTS) two of several sites selected. Also, sites throughout the United States with large formations of salt or granite were examined.
- **1981** - Winograd again proposes use of thick unsaturated alluvium in the desert for HLW disposal. Leads to use of unsaturated zone by Yucca Mt. Project and disposal of TRU waste at Greater Confinement Disposal (GCD) facility at NTS.

- **1982** - Congress passes Nuclear Waste Policy Act (NWPA): (a) requires DOE to identify two repository sites (unstated agreement was one in west and one elsewhere), (b) sets up trust fund, funded by utilities, to pay for SNF and HLW disposal, (c) establishes office within DOE responsible for designing, building, and operating one of two repositories identified, (d) suggests 1000 deaths/10,000 yr criterion, (e) sets strict timetable opening 1st repository for commercial and defense spent nuclear fuel (SNF) and HLW, and (f) suggests Monitored Retrievable Storage (MRS). **Dec:** NRC promulgates shallow land disposal requirements for low-level waste (10 CFR 61).

- **1983** - NRC promulgates technical criteria in 10 CFR 60: (a) includes by reference the yet-to-be promulgated 40 CFR 191 and (b) sets deterministic criteria on subsystems of disposal system. **Feb:** Parts of ONWI become Office of Civilian Radioactive Waste Management (OCRWM) of DOE as mandated by NWPA of 1982; program formally identifies 9 sites.
- **1984 - Dec:** DOE recommends Hanford, Washington, Yucca Mt., Nevada, and Deaf Smith, Texas, as potential sites in draft EIS. Ensuing controversy calls for another evaluation. SNL conducts scoping calculation of YMP repository showing ^{99}Tc, ^{129}I, and ^{237}Np are important radioisotopes for evaluating compliance.
- **1986 - Jun:** DOE issues environmental assessment of each of five potential sites for commercial spent nuclear fuel. Basalt at Hanford reservation, volcanic tuff at Nevada, and bedded salt in Texas and Utah for further characterization. **Jul:** NRC proposes to explicitly incorporate 40 CFR 191 requirements directly into 10 CFR 60-never adopted because of court remand of 40 CFR 191.

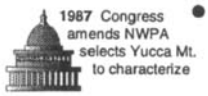

- **1987 - Jan:** Multi-attribute utility decision analysis applied to selecting nuclear waste disposal sites and applied to concept of lowering program risk with a "portfolio" of sites; same 3 sites as recommended by DOE in 1984. **Dec:** U.S. Congress passes Nuclear Waste Policy Amendments Act (NWPAA): (a) selects Yucca Mt. for first site to be characterized for potential SNF and HLW disposal, (b) revises time table for opening first site, and (c) greatly restricts MRS (can't construct until repository being constructed).

- **1988** - SNL publishes Site Characterization Plan (SCP) of Yucca Mt. – several aspects of PA described (e.g., scenario development); repository placed in unsaturated zone.
- **1990 - Oct:** Electrical Power Research Institute (EPRI), representing nuclear utilities, completes 1st PA of Yucca Mt. repository.
- **1991** - Collection of analyses (PACE-90) shows little radioisotope movement in unsaturated zone over 10^4 yr when infiltration 0.01 mm/yr.
- **1992 - May:** EPRI completes 2nd PA of Yucca Mt. Congress asks NAS to recommend to EPA and NRC disposal criteria for Yucca Mt. strongly suggesting maximum individual dose. **Jul:** SNL completes 1st PA on Yucca Mt. (TSPA-91) manually connecting two alternative, 1-d, fluid-flow codes in the unsaturated zone. NRC completes own PA of Yucca Mt. repository.
- **1993** - SNL performs PA on DOE-owned SNF disposed in salt and granite to help with decisions on treatment. SNL performs 1st PA on greater than class-C waste disposal at GCD facility at NTS using readily available data.

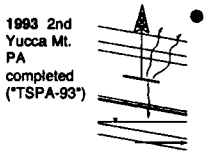

- **1994 - Apr:** SNL completes 2nd PA on commercial SNF disposal at Yucca Mt. using better data set (some distributions developed through PA group consensus), and improvements in the source-term model (e.g., inclusion of corrosion and thermal effects) (TSPA-93). SNL performs 2nd PA on Greater Confinement Disposal (GCD) repository, located at NTS, after collecting site specific data.
- **1995 - Mar:** SNL performs PA on DOE-owned SNF disposed in tuff to help with decision on direct disposal and concern with critical conditions. NAS recommends guidance on developing regulation for potential repository at Yucca Mt. that includes risk calculation based on dose over 10^6 yr period. **Nov:** YMP M&O completes 3rd PA of Yucca Mt. using simplified codes and linkage system (RIP) (TSPA-95); SNF closely packed to drive water from repository in 1st 10^3 yr.
- **1996 - Dec:** EPRI completes PA on Yucca Mt. repository using a logic tree approach.

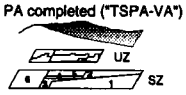

- **1998 - Nov:** YMP M&O completes 4th major PA (TSPA-VA) of transport of radioisotopes to wells in the Amargosa Valley 20 km from the potential site over 10^6 yr period. PA includes influence of zircalloy cladding reduced Np solubility, increased infiltration (7 mm/yr current average, 40 mm/yr, long-term average), and greatly reduced dispersion in saturated zone. ^{99}Tc most important radioisotope at 10^4 yr, ^{237}Np at 10^5 yr. EPRI completes 4th PA of YMP.

Fig. 12. Application of performance assessment at the YMP.

In the United States, the NRC is responsible for ensuring that a disposal system for commercial-generated spent nuclear fuel meets the requirements of EPA's standards for commercial nuclear waste, such as 40 CFR 191. In 1983, prior to final promulgation of 40 CFR 191, but cognizant of its likely contents, the NRC promulgated 10 CFR 60 (46 FR 13971; 48 FR 28194; 10 CFR 60) that incorporated the EPA standard by reference but also set deterministic technical criteria on subsystems of the waste disposal system (Fig. 12). In 10 CFR 60, the technical criteria established stringent minimum requirements for disposal subsystems: 1,000-year groundwater travel requirement on the geologic barrier 300-year container life without substantial failure, and a maximum release rate from the container after initial failure. These criteria were not probabilistic, despite the NRC's support of PRAs in the late 1970s (see Section

4.2). In 1986, the NRC proposed to explicitly incorporate the requirements of the EPA standard, 40 CFR 191, into 10 CFR 60 but the changes were never adopted (51 FR 22288) because 40 CFR 191 was remanded by the courts (824 F. 2d. 1258). The NRC proposed 10 CFR 63 in February 1999 (64 FR 8640) for the repository at Yucca Mountain, again cognizant of the likely contents of the EPA Standard, 40 CFR 197 recently proposed in August 1999 (64 FR 46977). The NRC regulation proposes a dose limit of 25 mrem/yr during a 10,000-year period from drinking water and consumption of vegetables, given a small community well about 20-kilometer downgradient from the site. The NRC eliminated all subsystem requirements since they could cause expensive suboptimal designs (64 FR 8640).

System Characterization

Although salt was an appealing disposal medium for commercially generated nuclear waste, the DOE began an intensive search in 1976 for repositories in several types of rock in 36 states. By 1980, the DOE's Nuclear Waste Terminal Storage Program had settled on nine sites, including volcanic tuff at Yucca Mountain near the Nevada Test Site.[36] DOE ownership of the land, the adsorptive capability of the tuff (especially the zeolitized portions), the belief at that time that spent nuclear fuel could be easily retrieved from tunnels for reuse or disposal elsewhere, and the extremely dry climate were important reasons for consideration of this site.[36,132] As with the WIPP, a PA was not used directly in site selection. Rather, a comprehensive study was published in 1986. (Although it caused confusion, the study was called an Environmental Assessment [EA] but was not related to the EA defined in 40 CFR 1501 regulations promulgated in 1979 to implement NEPA.) Under 10 CFR 60, the NRC required the DOE to prepare a site characterization plan (SCP) (46 FR 13971; 48 FR 28194; 10 CFR 60), which was completed in 1988.[133] The massive SCP described almost every experiment or study that might be required to characterize the highly fractured tuff and generate mathematical models of waste dissolution and movement of radioisotopes in groundwater. As with most aspects of the YMP, the characterization studies were conducted by several research organizations in addition to Sandia, including the USGS, Los Alamos National Laboratory, Lawrence Livermore National Laboratory, Lawrence Berkeley National Laboratory, Argonne National Laboratory, PNL, and contracting organizations such as SAIC, Inc.; Raytheon, Inc.; Reynolds, Inc.; and later TRW, Inc.

The design of the repository at Yucca Mountain has varied considerably over the life of the project. Initially, the repository was placed in the saturated zone, but arguments in 1981 for disposal of high-level waste in unsaturated alluvium derived from tuff deposits[134] prompted consideration of the unsaturated zone at Yucca Mountain. By 1988, the SCP envisioned a repository in the unsaturated zone. Even though construction of the repository was far off, DOE awarded a management and operations (M& O) contract in 1993. Shortly afterwards, the design was modified to include large disposal containers emplaced directly in the drifts to reduce mining and operating costs. Also, by 1995, the project seriously considered closely packing the wastes such that the heat would dry out the unsaturated zone for ~1,000 years,[135] instead of keeping temperatures low such that perturbations to the geologic environment would be small, as envisioned by the NAS in 1957.[71] Although tunneling costs were reduced, acquiring sufficient understanding of the geologic environment to confidently predict the benefits of drying out the host tuff effects in turn necessitated gathering more characterization data, an expensive undertaking. The most recent design envisions closely spaced containers to dry out the tunnel, but widely spaced tunnels to keep the area between tunnels cool, and thereby allowing water drainage.

Hazard Identification and Scenario Development

As with the WIPP, hazard identification for YMP examined what features, events, or processes could negate the initially perceived advantages of the site. The hazard identification and scenario development process for this and later PAs generally recognized volcanism, seismicity, and human intrusion as important events and climate change as an important process to consider. Elaborate event trees with many changes in physical processes in addition to basic events(136) were developed in 1995 to promote a qualitative understanding of the issues and were similar to the event trees developed for the 1979 Draft EIS on the WIPP. However, the event trees were not used directly in simulations. Rather, only small portions of the trees were considered. Kessler and McGuire report on more extensive use of logic trees for a PA of the Yucca Mountain repository in this

special issue.[137] Currently, the YMP has adopted a hazard identification and scenario development procedure identical to that used by the WIPP Project in the 1990s, which in turn had been proposed to the NRC in 1981.[82,122,138]

Consequence Analysis

Simple analytical calculations to determine the relative importance of various phenomena present at Yucca Mountain were conducted in 1984 (which identified ^{99}Tc, ^{129}I, and ^{237}Np as important radioisotopes for evaluating compliance)[139] and 1988 (performed in conjunction with the SCP).[133] The first large-scale analysis of fluid movement through the unsaturated zone occurred in 1990.[140] Shortly thereafter, a series of deterministic calculations using best estimates for model parameters were run by several organizations—Sandia, PNL, and Los Alamos National Laboratory—to simulate the expected performance of the disposal system in the unsaturated zone. Percolation was set at 0.01 mm/yr and four radioisotopes were transported through a 19-layer one-dimensional model of the mountain. No radioisotopes reached the underlying aquifer ~300 meters below the repository.[141]

Initial Performance Assessments. In 1992 (16 years after a search was begun and 11 years after site selection), the YMP completed the first probabilistic PA[16] of the Yucca Mountain disposal system that evaluated releases to a 5-kilometer boundary (TSPA-91),[142] generally following the process outlined in the 1988 SCP.[133] For fluid flow in TSPA-91, Sandia used a one-dimensional model and PNL a two-dimensional model. For the first time, gaseous flow of ^{14}C and a probability distribution (exponential distribution with mean of 1 mm/yr) for percolation that was believed to incorporate future climatic changes were included.

The second PA (TSPA-93)[143] included an improved source-term model and a saturated zone model. The analysis also greatly expanded the data used for defining distributions for hydrologic and geochemical parameters. Percolation was divided into two distributions: one for the current dry climate (exponential distribution with mean of 0.5 mm/yr) and one for a hypothetical wet climate (exponential distribution with mean of 10 mm/yr).

Also, the Electric Power Research Institute (EPRI) conducted two early PAs in 1990[144] and 1992,[145] and PNL conducted a PA that used detailed multidimensional models of flow and transport, but evaluated consequences for only a limited number of different model parameters. In 1996, EPRI completed a third iteration of their PA,[146] described further in this special issue.[137] Similar to some international regulatory agencies,[147] the NRC has developed an independent capability to perform a PA.[148] The NRC completed their initial PA in 1992[149] and a second in 1995.[150]

Studies for Design Options. Between 1992 and 1995, the YMP reported each year on a fairly simple modeling system (Repository Integration Program [RIP][151]) originally intended to rapidly simulate the behavior of the disposal system to evaluate design systems. The system used a variety of techniques such as curve fits to previous results and selection of distributions for particular data (e.g., percolation fluxes) to incorporate previous results.[152] That is, RIP used simplified model types, $f_\alpha(\cdot)$, for most of the necessary components (designated by α) of the exposure pathway model, $C(\cdot)$. For instance, in the unsaturated zone in 1992 and 1994, a one-dimensional phenomenological model was used and, in 1995, analysts developed steady-state velocity fields and percolation flux distributions, from a few simulations using phenomenological models. This simplified modeling style, called "abstraction," had been originally proposed in the 1988 SCP[133] as the culmination of sensitivity analysis on process models. A purported advantage of this approach is that it allows for rapid calculations and thus potentially helped managers allocate resources for further characterization studies. The analyses using RIP were the only PAs performed by the YMP from 1995 to 1997.[135,153,154] During this time, the choice of corrosion-resistant material for the disposal container shifted from Inconel 625 to Incoloy 825 to Hastelloy C-22. Furthermore, the 100-mm layer of carbon steel, which was to serve as corrosion-allowance, has been replaced with 50-mm layer of stainless steel, which is to serve primarily for structural strength.

Licensing Studies. In 1997, Congress mandated in its energy appropriation bill that the YMP evaluate

[16] The YMP calls its PAs "total system PAs (TSPA)" to emphasize that the assessment includes all the major subsystems and components of the disposal system. Because of the definition of PA used within this report, the term is unnecessary here. However, the term "total system" does serve to explicitly connect performance assessment to systems engineering, a connection that was recognized in the 1970s (e.g., Rowe's book, *Anatomy of Risk*,[81] was part of the engineering systems analysis series of Wiley-Interscience).

the likelihood that the potential Yucca Mountain disposal system would meet EPA and NRC requirements (Public Law 104-206). A viability PA (TSPA-VA) was thus initiated using anticipated new NRC regulatory criteria (10 CFR 63); TSPA-VA was completed in November 1998.[155] Although TSPA-VA used RIP, numerous changes and additions were made to the TSPA-95 models, including the addition of more phenomenological models. Some of these changes included the influence of the zircaloy cladding on commercial spent nuclear fuel, evaluation and inclusion of geochemistry changes near the waste package, colloid formation and transport, and a factor of 100 reduction in solubility of Np. Numerical dispersion in codes modeling the saturated zone was avoided by using six stream tubes; the infiltration of moisture was increased a factor of 10 to a current mean of 7 mm/yr and a long-term average of ~40 mm/yr; and a new risk measure, dose to a 100-member farming community 20 kilometers from the site, was calculated. Similar to past analyses, the TSPA-VA found that the amount of seepage and the distribution of this seepage were the most important aspects determining failure of waste packages and releases of radioisotopes. EPRI also produced a fourth iteration of their PA.[156] Future licensing analyses currently planned include (1) a Draft EIS to be completed by the end of July 1999, (2) a site recommendation PA (TSPA-SR) to be submitted to the president by July 2001, and (3) the license application to be submitted to the NRC by March 2002.

Probability Evaluation

In its first probabilistic assessment of the potential Yucca Mountain disposal system as reported in 1992 (TSPA-91),[142] the YMP was at a relatively early stage in conceptual model development. Thus, TSPA-91 was similar in formality to the 1989 WIPP PA with regard to assigning probability distributions to the uncertain parameters or probabilities for specific scenarios. The probability of human intrusion was evaluated with the Poisson distribution, and the probability of volcanism was based on consensus of analysts within the YMP PA group. Parameter values and distributions were determined primarily by individual PA analysts. The formality increased when uncertain parameters were evaluated in YMP's second PA (TSPA-93), reported on in 1994,[143] in that distributions for many more parameters were developed and were more often based on the consensus of several PA analysts, accompanied by input from site characterization scientists. The basic information on parameter distributions reported in TSPA-93 was then used for subsequent simplified PAs in 1995, 1996, and 1997,[135,153–154] although values were sometimes changed for parametric sensitivity analysis. Improved data for a few parameters (e.g., solubility of neptunium) were incorporated into the TSPA-VA. However, many parameter values that were estimated in the early 1990s have not yet been confirmed. However, the requirement to conduct the TSPA-VA spurred the process of developing an analysis that could withstand regulatory scrutiny, and have generated numerous quality assurance (QA) procedures were applied.

6.3. Other Assessments for Repositories

Other Performance Assessments in the United States

Besides PAs conducted specifically for the WIPP and the YMP, other PAs were conducted by the United States. Three projects in the United States that benefited from PA were (1) a reexamination of deep seabed disposal of nuclear waste in 1977 that concluded in 1988 and that applied some techniques, such as embedded models, that were later adopted for the WIPP Project[157]; (2) an exploration of the feasibility of demonstrating compliance for greater-than-class C low-level waste (e.g., tritium) and other transuranic waste, which was disposed of at the Nevada Test Site in 1981[158,159]; and (3) analyses in 1993 and 1995 of the behavior of DOE-owned spent nuclear fuel to test the viability of direct disposal of the waste in salt, granite, and tuff that used tools developed for the WIPP[9,160] (Fig. 11).

International Assessments

In contrast to the United States, most countries have anticipated relatively long-term surface storage of spent nuclear fuel and high-level waste, so there has been less motivation to follow a strict timetable for permanent disposal.[161] The Canadians and British support probabilistic assessments, but most other international PAs tend to be deterministic. Other differences include the omission or inclusion of future human intrusion and the length of the regulatory period. For example, Germany does not consider human intrusion in its assessments nor specify

a regulatory time period. Also, countries other than the United States sometimes place greater emphasis on analog models in addition to mathematical models for predictions of future behavior[15,16] and use a dose (or individual risk) rather than a cumulative release limit. Figure 13 is a summary depiction of analysis and disposal criteria in several international assessments of nuclear waste disposal. B.G.J. Thompson reports on various regulatory issues addressed in the international community in this special issue.[147]

7. SUMMARY

7.1. Common Foundations and Comparisons Between Risk Assessments

Risk assessment has evolved from hazard identification for relatively straightforward problems to methods that incorporate probability and uncertainty of knowledge for more complex situations, when society is unsure about how to either interpret or respond

- **1967** - West Germany begin experiments for radioactive waste disposal in abandoned Asse salt/potash mine.
- **1975 - Oct:** International Nuclear Energy Agency (NEA) forms Radioactive Waste Management Committee to foster exchange of information on nuclear waste disposal.
- **1977** - Sweden begins underground research at Stripa mine. IAEA recommends site selection criteria for geologic disposal sites.
- **1978** - Canada announces Atomic Energy of Canada, Ltd. (AECL), given task of developing nuclear waste disposal concept. West Germany starts suitability study of abandoned Konrad iron ore mine for disposing of radioactive waste with no heat (primarily low and intermediate level waste [LLW & ILW]). Sandia WIPP project begins technical exchange with German salt disposal project at Asse salt mine.
- **1979** - West Germans start investigating high-level waste disposal in salt dome at Gorleben, near East-W est boarder.
- **1980** - Swedes reject nuclear power in national referendum, must find source for 50% of electric power needs by 2010. Switzerland regulator (HSK) sets max individual dose at 0.1 mSv/yr for HLW without time limit.

1981 Canadians publish SYVAC-1

1981 East Germans start disposing LLW & ILW at Morsleben

- **1981 - Apr:** East Germans start disposing low and intermediate alpha-emitting radioactive waste in Morsleben, abandoned mine in domal salt, near Gorleben under 5 yr license. Canada announces no site selection until after EIS on disposal concept. Canadians proponents (AECL) develop SYVAC-1, single set of primarily analytic models for total-system geologic and subseabed disposal (concept expanded on by CAMCON). IAEA recommends procedure for PA and potential list for scenarios.
- **1982** - U.K.'s regulator (HMIP) adapts SYVAC-1 for use in low-, inter- mediate-, and high-level waste disposal. Germans complete suitability study of Konrad and start developing license application.
- **1983** - Commission of European Communities (CEC) develops LISA PA code. To continue developing nuclear power, Swedes publish PA of disposal of HLW in fractured granite using copper canister and bentonite backfill. German regulator (BMU) promulgate radioactive standards, mostly qualitative except for maximum dose limit of 0.3 mSv/yr without time limit.
- **1984** - NEA sets up group from various countries to exchange ideas on PA. NEA suggests maximum individual human health risk of 10^{-5} cancers per year from HLW. Swiss begin field tests in fractured granite in Swiss Alps at Grimsel.
- **1985** - Canadians complete second interim assessment on conceptual design using SYVAC-2 and begin underground research at Lac du Bonnet, Winnipeg. Swiss proponents (NAGRA) publish Project Gewahr PA of vitrified HLW in a 1200-m deep repository in granite. Spain's nuclear safety council publishes safety criteria.. Sweden nuclear waste studies at Äspö Laboratory.
- **1986** - East Germans grant Morsleben permanent disposal license. West Germany begins construction of 2 shafts in Gorleben salt dome. Swedish Nuclear Power Inspectorate (SKI) starts "Project-90" to examine hypothetical granite repository with 100-mm thick copper canister. U.K. simulates glacial climate changes in PA.
- **1987** - Canada sets maximum individual risk at 10^{-6}/yr for 10^{4} yr for HLW disposal.
- **1988** - Canada's proponent AECL announces disposal concept ready for EIS review.
- **1989** - U. K. develop VANDAL, combination of SYVAC and precursor of NEFTRAN, as PA tool. NEA holds major symposium on state-of-the-art nuclear waste disposal.
- **1990** - Sweden's regulator complete Project 90 (deterministic PA on "what if" conditions).

1991 Sweden complete major PA

- **1991** - Swedish proponents publish assessment focusing on role of geosphere ("SKB-91"). Finland sets maximum individual dose at 0.1 mSv/yr for normal and 5 mSv/yr for accident conditions without time limit. Administrative count issues preliminary injunction to stop waste emplacement at Morsleben.

1992 U.K. complete "Dry Run 3" PA

- **1992** - Canada's Minister of Natural Resources issues guidelines for EIS on disposal concept to AECL. Finland publishes deterministic PA of disposal concept ("TVO-92"). U.K.'s regulator (HMIP) completes "Dry Run 3" – full probabilistic PA including long-term glaciation of site using VANDAL, a network simulation code. First integrated PA of HLW disposal is performed in Japan.
- **1993** - U.K.'s regulator (HMIP) sets 10^{-6}/yr for individual risk or 0.1 mSv/yr dose without time limit.

1994 Canadians publish EIS on HLW repository concept

- **1994** - Canada's proponent AECL publishes EIS for disposal concept recommending siting phase. Netherlands publishes probabilistic PA of disposal of vitrified HLW in salt domes. Swiss proponents (NAGRA) update their 1985 PA in Kristallin I. German court lifts injunction and waste emplacement begins again at Morsleben.
- **1996** - Sweden's regulator completes SITE 94 (large study of features, events, and processes) for a hypothetical repository with geologic characteristics derived from the Äspö laboratory.
- **1998 - Jun:** Final signatory of Konrad license application refuses to sign license until after German elections. **Sep:** Superior Administrative Court orders emplacement of waste to stop at Morsleben's "eastern field" however, all emplacement stopped voluntarily. **Dec:** Germans elect socialist Green coalition to power that vows to stop reliance on all nuclear power over next 4 yr (33% of energy use, plants represent 61 billion in assets); want all waste disposal to stop until reevaluation of sites and one site selected.

Fig. 13. Standards and assessments in the international community for nuclear waste disposal.

to an identified hazard for which there is only limited experience. Furthermore, risk management decisions often are constrained to use (through regulations) different kinds of risk information and, thereby, encompass varying degrees of detail.

Definition of Risk Criteria

Until a regulatory environment has been established, any risk assessment must deal with defining risk criteria and goals. Initially, Congress decreed zero probability of cancer from food additives in the "Delaney clause" in 1958 (Figs. 1 and 9). However, in the 1970s and 1980s, several technological and environmental risk goals were defined. In 1973, the FDA proposed evaluating cancer risks (Figs. 1 and 9), and in 1977, the FDA proposed a probability of less than 10^{-6} cancers per year as a risk goal (42 FR 10412; 52 FR 49572), assuming dose–response models with plausible upper bounds. (That is, the risk criteria are dependent on the methods used to assess the risk.) The Supreme Court endorsed a similar risk goal for OSHA in 1980 (100 S. Ct. 2844). From 1977 to 1985, the radiation program within the EPA set about establishing risk limits for radioactive waste repositories to promulgate 40 CFR 191 (50 FR 38066). The EPA is currently establishing site-specific risk limits for a potential site at Yucca Mountain in 40 CFR 197 (64 FR 46976).

Characterization of System

In antiquity through the 1930s, system definition and characterization was relatively informal and primarily based on experience with an activity or technology. System characterization is necessary for any scientific modeling of a natural system, whether its purpose is to gain insight or illustrate possible future behavior. Hence, even before safety goals and a compliance process were established for radioactive waste disposal, characterization of the WIPP near Carlsbad, New Mexico, was undertaken for the EIS in the late 1970s (Figs. 1 and 11).

Identification of Hazards and Development of Scenarios

Many practical risk management techniques have been rapidly and inexpensively deployed to reduce risks by means of a hazard assessment. Simple hazard identification and appropriate risk management, such as linking cholera to contaminated well water (Figs. 1 and 3) and later purified water supplies,[25] improved sanitation, and medical services, were responsible for the dramatic rise in human longevity from about 25 years at the time of the Roman Empire to about 63 years in 1940. Applied risk management, such as improved medical services, in turn lead to identifying new hazards (e.g., radium paint; Figs. 1 and 4).[19] Although, NASA abandoned tools of probability and consequence assessments for the Apollo Program in the 1970s, it retained hazard assessment through Failure Mode/Effects Analysis.[66] The initial assessment of an abandoned chemical waste site for emergency response under CERCLA is a hazard assessment.

Evaluation of Probability

From its inception around 1660, probability theory has been intimately involved with individual and societal decisions about actions that can be taken today, such as insuring life or property (e.g., the Dutch), to mitigate possible unwanted future outcomes (Figs. 1 and 2).[1] Reliability/system analysis became important during development of aircraft technology in the 1930s and missile technology in the 1940s and 1950s (Figs. 1 and 5).[40] For these technologies, a trial-and-error, design-and-construction approach was insufficient.

A major difference among types of risk assessments is whether uncertainties in knowledge of parameters and model forms are included. For a deterministic evaluation, the risk assessment displays only a conditional result $C(\mathbf{x})$, where $\mathbf{x}$ are expected or best estimate values of parameters or, more often, plausible upper bounds. Unless the system under study is linear, the use of expected parameter values in models will not necessarily result in expected values of the consequence—a measure of risk promoted in the early 1980s (e.g., Ref. 162). The use of plausible upper-bound parameter values can present additional problems because the location of the conservative result with regard to distribution is not known and the degree of conservatism in risk from different hazards can differ greatly, as pointed out as early as 1985.[74] Furthermore, comparison of *mean* benefits to *conservative* risks for various options is problematic when making decisions.[17,74] Even though encouraged in the early 1980s (Figs. 1 and 10), the absence of a

mandate to include uncertainty in risk assessments for hazardous waste disposal contributed to the inconsistent use of uncertainty analysis into the mid-1990s.[93]

A PRA displays the entire distribution function and avoids the dilemma in which events of low probability and high consequence are equated to events of high probability and low consequence, although conservative models and parameters are still incorporated, as in the dose–response assessment and conditions of future society. Until uncertainty is included in the risk assessment, the risk measure will likely diverge from a common historical meaning of the word risk, associated with variance, and thus contribute to misunderstanding. Requiring explicit, quantitative inclusion of uncertainty by the EPA in 40 CFR 191 was a natural progression from the 1975 *Reactor Safety Study* (which, in turn, had progressed from smaller studies in the late 1960s; Fig. 1). The stochastic analyses for nuclear facilities have yielded (and continue to yield) by far the largest analysis of uncertainty in mathematical modeling.

Evaluation of Consequence

A consequence evaluation determines the effects of realizing a hazard through a dose–response assessment and an exposure pathway assessment. Initially, in the early 1900s, scientists assumed a model of human dose response with a threshold below which there was zero risk of toxicity. By the 1940s, however, observed effects of radiation and radioisotope toxicity studies (Figs. 1 and 4) brought into question whether a practical threshold existed for radiation[17,35] and, in 1948, the NCRP recommended an ALARA policy for radiation. By the mid-1970s, the FDA and EPA were adopting non-threshold guidelines for developing bounding dose—response curves as risk analysis was introduced for carcinogenic chemicals (Figs. 1 and 10). According to current EPA guidelines, PA and PRA included, the dose–response assessment (i.e., modeling internal to the human body) uses plausible upper bounds for parameter values, but uncertainty in radiogenic dose–response has been explored (62 FR 55249; 63 FR 36677).

The prediction of consequences along exposure pathways external to humans became important as society grew concerned about the consequences of technologies or activities of which little was known. Soon after passage of the Atomic Energy Act of 1954 (Public Law 83-703 [68 Stat. 919]), the financial risk to the federal government from a calamity at a nuclear power plant motivated an examination of consequences in the late 1950s.[20,50] The *Reactor Safety Study* in 1975 investigated risks from the nuclear power plant by combining concepts of reliability analysis, exposure pathway analysis, and radiation pharmacology, thus inaugurating the concept of a PRA on a grand scale. This study was later updated in 1990 (Figs. 1 and 6).

In assessing the safety of a geologic disposal system for the first time in the mid 1970s (Figs. 1 and 7), a new challenge was understanding long-term behavior of system components (e.g., waste containers and their interaction with the host rock environment). Especially in the United States, a PA became intimately tied to the process of building a mathematical model of the system. The passage of stringent risk criteria required a more realistic, rather than a highly conservative but simple, analysis. In turn, the realistic analysis required evaluating the uncertainty associated with stylized situations for regulatory analysis. Monte Carlo analysis, originally developed and applied in 1947 for nuclear weapon design on the first computers (Figs. 1 and 5). LHS has been frequently used for sensitivity and uncertainty analysis of several linked models in the United States.[11,115] The LHS technique, a simple scheme developed in 1975[57] to judiciously sample the parameter domain in Monte Carlo Analysis, was used to gain insight about the pipe ruptures in nuclear power plants in 1975[57] and important parameters of a geologic disposal system in 1978 in PAs and PRAs.[86,87]

Evaluation of Risk Measure and Comparison with Risk Goals

A significant difference between a PA for radioactive disposal and other policy analyses is that the PA (by definition), is designed to test *compliance* to a set of standards rather than just elucidate understanding. Certainly, PA can be used to enhance understanding through sensitivity analysis; however, the assessment for radioactive waste disposal is essential to determine whether the selected risk management technique, deep geologic disposal of nuclear waste, is likely to meet the selected risk limits using stylized circumstances selected by the regulator. Although the disposal assessment does not represent a complete examination of intergenerational equity, it is unique among regulations in the United States in at least indirectly acknowledging the issue (40 CFR 191;

50 FR 58196).[92] Building on the work conducted at Sandia in the late 1970s and 1980s,[62,63,75–77,157] the assessment for the WIPP in 1996 consisted of a PA that included many quantifiable uncertainties (Figs. 1 and 11). The distribution of cumulative radioisotope release results, expressed as a CCDF, was compared with probabilistic regulatory criteria.[109–114]

In contrast, for an active hazardous waste disposal site, specified methods for treatment and disposal of the waste at a site with specific engineered features, such as plastic liners as required by regulations implementing RCRA (40 CFR Parts 260–281), are used to determine compliance. Furthermore, because a ready funding source is available from the DOE or users of electrical power generated by reactors, the resources that are marshaled and the costs incurred for evaluating consequences, incorporating uncertainty into the analysis, and demonstrating compliance with nuclear waste disposal regulations are one or two orders of magnitude greater than might be expected for clean up of an abandoned Superfund site (using the WIPP Project as an example).[70] Hence, several other aspects also differentiate chemical and nuclear waste risk assessments. More extensive site-specific information is produced for a nuclear waste site than for a chemical site[70]; the inventory of radionuclides is fairly well determined[111]; the feature, event, and process screening and scenario development are more detailed[72,88,119,122]; the exposure pathway assessment uses more detailed phenomenological models[113,114,127]; modeling assumptions are more consistent because of the use of database and computer control of the analysis[109,120]; several iterations of the analysis are performed and sensitivity analysis is extensive.[126,128] When evaluating mixed waste problems and disposal sites, analysts have had to resolve some of the differences in assessment assumptions,[105] but much more could be done.

7.2. Influence of Risk Assessments

The first two steps of a risk assessment, basically hazard assessment have clearly led to improvements in general human welfare since ancient times. Yet, the addition of consequence and probabilistic evaluation steps have also produced some valuable input for documenting administrative decisions for controversial projects likely to be reviewed by a court.[17] Basic risk evaluations have been used at OSHA since the U.S. Supreme Court ruled that a risk assessment was required before OSHA could promulgate an occupational exposure regulation (100 S. Ct. 2844). The FDA has used risk assessment to reach more reasoned decisions such as in 1980, when the FDA successfully argued that the risks from lead acetate, a possible carcinogen, were reasonable when used in hair coloring (45 FR 72112).

Sophisticated risk assessments, such as the PAs for the WIPP, blend information from multiple disciplines and thus multiple viewpoints, which can be a strength when dealing with large uncertainties, rather than relying on only one discipline, such as geology.[17] The NRC eventually became a staunch supporter of PRAs in managing risks at nuclear reactors and adopted them as the main tool for setting policies in 1995. Similarly, the EPA became convinced of the benefits of a PA for radioactive waste disposal. Nevertheless, except for PA and PRA for nuclear facilities and policy setting at OSHA and FDA, risk assessment has not been uniformly recognized as a valuable input to policy decisions, regulatory control of other environmental concerns within the EPA, possibly because of the inconsistent mandate provided by Congress and the courts.

Risk assessment has also been used to influence other types of policy decisions. For example, the federal government has used risk assessment results to examine dollars spent on risk management in proportion to potential lives saved.[17,93] Yet, just as conclusions of cost–benefit analysis are dependent on the assumed future interest rate or the value of a human life, the results from risk assessments can become dependent on basic assumptions about the conditions under investigation (e.g., assumptions concerning future human activities; such as exploratory drilling) and land use (such as a housing development). At the WIPP, this dependency was acknowledged when information about the geologic disposal site was deemed sufficient because assumptions on inadvertent human intrusion continued to dominate the risk results at the later stages of disposal characterization. Not acknowledging such a dependency can be detrimental if the decision makers assume that the assessment calculates an absolute risk such that comparisons of risks from different hazards and activities are valid. The latter situation could occur when comparing calculated risk from radioactive hazardous and waste disposal, even though the time frames of the analyses are very different and the assessment as-

[17] However, adequate documentation and competent peer review are required lest the risk assessment become less than the sum of the disciplines ("parts").

sumptions include the potential for human intrusion in one case but not in the other.

Although many have urged inclusion of uncertainty when quantifying risks, not all elements of uncertainty can properly or easily enter the assessment, and thus other factors must enter into a risk management decision. For example, the PA for disposal of radioactive waste at the WIPP, which included more than 80,000 pages of documentation, has not by itself produced a change in the public's basic beliefs about radioactive waste disposal in New Mexico that is politically significant.[60,163,164] That is, the assessment has not been considered by the public as a complete measure of the uncertainty of the repository. Rather, the public has used factors such as knowledge of the type of waste to be stored at the WIPP, its perception of risk associated with transporting the waste, and, as part of the overall uncertainty, its trust of public officials' personal acceptance or resistance to the WIPP repository. (The concept is similar to a banker's "risk premium" on interest rates.)

Furthermore, risk assessment cannot always lead to the desired understanding of the issues or to more reasoned decisions.[93] In some cases, risk assessments have inadvertently increased the public's concern over safety. For example, the initial assessment of risks at Times Beach, Missouri, overestimated risks, confirmed public fears, and contributed to the decision to evacuate residents. Subsequent studies by the Centers for Disease Control and Prevention, including a revised risk assessment in 1991, suggested that the first assessment exaggerated the risks and that a less drastic risk management choice such as paving dirt roads may have made the evacuation unnecessary.[99] Similarly, a questionable study of the cancer risk from asbestos in 1978[99] eventually led to the extreme risk management decision to remove all asbestos insulation in schools. A more moderate risk management approach, which left undisturbed asbestos insulation in good condition, was not instituted until the 1990s, and then only after prodding by scientists[165] and after billions had been spent. Finally, in 1989, the Natural Resources Defense Council (NRDC) used a risk assessment to challenge EPA's decision to phase out during an 18-month period the use of Alar (a growth stimulant regulated as a pesticide). The news story, which had started with results from the NRDC assessment, caused unnecessary public avoidance of apples and contributed to economic ruin of several small apple farmers.[166] Therefore, we should not as a profession expect too much of a "simple paper study" in its ability to further acceptance of a particular activity nor hastily conclude that a "simple paper study" cannot contribute to unintended harm.

ACKNOWLEDGMENTS

This work was performed by Sandia National Laboratories, which is a multiprogram laboratory operated by Sandia Corporation, a Lockheed-Martin Company for the U.S. Department of Energy (DOE) under Contract DE-AC04-94AL8500. The author is grateful to F. C. Allan and S. Halliday, librarians from Sandia who helped with searches, C. S. Crawford, ASAP, Inc., who verified references, and J. M. Chapman and S. K. Best of Tech Reps, Inc., who respectively edited this text and prepared the figures. M. S. Tierney and F. W. Bingham at Sandia National Laboratories carefully reviewed the test and called attention to additional historical facts.

REFERENCES

Note: See Ref. 8 for a more complete listing of primary references.

1. I. Hacking, *The Emergence of Probability: A Philosophical Study of Early Ideas About Probability, Induction and Statistical Inference* (Cambridge University Press, New York, 1975).
2. P. L. Bernstein, *Against the Gods: The Remarkable Story of Risk* (John Wiley & Sons, New York, 1996).
3. National Academy of Sciences/National Research Council (NAS/NRC), *Risk Assessment in the Federal Government: Managing the Process,* Committee on the Institutional Means for Assessment of Risks to Public Health, Commission on Life Sciences, National Research Council (National Academy Press, Washington, D.C., 1983).
4. W. W. Lowrance, *Of Acceptable Risk: Science and the Determination of Safety* (W. Kaufmann, Los Altos, CA, 1976).
5. M. W. Martin and R. Schinzinger, *Ethics in Engineering,* 2nd Ed. (McGraw-Hill, New York, 1989).
6. R. B. Cumming, "Editorial: Is Risk Assessment a Science?" *Risk Anal.* **1**(1), 1–3 (1981).
7. W. D. Ruckelshaus, "Science, Risk, and Public Policy," *Science* **221**(4615), 1026–1028 (1983).
8. R. P. Rechard, *Historical Relationship Between Performance Assessment and Other Types of Risk Assessment in the United States* (Sandia National Laboratories, Albuquerque, NM, in preparation).
9. R. P. Rechard (ed.), *Performance Assessment of the Direct Disposal in Unsaturated Tuff of Spent Nuclear Fuel and High-Level Waste Owned by U.S. Department of Energy,* SAND94-2563/1/2/3 (Sandia National Laboratories, Albuquerque, NM, 1995), pp. 1–3.
10. S. Kaplan and B. J. Garrick, "On the Quantitative Definition of Risk," *Risk Anal.* **1**(1), 11–27 (1981).
11. J. C. Helton, D. R. Anderson, M. G. Marietta, and R. P. Rechard, "Performance Assessment for the Waste Isolation Pilot Plant: From Regulation to Calculation for 40 CFR 191.13," *Oper. Res.* **45**(2), 157–177 (1997).

12. J. C. Helton, "Risk, Uncertainty in Risk, and the EPA Release Limits for Radioactive Waste Disposal," *Nucl. Technol.* **101**(1), 18–39 (1993).
13. M. G. Morgan, M. Henrion, and M. Small, *Uncertainty, A Guide to Dealing with Uncertainty in Quantitative Risk and Policy Analysis* (Cambridge University Press, New York, 1990), p. 292.
14. N. C. Rasmussen, *Reactor Safety Study: An Assessment of Accident Risks in U.S. Commercial Nuclear Power Plants,* NUREG-75/014, WASH-1400 (U.S. Nuclear Regulatory Commission, Washington, D.C., 1975), pp. 1–8.
15. Nuclear Energy Agency (NEA), *Disposal of High-Level Radioactive Wastes: Radiation Protection and Safety Criteria, Proceedings of an NEA Workshop, Paris, 5–7 November 1990* (NEA, Organisation for Economic Co-Operation and Development, Paris, 1991).
16. Nuclear Energy Agency (NEA), *Disposal of Radioactive Waste: Review of Safety Assessment Methods,* A Report of the Performance Assessment Advisory Group of the Radioactive Waste Management Committee, OECD Nuclear Energy Agency (NEA, Organisation for Economic Co-Operation and Development, Paris, 1991).
17. J. D. Graham, "Historical Perspective on Risk Assessment in the Federal Government," *Toxicology* **102**(1/2), 29–52 (1995).
18. K. Shrader-Frechette, *Science Policy, Ethics, and Economic Methodology: Some Problems of Technology Assessment and Environmental-Impact Analysis* (D. Reidel, Boston, 1985).
19. V. T. Covello and J. Mumpower, "Risk Analysis and Risk Management: An Historical Perspective," *Risk Anal.* **5**(2), 103–120 (1985).
20. J. N. Stannard, *Radioactivity and Health: A History,* DOE/RL/01830-T59 (Pacific Northwest Laboratory, Richland, WA, 1988).
21. N. Smith, *A History of Dams* (The Citadel Press, Secaucus, England, 1971), pp. 9, 230–234.
22. J. R. Newman, (ed.), *The World of Mathematics, A Small Library of the Literature of Mathematics from Ah mosé the Scribe to Albert Einstein* (Simon & Schuster, New York, 1956), pp. 1–3.
23. Random House, *Webster's College Dictionary,* Rev. Ed. (Random House, New York, pp. 1998).
24. R. W. Burchfield (ed.), *The Oxford English Dictionary* (Clarendon Press, Oxford, 1982), Vol. VIII, p. 714.
25. National Academy of Sciences/National Research Council (NAS/NRC), *Drinking Water and Health,* Safe Drinking Water Committee, Board on Toxicology and Environmental Health Hazards, Assembly of Life Science, National Research Council (National Academy Press, Washington, D.C., 1977).
26. E. R. Tufte, *Visual Explanations: Images and Quantities, Evidence and Narrative* (Graphics Press, Cheshire, CT, 1997).
27. P. B. Hutt, "Use of Quantitative Risk Assessment in Regulatory Decisionmaking Under Federal Health and Safety Statutes," in D. G. Hoel, R. A. Merrill, and F. P. Perera (eds.), *Risk Quantitation and Regulatory Policy, Proceedings of the Banbury Center Conference, Lloyd Harbor, May 13, 1994,* CONF-8405356, Banbury Report 19 (Cold Spring Harbor Laboratory, Cold Spring Harbor, 1985), pp. 15–29.
28. M. L. Dourson and J. F. Stara, "Regulatory History and Experimental Support of Uncertainty (Safety) Factors," *Regul. Toxicol. Pharmacol.* **3**, 224–238 (1983).
29. B. D. Goldstein, "The Problem with the Margin of Safety: Toward the Concept of Protection," *Risk Anal.* **10**(1), 7–10 (1990).
30. U.S. Environmental Protection Agency (EPA), *Background Information Document Final Rule for High-Level and Transuranic Radioactive Wastes,* EPA 520/1–85–023 (EPA, Office of Radiation Programs, Washington, D.C., 1985).
31. International Commission on Radiological Protection (ICRP), *Report of Committee II on Permissible Dose for Internal Radiation (1959): Recommendations of the International Commission on Radiological Protection,* ICRP Publication 2 (Pergamon Press, New York, 1959).
32. International Commission on Radiological Protection (ICRP), *Limits for Intakes of Radionuclides by Workers: A Report of Committee 2 of the International Commission on Radiological Protection,* ICRP Publication 30, Part 1, Annals of the ICRP, Vol. 2, No. 3/4 (Pergamon Press, New York, 1979).
33. R. D. Evans, "Inception of Standards for Internal Emitters, Radon and Radium," *Health Phys.* **41**(3), 437–448 (1981).
34. R. D. Evans, R. S. Harris, and J. W. M. Bunker, "Radium Metabolism in Rats and the Production of Osteogenic Sarcoma by Experimental Radium Poisoning," *Am. J. Roentgenol.* **52**, 353–373 (1944).
35. E. B. Lewis, "Leukemia and Ionizing Radiation," *Science* **125**(3255), 965–972 (1957).
36. L. J. Carter, *Nuclear Imperatives and Public Trust: Dealing with Radioactive Waste* (Resources for the Future, Washington, D.C., 1987).
37. E. Teller, "The Plowshare Program," *Proceedings of the Second Plowshare Symposium, San Francisco, CA, May 13–15, 1959, Part I, Phenomenology of Underground Nuclear Explosions,* Plowshare Series Report No. 2, UCRL-5675 (Lawrence Radiation Laboratory, Livermore, CA, 1959), pp. 8–13.
38. H. Kumamoto and E. J. Henley, *Probabilistic Risk Assessment and Management for Engineers and Scientists,* 2nd ed. (IEEE Press, New York, 1996), pp. 1–54.
39. N. Metropolis and S. M. Ulam, "The Monte Carlo Method," *J. Am. Statist. Assoc.* **44**(247), 335–341 (1949).
40. J. Neufeld, *The Development of Ballistic Missiles in the United States Air Force 1945–1960* (Office of Air Force History, U.S. Air Force, Washington, D.C., 1990), pp. 169, 215.
41. N. Wiener, *Cybernetics or Control and Communication in the Animal and the Machine,* 2nd Ed. (MIT Press, New York, 1961).
42. A. F. Hixenbaugh, *Fault Tree for Safety,* D6-53604 (Boeing Military Aircraft Product Development, Seattle, 1968).
43. J. R. Kahn, *The Economic Approach to Environmental and Natural Resources,* 2nd Ed. (The Dryden Press, Fort Worth, TX, 1998), pp. 110–113.
44. J. M. Hammersley and D. C. Handscomb, *Monte Carlo Methods* (John Wiley & Sons, New York, 1964).
45. D. B. Hertz, "Risk Analysis in Capital Investment," *Harvard Bus. Rev.* **42**(1), 95–106 (1964).
46. H. Raiffa, *Decision Analysis: Introductory Lectures on Choices Under Uncertainty* (Addison-Wesley, Reading, MA, 1968).
47. R. L. Keeney and H. Raiffa, *Decisions with Multiple Objectives: Preferences and Value Tradeoffs* (John Wiley & Sons, New York, 1976).
48. R. L. Keeney and K. Nair, "Selecting Nuclear Power Plant Sites in the Pacific Northwest Using Decision Analysis," in D. E. Bell, R. L. Keeney, and H. Raiffa (eds.), *Conflicting Objectives in Decisions* (John Wiley & Sons, New York, 1977), pp. 298–332.
49. M. W. Merkhofer and R. L. Keeney, "A Multiattribute Utility Analysis of Alternative Sites for the Disposal of Nuclear Waste," *Risk Anal.* **7**(2), 173–194 (1997).
50. Atomic Energy Commission (AEC), *Theoretical Possibilities and Consequences of Major Accidents in Large Nuclear Power Plants: A Study of Possible Consequences if Certain Assumed Accidents, Theoretically Possible But Highly Improbable, Were to Occur in Large Nuclear Power Plants,* WASH-740 (AEC, Washington, D.C., 1957).
51. G. E. Apostolakis, *Mathematical Methods of Probabilistic Safety Analysis,* UCLA-ENG-7464 (University of California

at Los Angeles, School of Engineering and Applied Science, Los Angeles, 1974).
52. C. Starr, "Social Benefit Versus Technological Risk: What Is Our Society Willing to Pay for Safety?" *Science* **165**, 1232–1238 (1969).
53. J. G. Arbuckle, M. E. Bosco, D. R. Case, E. P. Laws, J. C. Martin, M. L. Miller, R. D. Moran, R. V. Randle, D. M. Steinway, R. G. Stoll, T. F. P. Sullivan, T. A. Vanderver, Jr., and P. A. J. Wilson, *Environmental Law Handbook,* 11th Ed. (Government Institutes, Rockville, MD, 1991), pp. 328–369, 406–442, 471–628.
54. H. W. Lewis, R. J. Budnitz, H. J. C. Kouts, W. B. Lowenstein, W. D. Rowe, F. von Hippel, and F. Zachariasen, *Risk Assessment Review Group Report to the U.S. Nuclear Regulatory Commission,* NUREG/CR-0400 (U.S. Nuclear Regulatory Commission, Washington, D.C., 1978).
55. American Physical Society(APS), "Report to the American Physical Society by the Study Group on Light-Water Reactor Safety," *Rev. Mod. Phys.* **47**, Suppl. 1, S1–S124 (1975).
56. H. W. Lewis, "The Safety of Fission Reactors," *Sci. Am.* **242**(3), 53–65 (1980).
57. M. D. McKay, R. J. Beckman, and W. J. Conover, "A Comparison of Three Methods for Selecting Values of Input Variables in the Analysis of Output from a Computer Code," *Technometrics* **21**(2), 239–245 (1979).
58. J. F. Mason, "The Technical Blow-by-Blow. Details of the Three Mile Island Accident as Excerpted and Edited from Interviews with Nuclear Regulatory Commission Investigators," *IEEE Spectrum* **16**(11), 33–42 (1979).
59. B. Fischhoff, P. Slovic, and S. Lichtenstein, "Weighing the Risks: Which Risks Are Acceptable?" *Environment* **21**(4), 17–20, 32–38 (1979).
60. H. C. Jenkins-Smith and G. W. Bassett, Jr., "Perceived Risk and Uncertainty of Nuclear Waste: Differences Among Science, Business, and Environmental Group Members," *Risk Anal.* **14**(5), 851–856 (1994).
61. B. J. Garrick, "Lessons Learned from 21 Nuclear Plant PRAs," *International Topical Conference on Probabilistic Safety Assessment and Risk Management, Zurich, Switzerland, August 30--September 4, 1987,* CONF-870820 (Pickard, Lowe and Garrick, Newport Beach, CA, 1987.
62. R. J. Breeding, J. C. Helton, E. D. Gorham, and F. T. Harper, "Summary Description of the Methods Used in the Probabilistic Risk Assessments for NUREG-1150," *Nucl. Eng. Des.* **135**(1), 1–27 (1992).
63. U.S. Nuclear Regulatory Commission (NRC), *Severe Accident Risks: An Assessment for Five U.S. Nuclear Power Plants. Final Summary Report,* NUREG-1150 (NRC, Washington, D.C., 1990–1991), pp 1–3.
64. C. Perrow, *Normal Accidents: Living with High-Risk Technologies* (Basic Books, New York, 1984), pp. 108–112.
65. F. M. Bordewich, "The Lessons of Bhopal," *The Atlantic* **259**(3), 30–33 (1987).
66. B. J. Garrick, "The Approach to Risk Analysis in Three Industries: Nuclear Power, Space Systems and Chemical Process," in R. A. Knief (ed.), *Risk Management: Expanding Horizons in Nuclear Power and Other Industries* (Hemisphere, New York, 1991), pp. 173–181.
67. E. Marshall, "Feynman Issues His Own Shuttle Report, Attacking NASA Risk Estimates," *Science* **232**(4758), 1596 (1986).
68. U.S. Congress, *Investigation of the Challenger Accident,* Report of the Committee on Science and Technology, House of Representatives, Ninety-Ninth Congress, Second Session, House Report 99-1016 (U.S. Government Printing Office, Washington, D.C.,1986).
69. R. P. Rechard, *Milestones for Disposal of Radioactive Waste at the Waste Isolation Pilot Plant (WIPP) in the United States,* SAND98-0072 (Sandia National Laboratories, Albuquerque, NM, 1998).
70. R. P. Rechard, *Historical Background on Assessing the Performance of the Waste Isolation Pilot Plant,* SAND98-2708 (Sandia National Laboratories, Albuquerque, NM, 1999).
71. National Academy of Sciences/National Research Council (NAS/NRC), *The Disposal of Radioactive Waste on Land: Report of the Committee on Waste Disposal of the Division of Earth Sciences,* Publication 519 (NAS/NRC, Washington, D.C., 1957).
72. H. C. Claiborne and F. Gera, *Potential Containment Failure Mechanisms and Their Consequences at a Radioactive Waste Repository in Bedded Salt in New Mexico,* ORNL-TM-4639 (Oak Ridge National Laboratory, Oak Ridge, TN, 1974).
73. W. C. McClain and R. L. Bradshaw, "Status of Investigations of Salt Formations for Disposal of Highly Radioactive Power-Reactor Wastes," *Nucl. Saf.* **11**(2), 130–141 (1970).
74. M. E. Paté-Cornell, "Uncertainties in Risk Analysis: Six Levels of Treatment," *Reliab. Eng. Syst. Saf.* **54**(2/3), 95–111 (1996).
75. R. M. Cranwell, J. E. Campbell, J. C. Helton, R. L. Iman, D. E. Longsine, N. R. Ortiz, G. E. Runkle, and M. J. Shortencarier, *Risk Methodology for Geological Disposal of Radioactive Waste: Final Report,* SAND81-2573, NUREG/CR-2452 (Sandia National Laboratories, Albuquerque, NM, 1987).
76. J. E. Campbell and R. M. Cranwell, "Performance Assessment of Radioactive Waste Repositories," Science 239(4846), 1389–1392 (1988).
77. J. W. Bartlett, H. C. Burkholder, and W. K. Winegardner, "Safety Assessment of Geologic Repositories for Nuclear Waste," in J. B. Fussell and G. R. Burdick (eds.), *Nuclear Systems Reliability Engineering and Risk Assessment* (Society for Industrial and Applied Mathematics, Philadelphia, 1977), pp. 636–660.
78. S. E. Logan, *Workshop on Geologic Data Requirements for Radioactive Waste Management Assessment Models,* Santa Fe, NM, June 28–July 1, 1976, Y/OW1/SUB-76/81726 (University of New Mexico, College of Engineering, Albuquerque, 1976).
79. International Atomic Energy Agency (IAEA), *Site Selection Factors for Repositories of Solid High-Level and Alpha-Bearing Wastes in Geological Formations,* Technical Report Series No. 177 (International Atomic Energy Agency, Vienna, 1977).
80. R. C. Ewing, M. S. Tierney, L. F. Konikow, and R. P. Rechard, "Performance Assessments of Nuclear Waste Repositories: A Dialogue on Their Value and Limitations," *Risk Anal.* **19**(5), 933–958 (1999).
81. W. D. Rowe, *An Anatomy of Risk* (John Wiley & Sons, New York, 1977), pp. 11–27.
82. R. M. Cranwell, R. V. Guzowski, J. E. Campbell, and N. R. Ortiz, *Risk Methodology for Geologic Disposal of Radioactive Waste: Scenario Selection Procedure,* SAND80-1429, NUREG/CR-1667 (Sandia National Laboratories, Albuquerque, NM, 1990).
83. International Atomic Energy Agency (IAEA), *Safety Assessment for the Underground Disposal of Radioactive Wastes,* Safety Series No. 56 (International Atomic Energy Agency, Vienna, 1981).
84. R. L. Hunter, *Preliminary Scenarios for the Release of Radioactive Waste from a Hypothetical Repository in Basalt of the Columbia Plateau,* SAND83-1342, NUREG/CR-3353 (Sandia National Laboratories, Albuquerque, NM, 1983).
85. J. C. Helton, "Uncertainty and Sensitivity Analysis in the Presence of Stochastic and Subjective Uncertainty," *J. Stat. Comput. Simul.* **57**(1/4), 3–76 (1997).
86. R. L. Iman, J. C. Helton, and J. E. Campbell, *Risk Methodology for Geologic Disposal of Radioactive Waste: Sensitivity*

Analysis Techniques, SAND78-0912, NUREG/CR-0390 (Sandia National Laboratories, Albuquerque, NM, 1978).
87. R. L. Iman and W. J. Conover, "Small Sample Sensitivity Analysis Techniques for Computer Models, with an Application to Risk Assessment," *Commun. Stat.* **A9**(17), 1749–1842 (1980).
88. F. W. Bingham and G. E. Barr, "Development of Scenarios for the Long-Term Release of Radionuclides from the Proposed Waste Isolation Pilot Plant in Southeastern New Mexico," in C. J. M. Northrup, Jr. (ed.), *Scientific Basis for Nuclear Waste Management, Proceedings of the International Symposium, Boston, MA, November 27–30, 1979,* SAND79-0955C (Plenum Press, New York, 1980), Vol. **2**, pp. 771–778.
89. J. E. Campbell, R. T. Dillon, M. S. Tierney, H. T. Davis, P. E. McGrath, F. J. Pearson, Jr., H. R. Shaw, J. C. Helton, and F. A. Donath, *Risk Methodology for Geologic Disposal of Radioactive Waste: Interim Report,* SAND78-0029, NUREG/CR-0458 (Sandia National Laboratories, Albuquerque, NM, 1978).
90. E. J. Bonano, P. A. Davis, L. R. Shipers, K. F. Brinster, W. E. Beyeler, C. D. Updegraff, E. R. Shepherd, L. M. Tilton, and K. K. Wahi, *Demonstration of a Performance Assessment Methodology for High-Level Radioactive Waste Disposal in Basalt Formations,* SAND86-2325, NUREG/CR-4759 (Sandia National Laboratories, Albuquerque, NM, 1989).
91. Science Advisory Board(SAB), *Report on the Review of Proposed Environmental Standards for the Management and Disposal of Spent Nuclear Fuel, High-Level and Transuranic Radioactive Wastes (40 CFR 191),* (High-Level Radioactive Waste Disposal Subcommittee, Science Advisory Board, U.S. Environmental Protection Agency, Washington, D.C., 1984).
92. D. Okrent, "On the Intergenerational Equity and Its Clash with Intragenerational Equity and On the Need for Policies to Guide the Regulation of Disposal of Wastes and Other Activities Posing Very Long Term Risks," *Risk Anal.* **19**(5), 877–901 (1999).
93. National Academy of Public Administration NAPA), *Setting Priorities, Getting Results: A New Direction for the Environmental Protection Agency,* Report to Congress, 1st ed. (Washington, D.C., 1995).
94. H. J. Otway, "Risk Estimation and Evaluation," in *Proceedings of IIASA Planning Conference on Energy Systems, IIASA-PC-3, Baden, July 17–20, 1973,* CP-73-03 (International Institute for Applied Systems Analysis, Laxenburg, Austria, 1973), pp. 354–379.
95. N. Mantel and W. R. Bryan, " 'Safety' Testing of Carcinogenic Agents," *J. Nat. Cancer Inst.* **27**(2), 455–470 (1961).
96. J. Q. Wilson, *Bureaucracy: What Government Agencies Do and Why They Do It* (Basic Books, New York, 1989).
97. R. Carson, *Silent Spring,* 25th Anniversary Ed. (Houghton Mifflin; Boston, 1987).
98. E. L. Anderson and the Carcinogen Assessment Group of the U.S. Environmental Protection Agency, "Quantitative Approaches in Use to Assess Cancer Risk," *Risk Anal.* **3**(4), 277–295 (1983).
99. A. Wildavsky, *But Is It True? A Citizen's Guide to Environmental Health and Safety Issues* (Harvard University Press, Cambridge, MA, 1995).
100. U.S. Environmental Protection Agency (EPA), Respondents motion to determine whether or not the registration of mirex should be cancelled or amended, Attachment A (September 9, 1975).
101. W. D. Ruckelshaus, "Risk, Science, and Democracy," *Iss. Sci. Technol.* **1**(3), 19–38 (1985).
102. K. S. Crump, "An Improved Procedure for Low-Dose Carcinogenic Risk Assessment from Animal Data," *J. Environ. Pathol. Toxicol. Oncol.* **5**(4/5), 339–348 (1984).
103. National Academy of Sciences/National Research Council (NAS/NRC), *Science and Judgment in Risk Assessment,* Committee on Risk Assessment of Hazardous Air Pollutants, Board on Environmental Studies and Toxicology, Commission on Life Sciences, National Research Council (National Academy Press, Washington, D.C., 1994).
103a. U.S. Environmental Protection Agency (EPA), *Policy for Use of Probabilistic Analysis in Risk Assessment at the U.S. Environmental Protection Agency,* EPA/630/R-97/001. EPA, Washington, DC, 1997)
104. J. V. Rodricks, "Risk Assessment at Hazardous Waste Disposal Sites," *Hazard. Waste* **1**(3), 333–362 (1984).
105. R. P. Rechard and M. S. Y. Chu, "Use of Risk to Resolve Conflicts in Assessing Hazards at Mixed-Waste Sites," in A. A. Moghissi and G. A. Benda (eds.), *Mixed Waste, Proceedings at the First International Symposium, Baltimore, MD, August 26–29, 1991,* SAND91-0587C (University of Maryland, Baltimore, 1991), pp. 12.4.1–12.4.15.
106. R. Wilson, "Introduction," in R. Wilson and J. D. Spengler (eds.), *Particles in Our Air: Concentrations and Health Effects* (Harvard University Press, Cambridge, MA, 1996), pp. 1–14.
107. R. A. Merrill, "Legal Impediments to the Use of Risk Assessment by Regulatory Agencies," in D. G. Hoel, R. A. Merrill, and F. P. Perera (eds.), *Risk Quantitation and Regulatory Policy, Proceedings of the Banbury Center Conference, Lloyd Harbor, NY, May 13, 1994,* CONF-8405356, Banbury Report 19 (Cold Spring Harbor Laboratory, Cold Spring Harbor, 1985), pp. 41–52.
108. National Academy of Sciences/National Research Council (NAS/NRC), *Regulating Pesticides in Food: The Delaney Paradox,* Committee on Scientific and Regulatory Issues Underlying Pesticide Use Patterns and Agricultural Innovation, Board on Agriculture, National Research Council (National Academy Press, Washington, D.C., 1987).
109. R. P. Rechard, *Review and Discussion of Code Linkage and Data Flow in Nuclear Waste Compliance Assessments,* SAND87-2833 (Sandia National Laboratories, Albuquerque, NM, 1989).
110. M. G. Marietta, S. G. Bertram-Howery, D. R. Anderson, K. F. Brinster, R. V. Guzowski, H. Iuzzolino, and R. P. Rechard, *Performance Assessment Methodology Demonstration: Methodology Development for Evaluating Compliance with EPA 40 CFR 191, Subpart B, for the Waste Isolation Pilot Plant,* SAND89-2027 (Sandia National Laboratories, Albuquerque, NM, 1989).
111. R. P. Rechard, W. Beyeler, R. D. McCurley, D. K. Rudeen, J. E. Bean, and J. D. Schreiber, *Parameter Sensitivity Studies of Selected Components of the Waste Isolation Pilot Plant Repository/Shaft System,* SAND89-2030 (Sandia National Laboratories, Albuquerque, NM, 1990).
112. S. G. Bertram-Howery, M. G. Marietta, R. P. Rechard, P. N. Swift, D. R. Anderson, B. L. Baker, J. E. Bean, Jr., W. Beyeler, K. F. Brinster, R. V. Guzowski, J. C. Helton, R. D. McCurley, D. K. Rudeen, J. D. Schreiber, and P. Vaughn, *Preliminary Comparison with 40 CFR Part 191, Subpart B for the Waste Isolation Pilot Plant, December 1990,* SAND90-2347 (Sandia National Laboratories, Albuquerque, NM, 1990).
113. WIPP PA (Performance Assessment) Division, *Preliminary Comparison with 40 CFR Part 191, Subpart B for the Waste Isolation Pilot Plant, December 1991,* SAND91-0893/1/2/3/4 (Sandia National Laboratories, Albuquerque, NM, 1991/1992), pp. 1–4.
114. WIPP PA (Performance Assessment) Department, *Preliminary Performance Assessment for the Waste Isolation Pilot Plant, December 1992,* SAND92-0700/1/2/3/4/5 (Sandia National Laboratories, Albuquerque, NM, 1992/1993), pp. 1–5.
115. J. C. Helton, "Treatment of Uncertainty in Performance Assessments for Complex Systems," *Risk Anal.* **14**(4), 483–511 (1994).
116. J. C. Helton, M. G. Marietta, and R. P. Rechard, "Conceptual

Structure of Performance Assessments Conducted for the Waste Isolation Pilot Plant," in C. G. Interrante and R. T. Pabalan (eds.), *Scientific Basis for Nuclear Waste Management XVI, Materials Research Society Symposium Proceedings, Boston, MA, November 30–December 4, 1992,* SAND92-2285C (Materials Research Society, Pittsburgh, 1993), Vol. 294, 885–898.

117. U.S. Department of Energy(DOE), *Final Environmental Impact Statement, Waste Isolation Pilot Plant,* DOE/EIS-0026 (DOE, Washington, D.C., 1980), pp. 1–2.
118. Sandia [National] Laboratories, *Waste Isolation Pilot Plant (WIPP) Conceptual Design Report,* SAND77-0274 (Sandia [National] Laboratories, Albuquerque, NM, 1977).
119. R. L. Hunter, *Events and Processes for Constructing Scenarios for the Release of Transuranic Waste from the Waste Isolation Pilot Plant, Southeastern New Mexico,* SAND89-2546 (Sandia National Laboratories, Albuquerque, NM, 1989).
120. R. P. Rechard, "CAMCON: Computer System for Assessing Regulatory Compliance of the Waste Isolation Pilot Plant," in G. Apostolakis (ed.), *Probabilistic Safety Assessment and Management, Proceedings of the International Conference (PSAM), Beverly Hills, CA, February 4–7, 1991,* SAND90-2094C (Elsevier, New York, 1991), Vol. 2, pp. 899–904.
121. J. C. Helton, D. R. Anderson, H.-N. Jow, M. Marietta, and M. G. Basabilvazo, "Performance Assessment in Support of the 1996 Compliance Certification Application for the Waste Isolation Pilot Plant," *Risk Anal.* **19**(5), 959–986 (1999).
122. D. A. Galson and P. N. Swift, "Recent Progress in Scenario Development for the WIPP," *High Level Radioactive Waste Management 1995, Proceedings of the Sixth Annual International Conference, Las Vegas, NV, April 30–May 5, 1995,* SAND95-0117C (American Nuclear Society, La Grange Park, IL, 1995), pp. 391–396.
123. R. P. Rechard, *An Introduction to the Mechanics of Performance Assessment Using Examples of Calculations Done for the Waste Isolation Pilot Plant Between 1990 and 1992,* SAND93-1378 (Sandia National Laboratories, Albuquerque, NM, 1995).
124. B. G. J. Thompson and B. Sagar, "The Development and Application of Integrated Procedures for Post-Closure Assessment, Based Upon Monte Carlo Simulation: The Probabilistic Systems Assessment (PSA) Approach," *Reliab. Eng. Syst. Saf.* **42**(2/3), 125–160 (1993).
125. U.S. Department of Energy (DOE), *Draft Environmental Impact Statement: Waste Isolation Pilot Plant,* DOE/EIS-0026-D (DOE, Washington, D.C., 1979), pp. 1–2.
126. J. C. Helton, J. W. Garner, M. G. Marietta, R. P. Rechard, D. K. Rudeen, and P. N. Swift, "Uncertainty and Sensitivity Analysis Results Obtained in a Preliminary Performance Assessment for the Waste Isolation Pilot Plant," *Nucl. Sci. Eng.* **114**(4), 286–331 (1993).
127. J. C. Helton, D. R. Anderson, B. L. Baker, J. E. Bean, J. W. Berglund, W. Beyeler, J. W. Garner, H. J. Iuzzolino, M. G. Marietta, R. P. Rechard, P. J. Roache, D. K. Rudeen, J. D. Schreiber, P. N. Swift, M. S. Tierney, and P. Vaughn, "Effect of Alternative Conceptual Models in a Preliminary Performance Assessment for the Waste Isolation Pilot Plant," *Nucl. Eng. Des.* **154**(3), 251–344 (1995).
128. J. C. Helton, D. R. Anderson, B. L. Baker, J. E. Bean, J. W. Berglund, W. Beyeler, K. Economy, J. W. Garner, S. C. Hora, H. J. Iuzzolino, P. Knupp, M. G. Marietta, J. Rath, R. P. Rechard, P. J. Roache, D. K. Rudeen, K. Salari, J. D. Schreiber, P. N. Swift, M. S. Tierney, and P. Vaughn, "Uncertainty and Sensitivity Analysis Results Obtained in the 1992 Performance Assessment for the Waste Isolation Pilot Plant," *Reliab. Eng. Syst. Saf.* **51**(1), 53–100 (1996).
129. J. C. Helton, "Uncertainty and Sensitivity Analysis Techniques for Use in Performance Assessment for Radioactive Waste Disposal," *Reliab. Eng. Syst. Saf.* **42**(2/3), 327–367 (1993).
130. B. J. Garrick and S. Kaplan, "A Decision Theory Perspective on the Disposal of High Level Radioactive Waste," *Risk Anal.* **19**(5), 903–913 (1999).
131. National Academy of Sciences/National Research Council (NAS/NRC), *Technical Bases for Yucca Mountain Standards,* Committee on Technical Bases for Yucca Mountain Standards, Board on Radioactive Waste Management, Commission on Geosciences, Environment, and Resources, National Research Council (National Academy Press, Washington, D.C., 1995), p. 2.
132. R. W. Lynch, R. L. Hunter, D. R. Anderson, F. W. Bingham, J. M. Covan, G. F. Hohnstrieter, T. O. Hunter, R. D. Klett, E. E. Ryder, T. L. Sanders, and W. D. Weart, *Deep Geologic Disposal in the United States: The Waste Isolation Pilot Plant and Yucca Mountain Projects,* SAND90–1656 (Sandia National Laboratories, Albuquerque, NM, 1991).
133. U.S. Department of Energy (DOE), "Chapter 8, Section 8.3.5.13, Total System Performance," *Site Characterization Plan, Yucca Mountain Site, Nevada Research and Development Area, Nevada,* DOE/RW-0199 (DOE, Washington, D.C., 1988), pp. 8.3.5.13–1 – 8.3.5.13–148.
134. I. J. Winograd, "Radioactive Waste Disposal in Thick Unsaturated Zones," *Science* **212**(4502), 1457–1464 (1981).
135. Civilian Radioactive Waste Management System, Management and Operating Contractor (M&O), *Total System Performance Assessment—1995: An Evaluation of the Potential Yucca Mountain Repository,* Document No. B00000000-01717-2200-00136, Rev. 01 (M&O, Las Vegas, 1995).
136. G. E. Barr, R. L. Hunter, E. Dunn, and A. Flint, *Scenarios Constructed for Nominal Flow in the Presence of a Repository at Yucca Mountain and Vicinity,* SAND92-2186 (Sandia National Laboratories, Albuquerque, NM, 1995).
137. J. H. Kessler and R. K. McGuire, "Total System Performance Assessment for Waste Disposal Using a Logic Tree Approach," *Risk Anal.* **19**(5), 915–931 (1999).
138. P. Swift, G. Barr, R. Barnard, R. Rechard, A. Schenker, G. Freeze, and P. Burck, "Feature, Event, and Process Screening and Scenario Development for the Yucca Mountain Total System Performance Assessment," in *Proceedings of the NEA Workshop on Scenario Development, Madrid, Spain, May 10–12, 1999,* SAND98-2831C (Nuclear Energy Agency of the Organisation for Economic Co-Operation and Development, Paris, 1999).
139. S. Sinnock, Y. T. Lin, and J. P. Brannen, *Preliminary Bounds on the Expected Postclosure Performance of the Yucca Mountain Repository Site, Southern Nevada,* SAND84-1492 (Sandia National Laboratories, Albuquerque, NM, 1984).
140. R. W. Prindle and P. L. Hopkins, *On Conditions and Parameters Important to Model Sensitivity for Unsaturated Flow Through Layered, Fractured Tuff: Results of Analyses for HYDROCOIN Level 3 Case 2,* SAND89-0652 (Sandia National Laboratories, Albuquerque, NM, 1990).
141. R. W. Barnard and H. A. Dockery (eds.), *Technical Summary of the Performance Assessment Calculational Exercises for 1990 (PACE-90), Volume 1: "Nominal Configuration" Hydrogeologic Parameters and Calculational Results,* SAND90-2726 (Sandia National Laboratories, Albuquerque, NM, 1991).
142. R. W. Barnard, M. L. Wilson, H. A. Dockery, J. H. Gauthier, P. G. Kaplan, R. R. Eaton, F. W. Bingham, and T. H. Robey, *TSPA 1991: An Initial Total-System Performance Assessment for Yucca Mountain,* SAND91-2795 (Sandia National Laboratories, Albuquerque, NM, 1992).
143. M. L. Wilson, J. H. Gauthier, R. W. Barnard, G. E. Barr, H. A. Dockery, E. Dunn, R. R. Eaton, D. C. Guerin, N. Lu, M. J. Martinez, R. Nilson, C. A. Rautman, T. H. Robey, B. Ross, E. E. Ryder, A. R. Schenker, S. A. Shannon, L. H.

Skinner, W. G. Halsey, J. D. Gansemer, L. C. Lewis, A. D. Lamont, I. R. Triay, A. Meijer, and D. E. Morris, *Total-System Performance Assessment for Yucca Mountain—SNL Second Iteration (TSPA-1993),* SAND93-2675 (Sandia National Laboratories, Albuquerque, NM, 1994).

144. Electric Power Research Institute (EPRI), *Demonstration of a Risk-Based Approach to High-Level Waste Repository Evaluation,* EPRI NP-7057 (EPRI, Palo Alto, CA, 1990).
145. Electric Power Research Institute (EPRI), *Demonstration of a Risk-Based Approach to High-Level Waste Repository Evaluation: Phase 2,* EPRI TR-100384 (EPRI, Palo Alto, CA, 1992).
146. Electric Power Research Institute (EPRI), *Yucca Mountain Total System Performance Assessment, Phase 3,* EPRI TR-107191 (EPRI, Palo Alto, CA, 1996).
147. B. G. J. Thompson, "The Role of Performance Assessment in the Regulation of Underground Disposal of Radioactive Wastes: An International Perspective," *Risk Anal.* **19**(5), 809–846 (1999).
148. N. A. Eisenberg, M. P. Lee, T. J. McCartin, K. I. McConnell, M. Thaggard, and A. C. Campbell, "Development of a Performance Assessment Capability in the Waste Management Programs of the U.S. Nuclear Regulatory Commission," *Risk Anal.* **19**(5), 847–876 (1999).
149. R. Codell, N. Eisenberg, D. Fehringer, W. Ford, T. Margulies, T. McCartin, J. Park, and J. Randall, *Initial Demonstration of the NRC's Capability to Conduct a Performance Assessment for a High-Level Waste Repository,* NUREG-1327 (U.S. Nuclear Regulatory Commission, Washington, D.C., 1992).
150. R. G. Wescott, M. P. Lee, N. A. Eisenberg, T. J. McCartin, and R. B. Baca (eds.), *NRC Iterative Performance Assessment Phase 2. Development of Capabilities for Review of a Performance Assessment for a High-Level Waste Repository,* NUREG-1464 (Nuclear Regulatory Commission, Washington, D.C., 1995).
151. Golder Associates, *RIP Integrated Probabilistic Simulator for Environmental Systems: Theory Manual and User's Guide* (Golder Associates, Redmond, WA, November 1998).
152. R. W. Andrews, T. F. Dale, and J.A. McNeish, *Total System Performance Assessment—1993: An Evaluation of the Potential Yucca Mountain Repository,* Document No. B00000000-01717-2200-00099-01 (INTERA, Las Vegas, 1994).
153. Civilian Radioactive Waste Management System, Management and Operating Contractor (M&O), *Description of Performance Allocation Report,* Document No. B00000000-01717-2200-00177-00 (M&O, Las Vegas, 1996).
154. Civilian Radioactive Waste Management System, Management and Operating Contractor (M&O), *Total System Performance Assessment Sensitivity Studies of U.S. Department of Energy Spent Nuclear Fuel,* Document No. A00000000-01717-5705-00017-00 (M&O, Las Vegas, 1997).
155. Civilian Radioactive Waste Management System, Management and Operating Contractor (M&O), *Total System Performance Assessment-Viability Assessment (TSPA-VA) Analyses Technical Basis Document,* Document No. B00000000-01717-4301-00001, Rev. 01 (M&O, Las Vegas, 1998).
156. Electric Power Research Institute (EPRI), *Alternative Approaches to Assessing the Performance and Suitability of Yucca Mountain for Spent Fuel Disposal,* EPRI TR-108732 (EPRI, Palo Alto, CA, 1998).
157. M. G. Marietta and W. F. Simmons, *Feasibility of Disposal of High-Level Radioactive Waste into the Seabed, Volume 5—Dispersal of Radionuclides in the Oceans: Models, Data Sets, and Regional Descriptions,* SAND87-0753, INIS-XN-177 (Sandia National Laboratories, Albuquerque, NM, 1988).
158. L. L. Price, S. H. Conrad, D. A. Zimmerman, N. E. Olague, K. C. Gaither, W. B. Cox, J. T. McCord, and C. P. Harlan, *Preliminary Performance Assessment of the Greater Confinement Disposal Facility at the Nevada Test Site,* SAND91-0047 (Sandia National Laboratories, Albuquerque, NM, 1993), pp. 1–3.
159. T. A. Baer, L. L. Price, J. N. Emery, and N. E. Olague, *Second Performance Assessment Iteration of the Greater Confinement Disposal Facility at the Nevada Test Site,* SAND93-0089 (Sandia National Laboratories, Albuquerque, NM, 1994).
160. R. P. Rechard (ed.), *Initial Performance Assessment of the Disposal of Spent Nuclear Fuel and High-Level Waste Stored at Idaho National Engineering Laboratory,* SAND93-2330/1/2 (Sandia National Laboratories, Albuquerque, NM, 1993), 1–2.
161. General Accounting Office (GAO), *Nuclear Waste, Foreign Countries' Approaches to High-Level Waste Storage and Disposal,* United States General Accounting Office Report to the Honorable Richard H. Bryan, U.S. Senate, GAO-RCED-94-172 (GAO, Resources, Community, and Economic Development Division, Washington, D.C., 1994).
162. P. C. Fishburn, "Foundations of Risk Measurement. I. Risk as Probable Loss," *Manage. Sci.* **30**(4), 396–406 (1984).
163. University of New Mexico (UNM)), "Focus 1: WIPP," *Public Opinion Profile of New Mexico Citizens* (UNM, Institute for Public Policy Survey Research Center, Albuquerque, 1998), **10**(2), 1–6.
164. H. C. Jenkins-Smith and S. Cullipher, *Public Views of the WIPP Policy Debate in Bernalillo and Santa Fe Counties: December 1997–January* 1998 (University of New Mexico, Institute for Public Policy, Albuquerque, NM, 1998).
165. B. T. Mossman, J. Bignon, M. Corn, A. Seaton, and J. B. L. Gee, "Asbestos: Scientific Developments and Implications for Public Policy," *Science* **247**(4940), 294–301 (1990).
166. E. Marshall, "A is for Apple, Alar, and . . . Alarmist?" *Science* **254**(5028), 20–22 (1991).

This page intentionally left blank

Appendix B

Helton JC, Johnson JD, Sallaberry CJ, Storlie CB. Survey of Sampling-Based Methods for Uncertainty and Sensitivity Analysis. *Reliability Engineering and System Safety* 2006;91(10-11):1175-1209

This page intentionally left blank

Available online at www.sciencedirect.com
SCIENCE DIRECT®
Reliability Engineering and System Safety 91 (2006) 1175–1209
RELIABILITY ENGINEERING & SYSTEM SAFETY
www.elsevier.com/locate/ress

Survey of sampling-based methods for uncertainty and sensitivity analysis

J.C. Helton[a,*], J.D. Johnson[b], C.J. Sallaberry[c], C.B. Storlie[d]

[a]Department of Mathematics and Statistics, Arizona State University, Tempe, AZ 85287-1804, USA
[b]ProStat, Mesa, AZ 85204-5326, USA
[c]Sandia National Laboratories, Albuquerque, NM 87185-0776, USA
[d]Department of Statistics, Colorado State University, Fort Collins, CO 80523-1877, USA

Available online 18 January 2006

Abstract

Sampling-based methods for uncertainty and sensitivity analysis are reviewed. The following topics are considered: (i) definition of probability distributions to characterize epistemic uncertainty in analysis inputs, (ii) generation of samples from uncertain analysis inputs, (iii) propagation of sampled inputs through an analysis, (iv) presentation of uncertainty analysis results, and (v) determination of sensitivity analysis results. Special attention is given to the determination of sensitivity analysis results, with brief descriptions and illustrations given for the following procedures/techniques: examination of scatterplots, correlation analysis, regression analysis, partial correlation analysis, rank transformations, statistical tests for patterns based on gridding, entropy tests for patterns based on gridding, nonparametric regression analysis, squared rank differences/rank correlation coefficient test, two-dimensional Kolmogorov–Smirnov test, tests for patterns based on distance measures, top down coefficient of concordance, and variance decomposition.
© 2005 Elsevier Ltd. All rights reserved.

Keywords: Aleatory uncertainty; Epistemic uncertainty; Latin hypercube sampling; Monte Carlo; Sensitivity analysis; Uncertainty analysis

1. Introduction

Uncertainty analysis and sensitivity analysis are essential parts of analyses for complex systems [1–14]. Specifically, uncertainty analysis refers to the determination of the uncertainty in analysis results that derives from uncertainty in analysis inputs, and sensitivity analysis refers to the determination of the contributions of individual uncertain analysis inputs to the uncertainty in analysis results. The uncertainty under consideration here is often referred to as epistemic uncertainty; alternative designations for this form of uncertainty include state of knowledge, subjective, reducible, and type B [15–24]. Epistemic uncertainty derives from a lack of knowledge about the appropriate value to use for a quantity that is assumed to have a fixed value in the context of a particular analysis. In the conceptual and computational organization of an analysis, epistemic uncertainty is generally considered to be distinct from aleatory uncertainty, which arises from an inherent randomness in the behavior of the system under study [15–24]. Alternative designations for aleatory uncertainty include variability, stochastic, irreducible, and type A.

A number of approaches to uncertainty and sensitivity analysis have been developed, including differential analysis [25–33], response surface methodology [34–43], Monte Carlo analysis [44–55], and variance decomposition procedures [56–60]. Overviews of these approaches are available in several reviews [61–68].

The focus of this presentation is on Monte Carlo (i.e., sampling-based) approaches to uncertainty and sensitivity analysis. Sampling-based approaches to uncertainty and sensitivity analysis are both effective and widely used [69–83]. Analyses of this type involve the generation and exploration of a mapping from uncertain analysis inputs to uncertain analysis results. The underlying idea is that analysis results $\mathbf{y}(\mathbf{x}) = [y_1(\mathbf{x}), y_2(\mathbf{x}), \ldots, y_{nY}(\mathbf{x})]$ are functions of uncertain analysis inputs $\mathbf{x} = [x_1, x_2, \ldots, x_{nX}]$. In

*Corresponding author. Sandia National Laboratories, Department 6849, MS 0779, Albuquerque, NM, 87185-0779, USA.
Tel.: +1 505 284 4808; fax: +1 505 844 2348.
E-mail address: jchelto@sandia.gov (J.C. Helton).

0951-8320/$ - see front matter © 2005 Elsevier Ltd. All rights reserved.
doi:10.1016/j.ress.2005.11.017

turn, uncertainty in **x** results in a corresponding uncertainty in **y(x)**. This leads to two questions: (i) what is the uncertainty in **y(x)** given the uncertainty in **x**? and (ii) how important are the individual elements of **x** with respect to the uncertainty in **y(x)**? The goal of uncertainty analysis is to answer the first question, and the goal of sensitivity analysis is to answer the second question. In practice, the implementation of an uncertainty analysis and the implementation of a sensitivity analysis are very closely connected on both a conceptual and a computational level.

The following sections summarize and illustrate the five basic components that underlie the implementation of a sampling-based uncertainty and sensitivity analysis: (i) definition of distributions $D_1, D_2, \ldots, D_{nX}$ that characterize the epistemic uncertainty in the elements $x_1, x_2, \ldots, x_{nX}$ of **x** (Section 2), (ii) generation of a sample $\mathbf{x}_1, \mathbf{x}_2, \ldots, \mathbf{x}_{nS}$ from the **x**'s in consistency with the distributions $D_1, D_2, \ldots, D_{nX}$ (Section 3), (iii) propagation of the sample through the analysis to produce a mapping $[\mathbf{x}_i, \mathbf{y}(\mathbf{x}_i)]$, $i = 1, 2, \ldots, nS$, from analysis inputs to analysis results (Section 4), (iv) presentation of uncertainty analysis results (i.e., approximations to the distributions of the elements of **y** constructed from the corresponding elements of $\mathbf{y}(\mathbf{x}_i)$, $i = 1, 2, \ldots, nS$) (Section 5), and (v) determination of sensitivity analysis results (i.e., exploration of the mapping $[\mathbf{x}_i, \mathbf{y}(\mathbf{x}_i)]$, $i = 1, 2, \ldots, nS$) (Section 6). The presentation then ends with a concluding summary (Section 7).

Only probabilistic characterizations of uncertainty are considered in this presentation. Alternative uncertainty representations (e.g., evidence theory, possibility theory, fuzzy set theory, interval analysis) are active areas of research [84–92] but are outside the intended scope of this presentation.

2. Characterization of uncertainty

Definition of the distributions $D_1, D_2, \ldots, D_{nX}$ that characterize the epistemic uncertainty in the elements $x_1, x_2, \ldots, x_{nX}$ of **x** is the most important part of a sampling-based uncertainty and sensitivity analysis as these distributions determine both the uncertainty in **y** and the sensitivity of the elements of **y** to the elements of **x**. The distributions $D_1, D_2, \ldots, D_{nX}$ are typically defined through an expert review process [93–100], and their development can constitute a major analysis cost. A possible analysis strategy is to perform an initial exploratory analysis with rather crude definitions for $D_1, D_2, \ldots, D_{nX}$ and use sensitivity analysis to identify the most important analysis inputs; then, resources can be concentrated on characterizing the uncertainty in these inputs and a second presentation or decision-aiding analysis can be carried out with these improved uncertainty characterizations.

The scope of an expert review process can vary widely depending on the purpose of the analysis, the size of the analysis, and the resources available to carry out the analysis. At one extreme is a relatively small study in which a single analyst both develops the uncertainty characterizations (e.g., on the basis of personal knowledge or a cursory literature review) and carries out the analysis. At the other extreme, is a large analysis on which important societal decisions will be based and for which uncertainty characterizations are carried out for a large number of variables by teams of outside experts who support the analysts actually performing the analysis.

Given the breadth of analysis possibilities, it is beyond the scope of this presentation to provide an exhaustive review of how the distributions $D_1, D_2, \ldots, D_{nX}$ might be developed. However, as general guidance, it is best to avoid trying to obtain these distributions by specifying the defining parameters (e.g., mean and standard deviation) for a particular distribution type. Rather, distributions can be defined by specifying selected quantiles (e.g., 0.0, 0.1, 0.25, …, 0.9, 1.0) of the corresponding cumulative distribution functions (CDFs), which should keep the individual supplying the information in closer contact with the original sources of information or insight than is the case when a particular named distribution is specified (Fig. 1a). Distributions from multiple experts can be aggregated by averaging (Fig. 1b) [101].

This presentation draws most of its examples from an uncertainty and sensitivity analysis carried out for a two phase flow model (implemented in the BRAGFLO program) [102–104] in support of the 1996 Compliance Certification Application for the Waste Isolation Pilot Plant [105–107]. The uncertain variables considered in the example results (i.e., $x_1, x_2, \ldots, x_{nX}$ with $nX = 31$) and their associated distributions (i.e., $D_1, D_2, \ldots, D_{31}$) are summarized in Table 1. Additional information on the use of these variables in the two phase flow model and on the development of the associated uncertainty distributions is available in the original analysis documentation [102,108].

Additional information: Section 6.2, Refs. [46, 93–100,109–119]. As an example, Ref. [100] describes the approach used in the extensive expert review process that supported the US Nuclear Regulatory Commission's (NRC's) reassessment of the risk from commercial nuclear power plants (i.e., NUREG-1150; see Refs. [82,120–124]).

3. Generation of sample

Several sampling strategies are available, including random sampling, importance sampling, and Latin hypercube sampling [44,55] Latin hypercube sampling is very popular for use with computationally demanding models because its efficient stratification properties allow for the extraction of a large amount of uncertainty and sensitivity information with a relatively small sample size.

Latin hypercube sampling operates in the following manner to generate a sample of size nS from the distributions $D_1, D_2, \ldots, D_{nX}$ associated with the elements of $\mathbf{x} = [x_1, x_2, \ldots, x_{nX}]$. The range of each x_j is exhaustively divided into nS disjoint intervals of equal probability and one value x_{ij} is randomly selected from each interval. The nS values for x_1 are randomly paired without replacement

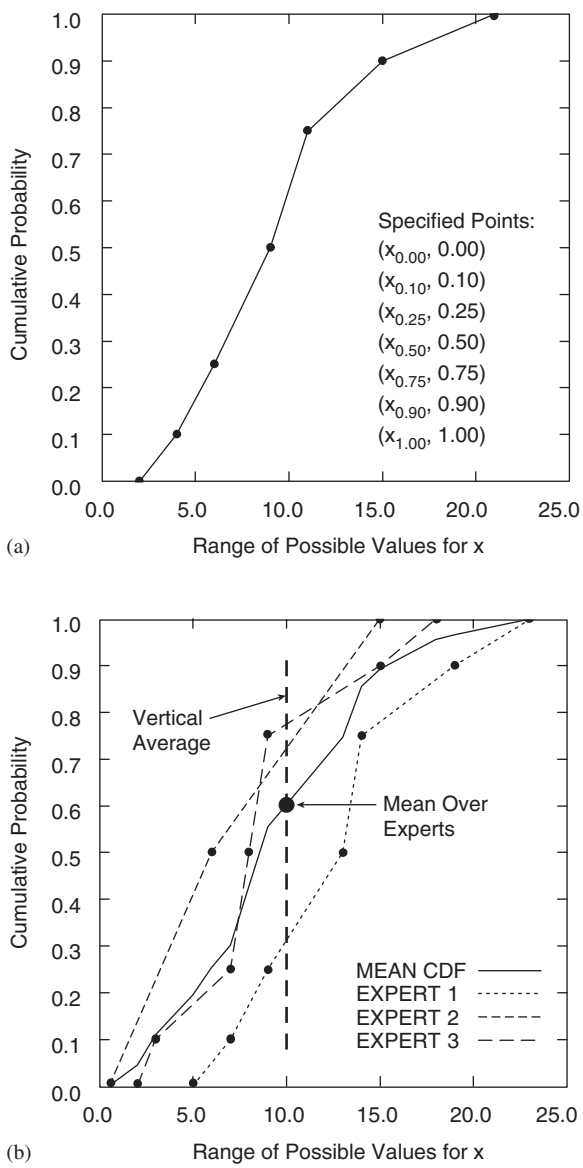

Fig. 1. Characterization of epistemic uncertainty: (a) construction of CDF from specified quantile values (Ref. [101, Fig. 4.1]), and (b) construction of mean CDF by vertical averaging of CDFs defined by individual experts with equal weight (i.e., $1/nE = 1/3$, where $nE = 3$ is the number of experts) given to each expert (Ref. [101, Fig. 4.2]).

with the nS value for x_2 to produce nS pairs. These pairs are then randomly combined without replacement with the nS values for x_3 to produce nS triples. This process is continued until a set of nS nX-tuples $\mathbf{x}_i = [x_{i1}, x_{i2}, \ldots, x_{i,nX}]$, $i = 1, 2, \ldots, nS$, is obtained, with this set constituting the Latin hypercube sample (Fig. 2).

Latin hypercube sampling is a good choice for a sampling procedure when computationally demanding models are being studied. The popularity of Latin hypercube sampling recently led to the original article being designated a *Technometrics* classic in experimental design [125]. When the model is not computationally demanding, many model evaluations can be performed and random sampling works as well as Latin hypercube sampling.

If large sample sizes are required to provide appropriate coverage of low probability/high consequence subsets of values for $\mathbf{x}$, then importance sampling may be a more effective sampling procedure than either random or Latin hypercube sampling [126–134]. However, importance sampling complicates sensitivity analysis (Section 6) as the individual sample elements do not have equal weight (i.e., likelihood of occurrence). Often, some type of importance sampling is used to sample from aleatory uncertainty (e.g., possibly implemented through the use of event trees as is typically the case in probabilistic risk assessments for complex engineered facilities such as nuclear plants) and Latin hypercube sampling is used to sample from epistemic uncertainty. The NUREG-1150 analyses (see Refs. [82,120–124]) are an example of this approach to the propagation of uncertainty.

Control of correlations is an important aspect of sample generation. Specifically, correlated variables should have correlations close to their specified values, and uncorrelated variables should have correlations close to zero. In general, the imposition of complex correlation structures is not easy. However, Iman and Conover have developed a broadly applicable procedure to impose rank correlations on sampled values that (i) is distribution free (i.e., does not depend on the assumed marginal distributions for the sampled variables), (ii) can impose complex correlation structures involving multiple variables, (iii) works with both random and Latin hypercube sampling, and (iv) preserves the intervals used in Latin hypercube sampling [135,136]. Details on the implementation of the procedure are available in the original reference; [135] illustrative results are provided in Fig. 3 [137].

The analysis involving the variables in Table 1 used three independently generated (i.e., replicated) Latin hypercube samples of size $nS = 100$ each. The purpose of the replication was to provide a basis for testing the stability of uncertainty and sensitivity analysis results obtained with Latin hypercube sampling (Ref. [108, Sections 7 and 8]). The Iman/Conover restricted pairing technique indicated in the preceding paragraph was used to control correlations within the individual samples. The analyses with the three replicated samples were sufficiently similar that each analysis would have independently lead to the same insights with respect to model behavior [138]. However, to make full use of all model evaluations, final presentation results [103,104] were calculated with the three replicated samples pooled together to produce a single sample of size $nS = 300$.

Additional information: Ref. [46, Section 6.3], Refs. [44,50,54,55,139].

4. Propagation of sample through the analysis

Propagation of the sample through the analysis to produce the mapping $[\mathbf{x}_i, \mathbf{y}(\mathbf{x}_i)]$, $i = 1, 2, \ldots, nS$, from

Table 1
Uncertain variables $x_1, x_2, \ldots, x_{31}$ and associated uncertainty distributions $D_1, D_2, \ldots, D_{31}$ used in illustration of uncertainty and sensitivity analysis procedures for two phase flow model (Ref. [138, Table 1])

ANHBCEXP—Brooks–Corey pore distribution parameter for anhydrite (dimensionless). Distribution: Student's with 5 degree of freedom. Range: 0.491–0.842. Mean, median: 0.644.
ANHBCVGP—Pointer variable for selection of relative permeability model for use in anhydrite. Distribution: Discrete with 60% 0, 40% 1. Value of 0 implies Brooks–Corey model; value of 1 implies van Genuchten–Parker model.
ANHCOMP—Bulk compressibility of anhydrite (PA^{-1}). Distribution: Student's with 3 degrees of freedom. Range: 1.09×10^{-11}–$2.75 \times 10^{-10}\,Pa^{-1}$. Mean, median: $8.26 \times 10^{-11}\,Pa^{-1}$. Correlation: −0.99 rank correlation [23] with *ANHPRM*. Variable 21 in LHS.
ANHPRM—Logarithm of anhydrite permeability (m^2). Distribution: Student's with 5 degrees of freedom. Range: −21.0–−17.1 (i.e., permeability range is 1×10^{-21}–$1 \times 10^{-17.1}\,m^2$). Mean, median: −18.9. Correlation: −0.99 rank correlation with *ANHCOMP*.
ANRBRSAT—Residual brine saturation in anhydrite (dimensionless). Distribution: Student's with 5 degrees of freedom. Range: 7.85×10^{-3}–1.74×10^{-1}. Mean, median: 8.36×10^{-2}.
ANRGSSAT—Residual gas saturation in anhydrite (dimensionless). Distribution: Student's with 5 degrees of freedom. Range 1.39×10^{-2}–1.79×10^{-1}. Mean, median: 7.71×10^{-2}.
BHPRM—Logarithm of borehole permeability (m^2). Distribution: Uniform. Range: −14 to −11 (i.e., permeability range is 1×10^{-14}–$1 \times 10^{-11}\,m^2$). Mean, median: −12.5.
BPCOMP—Logarithm of bulk compressibility of brine pocket (Pa^{-1}). Distribution: triangular. Range: −11.3 to −8.00 (i.e., bulk compressibility range is $1 \times 10^{-11.3}$–$1 \times 10^{-8}\,Pa^{-1}$). Mean, mode: −9.80, −10.0. Correlation: −0.75 rank correlation with *BPPRM*.
BPINTPRS—Initial pressure in brine pocket (Pa). Distribution: triangular. Range: 1.11×10^7–1.70×10^7 Pa. Mean, mode: 1.36×10^7, 1.27×10^7 Pa.
BPPRM—Logarithm of intrinsic brine pocket permeability (m^2). Distribution: triangular. Range: −14.7 to −9.80 (i.e., permeability range is $1 \times 10^{-14.7}$ $-1 \times 10^{-9.80}\,m^2$). Mean, mode: −12.1, −11.8. Correlation: −0.75 rank correlation with *BPCOMP*.
BPVOL–Pointer variable for selection of brine pocket volume. Distribution: discrete, with integer values 1, 2, …, 32 equally likely.
HALCOMP—Bulk compressibility of halite (Pa−1). Distribution: Uniform. Range: 2.94×10^{-12}–$1.92 \times 10^{-10}\,Pa^{-1}$. Mean, median: $9.75 \times 10^{-11}\,Pa^{-1}$, $9.75 \times 10^{-11}\,Pa^{-1}$. Correlation: −0.99 rank correlation with *HALPRM*.
HALPOR—Halite porosity (dimensionless). Distribution: Piecewise uniform. Range: 1.0×10^{-3}–3×10^{-2}. Mean, median: 1.28×10^{-2}, 1.00×10^{-2}.
HALPRM–Logarithm of halite permeability (m^2). Distribution: Uniform. Range: −24 to −21 (i.e., permeability range is 1×10^{-24} to $1 \times 10^{-21}\,m^2$). Mean, median: −22.5, −22.5. Correlation: −0.99 rank correlation with *HALCOMP*.
SALPRES–Initial brine pressure, without the repository being present, at a reference point located in the center of the combined shafts at the elevation of the midpoint of MB 139 (Pa). Distribution: Uniform. Range: 1.104×10^7–1.389×10^7 Pa. 1.247×10^7 Pa.
SHBCEXP—Brooke-Corey pore distribution parameter for shaft (dimensionless). Distribution: Piecewise uniform. Range: 0.11–8.10. Mean, median: 2.52, 0.94.
SHPRMASP—Logarithm of permeability (m^2) of asphalt component of shaft seal (m^2). Distribution: Triangular. Range: −21–−18 (i.e., permeability range is 1×10^{-21}–$1 \times 10^{-18}\,m^2$). Mean, mode: −19.7, −20.0.
SHPRMCLY—Logarithm of permeability (m^2) for clay components of shaft. Distribution: Triangular. Range: −21–−17.3 (i.e., permeability range is 1×10^{-21}–$1 \times 10^{-17.3}\,m^2$). Mean, mode: −18.9, −18.3.
SHPRMCON—Same as *SHPRMASP* but for concrete component of shaft seal for 0 − 400 yr.Distribution: Triangular. Range: −17.0–−14.0 (i.e., permeability range is 1×10^{-17}–$1 \times 10^{-14}\,m^2$). Mean, mode: −15.3, −15.0.
SHPRMDRZ–Logarithm of permeability (m^2) of DRZ surrounding shaft. Distribution: Triangular. Range: −17.0–−14.0 (i.e., permeability range is 1×10^{-17}–$1 \times 10^{-14}\,m^2$). Mean, mode: −15.3, −15.0.
SHPRMHAL–Pointer variable (dimensionless) used to select permeability in crushed salt component of shaft seal at different times. Distribution: Uniform. Range: 0–1. Mean, mode: 0.5, 0.5. A distribution of permeability (m^2) in the crushed salt component of the shaft seal is defined for each of the following time intervals: [0, 10 yr], [10,25 yr], [25,50 yr], [50,100 yr], [100,200 yr], [200,10,000 yr]10,200. *SHPRMHAL* is used to select a permeability value from the cumulative distribution function for permeability for each of the preceding time intervals with result that a rank correlation of 1 exists between the permeabilities used for the individual time intervals.
SHRBRSAT—Residual brine saturation in shaft (dimensionless). Distribution: Uniform. Range: 0–0.4. Mean, median: 0.2, 0.2.
SHRGSSAT—Residual gas saturation in shaft (dimensionless). Distribution: Uniform. Range: 0–0.4. Mean, median: 0.2, 0.2.
WASTWICK—Increase in brine saturation of waste owing to capillary forces (dimensionless). Distribution: Uniform: Range: 0–1. Mean, median: 0.5, 0.5.
WFBETCEL—Scale factor used in definition of stoichiometric coefficient for microbial gas generation (dimensionless). Distribution: Uniform. Range: 0–1. Mean, median: 0.5, 0.5.
WGRCOR–Corrosion rate for steel under inundated conditions in the absence of CO_2 (m/s). Distribution: Uniform. Range: 0–1.58×10^{-14} m/s. Mean, median: 7.94×10^{-15} m/s, 7.94×10^{-15} m/s.
WGRMICH—Microbial degradation rate for cellulose under humid conditions (mol/kg s). Distribution: Uniform. Range: 0–1.27×10^{-9} mol/kg s. Mean, median: 6.34×10^{-10} mol/kg s, 6.34×10^{-10} mol/kg s.
WGRMICI—Microbial degradation rate for cellulose under inundated conditions (mol/kg s). Distribution: Uniform. Range: 3.17×10^{-10}–9.51×10^{-9} mol/kg s. Mean, median: 4.92×10^{-9} mol/kg s, 4.92×10^{-9} mol/kg s.
WMICDFLG–Pointer variable for microbial degradation of cellulose. Distribution: Discrete, with 50% 0, 25% 1, 25% 2, *WMICDFLG* = 0, 1, 2, implies no microbial degradation of cellulose, microbial degradation of only cellulose, microbial degradation of cellulose, plastic and rubber.
WRBRNSAT—Residual brine saturation in waste (dimensionless). Distribution: Uniform. Range: 0–0.552. Mean, median: 0.276, 0.276.
WRGSSAT—Residual gas saturation i n waste (dimensionless). Distribution: Uniform. Range: 0–0.15. Mean, median: 0.075, 0.075.

analysis inputs to analysis results is often the most computationally demanding part of a sampling-based uncertainty and sensitivity analysis. The details of this propagation are analysis specific and can range from very simple for analyses that involve a single model to very complicated for large analyses that involve complex systems of linked models [82,107].

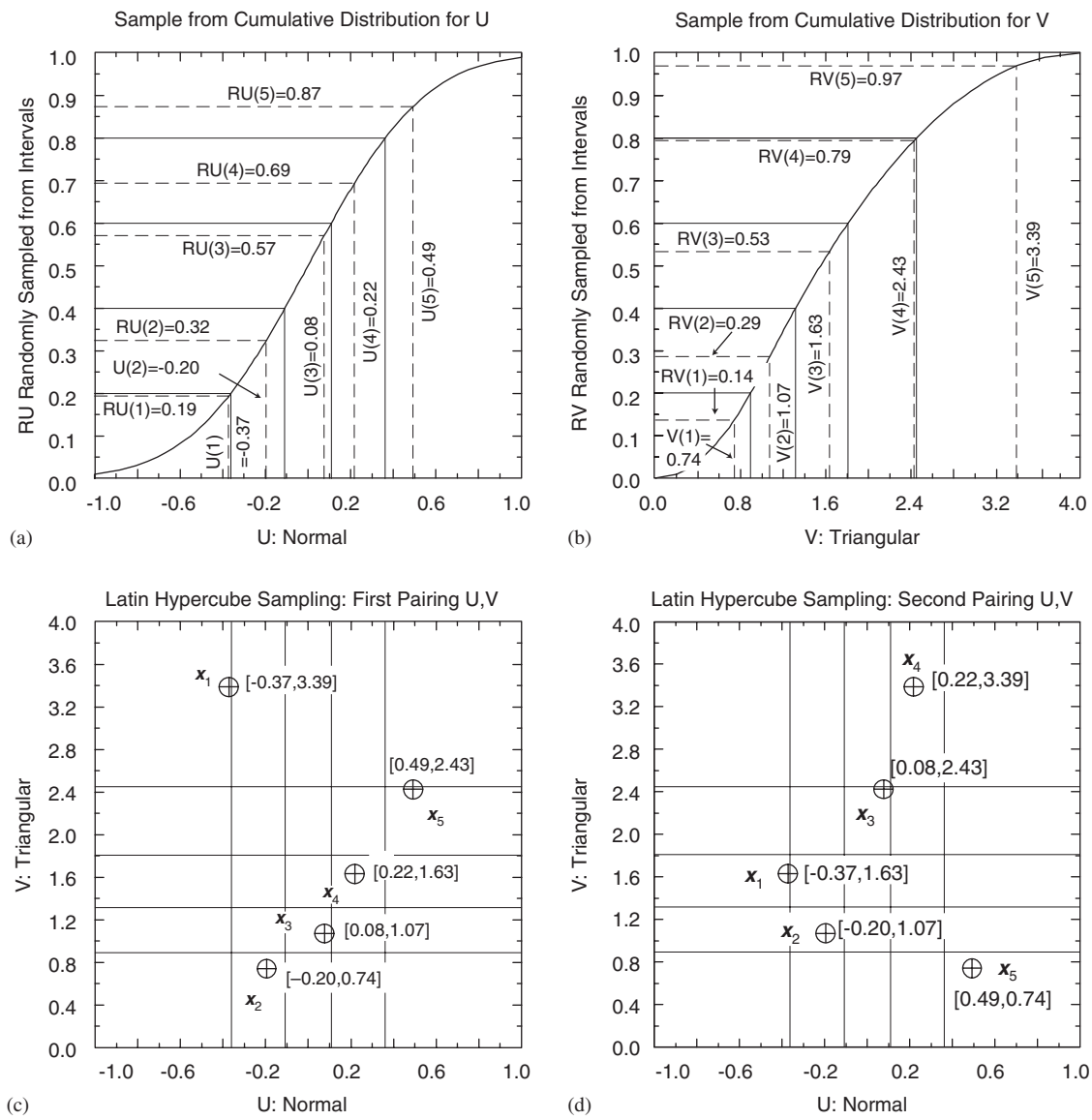

Fig. 2. Example of Latin hypercube sampling to generate a sample of size $nS = 5$ from $\mathbf{x} = [U, V]$ with U normal on $[-1, 1]$ (mean = 0.0; 0.01 quantile = −1; 0.99 quantile = 1) and V triangular on [0, 4] (mode = 1): (a, b) Upper frames illustrate sampling of values for U and V, and (c, d) Lower frames illustrate two different pairings of the sampled values of U and V in the construction of an LHS (Ref. [101, Fig. 5.3]).

When a single model is under consideration, this part of the analysis can involve little more than putting a DO loop around the model that (i) supplies the sampled input to the model, (ii) runs the model, and (iii) stores model results for later analysis. When more complex analyses with multiple models are involved, considerable sophistication may be required in this part of the analysis. Implementation of such analyses can involve (i) development of simplified models to approximate more complex models, (ii) clustering of results at model interfaces, (ii) reuse of model results through interpolation or linearity properties, and (iv) complex procedures for the storage and retrieval of analysis results.

Additional information: The NUREG-1150 analyses [82,93–100,109,119], the analyses carried out in support of the Compliance Certification Application for the Waste Isolation Pilot Plant [105–107], and analyses carried out in support of the Yucca Mountain Project's development of a facility for the deep geologic disposal of high level radioactive waste [140–142] provide examples of complex analyses that have used Latin hypercube sampling in the propagation of epistemic uncertainty.

5. Presentation of uncertainty analysis results

Presentation of uncertainty analysis results is generally straight forward and involves little more than displaying the results associated with the already calculated mapping $[\mathbf{x}_i,\ \mathbf{y}(\mathbf{x}_i)]$, $i = 1, 2, \ldots, nS$. Presentation possibilities include means and standard deviations, density functions, CDFs, complementary cumulative distribution functions (CCDFs), and box plots. Presentation formats such as

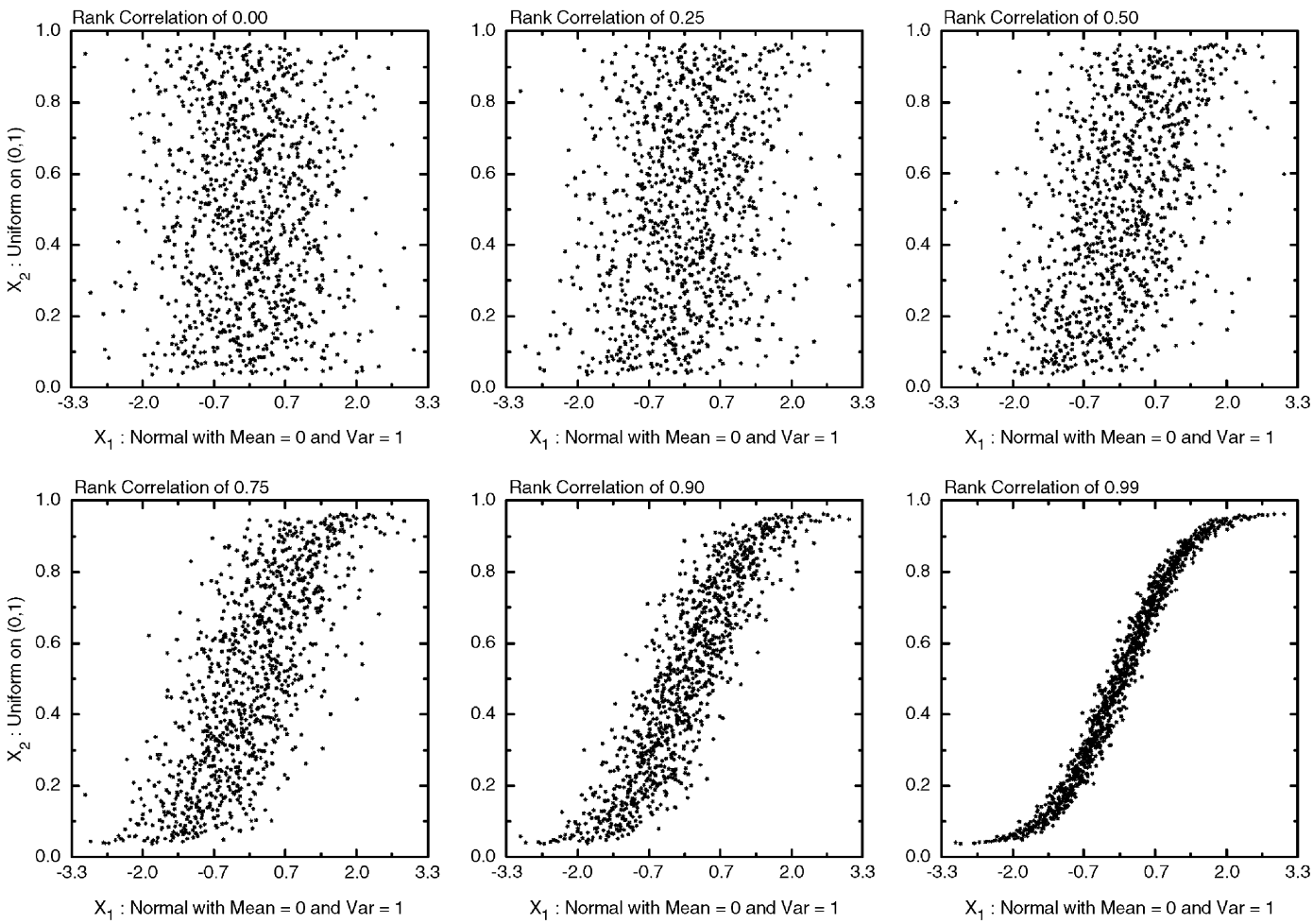

Fig. 3. Examples of rank correlations of 0.00, 0.25, 0.50, 0.75, 0.90 and 0.99 imposed with the Iman/Conover restricted pairing technique for an LHS of size $nS = 1000$ (Ref. [137, Fig. 5.1]).

CDFs (Fig. 4a), CCDFs (Fig. 4a) and box plots (Fig. 4b) are usually preferable to means and standard deviations because of the large amount of uncertainty information that is lost in the calculation of means and standard deviations (see Table 2 for definitions of dependent variables used to illustrate uncertainty and sensitivity analysis procedures). Owing to their flattened shape, box plots are particularly useful when it is desired to the display and compare the uncertainty in a number of related variables.

The representational challenge is more complex when the analysis outcome of interest is a function rather than a scalar. For example, time-dependent system properties are common analysis outcomes. As another example, a CCDF that summarizes the effects of aleatory uncertainty is a standard analysis outcome in risk assessments. An effective display format for such analysis outcomes is to use two plot frames, with first frame displaying the analysis results for the individual sample elements and the second frame displaying summary results for the outcomes in the first frame (e.g., quantiles and means) (Fig. 5).

Additional information: Ref. [46, Section 6.4]; Refs. [143,144].

6. Determination of sensitivity analysis results

Determination of sensitivity analysis results is usually more demanding than the presentation of uncertainty analysis results due to the need to actually explore the mapping $[\mathbf{x}_i, \mathbf{y}(\mathbf{x}_i)]$, $i = 1, 2, \ldots, nS$, to assess the effects of individual elements of $\mathbf{x}$ on the elements of $\mathbf{y}$. A number of approaches to sensitivity analysis that can be used in conjunction with a sampling-based uncertainty analysis are briefly summarized in this section. In this summary, (i) x_j is an element of $\mathbf{x} = [x_1, x_2, \ldots, x_{nX}]$, (ii) y is an element of $\mathbf{y}(\mathbf{x}) = [y_1(\mathbf{x}), y_2(\mathbf{x}), \ldots, y_{nY}(\mathbf{x})]$, (iii) $\mathbf{x}_i = [x_{i1}, x_{i2}, \ldots, x_{i,nX}]$, $i = 1, 2, \ldots, nS$, is a random or Latin hypercube sample from the possible values for $\mathbf{x}$ generated in consistency with the joint distribution assigned to the x_j's, (iv) $\mathbf{y}_i = \mathbf{y}(\mathbf{x}_i)$ for $i = 1, 2, \ldots, nS$, and (v) x_{ij} and y_i are elements of $\mathbf{x}_i$ and $\mathbf{y}_i$, respectively. Sensitivity analyses usually consider the effects of all elements of $\mathbf{x}$ on individual elements of $\mathbf{y}$;

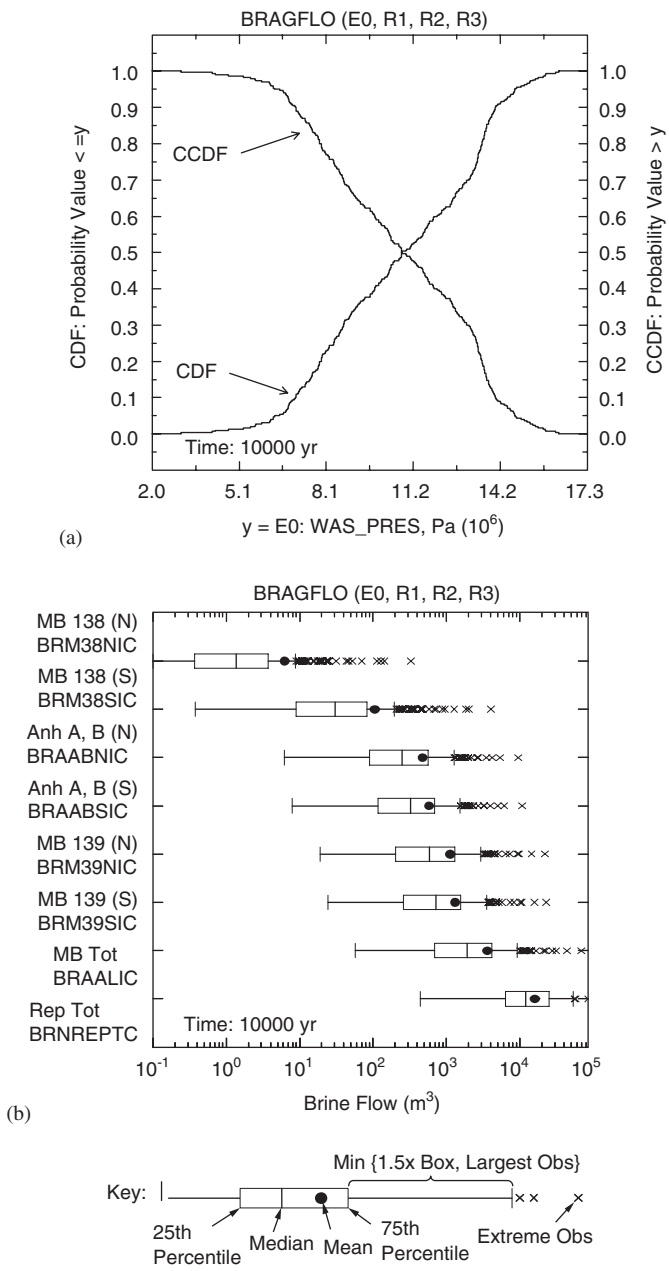

Fig. 4. Representation of uncertainty in scalar-valued analysis results: (a) CDFs and CCDFs (Ref. [101, Fig. 7.2]) and (b) box plots (Ref. [101, Fig. 7.4]).

for this reason and for notational simplification, the subscripted variables x_j, $j = 1, 2, \ldots, nX$, are used to represent the elements of $\mathbf{x}$ but the unsubscripted variable y is used to represent an arbitrary element of $\mathbf{y}$.

6.1. Scatterplots

A plot of the points $[x_{ij}, y_i]$ for $i = 1, 2, \ldots, nS$ (i.e., a scatterplot of y versus x_j) can reveal nonlinear or other unexpected relationships between analysis inputs and analysis results (Fig. 6). Scatterplots are a natural starting point in a complex analysis that can help in the development of a sensitivity analysis strategy using one or more additional techniques. Often, the examination of scatterplots is all that is needed to understand the relationships between the uncertainty in analysis inputs and the uncertainty in analysis results [145].

Most analyses start with two dimensional scatterplots. However, when strong three-way interactions between variables are present, three-dimensional scatterplots (i.e., scatterplots involving three variables) can provide informative displays of analysis results (Fig. 7). The three-dimensional scatterplot in Fig. 7 involves one sampled variable (i.e., $x_j = WPRTDIAM$) and two calculated variables (i.e., $y_k = WAS_PRES$ and $y_l = REL_VOL$). The result in Fig. 7 was calculated by a model that uses the calculated value for WAS_PRES under undisturbed conditions as an input and then determines the volume of material (i.e., REL_VOL) released to the surface at the time of a drilling intrusion due to a pressure-driven spallings event; $WPRTDIAM$ is one of the uncertain (i.e., sampled) variables used in this calculation [145] Specifically, Fig. 7 contains a plot of the points (x_{ij}, y_{ik}, y_{il}) for $i = 1, 2, \ldots, nS$. As examination of Fig. 7 shows, (i) WAS_PRES acts as a switch that determines if REL_PRES is nonzero, and (ii) $WPRTDIAM$ determines the magnitude of the nonzero values for REL_PRES. Because of the large number of possible three-way variable combinations in most analyses, some initial insights with respect to variable interactions usually needs to be developed before a reasonable selection of three-dimensional scatterplots can be made.

Additional information: Ref. [46, Section 6.6.1]; see Ref. [146] for additional plotting formats, including cobweb plots which provide a representation of multi-dimensional results (e.g., $[\mathbf{x}_i, y_i] = [x_{i1}, x_{i2}, \ldots, x_{i,nX}, y_i]$, $i = 1, 2, \ldots, nS$) in a two-dimensional plot.

6.2. Correlation

Correlation provides a measure of the strength of the linear relationship between x_j and y. Specifically, the (Pearson or sample) correlation coefficient (CC) $c(x_j, y)$ between x_j and y is defined by

$$c(x_j, y) = \frac{\sum_{i=1}^{nS}(x_{ij} - \bar{x}_j)(y_i - \bar{y})}{\left[\sum_{i=1}^{nS}(x_{ij} - \bar{x}_j)^2\right]^{1/2}\left[\sum_{i=1}^{nS}(y_i - \bar{y})^2\right]^{1/2}}, \tag{1}$$

where

$$\bar{x}_j = \sum_{i=1}^{nS} x_{ij}/nS \text{ and } \bar{y} = \sum_{i=1}^{nS} y_i/nS.$$

The CC $c(x_j, y)$ has a value between -1 and 1, with a positive value indicating that x_j and y tend to increase and decrease together and a negative value indicating that x_j and y tend to move in opposite directions. Further, gradations in the absolute value of $c(x_j, y)$ between 0 and 1 correspond to a trend from no linear relationship between x_j and y to an exact linear relationship between

Table 2
Definition of dependent variables calculated by BRAGFLO program for two phase flow and used in the illustration of uncertainty and sensitivity analysis procedures

BNBHDNUZ—Cumulative brine flow (m^3) down borehole at Market Bed (MB) 138 (i.e., from cell 223 to cell 575 in Ref. [102, Fig. 3]).
BRAABNIC—Cumulative brine flow (m^3) out of north anhydrites A and B into disturbed rock zone (DRZ) (i.e., from cells 556 to cell 527 in Ref. [102, Fig. 3]).
BRAABSIC—Cumulative brine flow (m^3) out of south anhydrites A and B into DRZ (i.e., from cell 555 to cell 482 in Ref. [102, Fig. 3]).
BRAALIC—Cumulative brine flow (m^3) out of all MBs into DRZ (i.e.,
BRAALIC = *BRM38NIC*+*BRAABNIC*+*BRM39NIC*+*BRM38SIC*+*BRAABSIC*+*BRM39SIC*).
BRM38NIC—Cumulative brine flow (m^3) out of north MB138 into DRZ (i.e., from cells 588 to 587 in Ref. [102, Fig. 3]).
BRM38SIC—Cumulative brine flow (m^3) out of south MB138 into DRZ (i.e., from cell 571 to cell 572 in Ref. [102, Fig. 3]).
BRM39NIC–Cumulative brine flow (m^3) out of north MB139 to DRZ (i.e., from cells 540 to 465 in Ref. [102, Fig. 3]).
BRM39SIC—Cumulative brine flow (m^3) out of south MB139 into DRZ (i.e., from cell 539 to cell 436 in Fig. 3, Ref. [102]).
BRNREPTC—Cumulative brine flow (m^3) into repository (i.e., into regions corresponding to cells 596–625, 638–640 in Ref. [102, Fig. 3]).
REP_SATB—Brine saturation in upper waste panels (i.e., average brine saturation calculated over cells 617–625 in Ref. [102, Fig. 3]).
WAS_PRES—Pressure (Pa) in lower waste panel (i.e., average pressure calculated over cells 596–616 in Ref. [102, Fig. 3]).
WAS_SATB—Brine saturation in lower waste panel (i.e., average brine saturation calculated over cells 596–616 in Ref. [102, Fig. 3])

The designator E0 is used to indicate results calculated for undisturbed conditions, and the designator E2 is used to indicate results calculated for disturbed conditions due to a drilling intrusion that penetrates the lower waste panel of the repository 1000 yr after repository closure. Further, the designator *R*1 indicates results calculated for the first of the three replicated Latin hypercube samples described in Section 3, and the designators *R*1, *R*2, *R*3 collectively are used to indicate results calculated with the three replicates pooled together.

x_j and y. As an example, the CCs associated with the scatterplots in Fig. 8 are $c(HALPOR,\ REP_SATB) = 0.75$ (Fig. 8a) and $c(WGRCOR,\ REP_SATB) = -0.41$ (Fig. 8b).

The CC $c(x_j,\ y)$ is closely related to results obtained in a linear regression relating y to x_j. Specifically, $c(x_j,\ y)$ is equal to the standardized regression coefficient (SRC) in the indicated regression, and the absolute value of $c(x_j,\ y)$ is equal to the square root of the corresponding R^2 value (see Section 6.3). As a correlation of 0 only indicates the absence of a linear association between x_j and y, it does not preclude the existence of a well-defined nonlinear relationship between x_j and y (e.g., $y = \sin x_j$).

Additional information: Ref. [46, Section 6.6.4].

6.3. Regression analysis

Regression analysis provides an algebraic representation of the relationships between y and one or more of the x_j's. Unless stated otherwise, regression analysis is usually assumed to involve the construction of linear models of the form

$$\hat{y} = b_0 + b_j x_j \tag{2}$$

for a single independent variable (i.e., x_j) and

$$\hat{y} = b_0 + \sum_{j=1}^{nX} b_j x_j \tag{3}$$

for multiple independent variables (i.e., $x_1,\ x_2,\ \ldots,\ x_{nX}$). The regression coefficients in Eqs. (2) and (3) are determined such that the sums

$$\sum_{i=1}^{nS} (y_i - \hat{y}_i)^2 = \sum_{i=1}^{nS} [y_i - (b_0 + b_j x_{ij})]^2 \tag{4}$$

and

$$\sum_{i=1}^{nS} (y_i - \hat{y}_i)^2 = \sum_{i=1}^{nS} \left[y_i - \left(b_0 + \sum_{j=1}^{nS} b_j x_{ij} \right) \right]^2, \tag{5}$$

respectively, are minimized. As a result, the regression models in Eqs. (2) and (3) are often referred to as least-squares models due to the minimization of the sums of squares in Eqs. (4) and (5).

As important property of least squares regression models is the equality

$$\sum_{i=1}^{nS} (y_i - \bar{y})^2 = \sum_{i=1}^{nS} (\hat{y}_i - \bar{y})^2 + \sum_{i=1}^{nS} (\hat{y}_i - y_i)^2. \tag{6}$$

For notational convenience, the preceding equality is often written

$$\mathrm{SS_{tot}} = \mathrm{SS_{reg}} + \mathrm{SS_{res}}, \tag{7}$$

where

$$\mathrm{SS_{tot}} = \sum_{i=1}^{nS} (y_i - \bar{y})^2, \quad \mathrm{SS_{reg}} = \sum_{i=1}^{nS} (\hat{y}_i - \bar{y})^2,$$

$$\mathrm{SS_{res}} = \sum_{i=1}^{nS} (\hat{y}_i - y)^2$$

and the three preceding summations are called the total sum of squares ($\mathrm{SS_{tot}}$), regression sum of squares ($\mathrm{SS_{reg}}$) and residual sum of squares ($\mathrm{SS_{res}}$), respectively.

Since $\mathrm{SS_{res}}$ provides a measure of variability about the regression model, the ratio

$$R^2 = \mathrm{SS_{reg}}/\mathrm{SS_{tot}} = \sum_{i=1}^{nS} (\hat{y}_i - \bar{y})^2 \Big/ \sum_{i=1}^{nS} (y_i - \bar{y})^2 \tag{8}$$

provides a measure of the extent to which the regression model can match the observed data. Specifically, when the

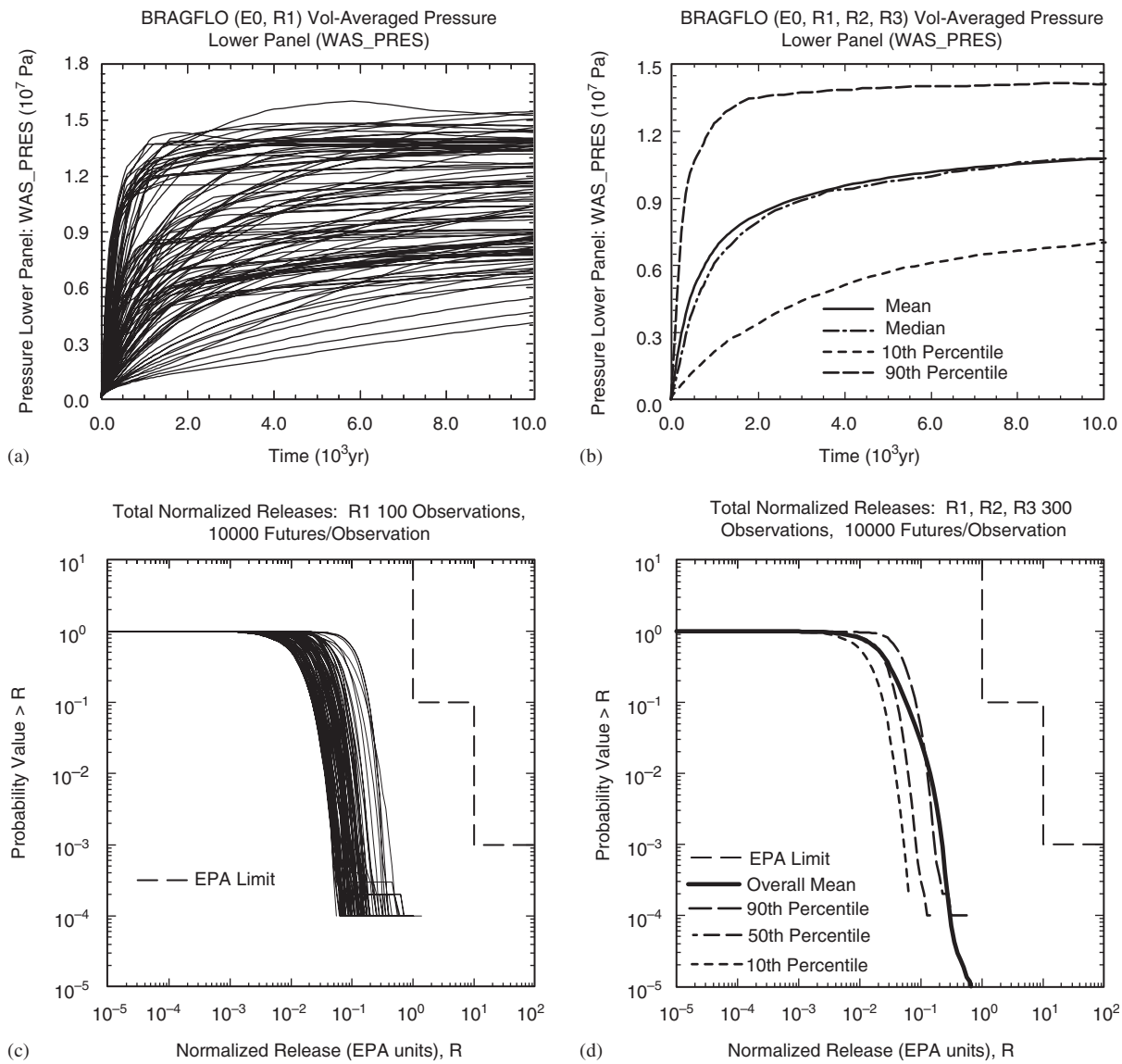

Fig. 5. Representation of uncertainty in analysis results that are functions: (a, b) Pressure as a function of time (Ref. [101, Figs. 7.5, 7.9]), and (c, d) effects of aleatory uncertainty summarized as a CCDF (Ref. [101, Fig. 10.5]).

variation about the regression model is small (i.e., SS_{res} is small relative to SS_{reg}), then the corresponding R^2 value is close to 1, which indicates that the regression model is accounting for most of the uncertainty in y. Conversely, an R^2 value close to 0 indicates that the regression model is not very successful in accounting for the uncertainty in y. When the individual x_j in the regression model in Eq. (3) are independent, the R^2 value for the regression model can be expressed as

$$R^2 = SS_{reg}/SS_{tot} = R_1^2 + R_2^2 + \cdots + R_{nX}^2, \tag{9}$$

where R_j^2 is the R^2 value that results from regressing y on only x_j. Thus, R_j^2 is equal to the contribution of x_j to the R^2 value for the regression model in Eq. (3) when the x_j's are independent.

The regression coefficients b_j, $j = 1, 2, \ldots, nX$, are not very useful in sensitivity analysis because each b_j is influenced by the units in which x_j is expressed and also does not incorporate any information on the distribution assigned to x_j. Because of this, the regression models in Eqs. (2) and (3) are usually reformulated as

$$(\hat{y} - \bar{y})/\hat{s} = (b_j \hat{s}_j/\hat{s})(x_j - \bar{x}_j)/\hat{s}_j \tag{10}$$

and

$$(\hat{y} - \bar{y})/\hat{s} = \sum_{j=1}^{nX} (b_j \hat{s}_j/\hat{s})(x_j - \bar{x}_j)/\hat{s}_j, \tag{11}$$

respectively, where

$$\hat{s} = \left[\sum_{i=1}^{nS} (y_i - \bar{y})^2/(nS-1)\right]^{1/2},$$

$$\hat{s}_j = \left[\sum_{i=1}^{nS} (x_{ij} - \bar{x}_j)^2/(nS-1)\right]^{1/2}$$

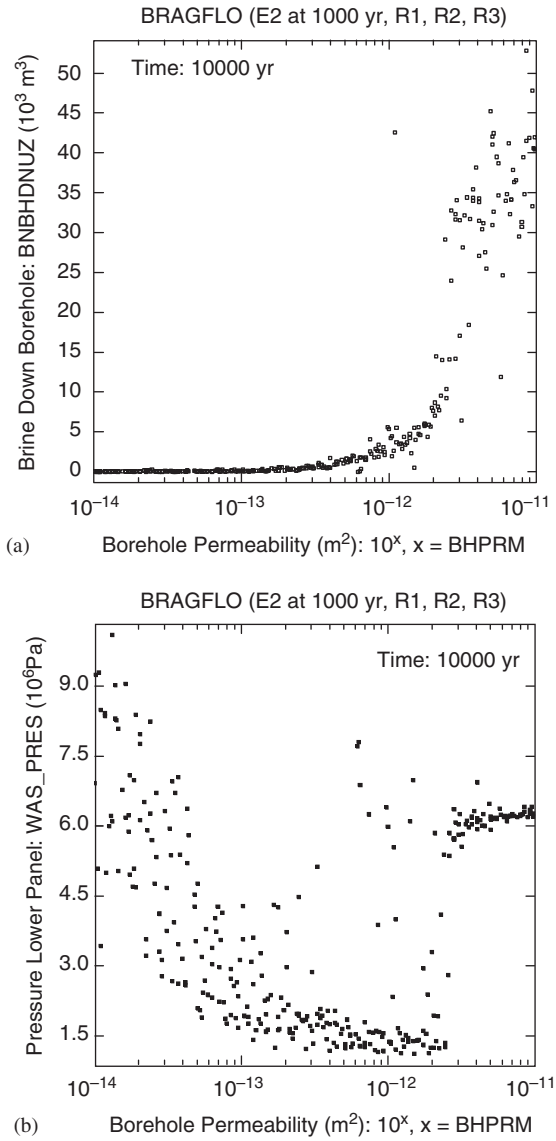

Fig. 6. Examples of scatterplots obtained in a sampling-based uncertainty/sensitivity analysis (Ref. [101, Figs. 8.1, 8.2]).

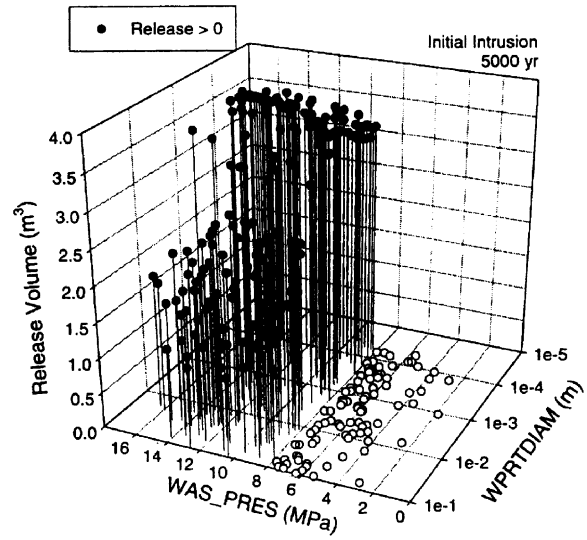

Fig. 7. Example of three-dimensional scatterplot obtained in a sampling-based uncertainty/sensitivity analysis (Ref. [145, Fig. 13]).

and $\bar{y}$ and $\bar{x}_j$ are defined in conjunction with Eq. (1). The coefficients $b_j\hat{s}_j/\hat{s}$ in Eqs. (10) and (11) are referred to as SRCs.

When the regression models in Eqs. (2) and (10) involving only x_j are under consideration, the SRC $b_j\hat{s}_j/\hat{s}$ provides a measure of variable importance based on the effect on y relative to the standard deviation $\hat{s}$ of y of moving x_j away from its expected value $\bar{x}_j$ by a fixed fraction of its standard deviation $\hat{s}_j$. Further, when the x_j's are independent, the inclusion or exclusion of an individual x_j from the regression models in Eqs. (3) and (11) has no effect on the SRCs for the remaining variables in the model. Thus, as long as the x_j's are independent, the SRCs $b_j\hat{s}_j/\hat{s}$ in Eq. (11) provide a useful measure of variable importance, with (i) the absolute values of the coefficients $b_j\hat{s}_j/\hat{s}$ providing a comparative measure of variable importance (i.e., variable x_u is more important than variable x_v if $|b_u\hat{s}_u/\hat{s}| > |b_v\hat{s}_v/\hat{s}|$) and (ii) the sign of $b_j\hat{s}_j/\hat{s}$ indicating whether x_j and y tend to move in the same direction or in opposite directions. However, when x_j's are not independent, SRCs do not provide reliable indications of variable importance (Ref. [46, Section 6.6.7]).

For purposes of sensitivity analysis, there is usually no reason to construct a regression model containing all the uncertain variables (i.e., $x_1, x_2, \ldots, x_{nX}$) as indicated in Eqs. (3) and (11). Rather, a more appropriate procedure is to construct regression models in a stepwise manner. With this procedure, a regression model is first constructed with the most influential variable (e.g., $\tilde{x}_1$ as determined based on R^2 values for regression models containing only single variables). Then, a regression model is constructed with $\tilde{x}_1$ and the next most influential variable (e.g., $\tilde{x}_2$ as determined based on R^2 values for regression models containing $\tilde{x}_1$ and each of the remaining variables). The process then repeats to determine $\tilde{x}_3$ in a similar manner and continues until no more variables with an identifiable effect on y can be found. Variable importance (i.e., sensitivity) is then indicated by the order in which variables are selected in the stepwise process, the changes in cumulative R^2 values as additional variables are added to the regression model, and the SRCs for the variables in the final regression model. An example of a sensitivity analysis of this form is presented in Table 3.

A display of regression results of the form shown in Table 3 is very unwieldy when results at a sequence of times are under consideration. In this situation, a more compact display of regression results is provided by plotting SRCs as functions of time for all x_j that appear to have a significant effect on y at some point in the time interval under consideration (Fig. 9a).

This section only considers linear regression models. However, linear regression models also include models of

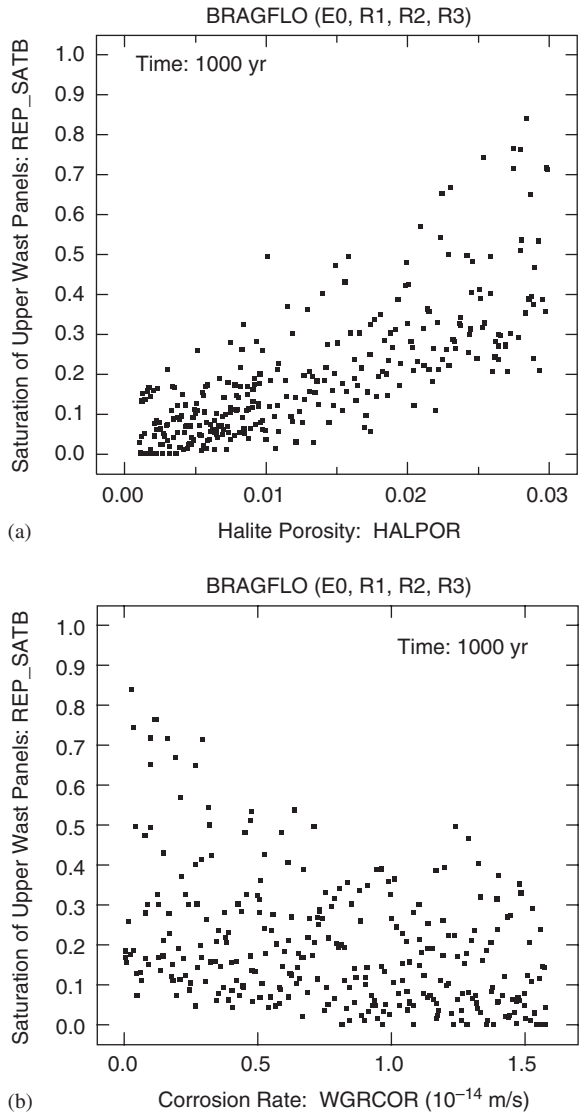

Fig. 8. Illustration of correlation coefficients: (a) $c(x_j, y) = 0.75$ with $x_j = HALPOR$ and $y = REP_SATB$ (left frame), and (b) $c(x_j, y) = -0.41$ with $x_j = WGRCOR$ and $y = REP_SATB$ (right frame).

Table 3
Example of stepwise regression analysis to identify uncertain variables affecting the uncertainty in pressure (*WAS_PRES*) at 10,000 yr in Fig. 5a (Ref. [101, Table 8.6])

Step[a]	Variable[b]	SRC[c]	R^{2d}
1	*WMICDFLG*	0.718	0.508
2	*HALPOR*	0.466	0.732
3	*WGRCOR*	0.246	0.792
4	*ANHPRM*	0.129	0.809
5	*SHRGSSAT*	0.070	0.814
6	*SALPRES*	0.063	0.818

[a]Steps in stepwise regression analysis.
[b]Variables listed in the order of selection in regression analysis.
[c]SRCs for variables in final regression model.
[d]Cumulative R^2 value with entry of each variable into regression model.

forms such as

$$\hat{y} = b_0 + \sum_{j=1}^{nX} b_j f_j(x_j) + \sum_{j=1}^{nX} \sum_{l=j}^{nX} b_{jl} f_{jl}(x_j, x_l). \tag{12}$$

This inclusion exists because the preceding model is linear in its coefficients (i.e., b_0, the b_j, the b_{jl}); in essence, the indicated transformations involving the x_j (i.e., $f_j(x_j)$, $f_{jl}(x_j, x_l)$) are simply defining a new set of analysis inputs to be used in a regression-based sensitivity analysis. Results can be improved in some analyses by well-chosen variable transformations of the form indicated in Eq. (12). However, in large analyses involving many uncertain analysis inputs (i.e., x_j) and many possibly time-dependent analysis results (i.e., many different elements of **y**), the a priori determination of suitable transformations can be difficult. Also, care can be taken to suitably account for any correlations that may be introduced by the chosen transformations (i.e., $f_j(x_j)$ and $f_{jl}(x_j, x_l)$ may be highly correlated).

Nonlinear regression provides an alternative to linear regression that can be useful in some analyses. In nonlinear regression, at least some of the model coefficients are operated on by nonlinear functions. For example,

$$\hat{y} = b_0 + b_1 \exp(b_2 x_1) + b_3 \sin(b_4 x_2) \tag{13}$$

is a nonlinear model because b_2 and b_4 appear in expressions that are operated on by nonlinear functions. A major challenge in the use of nonlinear regression in sensitivity analysis is the determination of a suitable form for the nonlinear regression model. The following two alternatives to nonlinear regression for use in the presence of nonlinear relationships between model inputs (i.e., the x_j) and model results (i.e., the elements of **y**) that place fewer a priori demands on the analyst are described later in this presentation: rank transformations (Section 6.5) and nonparametric regression (Section 6.8).

Additional information: Ref. [46, Sections 6.6.2, 6.6.3, and 6.6.5]. Further, general information on regression analysis is available in a number of texts (e.g., Refs. [147–151]).

6.4. Partial correlation

The partial correlation coefficient (PCC) between x_j and y can be defined in the following manner. First, the two regression models indicated below are constructed:

$$\hat{x}_j = c_0 + \sum_{\substack{p=1 \\ p \neq j}}^{nX} c_p x_p \quad \text{and} \quad \hat{y} = b_0 + \sum_{\substack{p=1 \\ p \neq j}}^{nX} b_p x_p. \tag{14}$$

Then, the results of the two preceding regressions are used to define the new variables $x_j - \hat{x}_j$ and $y - \hat{y}$. The PCC between x_j and y is the CC $c(x_j - \hat{x}_j, y - \hat{y})$ (see Eq. (1)) between $x_j - \hat{x}_j$ and $y - \hat{y}$. As for SRCs, PCCs are often defined for variables that are functions of time and presented as time-dependent plots (Fig. 9b).

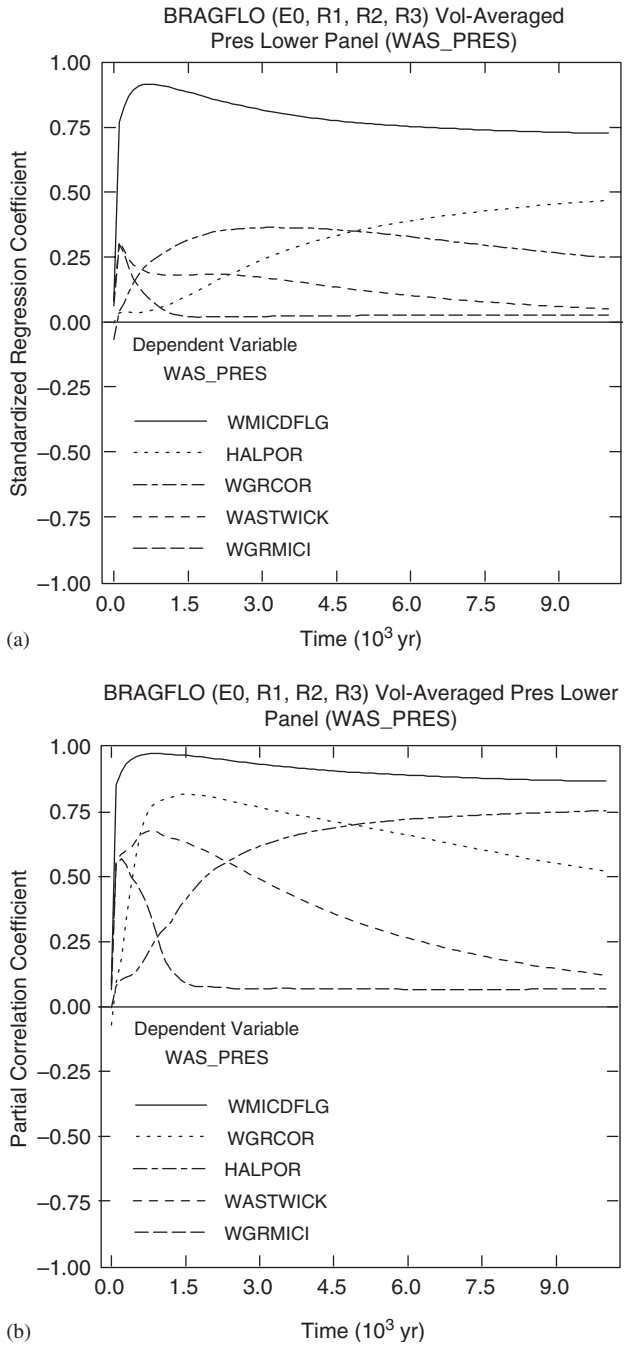

Fig. 9. Time-dependent sensitivity analysis results for uncertain pressure curves in Fig. 5a: (a) SRCs as a function of time, and (b) PCCs as a function of time (Ref. [101, Fig. 8.3]).

The PCC characterizes the linear relationship between x_j and y after a correction has been made for the linear effects on y of the remaining elements of $\mathbf{x}$, and the SRC characterize the effect on y that results from perturbing x_j by a fixed fraction of its standard deviation. Thus, PCCs and SRCs provide related, but not identical, measures of variable importance. In particular, the PCC between x_j and y provides a measure of variable importance that tends to exclude the effects of the other elements of $\mathbf{x}$, the assumed distribution for x_j, and the magnitude of the impact of the uncertainty in x_j on the uncertainty in y. In contrast, the SRC relating x_j to y is more influenced by the distribution assigned to x_j and the magnitude of the impact of the uncertainty in x_j on the uncertainty in y. However, when the elements of $\mathbf{x}$ are independent, PCCs and SRCs give the same rankings of variable importance. Specifically, an ordering of variable importance based on the absolute value of PCCs is the same as an ordering based on either the absolute value of CCs or the absolute value of SRCs (Ref. [46, Section 6.6.4]). A cosmetic benefit of using PCCs is that PCCs tend to be spread out in value more than SRCs and thus produce results that are easier to read (e.g., compare Figs. 9a and b); however, the downside to this is that a variable can appear to have a larger effect on the uncertainty in y than is actually the case.

As for analyses based on SRCs, analyses based on PCCs can give very misleading results when correlations exist between the elements of $\mathbf{x}$. Specifically, if $\mathbf{x}$ contains two highly correlated variables, then each variable will cancel the other's effect when PCCs with y are calculated.

Additional information: Ref. [46, Section 6.6.4]; Ref. [152].

6.5. Rank transformations

A rank transformation can be used to convert a nonlinear but monotonic relationship between the x_j and y into a linear relationship. With this transformation, the values for the x_j and y are replaced by their corresponding ranks. Specifically, the smallest value for a variable is assigned a rank of 1; the next largest value is assigned a rank of 2; tied values are assigned their average rank; and so on up to the largest value, which is assigned a rank of nS. Use of the rank transformation results in rank (i.e., Spearman) correlation coefficients (RCCs), rank regressions, standardized rank regression coefficients (SRRCs) and partial rank correlation coefficients (PRCCs). In the presence of nonlinear but monotonic relationships between the x_j and y, use of the rank transform can substantially improve the resolution of sensitivity analysis results (Table 4).

Additional information: Ref. [46, Section 6.6.6]; Ref. [153].

6.6. Statistical tests for patterns based on gridding

Analyses based on raw or rank-transformed data can fail when the underlying relationships between the x_j and y are nonlinear and nonmonotonic (Fig. 10). The scatterplot in Fig. 6b is for the pressure at 10,000 yr in Fig. 10a versus the uncertain variable *BHPRM*. The partial correlation analyses summarized in Fig. 10b fail at later times because the pattern appearing in Fig. 6b is too complex to be captured with a partial correlation analysis based on raw or rank-transformed data; analyses with SRCs or SRRCs also fail for the same reason. An alternative analysis strategy for

Table 4
Comparison of stepwise regression analyses with raw and rank-transformed data for cumulative brine inflow to vicinity of repository over 10,000 yr from anhydrite marker beds (*BRAALIC*) under undisturbed (i.e., E0) conditions in Fig. 4b (Ref. [101, Table 8.8])

Step[a]	Raw data			Rank-transformed data		
	Variable[b]	SRC[c]	R^{2d}	Variable[b]	SRRC[e]	R^{2d}
1	*ANHPRM*	0.562	0.320	*WMICDFLG*	−0.656	0.425
2	*WMICDFLG*	−0.309	0.423	*ANHPRM*	0.593	0.766
3	*WGRCOR*	−0.164	0.449	*HALPOR*	−0.155	0.802
4	*WASTWICK*	−0.145	0.471	*WGRCOR*	−0.152	0.824
5	*ANHBCEXP*	−0.120	0.486	*HALPRM*	0.143	0.845
6	*HALPOR*	−0.101	0.496	*SALPRES*	0.120	0.860
7				*WASTWICK*	−0.010	0.869

[a]Steps in stepwise regression analysis.
[b]Variables listed in order of selection in regression analysis.
[c]SRCs for variables in final regression model.
[d]Cumulative R^2 value with entry of each variable into regression model.
[e]SRRCs for variables in final regression model.

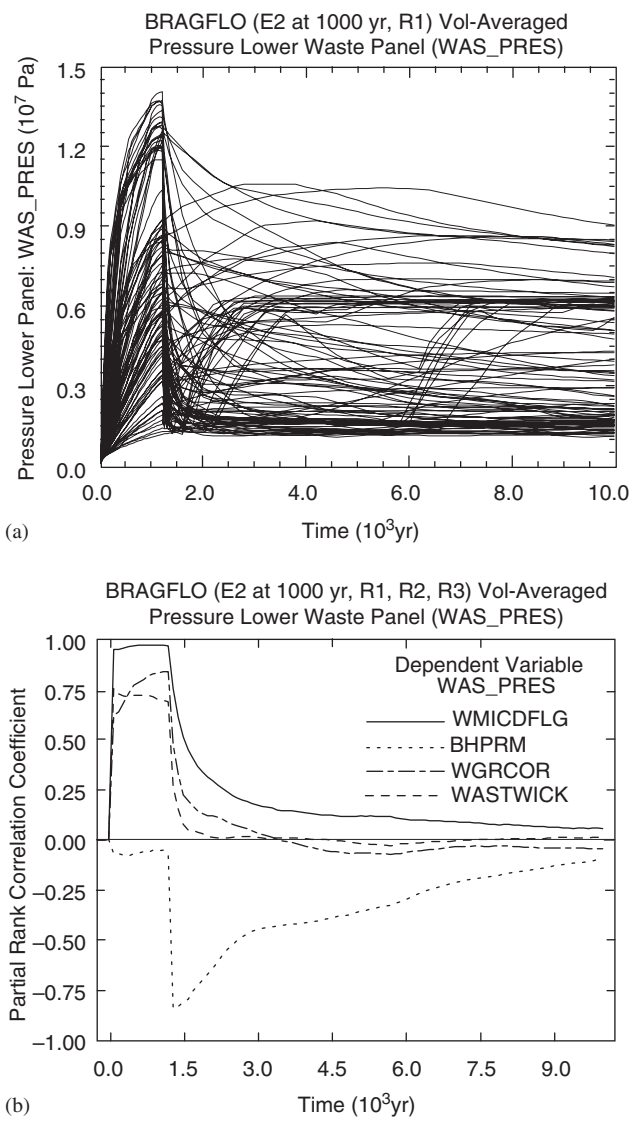

Fig. 10. Illustration of failure of a sensitivity analysis based on rank-transformed data: (a) pressures as a function of time and (b) PRCCs as a function of time (Ref. [101, Fig. 8.7]).

situations of this type is to place grids on the scatterplot for y and x_j and then perform various statistical tests to determine if the distribution of points across the grid cells appears to be nonrandom. Appearance of a nonrandom pattern indicates that x_j has an effect on y. Possibilities include tests for (i) common means (CMNs), (ii) common distributions or locations (CLs), (iii) common medians (CMDs), and (iv) statistical independence (SI). Descriptions of these tests follow.

The CMNs test is based on dividing the values of x_j (i.e., x_{ij}, $i = 1, 2, \ldots, nS$) into nI classes and then testing to determine if y has a CMN across these classes (Ref. [154, Section 3.1]). The required classes are obtained by dividing the range of x_j into a sequence of mutually exclusive and exhaustive subintervals containing equal numbers of sampled values (Fig. 11a). If x_j is discrete, individual classes are defined for each of the distinct values. For notational convenience, let c, $c = 1, 2, \ldots, nI$, designate the individual classes into which the values of x_j have been divided; let X_c designate the set such that $i \in \mathrm{X}_c$ only if x_{ij} belongs to class c; and let nI_c equal the number of elements contained in X_c (i.e., the number of x_{ij}'s associated with class c).

The F-test can be used to test for the equality of the mean values of y for the classes into which the values of x_j have been divided (e.g., the intervals defined on the abscissa of the scatterplot in Fig. 11a). Specifically, if the y values conditional on each class of x_j values are normally distributed with equal expected values, then

$$F = \frac{\left[\sum_{c=1}^{nI} nI_c \bar{y}_c^2 - nS\bar{y}^2\right] \Big/ (nI - 1)}{\left[\sum_{i=1}^{nS} y_i^2 - \sum_{c=1}^{nI} nI_c \bar{y}_c^2\right] \Big/ (nS - nI)} \tag{15}$$

follows an F-distribution with (nI–1, nS–nI) degrees of freedom, where $\bar{y}_c = \sum_{i \in X_c} y_i / nI_c$ and $\bar{y}$ is defined in conjunction with Eq. (1). Given that the indicated

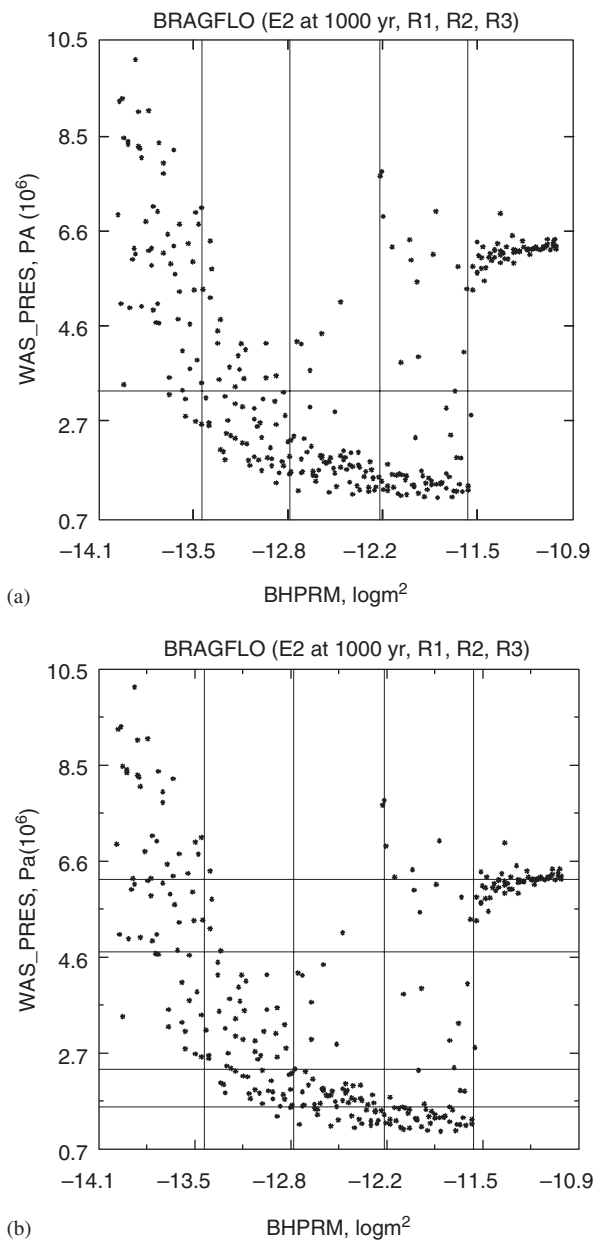

Fig. 11. Grids used to test for nonrandom patterns: (a) partitioning of range of x_j for CMNs and CLs tests and ranges of x_j and y for CMDs test (Ref. [101, Fig. 8.8]), and (b) partitioning of ranges of x_j and y for SI (Ref. [101, Fig. 8.9]).

assumptions hold, the probability $\text{prob}_F(\tilde{F} > F|\ nI\text{–}1, nS\text{–}nI)$ of obtaining an F-statistic of value $\tilde{F}$ that exceeds the value of F in Eq. (15) can be obtained from an F-distribution with (nI–1, nS–nI) degrees of freedom. A low probability (i.e., p-value) of obtaining a larger value for F suggests that the observed pattern involving x_j and y did not arise by chance and hence that x_j has an effect on the behavior of y.

The CLs test employs the Kruskal–Wallis test statistic T, which is based on rank-transformed data and uses the same classes of x_j values as the F-statistic in Eq. (15) Ref. [155, pp. 229–230]). Specifically,

$$T = \left[\sum_{c=1}^{nI}(R_c^2/nI_c) - nS(nS+1)^2/4\right] \Big/ s^2, \tag{16}$$

where

$$R_c = \sum_{i \in X_c} r(y_i), s^2 = \left[\sum_{i=1}^{nS} r(y_i)^2 - nS(nS+1)^2/4\right] \Big/ (nS-1)$$

and $r(y_i)$ denotes the rank of y_i. If the y values conditional on each class of x_j values have the same distribution, then the statistic T in Eq. (16) approximately follows a χ^2 distribution with nI–1 degrees of freedom (Ref. [155, pp. 230–231]). Thus, the probability $\text{prob}_{\chi^2}(\tilde{T} > T|nI-1)$ of obtaining a value $\tilde{T}$ that exceeds T in the presence of identical y distributions for the individual classes can be obtained from a χ^2 distribution with nI–1 degrees of freedom. A small value for $\text{prob}_{\chi^2}(\tilde{T} > T|nX-1)$ (i.e., a p-value) indicates that the values for y's conditional on individual classes have different distributions and thus, most likely, different means and medians. Hence, a small p-value indicates that x_j has an effect on y.

The CMDs test is based on the χ^2-test for contingency tables, which can be used to test for the equality of the median values of y for the classes into which the values of x_j have been divided (Ref. [155, pp. 143–178]). First, the median $y_{0.5}$ for y is estimated for all nS observations. Specifically,

$$y_{0.5} = \begin{cases} y_{(0.5nS)} & \text{if } 0.5nS \text{ is an integer,} \\ [y_{([0.5nS])} + y_{([0.5nS]+1)}]/2 & \text{otherwise,} \end{cases} \tag{17}$$

where $y_{(i)}$, $i = 1, 2, \ldots, nS$, denotes the ordering of the y-values such that $y_{(i)} \leqslant y_{(i+1)}$ and [~] designates the greatest integer function. The individual classes of x_j values are then further subdivided on the basis of whether y values fall above or below $y_{0.5}$ (Fig. 11a). For class c, let nI_{1c} equal the number of y values that exceed $y_{0.5}$, and let nI_{2c} equal the number of y values that are less than or equal to $y_{0.5}$.

The result of this partitioning is a $2 \times nI$ contingency table with nI_{rc} observations in each cell (i.e., in cell (r, c), where r and c designate "row" and "column," respectively, in the corresponding contingency table). The following statistic can now be defined:

$$T = \sum_{c=1}^{nI}\sum_{r=1}^{2}(nI_{rc} - nE_{rc})^2/nE_{rc}, \tag{18}$$

where

$$nE_{rc} = \left(\sum_{p=1}^{2} nI_{pc}/nS\right)\left(\sum_{q=1}^{nI} nI_{rq}/nS\right)nS = \left(\sum_{p=1}^{2} nI_{pc}\right)\left(\sum_{q=1}^{nI} nI_{rq}\right) \Big/ nS$$

and corresponds to the expected number of observations in cell (r, c). If the individual classes of x_j values have equal

medians, then T approximately follows a χ^2 distribution with $(nI-1)(2-1) = nI-1$ degrees of freedom (Ref. [155, p. 156]). Thus, the probability of obtaining a value $\tilde{T}$ that exceeds T in the presence of equal medians is given by $\text{prob}_{\chi^2}(\tilde{T} > T|nI-1)$. A small value (i.e., p-value) for $\text{prob}_{\chi^2}(\tilde{T} > T|nI-1)$ indicates that the y's conditional on individual classes have different medians and hence that x_j has an influence on y.

The SI test also uses the χ^2-test to indicate if the pattern appearing in a scatterplot appears to be nonrandom. The SI test uses the same partitioning of x_j values as used for the CMNs, CLs and CMDs tests. In addition, the y values are also partitioned in a manner analogous to that used for the x_j values (Fig. 11b). For notational convenience, let r, $r = 1, 2, \ldots, nD$, designate the individual classes into which the values of y are divided; let Y_r designate the set such that $i \in \mathrm{Y}_r$ only if y_i belongs to class r; and let nD_r equal the number of elements contained in Y_r (i.e., the number of y_i's associated with class r).

The partitioning of x_j and y into nI and nD classes in turn partitions (x_j, y) into $nI\ nD$ classes (Fig. 11a), where (x_{ij}, y_i) belongs to class (r, c) only if x_{ij} belongs to class c of the x_j values (i.e., $i \in \mathrm{X}_c$) and y_i belongs to class r of the y values (i.e., $i \in Y_r$). For notational convenience, let O_{rc} denote the set such that $x_{ij} \in O_{rc}$ only if $i \in X_c$ (i.e., x_{ij} is in class c of x_j values) and also $i \in Y_r$ (i.e., y_i is in class r of y values), and let nO_{rc} equal the number of elements contained in O_{rc}. Further, if x_j and y are independent, then

$$nE_{rc} = (nD_r/nS)(nI_c/nS)nS = nD_r\, nI_c/nS \tag{19}$$

is an estimate of the expected number of observations (x_j, y) that should fall in class (r, c).

The following statistic can be defined:

$$T = \sum_{c=1}^{nI}\sum_{r=1}^{nD}(nO_{rc} - nE_{rc})^2/nE_{rc}. \tag{20}$$

Asymptotically, T follows a χ^2-distribution with $(nI–1)(nD–1)$ degrees of freedom when x_j and y are independent (Ref. [155, pp. 158–153]). Thus, $\text{prob}_{\chi^2}[\tilde{T} > T|(nI-1)(nD-1)]$ is the probability (i.e., p-value) of obtaining a value of $\tilde{T}$ that exceeds T when x_j and y are independent. A small p-value indicates that the pattern in the scatterplot arose from some underlying relationship involving x_j and y rather than from chance alone. As shown by comparison of Eqs. (18) and (20), the CMDs and SI tests differ only in the partitionings used for the y values.

The four tests described in this section are illustrated in Table 5 for $y = WAS_PRES$ at 10,000 yr under undisturbed conditions (Fig. 5a) and disturbed conditions (Fig. 10a). Scatterplots illustrating the partitioning for $x_j = BHPRM$ and $y = WAS_PRES$ under disturbed conditions are given in Fig. 11. For perspective, rankings based on CCs and RCCs are also presented in Table 4. The relationships between $y = WAS_PRES$ and the dominant sampled variables under undisturbed conditions are fairly linear, with the result that all ranking procedures (i.e., CMNs, CLs, CMDs, SI, CCs, RCCs) give the same ordering of variable importance for the top four variables. In contrast, the relationship between $y = WAS_PRES$ and $x_j = BHPRM$ under disturbed conditions is both nonlinear and nonmonotonic (Fig. 11), with the result that the tests based on gridding (i.e., CMNs, CLs, CMDs, SI) all identify $BHPRM$ as being the dominant variable influencing the uncertainty in WAS_PRES; in contrast, the effect of $BHPRM$ was completely missed by tests based on CCs and RCCs. (Table 5).

The CMNs, CLs, CMDs and SI tests discussed in this section are all based on p-values that derive from statistical tests predicated on assumptions that are certainly not satisfied in their entirety in sampling-based sensitivity analyses. Thus, it is possible that the violation of these assumptions could be leading to misrankings of variable importance. Such a possibility can be explored by using a Monte Carlo procedure to assess if the use of formal statistical procedures to determine p-values is producing misleading results (Ref. [156]; Ref. [157, Section 14.5]). Specifically, nR samples of the form

$$(x_{ij}, y_i), \quad i = 1, 2, \ldots, nS \tag{21}$$

can be generated by pairing the nS values for x_j randomly and without replacement with the nS values for y. This random assignment is repeated nR times to produce nR samples of the form in Eq. (21) for each uncertain input x_j under consideration. In this example, $nR = 10,000$ and $nS = 300$. For a given procedure (i.e., CMNs, CLs, CMDs, SI), each of the nR samples can be used to calculate the value of the statistic used to determine the corresponding p-value. The resulting empirical distribution of the statistic can then be used to estimate the p-value for the statistic actually observed in the analysis. Comparison of the p-value obtained for a given set of statistical assumptions with the p-value obtained from the empirical distribution of the corresponding statistic provides an indication of the robustness of the variable rankings with respect to possible deviations from the assumptions underlying the formal statistical procedure. As examination of Table 6 shows, the variable rankings illustrated in this section are quite robust with respect to possible deviations from the underlying statistical assumptions on which they are predicated.

Additional Information: Ref. [46, Sections 6.6.8 and 6.6.9]; Refs. [47,158–160].

6.7. Entropy tests for patterns based on gridding

Measures of entropy provide another grid-based procedure to assess the strength of nonlinear relationships between the x_j and y. Specifically, the following quantities can be defined (Ref. [157, pp. 480–484]):

$$H(y) = -\sum_{r=1}^{nD}(nD_r/nS)\ln(nD_r/nS), \tag{22}$$

Table 5
Comparison of statistical tests for patterns based on gridding for pressure (*WAS_PRES*) at 10,000 yr under undistributed (i.e., *E*0) conditions (Fig. 5a) and disturbed (i.e., *E*2) conditions (Fig. 10a) (adapted from Ref. [47, Tables 4 and 21])

Variable[a]	CMNs: 1×5[b]		CLs: 1×5[c]		CMDs: 2×5[d]		SI: 5×5[e]		CCs[f]		RCCs[g]	
	Rank	*p*-Val	*Rank*	p-Val	Rank	*p*-Val	Rank	*p*-Val	Rank	*p*-Val	Rank	*p*-Val
Pressure, undisturbed (i.e., *E*0) conditions at 10,000 yr (Fig. 5a)												
WMICDFLG	1	0.0000	1	0.0000	1	0.0000	1	0.0000	1	0.0000	1	0.0000
HALPOR	2	0.0000	2	0.0000	2	0.0000	2	0.0000	2	0.0000	2	0.0000
WGRCOR	3	0.0000	3	0.0000	3	0.0025	3	0.0003	3	0.0000	3	0.0000
ANHPRM	4	0.0195	4	0.0187	4	0.0663	4	0.0049	4	0.0241	4	0.0268
ANHBCVGP	18	0.8062	16	0.7686	14	0.6442	5	0.0194	20	0.8084	15	0.7686
Pressure, disturbed (i.e., *E*2) conditions at 10,00 yr (Fig. 10a)												
BHPRM	1	0.0000	1	0.0000	1	0.0000	1	0.0000	10	0.3651	6	0.1704
HALPRM	2	0.0000	2	0.0000	2	0.0000	2	0.0002	1	0.0000	1	0.0000
ANHPRM	3	0.0002	3	0.0000	3	0.0007	4	0.0049	2	0.0000	2	0.0000
ANHBCEXP	4	0.0405	4	0.0602	4	0.0595	14	0.4414	7	0.1786	8	0.2373
HALPOR	5	0.0415	5	0.0940	5	0.0700	11	0.3142	3	0.0090	3	0.0184
WGRCOR	17	0.5428	9	0.2242	14.5	0.5249	3	0.0002	20	0.7676	17	0.6560

[a]Table includes only variables that had a *p*-value less than 0.05 for at least one of the procedures although the variable rankings for a specific procedure are based on the *p*-values obtained for that procedure for all variables considered in the analysis (see Table 1; variable *BHPRM* not included in analyses for undisturbed conditions).
[b]Variable ranks and *p*-values for CMNs test with 1×5 grid; see Eq. (15). Exceptions for CMNs, CLs, CMDs and SI tests: because variables *ANHBCVGP* and *WMICDFLG* are discrete with 2 and 3 values, respectively (see Table 1), $nI = 2$ and 3 rather than 5 for these two variables.
[c]Variable ranks and *p*-values for CLs test with 1×5 grid; see Eq. (16).
[d]Variable ranks and *p*-values for CMDs test with 2×5 grid; see Eq. (18).
[e]Variable ranks and *p*-values for SI test with 5×5 grid; see Eq. (20).
[f]Variable ranks and *p*-values for CC; see Eq. (24), Ref. [47].
[g]Variable ranks and *p*-values for RCC; see Eq. (38), Ref. [47].

$$H(x_j) = -\sum_{c=1}^{nI}(nI_c/nS)\ln(nI_c/nS), \tag{23}$$

$$H(y, x_j) = -\sum_{r=1}^{nD}\sum_{c=1}^{nI}(nO_{rc}/nS)\ln(nO_{rc}/nS), \tag{24}$$

$$\begin{aligned} H(x_j|y) &= \sum_{r=1}^{nD}\left\{\frac{nD_r}{nS}\right\} \times\left\{-\sum_{c=1}^{nI}[(nO_{rc}/nS)/nD_r/nS] \times\ln[(nO_{rc}/nS)/nD_r/nS]\right\} \\ &= -\sum_{r=1}^{nD}\sum_{c=1}^{nI}(nO_{rc}/nS)\ln(nO_{rc}/nD_r) \\ &= H(y, x_j) - H(y), \end{aligned} \tag{25}$$

$$\begin{aligned} H(y|x_j) &= \sum_{c=1}^{nI}\left\{\frac{nI_c}{nS}\right\} \times\left\{-\sum_{r=1}^{nD}[(nO_{rc}/nS)/(nI_c/nS)] \times\ln[(nO_{rc}/nS)/(nI_c/nS)]\right\} \\ &= -\sum_{c=1}^{nI}\sum_{r=1}^{nD}(nO_{rc}/nS)\ln(nO_{rc}/nI_c) \\ &= H(y, x_j) - H(x_j), \end{aligned} \tag{26}$$

$$\begin{aligned} U(x_j|y) &= [H(x_j) - H(x_j|y)]/H(x_j) \\ &= [H(y) + H(x_j) - H(y, x_j)]/H(x_j), \end{aligned} \tag{27}$$

$$\begin{aligned} U(y|x_j) &= [H(y) - H(y|x_j)]/H(y) \\ &= [H(y) + H(x_j) - H(y, x_j)]/H(y), \end{aligned} \tag{28}$$

$$\begin{aligned} U(y, x_j) &= 2[H(y) + H(x_j) - H(y, x_j)]/[H(y) + H(x_j)] \\ &= [H(y)U(y|x_j) + H(x)U(x_j|y)]/[H(y) + H(x_j)], \end{aligned} \tag{29}$$

where (i) $H(y)$ and $H(x_j)$ are estimates of the entropy associated with y and x_j, respectively, (ii) $H(y, x_j)$ is an estimate of the entropy associated with y and x_j, (iii) $H(x_j|y)$ and $H(y|x_j)$ are estimates of the expected entropy of x_j conditional on y and the expected entropy of x_j conditional on y, respectively, (iv) $U(x_j|y)$ and $U(y|x_j)$ are measures (i.e., uncertainty coefficients) of the contributions of y to the entropy associated with x_j and of x_j to the entropy associated with y, respectively, (v) $U(y,x)$ is an entropy-based measure of the strength of the association between x_j and y, (vi) the remaining expressions are the same as defined in Section 6.6, and (vii) the defined

Table 6
Comparison of variable rankings obtained with formal statistical procedures and Monte Carlo procedures for statistical tests for patterns based on gridding for pressure (*WAS_PRES*) at 10,000 yr under undisturbed (i.e., E0) conditions (Adapted from Ref. [47, Table 8]; see Ref. [47, Table 23], for a similar comparison for pressure at 10,000 yr under disturbed (i.e., E2) conditions)

Variable name[a]	CMN: 1×5[b]		CMNMC: 1×5[c]		Variable name[a]	CL: 1×5[b]		CLMC: 1×5[c]	
	Rank	*p*-Val	Rank	*p*-Val		Rank	*p*-Val	Rank	*p*-Val
WMICDFLG	1.0	0.0000	2.0	0.0000	*WMICDFLG*	1.0	0.0000	2.0	0.0000
HALPOR	2.0	0.0000	2.0	0.0000	*HALPOR*	2.0	0.0000	2.0	0.0000
WGRCOR	3.0	0.0000	2.0	0.0000	*WGRCOR*	3.0	0.0000	2.0	0.0000
ANHPRM	4.0	0.0195	4.0	0.0214	*ANHPRM*	4.0	0.0187	4.0	0.0212
SHPRMASP	5.0	0.1439	5.0	0.1495	*SHPRMASP*	5.0	0.1237	5.0	0.1277
WRBRNSAT	6.0	0.1506	6.0	0.1526	*WRBRNSAT*	6.0	0.2042	6.0	0.2053
SHRGSSAT	7.0	0.2488	7.0	0.2497	*ANRBRSAT*	7.0	0.2710	7.0	0.2710
ANRBRSAT	8.0	0.3034	8.0	0.3027	*SHRGSSAT*	8.0	0.3153	8.0	0.3167
…	…	…	…	…	…	…	…	…	…
WGRMICI	23.0	0.9705	23.0	0.9717	*WGRMICI*	23.0	0.9649	23.0	0.9663
WGRMICH	24.0	0.9975	24.0	0.9973.	*WGRMICH*	24.0	0.9865	24.0	0.9839
TDCC[d]			0.970		TDCC[d]			0.971	
Variable name[a]	CMD: 2×5[b]		CMDMC: 2×5[c]		Variable name[a]	SI: 5×5[b]		SIMC: 5×5[c]	
	Rank	*p*-Val	Rank	*p*-Val		Rank	*p*-Val	Rank	*p*-Val
WMICDFLG	1.0	0.0000	1.5	0.0000	*WMICDFLG*	1.0	0.0000	1.5	0.0000
HALPOR	2.0	0.0000	1.5	0.0000	*HALPOR*	2.0	0.0000	1.5	0.0000
WGRCOR	3.0	0.0025	3.0	0.0018	*WGRCOR*	3.0	0.0003	3.0	0.0003
ANHPRM	4.0	0.0663	4.0	0.0690	*ANHPRM*	4.0	0.0049	4.0	0.0038
SHPRMASP	5.0	0.2427	5.0	0.2401	*ANHBCVGP*	5.0	0.0194	5.0	0.0178
SHPRMCON	6.0	0.2674	6.0	0.2718	*WRGSSAT*	6.0	0.1229	6.0	0.1196
ANRBRSAT	7.0	0.3386	7.0	0.3329	*SHPRMCON*	7.0	0.1487	7.0	0.1529
HALPRM	8.0	0.3883	8.0	0.3967	*WASTWICK*	8.0	0.1850	8.0	0.1829
…	…	…	…	…	…	…	…	…	…
WGRMICH	23.0	0.9554	23.0	0.9439	*WGRMICH*	23.0	0.9437	23.0	0.9429
WGRMICI	24.0	0.9702	24.0	0.9664	*ANRGSSAT*	24.0	0.9763	24.0	0.9791
TDCC[d]			0.986		TDCC[d]			0.988	

[a]Twenty-four (24) variables included in analysis; highly correlated variables and variables not relevant to E0 conditions not included.
[b]Variable rankings obtained with a maximum of five classes of x values (i.e., $nI = 5$; see footnote b, Table 5) and analytic determination of p-values.
[c]Variable rankings obtained with a maximum of five classes of x values (i.e., $nI = 5$; see footnote b, Table 5) and Monte Carlo determination of p-values.
[d]Top down coefficient of concordance (TDCC, see Section 6.12) with variable rankings obtained with a maximum of five classes of x values (i.e., $nI = 5$; see footnote b, Table 5) and analytic determination of p-values.

quantities in Eqs. (22)–(29) are conditional on the grid structure in use.

The quantities $U(y|x_j)$ and $U(y, x_j)$ can be used as sensitivity measures, with $U(y|x_j)$ providing a measure of the effect of the uncertainty in x_j on the uncertainty in y and $U(y, x_j)$ providing a measure of the joint behavior of x_j and y. Both quantities equal zero when there is no relationship between y and x_j that is identifiable with the grid structure in use and equal one when there is a perfect association between y and x_j with the grid structure in use. Values between zero and one are indicative of intermediate levels of association. Specifically,

$$U(y|x_j) = U(y, x_j) = 0 \tag{30}$$

if

$$nO_{rc} = nS/(nD_r nI_c) \tag{31}$$

for $r = 1, 2, \ldots, nD$ and $c = 1, 2, \ldots, nI$, and

$$U(y|x_j) = U(y, x_j) = 1 \tag{32}$$

if each interval of values for x_j is associated with only one interval of values for y and each interval of values for y is associated with only one interval of values for x_j. Necessary, but not sufficient, conditions for the equality in Eq. (31) are (i) $nI = nD$, and (ii) $nIc = nDc$, $c = 1, 2, \ldots, nI(= nD)$.

When the nI and nD intervals into which the values for x_j and y are divided contain equal numbers of sampled values (i.e., nS/nI and nS/nD values for the intervals associated with x_j and y, respectively), then the following simpler expressions result:

$$H(x_j) = \ln(nI), H(y) = \ln(nD), \tag{33}$$

$$H(y|x_j) = H(y, x_j) - \ln(nI), H(x|y) = H(y, x_j) - \ln(nD), \tag{34}$$

$$U(y|x_j) = [\ln(nI) + \ln(nD) - H(y, x_j)]/\ln(nD), \tag{35}$$

$$U(x_j|y) = [\ln(nI) + \ln(nD) - H(y, x_j)]/\ln(nI), \tag{36}$$

$$U(y, x_j) = 2[\ln(nI) + \ln(nD) - H(y, x_j)]/[\ln(nI) + \ln(nD)]. \quad (37)$$

Further,

$$U(y|x_j) = U(x_j|y) = U(y, x_j) = 2 - H(y, x_j)/\ln(nI) \quad (38)$$

if $nI = nD$.

As shown by comparison of Eqs. (35) and (37), use of either $U(y|x_j)$ or $U(y, x_j)$ will produce identical rankings of variable importance based on the size of $H(y, x_j)$ when the same values for nI and nD and also for $nIc = nS/nI$ and $nDr = nS/nD$ are used in the determination of $U(y|x_j)$ and $U(y, x_j)$ for each of the independent variables under consideration. Specifically, $U(y|x_j)$ and $U(y, x_j)$ increase in size as the entropy $H(y, x_j)$ associated with joint distribution for x_j and y decreases. Thus, $U(y|x_j)$ and $U(y, x_j)$ are really sensitivity measures that quantify variable importance on the basis of the entropy $H(y, x_j)$ associated with x_j and y. Specifically, the smaller the entropy $H(y, x_j)$, the more important x_j is assessed to be in affecting the value of y. As shown in Eq. (38), $U(y|x_j)$ and $U(y, x_j)$ have identical numerical values when $nI = nD$ and $nI_c = nD_r = nS/nD$.

A closely related measure of association is given by

$$R(y, x_j) = \{1 - \exp(-2[H(x_j) + H(y) - H(y, x_j)])\}^{1/2}, \quad (39)$$

which has (i) a value of zero if there is no association between x_j and y in the sense indicated in Eq. (30), (ii) a value that approaches one as nI and nD increase if there is perfect association between x_j and y in the sense indicated in conjunction with Eq. (32), and (iii) intermediate values for intermediate levels of association (Ref. [161]). If x_j and y have a bivariate normal distribution, then $R(y, x_j)$ approaches the absolute value of the correlation coefficient between x_j and y as the sample and grid sizes increase [161].

As suggested by Mishra and Knowlton [162], the SI test (i.e., a χ^2-test on the same grid used to define entropy measures) can be used to identify important variables, and then the entropy measures $U(y, x_j)$, $U(y|x_j)$ and $R(y, x_j)$ can be used to provide a numerical representation of variable importance. The result of this approach is illustrated in Table 7, with the top two sets of results corresponding to the use of $nI = nD = 5$, and the lower two sets corresponding to the use of $nI = 10$ and $nD = 5$. As should be the case, the values for $U(y, x_j)$ and $U(y|x_j)$ are the same when $nI = nD$ and are somewhat different when $nI \neq nD$. Further, there is little difference in the variable rankings based on the SI test and on the entropy measures $U(y, x_j)$, $U(y|x_j)$ and $R(y, x_j)$. Although $U(y, x_j)$, $U(y|x_j)$ and $R(y, x_j)$ result in the same rankings of variable importance because of the underlying dependence on $H(y, x_j)$, the normalization associated with the definition of $R(y, x_j)$ produces results that are more widely spread over the interval [0,1]. Although not presented, similar normalizations referred to as Cramer's V and the contingency coefficient, respectively, are also possible for the χ^2statistic T in Eq. (20) associated with SI test (see Ref. [157, Section 13.6]). The right-most columns in Table 7 labeled "KS Test" and "KSMC Test" relate to a sensitivity analysis procedure based on a two-dimensional Kolmogorov–Smirnov (KS) test that will be discussed in Section 6.10.

The similarity between the ranking of variable importance with the SI test and with entropy-based measures is quite striking (Table 8). For all practical purposes, the χ^2 statistic T defined in Eq. (20) associated with the SI test and the entropy-based measures $U(y, x_j)$, $U(y|x_j)$ and $R(y, x_j)$ defined in Eqs. (28), (29) and (39) give the same rankings of variable importance. However, when discrete variables such as *ANHBCVGP* and *WMICDFLG* are under consideration, there can be some differences between rankings based on p-values for the χ^2 statistic and rankings based on either the χ^2 statistic itself or entropy measures because of the effects of the resultant different degrees of freedom associated with different variables on the p-values for the χ^2 statistic. Clearly, there is a close algebraic connection between T and the entropy-based measures $U(y, x_j)$, $U(y|x_j)$ and $R(y, x_j)$. As previously illustrated, p-values for the χ^2 statistic provide a way to discern influential from noninfluential variables for both the SI test and the entropy-based measures. Although not illustrated, the Monte Carlo procedure discussed in conjunction with Eq. (21) and Table 6 for the empirical determination of p-values could be used to directly determine p-values for $U(y, x_j)$, $U(y|x_j)$ and $R(y, x_j)$.

Additional information: Ref. [157, pp. 480–484]; Refs. [161–164].

6.8. Nonparametric regression

There are drawbacks to the parametric regression techniques indicated in Section 6.3 that can reduce their effectiveness in some sensitivity analyses. First, it is necessary to provide an a priori specification of the form of the regression model (e.g., linear as in Eqs. (3) and (12), nonlinear as in Eq. (13), or linear with rank transformed data as discussed in Section 6.5). Unfortunately, when complex patterns of behavior are present, it can be difficult to determine the appropriate form for a regression model. Such determinations can be a particular challenge in exploratory analyses that can involve 10 s or even 100 s of analysis results, with each result potentially requiring the specification of a different regression model. Second, the specified form for the regression is required to hold across the entire mapping from analysis inputs to analysis results, which makes the representation of local behavior and/or asymptotes difficult. In addition, the grid-based procedures discussed in Sections 6.6 and 6.7 have the drawback that the associated sensitivity results can be dependent on the particular grid selected for use. Unfortunately, the most appropriate grid for use with these procedures is not always apparent.

Nonparametric regression procedures provide an alternative to parametric regression procedures and grid-based procedures that can mitigate the potential problems

Table 7
Examples of entropy measures to identify uncertain variables affecting the uncertainty in pressure (*WAS_PRES*) at 10,000 yr under undisturbed (i.e., E0) Conditions (Fig. 5a) and Disturbed (i.e., E2) conditions (Fig. 10a)

Variable[a]	SI test[b]			Entropy[c]		Cond. entropy[d]		*R*-statistic[e]	
	χ^2	*p*-Value	Rank	$U(y, x_j)$	Rank	$U(y\|x_j)$	Rank	$R(y, x_j)$	Rank
Pressure, undisturbed (i.e., *E*0) conditions at 10,000 yr (Fig. 5a): $nI = 5$, $nD = 5$									
WMICDFLG	198.6	0.0000	1	0.2868	1	0.2361	1	0.7296	1
HALPOR	127.2	0.0000	2	0.1350	2	0.1350	2	0.5930	2
WGRCOR	42.5	0.0003	3	0.0485	3	0.0485	3	0.3800	3
ANHPRM	34.3	0.0049	4	0.0420	4	0.0420	4	0.3560	4
ANHBCVGP	11.7	0.0194	5	0.0172	15.5	0.0123	25	0.1970	25
Pressure, disturbed (i.e., *E*2) conditions at 10,000 yr (Fig. 10a): $nI = 5$, $nD = 5$									
BHPRM	337.2	0.0000	1	0.3700	1	0.3700	1	0.8340	1
HALPRM	43.7	0.0002	2	0.0526	2	0.0526	2	0.3940	2
WGRCOR	43.7	0.0002	3	0.0456	3	0.0456	3	0.3690	3
ANHPRM	34.3	0.0049	4	0.0405	4	0.0405	4	0.3500	4
Pressure, undisturbed (i.e., *E*0) conditions at 10,000 yr (Fig. 5a): $nI = 10$, $nD = 5$									
WMICDFLG	198.6	0.0000	1	0.1868	1	0.2361	1	0.7296	1
HALPOR	140.2	0.0000	2	0.1240	2	0.1510	2	0.6200	2
WGRCOR	56.3	0.0167	3	0.0515	4.	0.0626	4	0.4270	4
ANHPRM	53.3	0.0314	4	0.0547	3	0.0664	3	0.4390	3
Pressure, disturbed (i.e., *E*2) conditions at 10,000 yr (Fig. 10a); $nI = 10$, $nD = 5$									
BHPRM	402.3	0.0000	1	0.3490	1	0.4240	1	0.8630	1
WGRCOR	69.0	0.0008	2	0.0616	2	0.0749	2	0.4630	2
HALPRM	63.0	0.0035	3	0.0601	3	0.0731	3	0.4580	3
ANHPRM	63.0	0.0035	4	0.0594	4	0.0722	4	0.4550	4

[a]Table includes only variables that had a *p*-value less than 0.05 for SI test.
[b]χ^2 value, *p*-value and variable rank for SI test with 5×5 grid for $nI = 5$, $nD = 5$ and 10×5 grid for $nI = 10$, $nD = 5$; see Eq. (20). Exception: because variables *ANHBCVGP* and *WMICDFLG* are discrete with 2 and 3 values, respectively (see Table 1), $nI = 2$ and 3 rather than 5 for these two variables.
[c]Entropy $U(y, x_j)$ and variable rank; see Eq. (29).
[d]Conditional entropy and variable rank; see Eq. (28).
[e]*R*-statistic ($R(y, x_j)$ and variable rank; see Eq. (39).

indicated in the preceding paragraph. With nonparametric regression procedures, an a priori specification of the exact algebraic form of the regression model is not required. Rather, an iterative procedure is used to construct a model that captures the relationships that are present in the mapping between analysis inputs and a particular analysis result. This iterative construction procedure does not require the use of a grid and produces a model that can represent local patterns of behavior. Nonparametric regression is often referred to as smoothing. Popular nonparametric regression procedures include (i) locally weighted regression (LOESS), (ii) generalized additive models (GAMs), (iii) projection pursuit regression (PP_REG), and (iv) recursive partitioning regression (RP_REG). These procedures are briefly described below.

The LOESS technique is based on the assumption that the relationship between y and $\mathbf{x}$ is of the form

$$y = f(\mathbf{x}) = \alpha(\mathbf{x}) + \beta(\mathbf{x})\mathbf{x}, \tag{40}$$

where $\boldsymbol{\beta}(\mathbf{x}) = [\beta 1(\mathbf{x}), \beta 2(\mathbf{x}), \ldots, \beta nX(\mathbf{x})]$ and $\mathbf{x} = [x1, x2, \ldots, xnX]^{\mathrm{T}}$. In turn, an approximate relationship of the form

$$\hat{y} = \hat{f}(\mathbf{x}) = \hat{\alpha}(\mathbf{x}) + \hat{\beta}(\mathbf{x})\mathbf{x} \tag{41}$$

is sought with LOESS. The quantities $\hat{\alpha}(\mathbf{x})$ and $\hat{\boldsymbol{\beta}}(\mathbf{x})$ for a given value of $\mathbf{x}$ are defined to be the values for α and $\boldsymbol{\beta} = [\beta 1, \beta 2, \ldots, \beta nX]$ that minimize the sum

$$\sum_{i=1}^{nS} (\alpha + \boldsymbol{\beta}\mathbf{x}_i - y_i)^2 \left[1 - \left(\frac{\|\mathbf{x} - \mathbf{x}_i\|}{d_r(\mathbf{x})}\right)^3\right]^3 I_{[0,d_r(\mathbf{x}))}(\|\mathbf{x} - \mathbf{x}_i\|), \tag{42}$$

where (i) $d_r(\mathbf{x})$ is the distance to the rth nearest neighbor (NN) of $\mathbf{x}$ in nX-dimensional Eulidean space, (ii) $I_{[0,dr(\mathbf{x}))}(\|\mathbf{x}–\mathbf{x}_i\|$ equals 1 if $\|\mathbf{x}–\mathbf{x}_i\| < d_r(\mathbf{x})$ and equals 0 otherwise, and (iii) the individual independent variables (i.e., x_1, x_2, …, x_{nX}) are normalized to mean zero and standard deviation one so that the value of the norm $\| \cdot \|$ is not dominated by the units used for these variables. The determination of α and $\boldsymbol{\beta}$ is straightforward with the use of appropriate matrix techniques (Ref. [165, p. 139]).

For GAMs, the function $f(\mathbf{x})$ is assumed to have the form

$$f(\mathbf{x}) = \sum_{j=1}^{nX} f_j(x_j), \tag{43}$$

Table 8
Detailed comparison of χ^2 statistic T and entropy $U(y, x_j)$ used to identify uncertain variables affecting the uncertainty in pressure (*WAS_PRES*) at 10,000 yr under undisturbed (i.e., *E*0) conditions (Fig. 5a) and disturbed (i.e., *E*2) conditions (Fig. 10a)

Variable[a]	Pressure, undisturbed (i.e., *E*0) conditions at 10,000 yr (Fig. 5a): $nI = 5$, $nD = 5$				Variable[a]	Pressure, disturbed (i.e., *E*2) conditions at 10,000 yr (Fig. 10a): $nI = 5$, $nD = 5$			
	SI test			Entropy		SI test			Entropy
	χ^2 [b]	df[c]	*p*-Value	$U(y, x_j)$[d]		χ^2 [b]	df[c]	*p*−Value	$U(y, x_j)$[d]
WMICDFLG	198.6 (1.0)	8	0.0000 (1.0)	0.2868 (1.0)	*BHPRM*	337.2 (1.0)	16	0.0000 (1.0)	0.3700 (1.0)
HALPOR	127.0 (2.0)	16	0.0000 (1.0)	0.1350 (2.0)	*WGRCOR*	43.7 (2.0)	16	0.0002 (2.0)	0.0456 (3.0)
WGRCOR	42.5 (3.0)	16	0.0003 (3.0)	0.0485 (3.0)	*HALPRM*	43.7 (3.0)	16	0.0002 (3.0)	0.0526 (2.0)
ANHPRM	34.3 (4.0)	16	0.0049 (4.0)	0.0420 (4.0)	*ANHPRM*	34.3 (4.0)	16	0.0049 (4.0)	0.0405 (4.0)
WRGSSAT	22.7 (5.0)	16	0.1229 (6.0)	0.0230 (5.0)	*SHRGSSAT*	25.0 (5.0)	16	0.0698 (5.0)	0.0268 (5.0)
SHPRMCON	21.8 (6.0)	16	0.1487 (7.0)	0.0228 (6.0)	*SHBCEXP*	23.5 (6.0)	16	0.1010 (6.0)	0.0260 (6.0)
WASTWICK	20.8 (7.0)	16	0.1850 (8.0)	0.0223 (7.0)	*WGRMICI*	20.5 (7.0)	16	0.1985 (7.0)	0.0213 (7.0)
SHBCEXP	19.5 (8.0)	16	0.2436 (9.0)	0.0212 (8.0)	*WRBRNSAT*	19.5 (8.0)	16	0.2436 (9.0)	0.0198 (8.0)
SHPRNHAL	19.3 (9.0)	16	0.2518 (10.0)	0.0200 (10.0)	*ANRBRSAT*	19.3 (9.0)	16	0.2518 (10.0)	0.0197 (9.0)
SHPRMSAP	19.2 (10.0)	16	0.2601 (11.0)	0.0190 (12.0)	*SHRBRSAT*	18.2 (10.5)	16	0.3142 (11.5)	0.0186 (11.0)
SHPRMDRZ	18.2 (11.0)	16	0.3142 (12.0)	0.0204 (9.0)	*HALPOR*	18.2 (10.5)	16	0.3142 (11.5)	0.0190 (10.0)
WGRMICI	18.0 (12.0)	16	0.3239 (13.0)	0.0191 (11.0)	*WFBETCEL*	16.8 (12.0)	16	0.3965 (13.0)	0.0175 (12.0)
ANHBCEXP	17.7 (13.0)	16	0.3438 (14.0)	0.0179 (13.5)	*ANHBCEXP*	16.2 (13.0)	16	0.4414 (14.0)	0.0170 (13.0)
WFBETCEL	17.0 (14.0)	16	0.3856 (15.0)	0.0179 (13.5)	*WASTWICK*	15.2 (14.0)	16	0.5125 (15.0)	0.0164 (14.0)
SHRBRSAT	16.3 (15.0)	16	0.4299 (16.0)	0.0169 (17.0)	*WGRMICH*	14.7 (15.0)	16	0.5492 (16.0)	0.0148 (15.5)
ANRBRSAT	15.7 (16.0)	16	0.4765 (17.0)	0.0172 (15.5)	*SHPRMDRZ*	13.8 (16.0)	16	0.6111 (17.0)	0.0148 (15.5)
HALPRM	13.7 (17.0)	16	0.6235 (18.0)	0.0156 (18.0)	*SHPRMCLY*	13.3 (18.0)	16	0.6482 (19.0)	0.0133 (20.0)
SHRGSSAT	13.3 (18.0)	16	0.6482 (19.0)	0.0141 (19.0)	*ANRGSSAT*	13.3 (18.0)	16	0.6482 (19.0)	0.0137 (19.0)
WRBRNSAT	12.8 (19.0)	16	0.6849 (20.0)	0.0131 (20.0)	*SHPRMSAP*	13.3 (18.0)	16	0.6482 (19.0)	0.0145 (17.5)
SALPRES	11.8 (20.0)	16	0.7554 (21.0)	0.0125 (21.0)	*SALPRES*	12.5 (20.0)	16	0.7089 (21.0)	0.0145 (17.5)
ANHBCVGP	11.7 (21.0)	4	0.0197 (5.0)	0.0172 (15.5)	*WRGSSAT*	10.2 (21.0)	16	0.8578 (22.0)	0.0102 (21.0)
SHPRMCLY	8.7 (22.0)	16	0.9265 (22.0)	0.0093 (22.0)	*SHPRNHAL*	9.2 (22.0)	16	0.9064 (24.0)	0.0099 (22.0)
WGRMICH	8.2 (23.0)	16	0.9437 (23.0)	0.0085 (23.0)	*SHPRMCON*	5.8 (23.0)	16	0.9898 (25.0)	0.0059 (24.0)
ANRGSSAT	6.8 (24.0)	16	0.9763 (24.0)	0.0072 (24.0)	*ANHBCVGP*	5.5 (24.0)	4	0.2427 (8.0)	0.0080 (23.0)
					WMICDFLG	3.7 (25.0)	8	0.8859 (23.0)	0.0045 (25.0)

p-Value for χ^2 statistic and variable rank based on *p*-value for χ^2 statistic.
[a]Variables ordered by χ^2 statistic for SI test.
[b]χ^2 statistic for SI test with 5×5 grid (see footnote b, Tables 5 and 7, and Eq. (20)) and variable rank based on values of χ^2 statistic.
[c]Degrees of freedom for χ^2 statistic.
[d]Entropy $U(y, x_j)$ based on 5×5 grid (see footnote b, Tables 5 and 7, and Eq. (29)) and variable rank based on $U(y, x_j)$.

where the f_j are arbitrary functions that will be determined as part of the analysis process. In turn, the observed values for y are assumed to be of the form

$$y_i = f(\mathbf{x}_i) = \sum_{j=1}^{nX} f_j(x_{ij}). \tag{44}$$

Given initial estimates, $\hat{f}_2, \hat{f}_3, \ldots, \hat{f}_{nX}$ for $f_2, f_3, \ldots, f_{nX}$, an estimate $\hat{f}_1$ for f_1 can be obtained through use of the relationship

$$y_i - \sum_{j=2}^{nX} \hat{f}_j(x_{ij}) \cong f_1(x_{i1}) \tag{45}$$

for $i = 1, 2, \ldots, nS$. In particular, a scatterplot smoother (e.g., LOESS with only one independent variable) can be used to smooth the partial residuals on the left-hand side of Eq. (45) across x_1. This produces an estimate $\hat{f}_1$ for f_1 defined across the range of values for x_1. Given this estimate for f_1, the estimate $\hat{f}_2$ for f_2 can be refined in the same manner across the range of values for x_2 with $\hat{f}_1, \hat{f}_3, \hat{f}_4, \ldots, \hat{f}_{nX}$. This procedure then continues and repetitively cycles through the variables. The cycling continues until convergence is achieved. The result is $\hat{f}_j$ defined at $x_{1j}, x_{2j}, \ldots, x_{nS,j}$ for $j = 1, 2, \ldots, nX$. Additional detail is available elsewhere (Ref. [166, pp. 90–91]; Ref. [167, pp. 300–302]).

The PP_REG procedure involves both dimension reduction and additive modeling and is based on the assumption that $f(\mathbf{x})$ has the form

$$f(\mathbf{x}) = \sum_{s=1}^{nD} g_s(\alpha_s x), \tag{46}$$

where $\boldsymbol{\alpha}_s = [\boldsymbol{\alpha}_{1s}, \boldsymbol{\alpha}_{2s}, \ldots, \boldsymbol{\alpha}_{nX,s}]$, $\mathbf{x} = [x_1, x_2, \ldots, x_{nX}]^{\mathrm{T}}$, $\boldsymbol{\alpha}_s\mathbf{x}$ corresponds to a linear combination of the elements of $\mathbf{x}$, and g_s is an arbitrary function. Values for g_s, $\boldsymbol{\alpha}_s$ and nD are determined as part of the analysis procedure. The expression in Eq. (46) is an additive model with the quantities $\boldsymbol{\alpha}_s\mathbf{x}$ replacing the elements x_j of $\mathbf{x}$ as the independent variables. Further, this expression involves a reduction in dimension as nD is usually smaller than nX. The entities $\hat{\boldsymbol{\alpha}}_1, \hat{\boldsymbol{\alpha}}_2, \ldots, \hat{\boldsymbol{\alpha}}_{nD}$ and $\hat{g}_1, \hat{g}_2, \ldots, \hat{g}_{nD}$ are estimated as part of

the construction process. This is accomplished by first estimating $\boldsymbol{\alpha}_1$ and g_1. Specifically, $\hat{\boldsymbol{\alpha}}_1$ and $\hat{g}_1$ are defined to be the values for $\boldsymbol{\alpha}$ and $g_{\boldsymbol{\alpha}}$ that minimize the sum

$$\sum_{i=1}^{nS}[y_i - g_{\alpha}(\alpha x_i)]^2, \tag{47}$$

where $\boldsymbol{\alpha} \in R^{nX}$, $\|\boldsymbol{\alpha}\| = 1$, and $g_{\boldsymbol{\alpha}}$ is the outcome of using a scatterplot smoother (e.g., LOESS) on the points $[y_i, \boldsymbol{\alpha}\mathbf{x}_i]$, $i = 1, 2, \ldots, nS$. Once $\hat{\boldsymbol{\alpha}}_1$ and $\hat{g}_1$ are estimated, the partial residuals $y_i - g_1(\hat{\boldsymbol{\alpha}}_1\mathbf{x}_i)$, $i = 1, 2, \ldots, nS$, are used to obtain $\hat{\boldsymbol{\alpha}}_2$ and $\hat{g}_2$. Specifically, $\hat{\boldsymbol{\alpha}}_2$ and $\hat{g}_2$ are defined to be the values for $\boldsymbol{\alpha}$ and $g_{\boldsymbol{\alpha}}$ that minimize the sum

$$\sum_{i=1}^{nS}\{[y_i - \hat{g}_1(\hat{\boldsymbol{\alpha}}_1\mathbf{x}_i) - g_{\boldsymbol{\alpha}}(\alpha x_i)]\}^2, \tag{48}$$

where $\boldsymbol{\alpha} \in R^{nX}$, $||\boldsymbol{\alpha}|| = 1$, and $g_{\boldsymbol{\alpha}}$ is the outcome of using a scatterplot smoother on the points $[y_i - \hat{g}_1(\hat{\mathbf{a}}_1 \ \mathbf{x}_i), \boldsymbol{\alpha}\mathbf{x}_i]$, $i = 1, 2, \ldots, nS$. This process continues until no appreciable improvement based on a relative error criterion is observed.

The RP_REG procedure is based on splitting the data into subgroups where observations within each subgroup are more homogeneous than they are over the set of all observations. Then, $f(\mathbf{x})$ is estimated with regression models defined for each subgroup. Specifically, $f(\mathbf{x})$ is estimated by

$$\hat{f}(\mathbf{x}) = \sum_{s=1}^{nP}(\hat{\alpha}_s + \hat{\boldsymbol{\beta}}_s\mathbf{x})I_s(\mathbf{x}), \tag{49}$$

where (i) A_s, $s = 1, 2, \ldots, nP$, designate the subgroups into which the data are partitioned, (ii) $= {}_s + \boldsymbol{\beta}_s\mathbf{x}$ is the least-squares approximation to y associated with A_s, and (iii) I_s is the indicator functions such $I_s(\mathbf{x}) = 1$ if $\mathbf{x}$ is associated with A_s and $I_s(\mathbf{x}) = 0$ otherwise. The subgroups A_s, $s = 1, 2, \ldots, nP$, are developed algorithmically from the observations $[\mathbf{x}_i, y_i]$, $i = 1, 2, \ldots, nS$.

The preceding procedures can all be carried out in a stepwise manner to determine variable importance, with (i) the most important variable $\tilde{x}_1$ being the variable that results in the single-variable model with the most predictive capability, (ii) the second-most important variable $\tilde{x}_2$ being the variable that in conjunction with $\tilde{x}_1$ results in the two-variable model with the most predictive capability, and so on until (iii) some stopping criteria is reached that indicates that the consideration of additional variables does not produce models with improved predictive capability. Order of selection in the stepwise construction process and fraction of variability explained (i.e., R^2 as defined in Eq. (8)) can be used to indicate variable importance. The F-statistic with appropriate degrees of freedom (a topic too complicated for consideration here; see Ref. [168] and Ref. [169, Section 3.13]) can be used to determine a stopping point in the stepwise variable selection procedure.

Nonparametric regression procedures are illustrated in Table 9 for the pressures in Figs. 5a and 10a at 10,000 yr. For comparison, Table 9 also contains results obtained with parametric regression procedures, with LIN_REG indicating linear regression (see Eq. (3)), RANK_REG indicating rank regression (see Section 6.5), and RS_REG indicating response surface regression (i.e., the regression model in Eq. (12) with $f_j(x_j) = x_j$ and $f_{jl}(x_j, x_l) = x_jx_l$). For the result in Fig. 5a (i.e., pressure at 10,000 yr under undisturbed conditions), the relationship between pressure and the dominant independent variables is fairly monotonic, with the result that all the regression procedures perform reasonably well (i.e., R^2 values between 0.80 and 0.97 for the first five variables selected in the individual regressions). As shown in Fig. 6b, there is a strong nonlinear relationship between the result in Fig. 10a (i.e., pressure at 10,000 yr under disturbed conditions) and the variable *BHPRM*. The stepwise regressions with the four nonparametric procedures all identify *BHPRM* as the most important variable. In contrast, the linear regressions with raw and rank-transformed data fail to identify an effect for *BHPRM*. For this particular variable, the parametric response surface regression (i.e., RS_REG in Table 9) also performs well and results in a regression model with an R^2 value of 0.87; however, in many situations the nonparametric regression procedures will outperform response surface regression.

Additional information: A more detailed discussion of the use of nonparametric regression in sensitivity is given in Ref. [168]. General discussions of nonparametric regression procedures appear in Refs. [165–167,169]. The use of regression trees [170] in sensitivity analysis is discussed and illustrated in Ref. [171].

6.9. Squared rank differences/rank correlation coefficient (SRD/RCC) test

The SRD/RCC test is the result of combining a test for nonrandomness in the relationship between an independent and a dependent variable called the SRD test with the Spearman RCC [172]. This test is effective at identifying linear and very general nonlinear patterns in analysis results. However, unlike the regression procedures introduced in Sections 6.3 and 6.8, the SRD/RCC test does not involve the development of a model that approximates the relationship between independent and dependent variables. Further, unlike the grid-based procedures introduced in Sections 6.6 and 6.7, the SRD/RCC test does not require the introduction and use of a grid.

A brief description of the SRD/RCC test follows. The test is used to assess the relationships between individual elements x_j of $\mathbf{x} = [x_1, x_2, \ldots, x_{nX}]$ and a predicted variable y of interest for a random or LHS and a functional relationship of the form $y = f(\mathbf{x})$. The SRD component of the test is based on the statistic

$$Q_j = \sum_{i=1}^{nS-1}(r_{i+1,j} - r_{ij})^2, \tag{50}$$

Table 9
Comparison of variable rankings obtained with parametric regression (i.e., LIN_REG, RANK_REG, RS_REG), nonparametric regression (i.e., LOESS, PP_REG, RP_REG, GAMs), and the squared rank differences/rank correlation (SRD/RCC) test for pressure at (*WAS_PRES*) 10,000 yr under undisturbed (i.e., *E*0) conditions (Fig. 5a) and disturbed (i.e., *E*2) conditions (Fig. 10a)

Variable[a]	R^{2b}	df[c]	*p*-Val[d]	Variable	R^2	df	*p*-Val	Variable	R^2	df	*p*-Val
Pressure, undisturbed (i.e., *E*0) conditions at 10,000 yr (Fig. 5a)											
	LIN_REG				RANK_REG				RS_REG		
WMICDFLG	0.5076	1.0	0.0000	*WMICDFLG*	0.5226	1.0	0.0000	*WMICDFLG*	0.5098	2.0	0.0000
HALPOR	0.7316	1.0	0.0000	*HALPOR*	0.7320	1.0	0.0000	*HALPOR*	0.7462	3.0	0.0000
WGRCOR	0.7923	1.0	0.0000	*WGRCOR*	0.7859	1.0	0.0000	*WGRCOR*	0.8812	4.0	0.0000
ANHPRM	0.8088	1.0	0.0000	*ANHPRM*	0.7975	1.0	0.0001	*ANHPRM*	0.9160	5.0	0.0000
SHRGSSAT	0.8137	1.0	0.0056	*SALPRES*	0.8027	1.0	0.0058	*WASTWICK*	0.9304	6.0	0.0000
SALPRES	0.8177	1.0	0.0119	*SHRGSSAT*	0.8064	1.0	0.0187	*SALPRES*	0.9383	7.0	0.0000
	LOESS				PP_REG			*ANHBCEXP*	0.9427	8.0	0.0119
WMICDFLG	0.5098	2.0	0.0000	*WMICDFLG*	0.5098	2.0	0.0000		RP_REG		
HALPOR	0.7662	6.1	0.0000	*HALPOR*	0.7617	5.4	0.0000	*WMICDFLG*	0.5076	1.0	0.0000
WGRCOR	0.9186	33.1	0.0000	*WGRCOR*	0.9236	21.5	0.0000	*HALPOR*	0.8205	17.0	0.0000
ANHPRM	0.9477	25.1	0.0000	*ANHPRM*	0.9623	11.3	0.0000	*WGRCOR*	0.9220	3.0	0.0000
	GAM			*WASTWICK*	0.9711	10.1	0.0000	*ANHPRM*	0.9662	16.0	0.0000
WMICDFLG	0.5098	2.0	0.0000	*ANYBCVGP*	0.9755	9.1	0.0000	*WASTWICK*	0.9823	40.0	0.0000
HALPOR	0.7448	4.0	0.0000	*WRBRNSAT*	0.9813	10.5	0.0000	SRD/RCC TEST			
WGRCOR	0.8556	4.0	0.0000	*WFBETCEL*	0.9851	11.6	0.0000	*WMICDFLG*	NA[e]	4.0	0.0000
ANHPRM	0.8854	4.0	0.0000	*HALPRM*	0.9874	9.3	0.0000	*HALPOR*	NA	4.0	0.0000
WASTWICK	0.8921	4.0	0.0019	*SALPRES*	0.9901	8.2	0.0000	*WGRCOR*	NA	4.0	0.0001
SHRGSSAT	0.9007	10.0	0.0116	*SHPRMCLY*	0.9929	13.3	0.0000				
SALPRES	0.9042	1.0	0.0018	*SHRBRSAT*	0.9944	9.4	0.0000				
				SHPRMDRZ	0.9969	10.1	0.0000				
Pressure, disturbed (i.e., *E*2) conditions at 10,000 yr (Fig. 10a)											
	LIN_REG				RANK_REG				RS_REG		
HALPRM	0.1410	1.0	0.0000	*HALPRM*	0.1289	1.0	0.0000	*BHPRM*	0.6098	2.0	0.0000
ANHPRM	0.1999	1.0	0.0000	*ANHPRM*	0.1866	1.0	0.0000	*HALPRM*	0.7006	3.0	0.0000
HALPOR	0.2203	1.0	0.0057	*HALPOR*	0.2049	1.0	0.0094	*ANHPRM*	0.7902	4.0	0.0000
LOESS				PP_REG				*HALPOR*	0.8291	5.0	0.0000
BHPRM	0.6625	8.8	0.0000	*BHPRM*	0.6646	9.0	0.0000	*ANHBCVGP*	0.8400	6.0	0.0023
ANHPRM	0.7321	12.8	0.0000	*ANHPRM*	0.7603	10.7	0.0000	*WGRCOR*	0.8532	7.0	0.0013
HALPRM	0.7894	10.5	0.0000	*HALPRM*	0.8440	9.8	0.0000	*SHRBRSAT*	0.8654	8.0	0.0030
ANHBCVGP	0.8286	28.9	0.0058	*HALPOR*	0.8965	10.4	0.0000		RP_REG		
	GAM							*BHPRM*	0.7163	17.0	0.0000
BHPRM	0.6654	10.0	0.0000					*HALPRM*	0.8474	15.0	0.0000
ANHPRM	0.7555	4.0	0.0000					*ANHPRM*	0.8894	-9.0	0.0000
HALPRM	0.8242	2.0	0.0000					*ANRGSSAT*	0.9726	81.0	0.0000
HALPOR	0.8590	2.0	0.0000					SRD/RCC TEST			
								BHPRM	NA	4.0	0.0000
								HALPRM	NA	4.0	0.0000
								ANHPRM	NA	4.0	0.0001
								SHPRMDRZ	NA	4.0	0.0150

[a]Variables listed in order of selection.
[b]Cumulative R^2 value with entry of each variable into model.
[c]Incremental degrees of freedom with entry of each variable into model for all cases except SRD/RCC test; df fixed at 4.0 for all variables for SRD/RCC test.
[d]*p*-Value for model with addition of each new variable. Stepwise procedure terminates at a *p*-value of 0.02.
[e]NA indicates that result is not applicable.

where r_{ij}, $i = 1, 2, \ldots, nS$, is the rank of y obtained with the sample element in which x_j has rank i. Under the null hypothesis of no relationship between x_j and y, the quantity

$$S_j = \{Q_j - [nS(nS^2 - 1)/6]\} / \left\{ \sqrt{nS^5}/6 \right\} \tag{51}$$

approximately follows a standard normal distribution for $nS > 40$. Thus, a p-value p_{rj} indicative of the strength of the nonlinear relationship between x_j and y can be obtained from Q_j. Specifically, p_{rj} is the probability that a value $\tilde{Q}_j > Q_j$ would occur due to chance if there was no relationship between x_j and y.

The RCC component of the test is based on the rank (i.e., Spearman) correlation coefficient

$$rc(x_j, y) = \frac{\sum_{i=1}^{nS}[r(x_{ij}) - (nS+1)/2][r(y_i) - (nS+1)/2]}{\left\{\sum_{i=1}^{nS}[r(x_{ij}) - (nS+1)/2]^2\right\}^{1/2}\left\{\sum_{i=1}^{nS}[r(y_i) - (nS+1)/2]^2\right\}^{1/2}}, \tag{52}$$

where $r(x_{ij})$ and $r(y_i)$ are the ranks associated x_j and y for sample element i. Under the null hypothesis of no rank correlation between x_j and y, the quantity $rc(x_j, y)$ has a known distribution (Ref. [155, Table 10]). Thus, a p-value p_{cj} indicative of the strength of the monotonic relationship between x_j and y can be obtained from $rc(x_j, y)$.

The SRD/RCC test is obtained from combining the p-values p_{rj} and p_{cj} to obtain the statistic

$$\chi_4^2 = -2[\ln(p_{rf}) + \ln(p_{cj})], \tag{53}$$

which has a χ^2-square distribution with four degrees of freedom. The p-value associated with χ_4^2 constitutes the SRD/RCC test for the strength of the relationship between x_j and y.

Results obtained with SRD/RCC test are illustrated in Table 9. Like the nonparametric regression procedures, the SRD/RCC test is able to identify the nonlinear effect associated with *BHPRM* for the result in Fig. 10a (i.e., pressure at 10,000 yr under disturbed conditions), which is completely missed with the linear regression procedures with raw and rank-transformed data.

Additional information: A detailed description of the SRD/RCC test and the determination of the associated p-value is available in the original article [172].

6.10. Two-dimensional Kolmogorov–Smirnov (KS) test

The two dimensional KS test provides a way to test for a pattern in a scatterplot without the use of a grid [173–175]. With this test, each point $[x_{ij}, y_i]$ in the sample $[x_{ij}, y_i]$, $i = 1, 2, \ldots, nS$, is used to divide the $x_j y$ plane into four quadrants (Fig. 12):

$$Q_{i1} = \{(x_j, y) : x_{ij} < x_j, y_i < y\}, \tag{54}$$

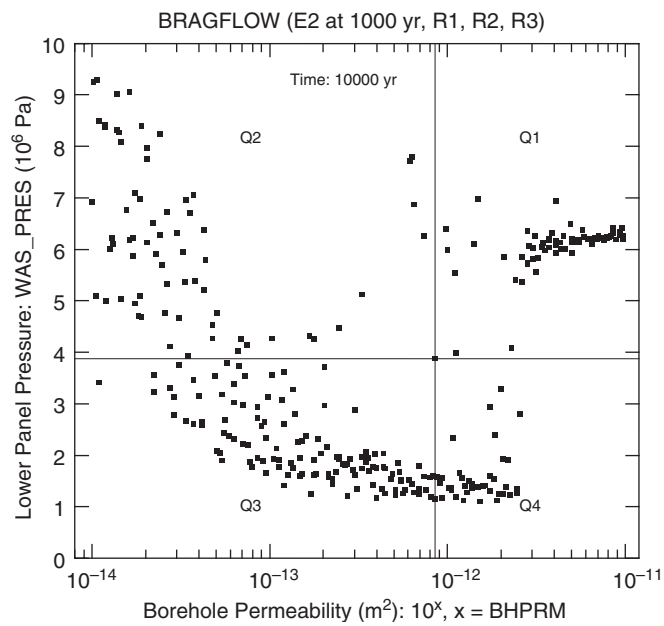

Fig. 12. Illustration of quadrants used with the two-dimensional KS test for the variable *WAS_PRES* at 10,000 yr.

Table 10
Comparison of formal statistical and Monte Carlo Determination of p-values for the SI Test and the two dimensional KS test for pressure (*WAS_PRES*) at 10,000 yr under undisturbed (i.e., *E*0) conditions (Fig. 5a) and disturbed (i.e., *E*2) conditions (Fig. 10a)

Variable[a]	SI test: 5 × 5[b]		SIMC test: 5 × 5[c]		KS test[d]		KSMC test[e]	
	p-Value	Rank	p-Value	Rank	p-Value	Rank	p-Value	Rank
Pressure, undisturbed (i.e., *E*0) conditions at 10,000 yr (Fig. 5a)								
WMICDFLG	0.0000	1	0.0000	1.5	0.0001	1	0.0000	1.5
HALPOR	0.0000	2	0.0000	1.5	0.0077	2	0.0000	1.5
WGRCOR	0.0003	3	0.0003	3	0.2979	3	0.0002	3
ANHPRM	0.0049	4	0.0031	4	0.8228	4	0.0257	4
ANHBCVGP	0.0194	5	0.0181	5	1.0000	24	0.4975	16
Pressure, disturbed (i.e., *E*2) conditions at 10,000 yr (Fig. 10a)								
BHPRM	0.0000	1	0.0000	1	0.0048	1	0.0000	1.5
HALPRM	0.0002	2	0.0003	3	0.1302	2	0.0000	1.5
WGRCOR	0.0002	3	0.0001	2	0.9609	5	0.1540	6
ANHPRM	0.0049	4	0.0039	4	0.6102	3	0.0023	3
HALPOR	0.3142	12	0.3164	12	0.7830	4	0.0178	4

[a]Variables ordered by p-values for SI test. Table includes only variables that had a p-value less than 0.05 for at least one of the procedures.
[b]p-Values and variable ranks for SI test with 5 × 5 grid (see Footnote b in Tables 5 and 7) determined from χ^2 distribution; see Eq. (20).
[c]p-Values and variable ranks for SI test with 5 × 5 grid (see Footnote b in Tables 5 and 7) determined with Monte Carlo procedure; see discussion associated with Eq. (21).
[d]p-Values and variable ranks for KS test determined from Eq. (61).
[e]p-Values and variable ranks for KS test determined with Monte Carlo procedure; see discussion associated with Eq. (21).

$$Q_{i2} = \{(x_j, y) : x_j < x_{ij}, y_i < y\}, \tag{55}$$

$$Q_{i3} = \{(x_j, y) : x_j < x_{ij}, y < y_i\}, \tag{56}$$

$$Q_{i4} = \{(x_j, y) : x_{ij} < x_j, y < y_i\}. \tag{57}$$

In turn, two fractions are defined for each quadrant:

$$fE_{ik} = \text{expected fraction of observations in quadrant } Q_{ik} \text{ if there is no relationship between } x_j \text{ and } y, \tag{58}$$

$$fO_{ik} = \text{observed fraction of observations in quadrant } Q_{ik}. \tag{59}$$

The quantity

$$D = \max\{|fE_{ik} - fO_{ik}|, k = 1,\ 2,\ 3,\ 4,\ i = 1,\ 2,\ \ldots,\ nS\} \tag{60}$$

is the KS statistic for the scatterplot.

The probability prob($\tilde{D} > D$) of exceeding D given that there is no relationship between x_j and y can be approximated by

$$\text{prob}(\tilde{D} > D) \cong Q_{\text{KS}}\left(\frac{D\sqrt{nS}}{1 + [1 - c(x_j, y)]^{1/2}\left[0.25 - 0.75/\sqrt{nS}\right]}\right), \tag{61}$$

where Q_{KS} is the function defined by

$$Q_{\text{KS}}(\lambda) = 2\sum_{j=1}^{\infty}(-1)^{j-1}\exp(-2j^2\lambda^2) \tag{62}$$

and $c(x_j, y)$ is the estimated CC between x_j and y (Ref. [157, Section 14.7]). Alternatively, prob($\tilde{D} > D$) can be estimated by a Monte Carlo procedure in which D is repeatedly estimated with randomly shuffled values (without replacement) of the x_{ij}'s and y_i's as previously illustrated in conjunction with Eq. (21) and Table 6 for the CMNs, CLs, CMDs and SI tests.

The result of applying the KS test is illustrated in Table 10, with p-values being calculated as indicated in Eq. (61) and also calculated with the previously indicated Monte Carlo procedure. This table also presents the results of using the SI test with a 5×5 grid. The direct calculation of p-values as indicated in Eq. (61) performs rather poorly and produces p-values that are much larger than those obtained with the Monte Carlo procedure. In contrast, the Monte Carlo calculation of p-values for the KS test produces results that are generally similar to, but not the same as, the results obtained with the SI test. In particular, the KS test with Monte Carlo calculation of p-values and the SI test agree on the most important variables but show some differences on the less-important variables.

Additional information: Ref. [157]; Refs. [173–175].

6.11. Tests for patterns based on distance measures

Tests for patterns based on distance measures provide possible alternatives to tests based on gridding as described in Sections 6.6 and 6.7. Distance-based tests for patterns have a potential advantage over grid-based tests in that they do not require the definition and use of a grid that can possibly influence the outcome of the test. Such tests have a long history of use in the ecological sciences [176–189].

Three distance-based tests will be illustrated: NN test, total distance (TD) test, and coefficient of aggregation (CA) test. Each of these tests involves the consideration of a set of points of the form $[x_{ij}, y_i]$, $i = 1, 2, \ldots, nS$. Further, the x_{ij}'s and y_i's are assumed to be normalized to mean zero and standard deviation one.

The NN test [190] is based on the statistic

$$d_j = \sum_{i=1}^{nS} d_{ij}/nS, \tag{63}$$

where d_{ij} is the distance from the point (x_{ij}, y_i) to its NN among the points (x_{kj}, y_k) for $k = 1, 2, \ldots, nS$ and $k \neq i$. If x_j has an effect on y, then the value for d_j should tend to be smaller than would be the case if x_j had no effect on y. Determination of values $\tilde{d}_j$ for samples $(\tilde{x}_{ij}, \tilde{y}_i)$, $i = 1, 2, \ldots, nS$, obtained by randomly pairing, without replacement, the values for the x_{ij}'s and y_i's in the original sample allows the determination of a distribution for d_j under the null hypothesis that there is no relationship between x_j and y. Thus, conditional on the observed distributions for x_j and y, the probability (i.e., a p-value) of obtaining a smaller value $\tilde{d}_j$ than the observed value d_j by chance alone can be determined. A small value for this probability (e.g., <0.01) indicates that x_j does indeed have an effect on y.

The TD test is a variant of the NN test and is based on the statistic

$$d_{tj} = \sum_{i=1}^{nS}\sum_{k=i+1}^{nS} d_{ik}/nD, \tag{64}$$

where d_{ik} is the distance between the points (x_{ij}, y_i) and (x_{kj}, y_k) and $nD = nS(nS-1)/2$ is the total number of distances d_{ik}. As for the NN statistic d_j, the value for d_{tj} will tend to be smaller than would otherwise be the case if x_j has an effect on y. Similarly to d_j, a Monte Carlo procedure can be used to develop a distribution for d_{tj} under the assumption that x_j has no effect on y. Then, conditional on the observed distributions for x_j and y, the probability of obtaining a smaller value for d_{tj} by chance alone can be estimated.

The CA test [179,191] is based on the statistic

$$A_j = \sum_{i=1}^{nS}\tilde{d}_{ij}^2 \Bigg/ \left[\sum_{i=1}^{nS} d_{ij}^2 + \sum_{i=1}^{nS}\tilde{d}_{ij}^2\right], \tag{65}$$

where d_{ij} is defined the same as in Eq. (63) for the NN test and $\tilde{d}_{ij}$ is defined similarly but for a sample $(\tilde{x}_{ij}, \tilde{y}_i)$, $i = 1, 2, \ldots, nS$, obtained by randomly permuting the values for the x_{ij}'s and y_i's in the sample (x_{ij}, y_i), $i = 1, 2, \ldots, nS$. If x_j has an effect on y, then the value for A_j will tend to be larger than would otherwise be the case

because of the presence of $\sum_i d_{ij}^2$ in the denominator in the definition of A_j. A Monte Carlo procedure involving repeated calculations of A_j with two different random permutations of the x_{ij}'s and y_i's in the sample (x_{ij}, y_i), $i = 1, 2, \ldots, nS$, can be used to estimate a distribution for A_j under the assumption that x_j has no effect on y. Then, conditional on the observed distributions for x_j and y, the probability of obtaining a larger value for $\tilde{A}_j$ for A_j than the observed value by chance alone can be estimated.

The SI, NN, TD and CA tests are illustrated in Table 11. On the whole, the results obtained with the distance-based tests show considerable disagreement with results obtained with the SI test and also with other grid-based techniques illustrated in Table 5. Of the distance-based tests, the TD test compares best with results obtained with the grid-based techniques. Thus, this comparison suggests that the NN, TD and CA tests are less effective sensitivity analysis procedures than some of the other techniques introduced in this survey. However, the idea of using a grid-free, distance-based measure of sensitivity is very appealing. It is certainly possible that more appropriate distance-based measures of sensitivity can be found than those used in the presented tests. This is an area that merits additional investigation. For example, the use of rank-transformed data might yield more informative results.

Additional information: Refs. [176–189]; Ref. [192, Section 8.2.5].

6.12. Top down coefficient of concordance (TDCC)

The TDCC was introduced by Iman and Conover as a way to test agreement between different sensitivity analysis procedures [193]. However, it also provides a way to identify significant sets of variables in a sampling-based sensitivity analysis that does not rely on statistical tests predicated on distributional assumptions that may not be satisfied. In this application, the TDCC is used in a stepwise manner to test for agreement of sensitivity results obtained when a particular sensitivity analysis procedures is applied individually to each sample in a sequence of replicated samples of the same size. The significant variables are those which the TDCC indicates are identified as being important across all replicates.

The TDCC is based on the consideration of arrays of the form

$$\begin{array}{cccccc} & R_1 & R_2 & \ldots & R_{nR} \\ x_1 & r(O_{11}) & r(O_{12}) & \ldots & r(O_{1,nR}) \\ x_2 & r(O_{21}) & r(O_{22}) & \ldots & r(O_{2,nR}) \\ \vdots & \vdots & \vdots & \ldots & \vdots \\ x_{nX} & r(O_{nX,1}) & r(O_{nX,2}) & \ldots & r(O_{nX,nR}), \end{array} \tag{66}$$

where (i) $x_1, x_2, \ldots, x_{nX}$ are the variables under consideration, (ii) $R_1, R_2, \ldots, R_{nR}$ designate the replicates, (iii) O_{jk} is the outcome (i.e., sensitivity measure) for variable x_j and replicate R_k, and (iv) $r(O_{jk})$, $j = 1, 2, \ldots, nX$, are the ranks assigned to the outcomes associated with replicate R_k. In the assigning of ranks, (i) a rank of 1 is assigned to the outcome O_{jk} with the largest value for $|O_{jk}|$, (ii) a rank of 2 is assigned the outcome O_{jk} with the second largest value for $|O_{jk}|$, and so on, and (iii) averaged ranks are assigned to equal values of O_{jk}. This is the reverse of the procedure used to assign ranks for use in rank regression.

Table 11
Comparison of tests for patterns based on distance measures for pressure (*WAS_PRES*) at 10,000 yr under undisturbed (i.e., *E*0) conditions (Fig. 5a) and disturbed (i.e., *E*2) conditions (Fig. 10a)

Variable[a]	SI test: 5×5[b]		NN test[c]		TD test[d]		CA test[e]	
	p-Value	Rank	*p*-Value	Rank	*p*-Value	Rank	*p*-Value	Rank
Pressure, undisturbed (i.e., *E*0) conditions at 10,000 yr (Fig. 5a)								
WMICDFLG	0.0000	1	0.0001	2	0.0000	2	0.6664	21
HALPOR	0.0000	2	0.0000	1	0.0000	2	0.0014	1
WGRCOR	0.0003	3	0.0327	3	0.0000	2	0.0049	2
ANHPRM	0.0049	4	0.3669	15	0.6348	21	0.3302	9
ANHBCVGP	0.0194	5	0.4745	7	0.4563	14	0.7544	24
Pressure, disturbed (i.e., *E*2) conditions at 10,000 yr (Fig. 10a)								
BHPRM	0.0000	1	0.0000	1	0.0000	2	0.0020	2
HALPRM	0.0002	2	0.3511	13	0.0000	2	0.0752	4
WGRCOR	0.0002	3	0.0095	2	0.7210	22	0.3420	12
ANHPRM	0.0049	4	0.0732	4	0.0000	2	0.0018	1
HALPOR	0.3142	12	0.2280	8	0.0210	4	0.2245	9

[a]Variables ordered by *p*-values for SI test. Table includes only variables that had a *p*-value less than 0.05 for at least one of the procedures.
[b]*p*-Values and variable ranks for SI test with 5×5 grid (see footnote b in Tables 5 and 7) determined from χ^2 distribution; see Eq. (20).
[c]*p*-Values and variable ranks for NN test (see Eq. (63)) determined with Monte Carlo procedures; see discussion associated with Eq. (21).
[d]Same as c but for TD test (see Eq. (64)).
[e]Same as c but for CA test (see Eq. (65)).

The TDCC is a measure of agreement between multiple rankings that emphasizes agreement between rankings assigned to important variables and deemphasizes disagreement between rankings assigned to less important/unimportant variables. For the TDCC, the ranks $r(O_{jk})$ in Eq. (66) are replaced by the corresponding Savage scores $ss(O_{ij})$, where

$$ss(O_{jk}) = \sum_{j=r(O_{jk})}^{nX} 1/j \tag{67}$$

and average Savage scores are assigned in the event of ties. The result is an array of the form

$$\begin{array}{cccccc} & R_1 & R_2 & \dots & R_{nR} \\ x_1 & \mathrm{ss}(O_{11}) & \mathrm{ss}(O_{12}) & \dots & \mathrm{ss}(O_{1,nR}) \\ x_2 & \mathrm{ss}(O_{21}) & \mathrm{ss}(O_{22}) & \dots & \mathrm{ss}(O_{2,nR}) \\ \vdots & \vdots & \vdots & \dots & \vdots \\ x_{nX} & \mathrm{ss}(O_{nX,1}) & \mathrm{ss}(O_{nX,2}) & \dots & \mathrm{ss}(O_{nX,nR}), \end{array} \tag{68}$$

which has the same form as the array in Eq. (66) except that the ranks $r(O_{jk})$ have been replaced by the corresponding Savage scores $ss(O_{jk})$.

The TDCC is defined by

$$C_T = \frac{\{\sum_{j=1}^{nX}[\sum_{k=1}^{nR}\mathrm{ss}(O_{jk})]^2 - nR^2nX\}}{\{nR^2(nX - \sum_{j=1}^{nX}1/j)\}} \tag{69}$$

and is equivalent to Kendall's coefficient of concordance (Ref. [155, p. 305]) calculated with Savage scores rather than ranks. Under repeated random assignment of the integers in the columns of Eq. (66),

$$T = nR(nX-1)C_T \tag{70}$$

approximately follows a χ^2-distribution with nX–1 degrees of freedom and thus provides the basis for a statistical test of agreement.

The procedure to identify a significant set of variables with the TDCC operates in the following manner: (i) The sensitivity analysis technique in use (e.g., stepwise regression analysis) is applied to each replicate to rank variable importance. (ii) The TDCC is applied to the variable rankings obtained with each replicate to determine if there is a significant agreement between the replicates (e.g., as defined by a specified p-value for the TDCC). (iii) If there is significant agreement, the top ranked variable (i.e., rank 1) for each replicate is removed from consideration for all replicates; this results in the removal of one variable if all replicates assign the same variable a rank of 1 and more than one variable if different variables are assigned a rank of 1 in different replicates. (iv) A new sensitivity analysis is then performed for each replicate with the remaining variables, the remaining variables are reranked for each replicate, and Steps (ii) and (iii) are repeated with the reduced set of variables. (v) The process is continued until the deleted variable result in the analysis reaches a point at which the TDCC indicates that there is no significant agreement between the variable rankings obtained with the individual replicates. (vi) At this point, the analysis ends, and the significant set of variables are those deleted before the TDCC indicated no significant agreement between the variable rankings obtained with the individual replicates.

This procedure is illustrated for rank regression analysis with the three replicated random samples (i.e., RS1, RS2, RS3) from the variables in Table 1 for cumulative brine flow into the repository (*BRNREPTC*) at 1000 yr. The individual regression analyses all rank *HALPOR* as the most important variable (Table 12) and have a TDCC of 0.80 with a p-value of 5.2E-5 (Table 13). As a result, *HALPOR* is removed from consideration, which reduces the number of independent variables from 29 to 28. A new rank regression is then performed for each replicate with the remaining 28 variables, and the variables are reranked (i.e., from 1 to 28) on the basis of their SRRCs, with *ANHPRM* having a rank of 1 in one replicate and *WMICDFLG* having a rank of 1 in two replicates. For this new ranking (i.e., without *HALPOR*), the TDCC has a value of 0.71 with a p-value of 5.0E-4 (Table 13). As this is considered to be significant agreement, *ANHPRM* and *WMICDFLG* are dropped; the remaining 26 variables are reranked; new regressions are performed for each replicate; and a resultant TDCC of 0.46 with a p-value of 9.8E-2 is calculated (Table 13). If a p-value of 9.8E-2 is considered to be insignificant, then the analysis ends, and the set of significant variables is taken to be {*HALPOR*, *ANHPRM*, *WMICDFLG*}.

If a p-value of 9.8E-2 is considered to be significant (e.g., if the analysis was using 0.1 as the p-value above which the analysis stopped), then the analysis would continue with the top ranked variables in the individual replicates being dropped (i.e., *SALPRES*, *HALPRM*, *BPPRM*) and the TDCC recalculated for the remaining 23 variables. This process would continue until either an insignificant value for the TDCC was obtained or all variables were dropped, with the latter being an unlikely outcome.

Additional information: Refs. [138,193]. Content of this section is an adaptation of material contained in of Ref. [138, Sections 5 and 6].

6.13. Variance decomposition

An informative, but potentially computationally expensive, sensitivity analysis procedure is based on a complete variance decomposition of the uncertainty associated with y [56–59] With this procedure, the variance $V(y)$ of y is expressed as

$$V(y) = \sum_{j=1}^{nX} V_j + \sum_{j=1}^{nX}\sum_{k=j+1}^{nX} V_{jk} + \cdots + V_{12,\dots,nX}, \tag{71}$$

where V_j is the contribution of x_j to $V(y)$, V_{jk} is the contribution of the interaction of x_j and x_k to $V(y)$, and so on up to $V_{12,\dots,nX}$, which is the contribution of the interaction of x_1, x_2, …, x_{nX} to $V(y)$. Sensitivity measures

Table 12
Sensitivity analysis results based on SRRCs for three replicated random samples (RS1 RS2, RS3) of size 100 for cumulative brine flow into repository (*BRNREPTC*) at 1000 yr under undisturbed (i.e., *E*0) conditions (adapted from Ref. [138, Table 8])

Variable[a]	RS1[b]	RS2	RS3
HALPOR	9.93E−01(1)[c]	9.67E−01(1)	9.73E−01(1)
WMICDFLG	−9.72E-02(2)	−6.92E−02(4)	−1.13E−01(2)
ANHPRM	6.49E-02(3)	1.33E−01(2)	9.84E−02(3)
SALPRES	−4.00E−02(4)	$-2.70^{E}-03$(26)	−1.41E−02(13)
HALPRM	3.53E−02(5)	7.67E−02(3)	4.05E−02(5)
WRBRNSAT	−3.08E−02(6)	$-1.79^{E}-02$(14)	9.13E−03(17)
WASTWICK	−2.82E−02(7)	−2.27E−02(10)	−4.47E−03(21)
BPCOMP	−2.61E−02(8)	2.36E−02(9)	−8.05E−04(29)
SHPRMDRZ	2.29E−02(9)	$-1.37^{E}-02$(17)	2.58E−02(8)
BPPRM	−1.85E−02(10)	1.27E−02(19)	5.08E−02(4)
…	…	…	…
BPVOL	−1.58E−03(27)	6.54E−03(23)	4.64E−03(20)
ANHBCEXP	−1.30E−03(28)	4.32E−03(25)	2.88E−02(6)
WRGSSAT	−1.19E−03(29)	1.32E−02(18)	−5.33E−03(19)

[a]Variables in regression model ordered by SRRCs for sample RS1.
[b]SRRC in model containing all variables for indicated sample.
[c]Variable rank based on absolute value of SRRC for indicated sample.

Table 13
Sensitivity analysis with the TDCC for three replicated random samples of size 100 for cumulative brine flow into repository (*BRNREPTC*) at 1000 yr under undisturbed (i.e., *E*0) conditions (adapted from Ref. [138, Table 9])

Step[a]	TDCC[b]	*p*-Value[c]	Variable(s) removed[d]
1	0.80	5.2E-05	*HALPOR*
2	0.71	5.0E-04	*WMICDFLG, ANHPRM*
3	0.46	9.8E-02	*SALPRES, HALPRM, BPPRM*

[a]Steps in analysis.
[b]TDCC at beginning of step.
[c]*p*-Value for TDCC at beginning of step.
[d]Variable(s) removed at end of step.

are provided by

$$s_j = V_j/V(y) \text{ and } s_{jT} = \frac{V_j + \sum_{\substack{k=1\\k\neq j}}^{nX} V_{jk} + \cdots + V_{12,\ldots,nX}}{V(v)}, \tag{72}$$

where s_j is the fraction of $V(y)$ contributed by x_j alone and s_{jT} is the fraction of $V(y)$ contributed x_j and interactions of x_j with other variables.

The contributions to variance V_j, V_{jk}, …, $V_{12,\cdots,nX}$ in Eqs. (71) and (72) are defined by multidimensional integrals involving $y = f(\mathbf{x})$ and the individual elements x_j of $\mathbf{x}$. Specifically,

$$E(y) = \int_X f(\mathbf{x}) \prod_{j=1}^{nX} d_j(x_j) \prod_{j=1}^{nX} dx_j, \tag{73}$$

$$V(y) = \int_X [f(x) - E(y)]^2 \prod_{j=1}^{nX} d_j(x_j) \prod_{j=1}^{nX} dx_j = \int_X f^2(x) \prod_{j=1}^{nX} d_j(x_j) \prod_{j=1}^{nX} dx_j - E^2(y), \tag{74}$$

$$V_j = \int_{X_j} \left[\int_{X_{-j}} f(x) \prod_{\substack{k=1\\k\neq j}}^{nX} d_k(x_k) \prod_{\substack{k=1\\k\neq j}}^{nX} d_k x_k \right]^2 \times d_j(x_j) dx_j - E^2(y), \tag{75}$$

$$V_{jk} = \int_{X_j} \int_{X_k} \left[\int_{X_{-j,k}} f(x) \prod_{\substack{l=1\\l\neq j,k}}^{nX} d_l(x_l) \prod_{\substack{l=1\\l\neq j,k}}^{nX} dx_l \right]^2 \times d_j(x_j) d_k(x_k) dx_j dx_k - E^2(y) - V_j - V_k \tag{76}$$

and

$$V_j + \sum_{\substack{k=1\\k\neq j}}^{nX} V_{jk} + \cdots + V_{12,\ldots,nX} = V(f) - \left\{ \left[\int_{X_{-j}} \int_{X_j} \int_{\tilde{X}_j} f(\mathbf{x})\ f(\tilde{\mathbf{x}}) d_j(\tilde{x}_j) d_j(x_j) \prod_{\substack{k=1\\k\neq j}}^{nX} d_k(x_k) \right] \times d\tilde{x}_j dx_j \prod_{\substack{k=1\\k\neq j}}^{nX} dx_k - E^2(y) \right\}, \tag{77}$$

where (i) X_j is the sample space for x_j, $d_j(x_j)$ is the density function for x_j and the resultant quantities

$$X = \prod_{j=1}^{nX} X_j \text{ and } d(\mathbf{x}) = \prod_{j=1}^{nX} d_j(x_j)$$

are the sample space and density function, respectively, for $\mathbf{x}$, (ii) X_{-j} and $X_{-\mathrm{j,k}}$ correspond to the reduced sample spaces defined by

$$X_{-j} = \prod_{\substack{k=1\\k\neq j}}^{nX} X_k \text{ and } X_{-j,k} = \prod_{\substack{l=1\\l\neq j,k}}^{nX} X_l$$

and (iii) $X_j = \tilde{X}_j$ in Eq. (77) with the value for $\tilde{x}_j \in \tilde{X}_j$ replacing the value for $x_j \in X_j$ in the vector $\tilde{\mathbf{x}}$ (i.e., the variables x_j and $\tilde{x}_j$ associated with X_j and $\tilde{X}_j$ have identical distributions but are assumed to be independent and the vectors $\mathbf{x}$ and $\tilde{\mathbf{x}}$ are the same except that x_j appears as element j in $\mathbf{x}$ and $\tilde{x}_j$ appears as element j in $\tilde{\mathbf{x}}$).

As a result, the determination of s_j and s_{jT} is a problem in the evaluation of multidimensional integrals. In practice, this evaluation is carried out with sampling-based methods of the form indicated in the following algorithm.

Step 1: Generate a random or LHS

$$\mathbf{x}_i = [x_{i1},\ x_{i2}, \ldots,\ x_{i,nX}], \quad i = 1,\ 2,\ \ldots,\ nS \tag{78}$$

from $\mathbf{x} = [x1, x2, \ldots, xnX]$ in consistency with the distributions assigned to the individual x_j.

Step 2: Estimate the mean and variance for y with the approximations

$$\hat{E}(y) = \sum_{i=1}^{nS} f(x_i)/nS \tag{79}$$

and

$$\hat{V}(y) = \sum_{i=1}^{nS} [f(x_i) - \hat{E}(y)]^2/nS = \sum_{i=1}^{nS} f^2(x_i)/nS - \hat{E}^2(y). \tag{80}$$

The estimation of $\hat{E}(y)$ and $\hat{V}(y)$ requires nS evaluations of the function f.

Step 3: Generate a second random or LHS

$$\mathbf{r}_i = [r_{i1},\ r_{i2},\ \ldots,\ r_{i,nX}], \quad i = 1,\ 2,\ \ldots,\ nS \tag{81}$$

by randomly permuting, without replacement, the individual variable values associated with the sample generated in Step 1.

Step 4: For each variable x_j, generate a reordering

$$\mathbf{r}_{ij} = [r_{ij1},\ r_{ij2},\ \ldots,\ r_{ij,nX}], \quad i = 1,\ 2,\ \ldots,\ nS \tag{82}$$

of the sample generated in Step 3 such that $r_{ijj} = x_{ij}$. This step only involves a change in the numbering associated with the sample generated in Step 3 for each x_j; no changes to the sample itself are involved.

Step 5: For each variable x_j, estimate s_j by

$$s_j \cong \left[\sum_{i=1}^{nS} f(\mathbf{x}_i) f(\mathbf{r}_{ij})/nS - \hat{E}^2(y)\right] \Big/ \hat{V}(y). \tag{83}$$

The estimation of s_j for all x_j requires only nS additional evaluations of the function f as a result of the efficient reuse of the function evaluations for the sample generated in Step 3.

Step 6: For each variable x_j, generate an additional sample

$$\mathbf{x}_{ij} = [x_{ij1},\ x_{ij2},\ \ldots,\ x_{ij,nX}], \quad i = 1,\ 2,\ \ldots,\ nS, \tag{84}$$

where x_{ijj} is generated as a random or LHS from x_j and $x_{ijk} = x_{ik}$ for $k \neq j$. The sample generated for x_j in this step differs from the sample generated in Step 1 only in the values associated with x_j.

Step 7: Estimate s_{jT} by

$$s_{jT} \cong \sum_{i=1}^{nS} f(\mathbf{x}_i)[f(\mathbf{x}_i) - f(\mathbf{x}_{ij})]/[nS\hat{V}(y)] \tag{85}$$

for each x_j. The estimation of s_{jT} for all x_j requires an additional $(nX)(nS)$ evaluations of the function f.

Although the sensitivity measures s_j and s_{jT} provide valuable sensitivity information, their determination can be computationally expensive due to the large number of function evaluations that could be required. Specifically, $2(nS)$, $(nX+1)(nS)$ and $(nX+2)(nS)$ function evaluations are required to estimate s_j, s_{jT} and both s_j and s_{jT}, respectively, for nX uncertain variables. Further, because integrals are being approximated, the basic sample size nS required for the preceding algorithm to produce acceptable approximations to s_j and s_{jT} is likely to be larger than the sample sizes required for other sampling-based sensitivity measures.

Sensitivity analysis based on variance decomposition is illustrated with a simple test function introduced as part of a review of uncertainty and sensitivity analysis procedures (Ref. [194, Model 9]). Specifically, this test function is defined by

$$\begin{aligned} y &= f(x), x = [x_1,\ x_2,\ x_3] \\ &= \sin x_1 + A \sin^2 x_2 + B x_3^4 \sin x_1 \end{aligned} \tag{86}$$

with $A = 7$, $B = 0.1$ and each x_j uniform on $[-\pi, \pi]$. Unfortunately, the fluid flow model that has been used to illustrate other sensitivity analysis procedures is too computationally demanding for use with the procedures discussed in this section. Values of s_j and s_{jT} obtained with a base sample size of $nS = 10,000$ are

$$S_1 = 0.30,\ s_2 = 0.46,\ s_3 = 0.00 \tag{87}$$

and

$$s_{1\,T} = 0.53,\ s_{2\,T} = 0.45,\ s_{3\,T} = 0.23. \tag{88}$$

Further, results obtained with different values for nS are illustrated in Table 14 and suggest that the approximations of the integrals appearing in the definitions of s_j and s_{jT} are close to being converged with $nS = 10,000$.

For perspective, sensitivity results based on CCs, RCCs, CMNs, CLs, CMDs and SI are presented in Table 15 and scatterplots for x_1, x_2 and x_3 are given in Fig. 13. The model in Eq. (86) was constructed to have patterns that would be difficult to identify with regression-based sensitivity analysis procedures. Thus, although x_2 is a major contributor to the uncertainty in y, this effect is completely missed by the analyses based on CCs and RCCs in Table 15 owing to the oscillatory relationship between x_2 and y (Fig. 13b). Similarly, the CMDs test does not identify x_3 as having an effect on y owing to the constancy of the median values for y across the range of x_3 (Fig. 13c). Of the tests presented in Table 15, the SI test has the best performance and gives a reasonable indication of the importance of x_1, x_2 and x_3 with respect to the uncertainty in y for $nS = 100$ and 1000. This is not surprising as the SI test is effective at identifying nonlinear relationships. Fullest representation of the effects of x_1, x_2 and x_3 on uncertainty in y is given by the variance decomposition results in Eqs. (87) and (88). However, this enhanced resolution comes at a cost as the results in Eqs. (87) and (88) required more function evaluations (i.e., $nS = 10,000$) than the SI results (i.e., $nS = 100$ and $nS = 1000$) in Table 15.

Additional Information: Refs. [56–60,195–210].

Table 14
Evaluation of variance decompositions s_j and s_{jT} for model in Eq. (86) with different sample sizes

nS[a]	$\hat{E}(y)$[b]	$\hat{V}(y)$[c]	$\hat{s}_1$[d]	$\hat{s}_2$[d]	$\hat{s}_3$[d]	$\hat{s}_{1T}$[e]	$\hat{s}_{2T}$[e]	$\hat{s}_{3T}$[e]
10	3.7	16.5	0.70	0.65	−0.04	0.84	−0.09	−0.24
100	3.9	13.1	0.10	0.37	−0.24	0.79	0.80	0.45
1000	3.5	14.2	0.30	0.44	−0.02	0.56	0.53	0.24
10,000	3.5	14.0	0.30	0.46	0.00	0.53	0.45	0.23
100,000	3.5	13.9	0.32	0.44	−0.00	0.56	0.44	0.24
1,000,000	3.5	13.8	0.32	0.44	0.00	0.56	0.44	0.24

[a]Sample size.
[b]Estimate for expected value of y; see Eqs. (74) and (79).
[c]Estimate for variance of y; see Eqs. (74) and (80).
[d]Estimate for contribution of x_j, $j = 1, 2, 3$, to variance of y; see Eqs. (72) and (83).
[e]Estimate for contribution of x_j, $j = 1, 2, 3$, and its interactions with the other two variables to the variance of y; see Eqs. (72) and (85).

Table 15
Sensitivity results based on CCs, RCCs, CMNs, CLs, CMDs and SI for model in Eq. (86) (Ref. [101, Table 9.14])

Variable name[a]	CC[b]		RCC[c]		CMN: 1×5[d]		CL: 1×5[e]		CMD: 2×5[f]		SI: 5×5[g]	
	Rank	p-Val	Rank	p-Val	Rank	p-Val	Rank	p-Val	Rank	p-Val	Rank	p-Val
Sample size $nLHS = 100$												
x_1	1.0	0.0000	1.0	0.0000	1.0	0.0000	1.0	0.0000	2.0	0.0001	1.0	0.0000
x_3	2.0	0.5667	2.0	0.6361	3.0	0.6917	3.0	0.5495	3.0	0.9384	3.0	0.0615
x_2	3.0	0.8327	3.0	0.8393	2.0	0.0000	2.0	0.0000	1.0	0.0000	2.0	0.0008
Sample size $nLHS = 1000$												
x_1	1.0	0.0000	1.0	0.0000	1.5	0.0000	1.5	0.0000	2.0	0.0000	1.5	0.0000
x_3	2.0	0.0162	2.0	0.0187	3.0	0.0438	3.0	0.0347	3.0	0.1446	3.0	0.0000
x_2	3.0	0.9799	3.0	0.9999	1.5	0.0000	1.5	0.0000	1.0	0.0000	1.5	0.0000

[a]Variables ordered by p-values for CCs.
[b]Ranks and p-values for CCs; see Eq. (24), Ref. [47].
[c]Ranks and p-values for RCCs; see Eq. (38), Ref. [47].
[d]Ranks and p-values for CMNs test with 1×5 grid; see Eq. (15).
[e]Ranks and p-values for CLs test with 1×5 grid; see Eq. (16)
[f]Ranks and p-values for CMDs test with 2×5 grid; see Eq. (18).
[g]Ranks and p-values for SI test with 5×5 grid; see Eq. (20).

7. Summary

Sampling-based uncertainty and sensitivity analysis is widely used, and as a result, is a fairly mature area of study. However, there remain a number of important challenges and areas for additional study. For example, there is a need for sensitivity analysis procedures that are more effective at revealing nonlinear relations than the parametric regression procedures (Section 6.3) and partial correlation procedures (Section 6.4) currently in wide use. Among the approaches to sensitivity analysis described in the preceding section, statistical tests for patterns based on gridding (Section 6.6), nonparametric regression (Section 6.8), the SRD/rank correlation test (Section 6.9), the two dimensional KS test (Section 6.10), and complete variance decomposition (Section 6.13) have not been as widely used as approaches based on parametric regression and partial correlation and merit additional investigation and use. As another example, sampling-based procedures for uncertainty and sensitivity analysis usually use probability as the model, or representation, for uncertainty. However, when limited information is available with which to characterize uncertainty, probabilistic characterizations can give the appearance of more knowledge than is really present. Alternative representations for uncertainty such as evidence theory and possibility theory merit consideration for their potential to represent uncertainty in situations where little information is available [84–92]. Finally, a significant challenge is the education of potential users of uncertainty and sensitivity analysis about (i) the importance of such analyses and their role in both large and small analyses, (ii) the need for appropriate separation of aleatory and epistemic uncertainty in the conceptual and computational implementation of analyses of complex systems [15–24], (iii) the need for a clear conceptual view of what an analysis is intended to represent and a computational design that is consistent with that view [15,124,211,212], (iv) the role that uncertainty and sensitivity analysis plays in model and

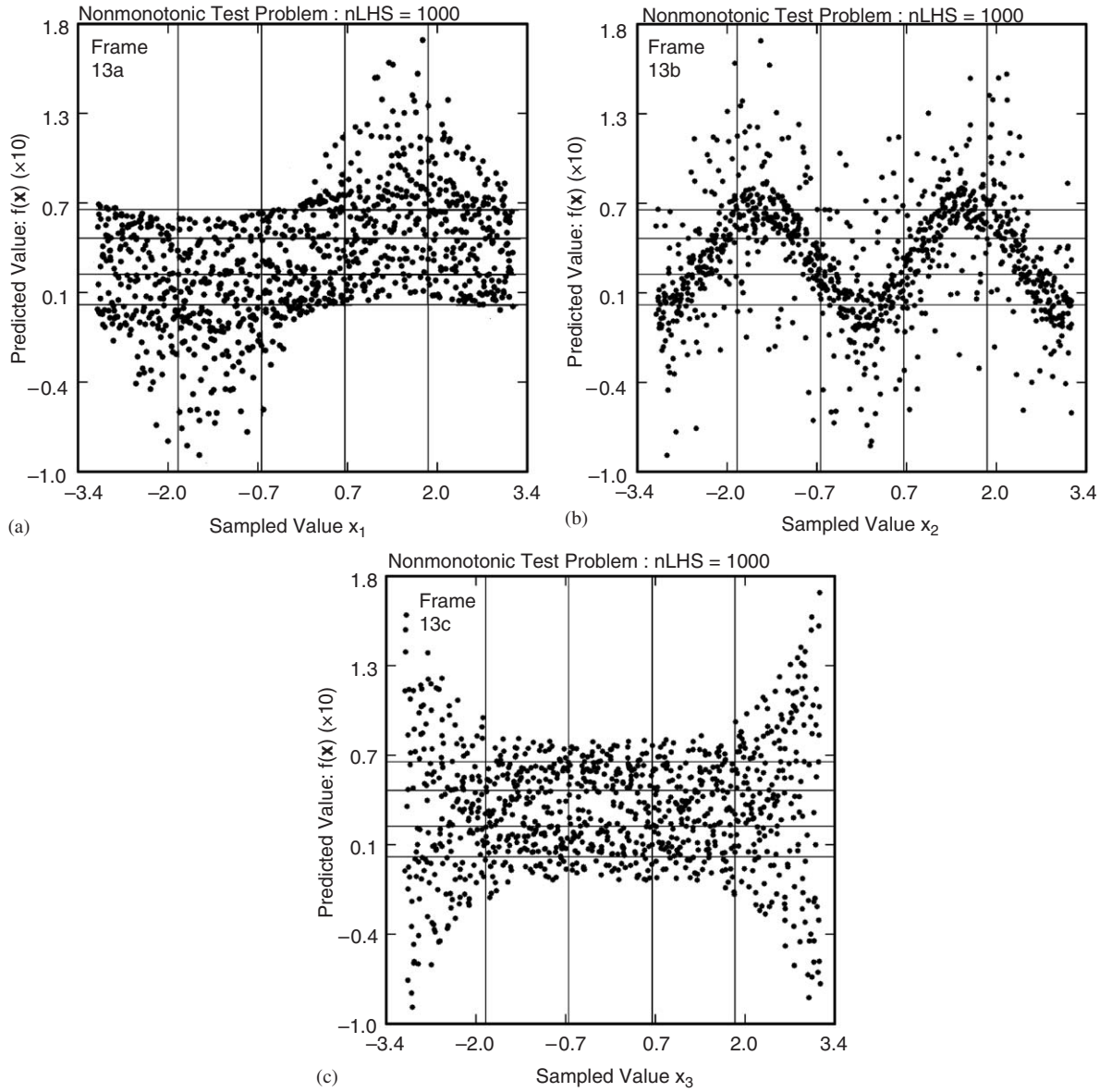

Fig. 13. Scatterplots for model in Eq. (86) with grid for SI test with $nI = nD = 5$ (adapted from Ref. [101, Fig. 9.15]).

analysis verification [5,6], and (v) the importance of avoiding deliberately conservative assumptions if meaningful uncertainty and sensitivity analysis results are to be obtained [213–217].

Acknowledgements

Work performed for Sandia National Laboratories (SNL), which is a multiprogram laboratory operated by Sandia Corporation, a Lockheed Martin Company, for the United States Department of Energy's National Security Administration under contract DE-AC04-94AL-85000. Review at SNL provided by Tony Giunta and Brian Rutherford. Editorial support provided by F. Puffer, K. Best and J. Ripple of Tech Reps, a division of Ktech Corporation.

References

[1] Christie MA, Glimm J, Grove JW, Higdon DM, Sharp DH, Wood-Schultz MM. Error analysis and simulations of complex phenomena. Los Alamos Sci 2005;29:6–25.
[2] Nikolaidis E, Ghiocel DM, Singhal S, editors. Engineering design reliability handbook. Boca Raton, FL: CRC Press; 2004.
[3] Sharp DH, Wood-Schultz MM. QMU and nuclear weapons certification: what's under the hood? Los Alamos Sci 2003;28:47–53.
[4] Wagner RL. Science, uncertainty and risk: the problem of complex phenomena. APS News 2003;12(1):8.
[5] Oberkampf WL, DeLand SM, Rutherford BM, Diegert KV, Alvin KF. Error and uncertainty in modeling and simulation. Reliab Eng Syst Safety 2002;75(3):333–57.
[6] Roache PJ. Verification and validation in computational science and engineering. Albuquerque, NM: Hermosa Publishers; 1998.
[7] Ayyub BM, editor. Uncertainty modeling and analysis in civil engineering. Boca Raton, FL: CRC Press; 1997.
[8] Risk Assessment Forum. Guiding principles for Monte Carlo analysis, EPA/630/R-97/001. Washington, DC: RiskAssessmentForum

Environmental Protection Agency; 1997 Available from the NTIS as PB97-188106/XAB.
[9] NCRP (National Council on Radiation Protection and Measurements). A guide for uncertainty analysis in dose and risk assessments related to environmental contamination, NCRP Commentary No. 14. Bethesda, MD: National Council on Radiation Protection and Measurements; 1996.
[10] NRC (National Research Council). Science and judgment in risk assessment. Washington, DC: National Academy Press; 1994.
[11] NRC (National Research Council). Issues in risk assessment. Washington, DC: National Academy Press; 1993.
[12] US EPA (US Environmental Protection Agency). An SAB Report: multi-media risk assessment for radon, review of uncertainty analysis of risks associated with exposure to radon, EPA-SAB-RAC-93-014. Washington, DC: US Environmental Protection Agency; 1993.
[13] IAEA (International Atomic Energy Agency). Evaluating the reliability of predictions made using environmental transfer models, safety series no. 100. Vienna: International Atomic Energy Agency; 1989.
[14] Beck MB. Water-quality modeling: a review of the analysis of uncertainty. Water Resour Res 1987;23(8):1393–442.
[15] Helton JC. Uncertainty and sensitivity analysis in the presence of stochastic and subjective uncertainty. J Stat Comput Simul 1997;57(1–4):3–76.
[16] Helton JC, Burmaster DE, editors. Guest editorial: treatment of aleatory and epistemic uncertainty in performance assessments for complex systems. Reliab Eng Syst Safety 1996;54(2–3):91–4.
[17] Paté-Cornell ME. Uncertainties in Risk Anal: six levels of treatment. Reliab Eng Syst Safety 1996;54(2–3):95–111.
[18] Winkler RL. Uncertainty in probabilistic risk assessment. Reliab Eng Syst Safety 1996;54(2–3):127–32.
[19] Hoffman FO, Hammonds JS. Propagation of uncertainty in risk assessments: the need to distinguish between uncertainty due to lack of knowledge and uncertainty due to variability. Risk Anal 1994;14(5):707–12.
[20] Helton JC. Treatment of uncertainty in performance assessments for complex systems. Risk Anal 1994;14(4):483–511.
[21] Apostolakis G. The concept of probability in safety assessments of technological systems. Science 1990;250(4986):1359–64.
[22] Haan CT. Parametric uncertainty in hydrologic modeling. Trans ASAE 1989;32(1):137–46.
[23] Parry GW, Winter PW. Characterization and evaluation of uncertainty in probabilistic Risk Anal. Nucl Safety 1981;22(1): 28–42 [DIRS 159059].
[24] Kaplan S, Garrick BJ. On the quantitative definition of risk. Risk Anal 1981;1(1):11–27.
[25] Cacuci DG. Sensitivity and uncertainty analysis, vol. 1: theory. Boca Raton, FL: Chapman & Hall/CRC Press; 2003.
[26] Griewank A. Evaluating derivatives: principles and techniques of algorithmic differentiation. Philadelphia, PA: Society for Applied and Industrial Mathematics; 2000.
[27] Berz M, Bischof C, Corliss G, Griewank A. Computational differentiation: techniques, applications, and tools. Philadelphia, PA: Society for Industrial and Applied Mathematics; 1996.
[28] Cacuci DG, Schlesinger ME. On the application of the adjoint method of sensitivity analysis to problems in the atmospheric sciences. Atmósfera 1994;7(1):47–59.
[29] Turányi T. Sensitivity analysis of complex kinetic systems, tools and applications. J Math Chem 1990;5(3):203–48.
[30] Rabitz H, Kramer M, Dacol D. Sensitivity analysis in chemical kinetics. In: Rabinovitch BS, Schurr JM, Strauss HL, editors. Annual review of physical chemistry, vol. 34. Palo Alto, CA: Annual Reviews Inc.; 1983. p. 419–61.
[31] Lewins J, Becker M, editors. Sensitivity and uncertainty analysis of reactor performance parameters. Advances in nuclear science and technology, vol. 14. New York, NY: Plenum Press; 1982.
[32] Frank PM. Introduction to system sensitivity theory. New York, NY: Academic Press; 1978.
[33] Tomovic R, Vukobratovic M. General sensitivity theory. New York, NY: Elsevier; 1972.
[34] Myers RH, Montgomery DC, Vining GG, Borror CM, Kowalski SM. Response surface methodology: a retrospective and literature review. J Quality Technol 2004;36(1):53–77.
[35] Myers RH. Response surface methodology—current status and future directions. J Quality Technol 1999;31(1):30–44.
[36] Andres TH. Sampling methods and sensitivity analysis for large parameter sets. J Stat Comput Simul 1997;57(1–4):77–110.
[37] Kleijnen JPC. Sensitivity analysis and related analyses: a review of some statistical techniques. J Stat Comput Simul 1997;57(1–4): 111–42.
[38] Kleijnen JPC. Sensitivity analysis of simulation experiments: regression analysis and statistical design. Math Comput Simul 1992;34(3–4):297–315.
[39] Myers RH, Khuri AI, Carter J, Walter H. Response surface methodology: 1966–1988. Technometrics 1989;31(2):137–57.
[40] Sacks J, Welch WJ, Mitchel TJ, Wynn HP. Design and analysis of computer experiments. Stat Sci 1989;4(4):409–35.
[41] Morton RH. Response surface methodology. Math Sci 1983; 8:31–52.
[42] Mead R, Pike DJ. A review of response surface methodology from a biometric viewpoint. Biometrics 1975;31:803–51.
[43] Myers RH. Response surface methodology. Boston, MA: Allyn & Bacon; 1971.
[44] Helton JC, Davis FJ. Latin hypercube sampling and the propagation of uncertainty in analyses of complex systems. Reliab Eng Syst Safety 2003;81(1):23–69.
[45] Helton JC, Davis FJ. Illustration of sampling-based methods for uncertainty and sensitivity analysis. Risk Anal 2002;22(3):591–622.
[46] Helton JC, Davis FJ. Sampling-based methods. In: Saltelli A, Shan K, Scott EM, editors. Sensitivity analysis. New York, NY: Wiley; 2000. p. 101–53.
[47] Kleijnen JPC, Helton JC. Statistical analyses of scatterplots to identify important factors in large-scale simulations, 1: review and comparison of techniques. Reliab Eng Syst Safety 1999;65(2): 147–85.
[48] Blower SM, Dowlatabadi H. Sensitivity and uncertainty analysis of complex models of disease transmission: an HIV model, as an example. Int Stat Rev 1994;62(2):229–43.
[49] Saltelli A, Andres TH, Homma T. Sensitivity analysis of model output. An investigation of new techniques. Comput Stat Data Anal 1993;15(2):445–60.
[50] Iman RL. Uncertainty and sensitivity analysis for computer modeling applications. In: Cruse TA, editor. Reliability technology—1992, the winter annual meeting of the American society of mechanical engineers, Anaheim, California, November 8–13, vol. 28. New York, NY: American Society of Mechanical Engineers, Aerospace Division; 1992. p. 153–68.
[51] Saltelli A, Marivoet J. Non-parametric statistics in sensitivity analysis for model output. A comparison of selected techniques. Reliab Eng Syst Safety 1990;28(2):229–53.
[52] Iman RL, Helton JC, Campbell JE. An approach to sensitivity analysis of computer models, Part 1. Introduction, input variable selection and preliminary variable assessment. J Quality Technol 1981;13(3):174–83.
[53] Iman RL, Helton JC, Campbell JE. An approach to sensitivity analysis of computer models, Part 2. Ranking of input variables, response surface validation, distribution effect and technique synopsis. J Quality Technol 1981;13(4):232–40.
[54] Iman RL, Conover WJ. Small sample sensitivity analysis techniques for computer models, with an application to risk assessment. Commun Stat: Theory Methods A 1980;9(17):1749–842.
[55] McKay MD, Beckman RJ, Conover WJ. A comparison of three methods for selecting values of input variables in the analysis of output from a computer code. Technometrics 1979;21(2):239–45.

[56] Li G, Rosenthal C, Rabitz H. High-dimensional model representations. J Phys Chem 2001;105(33):7765–77.
[57] Rabitz H, Alis OF. General foundations of high-dimensional model representations. J Math Chem 1999;25(2–3):197–233.
[58] Saltelli A, Tarantola S, Chan KP-S. A quantitative model-independent method for global sensitivity analysis of model output. Technometrics 1999;41(1):39–56.
[59] Sobol' IM. Sensitivity estimates for nonlinear mathematical models. Math Modeling Comput Exp 1993;1(4):407–14.
[60] Cukier RI, Levine HB, Shuler KE. Nonlinear sensitivity analysis of multiparameter model systems. J Comput Phys 1978;26(1): 1–42.
[61] Ionescu-Bujor M, Cacuci DG. A comparative review of sensitivity and uncertainty analysis of large-scale systems–I: deterministic methods. Nucl Sci Eng 2004;147(3):189–2003.
[62] Cacuci DG, Ionescu-Bujor M. A comparative review of sensitivity and uncertainty analysis of large-scale systems–II: statistical methods. Nucl Sci Eng 2004;147(3):204–17.
[63] Frey HC, Patil SR. Identification and review of sensitivity analysis methods. Risk Anal 2002;22(3):553–78.
[64] Saltelli A, Chan K, Scott EM, editors. Sensitivity analysis. New York, NY: Wiley; 2000.
[65] Hamby DM. A review of techniques for parameter sensitivity analysis of environmental models. Environ Monitor Assess 1994; 32(2):135–54.
[66] Helton JC. Uncertainty and sensitivity analysis techniques for use in performance assessment for radioactive waste disposal. Reliab Eng Syst Safety 1993;42(2–3):327–67.
[67] Ronen Y. Uncertainty analysis. Boca Raton, FL: CRC Press, Inc.; 1988.
[68] Iman RL, Helton JC. An investigation of uncertainty and sensitivity analysis techniques for computer models. Risk Anal 1988;8(1): 71–90.
[69] Blower SM, Gershengorn HB, Grant RM. A tale of two futures: HIV and antiretroviral therapy in San Francisco. Science 2000; 287(5453):650–4.
[70] Cohen C, Artois M, Pontier D. A discrete-event computer model of feline herpes virus within cat populations. Prevent Vet Med 2000;45(3–4):163–81.
[71] Hofer E. Sensitivity analysis in the context of uncertainty analysis for computationally intensive models. Comput Phys Commun 1999;117(1–2):21–34.
[72] Caswell H, Brault S, Read AJ, Smith TD. Harbor porpoise and fisheries: an uncertainty analysis of incidental mortality. Ecol Appl 1998;8(4):1226–38.
[73] Sanchez MA, Blower SM. Uncertainty and sensitivity analysis of the basic reproductive rate: tuberculosis as an example. Am J Epidemiol 1997;145(12):1127–37.
[74] Chan MS. The consequences of uncertainty for the prediction of the effects of schistosomiasis control programmes. Epidemiol Infect 1996;117(3):537–50.
[75] Gwo JP, Toran LE, Morris MD, Wilson GV. Subsurface stormflow modeling with sensitivity analysis using a latin-hypercube sampling technique. Ground Water 1996;34(5):811–8.
[76] Helton JC, Anderson DR, Baker BL, Bean JE, Berglund JW, Beyeler W, et al. Uncertainty and sensitivity analysis results obtained in the 1992 performance assessment for the waste isolation pilot plant. Reliab Eng Syst Safety 1996;51(1):53–100.
[77] Kolev NI, Hofer E. Uncertainty and sensitivity analysis of a postexperiment simulation of nonexplosive melt-water interaction. Exp Thermal Fluid Sci 1996;13(2):98–116.
[78] Whiting WB, Tong T-M, Reed ME. Effect of uncertainties in thermodynamic data and model parameters on calculated process performance. Ind Eng Chem Res 1993;32(7):1367–71.
[79] Ma JZ, Ackerman E, Yang J-J. Parameter sensitivity of a model of viral epidemics simulated with Monte Carlo techniques. I. Illness attack rates. Int J Biomed Comput 1993;32(3–4):237–53.
[80] Ma JZ, Ackerman E. Parameter sensitivity of a model of viral epidemics simulated with Monte Carlo techniques. II. Durations and peaks. Int J Biomed Comput 1993;32(3–4):255–68.
[81] Breshears DD, Kirchner TB, Whicker FW. Contaminant transport through agroecosystems: assessing relative importance of environmental, physiological, and management factors. Ecol Appl 1992; 2(3):285–97.
[82] Breeding RJ, Helton JC, Gorham ED, Harper FT. Summary description of the methods used in the probabilistic risk assessments for NUREG-1150. Nucl Eng Des 1992;135(1):1–27.
[83] MacDonald RC, Campbell JE. Valuation of supplemental and enhanced oil recovery projects with risk analysis. J Petroleum Technol 1986;38(1):57–69.
[84] Helton JC, Johnson JD, Oberkampf WL. An exploration of alternative approaches to the representation of uncertainty in model predictions. Reliab Eng Syst Safety 2004;85(1–3):39–71.
[85] Klir GJ. Generalized information theory: aims, results, and open problems. Reliab Eng Syst Safety 2004;85(1–3):21–38.
[86] Ross TJ. Fuzzy logic with engineering applications. 2nd ed. New York, NY: Wiley; 2004.
[87] Halpern JY. Reasoning about uncertainty. Cambridge, MA: MIT Press; 2003.
[88] Ross TJ, Booker JM, Parkinson WJ, editors. Fuzzy logic and probability applications: bridging the gap. Philadelphia, PA: Society for Industrial and Applied Mathematics; 2002.
[89] Jaulin L, Kieffer M, Didrit O, Walter E. Applied interval analysis. New York, NY: Springer; 2001.
[90] Wolkenhauer O. Data engineering: fuzzy mathematics in systems theory and data analysis. New York, NY: Wiley; 2001.
[91] Klir GJ, Wierman MJ. Uncertainty-based information. New York, NY: Physica-Verlag; 1999.
[92] Yager RR, Kacprzyk J, Fedrizzi M, editors. Advances in the dempster-shafer theory of evidence. New York, NY: Wiley; 1994.
[93] Cooke RM, Goossens LHJ. Expert judgement elicitation for risk assessment of critical infrastructures. J Risk Res 2004;7(6):643–56.
[94] Ayyub BM. Elicitation of expert opinions for uncertainty and risks. Boca Raton, FL: CRC Press; 2001.
[95] McKay M, Meyer M. Critique of and limitations on the use of expert judgements in accident consequence uncertainty analysis. Radiat Protect Dosim 2000;90(3):325–30.
[96] Budnitz RJ, Apostolakis G, Boore DM, Cluff LS, Coppersmith KJ, Cornell CA, et al. Use of technical expert panels: applications to probabilistic seismic hazard analysis. Risk Anal 1998;18(4):463–9.
[97] Thorne MC, Williams MMR. A review of expert judgement techniques with reference to nuclear safety. Progr Nucl Safety 1992;27(2–3):83–254.
[98] Cooke RM. Experts in uncertainty: opinion and subjective probability in science. Oxford; NY: Oxford University Press; 1991.
[99] Meyer MA, Booker JM. Eliciting and analyzing expert judgment: a practical guide. New York, NY: Academic Press; 1991.
[100] Hora SC, Iman RL. Expert opinion in risk analysis: the NUREG-1150 methodology. Nucl Sci Eng 1989;102(4):323–31.
[101] Helton JC, Davis FJ. Sampling-based methods for uncertainty and sensitivity analysis, SAND99-2240. Albuquerque, NM: Sandia National Laboratories; 2000.
[102] Vaughn P, Bean JE, Helton JC, Lord ME, MacKinnon RJ, Schreiber JD. Representation of two-phase flow in the vicinity of the repository in the 1996 performance assessment for the waste isolation pilot plant. Reliab Eng Syst Safety 2000;69(1–3): 205–26.
[103] Helton JC, Bean JE, Economy K, Garner JW, MacKinnon RJ, Miller J, et al. Uncertainty and sensitivity analysis for two-phase flow in the vicinity of the repository in the 1996 performance assessment for the waste isolation pilot plant: undisturbed conditions. Reliab Eng Syst Safety 2000;69(1–3):227–61.
[104] Helton JC, Bean JE, Economy K, Garner JW, MacKinnon RJ, Miller J, et al. Uncertainty and sensitivity analysis for two-phase flow in the vicinity of the repository in the 1996 performance

assessment for the waste isolation pilot plant: disturbed conditions. Reliab Eng Syst Safety 2000;69(1–3):263–304.
[105] US DOE (US Department of Energy). Title 40 CFR Part 191 compliance certification application for the waste isolation pilot plant, DOE/CAO-1996–2184. US Department of Energy, Carlsbad Area Office,; 1996 [DIRS 100975].
[106] Helton JC, Bean JE, Berglund JW, Davis FJ, Economy K, Garner JW, et al. Uncertainty and sensitivity analysis results obtained in the 1996 performance assessment for the waste isolation pilot plant, SAND98-0365. Albuquerque, NM: Sandia National Laboratories; 1998.
[107] Helton JC, Marietta MG. Special issue: the 1996 performance assessment for the waste isolation pilot plant. Reliab Eng Syst Safety 2000;69(1–3):1–451.
[108] Helton JC, Martell M-A, Tierney MS. Characterization of subjective uncertainty in the 1996 performance assessment for the waste isolation pilot plant. Reliab Eng Syst Safety 2000;69(1–3): 191–204.
[109] Goossens LHJ, Harper FT, Kraan BCP, Metivier H. Expert judgement for a probabilistic accident consequence uncertainty analysis. Radiat Protect Dosim 2000;90(3):295–301.
[110] Goossens LHJ, Harper FT. Joint EC/USNRC expert judgement driven radiological protection uncertainty analysis. J Radiol Protect 1998;18(4):249–64.
[111] Siu NO, Kelly DL. Bayesian parameter estimation in probabilistic risk assessment. Reliab Eng Syst Safety 1998;62(1–2):89–116.
[112] Evans JS, Gray GM, Sielken Jr RL, Smith AE, Valdez-Flores C, Graham JD. Use of probabilistic expert judgement in uncertainty analysis of carcinogenic potency. Regul Toxicol Pharmacol 1994;20(1, pt. 1):15–36.
[113] Chhibber S, Apostolakis G, Okrent D. A taxonomy of issues related to the use of expert judgments in probabilistic safety studies. Reliab Eng Syst Safety 1992;38(1–2):27–45.
[114] Kaplan S. Expert information versus expert opinions: another approach to the problem of eliciting combining using expert knowledge in PRA. Reliab Eng Syst Safety 1992;35(1):61–72.
[115] Otway H, Winterfeldt DV. Expert judgement in risk analysis and management: process, context, and pitfalls. Risk Anal 1992;12(1): 83–93.
[116] Bonano EJ, Apostolakis GE. Theoretical foundations and practical issues for using expert judgments in uncertainty analysis of high-level radioactive waste disposal. Radioactive Waste Manage Nucl Fuel Cycle 1991;16(2):137–59.
[117] Keeney RL, Winterfeldt DV. Eliciting probabilities from experts in complex technical problems. IEEE Trans Eng Manage 1991;38(3): 191–201.
[118] Svenson O. on expert judgments in safety analyses in the process industries. Reliab Eng Syst Safety 1989;25(3):219–56.
[119] Mosleh A, Bier VM, Apostolakis G. A critique of current practice for the use of expert opinions in probabilistic risk assessment. Reliab Eng Syst Safety 1988;20(1):63–85.
[120] Breeding RJ, Helton JC, Murfin WB, Smith LN, Johnson JD, Jow H-N, et al. The NUREG-1150 probabilistic risk assessment for the surry nuclear power station. Nucl Eng Des 1992;135(1):29–59.
[121] Payne Jr AC, Breeding RJ, Helton JC, Smith LN, Johnson JD, Jow H-N, et al. The NUREG-1150 probabilistic risk assessment for the peach bottom atomic power station. Nucl Eng Des 1992;135(1): 61–94.
[122] Gregory JJ, Breeding RJ, Helton JC, Murfin WB, Higgins SJ, Shiver AW. The NUREG-1150 probabilistic risk assessment for the sequoyah nuclear plant. Nucl Eng Des 1992;135(1):92–115.
[123] Brown TD, Breeding RJ, Helton JC, Jow H-N, Higgins SJ, Shiver AW. The NUREG-1150 probabilistic risk assessment for the grand gulf nuclear station. Nucl Eng Des 1992;135(1):117–37.
[124] Helton JC, Breeding RJ. Calculation of reactor accident safety goals. Reliab Eng Syst Safety 1993;39(2):129–58.
[125] Morris MD. Three technometrics experimental design classics. Technometrics 2000;42(1):26–7.
[126] Evans M, Swartz T. Approximating integrals via Monte Carlo and deterministic methods. Oxford, NY: Oxford University Press; 2000.
[127] Hurtado JE, Barbat AH. Monte Carlo techniques in computational stochastic mechanics. Arch Comput Methods Eng 1998;5(1):3–330.
[128] Nicola VF, Shahabuddin P, Nakayama MK. Techniques for fast simulation of models of highly dependable systems. IEEE Trans Reliab 2001;50(3):246–64.
[129] Owen A, Zhou Y. Safe and effective importance sampling. J Am Stat Assoc 2000;95(449):135–43.
[130] Heidelberger P. Fast simulation of rare events in queueing and reliability models. ACM Trans Modeling Comput Simul 1995; 5(1):43–85.
[131] Shahabuddin P. Importance sampling for the simulation of highly reliable Markovian systems. Manage Sci 1994;40(3):333–52.
[132] Goyal A, Shahabuddin P, Heidelberger P, Nicola VF, Glynn PW. A unified framework for simulating Markovian models of highly dependable systems. IEEE Trans Comput 1992;41(1):36–51.
[133] Melchers RE. Search-based importance sampling. Struct Safety 1990;9(2):117–28.
[134] Glynn PW, Iglehart DL. Importance sampling for stochastic simulations. Manage Sci 1989;35(11):1367–92.
[135] Iman RL, Conover WJ. A distribution-free approach to inducing rank correlation among input variables. Commun Stat: Simul Comput B 1982;11(3):311–34.
[136] Iman RL, Davenport JM. Rank correlation plots for use with correlated input variables. Commun Stat: Simul Comput B 1982;11(3):335–60.
[137] Helton JC, Davis FJ. Latin hypercube sampling and the propagation of uncertainty in analyses of complex systems, SAND2001-0417. Albuquerque, NM: Sandia National Laboratories; 2002.
[138] Helton JC, Davis FJ, Johnson JD. A comparison of uncertainty and sensitivity analysis results obtained with random and Latin hypercube sampling. Reliab Eng Syst Safety 2005;89(3):305–30.
[139] Kleinjen JPC. An overview of the design and analysis of simulation experiments for sensitivity analysis. Europ J Operat Res 2005; 164(2):287–300.
[140] CRWMS M&O (Civilian Radioactive Waste Management System Management and Operating Contractor). Total system performance assessment (TSPA) model for site recommendation, MDL-WIS-PA-000002 REV 00. Las Vegas, Nevada: CRWMS M&O; 2000.
[141] CRWMS M&O (Civilian Radioactive Waste Management System Management and Operating Contractor). Total system performance assessment for the site recommendation, TDR-WIS-PA-000001 REV 00. Las Vegas, Nevada: CRWMS M&O; 2000.
[142] U.S. DOE (U.S. Department of Energy). Viability assessment of a repository at Yucca mountain, DOE/RW-0508. Washington, DC: US Department of Energy, Office of Civilian Radioactive Waste Management; 1998.
[143] Ibrekk H, Morgan MG. Graphical communication of uncertain quantities to nontechnical people. Risk Anal 1987;7(4):519–29.
[144] Tufte ER. The visual display of quantitative information. Cheshire, CN: Graphics Press; 1983.
[145] Berglund JW, Garner JW, Helton JC, Johnson JD, Smith LN. Direct releases to the surface and associated complementary cumulative distribution functions in the 1996 performance assessment for the waste isolation pilot plant: cuttings, cavings and spallings. Reliab Eng Syst Safety 2000;69(1–3):305–30.
[146] Cooke RM, van Noortwijk JM. Graphical methods. In: Saltelli A, Chan K, Scott EM, editors. Sensitivity analysis. New York, NY: Wiley; 2000. p. 245–64.
[147] Myers RH. Classical and modern regression with applications. 2nd ed. Boston, MA: Duxbury Press; 1989.
[148] Draper NR, Smith H. Applied regression analysis. 2nd ed. New York, NY: Wiley; 1981.
[149] Daniel C, Wood FS, Gorman JW. Fitting equations to data: computer analysis of multifactor data. 2nd ed. New York, NY: Wiley; 1980.
[150] Seber GA. Linear regression analysis. New York, NY: Wiley; 1977.

[151] Neter J, Wasserman W. Applied linear statistical models: regression, analysis of variance, and experimental designs. Homewood: Richard D. Irwin; 1974.
[152] Iman RL, Shortencarier MJ, Johnson JD. A FORTRAN 77 program and user's guide for the calculation of partial correlation and standardized regression coefficients, NUREG/CR-4122, SAND85-0044. Albuquerque: Sandia National Laboratories; 1985.
[153] Iman RL, Conover WJ. The use of the rank transform in regression. Technometrics 1979;21(4):499–509.
[154] Scheffé H. The analysis of variance. New York, NY: Wiley; 1959.
[155] Conover WJ. Practical nonparametric statistics. 2nd ed. New York, NY: Wiley; 1980.
[156] Barnard GA. Contribution to the discussion of professor Bartlett's paper. J R Stat Soc Ser B 1963;26:294.
[157] Press WH, Teukolsky SA, Vetterling WT, Flannery BP. Numerical recipes in FORTRAN: the art of scientific computing. 2nd ed. Cambridge, NY: Cambridge University Press; 1992.
[158] Kleijnen JPC, Helton JC. Statistical analyses of scatterplots to identify important factors in large-scale simulations, 2: robustness of techniques. Reliab Eng Syst Safety 1999;65(2):187–97.
[159] Kleijnen JPC, Helton JC. Statistical analyses of scatterplots to identify important factors in large-scale simulations, SAND98-2202. Albuquerque: Sandia National Laboratories; 1999.
[160] Wagner HM. Global sensitivity analysis. Oper Res 1995;43:948–69.
[161] Granger C, Lin J-L. Using the mutual information coefficient to identify lags in nonlinear models. J Time Ser Anal 1994;15(4): 371–84.
[162] Mishra S, Knowlton RG. Testing for input–output dependence in performance assessment models. In: Proceedings of the 10th international high-level radioactive waste management conference (IHLRWM), March 30–April 2, 2003. Las Vegas, Nevada. La Grange Park, IL: American Nuclear Society; p. 882–7.
[163] Bonnlander BV, Weigend AS. Selecting input variables using mutual information and nonparametric density estimation. In: Proceedings of the international symposium on artificial neural networks (ISANN'94), Tainan, Taiwan, 1994. p. 42–50.
[164] Moddemeijer R. On the estimation of entropy and mutual information of continuous distributions. Signal Process 1989; 16(3):233–48.
[165] Simonoff JS. Smoothing methods in statistics. New York, NY: Springer; 1996.
[166] Hastie TJ, Tibshirani RJ. Generalized additive models. London: Chapman & Hall; 1990.
[167] Chambers JM, Hastie TJ. Statistical models in S. Pacific Grove, CA: Wadsworth & Brooks; 1992.
[168] Storlie CB, Helton JC. Multiple Predictor smoothing methods for sensitivity analysis, SAND2005-???? Albuquerque, NM: Sandia National Laboratories; to appear.
[169] Ruppert D, Ward MP, Carroll RJ. Semiparametric regression. Cambridge, MA: Cambridge University Press; 2003.
[170] Breiman L, Friedman JH, Olshen RA, Stone CJ. Classification and regression trees. Belmont, CA: Wadsworth Intl; 1984.
[171] Mishra S, Deeds NE, RamaRao BS. Application of classification trees in the sensitivity analysis of probabilistic model results. Reliab Eng Syst Safety 2003;79(2):123–9.
[172] Hora SC, Helton JC. A distribution-free test for the relationship between model input and output when using Latin hypercube sampling. Reliab Eng Syst Safety 2003;79(3):333–9.
[173] Peacock JA. Two-dimensional goodness-of-fit testing in astronomy. Monthly Notices R Astronom Soc 1983;202(2):615–27.
[174] Fasano G, Franceschini A. A multidimensional version of the Kolmogorov–Smirnov test. Monthly Notices R Astronom Soc 1987;225(1):155–70.
[175] Garvey JE, Marschall EA, Wright RA. From star charts to stoneflies: detecting relationships in continuous bivariate data. Ecology 1998;79(2):442–7.
[176] Ripley BD. Spatial point pattern analysis in ecology. In: Legendre P, Legendre L, editors. Developments in numerical ecology. NATO ASI series, series G: ecological sciences, vol. 14. Berlin; NY: Springer; 1987. p. 407–30.
[177] Zeng G, Dubes RC. A comparison of tests for randomness. Pattern Recogn 1985;18(2):191–8.
[178] Diggle PJ. Statistical analysis of spatial point patterns. New York, NY: Academic Press; 1983.
[179] Diggle PJ, Cox TF. Some distance-based tests of independence for sparsely sampled multivariate spatial point patterns. Int Stat Rev 1983;51(1):11–23.
[180] Byth K. On robust distance-based intensity estimators. Biometrics 1982;38(1):127–35.
[181] Byth K, Ripley BD. On sampling spatial patterns by distance methods. Biometrics 1980;36(2):279–84.
[182] Diggle PJ. On parameter estimation and goodness-of-fit testing for spatial point patterns. Biometrics 1979;35(1):87–101.
[183] Diggle PJ. Statistical methods for spatial point patterns in ecology. In: Cormack RM, Ord JK, editors. Spatial and temporal analysis in ecology. Fairfield, MD: International Co-operative Publishing House; 1979. p. 95–150.
[184] Ripley BD. Tests of randomness for spatial point patterns. J R Stat Soc 1979;41(3):368–74.
[185] Besag J, Diggle PJ. Simple Monte Carlo tests for spatial pattern. Appl Stat 1977;26(3):327–33.
[186] Diggle PJ, Besag J, Gleaves JT. Statistical analysis of spatial point patterns by means of distance methods. Biometrics 1976;32:659–67.
[187] Cox TF, Lewis T. A conditioned distance ratio method for analyzing spatial patterns. Biometrika 1976;63(3):483–91.
[188] Holgate P. The use of distance methods for the analysis of spatial distribution of points. In: Lewis PAW, editor. Stochastic point processes: statistical analysis, theory, and applications. New York: Wiley-Interscience; 1972. p. 122–35.
[189] Holgate P. Tests of randomness based on distance methods. Biometrika 1965;52(3–4):345–53.
[190] Clark PJ, Evans FC. Distance to nearest neighbour as a measure of spatial relationships in populations. Ecology 1954;35:23–30.
[191] Hopkins B, Shellam JG. A new method for determining the type of distribution of plant individuals. Ann Botany 1954;18(70): 213–27.
[192] Cressie NAC. Statistics for spatial data. New York, NY: Wiley; 1993.
[193] Iman RL, Conover WJ. A measure of top-down correlation. Technometrics 1987;29(3):351–7.
[194] Campolongo F, Saltelli A, Sorensen T, Tarantola S. Hitchhiker's guide to sensitivity analysis. In: Saltelli A, Chan K, Scott M, editors. Sensitivity analysis. New York: Wiley; 2000. p. 15–47.
[195] Saltelli A, Tarantola S, Campolongo F, Ratto M. Sensitivity analysis in practice. New York, NY: Wiley; 2004.
[196] Cukier RI, Fortuin CM, Shuler KE, Petschek AG, Schiably JH. Study of the sensitivity of coupled reaction systems to uncertainties in rate coefficients, I. Theory. J Chem Phys 1973;59(8):3873–8.
[197] Schaibly JH, Shuler KE. Study of the sensitivity of coupled reaction systems to uncertainties in rate coefficients, II. Applications. J Chem Phys 1973;59(8):3879–88.
[198] McRae GJ, Tilden JW, Seinfeld JH. Global sensitivity analysis—a computational implementation of the Fourier amplitude sensitivity test (FAST). Comput Chem Eng 1981;6(1):15–25.
[199] Saltelli A, Sobol' IM. About the use of rank transformation in sensitivity analysis of model output. Reliab Eng Syst Safety 1995;50(3):225–39.
[200] Homma T, Saltelli A. Importance measures in global sensitivity analysis of nonlinear models. Reliab Eng Syst Safety 1996; 52(1):1–17.
[201] Archer GEB, Saltelli A, Sobol' IM. Sensitivity measures, ANOVA-like techniques and the use of bootstrap. J Stat Comput Simul 1997;58(2):99–120.
[202] Saltelli A, Bolado R. An alternative way to compute Fourier amplitude sensitivity test (FAST). Comput Stat Data Anal 1998; 26(4):267–79.

[203] Saltelli A, Tarantola S, Campolongo F. Sensitivity analysis as an ingredient of modeling. Stat Sci 2000;15(4):377–95.
[204] Chan K, Saltelli A, Tarantola S. Winding stairs: a sampling tool to compute sensitivity indices. Stat Comput 2000;10(3):187–96.
[205] Rabitz H, Alis OF, Shorter J, Shim K. Efficient input–output model representations. Comput Phys Commun 1999;117(1–2):11–20.
[206] Jansen MJW, Rossing WAH, Daamen RA. Monte Carlo estimation of uncertainty contributions from several independent multivariate sources. In: Grasman J, van Straten G, editors. Predictability and nonlinear modeling in natural sciences and economics. Boston: Kluwer Academic Publishers; 1994. p. 334–43.
[207] Jansen MJW. Analysis of variance designs for model output. Comput Phys Commun 1999;117(1–2):35–43.
[208] McKay MD. Evaluating prediction uncertainty, LA-12915-MS; NUREG/CR-6311. Los Alamos, NM: Los Alamos National Laboratory; 1995.
[209] McKay MD. Nonparametric variance-based methods of assessing uncertainty importance. Reliab Eng Syst Safety 1997;57(3):267–79.
[210] McKay MD, Morrison JD, Upton SC. Evaluating prediction uncertainty in simulation models. Comput Phys Commun 1999; 117(1–2):44–51.
[211] Helton JC. Mathematical and numerical approaches in performance assessment for radioactive waste disposal: dealing with uncertainty. In: Scott EM, editor. Modelling radioactivity in the environment. New York, NY: Elsevier Science; 2003. p. 353–90.
[212] Helton JC, Anderson DR, Basabilvazo G, Jow H-N, Marietta MG. Conceptual structure of the 1996 performance assessment for the waste isolation pilot plant. Reliab Eng Syst Safety 2000;69(1–3): 151–65.
[213] Diaz NJ. Realism and conservatism, remarks by chairman diaz at the 2003 nuclear safety research conference. NRC News. No. S-03-023, Washington, DC: US Nuclear Regulatory Commission; October 20, 2003.
[214] Paté-Cornell E. Risk and uncertainty analysis in government safety decisions. Risk Anal 2002;22(3):633–46.
[215] Caruso MA, Cheok MC, Cunningham MA, Holahan GM, King TL, Parry GW, et al. An approach for using risk assessment in risk-informed decisions on plant-specific changes to the licensing basis. Reliab Eng Syst Safety 1999;63:231–42.
[216] Sielken Jr RL, Bretzlaff RS, Stevenson DE. Challenges to default assumptions stimulate comprehensive realism as a new tier in quantitative cancer risk assessment. Regul Toxicol Pharmacol 1995;21:270–80.
[217] Nichols AL, Zeckhauser RJ. The perils of prudence: how conservative risk assessments distort regulation. Regul Toxicol Pharmacol 1988;8:61–75.

This page intentionally left blank

Appendix C

Helton JC, Breeding RJ. Calculation of Reactor Accident Safety Goals. *Reliability Engineering and System Safety* 1993;39(2):129-158

This page intentionally left blank

Reliability Engineering and System Safety **39** (1993) 129–158

Calculation of reactor accident safety goals*

Jon C. Helton

Department of Mathematics, Arizona State University, Tempe, Arizona 85287, USA

&

Roger J. Breeding

Special Projects Division 6411, Sandia National Laboratories, Albuquerque, New Mexico 87185, USA

The US Nuclear Regulatory Commission is in the process of developing safety goals for the operation of nuclear power plants. At present, two safety goals (individual early fatality risk and individual latent cancer fatality risk) and three quantitative risk goals (severe accident frequency, conditional probability of containment failure, and large release frequency) are emerging from this development. Each of these goals requires that the expected value for a quantity be less than a specified value, where the expectation is calculated over imprecisely known parameters required in the analysis. This presentation provides a description of the calculations involved in the determination of these goals, including uncertainty analysis, sensitivity analysis and estimation of expected values. Results obtained in a probabilistic risk assessment performed for internally initiated accidents at the Surry Nuclear Power Station as part of the NUREG-1150 analyses are used for illustration.

1 INTRODUCTION

The US Nuclear Regulatory Commission (NRC) is in the process of developing safety goals for the operation of nuclear power plants.[1–4] At present, two safety goals for individual fatality risk and three quantitative risk goals for accident frequency are emerging from this development. These goals are of the following form:

- *Individual early fatality risk*: the expected value for average individual early fatality risk in the region between the plant site boundary and 1609·3 m (1 mi) beyond this boundary will be less than 5×10^{-7} year^{-1}. (SG1)
- *Individual latent cancer fatality risk*: the expected value for average individual latent cancer fatality risk in the region between the plant site boundary and 16 093 m (10 mi) beyond this boundary will be less than 2×10^{-6} year.$^{-1}$ (SG2)
- *Severe accident frequency*: the expected value for the frequency of a severe accident will be less than 1×10^{-4} year.$^{-1}$ (QRG1)
- *Conditional probability of containment failure*: the expected value for the probability of containment failure given the occurrence of a severe accident will be less than 0·1. (QRG2)
- *Large release frequency*: the expected value for the frequency of a large release will be less than 1×10^{-6} year.$^{-1}$ (QRG3)

Furthermore, a severe accident as used in (QRG1) is taken to be an accident involving core damage. In contrast, several possibilities exist for the definition of a severe accident in (QRG2); for example, this goal may be more meaningful for accidents that involve vessel breach. For (QRG3), a large radionuclide release is defined to be a release that has a potential for causing an early fatality in the population outside the plant site boundary.

For the individual risk goals (i.e. SG1 and SG2), average individual risk is defined to be the sum of the risks incurred by the individuals within the region

* This work was supported in part by the US Nuclear Regulatory Commission and was performed at Sandia National Laboratories, which is operated for the US Department of Energy under Contract Number DE-AC04-76DP00789.

under consideration divided by the number of individuals in the region. Mathematically, these goals can be represented by

$$\sum_{i=1}^{nI(b,b+1)} fT_i rEF_i \Big/ \sum_{i=1}^{nI(b,b+1)} fT_i < 5 \times 10^{-7}\ \text{year}^{-1} \quad (1)$$

and

$$\sum_{i=1}^{nI(b,b+10)} fT_i rLCF_i \Big/ \sum_{i=1}^{nI(b,b+10)} fT_i < 2 \times 10^{-6}\ \text{year}^{-1} \quad (2)$$

respectively, where

$nI(b, b+1)$ = number of individuals within 1609·3 m (1 mi) of the plant site boundary (dimensionless),
$nI(b, b+10)$ = number of individuals within 16 093 m (10 mi) of the plant site boundary (dimensionless),
fT_i = fraction of time that individual i is present in the region under consideration (dimensionless),
rEF_i = annual early fatality risk to individual i due to severe accidents at the reactor facility (year^{-1}), and
$rLCF_i$ = annual latent cancer fatality risk to individual i due to severe accidents at the reactor facility (year^{-1}).

The risks rEF_i and $rLCF_i$ are based on the assumption that the individual is always present in the region under consideration before an accident; the multiplier fT_i corrects for the amount of time the individual actually spends in this region. The summations in the denominators of eqns (1) and (2) define effective population sizes that incorporate how long each individual spends in the region of interest. Average individual risk could also be calculated with total population size by replacing the denominators in eqns (1) and (2) with $nI(b, b+1)$ and $nI(b, b+10)$, respectively.

Each goal involves a requirement that the expected value for a quantity be less than a specified value. The NRC indicates that this expected value is to be with respect to imprecisely known variables required in the calculation of the goals (Ref. 2, p. 30031). Thus, for example, the goals appearing in eqns (1) and (2) are actually of the form

$$E\left(\sum_{i=1}^{nI(b,b+1,\mathbf{X})} fT_i(\mathbf{X}) rEF_i(\mathbf{X}) \Big/ \sum_{i=1}^{nI(b,b+1,\mathbf{X})} fT_i(\mathbf{X})\right) < 5 \times 10^{-7}\ \text{year}^{-1} \quad (3)$$

and

$$E\left(\sum_{i=1}^{(nI(b,b+10,\mathbf{X})} fT_i(\mathbf{X}) rLCF_i(\mathbf{X}) \Big/ \sum_{i=1}^{nI(b,b+10,\mathbf{X})} fT_i(\mathbf{X})\right) < 2 \times 10^{-7}\ \text{year}^{-1} \quad (4)$$

respectively, where the vector $\mathbf{X}$ represents imprecisely known variables required in the analysis and E represents expected value calculated over the set of all possible values for $\mathbf{X}$.

The purpose of this presentation is to describe how the safety goals and associated risk goals might be calculated. Due to the central role that the treatment of uncertainties plays in the calculation of these goals, uncertainties in probabilistic risk assessments (PRAs) for nuclear facilities will be discussed first. Then, the calculation of the risk goals within a PRA will be discussed. For the purpose of this calculation, a PRA will be viewed as consisting of the following parts: accident frequency analysis, accident progression analysis, source term analysis and consequence analysis. A matrix formalism[5–8] will be used to show how these parts are assembled to produce a complete PRA and how the safety goals can be calculated within this assembly. Further, a PRA performed for internally-initiated accidents at the Surry nuclear power station[9] as part of the NUREG-1150 risk study[10] will be used for illustration.

Additional background on the development of the safety goals is available elsewhere.[11–21]

2 UNCERTAINTIES IN PROBABILISTIC RISK ASSESSMENT

A number of factors affect the uncertainty in PRA results, including completeness, aggregation, model selection, imprecisely known variables, and stochastic variation. The nature of these factors can be seen by defining risk to be a set R of ordered triples[22] of the form

$$R = \{(A_i, fA_i, cA_i), i = 1, \ldots, nA\} \quad (5)$$

where

A_i = a set of similar accidents,
fA_i = sum of the frequencies (year^{-1}) of the accidents in A_i,
cA_i = vector of accident consequences associated with A_i, and
nA = number of accident sets.

As will be illustrated later, the set R is typically defined in several different ways within a PRA.

Completeness refers to the extent that the PRA includes all possible accidents at the facility under consideration. In terms of the risk representation in eqn (5) completeness deals with whether or not all possible accidents are included in the union of the sets A_i (i.e. in $\bigcup_i A_i$). Aggregation refers to the division of the possible accidents into the sets A_i. Resolution is lost if the A_i are defined too coarsely (i.e. nA is too small) or in some other inappropriate manner. Model selection refers to the actual choice of the models for use in a PRA. Appropriate model choice is sometimes

unclear and can affect both fA_i and cA_i. Similarly, once the models for use have been selected, imprecisely known variables required as input by these models can also affect both fA_i and cA_i. Due to the complex nature of PRAs, model selection and imprecisely known variables can also affect the definition of the A_i. Stochastic variation is incorporated into the frequencies fA_i and involves factors such as the frequency of initiating events, the probability that safety systems will operate as designed, and the type of weather existing at the time of an accident.

Although the set R defined in eqn (5) provides a convenient conceptual representation for risk, it is difficult to directly inspect the information contained in R. As a result, exceedance frequency curves and annual risks are often used to summarize the information contained in R. An exceedance frequency curve is a plot in which the values for a consequence variable appear on the abscissa and the frequencies at which these values are exceeded appear on the ordinate. If cA_i represents the value for a specific consequence variable (e.g. number of latent cancer fatalities) contained in cA_i and the cA_i are ordered so that $cA_i \leq cA_{i+1}$, then the exceedance frequency curve for this variable is defined by the points

$$\left(cA_i, \sum_{j=i+1}^{nA} fA_i\right), \quad i = 1, 2, \ldots, nA \tag{6}$$

An example of an exceedance frequency curve is given in Fig. 1. The annual risk rA for a consequence variable is given by

$$rA = \sum_{i=1}^{nA} fA_i cA_i \tag{7}$$

The calculation of an annual risk is equivalent to reducing an exceedance frequency curve to a single number. For example, the annual risk associated with the curve in Fig. 1 is $5{\cdot}2 \times 10^{-3}$ latent cancer fatalities/year. In addition, more complex annual risks of the form

$$rA = \sum_{i=1}^{nA} fA_i f(A_i, fA_i, cA_i) \tag{8}$$

are also possible, where f is an appropriately defined function. Other types of results (e.g. conditional probabilities) can also be calculated with the information contained in R.

The quantities appearing in (SG1) through (QRG3) can all be defined and calculated in the context of the representation for risk given in eqn (5). The average individual risks in (SG1) and (SG2) are annual risks as defined in eqn (7); in this case, cA_i would be the conditional probability of an individual becoming an early fatality or a latent cancer fatality, respectively. The core damage frequency in (QRG1) involves a summation of the frequencies fA_i in eqn (5). The

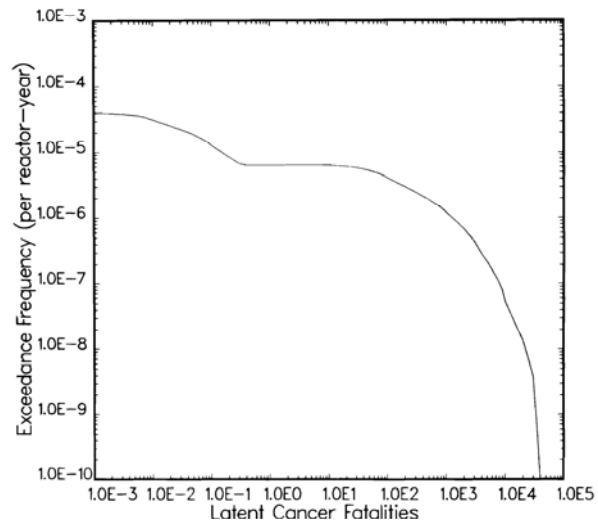

Fig. 1. Example exceedance frequency curve.

conditional probability in (QRG2) is obtained from a calculation that involves the fA_i and cA_i. The large release frequency in (QRG3) is defined by a point on an exceedance frequency curve for early fatalities. These ideas will be discussed and illustrated in more detail later.

The goals in (SG1) through (QRG3) each specify that the expected value for a quantity will be less than a stated value. The calculation of these goals requires many imprecisely known quantities, and the indicated expectations are over these quantities. These quantities all have the property that the analysis structure requires a single value for them but it is not known with exactness what these values should be. For convenience, these quantities can be represented by the vector

$$\mathbf{X} = [X_1, X_2, \ldots, X_{nV}] \tag{9}$$

where nV is the number of imprecisely known quantities or variables required in the analysis. As an example, the analysis performed for Surry identified 130 variables (i.e. $nV = 130$) for inclusion in an uncertainty study (Ref. 9, Tables 2.2-9, 2.2-10, 2.3-2 and 3.2-1).

The individual variables X_j in $\mathbf{X}$ can relate to completeness uncertainty (e.g. the value for a frequency cutoff used to drop low frequency accidents from the analysis), aggregation uncertainty (e.g. a bound on the value for nA), model uncertainty (e.g. a 0–1 variable that indicates which of two alternative models should be used), variable uncertainty (e.g. the failure pressure for the reactor containment), or stochastic uncertainty (e.g. the frequency for an initiating event or the probability that a safety system will operate on demand). Once these variables, and hence $\mathbf{X}$, have been specified, it is possible to

determine the set R in eqn (5). To emphasize this dependency, R can be represented as a function of $\mathbf{X}$:

$$R(\mathbf{X}) = \{(A(\mathbf{X}), fA_i(\mathbf{X}), cA_i(\mathbf{X})), \quad i = 1, \ldots, nA(\mathbf{X})\} \quad (10)$$

As $\mathbf{X}$ changes, the set $R(\mathbf{X})$ and the summary measures that can be calculated from it change. Included in these summary measures are the quantities in the safety and quantitative risk goals. By specifying expected values, these goals are, in essence, requiring that each set $R(\mathbf{X})$ and its associated summary measures be weighted by the likelihood that $\mathbf{X}$ contains the appropriate values for use in the analysis.

The calculation of expected values requires that a joint probability distribution be assigned to the X_j. Formally, this assignment involves the development of a set Ω that contains all the possible values for $\mathbf{X}$ and the definition of a density function p on Ω. Expected values are then obtained by integrations over Ω. For example, the formal representations for the expected values in eqns (3) and (4) would be

$$\int_\Omega \left(\sum_{i=1}^{nI(b,b+1,\mathbf{X})} fT_i(\mathbf{X}) rEF_i(\mathbf{X}) \Big/ \sum_{i=1}^{nI(b,b+1,\mathbf{X})} fT_i(\mathbf{X}) \right) p(\mathbf{X})\, d\mathbf{X} < 5 \times 10^{-7}\ \text{year}^{-1} \quad (11)$$

and

$$\int_\Omega \left(\sum_{i=1}^{nI(b,b+10,\mathbf{X})} fT_i(\mathbf{X}) rLCF_i(\mathbf{X}) \Big/ \sum_{i=1}^{nI(b,b+10,\mathbf{X})} fT_i(\mathbf{X}) \right) p(\mathbf{X})\, d\mathbf{X} < 2 \times 10^{-6}\ \text{year}^{-1} \quad (12)$$

respectively. In practice, the preceding integrals would not be calculated directly. Rather, Monte Carlo techniques would be used to determine approximations to them.

Development of the set Ω and the associated density function p is a major undertaking. As part of the NUREG-1150 PRAs, panels of outside experts were assembled and used to develop Ω and p. These panels developed subjective distributions for the X_j which characterized their beliefs as to where the appropriate values to use for these variables fell. In the development of this information, the panels took into account past observational data, experimental data, mechanistic code calculations, theoretical calculations, and level of resolution within the individual PRAs. Taken collectively, the ranges and distributions specified by these panels define Ω and p. This process is described in greater detail elsewhere.[23–31]

Once a joint distribution is developed for the variables shown in eqn (9) Monte Carlo procedures can be used to estimate the integrals shown in eqns (11) and (12) and other quantities of interest. With this approach, a sample

$$\mathbf{X}_s = [X_{s1}, X_{s2}, \ldots, X_{s,nV}], \quad s = 1, 2, \ldots, nS \quad (13)$$

is generated from the $\mathbf{X}$ values according to the assigned distribution, where nS is the number of elements in the sample. Latin hypercube sampling is a likely candidate for use in the generation of this sample due to the efficient manner in which it stratifies across the ranges of the individual variables contained in $\mathbf{X}$.[32,33]

Once the sample is generated, the set R shown in eqn (5) is evaluated for each sample element. This creates a sequence of results of the form

$$R(\mathbf{X}_s) = \{(A_i(\mathbf{X}_s), fA_i(\mathbf{X}_s), cA_i(\mathbf{X}_s)), \quad s = 1, \ldots, nA(\mathbf{X}_s)\} \quad (14)$$

for $s = 1, \ldots, nS$. For the Surry analysis, a sample size of $nS = 200$ was used (Ref. 9, Appendix E). Exceedance frequency curves, annual risks, and other quantities can be calculated for each set $R(\mathbf{X}_s)$. This yields distributions of results as shown in Figs 2 and 3.

Mean results can be obtained by summing over all sample elements and then dividing by the sample size nS. For example, the mean value of the annual early fatality risk associated with the 200 observations in Fig. 3 is $2{\cdot}0 \times 10^{-6}$ early fatalities/year. Such mean values are approximations to the expected value that would be obtained by integrating over Ω. For example, the representations for (SG1) and (SG2) in

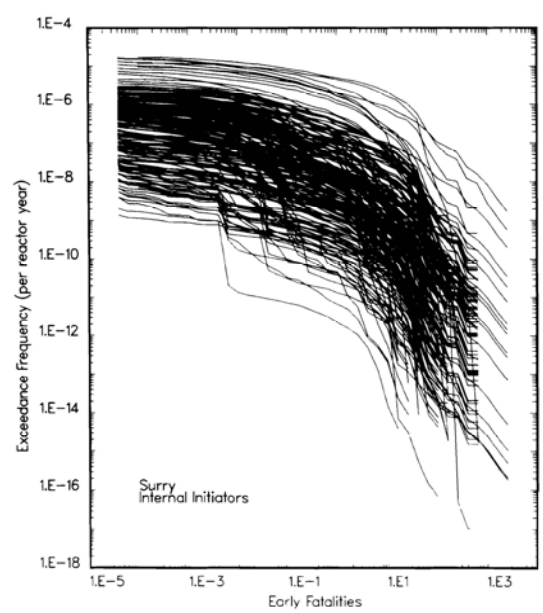

Fig. 2. Exceedance frequency curves for early fatalities due to accidents resulting from internal initiators at Surry (Ref. 9, Fig. D.1). Each curve corresponds to one sample element.

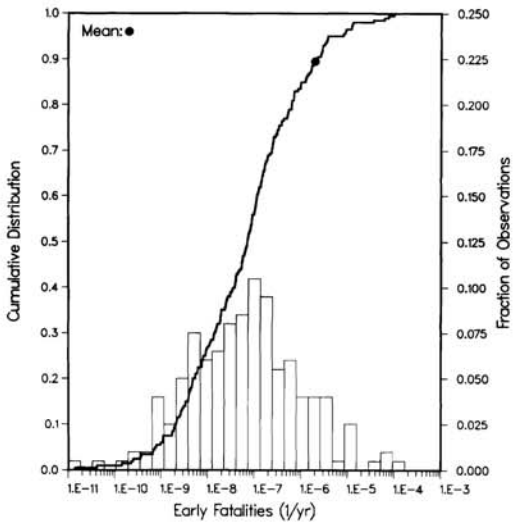

Fig. 3. Distribution of annual early fatality risk due to accidents resulting from internal initiators at Surry (replotted from Ref. 9, Fig. 5.1-2). The 200 annual risks on which this figure is based result from reducing each of the exceedance frequency curves in Fig. 2 to a single annual risk.

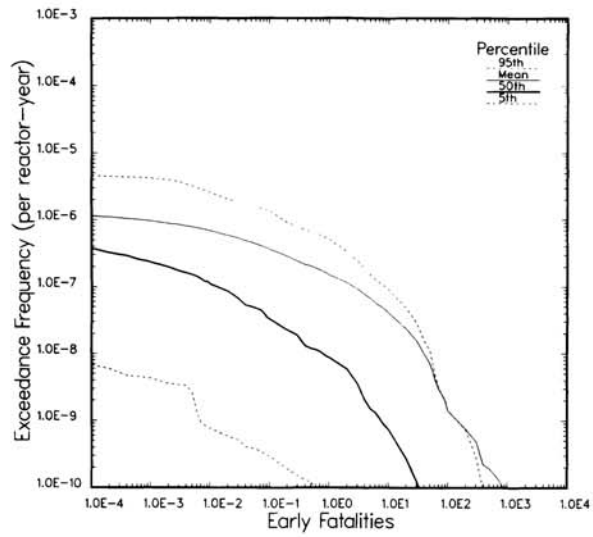

Fig. 4. Mean and percentile curves for exceedance frequencies for early fatalities due to accidents resulting from internal initiators at Surry (Ref. 9, Figure 5.1-1).

eqns (11) and (12) become

$$\sum_{s=1}^{nS}\left(\sum_{i=1}^{nI(b,b+1,\mathbf{X}_s)} fT_i(\mathbf{X}_s)rEF_i(\mathbf{X}_s)\Big/\sum_{i=1}^{nI(b,b+1,\mathbf{X}_s)} fT_i(\mathbf{X}_s)\right)\Big/ nS < 5\times10^{-7}\ \text{year}^{-1} \quad (15)$$

and

$$\sum_{s=1}^{nS}\left(\sum_{i=1}^{nI(b,b+10,\mathbf{X}_s)} fT_i(\mathbf{X}_s)rLCF_i(\mathbf{X}_s)\Big/\sum_{i=1}^{nI(b,b+10,\mathbf{X}_s)} fT_i(\mathbf{X}_s)\right)\Big/ nS < 2\times10^{-6}\ \text{year}^{-1} \quad (16)$$

respectively, when this approximation is used.

It is also possible to calculate mean exceedance frequency curves by summing the frequencies associated with individual consequence values and then dividing by the sample size. Figure 4 shows the result of this calculation for the exceedance frequency curves in Fig. 2. Also shown in Fig. 4 are the curves that result from calculating the 5th, 50th and 95th percentiles of the exceedance frequencies associated with each consequence value.

Due to the important role that expected values play in the safety and quantitative risk goals, this section has discussed uncertainties in PRAs and how expected values are generated from these uncertainties. The next four sections will show how these goals fit into the overall calculations that must be performed in a PRA. The ideas introduced in this section will continue to be used in this development. Additional discussion of the ideas underlying the NUREG-1150 PRAs is available elsewhere.[34,35]

3 ACCIDENT FREQUENCY ANALYSIS

Accident frequency analyses are typically performed with event tree and fault tree techniques to obtain characterizations of accidents that lead from initiating events to core damage.[36,37] These accidents are often referred to as severe accidents in the terminology used with the quantitative risk goals.

The starting point in the accident frequency analysis is a sequence of initiating events

$$IE_1, IE_2, \ldots, IE_{nIE} \quad (17)$$

where nIE is the number of initiating events selected for consideration. In practice, each initiating event is a set of similar accident initiators rather than a single unique event. The $nIE = 11$ initiating events considered in the analysis for internally initiated accidents at Surry are listed in Table 1.

Typically, an event tree is developed for each initiating event that indicates how an accident could progress from that initiating event to core damage. The events in these trees are usually high level and relate to whether or not specific safety systems operate. Each path through a tree that leads to core damage defines a set of similar accidents called an accident sequence. The result of this analysis is a collection

$$AS_1, AS_2, \ldots, AS_{nAS} \quad (18)$$

of accident sequences, where nAS is the total number of accident sequences identified for all initiating events. The $nAS = 28$ accident sequences selected for

Table 1. Initiating events considered in analysis for accidents resulting from internal initiators at Surry (Ref. 38, Table 4.3-1). Abbreviations are defined in Table 2

Initiating event	Mean annual frequency (year^{-1})
Loss of offsite power	$7{\cdot}7 \times 10^{-2}$
Transients with loss of MFW	$9{\cdot}4 \times 10^{-1}$
Transients with MFW initially available	7·3
Non-recoverable loss of DC Bus A	$5{\cdot}0 \times 10^{-3}$
Non-recoverable loss of DC Bus B	$5{\cdot}0 \times 10^{-3}$
Steam generator tube rupture	$1{\cdot}0 \times 10^{-2}$
Large LOCA, 6–29 inch[a]	$5{\cdot}0 \times 10^{-4}$
Medium LOCA, 2–6 inch	$1{\cdot}0 \times 10^{-3}$
Small LOCA, $\frac{1}{2}$–2 inch	$1{\cdot}0 \times 10^{-3}$
Very small LOCA, less than $\frac{1}{2}$ inch	$1{\cdot}3 \times 10^{-2}$
Interfacing LOCA	$1{\cdot}6 \times 10^{-6}$

[a]1 inch = 2·54 cm

inclusion in the integrated analysis for internally initiated accidents at Surry are summarized in Table 3.

The frequency of the accident sequences can be represented by the matrix product

$$\mathbf{fAS} = \mathbf{fIE}\ \mathbf{P}(AS \mid IE) \tag{19}$$

where

$\mathbf{fIE} = [fIE_1, \ldots, fIE_{nIE}]$

fIE_i = frequency (year^{-1}) for initiating event i,

$\mathbf{fAS} = [fAS_1, \ldots, fAS_{nAS}]$

Table 2. Abbreviations appearing in Tables 1, 3, 4 and 6

Abbreviation	Definition
AC	Alternating current
AFW	Auxiliary feedwater
ATWS	Anticipated transient without scram
BMT	Basemat melt-through
CCI	Core concrete interaction
CHR	Containment heat removal
DC	Direct current
ECCS	Emergency core cooling system
E-AFWS	Electric motor driven auxiliary feedwater system
Event V	Interfacing system loss of coolant accident
HPME	High pressure melt ejection
LOCA	Loss of coolant accident
LPIS	Low pressure injection system
MFW	Main feedwater
PORV	Power operated relief valve
RCP	Reactor coolant pump
RCS	Reactor coolant system
RWST	Refueling water storage tank
S-AFWS	Steam turbine driven auxiliary feedwater system
SBO	Station blackout
SG	Steam generator
SGTR	Steam generator tube rupture
SRV	Safety relief valve
SW	Service water
VB	Vessel breach

Table 3. Summary description of accident sequences selected for inclusion in Surry analysis for accidents resulting from internal initiators (Ref. 9, Table 5-3). Abbreviations are defined in Table 2

Description	Mean annual frequency (year^{-1})
Station blackout: battery depletion	$1{\cdot}1 \times 10^{-5}$
Station blackout: RCP seal LOCA	$5{\cdot}3 \times 10^{-6}$
Station blackout: AFW failure	$4{\cdot}7 \times 10^{-6}$
Station blackout: RCP seal LOCA	$3{\cdot}3 \times 10^{-6}$
Station blackout: stuck open PORV	$2{\cdot}2 \times 10^{-6}$
Medium LOCA: recirculation failure	$1{\cdot}7 \times 10^{-6}$
Interfacing System LOCA (Event V)	$1{\cdot}6 \times 10^{-6}$
SGTR: no depressurization: SG integrity fails	$1{\cdot}4 \times 10^{-6}$
Loss of MFW/AFW: feed and bleed fails	$9{\cdot}8 \times 10^{-7}$
Medium LOCA: injection failure	$8{\cdot}6 \times 10^{-7}$
ATWS: unfavorable moderation temperature coefficient	$8{\cdot}2 \times 10^{-7}$
Large LOCA: recirculation failure	$8{\cdot}2 \times 10^{-7}$
Loss of MFW/AFW: feed and bleed fails	$7{\cdot}4 \times 10^{-7}$
Medium LOCA: injection failure	$6{\cdot}7 \times 10^{-7}$
SBO: AFW failure	$6{\cdot}5 \times 10^{-7}$
Large LOCA: accumulator failure	$6{\cdot}4 \times 10^{-7}$
ATWS: emergency boration failure	$6{\cdot}4 \times 10^{-7}$
Very small LOCA: injection failure	$6{\cdot}3 \times 10^{-7}$
Small LOCA: injection failure	$4{\cdot}4 \times 10^{-7}$
SBO: battery depletion	$4{\cdot}3 \times 10^{-7}$
SBO: stuck open PORV	$3{\cdot}2 \times 10^{-7}$
Large LOCA: injection failure	$3{\cdot}1 \times 10^{-7}$
SGTR: injection failure; no depressurization	$2{\cdot}1 \times 10^{-7}$
Loss of DC BUS: AFW fails; no feed and bleed	$1{\cdot}3 \times 10^{-7}$
Loss of DC BUS: AFW fails; no feed and bleed	$1{\cdot}3 \times 10^{-7}$
SGTR: AFW failure	$1{\cdot}1 \times 10^{-7}$
SGTR: no depressurization: SG integrity Fails, PORV fails	$1{\cdot}1 \times 10^{-7}$
SGTR: ATWS	$1{\cdot}0 \times 10^{-7}$

fAS_j = frequency (year^{-1}) for accident sequence j

$$\mathbf{P}(AS \mid IE) = \begin{bmatrix} p(AS_1 \mid IE_1) & \cdots & p(AS_{nAS} \mid IE_1) \\ \vdots & & \vdots \\ p(AS_1 \mid IE_{nIE}) & \cdots & p(AS_{nAS} \mid IE_{nIE}) \end{bmatrix}$$

and

$p(AS_j \mid IE_i)$ = the (conditional) probability that accident sequence j will occur given that initiating event i has occurred.

In practice, evaluation of the preceding expression depends on a number of imprecisely known variables. When this is added to the notation, the representation for accident sequence frequency becomes

$$\mathbf{fAS(X)} = \mathbf{fIE(X)}\ \mathbf{P}(AS \mid IE, \mathbf{X}) \tag{20}$$

where $\mathbf{X}$ represents a vector of imprecisely known variables and the dependence of nIE, nAS, fIE_i, fAS_j and $p(AS_j \mid IE_i)$ on $\mathbf{X}$ can be represented analogously by $nIE(\mathbf{X})$, $nAS(\mathbf{X})$, $fIE_i(\mathbf{X})$, $fAS_j(\mathbf{X})$ and $p(AS_j \mid IE_i, \mathbf{X})$, respectively.

When the representation of risk by the set of ordered triples shown in eqn (5) is used, the results of a PRA carried through the accident frequency analysis (i.e. a level 1 PRA) can be expressed as

$$R = \{(IE_i, fIE_i, [p(AS_1 \mid IE_i), \ldots, p(AS_{nAS} \mid IE_i)]), \quad i = 1, \ldots, nIE\} \quad (21)$$

If the dependency on $\mathbf{X}$ is included as shown in eqn (9) this representation would become

$$R(\mathbf{X}) = \{(IE_i(\mathbf{X}), fIE_i(\mathbf{X}), [p(AS_1(\mathbf{X}) \mid IE_i(\mathbf{X}), \mathbf{X}), \ldots, p(AS_{nAS(X)}(\mathbf{X}) \mid IE_i(\mathbf{X}), \mathbf{X})]), \quad i = 1, \ldots, nIE(\mathbf{X})\} \quad (22)$$

As indicated by the preceding notation, it is possible for the initiating events and accident sequences themselves, as well as their frequencies, to depend on imprecisely known variables.

The first quantitative risk goal (i.e. QRG1) involves the risk results shown in eqn (22). Specifically, this goal requires that

$$E\left(\sum_{i=1}^{nIE(\mathbf{X})} fIE_i(\mathbf{X})\left[\sum_{j=1}^{nAS(\mathbf{X})} p(AS_j(\mathbf{X}) \mid IE_i(\mathbf{X}), \mathbf{X})\right]\right) < 1 \times 10^{-4}\ \text{year}^{-1} \quad (23)$$

In this goal, a bound is being placed on the expected value for an annual risk of the form defined in eqn (8).

The event trees used in the development of the accident sequences usually do not contain sufficient detail to permit a determination of the matrix $\mathbf{P}(AS \mid IE)$. Therefore, additional analysis is necessary before the expression in eqn (23) can be evaluated. Typically, fault trees are developed for the top events (i.e. the individual safety systems) appearing in the event trees that lead from individual initiating events to core damage. The fault trees provide a detailed characterization of the ways in which the individual safety systems might fail. The bottom events on the fault trees are failures of individual components that can be quantified. Once the fault trees are developed, the next step is to combine the event trees and fault trees (e.g. with the SETS program)[39] to obtain sequences of individual component failures, called minimal cut sets,[37] that lead from initiating events to core damage.

Each minimal cut set defines a set of accidents that involve similar failures at the individual component level rather than at the safety system level as with accident sequences. These sets can be represented by

$$MCS_1, MCS_2, \ldots, MCS_{nMCS} \quad (24)$$

where MCS_k is the set of accidents associated with the kth minimal cut set and $nMCS$ is the total number of minimal cut sets identified in the analysis. In practice, the accidents in the sets shown in eqn (24) are never fully identified; rather, the importance of these sets lies in the fact that the minimal cut sets were constructed in a way that makes it possible to calculate a frequency for each set MCS_k. For convenience in later discussions, the sets in eqn (24) will be referred to as minimal cut sets although, technically, a minimal cut set is a description for a sequence of failures rather than the set of accidents in which these failures actually occur. The Surry analysis for internally initiated accidents identified $nMCS =$ 2774 minimal cut sets for the accident sequences listed in Table 3. The most important of these cut set are listed in Table 5-1 of Ref. 38.

The outcome of identifying the minimal cut sets and calculating frequencies for the sets in eqn (24) can be represented by

$$\mathbf{fMCS} = \mathbf{fIE}\ \mathbf{P}(MCS \mid IE) \quad (25)$$

where

$$\mathbf{fMCS} = [fMCS_1, \ldots, fMCS_{nMCS}]$$

$fMCS_k$ = frequency (year^{-1}) for minimal cut set k

$$\mathbf{P}(MCS \mid IE) = \begin{bmatrix} p(MCS_1 \mid IE_1) & \cdots & p(MCS_{nMCS} \mid IE_1) \\ \vdots & & \vdots \\ p(MCS_1 \mid IE_{nIE}) & \cdots & p(MCS_{nMCS} \mid IE_{nIE}) \end{bmatrix}$$

where $p(MCS_k \mid IE_1)$ = the (conditional) probability that cut set k will occur given that initiating event i has occurred; all other symbols have been defined previously.

Each accident sequence AS_j is actually the union of one or more of the sets appearing in eqn (24). As a result, it is possible to obtain the matrix $\mathbf{P}(AS \mid IE)$ from the matrix $\mathbf{P}(MCS \mid IE)$. Specifically,

$$\mathbf{P}(AS \mid IE) = \mathbf{P}(MCS \mid IE)\ \mathbf{P}(AS \mid MCS) \quad (26)$$

where

$$\mathbf{P}(AS \mid MC) = \begin{bmatrix} p(AS_1 \mid MCS_1) & \cdots & p(AS_{nAS} \mid MCS_1) \\ \vdots & & \vdots \\ p(AS_1 \mid MCS_{nMCS}) & \cdots & p(AS_{nAS} \mid MCS_{nMCS}) \end{bmatrix}$$

$p(AS_j \mid MCS_k)$ = the (conditional) probability that accident sequence j will occur given that minimal cut set k has occurred

$$= \begin{cases} 1 & \text{if } MCS_k \subset AS_j \\ 0 & \text{otherwise} \end{cases}$$

and all other symbols have been previously defined.

The results in eqns (19) and (26) yield the following representation for the frequency of the accident sequences:

$$\mathbf{fAS} = \mathbf{fIE}\ \mathbf{P}(MCS \mid IE)\ \mathbf{P}(AS \mid MCS) \quad (27)$$

Further, when the dependency on $\mathbf{X}$ is added, this representation becomes

$$\mathbf{fAS(X)} = \mathbf{fIE(X)}\,\mathbf{P}(MCS \mid IE, \mathbf{X})\,\mathbf{P}(AS \mid MCS, \boldsymbol{X}) \quad (28)$$

The preceding decompositions are important because they provide a relation between minimal cut set frequency, which can be calculated directly, and accident sequence frequency, which cannot be calculated directly. As will now be illustrated, the Surry analysis used this decomposition to calculate the first quantitative risk goal shown in eqn (23).

The integrated analysis for internally-initiated accidents at Surry selected $nV = 41$ imprecisely known variables for inclusion in the accident frequency analysis (Ref. 9, Table 2.2-9) on the basis of results obtained in a sensititivity study involving a larger number of independent variables.[38] Latin hypercube sampling[32,33] was used to generate a sample of size $nS = 200$ from these variables; the general form of this sample is shown in eqn (13) As will be discussed later, this sample also contained variables from the accident progression and source term analyses.

The initiating events, minimal cut sets, and the accident sequences to which the minimal cut sets were assigned did not change during the analysis. Rather, the individual sample elements were used to recalculate the frequencies for the initiating events and minimal cut sets. The conceptual form of the analysis for each sample element $\mathbf{X}_s$ can be represented as

$$\begin{aligned}\mathbf{fAS}(\mathbf{X}_s) &= \mathbf{fIE}(\mathbf{X}_s)\,\mathbf{P}(MCS \mid IE, \mathbf{X}_s)\,\mathbf{P}(AS \mid MCS)\\ &= \mathbf{fIE}(\mathbf{X}_s)\,\mathbf{P}(AS \mid IE, \mathbf{X}_s) \qquad (29)\end{aligned}$$

The actual evaluation of the preceding expression was performed by the TEMAC program.[40,41]

Each sample element $\mathbf{X}_s$ yields a set $R(\mathbf{X}_s)$ of the form shown in eqn (22). Actually, these sets are somewhat simpler than the one shown in eqn (22) since IE_i, AS_j, nIE and nAS are fixed in the Surry analysis and do not change from sample element to sample element. Each set $R(\mathbf{X}_s)$ yields an estimate for the annual frequency of a severe accident of the following form:

$$fSA(\mathbf{X}_s) = \sum_{i=1}^{nIE} fIE_i(\mathbf{X}_s)\left[\sum_{j=1}^{nAS} p(AS_j \mid IE_i, \mathbf{X}_s)\right] \quad (30)$$

The distribution of these estimates is shown in Fig. 5.

An estimate for the expected value of the annual frequency of severe accidents can be obtained from the individual values shown in Fig. 5. Specifically,

$$E(fSA) \doteq \sum_{s=1}^{nS} fSA(\mathbf{X}_s)/nS = 4{\cdot}1 \times 10^{-5}\ \text{years}^{-1} \quad (31)$$

For internally initiated accidents at Surry, the preceding value of $4{\cdot}1 \times 10^{-5}$ year^{-1} is an approximation to the expected value appearing in the statement

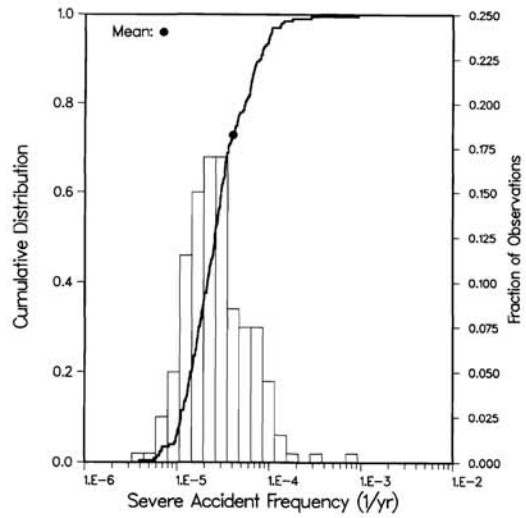

Fig. 5. Distribution of annual severe accident frequency due to accidents resulting from internal initiators at Surry (replotted from Ref. 9, Table 2.2-3).

of the first quantitative risk goal shown in eqn (23). Formally, this value is an approximation to the integral

$$E(fSA) = \int_{\Omega} \sum_{i=1}^{nIE} fIE_i(\mathbf{X})\left[\sum_{j=1}^{nAS} p(AS_j \mid IE_i, \mathbf{X})\right] p(\mathbf{X})\,\mathrm{d}\mathbf{X} \quad (32)$$

where Ω and p are, in essence, defined in Table 2.2-9 of Ref. 9. The mean (or expected) frequencies appearing in Tables 1 and 3 are obtained in a manner analogous to that shown in eqn (31).

The results presented in eqn (31) and elsewhere in this paper are for internally-initiated accidents only. A full calculation of the safety and quantitative risk goals requires the consideration of all accidents. However, the basic ideas in the necessary calculations are unchanged, and the results for internally-initiated accidents at Surry provide a tangible example of these calculations.

4 ACCIDENT PROGRESSION ANALYSIS

The accident progression analysis determines how severe accidents can progress from core damage to the release of radioactive material to the environment. This progression is typically studied with event tree techniques. Ultimately, the accident progression analyses will provide the information necessary to evaluate the second quantitative risk goal (QRG2) and also a link with the source term and consequence analyses that are required for the evaluation of the two safety goals (SG1 and SG2) and the third quantitative risk goal (QRG3).

The analysis performed for Surry provides a good

example of what a detailed accident progression analysis might entail. A detailed event tree was developed to represent accident progression. This tree had 71 questions. Further, some questions had more than two outcomes and other questions had outcomes that were functions of previous questions (Ref. 9, Chapter 2). Due to its size, it was not practical to evaluate this tree for every cut set or even every accident sequence. Therefore, the cut sets were formed into larger sets of accidents called plant damage states on the basis of the conditions that they presented to the accident progression analysis. The conditions considered in the development of the plant damage states are listed in Table 4. Initially, 25 plant damage states were developed. Then, these plant damage states were further grouped into the seven plant damage state groups shown in Table 5. These groups can be represented by

$$PDS_1, PDS_2, \ldots, PDS_{nPDS} \tag{33}$$

where $nPDS$ is the number of plant damage state groups (i.e. $nPDS = 7$) and each plant damage state group is composed of one or more of the minimal cut sets represented in eqn (24).

The frequencies for the plant damage state groups can be represented by

$$\begin{aligned} fPDS &= \mathbf{fIE}\,\mathbf{P}(PDS \mid IE) \\ &= \mathbf{fIE}\,\mathbf{P}(MCS \mid IE)\,\mathbf{P}(PDS \mid MCS) \end{aligned} \tag{34}$$

where

$$\mathbf{fPDS} = [fPDS_1, \ldots, fPDS_{nPDS}]$$

$fPDS_j$ = frequency (year^{-1}) for plant damage state group j

$$\mathbf{P}(PDS \mid IE) = \begin{bmatrix} p(PDS_1 \mid IE_1) & \cdots & p(PDS_{nPDS} \mid IE_1) \\ \vdots & & \vdots \\ p(PDS_1 \mid IE_{nIE}) & \cdots & \mathbf{p}(PDS_{nPDS} \mid IE_{nIE}) \end{bmatrix}$$

$p(PDS_j \mid IE_i)$ = the (conditional) probability that plant damage state group j will occur given that initiating event i has occurred

$$\mathbf{P}(PDS \mid MCS) = \begin{bmatrix} p(PDS_1 \mid MCS_1) & \cdots & \mathbf{p}(PDS_{nPDS} \mid MCS_1) \\ \vdots & & \vdots \\ p(PDS_1 \mid MCS_{nMCS}) & \cdots & \mathbf{p}(PDS_{nPDS} \mid MCS_{nMCS}) \end{bmatrix}$$

$p(PDS_j \mid MCS_k)$ = the (conditional) probability that plant damage state group j will occur given that minimal cut set k has occurred,

$$= \begin{cases} 1 & \text{if } MCS_k \subset PDS_j \\ 0 & \text{otherwise} \end{cases}$$

and all other symbols have been previously defined.

Table 4. Characteristics used to define plant damage states for pressurized water reactors in the NUREG-1150 PRAs (Ref. 9, Table 2.2-1) Abbreviations are defined in Table 2

1. Status of RCS at onset of core damage
   - T = no break (transient)
   - A = large break in the RCS pressure boundary
   - S_1 = medium break in the RCS pressure boundary
   - S_2 = small break in the RCS pressure boundary
   - S_3 = very small break in the RCS pressure boundary
   - G = steam generator tube rupture (SGTR)
   - H = SGTR with loss of secondary system integrity
   - V = large break in an interfacing system
2. Status of ECCS
   - B = operated in injection and now operating in recirculation
   - I = operated in injection only
   - R = not operating, but recoverable
   - N = not operating, not recoverable
   - L = LPIS available in both injection and recirculation modes
3. Containment heat removal
   - Y = operating or operable if/when initiated
   - R = not operating, but recoverable
   - N = never operated, not recoverable
   - S = sprays operable, but no CHR (no service water to heat exchangers)
4. AC power
   - Y = available
   - P = partially available
   - R = not available, but recoverable
   - N = not available, not recoverable
5. Contents of RWST
   - Y = injected into containment
   - R = not injected, but could be injected if power recovered
   - N = not injected, cannot be injected in the future
   - U = injected, but confined to upper compartment
6. Heat removal from the steam generators
   - X = at least one AFWS operating, SGs not depressurized
   - Y = at least one AFWS operating, SGs depressurized
   - S = S-AFWS failed at beginning, E-AFWS recoverable
   - C = S-AFWS operated until battery depletion, E-AFWS recoverable, SGs depressurized
   - D = S-AFWS operated until battery depletion, E-AFWS recoverable, SGs depressurized
   - N = no AFWS operating, no AFWS recoverable
7. Cooling for reactor coolant pump seals
   - Y = operating
   - R = not operating, but recoverable
   - N = not operating, not recoverable

Table 5. Plant damage state groups used in accident progression analysis for internally-initiated accidents at Surry (Ref. 9, Table 2.2-3).

Plant damage state group	Mean annual frequency (year^{-1})
Slow station blackout	$2{\cdot}2 \times 10^{-5}$
Loss of coolant accident (LOCA)	$6{\cdot}1 \times 10^{-5}$
Fast station blackout	$5{\cdot}4 \times 10^{-6}$
Interfacing system LOCA (Event V)	$1{\cdot}6 \times 10^{-6}$
Transients	$1{\cdot}8 \times 10^{-6}$
Anticipated transients without scram	$1{\cdot}4 \times 10^{-6}$
Steam generator tube rupture	$1{\cdot}8 \times 10^{-6}$

In the Surry analysis, the correspondence between plant damage state groups and minimal cut sets is fixed and does not change due to imprecisely known variables used in the analysis. Thus, when the sampled variables discussed in the preceding section are included, the representation for plant damage state group frequency becomes

$$\begin{aligned}\mathbf{fPDS}(\mathbf{X}_s) &= \mathbf{fIE}(\mathbf{X}_s)\,\mathbf{P}(PDS \mid IE, \mathbf{X}_s)\\ &= \mathbf{fIE}(\mathbf{X}_s)\,\mathbf{P}(MCS \mid IE, \mathbf{X}_s)\,\mathbf{P}(PDS \mid MCS)\end{aligned} \tag{35}$$

The mean frequencies appearing in Table 5 are obtained from the approximation

$$E(\mathbf{fPDS}) \approx \sum_{s=1}^{nS} \mathbf{fPDS}(\mathbf{X}_s)/nS \tag{36}$$

As comparison of eqns (30) and (36) shows, the only difference in the calculation of **fAS** and **fPDS** is the choice of the transition matrices $\mathbf{P}(AS \mid MCS)$ and $\mathbf{P}(PDS \mid MCS)$.

In the Surry analysis, the accident progression event tree was evaluated with the EVNTRE program[42] for each plant damage state group. Due to the size of the tree, it was not possible to save every path through it for subsequent source term and consequence analysis. Rather, the accidents associated with these paths were formed into groups called accident progression bins on the basis of conditions required in the source term analysis. These conditions are listed in Table 6. In essence, every vector of values for the 11 characteristics listed in Table 6 defines a set of accidents (i.e. all accidents for which those particular 11 values are satisfied) that present similar conditions to the source term analysis. To avoid having to save the tremendous number of paths through the tree for each plant damage state group, the probabilities associated with the individual accident progression bins are accumulated as the tree is evaluated without saving the paths themselves.

The accident progression analysis has two outcomes of interest here. The first outcome is a sequence of accident progression bins

$$APB_1, APB_2, \ldots, APB_{nAPB} \tag{37}$$

where $nAPB$ is the number of accident progression bins identified in the analysis. Further, associated with each accident progression bin is a vector

$$\mathbf{cAPB}_k = [cAPB_{k1}, \ldots, cAPB_{k.11}], \quad k = 1, \ldots, nAPB \tag{38}$$

that lists the values for the 11 characteristics in Table 6 which define the bin. The second outcome is a matrix $\mathbf{P}(APB \mid PDS)$ such that

$$\mathbf{fAPB} = fPDS\,\mathbf{P}(APB \mid PDS) \tag{39}$$

Table 6. Accident progress bin characteristics used in Surry analysis (Ref. 9, Section 2.4.2). Abbreviations are defined in Table 2

Characteristic 1—Containment failure time
- A Event V, break location not submerged.
- B Event V, break location submerged.
- C Containment failure before VB.
- D Containment failure at VB.
- E Late or very late containment failure (during CCI, nominally several hours after VB).
- F Containment failure in the final period (nominally about 24 h after VB).
- G No containment failure.

Characteristic 2—Sprays
- A The sprays operate only in the early period.
- B The sprays operate only in the early and intermediate periods.
- C The sprays operate only in the early, intermediate, and late periods.
- D The sprays always operate during the periods of interest for fission product removal.
- E The sprays operate only in the late period.
- F The sprays operate in the late and very late periods.
- G The sprays operate only in the very late period.
- H The sprays never operate during the accident, or operate only during the final period, which is not of interest for fission product removal.

Characteristic 3—Core–concrete interactions
- A CCI takes place promptly following VB. There is no overlaying water pool to scrub the releases.
- B CCI takes place promptly following VB. There is a shallow (about 4·5 ft) overlaying water pool to scrub the releases.
- C CCI does not take place.
- D CCI takes place promptly following VB. There is a deep (about 14 ft) overlying water pool to scrub the releases.
- E CCI takes place after a short delay. The debris bed is coolable, but the water in the cavity is not replenished. The delay is the time needed to boil off the accumulator water.
- F CCI takes place after a long delay. The debris bed is coolable, but the water in the cavity is not replenished. The delay is the time needed to boil off the water in a full cavity.

Characteristic 4—RCS pressure before vessel breach
- A System setpoint pressure (2 500 psia).
- B High pressure (1 000 to 2 000 psia).
- C Intermediate pressure (200 to 1000 psia).
- D Low pressure (less than 200 psia).

Characteristic 5—Mode of vessel breach
- A HPME occurs—direct heating always occurs to some extent.
- B The molten core pours out of the vessel, driven primarily by the effects of gravity.
- C Gross failure of a large portion of the bottom head of the vessel occurs, perhaps as a result of a circumstantial failure.
- D An alpha mode failure occurs resulting in containment failure as well as vessel failure.
- E A rocket mode failure occurs resulting in containment failure as well as vessel failure.
- F No vessel breach occurs.

Characteristic 6—Steam generator tube rupture
- A A SGTR occurs. The SRVs on the secondary system are not stuck open.
- B A SGTR occurs. The SRVs on the secondary system are stuck open.

Table 6.—*Continued*

C A SGTR does not occur.

Characteristic 7—Amount of core not in HPME available for CCI

A A CCI occurs and involves a large amount of the core (70–100%)

B A CCI occurs and involves a medium amount of the core (30–70%)

C A CCI occurs and involves a small amount of the core (0–30%)

D No CCI occurs.

Characteristic 8—Zirconium oxidation

A A low amount of the core zirconium was oxidized in the vessel prior to vessel breach. This implies a range from 0 to 40% oxidized, with a nominal value of 25%.

B A high amount of the core zirconium was oxidized in the vessel before VB. This implies that more than 40% of the zirconium was oxidized, with a nominal value of 65%.

Characteristic 9—High pressure melt ejection (HPME)

A A high fraction (>40%) of the core was ejected under pressure from the vessel at failure.

B A moderate fraction (20–40%) of the core was ejected under pressure from the vessel at failure.

C A low fraction (<20%) of the core was ejected under pressure from the vessel at failure.

D There was no HPME at vessel failure.

Characteristic 10—Containment failure size

A The containment failed by catastrophic rupture, resulting in a very large hole and gross structural failure.

B The containment failed by the development of a large hole or rupture; nominal hole size is 7 ft^2.

C The containment failed by the development of a leak (nominal size 0·1 ft^2) or BMT.

D The containment did not fail. It may have been bypassed.

Characteristic 11—Holes in the RCS

A There is only one large hole in the RCS following vessel breach, so there is no effective natural circulation through the RCS after breach.

B There are two large holes in the RCS following vessel breach, so there will be effective natural circulation through the RCS after breach.

1 foot = 0·3048 m
1 $foot^2$ = 0·0929 m^2
1 psia = $6{\cdot}895 \times 10^3$ Pa

where

$$\mathbf{fAPB} = [fAPB_1, \ldots, fAPB_{nAPB}]$$

$fAPB_k$ = frequency ($year^{-1}$) for accident progression bin k

$$\mathbf{P}(APB \mid PDS) = \begin{bmatrix} p(APB_1 \mid PDS_1) & \cdots & \mathbf{p}(APB_{nAPB} \mid PDS_1) \\ \vdots & & \vdots \\ p(APB_1 \mid PDS_{nPDS}) & \cdots & \mathbf{p}(APB_{nAPB} \mid PDS_{nPDS}) \end{bmatrix}$$

$p(APB_k \mid PDS_j)$ = the (conditional) probability that accident progression bin k will occur given that plant damage state j has occurred

and **fPDS** has been defined previously.

Many of the variables required in the accident progression analysis are imprecisely known. For the Surry analysis, $nV = 49$ such variables were identified for inclusion in the integrated study for internally-initiated accidents (Ref. 9, Table 2.3-2). These variables were included in the same sample of size $nS = 200$ discussed in the preceding section, and the accident progression analysis was performed with the EVNTRE program for each sample element. The result was a group of outcomes of the form discussed in the preceding paragraph for each sample element. Both the individual accident progression bins and the total number of accident progression bins varied from sample element to sample element. For the analysis over all sample elements, $nAPB$ varied from 54 to 157, the number of unique accident progression bins was 1906, and the total number of accident progression bins was 18 591. When this dependency is included, eqn (39) becomes

$$\mathbf{fAPB}(\mathbf{X}) = fPDS(\mathbf{X})\, \mathbf{P}(APB \mid PDS, \mathbf{X}) \quad (40)$$

where the vector $\mathbf{X}$ represents imprecisely known variables and other notation associated with eqn (39) can be modified in a similar manner to represent a dependency on $\mathbf{X}$.

With the representation for risk given in eqn (5) the results of a PRA carried through the accident progression analysis can be expressed as

$$R = \{(PDS_j, fPDS_j, [p(APB_1 \mid PDS_j), \ldots, p(APB_{nAPB} \mid PDS_j)]) \quad j = 1, \ldots, nPDS\} \quad (41)$$

When the dependency on $\mathbf{X}$ is included for the Surry analysis, this representation becomes

$$R(\mathbf{X}) = \{(PDS_j, fPDS_j(\mathbf{X}), [p(APB_1(\mathbf{X}) \mid PDS_j, \mathbf{X}), \ldots, p(APB)_{nAPB(\mathbf{X})}(\mathbf{X}) \mid PDS_j, \mathbf{X})]), \quad j = 1, \ldots, nPDS\} \quad (42)$$

Propagation of the sample through the accident frequency and accident progression analyses yielded 200 sets of results of the form shown in eqn (42).

The second quantitative risk goal (i.e. QRG2) involves the risk results shown in eqn (42). Specifically, the second goal requires that

$$E\left[\frac{\sum_{k \in S(\mathbf{X})} \sum_{j=1}^{nPDS} fPDS_j(\mathbf{X}) p(APB_k(\mathbf{X}) \mid PDS_j, \mathbf{X})}{\sum_{j=1}^{nPDS} fPDS_j(\mathbf{X})}\right] < 0{\cdot}1 \quad (43)$$

where $S(\mathbf{X})$ denotes the set such that $k \in S(\mathbf{x})$ only if accident progression bin k involves both a severe accident and containment failure in the sense intended for use with this goal.

The set $S(\mathbf{X})$ can be defined in several ways depending on exactly what is intended by the second

quantitative risk goal, including

$$S_1(\mathbf{X}) = \{k: cAPB_{kl} \neq G \text{ or } cAPB_{k6} = A \text{ or } B\} \quad (44)$$

$$S_2(\mathbf{X}) = \{k: cAPB_{k,10} = A \text{ or } B\} \quad (45)$$

and

$$S_3(\mathbf{X}) = \{k: cAPB_{k5} \neq F \text{ and } cAPB_{k,10} = A \text{ or } B\} \quad (46)$$

where the symbol $cAPB_{kl}$ is introduced in conjunction with eqn (38) and represents values for accident progression bin characteristics listed in Table 6. The set $S_1(\mathbf{X})$ designates all accident progression bins in which the containment fails (by a leak, rupture or catastrophic rupture), or a containment bypass occurs, or a steam generator tube rupture occurs. The set $S_2(\mathbf{X})$ designates all accident progression bins in which the containment fails by a rupture or a catastrophic rupture. The set $S_3(\mathbf{X})$ designates all accident progression bins in which the vessel fails and the containment fails by a rupture or a catastrophic rupture. The following ordering exists:

$$S_3(\mathbf{X}) \subset S_2(\mathbf{X}) \subset S_1(\mathbf{X}) \quad (47)$$

Other possibilities for $S(\mathbf{X})$ for use in the second quantitative risk goal also exist. For the Surry analysis, the sets S_2 and S_3 were the same.

Figure 6 shows the distributions of conditional containment failure probability that result from the use of S_1, S_2 and S_3, respectively, for S in the expression shown in eqn (43). Further, the mean value for conditional probability of containment failure corresponding to S_1, S_2 and S_3 are $8{\cdot}6 \times 10^{-3}$, $2{\cdot}4 \times 10^{-3}$ and $2{\cdot}4 \times 10^{-3}$, respectively. As discussed previously, these means are produced by summing over the sample and dividing by the sample size, and are approximations to the integrals used to define expected value.

The second quantitative risk goal as stated in eqn (43) is for containment failure conditional on core damage. A more restrictive, and possibly more meaningful, formulation of this risk goal would be for containment failure to be conditional on vessel failure. In this case, the second quantitative risk goal would require that

$$E\left(\frac{\sum_{k \in SC(\mathbf{X})} \sum_{j=1}^{nPDS} fPDS_j(\mathbf{X}) p(APB_k(\mathbf{X}) \mid PDS_j, \mathbf{X})}{\sum_{k \in SV(\mathbf{X})} \sum_{j=1}^{nPDS} fPDS_j(\mathbf{X}) p(APB_k(\mathbf{X}) \mid PDS_j, \mathbf{X})}\right) < 0{\cdot}1 \quad (48)$$

where $SV(\mathbf{X})$ denotes the set such that $k \in SV(\mathbf{X})$ only if accident progression bin k involves vessel breach and $SC(\mathbf{X})$ denotes the set such that $k \in SC(\mathbf{X})$ only if accident progression bin k involves both vessel breach and containment failure.

The set $SC(\mathbf{X})$ can be defined in several ways, including

$$SC_1(\mathbf{X}) = S_1(\mathbf{X}) \cap SV(\mathbf{X}) \quad (49)$$

$$SC_2(\mathbf{X}) = S_2(\mathbf{X}) \cap SV(\mathbf{X}) \quad (50)$$

and

$$SC_3(\mathbf{X}) = S_3(\mathbf{X}) \cap SV(\mathbf{X}) \quad (51)$$

where

$$SV(\mathbf{X}) = \{k: cAPB_{k^5} \neq F\} \quad (52)$$

The distributions for conditional containment failure probability that result from the use of SC_1, SC_2

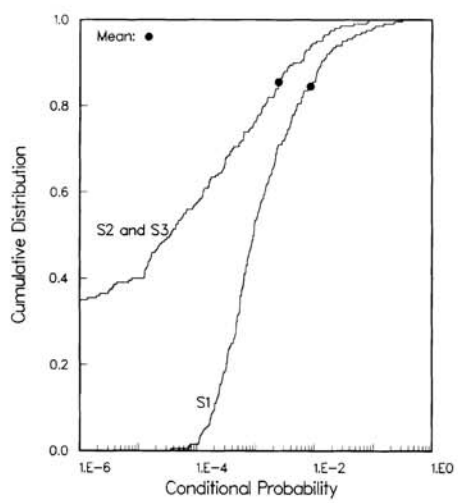

Fig. 6. Distribution of conditional probability of containment failure for accidents resulting from internal initiators at Surry (plotted from results obtained in analysis described in Ref. 9).

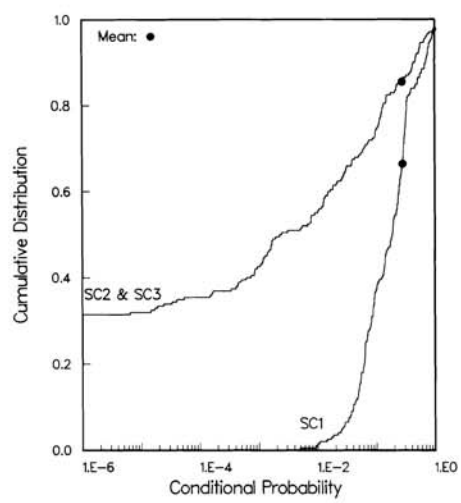

Fig. 7. Distribution of conditional probability of containment failure given vessel breach for accidents resulting from internal initiators at Surry (plotted from results obtained in analysis described in Ref. 9).

and SC_3 for SC in eqn (48) are shown in Fig. 7. Further, the mean values for conditional probability of containment failure corresponding to SC_1, SC_2 and SC_3 are 0·283, 0·279 and 0·279, respectively.

5 SOURCE TERM ANALYSIS

The source term analysis provides estimates of the radioactive releases that could occur due to the accidents identified in the accident progression analysis. If a limited number of accidents is under consideration, then it may be possible to estimate source terms for them with detailed programs such as STCP,[43] CONTAIN,[44] and MELCOR.[45] However, in practice, it is not possible to perform a detailed analysis for every accident. Two possibilities exist to deal with this problem. The first is to group the accidents in a small number of source term groups (on the order of 10) and then perform a single very detailed calculation for each group. The second is to use many sources of information and an appropriately defined algorithm to assign a source term to every accident progression bin identified in the accident progression analysis.

The second approach was used in the NUREG-1150 PRAs and will be used for illustration here. This approach consisted of three parts. In the first part, a database on severe accident source terms was developed for each plant considered in the study. This database was constructed from many sources of information, including experimental data, observational data, mechanistic code calculations, and theoretical derivations. Expert judgment played an important role in the assembly of a diverse body of knowledge into this database. In the second part, a correspondence or mapping was developed between the accident progression bin characteristics (e.g. see Table 6) and the information contained in the database. In the third part, an algorithm was written to develop source terms for the individual accident progression bins. This algorithm used the definition of the accident progression bins (see eqn (38) and Table 6) to identify appropriate information in the database and then to construct source terms from this information. This algorithm was implemented in a program called XSOR for an arbitrary plant[46] and SURSOR for the Surry analysis (Ref. 9, Chapter 3).

Many of the variables incorporated into the source term database for the NUREG-1150 PRAs are imprecisely known. For the Surry analysis, $nV = 12$ such variables were identified for inclusion in the integrated study (Ref. 9, Table 3.2-2). These variables were included in the same sample of size $nS = 200$ discussed in the preceding sections for the accident frequency and accident progression analyses. Actually, the 12 variables indicated in Table 3.2-2 of Ref. 9 are pointers to families of related source term variables. The total number of individual source term variables included in the analysis was several hundred.

In the NUREG-1150 PRAs, each source term is a vector of the form

$$\mathbf{ST} = [TW,\ T1,\ DT1,\ T2,\ DT2,\ ELEV,\ E1,\ (ST1_i,\ i = 1, \ldots, 9),\ E2,\ (ST2_i,\ i = 1, \ldots, 9)] \quad (53)$$

where

TW = time (s) at which warning is given (time 0 is taken to be scram time),
$T1$ = time (s) at which the first release segment begins,
$DT1$ = length (s) of the first release segment,
$T2$ = time (s) at which the second release segment begins,
$DT2$ = length (s) of second release segment,
$ELEV$ = elevation (m) of release,
$E1$ = energy release rate (J/s = W) during first release segment,
$ST1_i$ = release fraction for release class i, $i = 1, \ldots, 9$, in the first release segment (1, noble gas; 2, iodine; 3, cesium; 4, tellurium; 5, strontium; 6, ruthenium; 7, lanthanum; 8, cerium; 9, barium),
$E2$ = same as $E1$ but for the second release segment,
$ST2_i$ = same as $ST1_i$ but for the second release segment.

A source term was estimated for each accident progression bin. Thus, for example, 18 591 source terms were estimated in the analysis for internally-initiated accidents at Surry. Each source term was a function of the imprecisely known variables indicated in the preceding paragraph. Thus, a sequence

$$\mathbf{ST}_k(\mathbf{X}_s), \quad k = 1, \ldots, nAPB(\mathbf{X}_s) \quad (54)$$

of source terms was obtained for each sample element $\mathbf{X}_s$.

With the representation for risk given in eqn (5), the results of a PRA carried through the source term analysis (i.e. a level 2 PRA) can be expressed as

$$R = \{(APB_k, fAPB_k, \mathbf{ST}_k), \quad k = 1, \ldots, nAPB\} \quad (55)$$

When the dependency on $\mathbf{X}$ is included, this representation becomes

$$R(\mathbf{X}) = \{(APB_k(\mathbf{X}), fAPB_k(\mathbf{X}), ST_k(\mathbf{X})), \quad k = 1, \ldots, nAPB(\mathbf{X})\} \quad (56)$$

Propagation of the sample through the accident frequency, accident progression and source term analyses yields 200 sets of results of the form shown in eqn (56).

None of the safety goals or quantitative risk goals

are expressed in a form that uses the results of the source term analysis directly. The third quantitative risk goal (i.e. QRG3) requires that the expected frequency for a large release be less than 1×10^{-6} year^{-1}. However, the definition of a large release is expressed in terms of early fatalities. Thus, a consequence analysis must be performed before this frequency can be calculated.

Although the source terms are not used directly in the safety and quantitative risk goals, it is useful to examine them to determine the size and frequency of possible releases to the environment. This can be done with exceedance frequency curves as discussed in conjunction with eqn (6). For example, risk results of the form shown in eqn (56) can be used to generate an exceedance frequency curve for each radionuclide release class and each sample element. Figure 8 shows the 200 exceedance frequency curves that result for iodine for internally-initiated accidents at Surry. The release fraction appearing on the abscissa of Fig. 8 is the sum of the release fractions for the first and second release segments shown in eqn (56).

The large number of accident progression bins, and hence source terms, identified in the NUREG-1150 PRAs made it impractical to perform a consequence calculation for every source term. Therefore, a partitioning procedure[47,48] was used to group source terms on the basis of the conditions that they supplied to the consequence analysis. The final outcome of this procedure was a sequence

$$\mathbf{mST}_1, \mathbf{mST}_2, \ldots, \mathbf{mST}_{nSTG} \tag{57}$$

of frequency-weighted mean source terms and criteria for assigning individual source terms, and hence accident progression bins, to these mean source terms. The sets of accidents assigned to these mean source terms are called source term groups and are denoted by

$$STG_1, STG_2, \ldots, STG_{nSTG} \tag{58}$$

The membership in the preceding sets can change depending on the values assumed by imprecisely known variables (i.e. $\mathbf{X}$). Specifically, the same accident progression bin can be assigned to a different source term $\mathbf{mST}_l$, and hence a different set STG_l, for different values of $\mathbf{X}$. In contrast, the partitioning procedure used all source terms at one time to construct the mean source terms $\mathbf{mST}_l$ and the criteria

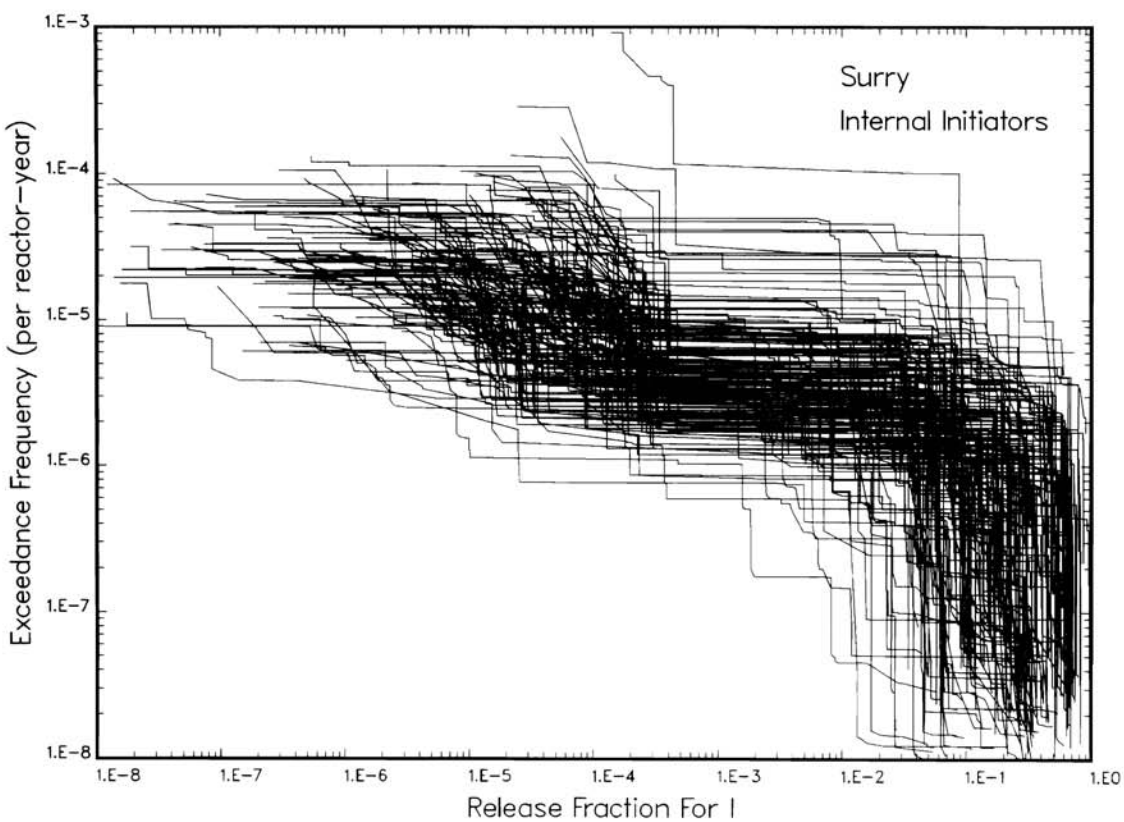

Fig. 8. Exceedance frequency curves for iodine release fractions due to accidents resulting from internal initiations at Surry (Ref. 9, Figure B.3-1).

for assigning individual source terms to the $\mathbf{mST}_l$. As an example, the 18 591 source terms calculated for internally-initiated accidents at Surry were partitioned into $nSTG = 54$ source term groups.

The frequencies for the source term groups can be represented by

$$\mathbf{fSTG} = \mathbf{fAPB}\ \mathbf{P}(STG \mid APB) \tag{59}$$

where

$$\mathbf{fSTG} = [fSTG_1, \ldots, fSTG_{nSTG}]$$

$fSTG_l$ = frequency (year^{-1}) for source term group l,

$$\mathbf{P}(STG \mid APB) = \begin{bmatrix} p(STG_l \mid APB_1) & \cdots & p(STG_{nSTG} \mid APB_1) \\ \vdots & & \vdots \\ p(STG_l \mid APB_{nAPB}) & \cdots & p(STG_{nSTG} \mid APB_{nAPB}) \end{bmatrix}$$

$p(STG_l \mid APB_k)$ = the (conditional) probability that source term group l will occur given that accident progression bin k has occurred

$$= \begin{cases} 1 & \text{if } APB_k \subset STG_l \\ 0 & \text{otherwise} \end{cases}$$

and **fAPB** is defined in eqn (39). When the dependency on **X** is included, the representation for **fSTG** becomes

$$\mathbf{fSTG(X)} = \mathbf{fAPB(X)}\ \mathbf{P}(STG \mid APB, \mathbf{X}) \tag{60}$$

with the other notation associated with eqn (59) being altered in a similar manner. Due to the sampling of source term variables, it is possible for the same accident progression bin to be assigned to different source term groups for different sample elements.

Once the source term partitioning is completed, the results of the source term analysis can be represented by

$$R(\mathbf{X}) = \{(STG_l(\mathbf{X}), fSTG_l(\mathbf{X}), \mathbf{mST}_l), \quad l = 1, \ldots, nSTG\} \tag{61}$$

This is the risk representation shown in eqn (5) and constitutes the actual link between the source term analysis and the consequence analysis. A sample of size $nS = 200$ is used in the Surry analysis to study the effects of imprecisely known variables. This results in 200 sets $R(\mathbf{X}_s)$ of the form shown in eqn (61). In each set, $STG_l(\mathbf{X}_s)$ and $fSTG_l(\mathbf{X}_s)$ change as a function of the sample element $\mathbf{X}_s$. However, $\mathbf{mST}_l$ and $nSTG$ remain fixed due to their construction from a pooling of the source term results from all sample elements.

6 CONSEQUENCE ANALYSIS

The consequences analysis provides estimates of the health and economic impacts that could occur as the result of radioactive releases to the environment. The starting points for the consequence analysis are the source terms identified in the source term analysis. In the NUREG-1150 PRAs, the MACCS program[49–52] was used to perform a detailed consequence calculation for each source term indicated in eqn (57).

Since the weather at the time of an accident can have a large effect on off-site consequences, reactor accident consequence calculations typically use site-specific weather data. These data can be characterized by vectors of the form

$$\mathbf{p}(WT \mid STG_l) = [p(WT_1 \mid STG_l), \ldots, p(WT_{nWT} \mid STG_l)] \tag{62}$$

where

$p(WT_m \mid STG_l)$ = the (conditional) probability that an accident involving weather type m will occur given that an accident in source term group l has occurred,

WT_m = set of all accidents that occur in conjunction with weather type m, and

nWT = number of weather types.

For the NUREG-1150 PRAs, $nWT = 2560$ and results from the use of 40 weather categories, 16 wind directions, and 4 variants within each weather category.

Expression (62) is stated for source term groups to be consistent with the NUREG-1150 analysis being used for illustration. However, if the consequence analysis was being performed for individual source terms, then the probabilities would be conditional on the occurrence of these source terms. Most PRAs including those performed for NUREG-1150 assume there is no relationship between source terms and weather. Thus, while a distribution of weather is considered, no correlation between weather and source term is assumed. This assumption is equivalent to assuming that the vector $\mathbf{p}(WT \mid STG_l)$ is independent of STG_l. In reality, there may be a dependence between weather and source term. For example, station blackouts are thought to be more likely during some types of weather than others.

The vectors $\mathbf{p}(WT \mid STG_l)$ appearing in eqn (62) can be used with the source term group frequencies in eqn (60) to determine the frequency at which accidents involving individual weather types occur in conjunction with individual source term groups. Specifically,

$$\mathbf{fWT} = \mathbf{fSTG}\ \mathbf{P}(WT \mid STG) \tag{63}$$

where

$$\mathbf{fWT} = [\mathbf{fWT}_1, \ldots, \mathbf{fWT}_{nSTG}]$$

$$\mathbf{fWT}_l = [\mathbf{fWT}_{l1}, \ldots, fWT_{l,nWT}]$$

fWT_{lm} = frequency (year^{-1}) at which an accident involving weather type m occurs in conjunction with source term group l

and

$$\mathbf{P}(WT \mid STG) = \begin{bmatrix} \mathbf{p}(WT \mid STG_1) & 0 & \cdots & 0 \\ 0 & \mathbf{p}(WT \mid STG_2) & \cdots & 0 \\ \vdots & \vdots & & \vdots \\ 0 & 0 & \cdots & \mathbf{p}(WT \mid STG_{nSTG}) \end{bmatrix}$$

The elements of **fWT** and $\mathbf{P}(WT \mid STG)$ are vectors. Each vector in **fWT** contains the frequencies at which accidents involving specific weather types occur in conjunction with a particular source term group.

A consequence calculation is performed for each weather type and each source term group. Conceptually, this is equivalent to performing a single consequence calculation for all accidents in each set

$$STG_l \cap WT_m \text{ for } l = 1, \ldots, nSTG \text{ and } m = 1, \ldots, nWT$$

The results of this calculation can be represented in two ways. The first way is with a vector of the form

$$\mathbf{cWT}_{lm} = [cWT_{lm1}, \ldots, cWP_{lm,nC}] \quad (64)$$

where cWT_{lmn} is the value for consequence measure n calculated for source term group l and weather type m and nC is the total number of consequence measures being calculated. The second way is with a vector of the form

$$\mathbf{cSTG}_{ln} = [cSTG_{l1n}, \ldots, cSTG_{l,nWT,n}] \quad (65)$$

where $cSTG_{lmn}$ is the value for consequence measure n calculated for source term group l and weather type m. Equation (64) organizes consequence results by weather type and source term group while eqn (65) organizes consequence results by source term group and individual consequence measure.

When consequence results are presented conditional on the occurrence of source term groups (or individual source terms), the individual consequence results shown in eqn (65) are usually used. Specifically, the pairs

$$(cSTG_{lmn}, p(WT_m \mid STG_l)),\ m = 1, \ldots, nWT \quad (66)$$

are used to construct an exceedance probability curve for each source term group and each consequence result of interest as indicated in conjunction with eqn (6). As these curves are conditional on the occurrence of a source term group, the ordinate displays conditional probabilities of exceedance. Figures 9–11 display exceedance curves of this type (also called complementary cumulative distribution functions or CCDFs) for the source term groups generated in the analysis for internally-initiated accidents at Surry and the consequence measures number of early fatalities, individual early fatality probability within 1609·3 m (1 mi) and individual latent cancer fatality probability within 16 093 m (10 mi). The last two consequence results were referred to as individual early fatality risk and individual latent cancer fatality risk in the NUREG-1150 PRAs (e.g. see Ref. 9, Fig. 4.3-1). These results are the conditional probability of becoming a fatality given that specified conditions exist and thus are more appropriately referred to as probabilities than as risks.

When consequence results are presented with the representation for risk given in eqn (5), the individual consequence results shown in eqn (64) are used. In this case, the representation for risk from a PRA carried through consequence analysis (i.e. a level 3 PRA) is

$$R = \{(STG_l \cap WT_m, fWT_{lm}, cWT_{lm}),\ l = 1, \ldots, nSTG,\ m = 1, \ldots, nWT\} \quad (67)$$

In practice, every term appearing in the preceding expression depends on imprecisely known variables. In the NUREG-1150 PRAs, imprecisely known variables were incorporated into the accident frequency, accident progression and source term analyses. However, such variables were not considered in the consequence analysis. When this is incorporated into the notation, the representation for risk becomes

$$R(\mathbf{X}) = \{(STG_l(\mathbf{X}) \cap WT_m(\mathbf{X}), fWT_{lm}(\mathbf{X}), cWT_{lm}),\ l = 1, \ldots, nSTG,\ m = 1, \ldots, nWT\} \quad (68)$$

Due to the use of a sample of size $nS = 200$ in the Surry analysis, 200 sets of the preceding form were generated.

As discussed in conjunction with eqn (6), exceedance frequency curves can be used to summarize the results contained in these sets. Examples of such curves from the Surry analysis for internally-initiated accidents appear in Figs 2, 12 and 13. The construction of these curves used the conditional results shown in Figs 9–11. The results appearing in Figs 2, 12 and 13 can also be summarized in the form shown in Figs 4, 14 and 15.

As discussed in conjunction with eqn (7), it is also possible to obtain annual risks from the representations given in eqns (67) and (68). This is equivalent to reducing each of the curves in Figs 2, 12 and 13 to a single number. Specifically, annual risk is given by

$$\mathbf{rC} = \mathbf{fWT}\ \mathbf{C}(WT, STG) \quad (69)$$

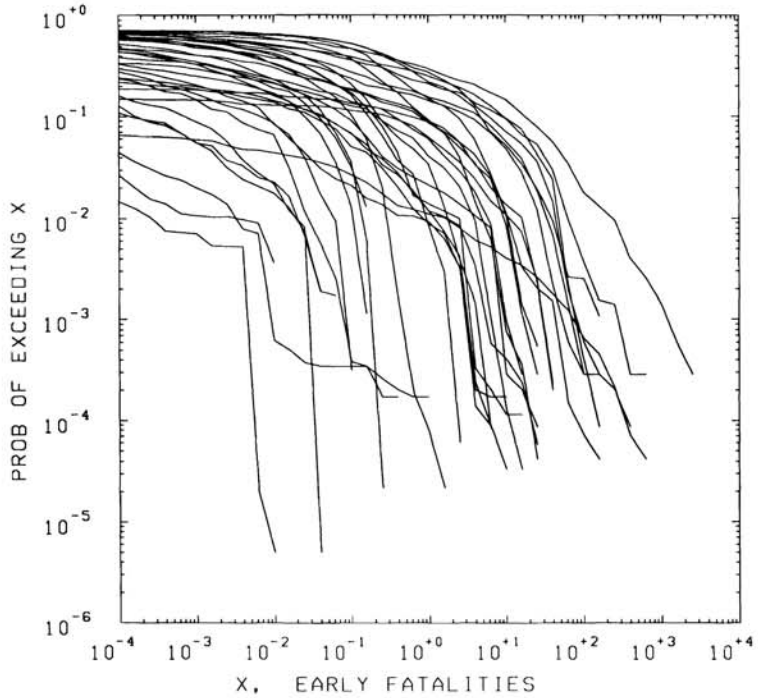

Fig. 9. Exceedance probability curves for early fatalities due to accidents resulting from internal initiators at Surry (Ref. 9, Figure 4.3-1). Each curve is conditional on the occurrence of a source term group.

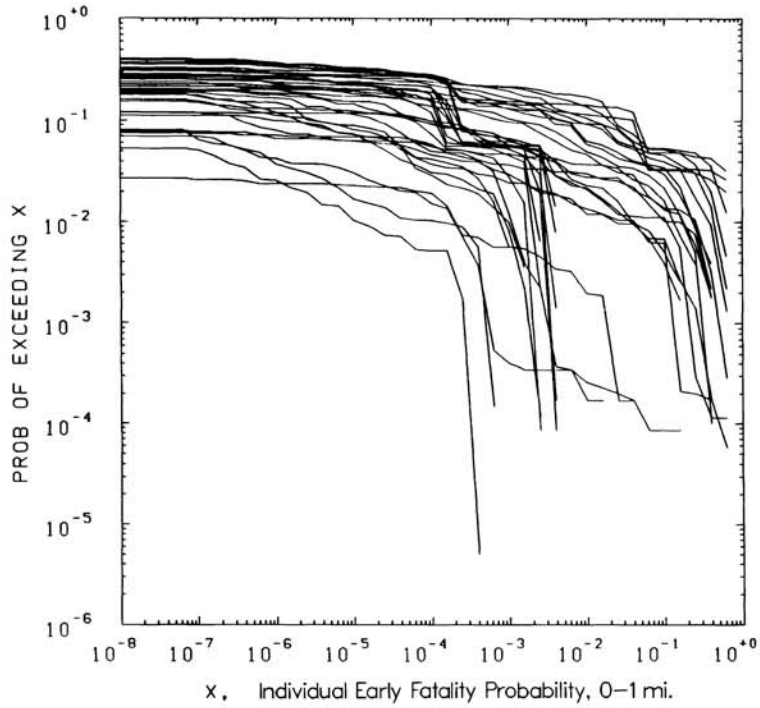

Fig. 10. Exceedance probability curves for individual early fatality probability within 1 mile = 1609·3 m (1 mi) of the site boundary due to accidents resulting from internal initiators at Surry (Ref. 9, Fig. 4.3-1). Each curve is conditional on the occurrence of one source term group.

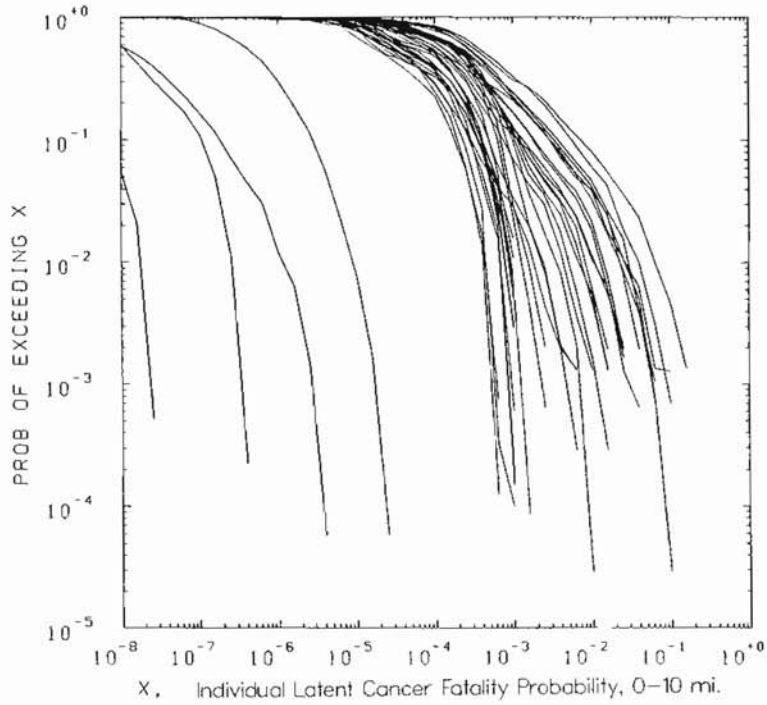

Fig. 11. Exceedance probability curves for individual latent fatality probability within 10 mi = 16 093 m (10 mi) of the site boundary due to accidents resulting from internal initiators at Surry (Ref. 9, Fig. 4.3-1). Each curve is conditional on the occurrence of one source term group.

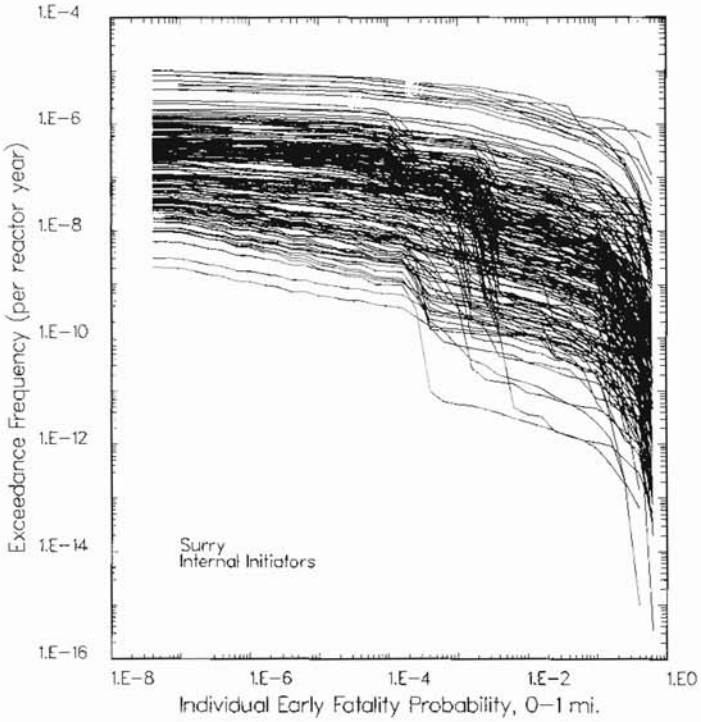

Fig. 12. Exceedance frequency curves for individual early fatality probability within 1 mi = 1609·3 m (1 mi) of the site boundary due to accidents resulting from internal initiators at Surry (Ref. 9, Fig. D.5). Each curve corresponds to one sample element.

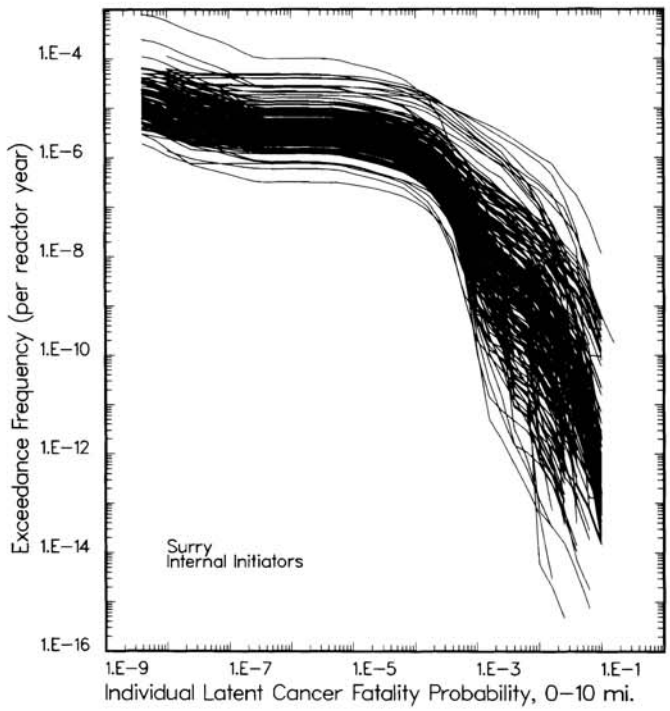

Fig. 13. Exceedance frequency curves for individual latent cancer fatality probability within 10 mi = 16 903 m (10 mi) of the site boundary due to accidents resulting from internal initiators at Surry (Ref. 9, Fig. D.6). Each curve corresponds to one sample element.

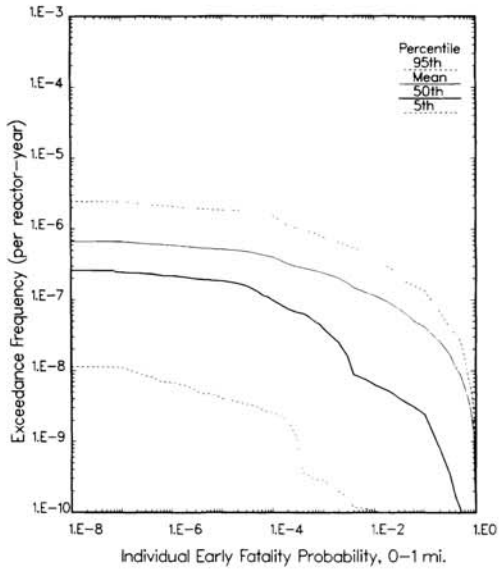

Fig. 14. Mean and percentile curves for exceedance frequencies for individual early fatality probability within 1 mi = 1609·3 m (1 mi) of the site boundary due to accidents resulting from internal initiators at Surry (Ref. 9, Fig. 5.1-1).

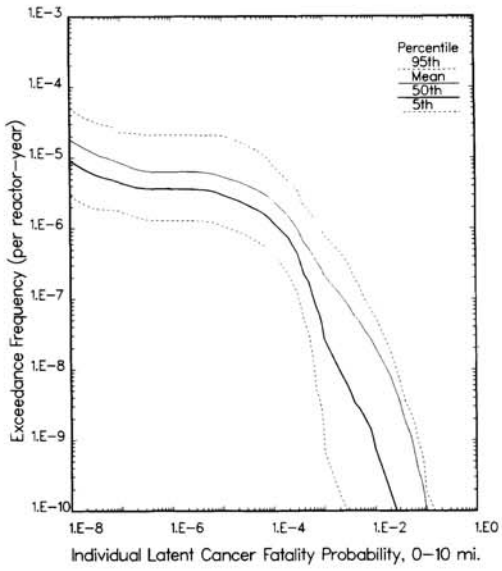

Fig. 15. Mean and percentile curves for exceedance frequencies for individual latent cancer fatality probability within 10 mi = 16 093 m (10 mi) of the site boundary due to accidents resulting from internal initiators at Surry (Ref. 9, Fig. 5.1-1).

where

$$\mathbf{rC} = [rC_1, \ldots, rC_{nC}]$$

rC_n = annual risk (consequence/year) for consequence measure n

$$\mathbf{C}(WT, STG) = \begin{bmatrix} \mathbf{cSTG}_{11}^T & \cdots & \mathbf{cSTG}_{1,nC}^T \\ \vdots & & \vdots \\ \mathbf{cSTG}_{nSTG,1}^T & \cdots & \mathbf{cSTG}_{nSTG,nC}^T \end{bmatrix}$$

Further, $\mathbf{fWT}$ and $\mathbf{cSTG}_{ln}$ are defined in eqns (63) and (65), respectively, and the superscript T appearing in the definition of $\mathbf{C}(WT, STG)$ is used to denote the transpose of the associated vector. When a dependency on imprecisely known variables is added, eqn (69) becomes

$$\mathbf{rC}(\mathbf{X}) = \mathbf{fWT}(\mathbf{X})\, \mathbf{C}(WT, STG, \mathbf{X}) \qquad (71)$$

In the NUREG-1150 PRAs, $\mathbf{C}(WT, STG)$ was not a function of imprecisely known variables since such variables were not considered in the consequence analysis.

The sample of size $nS = 200$ being used in the Surry analysis produced 200 annual risk estimates of the form shown in eqn (70). Figures 3, 16 and 17 give examples of the distributions of annual risk that resulted from this sample. Further, the mean values of the distributions appearing in Figs 3, 16 and 17 are $2{\cdot}0 \times 10^{-6}$ fatalities/year, $1{\cdot}6 \times 10^{-8}$ year^{-1} and $1{\cdot}7 \times 10^{-9}$ year^{-1}, respectively.

The two safety goals (i.e. SG1 and SG2) and the third quantitative risk goal (i.e. QRG3) involve the

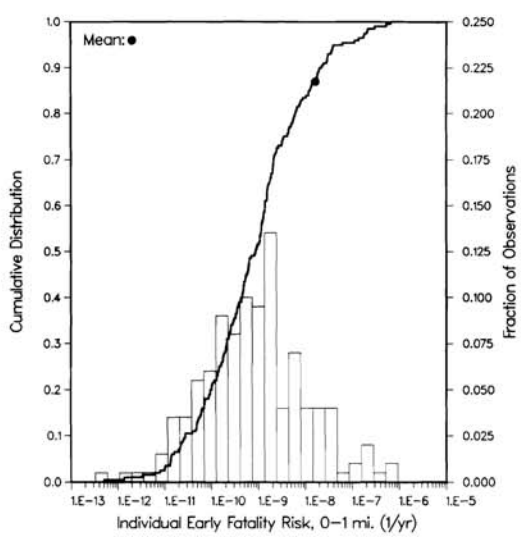

Fig. 16. Distribution of annual individual early fatality risk within 1 mi = 1609·3 m (1 mi) of the site boundary due to accidents resulting from internal initiators at Surry (replotted from Ref. 9, Fig. 5.1-2). The 200 annual risks on which this figure is based result from reducing each of the exceedance frequency curves in Fig. 12 to a single annual risk.

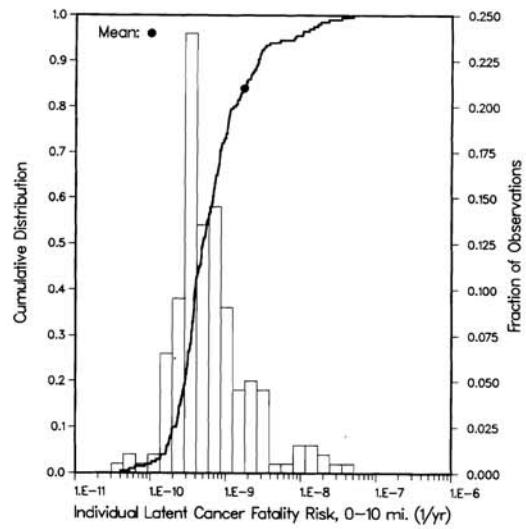

Fig. 17. Distribution of annual individual latent cancer fatality risk within 10 mi = 16 093 m (10 mi) of the site boundary due to accidents resulting from internal initiators at Surry (replotted from Ref. 9, Fig. 5.1-2). The 200 annual risks on which this figure is based result from reducing each of the exceedance frequency curves in Fig. 13 to a single annual risk.

risk results shown in eqns (67) and (68). Representations for the two safety goals are given in eqns (3) and (4) and again in eqns (11) and (12). Figures 16 and 17 give estimated distributions due to imprecisely known variables for the annual risks associated with these goals. The goals themselves apply to expected values, which can be estimated by summing over the results shown in these figures and dividing by the sample size. As previously indicated, this yields values of $1{\cdot}6 \times 10^{-8}$ year^{-1} and $1{\cdot}7 \times 10^{-9}$ year^{-1} for the early fatality and latent cancer fatality goals, respectively. In essence, these goals are based on reducing all the information in Figs 12 and 13 to single numbers.

The third quantitative risk goal uses the results shown in Fig. 2 and summarized in Fig. 4. This goal requires the expected value of the frequency of a large release to be less than 1×10^{-6} year^{-1}. In turn, a large release is defined to be a release that has the potential to cause an early fatality, although the word 'potential' has not been defined. However, potential can be associated with any number of fatalities on the abscissa in Figs 2 and 4 (e.g. 0·01, 0·1 or 1). Values of less than 1 early fatality appear in Figs 2 and 4 because low levels of radiation exposure have a probability of causing an early fatality which is considerably less than 1 and also because most of the population (i.e. 99·5%) participates in evacuation.

Figure 18 shows the distributions for large release frequencies that result when 'potential to cause an early fatality' is associated with 0·01, 0·1 and 1 early fatality, respectively. The frequencies shown in this

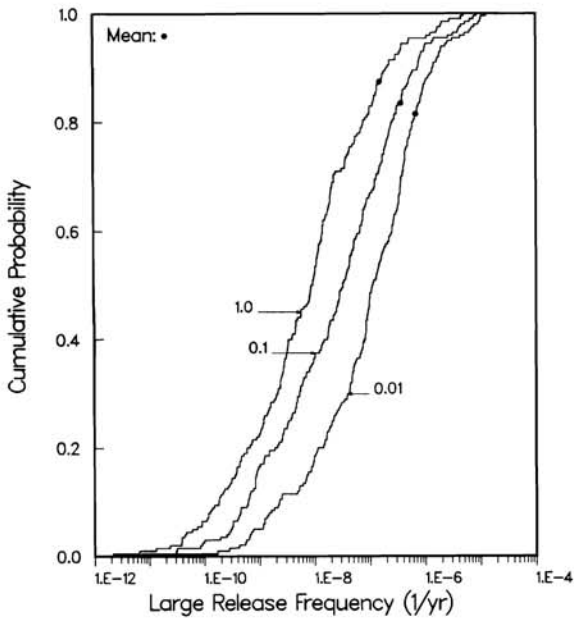

Fig. 18. Distributions of large release frequencies (year^{-1}) for internally-initiated accidents at Surry that result when potential to cause an early fatality is associated with 0·01, 0·1, and 1 early fatality (plotted from results obtained in analysis described in Ref. 9).

figure were obtained by drawing vertical slices through the curves above 0·01, 0·1 and 1 in Fig. 2. The third quantitative risk goal places a bound on the means associated with these distributions, which are $6{\cdot}8 \times 10^{-7}$ year^{-1}, $3{\cdot}7 \times 10^{-7}$ year^{-1} and $1{\cdot}5 \times 10^{-7}$ year^{-1}. Figure 18 provides a summary of the distributions of large release frequencies, including the mean values, that result from assigning 'potential to cause an early fatality' to different numbers of early fatalities. For the NUREG-1150 PRAs, 'potential to cause an early fatality' was associated with 1 early fatality.

7 SENSITIVITY ANALYSIS

The NRC intends that sensitivity analyses be performed in conjunction with the calculation of the safety goals (Ref. 2, p. 30031). The sampling-based approach to the calculation of the safety goals described in this presentation builds a mapping of the form

$$(\mathbf{X}_s, R(\mathbf{X}_s)), \quad s = 1, \ldots, nS \tag{71}$$

from analysis assumptions to analysis results, where $\mathbf{X}_s$ and $R(\mathbf{X}_s)$ are defined in eqns (13) and (14), respectively. Once generated and saved, this mapping can be explored in many ways with various sensitivity analysis techniques.

One approach is to use stepwise regression to investigate the relationships between sampled variables and selected dependent variables. In this approach, the importance of individual independent variables is indicated by the order in which they enter the regression model, the changes of R^2 values with the entry of successive variables into the model, and the standardized regression coefficients in the final model. Additional discussion of this approach is available elsewhere.[53–55] As an example, Figs 16 and 17 display the uncertainty in individual early and latent cancer fatality risk that results from imprecisely known variables. Table 7 shows the results of using stepwise regression to investigate the cause of the variation in the $nS = 200$ observations summarized in these figures. The independent variables appearing in Table 7 are defined in Table 8. The regressions in Table 7 were performed with the STEP programs[56] with rank-transformed variables[57] to reduce the effects of nonlinearities. Further, a variable was required to be significant at the 0·01 α-level to enter a regression model and to remain significant at the 0·05 α-level to be retained in a regression model. The PRESS criterion[58] was also used to check for overfitting of the data.

For individual early fatality risk, the stepwise regression selected the variable V-TRAIN first. As indicated by the R^2 value, V-TRAIN accounts for 58% of the variability in individual early fatality risk. After V-TRAIN, FISGFOSG and then FCOR were selected. Together, V-TRAIN, FISGFOSG and FCOR account for 67% of the variability in early fatality risk. After these three variables, the

Table 7. Stepwise regression analyses with rank-transformed variables for individual early fatality risk within 1 609·3 m (1 mi) of the site boundary and individual latent cancer fatality risk within 16 093 m (10 mi) of the site boundary due to accidents resulting from internal initiators at Surry (Ref. 9, Table 5.1-4)

Individual early fatality risk—1 609·3 m (1 mi)			Individual latent cancer fatality risk—16 093 m (10 mi)		
Variable[a]	SRC[b]	R^{2c}	Variable[a]	SRC[b]	R^{2c}
V-TRAIN	0·76	0·58	V-TRAIN	0·44	0·18
FISGFOSG	0·24	0·64	IE-SGTR	0·31	0·28
FCOR	0·19	0·67	FISGFOSG	0·22	0·34
IE-SGTR	0·13	0·69	IE-LOSP	0·19	0·38
VB-ALPHA	0·12	0·70	LATEI	0·16	0·40
FLATE	0·12	0·72	DG-FSTRT	0·16	0·43
DST	−0·12	0·73	FCOR	0·16	0·45
LATEI	0·10	0·74			

[a]Variables listed in the order that they entered the regression analysis.
[b]Standardized regression coefficients (SRCs) in final regression model.
[c]R^2 values with the entry of successive variables into the regression model.

Table 8. Sampled variables identified in the sensitivity analyses presented in Table 7 and Figs 19–21

Variable	Definition
V-TRAIN	Frequency (year^{-1}) of check valve failure in one of the low pressure injection system trains.
IE-LOSP	Frequency (year^{-1}) of loss of off-site power.
IE-SGTR	Frequency (year^{-1}) of a steam generator tube rupture (SGTR).
DG-FSTRT	Probability that a diesel generator fails to start, given a demand to start.
VB-ALPHA	Probability that an alpha mode containment failure occurs, given that the reactor coolant system (RCS) is at low pressure; one-tenth of this value is used for high pressure.
FCOR	Fraction of each fission product group released from the core to the vessel before or at vessel breach. There are two cases: high and low zirconium oxidation.
FCONV	Fraction of each fission product group in the containment from the RCS that is released from the containment in the absence of mitigating factors such as sprays. There is one distribution for each case, which applies to all radionuclide classes except inert gases. There are five cases: containment leak at or before vessel breach (VB) with sprays operating, containment leak at or before VB with sprays not operating, containment rupture at or before vessel breach, very late containment rupture, and Event V. The variable FCONV does not account for fission product removal by the sprays. The case differentiation on spray operation is to account for differences in containment atmosphere temperature and humidity between the two cases.
FCONC	Fraction of each fission product group in the containment from the core–concrete interaction release that is released from the containment in the absence of mitigating factors such as sprays. The five cases are the same as those for FCONV, but there are separate distributions for each radionuclide class.
LATEI	Fraction of the iodine deposited in the containment which is revolatilized and released to the environment late in the accident. This variable applies only to iodine.
FLATE	Fraction of the deposited amount of each fission product group in the RCS which revolatilized after VB and released to the containment. There are two cases: one large hole in the RCS, and two large holes in the RCS.
DST	Fraction of each fission product group in the core material that becomes aerosol particles in a direct containment heating event at VB that is released to the containment. There are two cases: VB at high pressure (1000 to 25 000 psia) and VB at intermediate pressure (200 to 1000 psia).
FISGFOSG	Fraction of each fission product group released from the reactor vessel to the steam generator, and from the steam generator to the environment, in a SGTR accident. There are two separate distributions, FISG and FOSG, each of which has two cases: SGTRs in which the secondary SRVs reclose, and SGTRs in which the secondary SRVs stick open.

1 psia = $6{\cdot}895 \times 10^3$ Pa

regression analysis identifies five more variables. These variables appear to have a small incremental impact on uncertainty (approximately 1% per variable). Collectively, all nine variables identified in the analysis account for approximately 74% of the variability in early fatality risk. As indicated by the signs of the standardized regression coefficients, there is a positive correlation between early fatality risk and each individual variable except for DST. Similar results are presented for individual latent cancer fatality risk. However, the regression model only accounts for 45% of the total variability. This relatively low percentage probably results from censoring effects due to emergency actions taken to mitigate the radiation exposure associated with individual accidents; specifically, these actions enable most individuals to avoid radiation exposure and thus remove (i.e. censor) the effect of individual variables.

The regressions in Table 7 indicate the variables that are important in causing variation in the early and latent cancer fatality safety goals. The values in these goals are derived from the results shown in Figs 12 and 13. More detailed sensitivity results can be obtained by analyzing the curves themselves rather than the summary results appearing in Figs 16 and 17. One way to do this is by performing a sensitivity analysis for the exceedance frequencies associated with each consequence value on the abscissa in Figs 12 and 13 and then plotting the sensitivity analysis results as functions of the consequence values. Figures 19 and 20 display sensitivity analysis results of this type obtained by calculating partial correlation coefficients between exceedance frequencies and the sampled variables. The independent variables shown in these figures are defined in Table 20. The analysis was performed with the PCCSRC program[59] with rank-transformed data. Further, to reduce the number of curves, a variable was included in Figs 19 and 20 only if its partial correlation coefficient had an absolute value that exceeded 0·5 for at least one value on the abscissa.

The analysis presented in Fig. 19 identified V-TRAIN, FISGFOSG, FCOR and IE-SGTR as being the dominant variables with respect to the frequency at which specified individual early fatality probabilities were exceeded. The variable V-TRAIN is the most important variable with respect to the frequency of accidents that involve high early fatality probabilities. The analysis presented in Fig. 20 identified six dominant variables with respect to the

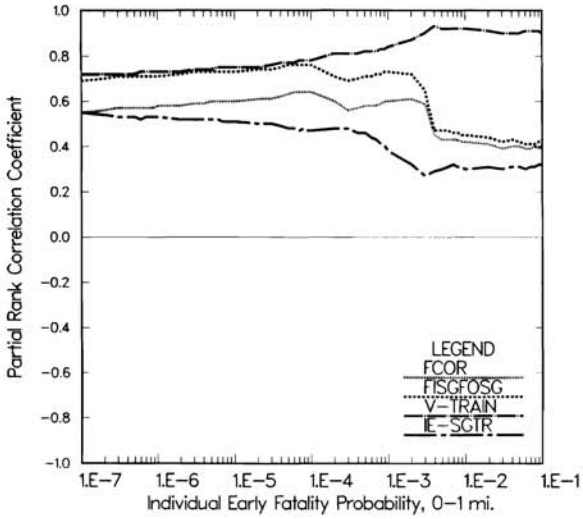

Fig. 19. Partial rank correlation analysis for the exceedance frequencies for individual early fatality probability within 1 mi of the site boundary due to accidents resulting from internal initiators at Surry (Ref. 9, Fig. 5.1-12).

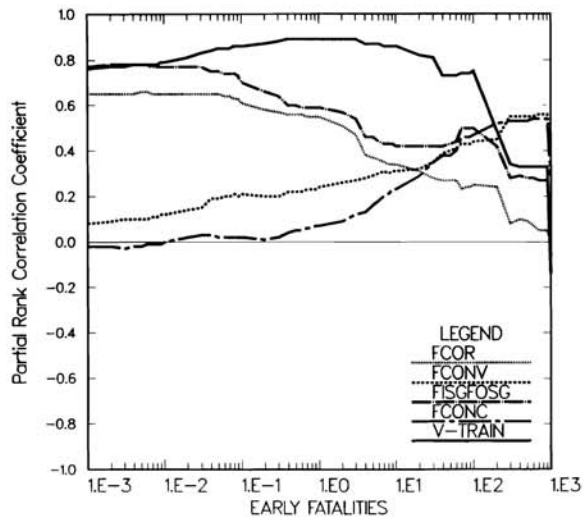

Fig. 21. Partial rank correlation analysis for the exceedance frequencies for a given number of early fatalities due to accidents resulting from internal initiators at Surry (Ref. 9, Fig. 5.1-8).

frequency at which specified individual latent cancer fatality probabilities were exceeded. Three variables (i.e. IE-SGTR, V-TRAIN and DG-FSTRT) dominated the frequencies at which low (i.e. $<1 \times 10^{-4}$) latent cancer fatality probabilities were exceeded, and four variables (i.e. V-TRAIN, FISGFOSG, VB-ALPHA and FCOR) dominated the frequencies at which the higher (i.e. $>1 \times 10^{-4}$) latent cancer fatality probabilities were exceeded.

The third quantitative risk goal is based on the frequency at which a specified number of early fatalities is exceeded. Figure 2 displays the individual exceedance frequency curves on which this goal is based. Figure 21 presents the results of analyzing these curves with the same procedure used in Figures 19 and 20. For less than one early fatality, V-TRAIN, FCONC and FCOR are the dominant variables with respect to the exceedance frequency on which the third quantitative risk goal is based. For more than 10 early fatalities, the variables FCONV and FCONC also emerge as being important.

The variation underlying the first and second

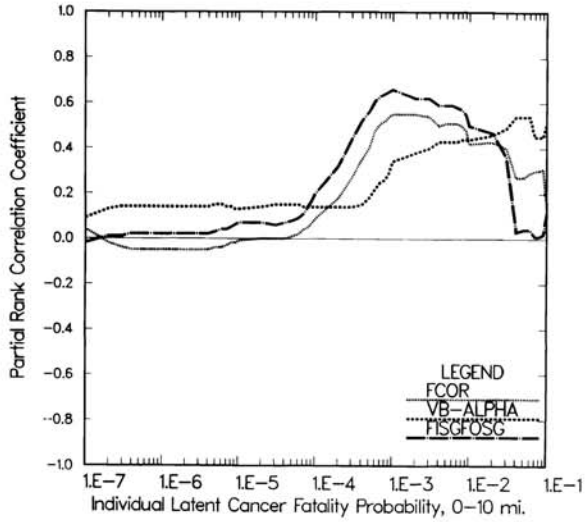

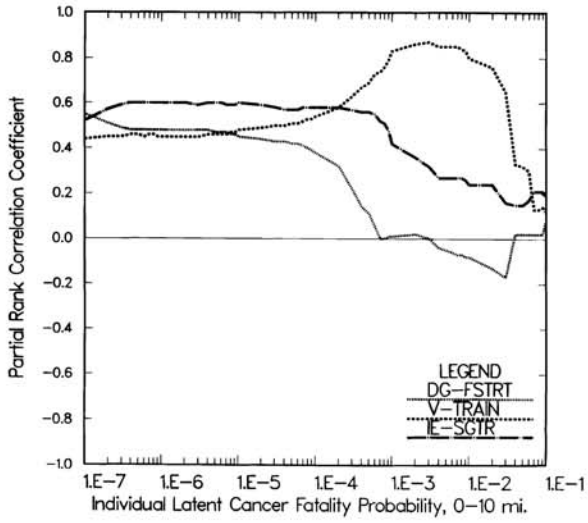

Fig. 20. Partial rank correlation analysis for the exceedance frequencies for individual latent cancer fatality probability within 10 mi of the site boundary due to accidents resulting from internal initiators at Surry (Ref. 9, Fig. 5.1-13).

quantitative risk goals is shown in Figs 5 and 6. This variation could be analyzed with stepwise regression in the same manner as shown in Table 7.

8 DISCUSSION

The safety goals listed in (SG1) through (QRG3) involve expected values over imprecisely known analysis variables. These variables are characterized by the fact that a PRA requires a single value for each of them but the appropriate values to use are not known with preciseness. Values for these variables can be developed from many sources of information, including experiments, observational data, theoretical calculations, and mechanistic code calculations. However, the final assembly of this information into probability distributions requires a process based on expert review and judgment. The resultant distributions provide a probabilistic summary of where the appropriate value to use for each variable is likely to fall in the collection of possible variable values. The importance of these distributions is that they provide a way of summarizing information from many sources into a form that facilitates additional analysis; in this case, the performance of a PRA.

This presentation has used a representation for risk based on a set R of ordered triples of the form shown in eqn (5). This representation formalizes the decomposition of risk into possible accidents (i.e. the A_i), accident frequencies (i.e. the fA_i), and accident consequences (i.e. the $\mathbf{cA}_i$). This representation also facilitates a conceptual decomposition of the factors that affect the uncertainty in PRA results, including completeness, aggregation, model selection, imprecisely known variables, and stochastic variation. It is possible for the uncertain variables in a PRA to relate to each of these sources of uncertainty.

In a broad sense, calculation of safety goals involves two types of uncertainty:[22,60–65] (1) uncertainty due to physical variability, which results in many different accidents being possible, and (2) uncertainty due to lack of knowledge, which results in an inability to determine the properties of individual accidents. The first type of uncertainty is characterized by the frequencies fA_i appearing in eqn (5). The second type of uncertainty is characterized by distributions assigned to quantities that are believed to be fixed (at least, within the resolution of the analyses being performed) but which are not known. These are the quantities that were assigned distributions and sampled in the analyses presented in this paper. In practice, it is common for there to be uncertainties of the second type in frequencies or probabilities used to characterize the first type of uncertainty. Simply put, the frequency fA_i may be a function of one or more quantities that are believed to be fixed but are unknown. Relationships of this type occur throughout the results presented in this paper.

The risk results presented in eqn (5) are typically summarized as exceedance frequency curves or as annual risks, which incorporate the first type of uncertainty. The inclusion of the second type of uncertainty in a PRA leads to families of such results. The expected values indicated in the safety goals result from the calculation of means over these families. Formally, this is equivalent to integrating over the probability space that characterizes imprecisely-known variables. In practice, Monte Carlo techniques are used to obtain approximations to the indicated expected values. Latin hypercube sampling is a likely candidate for use in such calculations due to the efficient manner in which it stratifies over the range of each variable.

It is important to recognize that safety goals based on expected values involve a loss of information. An expected value is the result of reducing an entire distribution to a single number. This number will always convey less information than the original distribution. The distributions that arise in PRAs are often highly skewed, with the result the expected value is in the upper tail of the distribution rather than close to the center of the distribution in a probabilistic sense.

The calculation of the safety goals is a complex process and requires careful organization. This is especially true since uncertainties must be propagated through the analysis in order to calculate expected values. Without careful planning, the performance of a PRA intended to estimate values for the safety goals can easily become computationally intractable.

One possibility is to subdivide a PRA into several parts, develop well-defined interfaces between these parts, perform the calculations for each part separately, and then assemble the results for the individual parts into a complete PRA. This presentation has illustrated an approach of this type in which an entire PRA was divided into an accident frequency analysis, an accident progression analysis, a source term analysis, and a consequence analysis. Further, careful interfaces were developed between these individual analysis parts. The results of the accident frequency analysis were grouped into plant damage states to form the interface with the accident progression analysis; the results of the accident progression analysis were grouped into accident progression bins to form the interface with the source term analysis; the results of the source term analysis were grouped into source term groups to form the interface with the consequence analysis.

Separate calculations were performed for each part of the analysis and then assembled to produce a

complete level 3 PRA. These calculations were repeated many times to provide a Monte Carlo propagation of uncertainty and the necessary results for the calculation of the expected values in the safety goals. Due to this large number of repeated calculations, the models used for the individual analysis parts must be relatively fast running. Otherwise, the total computational requirements of the analysis become unreasonable. Typically, these models serve to assemble information obtained from many sources rather than to perform first principle, mechanistic calculations. In the example given in this representation, the TEMAC, EVNTRE and SURSOR codes used for the accident frequency, accident progression and source term analyses, respectively, are models of this type.

The calculation of the safety goals falls at the interfaces in a well-planned analysis. In the example used in this presentation, the calculation of the severe accident frequency goal (QRG1) occurs at the interface between the accident frequency and accident progression analyses. The conditional probability of containment failure goal (QRG2) falls at the interface between the accident progression and source term analyses. The two individual fatality goals (SG1 and SG2) and the large release frequency goal (QRG3) follow the consequence analysis. As the goals are presently formulated, none of them are calculated immediately after the source term analysis. However, the source term analysis is necessary as the link between the accident progression analysis and the consequence analysis.

In general, PRAs are iterative. This is particularly true if they are being used as part of the design process for a nuclear facility or are being maintained as a 'living' PRA for an existing facility. The matrix formalism employed in this presentation provides a natural framework for the organization and assembly of a PRA that will be repeated many times. As a reminder, a PRA can be represented by a matrix product of the form

$$\mathbf{rC} = \mathbf{fIE}\,\mathbf{P}(PDS \mid IE)\,\mathbf{P}(APB \mid PDS)\,\mathbf{P}(STG \mid APB)\,\mathbf{C}(STG) \quad (72)$$

where

$\mathbf{rC}$ = vector of annual consequence risks (consequences/year),
$\mathbf{fIE}$ = vector of initiating event frequencies (year^{-1}),
$\mathbf{P}(PDS \mid IE)$ = matrix of transition probabilities from initiating events to plant damage states,
$\mathbf{P}(APB \mid PDS)$ = matrix of transition probabilities from plant damage states to accident progression bins,
$\mathbf{P}(STG \mid APB)$ = matrix of transition probabilities from accident progression bins to source term groups, and
$\mathbf{C}(STG)$ = matrix of mean (over weather variability) consequence results (consequences) conditional on the occurrence of source term groups.

Additional representations that are both more complex and less complex than this one, including representations that yield exceedance frequency curves rather than annual risks, are also possible.

The elements of the vectors and matrices in eqn (72) are functions of the many variables used in a PRA. When only some of these variables are being altered, it is possible to redefine the appropriate elements and recalculate the associated matrix products. This provides an efficient way to recalculate PRA results. Since the safety goals can be associated with these matrix products, they can also be recalculated. In the design phase of a nuclear facility, such recalculations might be performed as part of optimization studies in which the positive and negative impacts of various design options were investigated. Clearly, the assurance with which the safety goals could be met would be one of the criteria considered in such studies.

When the dependency on imprecisely known variables is included, the representation in eqn (72) becomes

$$\mathbf{rC(X)} = \mathbf{fIE(X)}\,\mathbf{P}(PDS \mid IE, \mathbf{X})\,\mathbf{P}(APB \mid PDS, \mathbf{X})\,\mathbf{P}(STG \mid APB, \mathbf{X})\,\mathbf{C}(STG, \mathbf{X}) \quad (73)$$

As the vector $\mathbf{X}$ of imprecisely known variables changes, so do the elements in the individual vectors and matrices. This creates a mapping from analysis inputs to analysis results. The calculation of the expected values that appear in the safety goals is based on this mapping. Further, this mapping forms the basis for sensitivity studies based on regression analysis. Such sensitivity studies can provide important insights into the relationships between analysis inputs and analysis results, including the impact of individual variables on the safety goals.

Several aspects of the individual safety goals are now considered. The populations used in the calculation of the two fatality risk goals (i.e. SG1 and SG2) must be clearly specified. In particular, it is necessary to know whether these goals apply only to a resident population or also include transient populations. In turn, this leads to the question of whether average individual risks should be calculated with a total population size or an effective population size which incorporates how long each individual spends in the region of interest. When a large transient population is involved, this can have a significant impact on individual risk results.

Two examples may help clarify the possibilities here. First, consider a nuclear facility close to a roadway on which many vehicles travel each day. One possibility is to calculate the early fatality risk to each passing individual. These risks would then be included with the risks to all other individuals in the vicinity of the facility and the population in the vicinity of the plant would be expanded to include the total number of individuals using the roadway. Each individual in this transient population would have a very small risk due to the brief time they were close to the nuclear facility and yet their total population size would be large if the roadway was heavily used. The result would be that this large transient population would reduce the average individual risk to a very small value even if the facility was unsafe and individuals spending a significant amount of time near it were exposed to an unacceptable level of risk. A second possibility would be to calculate an effective population size based on how many individuals used the roadway and how long these individuals were close to the facility. This effective population could then be assumed to be present at all times and risk results calculated accordingly. This could lead to risk results that would be very different from those obtained with the first approach. As a second example, consider the long time periods over which exposures leading to latent cancer fatalities can be incurred. The population exposed at the time of an accident may be quite different from the population experiencing exposure many years after the accident. Given this very real possibility, how should individual latent cancer fatality risk be calculated?

The first quantitative risk goal (QRG1) involves the frequency of a severe accident, which is equated to the occurrence of core damage. Conceptually, this goal is straightforward. This goal requires the expected value for the frequency of a severe accident to be less than 1×10^{-4} year^{-1}. Furthermore, 1×10^{-5} year^{-1} has been suggested as a goal for new plants. Recent PRAs (e.g. the NUREG-1150 studies) indicate that some existing plants may not meet the indicated goal for new plants. This is especially true when external initiators such as seismic events are included. Both the occurrence and effects of such initiators are not well established. This leads to wide uncertainty bands and expected values that are dominated by the upper tails of these bands. Thus, modifications to existing plant design philosophy may be required for new plants to have a core damage frequency of less than 1×10^{-5} year^{-1}.

The second quantitative risk goal (QRG2) involves conditional probability of containment failure. The NRC has indicated that containment failure is to be conditional on vessel breach.[1] If the purpose of this goal is to place a requirement on containment effectiveness, it is probably more appropriate to have failure conditional on vessel breach as suggested than on core damage. When failure is conditional on core damage, this probability can be affected by many factors (e.g. off-site power recovery) that are unrelated to containment effectiveness.

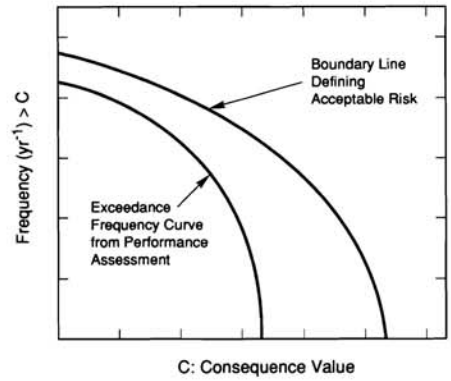

Fig. 22. Boundary line approach to specification of acceptable risk proposed by Farmer.[66]

F. R. Farmer[66] has proposed a 'boundary line' approach to the specification of acceptable risk for nuclear power plants. Specifically, this approach can be represented in the form shown in Fig. 22. The acceptable risk for a particular consequence is defined by the boundary line, with a facility having an acceptable level of risk if the exceedance frequency curve for the consequence falls below the boundary line. This approach to risk specification allows different consequence levels to be controlled with different levels of stringency (e.g. accidents resulting in large consequence values can be required to be less likely than accidents resulting in small consequence values). As illustrated in Fig. 23, the third quantitative risk goal (QRG3) can be presented in the form shown in Fig. 22, with the boundary line being defined by the single requirement that the annual frequency of

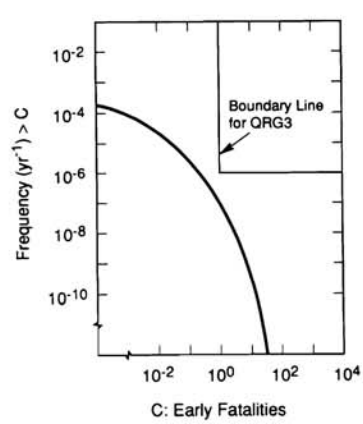

Fig. 23. Boundary line representation for third quantitative risk goal (QRG3).

exceeding 1 early fatality be less than 10^{-6}. A facility meets this requirement when the exceedance frequency curve for early fatalities falls below the boundary line indicated in Fig. 23.

This same approach to risk-based regulation appears in the US Environmental Protection Agency's (EPA) Standard for the disposal of high-level waste, transuranic waste and spent fuel (40 CFR 191).[55,67–69] As illustrated in Fig. 24, two points are used to define the boundary line for releases of radioactive material to the accessible environment. The facility is in compliance with the containment-requirement portions of the standard if the exceedance frequency curve for releases to the accessible environment falls below the boundary line shown in Fig. 24. Thus, the large release risk goal (QRG3) is conceptually the same as the EPA Standard for the disposal of high-level radioactive waste. The EPA Standard uses an appropriately defined 'weight' to define release size.[67,70] Use of this weight to define release size is conceptually equivalent to the use of the early fatality weight or some other measure to define release size for the third quantitative risk goal (QRG3).

A preliminary performance assessment conducted for the Waste Isolation Pilot Plant in southeastern New Mexico provides an extensive example of the calculation of exceedance frequency curves for comparison with the boundary line shown in Fig. 24.[71] As another example, safety criteria based on boundary lines are being used in The Netherlands to specify acceptable levels of public risk from industrial facilities.[72] Thus, the specification of the third quantitative risk goal (QRG3) as a bound on an exceedance frequency curve does not constitute an unusual risk criterion.

This presentation has used a PRA performed for internally-initiated accidents at the Surry Nuclear Power Station[9] as part of the NUREG-1150 risk study[10] for illustration. Similar results are also available for the other nuclear plants considered in the NUREG-1150 study (i.e. Peach Bottom, Grand Gulf, Sequoyah, Zion).[73–76]

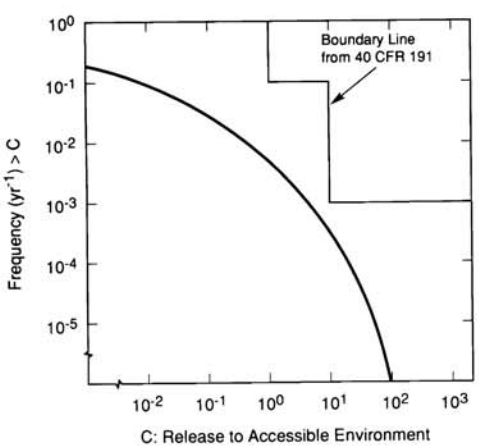

Fig. 24. Boundary line representation for EPA Standard for disposal of high-level waste, transuranic waste and spent fuel (40 CFR 191).

ACKNOWLEDGMENTS

The authors wish to acknowledge the support and cooperation of T. D. Brown, A. L. Camp, E. D. Gorham, J. J. Gregory, F. T. Harper, R. L. Iman, J. D. Johnson, A. C. Payne and other members of the NUREG-1150 analysis team. Special appreciation is extended to A. W. Shiver for assistance in figure preparation.

REFERENCES

1. US Nuclear Regulatory Commission, Implementation of safety goal policy. Letter from V. Stello to the Commissioners, Washington, DC, 30 March 1989.
2. US Nuclear Regulatory Commission, Safety Goals for the Operation of Nuclear Power Plants: Policy Statement; Correction and Republication. *Federal Register,* **51** (162) (21 August 1986) 30028–33.
3. US Nuclear Regulatory Commission, *Safety Goals for Nuclear Power Plant Operation.* NUREG-0880, Rev. 1, Washington, DC, 1983.
4. US Nuclear Regulatory Commission, *Safety Goals for Nuclear Power Plants: A Discussion Paper.* NUREG-0880, Washington, DC, 1982.
5. Iman, R. L., Johnson, J. D. & Helton, J. C., *PRAMIS: Probabilistic Risk Assessment Model Integration System.* NUREG/CR-5262, SAND88-3093, Sandia National Laboratories, Albuquerque, New Mexico, 1990.
6. Bley, D. D., Kaplan, S. & Garrick, B. J., Assembling and Decomposing PRA Results: A Matrix Formalism. In *Proceedings of the International Meeting on Thermal Nuclear Safety.* NUREG/CP-0027, Vol. 1, US Nuclear Regulatory Commission, Washington, DC, 1982, pp. 173–82.
7. Kaplan, S., Matrix theory formalism for event tree analysis: application to nuclear-risk analysis. *Risk Analysis,* **2** (1982) 9–18.
8. Sancaktar, S., An illustration of matrix formulation for a probabilistic risk-assessment study. *Risk Analysis,* **2** (1982) 137–47.
9. Breeding, R. J., Helton, J. C., Murfin, W. B. & Smith, L. N., *Evaluation of Severe Accident Risks: Surry Unit 1.* NUREG/CR-4551, SAND86-1309, Vol. 3, Rev. 1, Sandia National Laboratories, Albuquerque, New Mexico, 1990.
10. US Nuclear Regulatory Commission, *Severe Accident Risks: An Assessment for Five US Nuclear Power Plants.* NUREG-1150, Washington, DC, 1990.
11. Brooks, D. G., Using related samples in assessing conformance to safety goals: a nuclear reactor safety application. *Risk Analysis,* **10** (1990) 229–37.
12. Niehaus, F., Prospects for use of probabilistic safety criteria. *Nuclear Engineering and Design,* **115** (1989) 181–90.
13. Bier, V. M., The US Nuclear Regulatory Commission

Safety Goal Policy: a critical review. *Risk Analysis*, **8** (1988) 563–8.
14. Whipple, C. & Starr, C., Nuclear power safety goals in light of the Chernobyl accident. *Nuclear Safety*, **29** (1988) 20–8.
15. Cannell, W., Probabilistic reliability analysis, quantitative safety goals, and nuclear licensing in the United Kingdom. *Risk Analysis*, **7** (1987) 311–19.
16. Okrent, D., The safety goals of the US Nuclear Regulatory Commission. *Science*, **236** (1987) 296–300.
17. Rathbun, D. & Modarres, M., Development of safety goals for nuclear power plants. *Nuclear Safety*, **28** (1987) 155–63.
18. Martz, H. F. & Johnson, J. W., Assessing compatibility with reactor safety goals using uncertain risk analysis results with application to core melt. *Nuclear Safety*, **25** (1984) 305–16.
19. Kaplan, S., Safety goals and related questions. *Reliability Engineering*, **3** (1982) 267–77.
20. Griesmeyer, J. M. & Okrent, D., Risk management and decision rules for light water reactors. *Risk Analysis*, **1** (1981) 121–36.
21. Wall, I. B., Probabilistic risk assessment in nuclear power plant regulation. *Nuclear Engineering and Design*, **60** (1980) 11–24.
22. Kaplan, S. & Garrick, B. J., On the quantitative definition of risk. *Risk Analysis*, **1** (1981) 11–27.
23. Ortiz, N. R., Wheeler, T. A., Breeding, R. J., Hora, S., Meyer, M. A. & Keeney, R. L., Use of expert judgment in NUREG-1150. *Nuclear Engineering and Design*, **126** (1991) 313–31.
24. Hora, S. C. & Iman, R. L., Expert opinion in risk analysis: the NUREG-1150 methodology. *Nuclear Science and Engineering*, **102** (1989) 323–31.
25. Harper, F. T., Breeding, R. J., Brown, T. D., Gregory, J. J., Payne, A. C. Gorham, E. D. & Amos, C. N., *Evaluation of Severe Accident Risks: Quantification of Major Input Parameters: Experts' Determination of In-Vessel Issues*. NUREG/CR-4551, SAND86-1309, Vol. 2, Part 1, Rev. 1, Sandia National Laboratories, Albuquerque, New Mexico, 1990.
26. Harper, F. T., Amos, C. N., Breeding, R. J., Brown, T. D., Gregory, J. J., Gorham, E. D., Murfin, W., Payne, A. C. & Rightley, G. S., *Evaluation of Severe Accident Risks: Quantification of Major Input Parameters: Experts' Determination of Containment Loads and Molten Core-Concrete Issues*. NUREG/CR-4551, SAND86-1309, Vol. 2, Part 2, Rev. 1, Sandia National Laboratories, Albuquerque, New Mexico, 1991.
27. Breeding, R. J., Amos, C. N., Brown, T. D., Gorham, E. D., Gregory, J. J., Harper, F. T., Murfin, W. & Payne, A. C., *Evaluation of Severe Accident Risks: Quantification of Major Input Parameters: Experts' Determination of Structural Response Issues*. NUREG/CR-4551, SAND86-1309, Vol. 2, Part 3, Rev. 1, Sandia National Laboratories, Albuquerque, New Mexico, in preparation.
28. Harper, F. T., Amos, C. N., Boyd, G., Breeding, R. J., Brown, T. D., Gorham, E. D., Gregory, J. J., Helton, J. C., Jow, H.-N. & Payne, A. C., *Evaluation of Severe Accident Risks: Quantification of Major Input Parameters: Experts' Determination of Source Term Issues*. NUREG/CR-4551, SAND86-1309, Vol. 2, Part 4, Rev. 1, Sandia National Laboratories, Albuquerque, New Mexico, in preparation.
29. Harper, F. T. *et al.*, *Evaluation of Severe Accident Risks: Quantification of Major Input Parameters: Supporting Material*. NUREG/CR-4551, SAND86-1309, Vol. 2, Part 5, Rev. 1, Sandia National Laboratories, Albuquerque, New Mexico, in preparation.
30. Harper, F. T., Powers, D. A., Murata, K. K. & Allen, M. D., *Evaluation of Severe Accident Risks: Quantification of Major Input Parameters: Determination of Parameter Values Not Quantified by Expert Panels*. NUREG/CR-4551, SAND86-1309, Vol. 2, Part 6, Rev. 1, Sandia National Laboratories, Albuquerque, New Mexico, in preparation.
31. Wheeler, T. A., Hora, S. C., Cramond, W. R. & Unwin, S. D., *Analysis of Core Damage Frequency: Expert Judgment Elicitation*. NUREG/CR-4550, SAND86-2084, Vol. 2, Rev. 1, Sandia National Laboratories, Albuquerque, New Mexico, 1989.
32. Iman, R. L. & Shortencarier, M. J., *A FORTRAN 77 Program and User's Guide for the Generation of Latin Hypercube and Random Samples for Use With Computer Models*. NUREG/CR-3624, SAND83-2365, Sandia National Laboratories, Albuquerque, New Mexico, 1984.
33. McKay, M. D., Conover, W. J. & Beckman, R. J., A comparison of three methods for selecting values of input variables in the analysis of output from a computer code. *Technometrics*, **21** (1979) 239–45.
34. Gorham, E. D. *et al.*, *Evaluation of Severe Accident Risks: Methodology for the Containment, Source Term, Consequence and Risk Integration Analysis*. NUREG/CR-4551, SAND86-1309, Vol. 1, Rev. 1, Sandia National Laboratories, Albuquerque, New Mexico, in preparation.
35. Helton, J. C., Griesmeyer, J. M., Haskin, F. E., Iman, R. L., Amos, C. N. & Murfin, W. B., Integration of the NUREG-1150 analyses: calculation of risk and propagation of uncertainties. *Proceedings of the US Nuclear Regulatory Commission Fifteenth Water Reactor Safety Research Information Meeting*, Vol. 1. US Nuclear Regulatory Commission, Washington, DC, 1988, pp. 151–76.
36. Ericson, D. M., Wheeler, T. A., Sype, T. T., Drouin, M. T., Cramond, W. R., Camp, A. L., Maloney, K. J. & Harper, F. T., *Analysis of Core Damage Frequency: Internal Events Methodology*. Report No. NUREG/CR-4550, SAND86-2084, Vol. 1, Rev. 1, Sandia National Laboratories, Albuquerque, New Mexico, 1990.
37. Vesely, W. E., Goldberg, F. F., Roberts, N. H. & Haasl, D. F., *Fault Tree Handbook*, NUREG-0492, US Nuclear Regulatory Commission, Washington, DC, 1981.
38. Bertucio, R. C. & Julius, J. A., *Analysis of Core Damage Frequency: Surry, Unit 1, Internal Events*. NUREG/CR-4550, SAND86-2084, Vol. 1, Rev. 1, Sandia National Laboratories, Albuquerque, New Mexico, 1990.
39. Worrell, R. B., *SETS Reference Manual*. NUREG/CR-4213, SAND83-2675, Sandia National Laboratories, Albuquerque, New Mexico, 1985.
40. Iman, R. L., A matrix-based approach to uncertainty and sensitivity analysis for fault trees. *Risk Analysis*, **7** (1987) 21–33.
41. Iman, R. L. & Shortencarier, M. J., *A User's Guide for the Top Event Matrix Analysis Code (TEMAC)*. NUREG/CR-4598, SAND86-0960, Sandia National Laboratories, Albuquerque, New Mexico, 1986.
42. Griesmeyer, J. M. & Smith, L. N., *A Reference Manual for the Event Progression Analysis Code (EVNTRE)*.

NUREG/CR-5174, SAND88-1607, Sandia National Laboratories, Albuquerque, New Mexico, 1989.

43. Gieseke, J. A., Cybulskis, P., Jordan, H., Lee, K. W., Schumacher, P. M., Curtis, L. A., Wooton, R. O., Quayle, S. F. & Kogans, V., *Source Term Code Package: A User's Guide.* NUREG/CR-4587, BMI-2138, Battelle Columbus Division, Columbus, Ohio, 1986.
44. Bergeron, K. D., Clauser, M. J., Harrison, B. D., Murata, K. K., Rexroth, P. E., Schelling, F. J., Sciacca, F. W., Senglaub, M. E., Shire, P. R., Trebilcock, W. & Williams, D. C., *User's Manual for CONTAIN 1. 0. A Computer Code for Severe Reactor Accident Containment Analysis.* NUREG/CR-4085, SAND84-1204, Sandia National Laboratories, Albuquerque, New Mexico, 1985.
45. Summers, R. M., Cole, R. K., Boucheron, E. A., Carmel, M. K., Dingman, S. E. & Kelly, J. E. *MELCOR 1. 8. 0: A Computer Code for Severe Nuclear Reactor Accident Source Term and Risk Assessment Analyses.* NUREG/CR-5331, SAND90-0364, Sandia National Laboratories, Albuquerque, New Mexico, 1991.
46. Jow, H.-N., Murfin, W. B. & Johnson, J. D., *XSOR Codes User's Manual.* NUREG/CR-5350, SAND89-0943, Sandia National Laboratories, Albuquerque, New Mexico, in preparation.
47. Iman, R. L., Helton, J. C. & Johnson, J. D., *PARTITION: A Program for Defining the Source Term/Consequence Analysis Interface in the NUREG-1150 Probabilistic Risk Assessments.* NUREG/CR-5253, SAND88-2940, Sandia National Laboratories, Albuquerque, New Mexico, 1990.
48. Iman, R. L., Helton, J. C. & Johnson, J. D., A methodology for grouping source terms for consequence calculations in probabilistic risk assessments. *Risk Analysis,* **10** (1990) 507–20.
49. Chanin, D. I., Sprung, J. L., Ritchie, L. T. & Jow, H.-N., *MELCOR Accident Consequence Code System (MACCS): User's Guide.* NUREG/CR-4691, SAND86-1562, Vol. 1, Sandia National Laboratories, Albuquerque, New Mexico, 1990.
50. Jow, H.-N., Sprung, J. L., Rollstin, J. A., Ritchie, L. T. & Chanin, D. I., *MELCOR Accident Consequence Code System (MACCS): Model Description.* NUREG/CR-4691, SAND86-1562, Vol. 2, Sandia National Laboratories, Albuquerque, New Mexico, 1990.
51. Rollstin, J. A., Chanin, D. I. & Jow, H.-N., *MELCOR Accident Consequence Code System (MACCS): Programmer's Reference Manual.* NUREG/CR-1562, Vol. 3, Sandia National Laboratories, Albuquerque, New Mexico, 1990.
52. Sprung, J. L., Rollstin, J. A., Helton, J. C. & Jow, H.-N., *Evaluation of Severe Accident Risks: Quantification Major Input Parameters: MACCS Input.* NUREG/CR-4551, SAND86-1309, Vol. 2, Part 7, Rev. 1, Sandia National Laboratories, Albuquerque, New Mexico, 1990.
53. Helton, J. C., Iman, R. L., Johnson, J. D. & Leigh, C. D., Uncertainty and sensitivity analysis of a model for multicomponent aerosol dynamics. *Nuclear Technology,* **73** (1986) 320–42.
54. Helton, J. C. & Johnson, J. D., An uncertainty/sensitivity study for the station blackout sequence at a Mark I Boiling Water Reactor. *Reliability Engineering and System Safety,* **26** (1989) 293–328.
55. Helton, J. C., Garner, J. W., McCurley, R. D. & Rudeen, D. K., *Sensitivity Analysis Techniques and Results for Performance Assessment at the Waste Isolation Pilot Plant.* SAND90-7103, Sandia National Laboratories, Albuquerque, New Mexico, 1991.
56. Iman, R. L., Davenport, J. M., Frost, E. L. & Shortencarier, M. J., *Stepwise Regression With PRESS and Rank Regression (Program User's Guide).* SAND79-1472, Sandia National Laboratories, Albuquerque, New Mexico, 1980.
57. Iman, R. L. & Conover, W. J., The use of the rank transform in regression. *Technometrics,* **21** (1979) 499–509.
58. Allen, D. M., The prediction sum of squares as a criterion for selecting prediction variables. Report No. 23, Department of Statistics, University of Kentucky, Lexington, Kentucky, 1971.
59. Iman, R. L., Shortencarier, M. J. & Johnson, J. D., *A FORTRAN 77 Program and User's Guide for the Calculation of Partial Correlation and Standardized Regression Coefficients,* NUREG/CR-4122, SAND85-0044, Sandia National Laboratories, Albuquerque, New Mexico, 1985.
60. Vesely, W. E. & Rasmuson, D. M., Uncertainties in nuclear probabilistic risk analyses. *Risk Analysis,* **4** (1984) 313–22.
61. Stern, E. & Tadmor, J., Uncertainty bands in CCDF risk curves; their importance in decision making processes. *Proceedings of ANS/ENS International Topical Meeting on Probabilistic Safety Methods and Applications, San Francisco, CA, USA, February 24–March* 1, 1985, Vol. 1. American Nuclear Society, La Grange Park, IL, 1985, pp. 22.1–22.9.
62. Paté-Cornell, M. E., Probability and uncertainty in nuclear safety decisions. *Nuclear Engineering and Design,* **93** (1986) 319–27.
63. Parry, G. W., On the meaning of probability in probabilistic safety assessment. *Reliability Engineering and System Safety,* **23** (1988) 309–14.
64. International Atomic Energy Agency, Evaluating the reliability of predictions made using environmental transfer models. Safety Series Report No. 100, Vienna, 1989.
65. Apostolakis, G., The concept of probability in safety assessments of technological systems. *Science,* **250** (1990) 1359–64.
66. Farmer, F. R., Reactor safety and siting: a proposed risk criterion. *Nuclear Safety,* **8** (1967) 539–48.
67. US Environmental Protection Agency, Environmental standards for the management and disposal of spent nuclear fuel, high-level and transuranic radioactive waste; final rule. 40 CFR Part 191. *Federal Register,* **50** (1985) 38066–89.
68. Helton, J. C., Risk, uncertainty in risk and the EPA release limits for radioactive waste disposal. *Nuclear Technology,*
69. Helton, J. C. & Iuzzolino, H. J., Construction of complementary cumulative distribution functions for comparison with the EPA release limits for radioactive waste disposal. *Reliability Engineering and System Safety,* submitted for publication.
70. Helton, J. C., *Technical Assistance for Regulatory Development: Review and Evaluation of the Draft EPA Standard 40 CFR 191 for Disposal of High-Level Waste, Vol. 5. Health Effects Associated with Unit Radionuclide Releases to the Environment.* NUREG/CR-3235, SAND87-1557, Sandia National Laboratories, Albuquerque, New Mexico, 1983.
71. WIPP Performance Assessment Division, *Preliminary*

Comparison with 40 CFR 191, Subpart B for the Waste Isolation Pilot Plant, December 1991, Vol. 1–4. SAND91-0893/1, 2, 3, 4, Sandia National Laboratories, Albuquerque, New Mexico, 1991.

72. Versteeg, M. F., Showing compliance with probabilistic safety criteria and objectives. *Reliability Engineering and System Safety,* **35** (1992) 39–48.
73. Payne, A. C., Breeding, R. J., Jow, H.-N., Helton, J. C., Smith, L. N. & Shiver, A. W., *Evaluation of Severe Accident Risks: Peach Bottom Unit 2.* NUREG/CR-4551, SAND86-1309, Vol. 4, Rev. 1, Sandia National Laboratories, Albuquerque, New Mexico, 1990.
74. Gregory, J. J., Breeding, R. J., Muffin, W. B., Helton, J. C., Higgins, S. J. & Shiver, A. W., *Evaluation of Severe Accident Risks: Sequoyah Unit 1.* NUREG/CR-4551, SAND86-1309, Vol. 5, Rev. 1, Sandia National Laboratories, Albuquerque, New Mexico, 1990.
75. Brown, T. D., Breeding, R. J., Jow, H.-N., Helton, J. C., Higgins, S. J., Amos, C. N. & Shiver, A. W., *Evaluation of Severe Accident Risks: Grand Gulf Unit 1.* NUREG/CR-4551, SAND86-1309, Vol. 6, Rev. 1, Sandia National Laboratories, Albuquerque, New Mexico, 1990.
76. Park, C. K. *et al., Evaluation of Severe Accident Risks: Zion Unit 1.* NUREG/CR-4551, Vol. 7, Rev. 1, BNL/NUREG-5209, Brookhaven National Laboratory, Upton, NY. In preparation.

Appendix D

Helton JC, Anderson DR, Jow H-N, Marietta MG, Basabilvazo G. Performance Assessment in Support of the 1996 Compliance Certification Application for the Waste Isolation Pilot Plant. *Risk Analysis* 1999;19(5):959 - 986

This page intentionally left blank

Risk Analysis, Vol. 19, No. 5, 1999

Performance Assessment in Support of the 1996 Compliance Certification Application for the Waste Isolation Pilot Plant

J. C. Helton,[1] D. R. Anderson,[2] H.-N. Jow,[2] M. G. Marietta,[2] and G. Basabilvazo[3]

The conceptual and computational structure of a performance assessment (PA) for the Waste Isolation Pilot Plant (WIPP) is described. Important parts of this structure are (1) maintenance of a separation between stochastic (i.e., aleatory) and subjective (i.e., epistemic) uncertainty, with stochastic uncertainty arising from the many possible disruptions that could occur over the 10,000-year regulatory period that applies to the WIPP, and subjective uncertainty arising from the imprecision with which many of the quantities required in the analysis are known, (2) use of Latin hypercube sampling to incorporate the effects of subjective uncertainty, (3) use of Monte Carlo (i.e., random) sampling to incorporate the effects of stochastic uncertainty, and (4) efficient use of the necessarily limited number of mechanistic calculations that can be performed to support the analysis. The WIPP is under development by the U.S. Department of Energy (DOE) for the geologic (i.e., deep underground) disposal of transuranic (TRU) waste, with the indicated PA supporting a Compliance Certification Application (CCA) by the DOE to the U.S. Environmental Protection Agency (EPA) in October 1996 for the necessary certifications for the WIPP to begin operation. The EPA certified the WIPP for the disposal of TRU waste in May 1998, with the result that the WIPP will be the first operational facility in the United States for the geologic disposal of radioactive waste.

KEY WORDS: Aleatory uncertainty; compliance certification application; epistemic uncertainty; Latin hypercube sampling; performance assessment; radioactive waste; stochastic uncertainty; subjective uncertainty; transuranic waste; Waste Isolation Pilot Plant; 40 CFR 191; 40 CFR 194.

1. INTRODUCTION

The Waste Isolation Pilot Plant (WIPP) is under development by the U.S. Department of Energy (DOE) for the geologic disposal of transuranic (TRU) waste that has been generated at government defense installations in the United States.[1-3] The WIPP is located in southeastern New Mexico in an area of low population density approximately 42 km (26 mi) east of Carlsbad. Waste disposal will take place in excavated chambers (i.e., waste disposal panels) in a bedded salt formation, the Salado Formation (Fm), approximately 655 m (2,150 ft) below the land surface (Fig. 1). The Salado Fm is contained in the Delaware Basin, which is a large sedimentary basin located in southeastern New Mexico and western Texas (Ref. 4, Vol. 3, Section 1.5.3; Ref. 6, Chapter 2).

The sequence of events that led to the development of the WIPP by the DOE for the disposal of TRU waste in bedded salt began in 1955 when the Atomic Energy Commission (AEC), part of which later became the DOE, asked the National Academy

[1] Department of Mathematics, Arizona State University, Tempe, Arizona 85287-1804.
[2] Sandia National Laboratories, Albuquerque, New Mexico 87185-0779.
[3] U.S. Department of Energy, Carlsbad, New Mexico 88221.

0272-4332/99/1000-0959$16.00/1 © 1999 Society for Risk Analysis

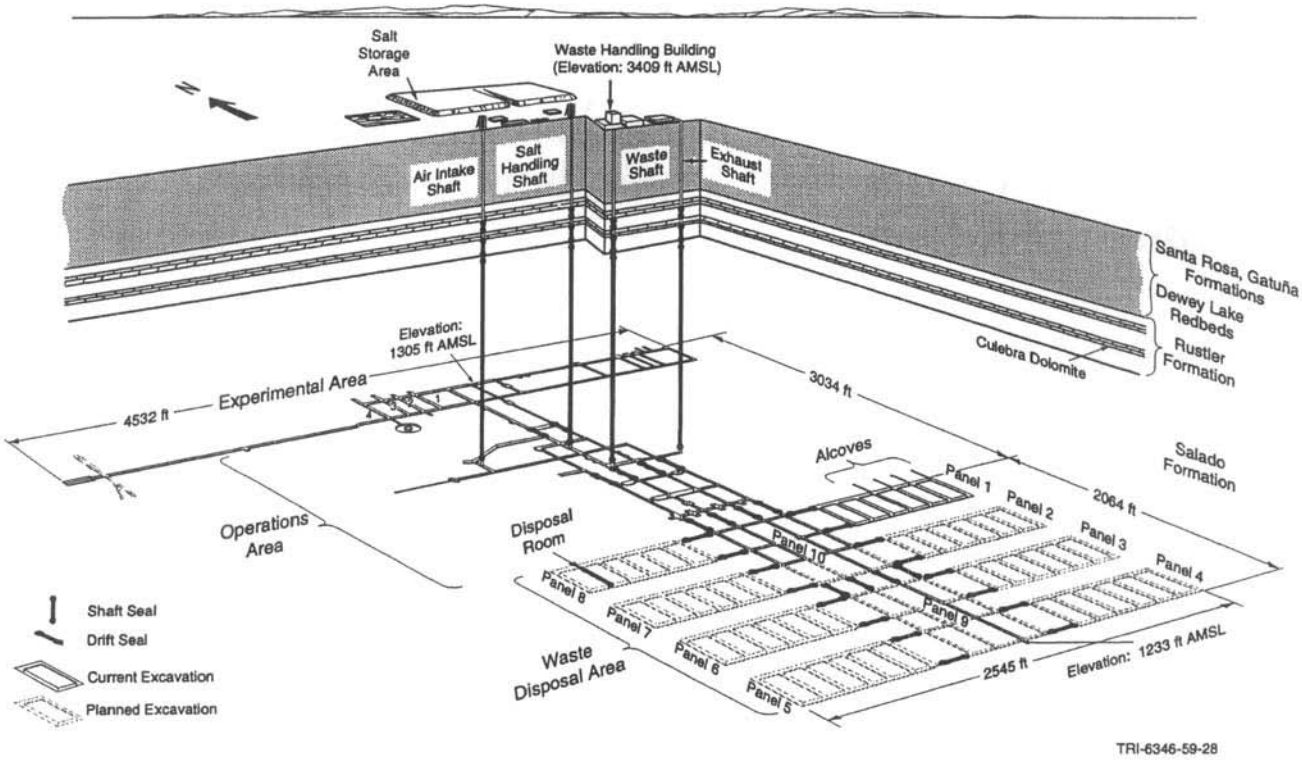

Fig. 1. Cross-sectional view of the WIPP (Fig. 1-9, Vol. 1, Ref. 4; see Section 2.2, Vol. 2, Ref. 5, for detailed stratigraphy).

of Science (NAS) to examine disposal options for radioactive waste (Ref. 7, Section 1.5.1; see Ref. 7, Tables 1.5-1 and 1.5-2 for more details on the historical development of the WIPP than can be presented here). In response, the NAS reported in 1957 that, while various options and disposal sites were feasible, disposal in bedded salt was the most promising disposal method.[8] From that point through the early 1970s, Oak Ridge National Laboratory conducted radioactive-waste disposal experiments, most notably Project Salt Vault in an abandoned salt mine near Lyons, Kansas.[9] Although the AEC considered using the mine as a repository, the discovery of boreholes in the nearby area prompted the AEC to search for more suitable sites.[10]

At the invitation of New Mexico's governor, the AEC investigated the Delaware Basin in the Carlsbad area of New Mexico. After an initial examination, a potential site was identified in the 1970s. The site was named the Waste Isolation Pilot Plant (WIPP) in January 1976.[11] The regional site-characterization phase of this potential waste disposal site[12] ended with the preparation of an Environmental Impact Statement (EIS) in 1980,[1] as required by the *National Environmental Policy Act of 1969* (NEPA).[13] In response to the EIS, the DOE decided to proceed with a preliminary design phase at this site.

During the 1970s, the mission of the WIPP, and thus the design,[14] varied between including and not including defense high-level waste (HLW) in addition to TRU waste. However, with passage of the *National Security and Military Applications of Nuclear Energy Authorization Act of 1980,*[15] Congress defined the WIPP as a research and development facility for the storage and disposal of TRU waste, and exempted the WIPP from regulation by the U.S. Nuclear Regulatory Commission.

In 1981, the "Stipulated Agreement" and "Consultation and Cooperation Agreement" defined the WIPP's relationship with the State of New Mexico and stipulated specific geotechnical experiments required by the state.[16] After much planning, construction of the WIPP began in 1983.[17,18] Experiments to characterize the local disposal system followed.[19-21] In preparation for the WIPP's opening, a Supplemental EIS was published in 1990.[2]

In the *Waste Isolation Pilot Plant Land Withdrawal Act of 1992* (LWA),[22] Congress defined the

process by which WIPP's compliance with applicable regulations would have to be evaluated, and transferred ownership of the WIPP site to the DOE. This act officially marked the transition from the construction and disposal-system characterization phase to the compliance and testing phases, although these phases had begun unofficially in 1985 when the EPA issued 40 CFR 191[23] and in 1989 when Sandia National Laboratories (SNL) first began to assess performance of the WIPP using the EPA standard.[24-26] Additional performance assessments (PAs) were carried out for the WIPP in 1990, 1991 and 1992,[4,5,27] with summaries of the 1991 and 1992 PAs available in the journal literature.[28-31]

The efforts to produce a PA for the WIPP to satisfy the requirements in 40 CFR 191 began in 1992, when Congress passed the LWA in which it established several mandates. First, Congress required that the DOE demonstrate compliance to the final disposal standards codified in 40 CFR Part 191, Subparts B and C, prior to opening the WIPP for the disposal of TRU waste.[23,32] Second, Congress mandated that the DOE submit an application to the EPA seeking certification of the DOE's compliance demonstration. Third, Congress mandated that the EPA issue certification criteria to judge the adequacy of the DOE's application. The EPA met this obligation in February 1996 with the issuance of 40 CFR Part 194.[33,34]

This presentation describes a PA carried out at SNL to support the Compliance Certification Application (CCA) made by the DOE to the EPA in October 1996 for the certification of the WIPP for the disposal of TRU waste as mandated in the LWA.[6] This PA will be referred to as the 1996 WIPP PA, with some documents also referring to it as the 1996 CCA PA or the 1996 WIPP CCA PA. This presentation is based in part on a preliminary description of the 1996 WIPP PA that was written in the summer of 1996 while the analysis was still in progress.[35] When appropriate, changes to this preliminary description are made to better indicate what was done in the final analysis and also to provide more detail on what was done. In addition, the presentation of results from the analysis is now possible, which could not be done in the summer of 1996 as such results were not yet available. The intent is to give a high-level overview of the conceptual and computational structure of the 1996 WIPP PA with approximately equal coverage given to the individual parts of this large analysis. Further, references to additional and more detailed sources of information are given.

2. REGULATORY REQUIREMENTS

The conceptual structure of the 1996 WIPP PA ultimately derives from the regulatory requirements imposed on this facility.[36,37] The primary regulation determining this structure is the U.S. EPA's standard for the geologic disposal of radioactive waste (40 CFR 191),[23,32] which is divided into three parts. Subpart A applies to a disposal facility prior to decommissioning and limits annual radiation doses to members of the public from waste management and storage operations. Subpart B applies after decommissioning and sets probabilistic limits on cumulative releases of radionuclides to the accessible environment for 10,000 years (40 CFR 191.13) and assurance requirements to provide confidence that 40 CFR 191.13 will be met (40 CFR 191.14). Subpart B also sets limits on radiation doses to members of the public in the onment for 10,000 years of undisturbed performance (40 CFR 191.15). Subpart C limits radioactive contamination of certain sources of groundwater for 10,000 years after disposal (40 CFR 191.24). The DOE must provide a reasonable expectation that the WIPP will comply with the requirements of Subparts B and C of 40 CFR 191.

The following is the central requirement in 40 CFR 191, Subpart B, and the primary determinant of the conceptual structure of the 1996 WIPP PA (Ref. 23, p. 38086):

> § 191.13 Containment requirements:
>
> (a) Disposal systems for spent nuclear fuel or high-level or transuranic radioactive wastes shall be designed to provide a reasonable expectation, based upon performance assessments, that cumulative releases of radionuclides to the accessible environment for 10,000 years after disposal from all significant processes and events that may affect the disposal system shall: (1) Have a likelihood of less than one chance in 10 of exceeding the quantities calculated according to Table 1 (Appendix A); and (2) Have a likelihood of less than one chance in 1,000 of exceeding ten times the quantities calculated according to Table 1 (Appendix A).
>
> (b) Performance assessments need not provide complete assurance that the requirements of 191.13(a) will be met. Because of the long time period involved and the nature of the events and processes of interest, there will inevitably be substantial uncertainties in projecting disposal system performance. Proof of the future performance of a disposal system is not to be had in the ordinary sense of the word in situations that deal with much shorter time frames. Instead, what is required is a reasonable expectation, on the basis of the record before the implementing agency, that compliance with 191.13(a) will be achieved.

Containment Requirement 191.13(a) refers to "quantities calculated according to Table 1 (App. A)," which means a normalized radionuclide release to the accessible environment based on the type of waste being disposed of, the initial waste inventory, and the release that takes place (Ref. 23, Appendix A). That table specifies allowable releases (i.e., release limits) for individual radionuclides and is reproduced as Table I of the present paper. The WIPP is intended for TRU waste, which is defined to be "waste containing more than 100 nanocuries of alpha-emitting transuranic isotopes, with half-lives greater than twenty years, per gram of waste" (Ref. 23, p. 38084). The normalized release R for transuranic waste is defined by

$$R = \sum_i (Q_i/L_i)(1 \times 10^6 \text{ Ci}/C) \qquad (1)$$

where Q_i is the cumulative release of radionuclide i to the accessible environment during the 10,000-year period following closure of the repository (Ci, curie), L_i is the release limit for radionuclide i given in Table I (Ci), 1×10^6 Ci is a normalization term, and C is the amount of transuranic waste emplaced in the repository (Ci). The normalized release R is unitless as a result of the release limit being scaled by the inventory of the repository; for convenience, R will be referred to as being in "EPA units." In the 1996 WIPP PA, $C = 3.44 \times 10^6$ Ci.[38] Further, accessible environment means (1) the atmosphere, (2) land surfaces, (3) surface waters, (4) oceans, and (5) all of the lithosphere that is beyond the controlled area; and controlled area means (1) a surface location, to be identified by passive institutional controls, that encompasses no more than 100 km^2 and extends horizontally no more than 5 km in any direction from the outer boundary of the original location of the radioactive wastes in a disposal system and (2) the subsurface underlying such a surface location.

Table I. Release Limits for the Containment Requirements[a]

Radionuclide	Release limit L_i per 1,000 MTHM[b] or other unit of waste[c]
Americium-241 or -243	100
Carbon-14	100
Cesium-135 or -137	1,000
Iodine-129	100
Neptunium-237	100
Plutonium-238, -239, -240, or -242	100
Radium-226	100
Strontium-90	1,000
Technetium-99	10,000
Thorium-230 or -232	10
Tin-126	1,000
Uranium-233, -234, -235, -236, or -238	100
Any other alpha-emitting radionuclide with a half-life greater than 20 years	100
Any other radionuclide with a half-life greater than 20 years that does not emit alpha particles	1,000

[a] Ref. 23, Appendix A, Table 1.
[b] Metric tons of heavy metal exposed to a burnup between 25,000 MW-days per metric ton of heavy metal (MWd/MTHM) and 40,000 MWd/MTHM.
[c] An amount of transuranic wastes containing one million Ci of alpha-emitting transuranic radionuclides with half-lives greater than 20 years.

As required by the LWA, the EPA also promulgated 40 CFR 194,[33] where the following elaboration on the intent of 40 CFR 191.13 is given (Ref. 33, pp. 5242–5243):

> § 194.34 Results of performance assessments.
> (a) The results of performance assessments shall be assembled into "complementary, cumulative distribution functions" (CCDFs) that represent the probability of exceeding various levels of cumulative release caused by all significant processes and events. (b) Probability distributions for uncertain disposal system parameter values used in performance assessments shall be developed and documented in any compliance application. (c) Computational techniques, which draw random samples from across the entire range of the probability distributions developed pursuant to paragraph (b) of this section, shall be used in generating CCDFs and shall be documented in any compliance application. (d) The number of CCDFs generated shall be large enough such that, at cumulative releases of 1 and 10, the maximum CCDF generated exceeds the 99th percentile of the population of CCDFs with at least a 0.95 probability. (e) Any compliance application shall display the full range of CCDFs generated. (f) Any compliance application shall provide information which demonstrates that there is at least a 95 percent level of statistical confidence that the mean of the population of CCDFs meets the containment requirements of § 191.13 of this chapter.

In addition to the requirements in 40 CFR 191.13 and 40 CFR 194.34 just quoted, 40 CFR 191 and 40 CFR 194 contain many additional requirements for the certification of the WIPP for the disposal of TRU waste. However, it is the indicated requirements that determine the overall structure of the 1996 WIPP PA and are the primary focus of this presentation. A complete description of the requirements that are placed on the WIPP and how these requirements

are addressed is available in the CCA (Ref. 6, pp. XWALK-1 to XWALK-36).

The results required in 191.13 and 194.34 determine the conceptual and computational structure of the 1996 WIPP PA and lead to an analysis based on three distinct entities (EN1, EN2, EN3): EN1 is a probabilistic characterization of the likelihood of different futures occurring at the WIPP site over the next 10,000 years; EN2 is a procedure for estimating the radionuclide releases to the accessible environment associated with each of the possible futures that could occur at the WIPP site over the next 10,000 years; and EN3 is a probabilistic characterization of the uncertainty in the parameters used in the definitions of EN1 and EN2. Together, EN1 and EN2 give rise to the CCDF specified in 191.13(a) (Fig. 2), and EN3 corresponds to the distributions indicated in 194.34(b).

The preceding entities arise from an attempt to answer three questions (Q1, Q2, Q3) about the WIPP: Q1 "What occurrences could take place at the WIPP site over the next 10,000 years?"; Q2, "How likely are the different occurrences that could take place at the WIPP site over the next 10,000 years?"; Q3, "What are the consequences of the different occurrences that could take place at the WIPP site over the next 10,000 years?". And one question (Q4) about the WIPP PA: Q4, "How much confidence should be placed in answers to the first three questions?". In the WIPP PA, EN1 provides answers to Q1 and Q2; EN2 provides an answer to Q3; and EN3 provides an answer to Q4.

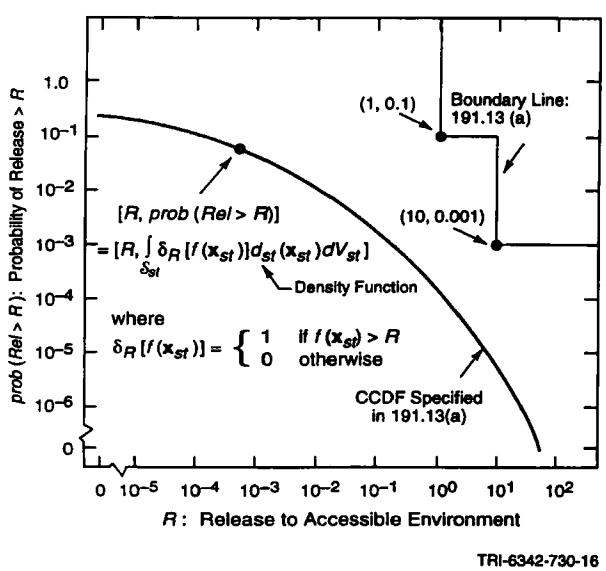

Fig. 2. Boundary line and associated CCDF specified in 40 CFR 191, Subpart B (Fig. 4, Ref. 39); see Sections 4 and 5 for a discussion of this CCDF as an integral involving a probability space ($\mathcal{S}_{st}$, $\mathcal{S}_{st}$, p_{st}) for stochastic uncertainty and a function f defined on $\mathcal{S}_{st}$.

3. SCREENING OF FEATURES, EVENTS, AND PROCESSES

As just indicated, the 1996 WIPP PA is based on three distinct entities. Careful definitions of how these entities are specified for the 1996 WIPP PA are given in Sections 4–6, and are necessary for the computational implementation of the analysis. However, the start of a PA for a complex system goes through a preliminary, and often rather ill-defined, phase in which it must be decided what is to be, and hence what is not to be, included in the analysis. It is from this work that the formal definitions of these entities ultimately emerge.

In a very real sense, this work has been going on for the WIPP since its development was initiated in the 1970s, and indeed goes back to the beginning of the consideration of geologic disposal for radioactive wastes in the 1950s. This development work and the early PAs carried out for the WIPP certainly led to general ideas about what would be important with respect to the performance of a waste repository in bedded salt. However, a PA that is to be used in a regulatory context requires a formal development and documentation of what is to be included in, and excluded from, the analysis. For the 1996 WIPP PA, this initial and fundamental work was carried out in an activity referred to as the identification and screening of features, events, and processes (FEPs) (Ref. 6, Section 6.2).

The regulatory requirements for an analysis of FEPs potentially important with respect to the WIPP derive from the following statement in 40 CFR 194 (Ref. 33, p. 5242):

> § 194.32 Scope of performance assessments.
>
> . . . (e) Any compliance application(s) shall include information which: (1) identifies all potential processes, events or sequences and combinations of processes and events that may occur during the regulatory time frame and may affect the disposal system; (2) Identifies the processes, events or sequences and combinations of processes and events included in performance assessments; and (3) Documents why any processes, events or sequences and combinations of processes and events identified pursuant to paragraph (e)(1) of this section were not included in performance assessment results provided in any compliance application.

To meet the preceding requirements, a formal FEPs screening was carried out as part of the 1996 WIPP PA.

As a starting point, a list of potentially relevant FEPs was assembled from a compilation developed for the Swedish Nuclear Power Inspectorate (SKI).[40] The SKI list is based on several FEP lists developed for other waste disposal programs and constituted the best documented and most comprehensive starting point for the WIPP PA. WIPP-specific FEPs were added to the SKI list, and the combined list was edited to remove redundancy and ambiguity, resulting in a FEPs list (Ref. 6, Attachment 1, Appendix SCR) that was appropriate for the WIPP (Ref. 6, Section 6.2.1).

This list was then carefully analyzed to identify the FEPs that should be incorporated into the computational structure of the 1996 WIPP PA and also the FEPs that did not require incorporation into this structure. Decisions to remove (i.e., screen out) FEPs from the computational structure used for the 1996 WIPP PA were based on the following criteria: regulatory exclusion (SO-R), low probability (SO-P), and low consequence (SO-C). The three screening criteria derive from specific regulatory requirements (Ref. 6, Section 6.2.2.1). In particular, the screening criterion SO-R arises because certain types of FEPs are specifically excluded from consideration in PAs to assess the compliance of the WIPP with 40 CFR 191 [e.g., the statement "Inadvertent and intermittent intrusion by drilling for resources (other than those resources provided by the waste in the disposal system or engineered barriers designed to isolate such waste) is the most severe human intrusion scenario" in 40 CFR 194.33 (Ref. 33, p. 5242) excludes many potential human disruptions of the WIPP from consideration]; the screening criterion SO-P arises because low-probability FEPs are specifically excluded from consideration in PAs to assess the compliance of the WIPP with 40 CFR 191 [i.e., the statement "Performance assessments need not consider processes and events that have less than one chance in 10,000 of occurring over 10,000 years" appears in 40 CFR 194.34 (Ref. 33, p. 5242)]; and the screening criterion SO-C arises because the occurrence of many FEPs has no effect on the location of the CCDF used to assess compliance with 40 CFR 191.13 [i.e., the statement "The results of performance assessments shall be assembled into "complementary cumulative distribution functions" (CCDFs) that represent the probability of exceeding various levels of cumulative release caused by all significant processes and events" appears in 40 CFR 194.34 (Ref. 33, p. 5242) and implies that it is acceptable to omit FEPs from the PA calculations when there is a reasonable expectation that the resultant CCDF for cumulative release would not be significantly changed by such omissions].

The FEPs not screened out were retained for inclusion in the PA and were classified as undisturbed performance (UP) or disturbed performance (DP) FEPs. As an example, a summary of the screening process for natural FEPs is given in Table II; in addition, waste- and repository-induced FEPs (Ref. 6, Table 6-46) and human-initiated events and processes (EPs) (Ref. 6, Table 6-56) were also considered. A detailed description of the screening process is available in Appendix SCR of Ref. 6.

4. EN1: PROBABILISTIC CHARACTERIZATION OF DIFFERENT FUTURES

The entity EN1 is the formal outcome of the FEPs process for determining what could happen at the WIPP. Specifically, EN1 provides a probabilistic characterization of the likelihood of different futures that could occur at the WIPP site over the 10,000-year period specified in 40 CFR 191. The entity EN1 is defined by a probability space $(\mathcal{S}_{st}, \mathcal{S}_{st}, p_{st})$, with the sample space $\mathcal{S}_{st}$ given by

$$\mathcal{S}_{st} = \{\mathbf{x}_{st}: \mathbf{x}_{st} \text{ is a possible 10,000 year sequence of occurrences at the WIPP}\} \quad (2)$$

The subscript *st* refers to stochastic (i.e., aleatory) uncertainty and is used because $(\mathcal{S}_{st}, \mathcal{S}_{st}, p_{st})$ is providing a probabilistic characterization of occurrences that may take place in the future.[41,42]

The introduction of the idea of a probability space may seem overly formal. However, this introduction provides a way to distinguish between the use of probability in the definition of EN1 (i.e., in the characterization of stochastic uncertainty) and the use of probability in the definition of EN3 (i.e., in the characterization of subjective uncertainty; see Section 6). As a reminder, a probability space $(\mathcal{S}, \mathcal{S}, p)$ consists of three components: a set $\mathcal{S}$ that contains everything that could occur for the particular "universe" under consideration, a suitably restricted set $\mathcal{S}$ of subsets of $\mathcal{S}$, and a function p defined for elements of $\mathcal{S}$ that actually defines probability.[43] In the terminology of probability theory, $\mathcal{S}$ is the sample space; the elements of $\mathcal{S}$ are elementary events; the

subsets of $\mathcal{S}$ contained in $\mathcal{S}$ are events; and p is a probability measure.

The FEPs development process for the WIPP identified drilling for natural resources as the only disruption with sufficient likelihood and consequence for inclusion in the definition of EN1 (Ref. 6, Appendix SCR). In addition, 40 CFR 194 specifies that the occurrence of mining within the land withdrawal boundary must be included in the analysis. The preceding considerations led to the elements $\mathbf{x}_{st}$ of $\mathcal{S}_{st}$ being vectors of the form

$$\mathbf{x}_{st} = [\underbrace{t_1, l_1, e_1, b_1, p_1, \mathbf{a}_1,}_{\text{1st intrusion}} \quad \underbrace{t_2, l_2, e_2, b_2, p_2, \mathbf{a}_2,}_{\text{2nd intrusion}} \quad \ldots, \underbrace{t_n, l_n, e_n, b_n, p_n, \mathbf{a}_n,}_{n\text{th intrusion}} \quad t_{min}] \tag{3}$$

in the 1996 WIPP PA, where n is the number of drilling intrusions, t_i is the time (years) of the ith intrusion, l_i designates the location of the ith intrusion, e_i designates the penetration of an excavated or nonexca-

Table II. Natural FEPs and Their Screening Classifications[a,b]

Geological FEPs (Section SCR.1.1, Ref. 6): 1. Stratigraphy. 1.1 Stratigraphy (UP). 1.2 Brine reservoirs (DP). 2. Tectonics. 2.1 Changes in regional stress (SO-C). 2.2 Regional tectonics (SO-C). 2.3 Regional uplift and subsidence (SO-C). 3. Structural FEPs. 3.1 Deformation. 3.1.1 Salt deformation (SO-P, UP near repository). 3.1.2 Diapirism (SO-P). 3.2 Fracture development. 3.2.1 Formation of fractures (SO-P, UP near repository). 3.2.2 Changes in fracture properties (SO-C, UP near repository). 3.3 Fault movement. 3.3.1 Formation of new faults (SO-P). 3.3.2 Fault movement (SO-P). 3.4 Seismic activity. 3.4.1 Seismic activity (UP). 4. Crustal processes. 4.1 Igneous activity. 4.1.1 Volcanic activity (SO-P). 4.1.2 Magmatic activity (SO-C). 4.2 Metamorphism 4.2.1 Metamorphic activity (SO-P). 5. Geochemical FEPs. 5.1 Dissolution. 5.1.1 Shallow dissolution (UP). 5.1.2 Lateral dissolution (SO-C). 5.1.3 Deep dissolution (SO-P). 5.1.4 Soluion chimneys (SO-P). 5.1.5 Breccia pipes (SO-P). 5.1.6 Collapse breccias (SO-P). 5.2 Mineralization. 5.2.1 Fracture infills (SO-C).

Subsurface hydrological FEPs (Section SCR.1.2, Ref. 6): 1. Groundwater characteristics. 1.1 Saturated groundwater flow (UP). 1.2 Unsaturated groundwater flow (UP, SO-C in Culebra). 1.3 Fracture flow (UP). 1.4 Density effects on groundwater flow (SO-C). 1.5 Effects of preferential pathways (UP, UP in Salado and Culebra. 2. Changes in groundwater flow. 2.1 Thermal effects on groundwater flow (SO-C). 2.2 Saline intrusion (SO-P). 2.3 Freshwater intrusion (SO-P). 2.4 Hydrological response to earthquakes (SO-C). 2.5 Natural gas intrusion (SO-P).

Subsurface geochemical FEPs (Section SCR.1.3, Ref. 6): 1. Groundwater geochemistry. 1.1 Groundwater geochemistry (UP). 2. Changes in groundwater chemistry. 2.1 Saline intrusion (SO-C). 2.2 Freshwater intrusion (SO-C). 2.3 Changes in groundwater Eh (SO-C). 2.4 Changes in groundwater pH (SO-C). 2.5 Effects of dissolution (SO-C).

Geomorphological FEPs (Section SCR.1.4, Ref. 6): 1. Physiography. 1.1 Physiography (UP). 2. Meteorite impact. 2.1 Impact of a large meteorite (SO-P). 3. Denudation. 3.1 Weathering. 3.1.1 Mechanical weathering (SO-C). 3.1.2 Chemical weathering. 3.2 Erosion. 3.2.1 Aeolian erosion (SO-C). 3.2.2 Fluvial erosion (SO-C). 3.2.3 Mass wasting (SO-C). 3.3 Sedimentation. 3.3.1 Aeolian deposition (SO-C). 3.3.2 Fluvial deposition (SO-C). 3.3.3 Lacustrine deposition (SO-C). 3.3.4 Mass wasting (SO-C). 4. Soil development. 4.1 Soil development (SO-C).

Surface Hydrological FEPs (Section SCR.1.5, Ref. 6): 1. Fluvial. 1.1 Stream and river flow (SO-C). 2. Lacustrine. 2.1 Surface water bodies (SO-C). 3. Groundwater recharge and discharge. 3.1 Groundwater discharge (UP). 3.2 Groundwater recharge (UP). 3.3 Infiltration (UP, UP for climate change effects). 4. Changes in surface hydrology. 4.1 Changes in groundwater recharge and discharge (UP). 4.2 Lake formation (SO-C). 4.3 River flooding (SO-C).

Climatic FEPs (Section SCR.1.6, Ref. 6): 1. Climate. 1.1 Precipitation (for example, rainfall) (UP). 1.2 Temperature (UP). 2. Climate change. 2.1 Meteorological. 2.1.1 Climate change (UP). 2.2 Glaciation. 2.2.1 Glaciation (SO-P). 2.2.2 Permafrost (SO-P).

Marine FEPs (Section SCR.1.7, Ref. 6): 1. Seas. 1.1 Seas and oceans (SO-C). 1.2 Estuaries (SO-C). 2. Marine sedimentology. 2.1 Coastal erosion (SO-C). 2.2 Marine sediment transport and deposition (SO-C). 3. Sea level changes. 3.1 Sea level changes (SO-C).

Ecological FEPs (Section SCR.1.8, Ref. 6): 1. Flora and fauna. 1.1 Plants (SO-C). 1.2 Animals (SO-C). 1.3 Microbes (SO-C, UP for colloidal effects and gas generation). 2. Changes in flora and fauna. 2.1 Natural ecological development (SO-C).

[a] Adapted from Ref. 6, Table 6-3.

[b] UP, FEPs accounted for in the assessment calculations for undisturbed performance for 40 CFR § 191.13 (as well as 40 CFR § 191.15 and Subpart C of 40 CFR Part 191); DP, FEPs accounted for (in addition to all UP FEPs) in the assessment calculations for disturbed performance for 40 CFR § 191.13; SO-R, FEPs eliminated from performance assessment calculations on the basis of regulations provided in 40 CFR Part 191 and criteria provided in 40 CFR Part 194; SO-C, FEPs eliminated from performance assessment (and compliance assessment) calculations on the basis of consequence; SO-P, FEPs eliminated from performance assessment (and compliance assessment) calculations on the basis of low probability of occurrence.

vated area by the ith intrusion, b_i designates whether or not the ith intrusion penetrates pressurized brine in the Castile Fm (see Ref. 5, Vol. 2, Section 2.2, for detailed stratigraphy), p_i designates the plugging procedure used with the ith intrusion, $\mathbf{a}_i$ designates the type of waste penetrated by the ith intrusion, and t_{min} is the time at which potash mining occurs within the land withdrawal boundary (Table III).

With respect to the questions indicated in Section 2, $\mathcal{S}_{st}$ provides an answer to Q1, while $\mathcal{S}_{st}$ and p_{st} provide an answer to Q2. In practice, Q2 is answered by the distributions specified for n, t_i, l_i, e_i, b_i, p_i, $\mathbf{a}_i$, and t_{min} (Table III), which in concept lead to definitions for $\mathcal{S}_{st}$ and p_{st}. The CCDF specified in 40 CFR 191 is obtained by evaluating an integral involving ($\mathcal{S}_{st}$, $\mathcal{S}_{st}$, p_{st}) (Fig. 2), with the probabilities associated with $\mathcal{S}_{st}$ and p_{st} being replaced symbolically by the corresponding density function d_{st}. The function f in Fig. 2 represents the environmental release associated with $\mathbf{x}_{st}$, corresponds to the second entity (i.e., EN2) in the 1996 WIPP PA, and is discussed in the next section.

Table III. Definitions and Distributions for Individual Elements t_i, l_i, e_i, b_i, p_i, $\mathbf{a}_i$, and t_{min} of Vectors $\mathbf{x}_{st}$ in Sample Space $\mathcal{S}_{st}$ for Stochastic Uncertainty

t_i: Time (years) of ith drilling intrusion within area marked by a berm as part of a system of passive institutional controls (Fig. 3, Ref. 39) with $t_1 \leq t_2 \leq \ldots \leq t_n \leq 10{,}000$ years and occurrence of individual drilling intrusions following a Poisson process with a time-dependent rate $\lambda_d(t)$ defined by $\lambda_d(t) = 0$ year^{-1} for $0 \leq t \leq 100$ years, $\lambda_d(t) = 2.94 \times 10^{-5}$ year^{-1} for $100 < t \leq 700$ years, and $\lambda_d(t) = 2.94 \times 10^{-3}$ year^{-1} for $700 < t \leq 10{,}000$ years. Base drilling rate defined to be 46.8 drilling intrusions/km^2/10^4 years after 700 years (Appendix DEL, Ref. 6), with no drilling intrusions possible between 0 and 100 years due to active institutional controls (Chapter 7, Ref. 6) and a two-order-of-magnitude reduction in drilling rate between 100 and 700 years due to passive institutional controls (Ref. 44). Additional information: Section 3.2, Ref. 45.

l_i: Integer designator for 144 discretized locations for drilling intrusions within area marked by a berm as part of a system of passive institutional controls (Fig. 3, Ref. 39). Probability pL_j that drilling intrusion i will occur at location L_j, $j = 1, 2, \ldots, 144$, in Fig. 3 of Ref. 39 is $pL_j = 1/144 = 6.94 \times 10^{-3}$. Additional information: Section 3.3, Ref. 45.

e_i: Integer designator for whether or not drilling intrusion i penetrates an excavated area of the respository (i.e., $e_i = 0, 1$ implies penetration of nonexcavated, excavated area, respectively). Corresponding probabilities pE_0, pE_1 for $e_i = 0, 1$ are $pE_0 = 0.791$, $pE_1 = 0.209$ and derive from excavated and nonexcavated areas within berm (Fig. 3, Ref. 39). Additional information: Section 3.4, Ref. 45.

b_i: Integer designator for whether or not drilling intrusion i penetrates pressurized brine in the Castile Fm (i.e., $b_i = 0, 1$ implies nonpenetration, penetration of pressurized brine; see Section 2.2, Vol. 2, Ref. 5, for detailed stratigraphy). Corresponding probabilities for $b_i = 0, 1$ are $pB_0 = 0.08$, $pB_1 = 0.92$. Additional information: Ref. 46; Section 3.5, Ref. 45.

p_i: Integer designator for plugging pattern used for drilling intrusion i, with (1) $p_i = 1$ corresponding to a full concrete plug through Salado Fm to Bell Canyon Fm with a permeability of 5×10^{-17} m^2, (2) $p_i = 2$ corresponding to a two-plug configuration with concrete plugs at Rustler/Salado interface and Castile/Bell Canyon interface, and (3) $p_i = 3$ corresponding to a three-plug configuration with concrete plugs at Rustler/Salado, Salado/Castile, and Castile/Bell Canyon interfaces. The probability that a given drilling intrusion will be sealed with plugging pattern j, $j = 1, 2, 3$, is given by pPL_j, where $pPL_1 = 0.02$, $pPL_2 = 0.68$, and $pPL_3 = 0.30$. Additional information: Ref. 47; Appendix DEL, Ref. 6; Section 3.6, Ref. 45.

$\mathbf{a}_i$: Designator for type of waste penetrated by drilling intrusion i. The waste intended for disposal at the WIPP is divided into 570 distinct waste streams (see Table 3.7.1, Fig. 3.7.1, Ref. 45), with 569 of these waste streams designated as contact-handled (CH)-TRU waste and one waste stream designated as remotely handled (RH)-TRU waste. Each waste drum emplaced at the WIPP will contain waste from a single CH-TRU waste stream. Given that the CH-TRU drums will be stacked three high, each drilling intrusion through CH-TRU waste will intersect three waste streams. In contrast, there is only one waste stream for RH-TRU waste with RH-TRU waste being emplaced separately from CH-TRU waste, and so each drilling intrusion through RH-TRU waste will intersect this single waste stream. Specifically, $\mathbf{a}_i = a_i = 0$ if $e_i = 0$ (i.e., if the ith drilling intrusion does not penetrate an excavated area of the repository); $\mathbf{a}_i = a_i = 1$ if $e_i = 1$ and RH-TRU waste is penetrated; and $\mathbf{a}_i = [2, iCH_{i1}, iCH_{i2}, iCH_{i3}]$ if $e_i = 1$ and CH-TRU waste is penetrated, where iCH_{i1}, iCH_{i2}, and iCH_{i3} are designators for the CH-TRU waste streams intersected by the ith drilling intrusion. Whether the ith intrusion penetrates a nonexcavated or excavated area is determined by the probabilities pE_0 and pE_1 defined in conjunction with e_i. Given that the ith intrusion penetrates an excavated area, the probabilities pCH and pRH of penetrating CH- and RH-TRU wastes are given by 0.876 and 0.124, respectively (Section 3.7, Ref. 45). The probabilities of the individual CH-TRU waste streams are indicated in Table 3.7.1 of Ref. 45. Additional information: Ref. 38; Section 3.7, Ref. 45.

t_{min}: Time (years) at which mining of potash deposits within land withdrawal boundary occurs. Assumed to follow a Poisson process (p. 5242, Ref. 33) with a time-dependent rate $\lambda_m(t)$ defined by $\lambda_m(t) = 0$ year^{-1} for $0 \leq t \leq 100$ years, $\lambda_m(t) = 1 \times 10^{-6}$ year^{-1} for $100 < t \leq 700$ years, and $\lambda_m(t) = 1 \times 10^{-4}$ year^{-1} for $700 < t \leq 10{,}000$ years, with no mining possible between 0 and 100 years due to active institutional controls (Chapter 7, Ref. 6) and a two-order-of-magnitude reduction in the mining rate between 100 and 700 years due to passive institutional control (Ref. 44). Additional information: Section 3.8, Ref. 45.

5. EN2: ESTIMATION OF RELEASES

The entity EN2 is the formal outcome of the FEPs process for determining what physical processes should be modeled at the WIPP, although most of the development of the mathematical representations for these physical processes took place outside of the FEPs process. Specifically, EN2 provides a way to estimate radionuclide releases to the accessible environment for the different futures (i.e., elements $\mathbf{x}_{st}$ of $\mathcal{S}_{st}$) that could occur at the WIPP. In concept, estimation of environmental releases corresponds to evaluation of the function f in Fig. 2; in practice, estimation of environmental releases and other system properties of interest involves evaluation of the models indicated in Fig. 3 and briefly described in Table IV.

When expressed in terms of the models indicated in Fig. 3 and Table IV, the function f in Fig. 2 is given by

$$\begin{aligned} f(\mathbf{x}_{st}) = {} & f_C(\mathbf{x}_{st}) + f_{SP}[\mathbf{x}_{st}, f_B(\mathbf{x}_{st})] \\ & + f_{DBR}\{\mathbf{x}_{st}, f_{SP}[\mathbf{x}_{st}, f_B(\mathbf{x}_{st})], f_B(\mathbf{x}_{st})\} \\ & + f_{MB}[\mathbf{x}_{st}, f_B(\mathbf{x}_{st})] \\ & + f_{DL}[\mathbf{x}_{st}, f_B(\mathbf{x}_{st})] + f_S[\mathbf{x}_{st}, f_B(\mathbf{x}_{st})] \\ & + f_{S\text{-}T}\{\mathbf{x}_{st,0}, f_{S\text{-}F}(\mathbf{x}_{st,0}), f_{N\text{-}P}[\mathbf{x}_{st}, f_B(\mathbf{x}_{st})]\} \end{aligned} \quad (4)$$

where $\mathbf{x}_{st}$ corresponds to the particular future under consideration; $\mathbf{x}_{st,0}$, a future involving no drilling intrusions but a mining event at the same time t_{min} as in $\mathbf{x}_{st}$; $f_C(\mathbf{x}_{st})$, cuttings and cavings release to accessible environment for $\mathbf{x}_{st}$ calculated with CUTTINGS_S; $f_B(x_{st})$, results calculated for $\mathbf{x}_{st}$ with BRAGFLO [in practice, $f_B(\mathbf{x}_{st})$ is a vector containing a large amount of information]; $f_{SP}[\mathbf{x}_{st}, f_B(\mathbf{x}_{st})]$, spallings release to accessible environment for $\mathbf{x}_{st}$ calculated with the spallings model contained in CUTTINGS_S [this calculation requires BRAGFLO results, i.e., $f_B(\mathbf{x}_{st})$, as input]; $f_{DBR}\{\mathbf{x}_{st}, f_{SP}[\mathbf{x}_{st}, f_B(\mathbf{x}_{st})], f_B(\mathbf{x}_{st})\}$, direct brine release to accessible environment for $\mathbf{x}_{st}$ calculated with a modified version of BRAGFLO designated BRAGFLO_DBR [this calculation requires spallings results obtained from CUTTINGS_S, i.e., $f_{SP}[\mathbf{x}_{st}, f_B(\mathbf{x}_{st})]$, and BRAGFLO results, i.e., $f_B(\mathbf{x}_{st})$, as input]; $f_{MB}[\mathbf{x}_{st}, f_B(\mathbf{x}_{st})]$, release through anhydrite marker beds to accessible environment for $\mathbf{x}_{st}$ calculated with NUTS [this calculation requires BRAGFLO results, i.e., $f_B(\mathbf{x}_{st})$, as input]; $f_{DL}[\mathbf{x}_{st}, f_B(\mathbf{x}_{st})]$, release through Dewey Lake Red Beds to accessible environment for $\mathbf{x}_{st}$ calculated with NUTS [this calculation requires BRAGFLO results, i.e., $f_B(\mathbf{x}_{st})$, as input]; $f_S[\mathbf{x}_{st}, f_B(\mathbf{x}_{st})]$, release to land surface due to brine flow up a plugged borehole for $\mathbf{x}_{st}$ calculated with NUTS or PANEL as appropriate [this calculation requires BRAGFLO results, i.e., $f_B(\mathbf{x}_{st})$, as input]; $f_{S\text{-}F}(\mathbf{x}_{st,0})$, flow field calculated for $\mathbf{x}_{st,0}$ with SECOFL2D; $f_{N\text{-}P}[\mathbf{x}_{st}, f_B(\mathbf{x}_{st})]$, release to Culebra for $\mathbf{x}_{st}$ calculated with NUTS or PANEL as appropriate [this calculation requires BRAGFLO results, i.e., $f_B(\mathbf{x}_{st})$, as input]; $f_{S\text{-}T}\{\mathbf{x}_{st,0}, f_{S\text{-}F}(\mathbf{x}_{st,0}), f_{N\text{-}P}[\mathbf{x}_{st}, f_B(\mathbf{x}_{st})]\}$, groundwater transport release through Culebra to accessible environment calculated with SECOTP2D [this calculation requires SECOFL2D results, i.e., $f_{S\text{-}F}(\mathbf{x}_{st,0})$, and NUTS or PANEL results, i.e., $f_{N\text{-}P}[\mathbf{x}_{st}, f_B(\mathbf{x}_{st})]$, as input; $\mathbf{x}_{st,0}$ is used as an argument to $f_{S\text{-}T}$ because drilling intrusions are assumed to cause no perturbations to the flow field in the Culebra].

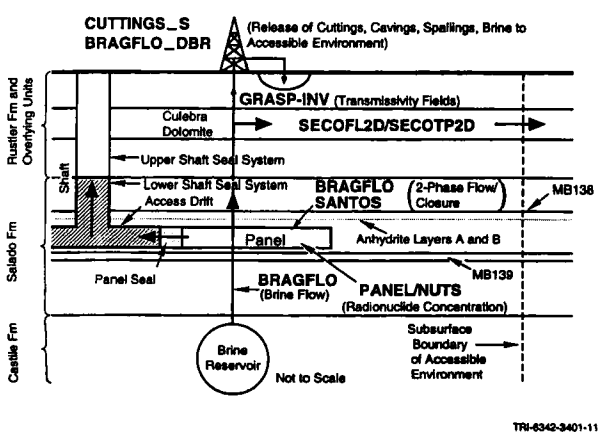

Fig. 3. Computer programs (models) used in 1996 WIPP PA (Fig. 5, Ref. 39).

The models in Fig. 3 and Table IV are too complex to permit a closed-form evaluation of the integral in Fig. 2 that defines the CCDF specified in 40 CFR 191. Instead, a Monte Carlo procedure was used in the 1996 WIPP PA.[61] With this approach, elements

$$\mathbf{x}_{st,i}, \qquad i = 1, 2. \ . \ . \ , nS \quad (5)$$

were randomly sampled from $\mathcal{S}_{st}$ in consistency with the definition of $(\mathcal{S}_{st}, \mathcal{S}_{st}, p_{st})$. Then the integral in Fig. 2, and hence the associated CCDF, was approximated by

$$prob(Rel > R)$$

$$= \int_{\mathcal{S}_{st}} \delta_R[f(\mathbf{x}_{st})] d_{st}(\mathbf{x}_{st})\, dV_{st} \doteq \sum_{i=1}^{nS} \delta_R[f(\mathbf{x}_{st,i})]/nS \quad (6)$$

where $\delta_R[f(\mathbf{x}_{st})] = 1$ if $f(\mathbf{x}_{st}) > R$ and 0 if $f(\mathbf{x}_{st}) \leq R$. The Monte Carlo CCDF construction procedure indicated in Eq. (6) and implemented by CCDFGF program[62,63] used a sample of size nS = 10,000 in the 1996 WIPP

Table IV. Summary of Computer Models Used in the 1996 WIPP PA[a]

BRAGFLO: Calculates multiphase flow of gas and brine through a porous, heterogeneous reservoir. Uses finite-difference procedures to solve system of nonlinear partial differential equations that describes the mass conservation of gas and brine along with appropriate constraint equations, initial conditions, and boundary conditions. Additional information: Ref. 48; Section 4.2, Ref. 45.
BRAGFLO_DBR: Special configuration of BRAGFLO model used in calculation of dissolved radionuclide releases to the surface (i.e., direct brine releases) at the time of a drilling intrusion. Uses initial value conditions obtained from calculations performed with BRAGFLO and CUTTINGS_S. Additional information: Ref. 49; Section 4.7, Ref. 45.
CUTTINGS_S: Calculates the quantity of radioactive material brought to the surface in cuttings and cavings and also in spallings generated by an exploratory borehole that penetrates a waste panel, where cuttings designates material removed by the drillbit, cavings designates material eroded into the borehole due to shear stresses resulting from the circular flow of the drilling fluid (i.e., mud), and spallings designates material carried to the borehole at the time of an intrusion due to the flow of gas from the repository to the borehole. Spallings calculation uses intial value conditions obtained from calculations performed with BRAGFLO. Outside reviewers expressed some concern over the spallings model incorporated into CUTTINGS_S,[50] but additional study led to the conclusion that this model was unlikely to have overestimated the size of the spallings release.[51] Additional information: Refs. 52, 53; Sections 4.5, 4.6, Ref. 45.
GRASP-INV: Generates transmissivity fields (estimates of transmissivity values) conditioned on measured transmissivity values and calibrated to steady-state and transient pressure data at well locations using an adjoint sensitivity and pilot-point technique. Additional information: Refs. 54, 55.
NUTS: Solves system of partial differential equations for radionuclide transport in vicinity of repository. Uses brine volumes and flows calculated by BRAGFLO as input. Additional information: Ref. 56; Section 4.3, Ref. 45.
PANEL: Calculates rate of discharge and cumulative discharge of radionuclides from a waste panel through an intruding borehole. Discharge is a function of fluid flow rate, elemental solubility, and radionuclide inventory. Uses brine volumes and flows calculated by BRAGFLO as input. Based on solution of system of linear ordinary differential equations. Additional information: Ref. 56; Section 4.4, Ref. 45.
SANTOS: Solves quasistatic, large-deformation, inelastic response of two-dimensional solids with finite-element techniques. Used to determine porosity of waste as a function of time and cumulative gas generation, which is an input to calculations performed with BRAGFLO. Additional information: Refs. 48, 57, 58; Section 4.2.3, Ref. 45.
SECOFL2D: Calculates single-phase Darcy flow for groundwater flow in two dimensions. The formulation is based on a single partial differential equation for hydraulic head using fully implicit time differencing. Uses transmissivity fields generated by GRASP-INV. Additional information: Refs. 59, 60; Section 4.8, Ref. 45.
SECOTP2D: Simulates transport of radionuclides in fractured porous media. Solves two partial differential equations: one provides two-dimensional representation for convective and diffusive radionuclide transport in fractures and the other provides one-dimensional representation for diffusion of radionuclides into rock matrix surrounding the fractures. Uses flow fields calculated by SECOFL2D. Additional information: Refs. 59, 60; Section 4.9, Ref. 45.

[a] Ref. 39, Table I.

PA. The individual programs in Fig. 3 do not run fast enough to allow this number of evaluations of f. As a result, it was necessary to evaluate the programs in Fig. 3 for a limited number of futures and then to use this limited number of evaluations to construct the releases for the large number of futures that must be considered in Eq. (6) (see Section 7).

With respect to the questions indicated in Section 2, the models in Fig. 3 and Table IV are providing an answer to Q3.

6. EN3: PROBABILISTIC CHARACTERIZATION OF PARAMETER UNCERTAINTY

The entity EN3 is the formal outcome of the data development effort for the WIPP. Specifically, EN3 provides a probabilistic characterization of the uncertainty in the parameters that underlie the WIPP PA. The entity EN3 is defined by a probability space $(\mathcal{S}_{su}, \mathcal{S}_{su}, p_{su})$, with the sample space $\mathcal{S}_{su}$ given by

$$\mathcal{S}_{su} = \{\mathbf{x}_{su}\text{: } \mathbf{x}_{su} \text{ is possibly the correct vector of parameter values to use in the WIPP PA models}\} \tag{7}$$

The subscript su refers to subjective (i.e., epistemic) uncertainty and is used because $(\mathcal{S}_{su}, \mathcal{S}_{su}, p_{su})$ is providing a probabilistic characterization of where the appropriate inputs to use in the WIPP PA are believed to be located.[41,42] The vectors $\mathbf{x}_{su}$ in $\mathcal{S}_{su}$ are of the form

$$\mathbf{x}_{su} = [x_1, x_2, \ldots, x_{nV}] \tag{8}$$

where each element x_j of $\mathbf{x}_{su}$ is an uncertain input to

Table V. Example Elements of $\mathbf{x}_{su}$ in the 1996 WIPP PA[a]

ANHPRM, Logarithm of anhydrite permeability (m^2). Used in BRAGFLO. Distribution: Student's t distribution with 5 degrees of freedom. Range: −21.0 to −17.1 (i.e., permeability range is 1×10^{-21} to $1 \times 10^{-17.1}$ m^2). Mean, median: −18.9, −18.9. Correlation: −0.99 rank correlation with *ANHCOMP* (bulk compressibility of anhydrite, Pa^{-1}).

BPCOMP, Logarithm of bulk compressibility of brine pocket (Pa^{-1}). Used in BRAGFLO. Distribution: Triangular. Range: −11.3 to −8.00 (i.e., bulk compressibility range is $1 \times 10^{-11.3}$ to 1×10^{-8} Pa^{-1}). Mean, mode: −9.80, −10.0. Correlation: −0.75 rank correlation with *BPPRM* (logarithm of brine pocket permeability, m^2).

HALPRM, Logarithm of halite permeability (m^2). Used in BRAGFLO. Distribution: Uniform. Range: −24 to −21 (i.e., permeability range is 1×10^{-24} to 1×10^{-21} m^2). Mean, median: −22.5, −22.5. Correlation: −0.99 rank correlation with *HALCOMP* (bulk compressibility of halite, Pa^{-1}).

WMICDFLG, Pointer variable for microbial degradation of cellulose. Used in BRAGFLO. Distribution: Discrete, with 50% 0, 25% 1, 25% 2. *WMICDFLG* = 0, 1, 2 implies no microbial degradation of cellulose, microbial degradation of only cellulose, microbial degradation of cellulose, plastic, and rubber.

WTAUFAIL, Shear strength of waste (Pa). Used in CUTTINGS_S. Distribution: Uniform. Range: 0.05–10 Pa. Mean, median: 5.03, 5.03 Pa.

[a] See Ref. 46, Appendix PAR and Ref. 45, Table 5.2.1 for a complete listing of the $nV = 57$ elements of $\mathbf{x}_{su}$ and sources of additional information.

the 1996 WIPP PA and nV is the number of such inputs (Table V).

The uncertainty in $\mathbf{x}_{su}$ is characterized by specifying a distribution

$$D_j, \qquad j = 1, 2, \ldots, nV \tag{9}$$

for each element x_j of $\mathbf{x}_{su}$ (Fig. 4). Correlations and other restrictions involving the elements of $\mathbf{x}_{su}$ are also possible. In the 1996 WIPP PA, rank correlations[65,66] were imposed on three pairs of variables (Fig. 5). The distributions D_j, $j = 1, 2, \ldots, nV$, and any associated conditions then give rise to the probability space $(\mathcal{S}_{su}, \mathcal{S}_{su}, p_{su})$.

In concept, individual elements of $\mathbf{x}_{su}$ can affect

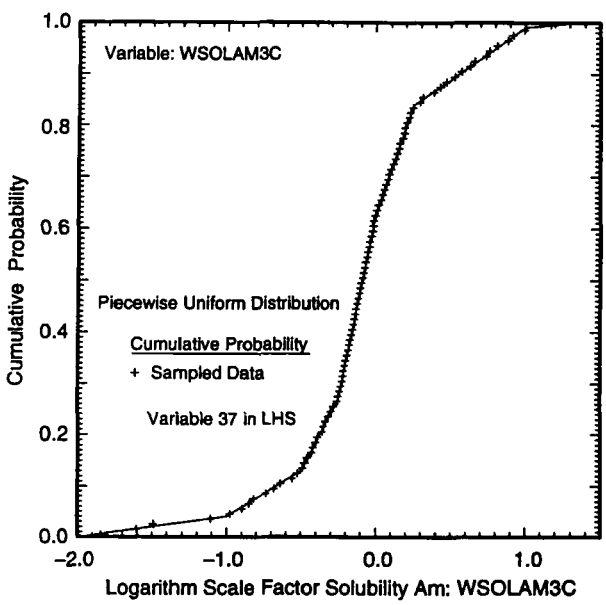

Fig. 4. Example of an uncertain variable, its associated distribution, and sampled values obtained with a Latin hybercube sample[64] of size 100 (see Appendix PAR, Ref. 6, for distributions of the $nV = 57$ variables in $\mathbf{x}_{su}$).

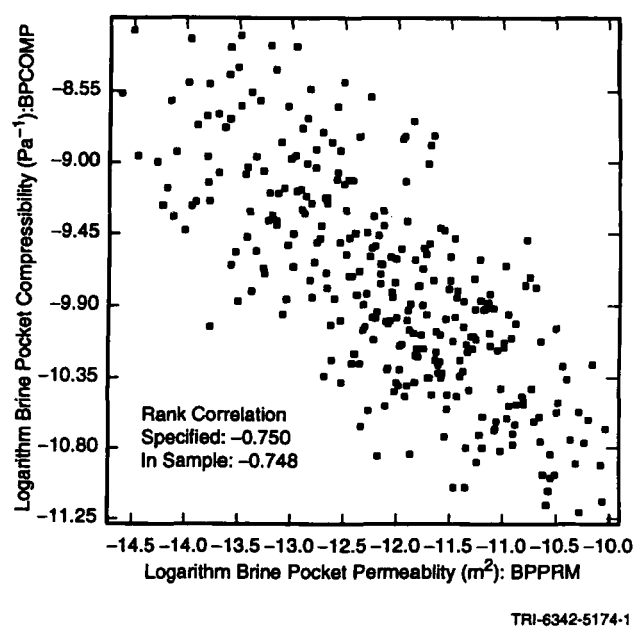

Fig. 5. Scatterplot illustrating correlation within the pair (*BPCOMP*, *BPPRM*); see Fig. 5.4.1, Ref. 45, for correlations within the pairs (*ANHCOMP*, *ANHPRM*) and (*HALCOMP*, *HALPRM*).

either the definition of $(\mathcal{S}_{st}, \mathcal{S}_{st}, p_{st})$ or the definition and/or evaluation of f. For example, the drilling rate or probability of penetrating pressurized brine in the Castile Fm could be treated as being uncertain, which would affect the definition of $(\mathcal{S}_{st}, \mathcal{S}_{st}, p_{st})$. Similarly, whether to use the Brooks–Corey or van Genuchten–Parker model for relative permeability or the appropriate value of a spatially averaged distribution coefficient (i.e., k_d value) could be treated as being uncertain, with the former affecting the definition of f and the latter defining a specific input parameter to f. All elements of $\mathbf{x}_{su}$ relate to the models in Fig. 2 in the 1996 WIPP PA. However, this does not have to be the case, and the probability of penetrating pressurized brine (i.e., pB_1 in Table III) was treated as being uncertain in a verification analysis associated with the 1996 WIPP PA carried out by SNL for the EPA.[67]

If $\mathbf{x}_{su}$ was known exactly, then the CCDF in Fig. 2 could be determined with certainty and an unambiguous comparison made with the boundary line specified in 40 CFR 191. However, given the complex physical processes that could take place at the WIPP site and the 10,000-year time period under consideration, $\mathbf{x}_{su}$ can never be known with certainty. Instead, uncertainty in $\mathbf{x}_{su}$ as characterized by $(\mathcal{S}_{su}, \mathcal{S}_{su}, p_{su})$ will lead to a distribution of possible CCDFs (Fig. 6), with a different CCDF resulting for each value that $\mathbf{x}_{su}$ can take on. As indicated in Fig. 6, f is now being viewed as a function of both $\mathbf{x}_{st}$ and $\mathbf{x}_{su}$, with $(\mathcal{S}_{st}, \mathcal{S}_{st}, p_{st})$ giving rise to a different CCDF for each value that $\mathbf{x}_{su}$ can take. In turn, $(\mathcal{S}_{su}, \mathcal{S}_{su}, p_{su})$ gives rise to a distribution of CCDFs. The proximity of this distribution to the boundary line in Fig. 2 provides an indication of the confidence with which 40 CFR 191 will be met.

The distribution of CCDFs in Fig. 6 can be summarized by distributions of exceedance probabilities conditional on individual release values (Fig. 7). For a given release value R, this distribution is defined by a double integral over $\mathcal{S}_{su}$ and $\mathcal{S}_{st}$.[42,68] In practice, this integral is too complex to permit a closed-form evaluation. Instead, the 1996 WIPP PA used Latin hypercube sampling[64] to evaluate the integral over $\mathcal{S}_{su}$ and, as indicated in Eq. (6), simple random sampling to evaluate the integral over $\mathcal{S}_{st}$. With this approach, a Latin hypercube sample (LHS) $\mathbf{x}_{su,k}$, $k = 1, 2, \ldots, nLHS$, is generated from $\mathcal{S}_{su}$ in consistency with the definition of $(\mathcal{S}_{su}, \mathcal{S}_{su}, p_{su})$, and a random sample $\mathbf{x}_{st,i}$, $i = 1, 2, \ldots, nS$, is generated from $\mathcal{S}_{st}$ in consistency with the definition of $(\mathcal{S}_{st}, \mathcal{S}_{st}, p_{st})$. The percentile values in Fig. 7 are then approximated by solving

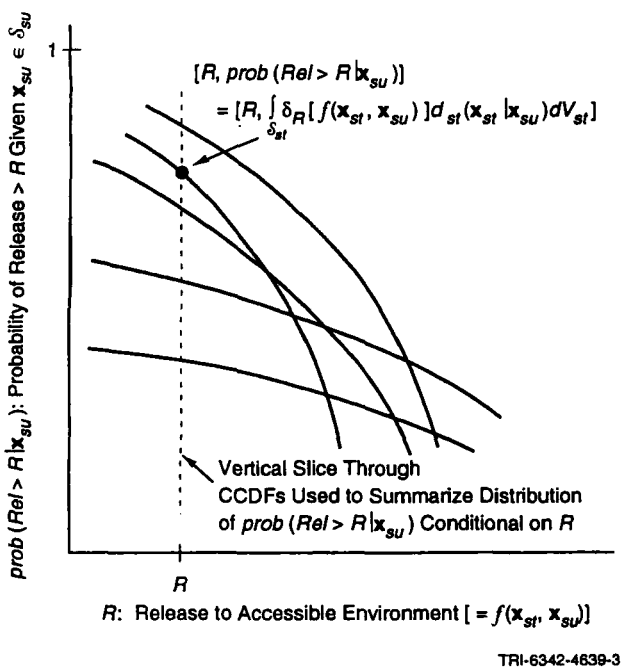

Fig. 6. Distribution of CCDFs resulting from possible values for $\mathbf{x}_{su} \in \mathcal{S}_{su}$ (adapted from Fig. 2, Ref. 42).

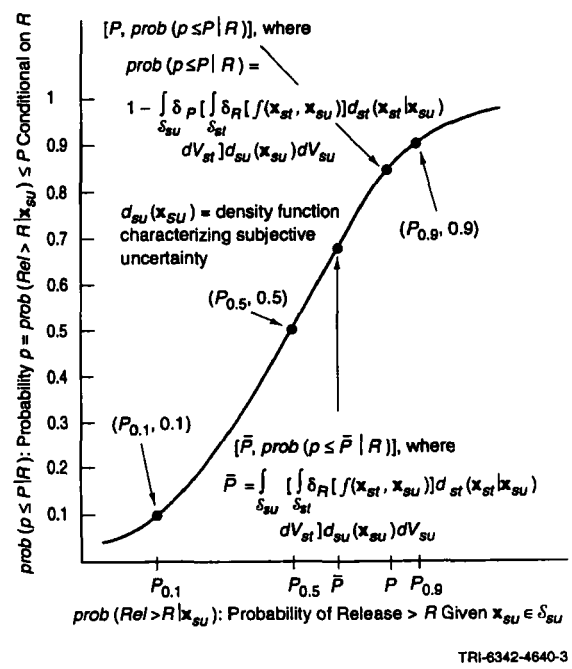

Fig. 7. Distribution of exceedance probabilities due to subjective uncertainty (adapted from Fig. 3, Ref. 42).

$$prob(p \le P|R) \doteq 1 - \sum_{k=1}^{nLHS} \delta_P \left[\sum_{i=1}^{nS} \delta_R[f(\mathbf{x}_{st,i}, \mathbf{x}_{su,k})]/nS \right] \Big/ nLHS \quad (10)$$

for P with $prob(p \le P|R) = 0.1$, 0.5, and 0.9, respectively, and the definition of δ_R, and hence the corresponding definition of δ_P, given in conjunction with Eq. (6). Similarly, the mean exceedance probability $\overline{P}$ is approximated by

$$\overline{P} \doteq \sum_{k=1}^{nLHS} \left[\sum_{i=1}^{nS} \delta_R[f(\mathbf{x}_{st,i}, \mathbf{x}_{su,k})]/nS \right] \Big/ nLHS \quad (11)$$

The results of the preceding calculations are typically displayed by plotting percentile values (e.g., $P_{0.1}$, $P_{0.5}$, $P_{0.9}$ in Fig. 7) and also mean values for exceedance probabilities (i.e., $\overline{P}$ in Fig. 7) above the corresponding release values (i.e., R) and then connecting these points to form continuous curves (Fig. 8). The proximity of these curves to the indicated boundary line provides an indication of the confidence with which 40 CFR 191 will be met.

With respect to the questions indicated in Section 2, ($\mathcal{S}_{su}$, $\mathcal{S}_{su}$, p_{su}) and results derived from ($\mathcal{S}_{su}$, $\mathcal{S}_{su}$, p_{su}) (e.g., the distributions in Figs. 6–8) are providing an answer to Q4.

7. COMPUTATIONAL DETAILS OF 1996 WIPP PA

The requirements in 194.34(c), (d), and (f) relate to the procedures used for a Monte Carlo integration over ($\mathcal{S}_{su}$, $\mathcal{S}_{su}$, p_{su}). The accuracy requirements in 194.34(d) can be satisfied with a simple random sample from $\mathcal{S}_{su}$ of size 300 (i.e., $1 - 0.99^n > 0.95$ yields $n = 298$). However, the 1996 WIPP PA decided to use Latin hypercube sampling[64] rather than simple random sampling for the required Monte Carlo integration on ($\mathcal{S}_{su}$, $\mathcal{S}_{su}$, p_{su}) due to the efficient stratification properties of Latin hypercube sampling.[69–71]

By using an LHS of size 300, the requirements in 194.34(c) and (d) can be met. Further, the confidence intervals required in 194.34(f) can be determined by generating the LHS with a replicated sampling procedure proposed by Iman.[72] In this procedure, the LHS $\mathbf{x}_{su,k}$, $k = 1, 2, \ldots, nLHS$, used in Eqs. (10) and (11) is repeatedly generated with different random seeds. These samples lead to a sequence $\overline{P}_r(R)$, $r = 1, 2, \ldots, nR$, of estimated mean exceedance probabilities, where $\overline{P}_r(R)$ defines the mean CCDF obtained for sample r [i.e., $\overline{P}_r(R)$ is the mean probability that a normalized release of size R will be exceeded] and nR is the number of independent LHSs generated with different random seeds. Then,

$$\overline{P}(R) = \sum_{r=1}^{nR} \overline{P}_r(R)/nR \quad (12)$$

and

$$SE(R) = \left\{ \sum_{r=1}^{nR} [\overline{P}_r(R) - \overline{P}(R)]^2/nR(nR-1) \right\}^{1/2} \quad (13)$$

provide an additional estimate of the mean CCDF and an estimate of the standard error associated with the mean exceedance probabilities. The t distribution with $nR - 1$ degrees of freedom can be used to place confidence intervals around the mean exceedance probabilities for individual R values [i.e., around $\overline{P}(R)$]. Specifically, the $1 - \alpha$ confidence interval is given by $\overline{P}(R) \pm t_{1-\alpha/2} SE(R)$, where $t_{1-\alpha/2}$ is the $1 -$

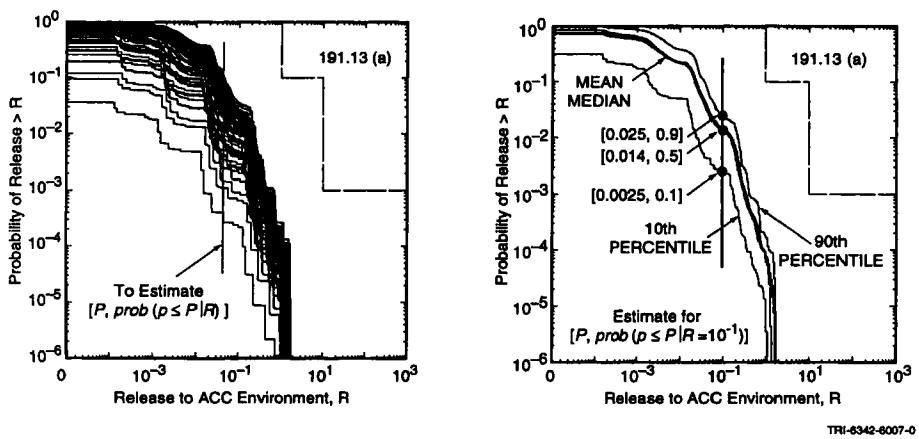

Fig. 8. Example CCDF distribution from 1992 WIPP PA (Fig. 10, Ref. 30).

$\alpha/2$ quantile of the t distribution with $nR - 1$ degrees of freedom (e.g., $t_{1-\alpha/2} = 4.303$ for $\alpha = 0.05$ and $nR = 3$).

To implement the preceding procedure, the 1996 WIPP PA used $nR = 3$ replicated LHSs of size $nLHS = 100$ each. This produced a total of 300 observations, which is approximately the same as the sample size of 298 indicated above. Each sample has the form

$$\mathbf{x}_{su,k} = [x_{k1}, x_{k2}, \ldots, x_{k,nV}], \quad k = 1, 2, \ldots, nLHS = 100 \tag{14}$$

and was generated with the restricted pairing technique developed by Iman and Conover[65] to induce specified rank correlations between correlated variables and also to assure that uncorrelated variables have correlations close to zero.

The calculations performed with the models in Fig. 3 and Table IV for the LHS elements in Eq. (14) had to be chosen very carefully. Otherwise, the total computational cost would have been prohibitive. In particular, a full set of model calculations to determine $f(\mathbf{x}_{st,i})$ in Eq. (6) could not be performed for each randomly sampled future $\mathbf{x}_{st,i}$. Rather, calculations were performed for a selected group of futures for each LHS element (Table VI), and then various interpolations and algebraic procedures were used to extend the results obtained with these futures to the large number of randomly sampled futures used in Eq. (6) (Ref. 45, Chapters 9–13). As an example, the procedures used to construct the spallings release [i.e., $f_{SP}(\mathbf{x}_{st,i})$ in Eq. (4)] will be described in Section 9; in addition, Section 6.6 of Ref. 45 provides a detailed description of the procedure used to sample the individual futures. Once values for $f(\mathbf{x}_{st,i})$ were determined, which correspond to the normalized release R in Eq. (1), the CCDF specified in 191.13(a) was readily constructed. Similarly, f_C, f_{SP}, f_{DBR}, f_{MB}, f_{DL}, f_S, and $f_{S\text{-}T}$ in Eq. (4) were used to estimate CCDFs for individual release modes.

Repetition of the preceding procedure for each LHS element yielded a distribution of CCDFs of the form in Fig. 8 for each of the $nR = 3$ replicates as requested in 194.34(e). Further, the replicated samples and the procedure in Eqs. (12) and (13) provided a basis for the estimation of confidence intervals as requested in 194.34(f).

8. INTERMEDIATE RESULTS

As indicated in Table VI, a large number of mechanistic calculations were performed as part of the 1996 WIPP PA. In turn, the outcomes of these calculations served as input to other mechanistic calculations or to algebraic procedures used in CCDF construction. The outcomes of a small number of these calculations are now presented, with more detailed presentations available in the original documentation for the 1996 WIPP PA.[45,48,49,53,55,56,60]

The first result required in the evaluation of $f(\mathbf{x}_{st})$ in Eq. (4) is the cuttings and cavings release (i.e., f_C). The volume of waste removed by cuttings and cavings was calculated by CUTTINGS_S (Fig. 9). As indicated in conjunction with $\mathbf{a}_i$ in Table III, this volume was then multiplied by an appropriate radionuclide concentration to obtain the actual radionuclide release to the surface. The sampling of the waste type (see $\mathbf{a}_i$ in Table III) and the individual waste streams if CH waste is penetrated is carried out within the Monte Carlo construction of individual CCDFs indicated in Eq. (6), with the cuttings and cavings release being dominated by intrusions through CH waste. In particular, the average concentration of CH waste is higher than that of RH waste (Fig. 10), and a drilling intrusion is more likely to penetrate CH waste than RH waste (se pCH and pRH in entry for $\mathbf{a}_i$ in Table III). Further, the variation in the radionuclide concentrations in the 569 waste streams for CH waste causes a wide range in the size of the releases associated with individual drilling intrusions through CH waste (Fig. 11).

The BRAGFLO model [i.e., f_B in Eq. (4)] produced results used by CUTTINGS_S, BRAGFLO_DBR, NUTS, and PANEL to estimate releases from the repository. An important result supplied by BRAGFLO and used by CUTTINGS_S and BRAGFLO_DBR to estimate spallings and direct brine releases, respectively, is repository pressure (Fig. 12). The pressure results in Fig. 12 are for replicate R1 and BRAGFLO calculations for two cases: (1) undisturbed (i.e., E0) conditions, and (2) a drilling intrusion at 1,000 years that penetrates pressurized brine in the Castile Fm (i.e., an E1 intrusion at 1,000 years). Each frame in Fig. 12 contains 100 individual pressure curves, with each curve calculated for one of the 100 LHS elements associated with replicate R1 [see Eq. (14)]. Thus, Fig. 12 displays results (i.e., pressure curves) obtained in 200 of the 1,800 calculations performed with BRAGFLO (Table VI).

The pressure in the repository under undisturbed conditions tends to increase monotonically toward an asymptote (Fig. 12a). In contrast, pressure tends to drop rapidly subsequent to a drilling intru-

Table VI. Mechanistic Calculations Performed as Part of the 1996 WIPP PA

BRAGFLO

Individual calculations (six cases): E0 (i.e., undisturbed conditions); E1 at 350, 1000 years (i.e., drilling intrusion through repository that penetrates pressurized brine in the Castile Fm); E2 at 350, 1000 years (i.e., drilling intrusion through repository that does not penetrate pressurized brine in the Castile Fm); E2E1 with E2 intrusion at 800 years and E1 intrusion at 2,000 years. Total calculations: 6 $nR\ nLHS = 6 \cdot 3 \cdot 100 = 1800$.

CUTTINGS_S

Individual calculations (52 cases): Intrusion into lower waste panel in previously unintruded (i.e., E0 conditions) repository at 100, 350, 1000, 3000, 5000, 10,000 years; intrusion into upper waste panel in previously unintruded repository at 100, 350, 1000, 3000, 5000, 10,000 years; initial E1 intrusion at 350 years followed by a second intrusion into the same waste panel at 550, 750, 2000, 4000, or 10,000 years; initial E1 intrusion at 350 years followed by a second intrusion into a different waste panel at 550, 750, 2000, 4000, or 10,000 years; initial E1 intrusion at 1000 years followed by a second intrusion into the same waste panel at 1200, 1400, 3000, 5000, or 10,000 years; initial E1 intrusion at 1000 years followed by a second intrusion into a different waste panel at 1200, 1400, 3000, 5000, or 10,000 years; same 23 cases for initial E2 intrusions as for initial E1 intrusions. Total calculations: 52 $nR\ nLHS = 52 \cdot 3 \cdot 100 = 15{,}600$.

BRAGFLO_DBR

Same computational cases as for CUTTINGS_S.

NUTS

Individual calculations (15 cases): E0; E1 at 100, 350, 1000, 3000, 5000, 7000, 9000 years; E2 at 100, 350, 1000, 3000, 5000, 7000, 9000 years. Screening calculations: 5 $nR\ nLHS = 1500$. Total NUTS calculations: 594. Note: Screening calculations were initially performed for each LHS element (i.e., E0, E1 at 350 and 1000 years, E2 at 350 and 1000 years, which produces the multiplier of 5 in the calculation of the number of screening calculations) to determine if the potential for a radionuclide release existed, with a full NUTS calculation only being performed when such a potential existed.

PANEL

Individual calculations (seven cases): E2E1 at 100, 350, 1000, 2000, 4000, 6000, 9000 years. Total calculations: 7 $nR\ nLHS = 7 \cdot 3 \cdot 100 = 2100$. Note: Additional PANEL calculations were also performed at 100, 125, 175, 350, 1000, 3000, 5000, 7500, and 10,000 years for Salado-dominated brines and also for Castile-dominated brines to determine dissolved radionuclide concentrations for use in the determinations of direct brine releases.

SECOFL2D

Individual calculations (two cases): Partially mined conditions in vicinity of repository (i.e., conditions before t_{min}); fully mined conditions in vicinity of repository (i.e., conditions after t_{min}). Total calculations: 2 $nR\ nLHS = 2 \cdot 3 \cdot 100 = 600$.

SECOTP2D

Individual calculations (two cases): Partially mined conditions in vicinity of repository; fully mined conditions in vicinity of repository. Total calculations: 2 $nR\ nLHS = 2 \cdot 3 \cdot 100 = 600$. Note: Each calculation is for four radionuclides: Am-241, Pu-239, Th-230, U-234. Further, calculations are done for unit releases at time 0 years, which can then be used to construct transport results for the Culebra for arbitrary time-dependent release rates into the Culebra (Ref. 45, Section 12.2).

sion due to gas flow up the borehole (Fig. 12b). Due to the relatively high permeability of the repository and the surrounding disturbed rock zone (DRZ), pressure gradients within the repository are small and pressure is almost constant throughout the repository at any given time.

Spallings results [i.e., f_{SP} in Eq. (4)] were calculated for both drilling intrusions into an undisturbed repository (i.e., E0 conditions) and drilling intrusions subsequent to an E1 or E2 intrusion (Table VI), with intrusions under undisturbed (Fig. 13) and disturbed (Fig. 14) repository conditions using pressure results of the form shown in Figs. 12a and 12b, respectively. Repository pressure at the time of the intrusion is used in the calculation of spallings releases with CUTTINGS_S. The calculations with CUTTINGS_S produced volumes of material released due to spallings (Figs. 13a, 14a), with these volumes then multiplied by the concentration of radionuclides in waste [EPA units/m^3 as defined in Eq. (1)] (Fig. 10) to produce radionuclide releases to the surface (Figs. 13b, 14b). Second and subsequent drilling intrusions often produce no spallings release (Fig. 14) due to low pressure in the repository (Fig. 12b). In particular, a column of drilling fluid at the depth of the repository exerts a pressure of approximately 8 MPa, and so both spallings releases and direct brine releases were assumed to have the potential to take place only when the pressure in the repository was above 8 MPa.[49]

Direct brine releases [i.e., f_{DBR} in Eq. (4)] were calculated for the same cases as spallings releases (Table VI). Similarly to the spallings calculation with CUTTINGS_S, a brine release was initially calculated by BRAGFLO_DBR (Fig. 15a), which was then multiplied by a radionuclide concentration (Fig. 16) to produce a direct brine release to the surface (Fig. 15b). Time-dependent radionuclide concentra-

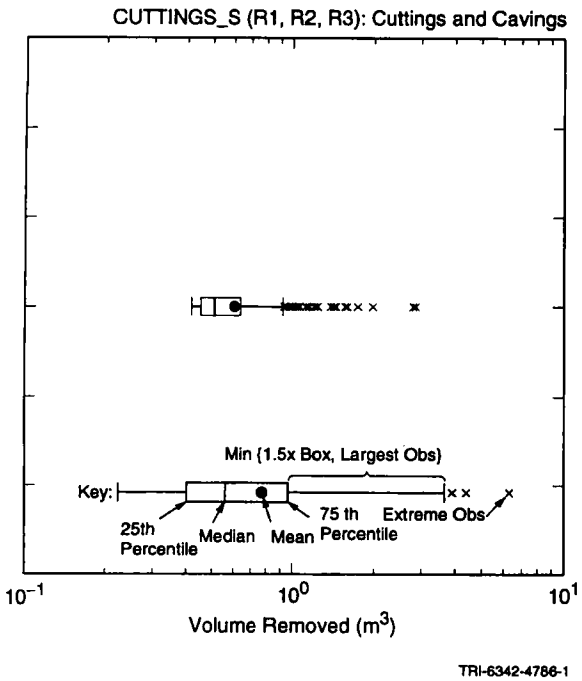

Fig. 9. Distribution over all 300 LHS elements for original (i.e., uncompacted) volume removed due to cuttings and cavings by a single drilling intrusion through CH-TRU waste.

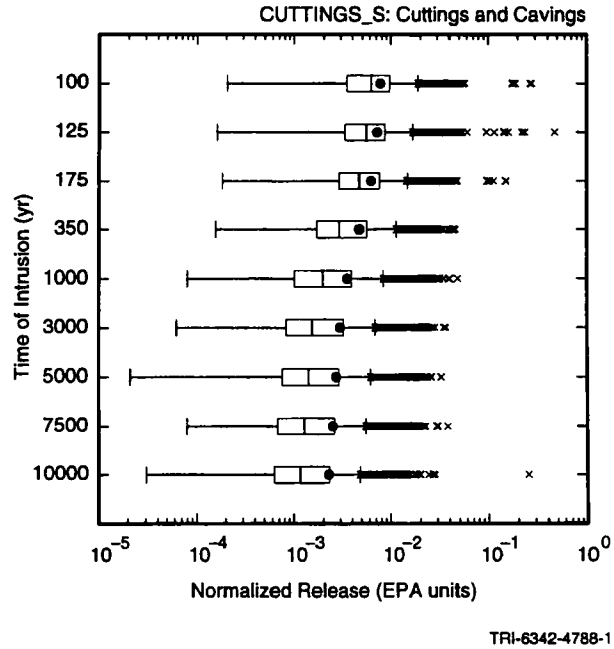

Fig. 11. Distribution of normalized release to accessible environment for cuttings removal from CH-TRU waste due to variation in intersected waste streams. Results calculated with median volume from Fig. 9 (i.e., 0.508 m^3), 38.6% of removed volume assumed to be CH-TRU waste, and a sample of size 10,000 at each time.

tions for Salado-dominated brine (Fig. 16a) and Castile-dominated brine (Fig. 16b) were used in the analysis because the chemistry of the brine and hence radionuclide solubilities are believed to be a function of brine source. The distributions of concentration

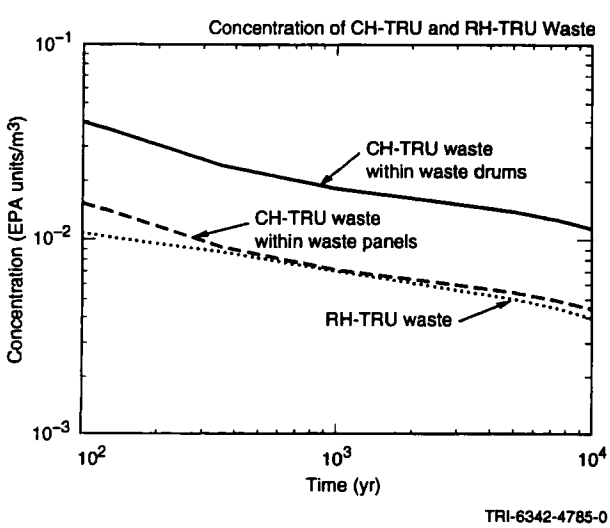

Fig. 10. Average concentration (EPA units/m^3) of CH- and RH-TRU waste.

curves in Fig. 16 result from uncertain variables contained in $\mathbf{x}_{su}$ and sampled in the LHS in Eq. (14). The calculations for direct brine releases subsequent to an initial drilling intrusion have the same case structure as for spallings releases (Table VI), with these releases often being zero due to either low pressure or low brine saturation in the repository (Ref. 45, Figs. 10.1.6, 10.1.7).

Another important result calculated by BRAGFLO is brine flow away from the repository, with such flows then used as input to NUTS and PANEL to determine radionuclide transport away from the repository by flowing brine. In terms of the representation for $f(\mathbf{x}_{st})$ in Eq. (4), these flows are used in the determination of f_{MB}, f_{DL}, f_S, and $f_{N\text{-}P}$. The releases represented by f_{MD}, f_{DL}, and f_S were determined by calculations performed with NUTS and were found to be zero for each of the 1,500 BRAGFLO calculations used to supply input for NUTS calculations (Table VI) due to limited or nonexistent brine flow from the repository to the marker beds, the Dewey Lake Red Beds, and the land surface. The only potentially significant brine flows away from the repository calculated by BRAGFLO were up an intruding borehole from the repository to the Culebra Dolomite

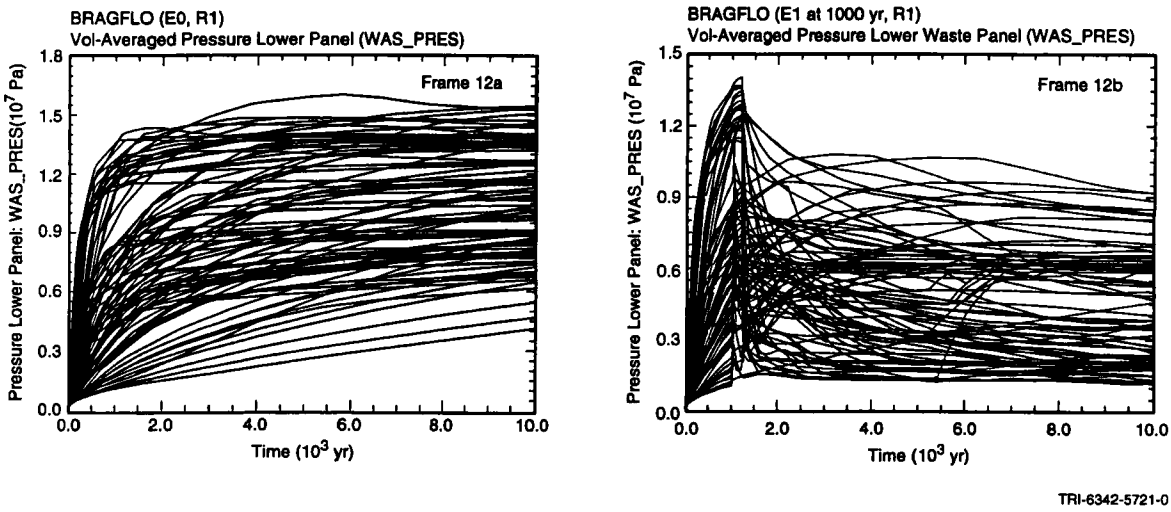

Fig. 12. Repository pressure for 100 LHS elements in replicate R1: (a) Undisturbed (i.e., E0) conditions, and (b) E1 intrusion at 1,000 years.

(Fig. 17), with these flows used in the determination of $f_{N\text{-}P}$ with NUTS or PANEL as appropriate (Table VI). However, most of these potentially important flows were also zero or very close to zero (Fig. 17).

The NUTS program was used to determine $f_{N\text{-}P}$ for cases involving a single drilling intrusion (i.e., an E1 or E2 intrusion), and the PANEL program was used to determine $f_{N\text{-}P}$ for cases involving both an E2 and an E1 intrusion into the same waste panel (i.e., an E2E1 intrusion). As an example, Fig. 18 shows releases of individual radionuclides for an E1 intrusion at 1,000 years (Fig. 18a) and total normalized

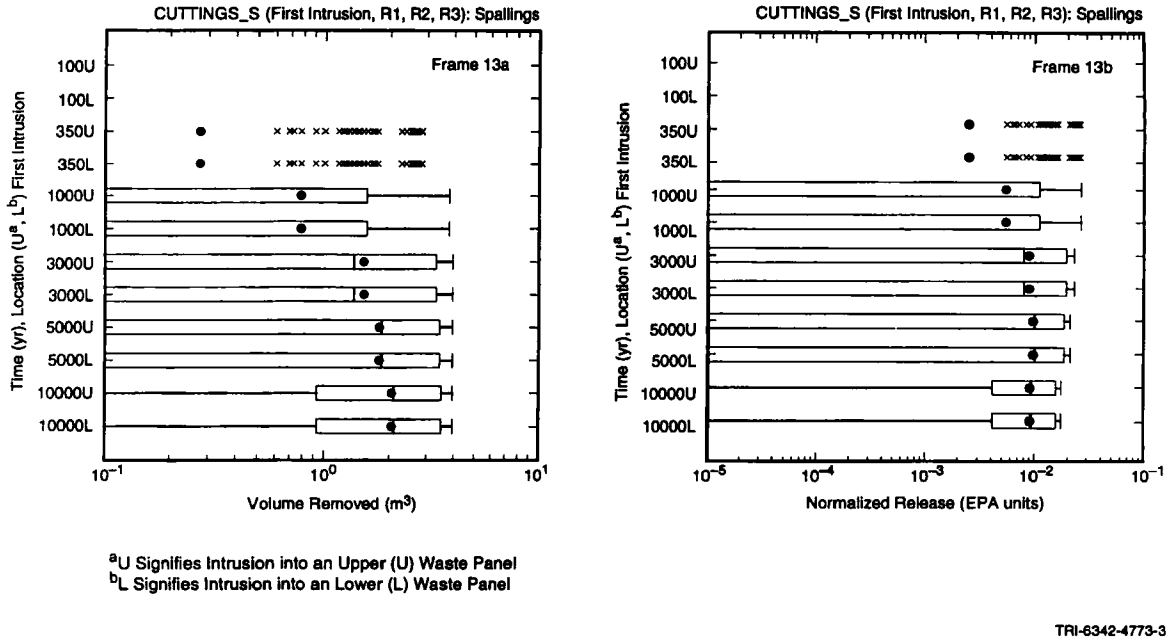

Fig. 13. Distribution over all 300 LHS elements for original (i.e., uncompacted) volume removed (m^3) and normalized release (EPA units) due to spallings for a single drilling intrusion into a previously unintruded repository that encounters CH-TRU waste.

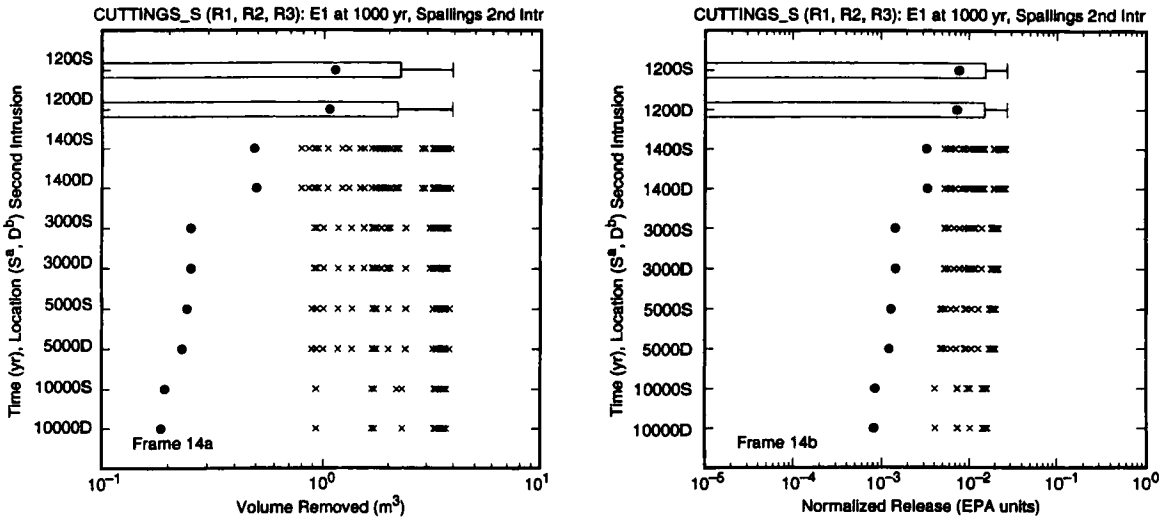

[a]S Signifies Second Intrusion Occurs in Same (S) Waste Panel as First Intrusion

[b]D Signifies Second Intrusion Occurs in Different (D) Waste Panel than First Intrusion

TRI-6342-4782-2

Fig. 14. Distribution over all 300 LHS elements for original (i.e., uncompacted) volume removed (m^3) and normalized release (EPA units) due to spallings for the second drilling intrusion into CH-TRU waste after an initial E1 intrusion at 1,000 years.

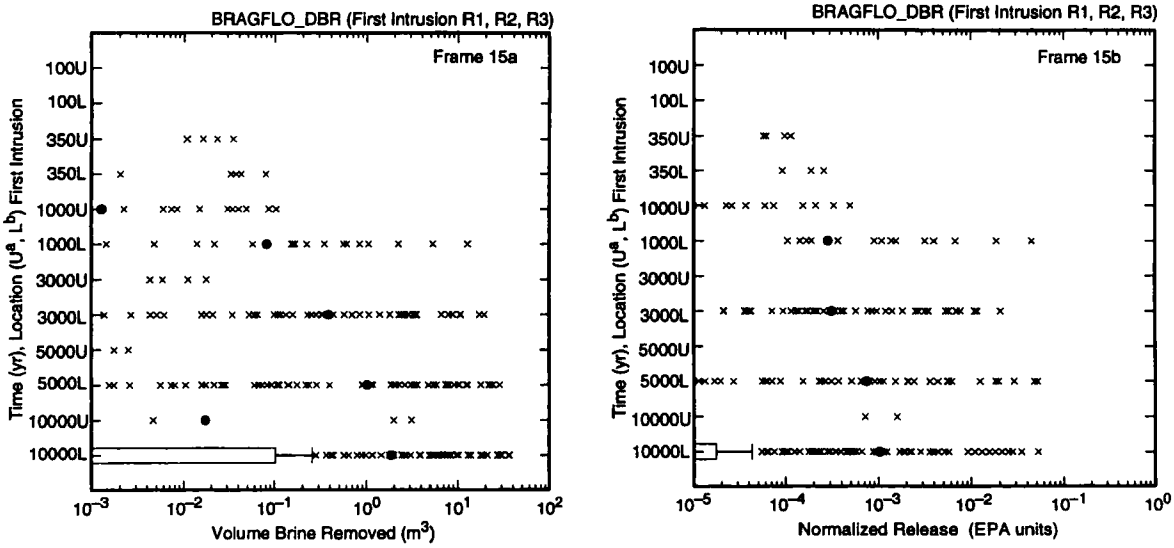

[a]U Signifies Intrusion into an Upper (U) Waste Panel

[b]L Signifies Intrusion into a Lower (L) Waste Panel

TRI-6342-4775-2

Fig. 15. Distribution over all 300 LHS elements for brine release (m^3) and normalized release (EPA units) due to direct brine release for a single drilling intrusion into a previously unintruded repository.

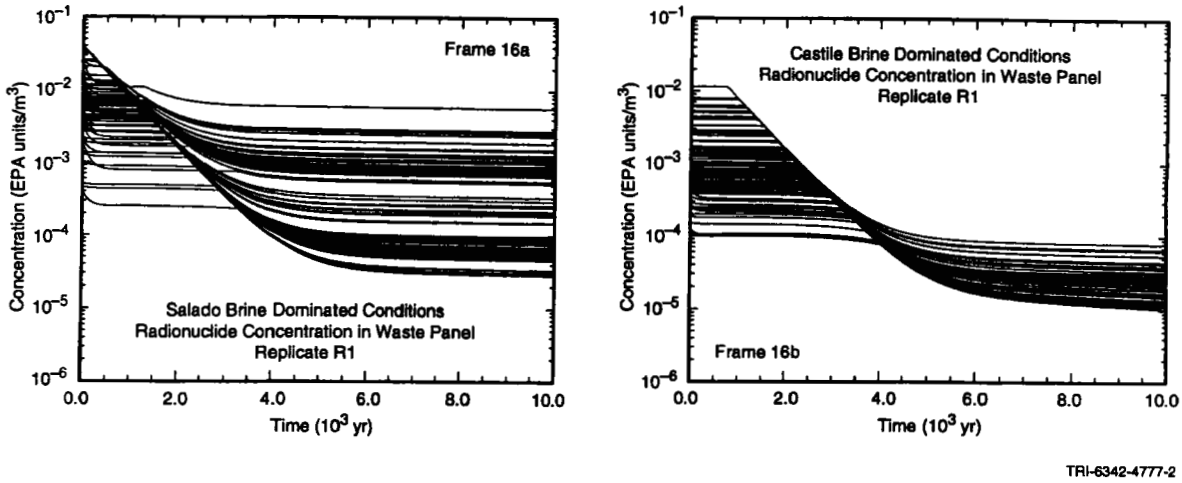

Fig. 16. Radionuclide concentration (EPA units/m^3) in repository with MgO backfill.

releases for E1 intrusions at different times (Fig. 18b). The large number of zero releases results from a failure of the repository to fill with brine, with the result that there is no brine flow from the repository to the Culebra. The results in Fig. 18 are cumulative (i.e., integrated) releases. As an example, the time-dependent cumulative releases for an E1 intrusion at 1,000 years are shown in Fig. 19, with the cumulative releases at 10,000 years corresponding to the total normalized releases for replicate R1 and an intrusion at 1,000 years in Figs. 18a and 18b.

The releases to the Culebra calculated by NUTS and PANEL provided input to SECO2DTP for transport through the Culebra to the accessible environment [i.e., for the evaluation of $f_{S\text{-}T}$ in Eq. (4)]. Also, Culebra flow fields were provided by calculations performed with SECO2DFL. The actual results available from NUTS and PANEL were time-dependent release rates of individual radionuclides to the Culebra (i.e., results of the form that were integrated to obtain the cumulative releases in Fig. 19, but for individual radionuclides).

To save on computational requirements, the 1996 WIPP PA performed SECO2DTP calculations for unit radionuclide releases to the Culebra, with the results of these calculations then being used to construct transport results for arbitrary time-dependent radionuclide releases to the Culebra (Ref. 45, Table 12.2.3). This computational strategy was possible because SECO2DTD is based on the solution of a system of linear partial differential equations. When the SECO2DTP calculations were performed for unit releases to the Culebra, the resultant transport to the accessible environment was found to be zero for all sample elements and all radionuclides except for U-234 for one sample element. However, that sample element had no radionuclide release to the Culebra. Thus, although radionuclide releases to the Culebra did take place for some sample elements, no radionuclide transport through the Culebra to the accessible environment took place in the analysis.

9. CONSTRUCTION OF CCDFs AND COMPARISONS WITH 40 CFR 191.13

The central result calculated in the 1996 WIPP PA is the CCDF for normalized radionuclide release to the accessible environment specified in 40 CFR 191.13 (Section 2). As indicated in Sections 4 and 5, individual CCDFs were constructed with Monte Carlo techniques for normalized releases defined by a function f of the form in Eq. (4), with such CCDFs characterizing the effects of stochastic uncertainty. Further, as indicated in Sections 6 and 7, distributions of CCDFs derive from subjective uncertainty and were estimated with procedures based on Latin hypercube sampling.

Of the components of f in Eq. (4), only f_C, f_{SP}, and f_{DBR} are nonzero in the 1996 WIPP PA, with the result that f has the simpler form

$$f(\mathbf{x}_{st}) = f_C(\mathbf{x}_{st}) + f_{SP}[\mathbf{x}_{st}, f_B(\mathbf{x}_{st})] + f_{DBR}\{\mathbf{x}_{st}, f_{SP}[\mathbf{x}_{st}, f_B(\mathbf{x}_{st})], f_B(\mathbf{x}_{st})\} \quad (15)$$

Although the CCDF specified in 40 CFR 191.13 is

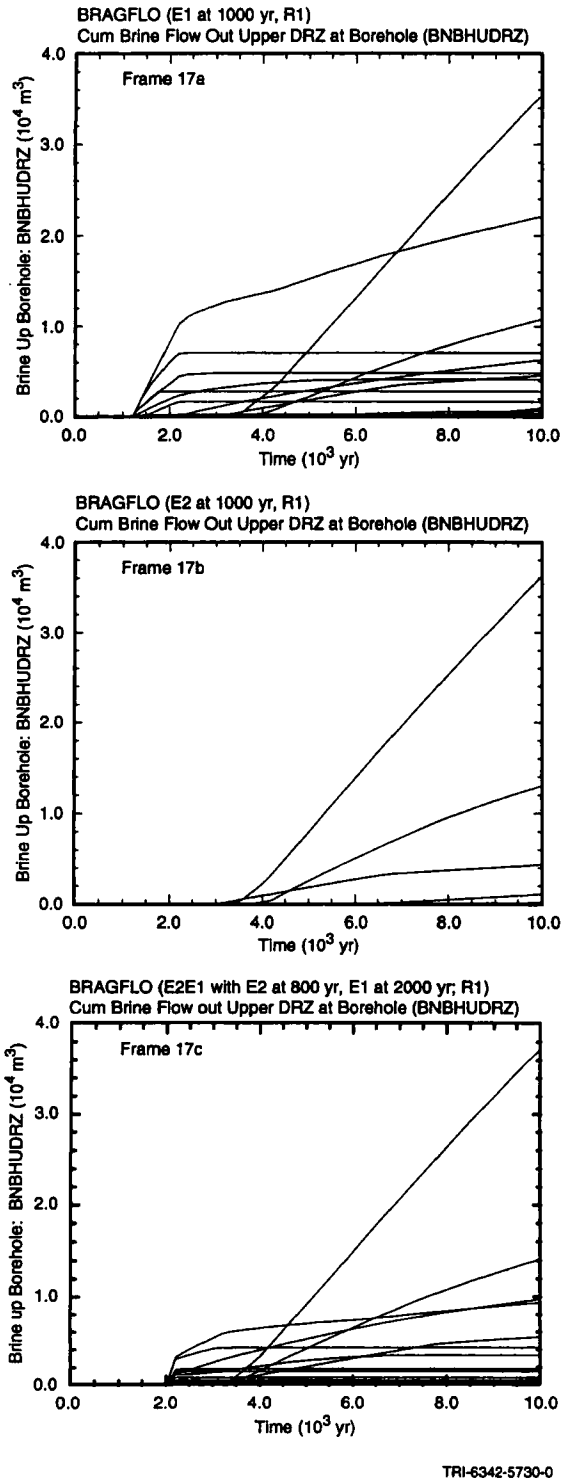

Fig. 17. Cumulative brine flow up borehole at top of DRZ for 100 LHS elements in Replicate R1: (a) E1 intrusion, (b) E2 intrusion, and (c) E2E1 intrusion.

for all release modes [i.e., is based on f as defined in Eqs. (4) and (15)], CCDFs can also be determined for the individual release modes [i.e., f_C, f_{SP}, and f_{DBR} in Eq. (15)], with such results helping provide perspective on what is determining the location of the CCDF for all release modes.

As an example, the construction of the CCDFs associated with spallings releases is now illustrated. This construction is based on the evaluation of $f_{SP}(\mathbf{x}_{st,i})$ for a sequence of randomly sampled futures $\mathbf{x}_{st,i}$, $i = 1, 2, \ldots, nS = 10{,}000$ [see Eqs. (5), (6)]. Specifically, the construction uses results obtained in a small number of calculations performed with CUTTINGS_S (Table VII) in conjunction with algebraic manipulations and interpolations (Table VIII) to estimate $f_{SP}(\mathbf{x}_{st,i})$ for each randomly sampled future $\mathbf{x}_{st,i}$. Once the $f_{SP}(\mathbf{x}_{st,i})$ are evaluated, the resultant CCDF can be constructed as indicated conceptually in Eq. (6), although in computational practice a somewhat different and more efficient procedure is used (Ref. 45, Section 6.7). The computational results described in Table VII are illustrated in Figs. 10, 13, and 14. The distributions in Figs. 13 and 14 are over all 300 LHS elements used in the analysis. However, the algorithm described in Table VIII to determine $f_{SP}(\mathbf{x}_{st,i})$, $i = 1, 2, \ldots, nS$, uses results obtained with one LHS element at a time [i.e., $\mathbf{x}_{su,k}$ in Eq. (14)], with the result that each constructed CCDF is conditional on the occurrence of a specific LHS element.

The resultant distribution of CCDFs for the spallings release for replicate R1 is shown in Fig. 20b. As each CCDF was constructed for a single LHS element, Fig. 20b potentially contains 100 CCDFs, although only 82 CCDFs appear in the plot because 18 LHS elements failed to produce spallings releases that exceeded 1×10^{-5} EPA units. The spread of the CCDFs in Fig. 20b provides an indication of confidence that the CCDF for spallings release does indeed fall below the boundary line specified in 40 CFR 191.13. As indicated by the location of all CCDFs to the left of the boundary line, a high degree of confidence exists that the CCDF for spallings releases meets the requirements imposed by 40 CFR 191.13.

Similar construction procedures were also used to determine CCDFs due to cuttings and cavings (Ref. 45, Section 9.2) and direct brine releases (Ref. 45, Section 10.3). Further, the cuttings and cavings, spallings, and direct brine releases were combined to determine a total release as indicated in Eq. (15). The CCDFs for the individual release modes and the total release fall substantially to the left of the boundary line specified in 40 CFR 191.13, with the

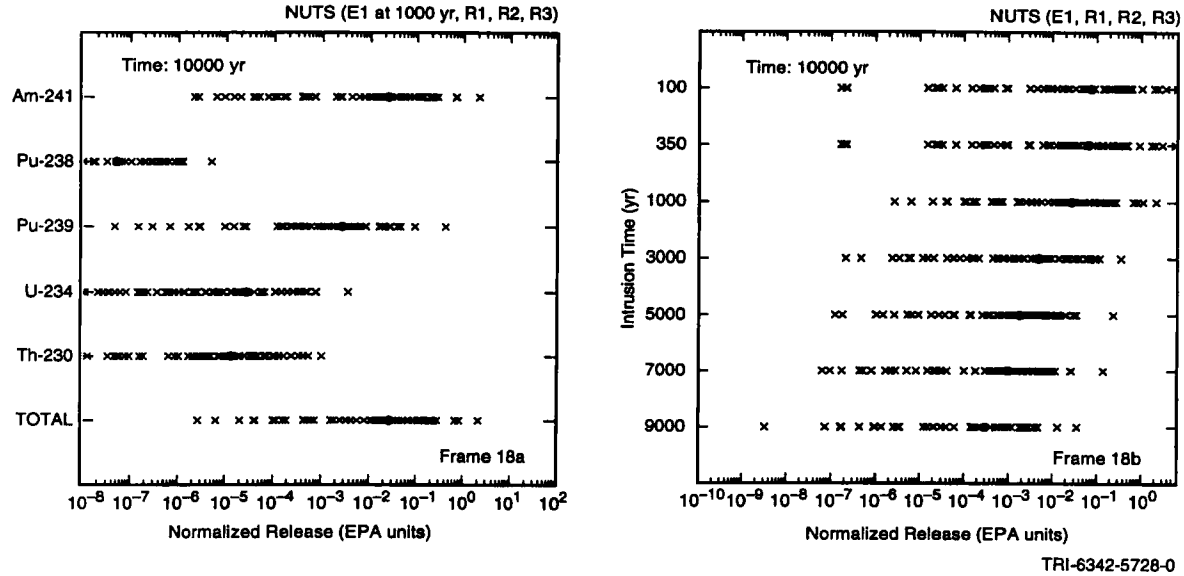

Fig. 18. Cumulative radionuclide transport over 10,000 years from repository to Culebra Dolomite for E1 intrusions: (a) Individual radionuclides with an E1 intrusion at 1000 years, and (b) total release for E1 intrusions at 100, 350, 1000, 3000, 5000, 7000, and 9000 years.

total release dominated by the cuttings and cavings component (Fig. 20).

The presentation of mean CCDFs and percentile curves as described in conjunction with Fig. 8 provides a more quantitative way to compare the distributions of CCDFs in Fig. 20 with the boundary line specified in 40 CFR 191.13. As an example, mean and percentile curves for the total release are shown in Fig. 21 and fall substantially to the left of the boundary line.

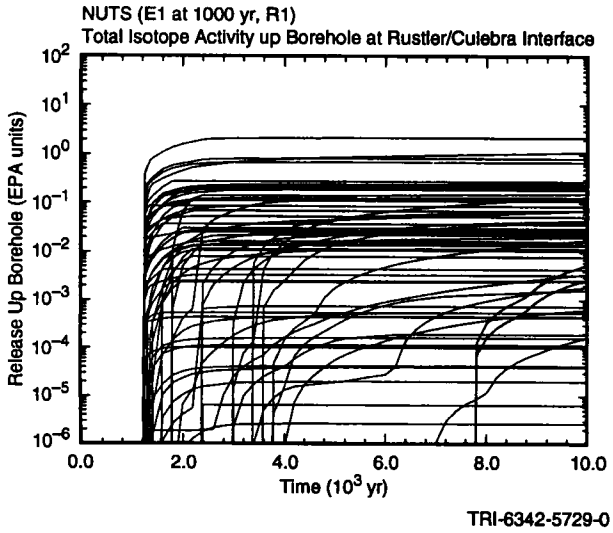

Fig. 19. Cumulative normalized release from repository to Culebra Dolomite for an E1 intrusion at 1,000 years.

The curves in Fig. 21 were obtained by pooling replicates R1, R2, and R3 (i.e., the mean CCDFs and percentile curves were constructed from the 300 CCDFs associated with replicates R1, R2, and R3). However, the results obtained with the individual replicates were quite stable, with little variation in the location of the mean CCDF and percentile curves from replicate to replicate. For the total release CCDFs, the results obtained with the individual replicates are almost indistinguishable (Fig. 22a).

The requirement in 40 CFR 194.34(f) mandates the determination of a 95% confidence interval on the mean CCDF (Section 2), which can be obtained from the three replicated samples with the technique described in conjunction with Eqs. (12) and (13). In particular, a very tight confidence interval exists around the mean CCDF (Fig. 22b), which is consistent with the stability of the mean CCDF across the three replicates (Fig. 22a).

10. DISCUSSION

The 1996 WIPP PA was carried out to support an application by the DOE to the EPA for the certi-

Table VII. Results Available for Each LHS Element $\mathbf{x}_{su,k}$ from Calculations with CUTTINGS_S for Use in CCDF Construction for Spallings Releases

$C_{CH}(\tau_k)$: Concentration (EPA units/m^3) in CH-TRU waste at time τ_k, where τ_k, $k = 1, 2, \ldots, 9$, corresponds to 100, 125, 175, 350, 1000, 3000, 5000, 7500, and 10,000 years, respectively. See curve "CH-TRU waste within waste panels" in Fig. 10. Source: Refs. 38, 73.

$VS_{E0,U}(\tau_k)$: Volume (m^3) of original (i.e., uncompacted) material released by a drilling intrusion into a previously unintruded repository at time τ_k that encounters CH-TRU waste in an upper waste panel, where τ_k, $k = 1, 2, \ldots, 6$, corresponds to 100, 350, 1000, 3000, 5000, and 10,000 years, respectively. See Fig. 13a. Source: CUTTINGS_S.

$VS_{E0,L}(\tau_k)$: Same as $VS_{E0,U}(\tau_k)$, but for intrusion into a lower waste panel.

$VS_{E1,S}(\tau_j, \Delta\tau_{jk})$: Volume (m^3) of original (i.e., uncompacted) material released by second drilling intrusion at time $\tau_j + \Delta\tau_{jk}$ into the same waste panel penetrated by an initial E1 intrusion at time τ_j, where (1) τ_j, $j = 1, 2$, corresponds to 350 and 1000 years; (2) $\tau_1 + \Delta\tau_{1k}$, $k = 1, 2, \ldots, 7$, corresponds to 350, 550, 750, 2000, 4000, 10,000, and 10,250 years (i.e., $\Delta\tau_{1k} = 0$, 200, 400, 1650, 3650, 9650, 9900 years), results for $k = 2, 3, \ldots, 6$ are summarized in Fig. 9.3.6 of Ref. 45, $VS_{E1,S}(\tau_1, \Delta\tau_{11}) = VS_{E1,S}(\tau_1, \Delta\tau_{12})$ [i.e., $VS_{E1,S}(350, 0) = VS_{E1,S}(350, 200)$], and $VS_{E1,S}(\tau_1, \Delta\tau_{16}) = VS_{E1,S}(\tau_1, \Delta\tau_{17})$ [i.e., $VS_{E1,S}(350, 9650) = VS_{E1,S}(350, 9900)$]; and (3) $\tau_2 + \Delta\tau_{2k}$, $k = 1, 2, \ldots, 6$, corresponds to 1000, 1200, 1400, 3000, 5000, and 10,000 years (i.e., $\Delta\tau_{2k} = 0$, 200, 400, 1000, 4000, 9000 years), results for $k = 2, 3, \ldots, 6$ are summarized in Fig. 14a, and $VS_{E1,S}(\tau_2, \Delta\tau_{21}) = VS_{E1,S}(\tau_2, \Delta\tau_{22})$ [i.e., $VS_{E1,S}(1000, 0) = VS_{E1,S}(1000, 200)$]. Source: CUTTINGS_S. The assignments $VS_{E1,S}(350, 0) = VS_{E1,S}(350, 200)$ and $VS_{E1,S}(1000, 0) = VS_{E1,S}(1000, 200)$ are made to bracket the time period between the occurrence of the first drilling intrusion and the failure of the plug at the Rustler/Salado interface (see Table 4.2.8, Ref. 45); the assignment $VS_{E1,S}(350, 9650) = VS_{E1,S}(350, 9900)$ is made to facilitate the use of $VS_{E1,S}(\tau_1, \Delta\tau_{1k})$ for initial intrusions before $\tau_1 = 350$ years.

$VS_{E1,S}(\tau_j, \Delta\tau_{jk})$: Same as $VS_{E1,S}(\tau_j, \Delta\tau_{jk})$, but for intrusion into different waste panel. See Fig. 9.3.6 of Ref. 45 for initial intrusions at 350 years and Fig. 14a of this presentation for initial intrusions at 1000 years.

$VS_{E2,S}(\tau_j, \Delta\tau_{jk})$: Same as $VS_{E1,S}(\tau_j, \Delta\tau_{jk})$, but for initial E2 intrusion. See Fig. 9.3.7, Ref. 45.

$VS_{E2,D}(\tau_j, \Delta\tau_{jk})$: Same as $VS_{E1,D}(\tau_j, \Delta\tau_{jk})$ but for initial E2 intrusion. See Fig. 9.3.7, Ref. 45.

fication of the WIPP for the disposal of TRU waste.[6] The most important result from a regulatory perspective calculated in this PA is a CCDF for normalized radionuclide release to the accessible environment, which is required to fall to the left of the boundary line specified in the EPA's regulation 40 CFR 191.13 (Section 2). Even when the effects of subjective uncertainty are taken into account, this CCDF was found to meet the requirements associated with 40 CFR 191.13 (Section 9).

Some individuals feel that the boundary line specified in 40 CFR 191.13 for the CCDF for normalized radionuclide release to the accessible environment (Fig. 2) is a novel concept. However, this boundary line is actually an example of the Farmer limit line approach to the definition of acceptable risk.[74–76] A similar construction appears in the U.S. Nuclear Regulatory Commission's proposed large release safety goal (Ref. 41, Fig. 20; Refs. 77, 78).

As is typical of large PAs, the 1996 WIPP PA was not a single isolated analysis, but rather the final outcome of a sequence of iterative PAs carried out over approximately 10 years.[4,5,25–27] By starting the PA process early in the development of the WIPP's CCA, important insights were obtained with respect to model and data needs and also with respect to the appropriate conceptual and computational structure of the PA itself. It is strongly recommended that any project that is required to produce a PA start the process as early as possible so that the associated experience and insights can be gained before carrying out the final PA.

The overall conceptual and computational structure of the 1996 WIPP PA derived from the requirement to maintain a separation between stochastic (i.e., aleatory) uncertainty and subjective (i.e., epistemic) uncertainty as mandated in 40 CFR 191 and 40 CFR 194 (Section 2). This distinction was maintained by defining separate probability spaces $(\mathcal{S}_{st}, \mathcal{S}_{st}, p_{st})$ and $(\mathcal{S}_{su}, \mathcal{S}_{su}, p_{su})$ for stochastic and subjective uncertainty, respectively, with individual CCDFs for comparison with the boundary line in 40 CFR 191.13 deriving from stochastic uncertainty and distributions of CCDFs deriving from subjective uncertainty (Sections 4–6). In the computational implementation of the PA, simple random sampling was used to determine the effects of stochastic uncertainty, and Latin hypercube sampling was used to determine the effects of subjective uncertainty (Sections 7–9).

The use of simple random sampling to assess the effects of stochastic uncertainty was made possible by performing a relatively small number of mechanistic calculations for each LHS element (Tables VI, VII) and then using algebraic procedures (Table VIII) to

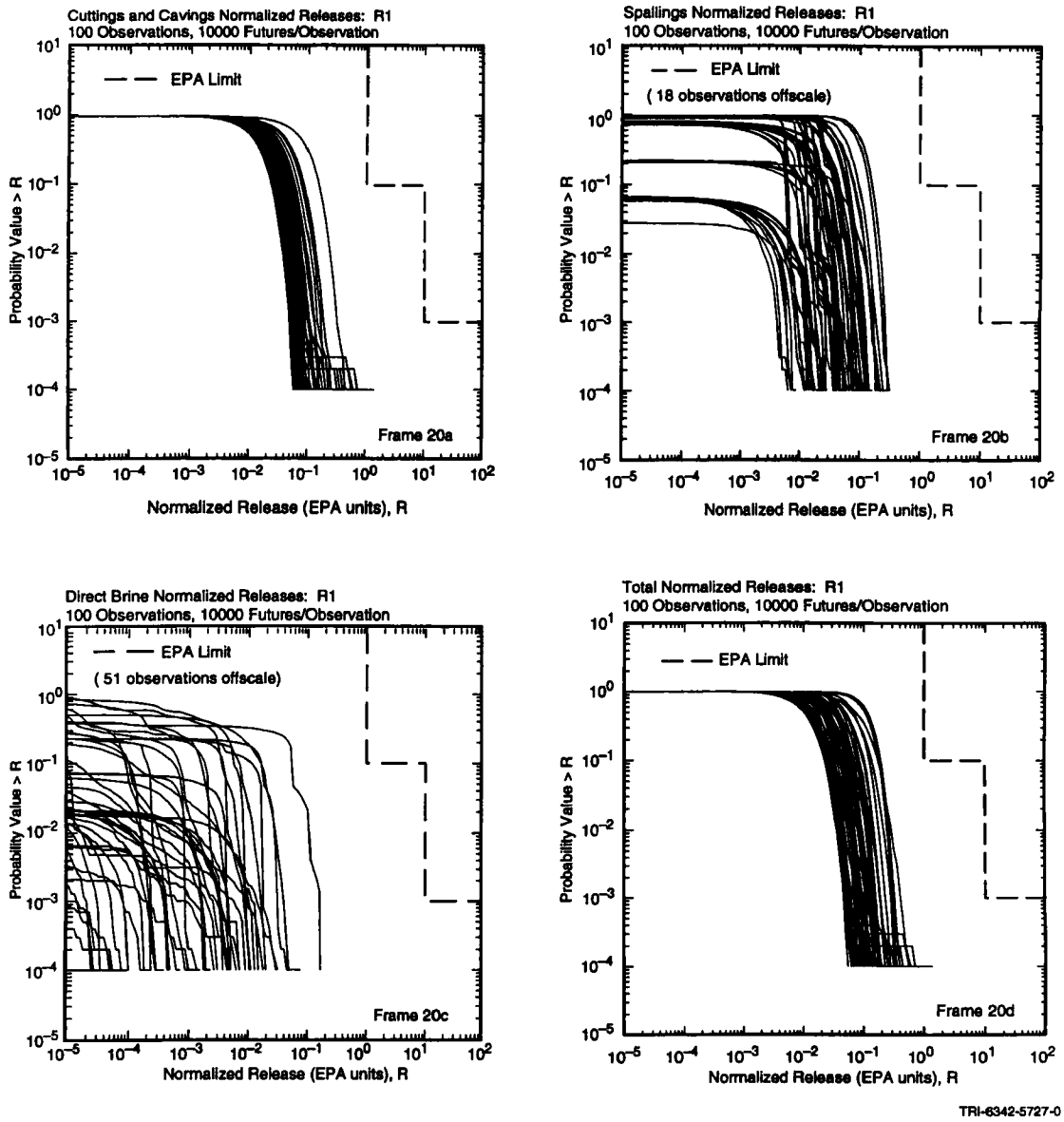

Fig. 20. Distributions of CCDFs for normalized release to the accessible environment over 10,000 years for replicate R1: (a) Cuttings and cavings, (b) spallings, (c) direct brine release, (d) total release (Figs. 6, 9, Ref. 39).

extend the results of these calculations to the large number of futures generated in random sampling from the probability space ($\mathcal{S}_{st}$, $\mathcal{S}_{st}$, p_{st}). The maintenance of an appropriate separation between stochastic and subjective uncertainty, as done in the 1996 WIPP PA, is widely recognized as an essential part of PAs for complex systems.[41,42,79–83]

Formal quality assurance (QA) procedures are essential in an analysis such as the 1996 WIPP PA that supports a major regulatory decision and, indeed, are specified by the EPA as part of the requirements that must be satisfied by the WIPP (see Ref. 33, Section 194.22, which specifies adherence to a QA program that implements the requirements of ASME NQA-1, ASME NQA-2a, and ASME NQA-3). Such procedures assure (1) adequate documentation of models and the computer programs that implement them, (2) adequate documentation of analysis assumptions and data used within the analysis, and (3) the traceability and archival storage of all calculations performed as part of the analysis. To this end, formal QA procedures based on guidance from the EPA[33]

Table VIII. Determination of Spallings Release $f_{SP}[\mathbf{x}_{st}, f_B(\mathbf{x}_{st})]$ for an Arbitrary Future $\mathbf{x}_{st}$

Notation:

nH_i = number of intrusions prior to intrusion i that penetrate pressurized brine and use plugging pattern 2 (i.e., two discrete plugs)

nD = number of intrusions required to deplete brine pocket (see *BPVOL* in Table 5.2.1, Ref. 45, for definition of nD in 1996 WIPP PA)

$\tilde{b}_i$ = 0 if intrusion i into (1) nonexcavated area or (2) excavated area and plugging pattern 1 used (i.e., continuous plug)

= 1 if intrusion i into excavated area, penetrates pressurized brine, plugging pattern 2 used, and $nH_i \le nD$

= 2 if intrusion i into excavated area and either (1) penetrates pressurized brine, plugging pattern 2 used, and $nH_i > nD$, (2) does not penetrate pressurized brine and plugging pattern 2 used, or (3) plugging pattern 3 used (i.e., three discrete plugs)

Release rSP_i for intrusion into nonexcavated area at time t_i:

$rSP_i = 0$

Release rSP_i for intrusion into pressurized repository at time t_i(i.e., $i = 1$ or $\tilde{b}_j = 0$ for $j = 1, 2, \ldots, i-1$):

$rSP_i = 0$ if intrusion penetrates RH-TRU waste

$= C_{CH}(t_i)VS_{E0,U}(t_i)$ if l_i in upper waste panel[a]

$= C_{CH}(t_i)VS_{E0,L}(t_i)$ if l_i in lower waste panel

Release rSP_i for intrusion into a depressurized repository at time t_i with no E1 intrusion in first $i-1$ intrusions (i.e., $\tilde{b}_k = 0$ for $k = 1, 2, \ldots, j-1$, $\tilde{b}_j = 2$, $\tilde{b}_k \ne 1$ for $k = j+1, j+2, \ldots, i-1$):

$rSP_i = 0$ if intrusion penetrates RH-TRU waste

$= C_{CH}(t_i)VS_{E2,S}(t_j, t_i - t_j)$ if l_j, l_i in same waste panel[b]

$= C_{CH}(t_i)VS_{E2,D}(t_j, t_i - t_j)$ if l_j, l_i in different waste panels

Release rSP_i for intrusion into a depressurized repository at time t_i with first E1 intrusion at time $t_j < t_i$ (i.e., $\tilde{b}_k \ne 1$ for $k = 1, 2, \ldots, j-1$, $b_j = 1$):

$rSP_i = 0$ if intrusion penetrates RH-TRU waste

$= C_{CH}(t_i)VS_{E1,S}(t_j, t_i - t_j)$ if l_j, l_i in same waste panel

$= C_{CH}(t_i)VS_{E1,D}(t_j, t_i - t_j)$ if l_j, l_i in different waste panels

Spallings release $f_{SP}[\mathbf{x}_{st}, f_B(\mathbf{x}_{st})]$:

$$f_{SP}[\mathbf{x}_{st}, f_B(\mathbf{x}_{st})] = \sum_{i=1}^{n} rSP_i$$

[a] Here and elsewhere, appearance of an undefined time implies linear interpolation between defined times in Table VII.

[b] Here and elsewhere, appearance of two undefined times implies two-dimensional linear interpolation between defined times in Table VII.

and the DOE[84] were implemented and followed as an integral part of the 1996 WIPP PA.

Although not emphasized in this presentation, regression-based sensitivity analysis played an important role in both the 1996 WIPP PA[45] and in earlier PAs (Ref. 4, Vol. 4; Ref. 5, Vols. 4, 5; Refs. 28–30, 85, 86) and helped provide many of the important insights gained in these PAs. In particular, the LHSs used to propagate subjective uncertainty lead to a mapping from uncertain analysis inputs to analysis results that can be explored with techniques based on examination of scatterplots, stepwise regression analysis, and partial correlation analysis.[87] Sensitivity analysis provides a way to identify which of the uncertain inputs to the analysis (Table V) are most important in determining the uncertainty in analysis outcomes. For example, the uncertainty characterized by the distribution of CCDFs in Fig. 20d for total normalized release to the accessible environment is dominated by the uncertainty in the shear strength of the waste (*WTAUFAIL* in Table V) and the extent to which microbial degradation of cellulose takes place (*WMICDFLG* in Table V), with smaller effects due to a number of additional variables (Ref. 45, Section. 13.2). Further, sensitivity analysis constitutes a powerful tool for analysis verification by providing a way to examine the effects of different inputs on a large number of analysis outcomes, with the possibility of an error being indicated when a variable has an observed effect that is not consistent with its anticipated effect (e.g., the observation that radionuclide release to the Culebra increases as radionuclide

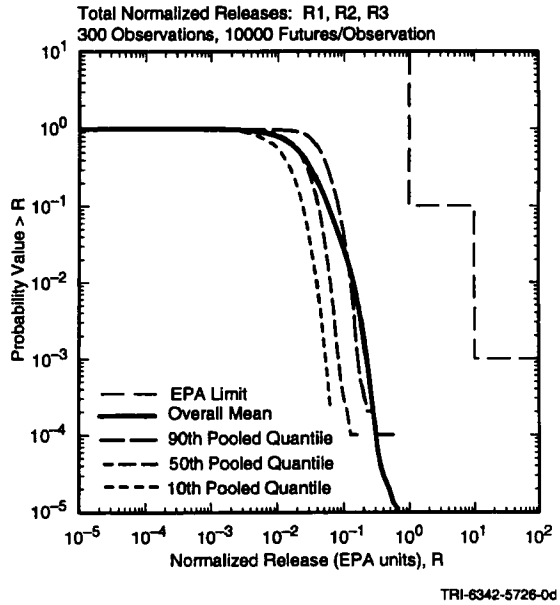

Fig. 21. Mean and percentile curves for total normalized release (i.e., cuttings, cavings, spallings and direct brine) to the accessible environment over 10,000 years obtained by pooling results for replicates R1, R2, and R3.

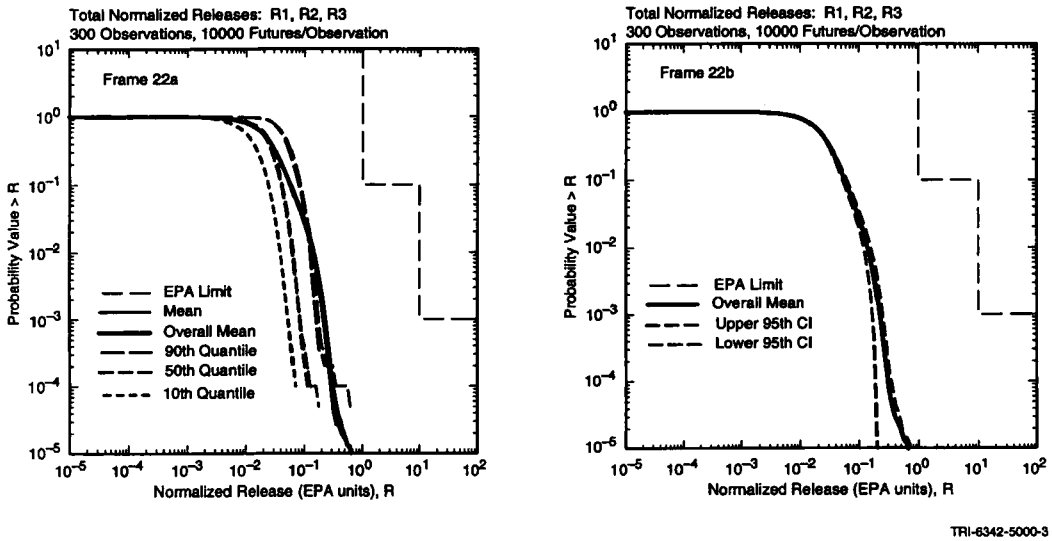

Fig. 22. Outcome of replicated sampling for distribution of CCDFs for total normalized release to the accessible environment over 10,000 years: (a) Mean and percentile curves for individual replicates, (b) confidence intervals (CIs) on mean curve obtained from the three replicates (Fig. 8, Ref. 39).

solubility decreases would suggest that there was probably an error in the implementation of the analysis). A high-level overview of sensitivity analysis in PA for the WIPP is given in Ref. 88.

The EPA certified the WIPP for the disposal of TRU waste in May 1998,[89] and at present (August 1998), it appears likely that the WIPP will be in operation by the end of 1998. The LWA[22] specifies that the WIPP must undergo a recertification every 5 years. These recertifications will require updates of the CCA PA described in this presentation that incorporate any new information or perspectives with respect to the WIPP that have been acquired since the implementation of the CCA PA.

ACKNOWLEDGMENTS

Work performed for Sandia National Laboratories (SNL), which is a multiprogram laboratory operated by Sandia Corporation, a Lockheed Martin Company, for the U. S. Department of Energy under contract DE-AC04-94AL85000. Many individuals at SNL and its contractors contributed to the results in this presentation, including K. Aragon, J. E. Bean, D. G. Bennet, J. W. Berglund, R. Blaine, M. B. Crawford, F. J. Davis, K. Economy, D. A. Galson, J. W. Garner, F. D. Hansen, T. W. Hicks, J. D. Johnson, M. K. Knowles, K. W. Larson, M. E. Lord, R. J. MacKinnon, J. Miller, D. G. O'Brien, J. L. Ramsey, L. C. Sanchez, J. Schatz, J. D. Schreiber, A. Shinta, L. N. Smith, D. M. Stoelzel, C. Stockman, P. N. Swift, T. W. Thompson, M. S. Tierney, P. Vaughn, M. Wallace, M. Williamson, and R. D. Wilmot. Review provided at SNL by M. Chavez, C. Crawford, and M. J. Shortencarier. Editorial support provided by L. Harrison, T. Allen, and H. Olmstead of Tech Reps, Inc.

REFERENCES

1. U.S. Department of Energy, *Final Environmental Impact Statement: Waste Isolation Pilot Plant*, DOE/EIS-0026 (Office of Environmental Restoration and Waste Management, Washington, D.C., 1980).
2. U.S. Department of Energy, *Final Supplement: Environmental Impact Statement, Waste Isolation Pilot Plant*, DOE/EIS-0026-FS (Office of Environmental Restoration and Waste Management, Washington, D.C., 1990).
3. National Research Council, *The Waste Isolation Pilot Plant: A Potential Solution for the Disposal of Transuranic Waste*, Committee on the Waste Isolation Pilot Plant, Board on Radioactive Waste Management, Commission on Geosciences, Environment, and Resources, National Research Council (National Academy Press, Washington, D.C., 1996).
4. WIPP Performance Assessment Division, *Preliminary Comparison with 40 CFR Part 191, Subpart B for the Waste Isolation Pilot Plant, December 1991*, Volumes 1–4, SAND91-0893/1-4 (Sandia National Laboratories, Albuquerque, New Mexico, 1991–1992).
5. WIPP Performance Assessment Department, *Preliminary Performance Assessment for the Waste Isolation Pilot Plant, De-*

cember 1992, Volumes 1–5, SAND92-0700/1-5 (Sandia National Laboratories, Albuquerque, New Mexico, 1992–1993).
6. U.S. Department of Energy, *Title 40 CFR Part 191 Compliance Certification Application for the Waste Isolation Pilot Plant*, DOE/CAO-1996-2184 (U.S. Department of Energy, Carlsbad Area Office, Carlsbad, New Mexico, 1996).
7. R. P. Rechard, *An Introduction to the Mechanics of Performance Assessment Using Examples of Calculations Done for the Waste Isolation Pilot Plant between 1990 and 1992*, SAND93-1378 (Sandia National Laboratories, Albuquerque, New Mexico, 1995).
8. National Academy of Sciences/National Research Council, *The Disposal of Radioactive Waste on Land: Report of the Committee on Waste Disposal of the Division of Earth Sciences*, Publication 519 (National Academy of Sciences/National Research Council, Washington, D.C., 1957).
9. R. L. Bradshaw and W. C. McClain (eds.), *Project Salt Vault: A Demonstration of the Disposal of High-Activity Solidified Wastes in Underground Salt Mines*, ORNL-4555 (Oak Ridge National Laboratory, Oak Ridge, Tennessee, 1971).
10. L. J. Carter, *Nuclear Imperatives and Public Trust: Dealing with Radioactive Waste* (Resources for the Future, Inc, Washington, D.C., 1987).
11. National Academy of Sciences/National Research Council, *Review of the Scientific and Technical Criteria for the Waste Isolation Pilot Plant (WIPP)*, DOE/DP/48015-1 (National Academy Press, Washington, D.C., 1984).
12. D. W. Powers *et al.* (eds.), *Geological Characterization Report, Waste Isolation Pilot Plant (WIPP) Site, Southeastern New Mexico*, Volumes 1–2, SAND78-1596 (Sandia National Laboratories, Albuquerque, New Mexico, 1978).
13. Public Law 91-190, *National Environmental Policy Act of 1969* (83 Stat. 852; 42 U.S.C. 1801 et seq.) (1970).
14. W. D. Weart, "WIPP: A Bedded Salt Repository for Defense Radioactive Waste in Southeastern New Mexico," in S. Fried (ed.), *Radioactive Waste in Geologic Storage, 176th Annual Meeting of the American Chemical Society, Miami, Beach, Florida, September 11–15, 1978*, (American Chemical Society, Washington, D.C., 1979).
15. Public Law 96-164, *Department of Energy National Security and Military Applications of Nuclear Energy Authorization Act of 1980* (93 Stat. 1259) (1979).
16. U.S. Department of Energy and State of New Mexico, *Agreement for Consultation and Cooperation on WIPP by the State of New Mexico and U.S. Department of Energy* (U.S. Department of Energy, Albuquerque, New Mexico, 1981).
17. U. S. Department of Energy, *Summary of the Results of the Evaluation of the WIPP Site and Preliminary Design Validation Program*, WIPP-DOE-161 (U.S. Department of Energy, Albuquerque, New Mexico, 1983).
18. U. S. Department of Energy, "Announcement of Decision to Proceed with Construction of the Waste Isolation Pilot Plant (WIPP)," *Fed. Reg.* **48**, 30427–30428 (1983).
19. A. R. Lappin, *Summary of Site-Characterization Studies Conducted from 1983 through 1987 at the Waste Isolation Pilot Plant (WIPP) Site, Southeastern New Mexico*, SAND88-0157 (Sandia National Laboratories, Albuquerque, New Mexico, 1988).
20. L. D. Tyler *et al.*, *Summary Report for the WIPP Technology Development Program for Isolation of Radioactive Waste*, SAND88-0844 (Sandia National Laboratories, Albuquerque, New Mexico, 1988).
21. R. W. Lynch *et al.*, *Deep Geologic Disposal in the United States: The Waste Isolation Pilot Plant and Yucca Mountain Projects*, SAND90-1656 (Sandia National Laboratories, Albuquerque, New Mexico, 1991).
22. Public Law 102-579, *Waste Isolation Pilot Plant Land Withdrawal Act* (106 Stat. 4777) (1992).
23. U.S. Environmental Protection Agency, "Environmental Standards for the Management and Disposal of Spent Nuclear Fuel, High-Level and Transuranic Radioactive Wastes; Final Rule, 40 CFR Part 191," *Fed. Reg.* **50**, 38066–38089 (1985).
24. S. G. Bertram-Howery *et al.*, *Draft Forecast of the Final Report for the Comparison to 40 CFR Part 191, Subpart B, for the Waste Isolation Pilot Plant*, SAND88-1452 (Sandia National Laboratories, Albuquerque, New Mexico, 1989).
25. M. G. Marietta *et al.*, *Performance Assessment Methodology Demonstration: Methodology Development for Evaluating Compliance with EPA 40 CFR 191, Subpart B, for the Waste Isolation Pilot Plant*, SAND89-2027 (Sandia National Laboratories, Albuquerque, New Mexico, 1989).
26. A. R. Lappin *et al.*, *Systems Analysis, Long-Term Radionuclide Transport, and Dose Assessments, Waste Isolation Pilot Plant (WIPP), Southeastern New Mexico; March 1989*, SAND89-0462 (Sandia National Laboratories, Albuquerque, New Mexico, 1989).
27. S. G. Bertram-Howery *et al.*, *Preliminary Comparison with 40 CFR Part 191, Subpart B for the Waste Isolation Pilot Plant, December 1990*, SAND90-2347 (Sandia National Laboratories, Albuquerque, New Mexico, 1990).
28. J. C. Helton *et al.*, "Uncertainty and Sensitivity Analysis Results Obtained in a Preliminary Performance Assessment for the Waste Isolation Pilot Plant," *Nucl. Sci. Eng.* **114**, 286–331 (1993).
29. J. C. Helton *et al.*, "Effect of Alternative Conceptual Models in a Preliminary Performance Assessment for the Waste Isolation Pilot Plant," *Nucl. Eng. Design* **154**, 251–344 (1995).
30. J. C. Helton *et al.*, "Uncertainty and Sensitivity Analysis Results Obtained in the 1992 Performance Assessment for the Waste Isolation Pilot Plant," *Reliability Eng. System Safety* **51**, 53–100 (1996).
31. J. C. Helton and K. M. Trauth, "Comments on an Evaluation of the 1992 Performance Assessment for the Waste Isolation Pilot Plant," *Nucl. Eng. Design* **168**, 339–360 (1997).
32. U. S. Environmental Protection Agency, "Environmental Radiation Protection Standards for the Management and Disposal of Spent Nuclear Fuel, High-Level and Transuranic Radioactive Wastes; Final Rule," 40 CFR Part 191, *Fed. Reg.* **58**, 66398–66416 (1993).
33. U. S. Environmental Protection Agency, "40 CFR Part 194: Criteria for the Certification and Re-Certification of the Waste Isolation Pilot Plant's Compliance with the 40 CFR Part 191 Disposal Regulations; Final Rule," *Fed. Reg.* **61**, 5224–5245 (1996).
34. U. S. Environmental Protection Agency, *Compliance Application Guidance for 40 CFR Part 194*. EPA 402-R-95-014 (U.S. Environmental Protection Agency, Office of Radiation and Indoor Air, Washington, D.C., 1996).
35. J. C. Helton, "Computational Structure of a Performance Assessment Involving Stochastic and Subjective Uncertainty," in J. M. Charnes *et al.* (eds.), *Proceedings of the 1996 Winter Simulation Conference* (Institute of Electrical and Electronics Engineers, Piscataway, New Jersey, 1996), pp. 239–247.
36. J. C. Helton, "Risk, Uncertainty in Risk, and the EPA Release Limits for Radioactive Waste Disposal," *Nucl. Technol.* **101**, 18–39 (1993).
37. J. C. Helton *et al.*, "Performance Assessment for the Waste Isolation Pilot Plant: From Regulation to Calculation for 40 CFR 191.13," *Operations Res.* **45**, 157–177 (1997).
38. L. C. Sanchez *et al.*, "WIPP PA Analysis Report for EPAUNI: Estimating Probability Distribution of EPA Unit Loading in the WIPP Repository for Performance Assessment Calculations," Version 1.01, Sandia WIPP Central Files WPO # 43843 (Sandia National Laboratories, Albuquerque, New Mexico, 1997).
39. J. C. Helton *et al.*, "Stochastic and Subjective Uncertainty in the Assessment of Radiation Exposure at the Waste Isolation Pilot Plant," *Hum. Ecol. Risk Assessment* **4**, 469–526 (1998).

40. M. J. Stenhouse *et al.*, *SITE-94 Scenario Development FEP Audit List Preparation: Methodology and Presentation*, SKI Technical Report 93:27 (Swedish Nuclear Power Inspectorate, Stockholm, 1993).
41. J. C. Helton, "Treatment of Uncertainty in Performance Assessments for Complex Systems," *Risk Anal.* **14,** 483–511 (1994).
42. J. C. Helton, "Uncertainty and Sensitivity Analysis in the Presence of Stochastic and Subjective Uncertainty," *J. Stat. Computation Simulation* **57,** 3–76 (1997).
43. W. Feller, *An Introduction to Probability Theory and Its Applications*, Volume II, 2nd ed. (Wiley, New York, 1971).
44. K. M. Trauth *et al.*, "Effectiveness of Passive Institutional Controls in Reducing Inadvertent Human Intrusion into the Waste Isolation Pilot Plant for Use in Performance Assessments," WIPP/CAO-96-3168, Revision 1, November 14, 1996 with Addendum of December 6, 1996 (U.S. Department of Energy, Carlsbad Area Office, Carlsbad, New Mexico, 1996).
45. J. C. Helton *et al.*, *Uncertainty and Sensitivity Analysis Results Obtained in the 1996 Performance Assessment for the Waste Isolation Pilot Plant*, SAND98-0365 (Sandia National Laboratories, Albuquerque, New Mexico, 1998).
46. D. W. Powers *et al.*, "Probability of Intercepting a Pressurized Brine Reservoir under the WIPP," Sandia WIPP Central Files WPO # 40199 (Sandia National Laboratories, Albuquerque, New Mexico, 1996).
47. T. W. Thompson *et al.*, "Inadvertent Intrusion Borehole Permeability, Final Draft," May 20, 1996, Sandia WIPP Central Files WPO # 41131 (Sandia National Laboratories, Albuquerque, New Mexico, 1996).
48. J. E. Bean *et al.*, "Analysis Package for the Salado Flow Calculations (Task 1) of the Performance Assessment Analysis Supporting the Compliance Certification Application (CCA)," Analysis package, SWCF-A:1.2.07.4.1:PA:QA:CCA, Sandia WIPP Central Files WPO # 40514 (Sandia National Laboratories, Albuquerque, New Mexico, 1996).
49. D. M. Stoelzel and D. G. O'Brien, "Analysis Package for the BRAGFLO Direct Release Calculations (Task 4) of the Performance Assessment Calculations Supporting the Compliance Certification Application (CCA), AP-029, Brine Release Calculations," Analysis package, SWCF-A:1.2.07.4.1:PA:QA, Sandia WIPP Central Files WPO #40520 (Sandia National Laboratories, Albuquerque, New Mexico, 1996).
50. C. Wilson *et al.* "Waste Isolation Pilot Plant Conceptual Models Peer Review Report," (Sandia Central Files WPO# 41805 July 1996); "Waste Isolation Pilot Plant Supplementary Conceptual Models Peer Review Report," Sandia Central Files WPO# 43153, (December 1996); "Waste Isolation Pilot Plant Secondary Supplementary Peer Review Report," Sandia Central Files WPO# 44536, (January 1997); (U.S. Department of Energy, Carlsbad Area Office, Office of Regulatory Compliance, Carlsbad, New Mexico).
51. F. D. Hansen *et al.*, *Description and Evaluation of a Mechanistically Based Conceptual Model for Spall.* SAND97-1369. (Sandia National Laboratories, Albuquerque, New Mexico, 1997).
52. J. W. Berglund, *Mechanisms Governing the Direct Removal of Wastes from the Waste Isolation Pilot Plant Repository Caused by Exploratory Drilling*, SAND92-7295 (Sandia National Laboratories, Albuquerque, New Mexico, 1992).
53. J. W. Berglund, "Analysis Package for the Cuttings and Spalling Calculations (Tasks 5 and 6) of the Performance Assessment Calculation Supporting the Compliance Certification Application (CCA), AP-015 and AP-016," Analysis package, SWCF-A:1.2.07.4.1:PA:CCA:QA, Sandia Central Files WPO # 40521 (Sandia National Laboratories, Albuquerque, New Mexico, 1996).
54. A. M. LaVenue and B. S. RamaRao, *A Modeling Approach to Address Spatial Variability Within the Culebra Dolomite Transmissivity Field*, SAND92-7306 (Sandia National Laboratories, Albuquerque, New Mexico, 1992).
55. A. M. LaVenue, "Analysis of the Generation of Transmissivity Fields for the Culebra Dolomite Compliance Certification Application (CCA)," Analysis package, SWCF-A:1.2.07.4.1:PA:QA, Sandia WIPP Central Files WPO #40517 (Sandia National Laboratories, Albuquerque, New Mexico, 1996).
56. C. Stockman *et al.*, "Analysis Package for the Salado Transport Calculations (Task 2) of the Performance Assessment Analyses Supporting the Compliance Certification Application (CCA), AP-023," Analysis package, SWCF-A:1.2.07.4.1: PA:QA:CCA, Sandia WIPP Central Files WPO #40515 (Sandia National Laboratories, Albuquerque, New Mexico, 1996).
57. C. M. Stone, *SANTOS—A Two-Dimensional Finite Element Program for the Quasistatic, Large Deformation, Inelastic Response of Solids*, SAND90-0543 (Sandia National Laboratories, Albuquerque, New Mexico, 1997).
58. C. M. Stone, *Final Disposal Room Structural Response Calculations*, SAND97-0795 (Sandia National Laboratories, Albuquerque, New Mexico, 1997).
59. P. J. Roache, "The SECO Suite of Codes for Site Performance Assessment," in *High Level Radioactive Waste Management, Proceedings of the Fourth Annual International Conference, Las Vegas, NV, April 26–30, 1993*, (American Nuclear Society, La Grange Park, Illinois, 1993), Vol. 2, pp. 1586–1594.
60. J. Ramsey and M. G. Wallace, "Analysis Package for the Culebra Flow and Transport Calculations (Task 3) of the Performance Assessment Calculations Supporting the Compliance Certification Application (CCA), Analysis Plan 019," Analysis package, SWCF-A:WA:1.2.07.4.1:QA, Sandia WIPP Central Files WPO #40516 (Sandia National Laboratories, Albuquerque, New Mexico, 1996).
61. J. C. Helton and A. W. Shiver, "A Monte Carlo Procedure for the Construction of Complementary Cumulative Distribution Functions for Comparison with the EPA Release Limits for Radioactive Waste Disposal," *Risk Anal.* **16,** 43–55 (1996).
62. L. N. Smith *et al.*, "Analysis Package for the CCDF Construction (Task 7) of the Performance Assessment Calculations Supporting the Compliance Certification Application (CCA), AP-AAD," Analysis package, SWCF-A:1.2.07.4.1:PA:QA, Sandia WIPP Central Files WPO # 40524 (Sandia National Laboratories, Albuquerque, New Mexico, 1996).
63. J. D. Johnson, "CCDFGF, Version 4.00, User's Manual," Sandia WIPP Central Files WPO # 47364 (Sandia National Laboratories, Albuquerque, New Mexico, 1997).
64. M. D. McKay *et al.*, "A Comparison of Three Methods for Selecting Values of Input Variables in the Analysis of Output from a Computer Code," *Technometrics* **21,** 239–245 (1979).
65. R. L. Iman and W. J. Conover. "A Distribution-Free Approach to Inducing Rank Correlation Among Input Variables," *Commun. Stat. Simulation Computation B* **11,** 311–334 (1982).
66. R. L. Iman and J. M. Davenport. "Rank Correlation Plots for Use with Correlated Input Variables," *Commun. Stat. Simulation Computation B* **11,** 335–360 (1982).
67. R. MacKinnon *et al.*, "Summary of EPA-Mandated Performance Assessment Verification Test (Replicate 1) and Comparison with the Compliance Certification Application Calculations," Technical Data Package, Sandia WIPP Central Files WPO # 46674 (Sandia National Laboratories, Albuquerque, New Mexico, 1997).
68. J. C. Helton, "Probability, Conditional Probability and Complementary Cumulative Distribution Functions in Performance Assessment for Radioactive Waste Disposal," *Reliability Eng. System Safety* **54,** 145–163 (1996).
69. R. L. Iman and J. C. Helton, "An Investigation of Uncertainty and Sensitivity Analysis Techniques for Computer Models," *Risk Anal.* **8,** 71–90 (1988).
70. R. L. Iman and J. C. Helton, "The Repeatability of Uncertainty

and Sensitivity Analyses for Complex Probabilistic Risk Assessments," *Risk Anal.* **11,** 591–606 (1991).
71. J. C. Helton *et al.*, "Robustness of an Uncertainty and Sensitivity Analysis of Early Exposure Results with the MACCS Reactor Accident Consequence Model," *Reliability Eng. System Safety* **48,** 129–148 (1995).
72. R. L. Iman, "Statistical Methods for Including Uncertainties Associated with Geologic Isolation of Radioactive Waste Which Allow for a Comparison with Licensing Criteria," in D. C. Kocher (ed.), *Proceedings of the Symposium on Uncertainties Associated with the Regulation of the Geologic Disposal of High-Level Radioactive Waste: March 9-13, 1981, Gatlinburg, TN,* NUREG/CP-0022, CONF-810372 (Oak Ridge National Laboratory, Oak Ridge, Tennessee, 1982), pp. 145–157.
73. U. S. Department of Energy, *Transuranic Waste Baseline Inventory Report (Revision 3)*, DOE/CAO-95-1121 (U.S. Department of Energy, Carlsbad Area Office, Carlsbad, New Mexico, 1996).
74. F. R. Farmer, "Reactor Safety and Siting: A Proposed Risk Criterion," *Nucl. Safety* **8,** 539–548 (1967).
75. D. C. Cox and P. Baybutt, "Limit Lines for Risk," *Nucl. Technol.* **57,** 320–330 (1982).
76. H. A. Munera and G. Yadigaroglu, "On Farmer's Line, Probability Density Functions, and Overall Risk," *Nucl. Technol.* **74,** 229–232 (1986).
77. J. C. Helton and R. J. Breeding, "Calculation of Reactor Accident Safety Goals," *Reliability Eng. System Safety* **39,** 129–158 (1993).
78. U. S. Nuclear Regulatory Commission, "Safety Goals for the Operation of Nuclear Power Plants: Policy Statement. Correction and Republication," *Fed. Reg.* **51,** 30028–30033 (1986).
79. S. Kaplan and B. J. Garrick, "On the Quantitative Definition of Risk," *Risk Anal.* **1,** 11–27 (1981).
80. F. O. Hoffman and J. S. Hammonds, "Propagation of Uncertainty in Risk Assessments: The Need to Distinguish Between Uncertainty Due to Lack of Knowledge and Uncertainty Due to Variability," *Risk Anal.* **14,** 707–712 (1994).
81. J. C. Helton and D. E. Burmaster, "Guest Editorial: Treatment of Aleatory and Epistemic Uncertainty in Performance Assessments for Complex Systems," *Reliability Eng. System Safety* **54,** 91–94 (1996).
82. M. E. Paté-Cornell, "Uncertainties in Risk Analysis: Six Levels of Treatment," *Reliability Eng. System Safety* **54,** 95–111 (1996).
83. K. M. Thompson and J. D. Graham, "Going Beyond the Single Number: Using Probabilistic Risk Assessment to Improve Risk Management," *Hum. Ecol. Risk Assessment* **2,** 1008–1034 (1996).
84. U. S. Department of Energy, *Quality Assurance Program Document*, CAO-94-1012, Rev. 1 (U.S. Department of Energy, Carlsbad Area Office, Carlsbad, New Mexico, 1996).
85. J. C. Helton *et al., Sensitivity Analysis Techniques and Results for Performance Assessment at the Waste Isolation Pilot Plant*, SAND90-7103 (Sandia National Laboratories, Albuquerque, New Mexico, 1991).
86. J. C. Helton *et al., Uncertainty and Sensitivity Analyses for Gas and Brine Migration at the Waste Isolation Pilot Plant, May 1992*, SAND92-2013 (Sandia National Laboratories, Albuquerque, New Mexico, 1993).
87. J. C. Helton, "Uncertainty and Sensitivity Analysis Techniques for Use in Performance Assessment for Radioactive Waste Disposal," *Reliability Eng. System Safety* **42,** 327–367 (1993).
88. J. C. Helton, "Uncertainty and Sensitivity Analysis in Performance Assessment for the Waste Isolation Pilot Plant," *Computer Phy. Commun.* **117,** 156–180 (1999).
89. U. S. Environmental Protection Agency, "Criteria for the Certification and Re-Certification of the Waste Isolation Pilot Plant's Compliance with the Disposal Regulations: Certification Decision; Final Rule," *Fed. Reg.* **63,** 27353–27406 (1998).

Appendix E

Helton JC, Hansen CW, Sallaberry CJ. Yucca Mountain 2008 Performance Assessment: Conceptual Structure and Computational Implementation. In. *Proceedings of the International High-Level Radioactive Waste Management Conference, September 7-11, 2008*: American Nuclear Society, 2008: 524–532

Sallaberry CJ, Aragon A, Bier A, Chen Y, Groves JW, Hansen CW, Helton JC, Mehta S, Miller SP, Min J, Vo P. Yucca Mountain 2008 Performance Assessment: Uncertainty and Sensitivity Analysis for Physical Processes. In. *Proceedings of the 2008 International High-Level Radioactive Waste Management Conference, September 7-11, 2008*: American Nuclear Society, 2008: 559–566

Hansen CW, Brooks K, Groves JW, Helton JC, Lee PL, Sallaberry CJ, Stathum W, Thom C. Yucca Mountain 2008 Performance Assessment: Uncertainty and Sensitivity Analysis for Expected Dose. In. *Proceedings of the 2008 International High-Level Radioactive Waste Management Conference, September 7-11, 2008*: American Nuclear Society, 2008: 567–574

This page intentionally left blank

YUCCA MOUNTAIN 2008 PERFORMANCE ASSESSMENT: CONCEPTUAL STRUCTURE AND COMPUTATIONAL ORGANIZATION

J.C. Helton, C.W. Hansen, C.J. Sallaberry

Sandia National Laboratories, Albuquerque, NM 87185-0776, jchelto@sandia.gov

The conceptual structure and computational organization of the 2008 total system performance assessment (TSPA) for the proposed high-level radioactive waste repository at Yucca Mountain, Nevada, are described. This analysis was carried out to support the License Application by the U.S. Department of Energy (DOE) to the U.S. Nuclear Regulatory Commission (NRC) for the indicated repository. In particular, the analysis was carried out to establish compliance with the postclosure requirements specified by the NRC in proposed 10 CFR Part 63. The requirements in 10 CFR Part 63 result in a performance assessment that involves three basic entities: (EN1) a characterization of the uncertainty in the occurrence of future events (e.g., igneous events, seismic events) that could affect the performance of the repository; (EN2) models for predicting the physical behavior and evolution of the repository (e.g., systems of ordinary and partial differential equations); and (EN3) a characterization of the uncertainty associated with analysis inputs that have fixed but imprecisely known values (e.g., the appropriate spatially-averaged value for a distribution coefficient). The designators aleatory and epistemic are commonly used for the uncertainties characterized by entities (EN1) and (EN3). The manner in which the preceding entities are defined and organized to produce the 2008 TSPA for the proposed Yucca Mountain repository are described.

I. INTRODUCTION

The appropriate disposal of radioactive waste from military and commercial activities is a challenge of national and international importance. As part of the solution to this challenge, a proposed deep geologic repository for high-level radioactive waste is under development by the U.S. Department of Energy (DOE) at Yucca Mountain (YM), Nevada. The development of the YM repository is the single most important radioactive waste disposal project currently being undertaken in the United States. The following presentation provides a description of the conceptual structure and computational organization of the 2008 total system performance assessment (TSPA) for the proposed YM repository.

II. REGULATORY BACKGROUND

As mandated in the Energy Policy Act of 1992,[1] the U.S. Environmental Protection Agency (EPA) is required to promulgate public health and safety standards for radioactive material stored or disposed of in the YM repository; the U.S. Nuclear Regulatory Commission (NRC) is required to incorporate the EPA standards into licensing standards for the YM repository; and the DOE is required to show compliance with the NRC standards. The regulatory requirements for the YM repository that resulted from these mandates have two primary sources: (i) *Public Health and Environmental Radiation Protection Standards for Yucca Mountain, NV; Final Rule* (40 CFR Part 197),[2] which has been promulgated by the EPA, and (ii) *Disposal of High-Level Radioactive Wastes in a Proposed Geologic Repository at Yucca Mountain, Nevada; Final Rule* (10 CFR Parts 2, 19, 20, etc.),[3] which has been promulgated by the NRC. In turn, the DOE is required to carry out a performance assessment for the YM repository that satisfies the requirements specified in the preceding documents. In addition, the NRC has published the *Yucca Mountain Review Plan; Final Report* (YMRP)[4] to guide assessing compliance with 10 CFR Parts 2, 19, 20, etc.

The initial EPA standard indicated above specified conditions that the YM repository was required to satisfy for the first 10^4 yr after its closure. In a subsequent suit,[5] it was ruled that the EPA did not follow guidance in a National Academy of Science (NAS) study[6] as mandated by Congress in the Energy Policy Act of 1992. In particular, it was ruled that the EPA had failed to follow the guidance in the NAS study that the regulatory period for the YM repository should extend over the period of geologic stability at the facility site, which was suggested to be 10^6 yr. As a result, the initial regulation for the YM facility was remanded to the EPA for revision.

In response to this remand, the EPA published 40 CFR Part 197, *Public Health and Environmental Radiation Protection Standards for Yucca Mountain, Nevada; Proposed Rule*,[7] which contained proposed revisions to the standards for the YM repository. Consistent with the EPA's proposed revisions, the NRC published proposed 10 CFR Part 63, *Implementation of a Dose Standard After 10,000 Years*.[8] The EPA's and

NRC's proposals in response to the remand left most of the requirements for the first 10^4 yr after repository closure unchanged. However, new conditions were proposed for the time interval from 10^4 yr through the period of geologic stability.

The overall structure of the YM 2008 TSPA derives from the individual protection standard specified by the EPA and the NRC. Specifically, the following standard is specified by the NRC (Ref. 8, p. 53319):

§ 63.311 Individual protection standard after permanent closure. (a) DOE must demonstrate, using performance assessment, that there is a reasonable expectation that the reasonably maximally exposed individual receives no more than the following annual dose from releases from the undisturbed Yucca Mountain disposal system: (1) 0.15 mSv (15 mrem) for 10,000 years following disposal; and (2) 3.5 mSv (350 mrem) after 10,000 years, but within the period of geologic stability. (b) DOE's performance assessment must include all potential environmental pathways of radionuclide transport and exposure. (NRC1)

Except for minor differences in wording, the preceding standard is the same as the proposed standard specified by the EPA (Ref. 7, p. 49063).

In turn, the NRC gives the following guidance on implementing the preceding individual protection standard (Ref. 8, p. 53319):

§ 63.303 Implementation of Subpart L. (a) Compliance is based upon the arithmetic mean of the projected doses from DOE's performance assessments for the period within 10,000 years after disposal for: (1) § 63.311(a)(1); and (2) §§ 63.321(b)(1) and 63.331, if performance assessment is used to demonstrate compliance with either or both of these sections. (b) Compliance is based upon the median of the projected doses from DOE's performance assessments for the period after 10,000 years of disposal and through the period of geologic stability for: (1) § 63.311(a)(2); and (2) § 63.321(b)(2), if performance assessment is used to demonstrate compliance. (NRC2)

Again, the preceding is the same as the corresponding guidance given by the EPA (Ref. 7, p. 49063).

As indicated in (NRC1) and (NRC2), the NRC expects the determination of mean and median dose to the reasonably maximally exposed individual (RMEI) to be based on a detailed performance assessment. This expectation is further emphasized by the following statement in the YMRP (Ref. 4, p. 2.2-1):

Risk-Informed Review Process for Performance Assessment—The performance assessment quantifies repository performance, as a means of demonstrating compliance with the postclosure performance objectives at 10 CFR 63.113. The U.S. Department of Energy performance assessment is a systematic analysis that answers the triplet risk questions: what can happen; how likely is it to happen; and what are the consequences. (NRC3)

For convenience, the preceding questions can be represented by (Q1) "What can happen?", (Q2) "How likely is it to happen?", and (Q3) "What are the consequences if it does happen?". The preceding questions provide the intuitive basis for the Kaplan/Garrick ordered triple representation for risk:

$$(\mathcal{S}_i, pS_i, \boldsymbol{cS}_i),\ i = 1, 2, \ldots, nS, \qquad (1)$$

where (i) $\mathcal{S}_i$ is a set of similar occurrences (i.e., the answer to Q1), (ii) pS_i is the probability of $\mathcal{S}_i$ (i.e., the answer to Q2), and (iii) $\boldsymbol{cS}_i$ is a vector of consequences associated with $\mathcal{S}_i$ (i.e., the answer to Q3).[9] Further, the $\mathcal{S}_i$ must be disjoint (i.e., $\mathcal{S}_i \cap \mathcal{S}_j = \varnothing$ for $i \neq j$); each $\mathcal{S}_i$ must be sufficiently homogeneous to allow use of a single representative consequence vector $\boldsymbol{cS}_i$; and $\cup_i \mathcal{S}_i$ must contain all risk significant occurrences for the facility under consideration.

In addition, there is a fourth basic question that underlies the YM 2008 TSPA and, indeed, all complete performance assessments: (Q4) "What is the uncertainty in the answers to the initial three questions?". The importance of answering this fourth question is emphasized in a number of statements by the NRC. For example:

For such long-term performance, what is required is reasonable expectation, making allowance for the time period, hazards, and uncertainties involved, that the outcome will conform with the objectives for postclosure performance for the geologic repository. Demonstrating compliance will involve the use of complex predictive models that are supported by limited data from field and laboratory tests, site-specific monitoring, and natural analog studies that may be supplemented with prevalent expert judgment. Compliance demonstrations should not exclude important parameters from assessments and analyses simply because they are difficult to precisely quantify to a high degree of confidence. The performance assessments and analyses should focus upon the full range of defensible and reasonable parameter distributions rather than only upon extreme physical situations and parameter values (Ref. 3, p. 55804). (NRC4)

Once again, although the criteria may be written in unqualified terms, the demonstration of compliance must take uncertainties and gaps in knowledge into account so that the Commission can make the specified finding with respect to paragraph (a)(2) of § 63.31 (Ref. 3, p. 55804). (NRC5)

Both the preceding statements clearly indicate that a reasonable treatment of uncertainty should be a fundamental part of a performance assessment used to support a licensing application for the YM repository.

III. CONCEPTUAL STRUCTURE

The YM 2008 TSPA was developed to satisfy requirements in 10 CFR Part 63 and has a structure that

involves three basic entities: (EN1) a characterization of the uncertainty in the occurrence of future events (e.g., igneous events, seismic events) that could affect the performance of the repository; (EN2) models for predicting the physical behavior and evolution of the repository (e.g., systems of ordinary and partial differential equations); and (EN3) a characterization of the uncertainty associated with analysis inputs that have fixed but imprecisely known values (e.g., the spatially-averaged value for a distribution coefficient).[10] The designators aleatory and epistemic are commonly used for the uncertainties characterized by (EN1) and (EN3).

In the preceding, aleatory uncertainty is used in the designation of randomness in the possible future conditions that could affect the YM repository. In concept, each possible future at the YM repository can be represented by a vector

$$\mathbf{a} = [a_1, a_2, \ldots, a_{nA}], \qquad (2)$$

where each a_i is a specific property of the future $\mathbf{a}$ (e.g., time of a seismic event, size of a seismic event, …). In turn, a subset $\mathcal{S}$ of the set $\mathcal{A}$ of all possible values for $\mathbf{a}$ constitutes what is referred to as a scenario class in the YM 2008 TSPA. As part of the YM 2008 TSPA development, a probabilistic structure is imposed on the set $\mathcal{A}$. Formally, this corresponds to defining a probability space ($\mathcal{A}$, $\mathbb{A}$, p_A) for aleatory uncertainty. Then, $\mathbb{A}$ is the set of all possible scenario classes, and p_A is the function that defines scenario class probability (i.e., scenario class $\mathcal{S}$ is an element of $\mathbb{A}$ and $p_A(\mathcal{S})$ is the probability of scenario class $\mathcal{S}$). As discussed in more detail in Sect. VI, the set $\mathbb{A}$ contains both disjoint and nondisjoint scenario classes. Formally, the probability space ($\mathcal{A}$, $\mathbb{A}$, p_A) provides a characterization of aleatory uncertainty and constitutes the first of the three basic mathematical entities that underlie the determination of expected (i.e., mean) dose.

TABLE I. Representation of Aleatory Uncertainty in the YM 2008 TSPA

Individual Futures:

$$\mathbf{a} = [nEW, nED, nII, nIE, nSG, nSF, \mathbf{a}_{EW}, \mathbf{a}_{ED}, \mathbf{a}_{II}, \mathbf{a}_{IE}, \mathbf{a}_{SG}, \mathbf{a}_{SF}]$$

where, for a time interval [a, b] (e.g., [0, 10^4 yr] or [0, 10^6 yr]), nEW = number of early waste package (WP) failures, nED = number of early drip shield (DS) failures, nII = number of igneous intrusive (II) events, nIE = number of igneous eruptive (IE) events, nSG = number of seismic ground (SG) motion events, nSF = number of seismic fault (SF) displacement events, $\mathbf{a}_{EW}$ = vector defining the nEW early WP failures, $\mathbf{a}_{ED}$ = vector defining the nED early DS failures, $\mathbf{a}_{II}$ = vector defining the nII igneous intrusive events, $\mathbf{a}_{IE}$ = vector defining the nIE igneous eruptive events, $\mathbf{a}_{SG}$ = vector defining the nSG seismic ground motion events, and $\mathbf{a}_{SF}$ = vector defining the nSF seismic fault displacement events.

Sample Space for Aleatory Uncertainty: $\mathcal{A} = \{\mathbf{a} : \mathbf{a} = [nEW, nED, nII, nIE, nSG, nSF, \mathbf{a}_{EW}, \mathbf{a}_{ED}, \mathbf{a}_{II}, \mathbf{a}_{IE}, \mathbf{a}_{SG}, \mathbf{a}_{SF}]\}$

Example Scenario Classes:

Nominal, $\mathcal{A}_N = \{\mathbf{a} : \mathbf{a} \in \mathcal{A} \text{ and } nEW = nED = nII = nIE = nSG = nSF = 0\}$

Early WP failure, $\mathcal{A}_{EW} = \{\mathbf{a} : \mathbf{a} \in \mathcal{A} \text{ and } nEW \geq 1\}$; Early DS failure, $\mathcal{A}_{ED} = \{\mathbf{a} : \mathbf{a} \in \mathcal{A} \text{ and } nED \geq 1\}$

Igneous intrusive, $\mathcal{A}_{II} = \{\mathbf{a} : \mathbf{a} \in \mathcal{A} \text{ and } nII \geq 1\}$; Igneous eruptive, $\mathcal{A}_{IE} = \{\mathbf{a} : \mathbf{a} \in \mathcal{A} \text{ and } nIE \geq 1\}$

Seismic ground motion, $\mathcal{A}_{SG} = \{\mathbf{a} : \mathbf{a} \in \mathcal{A} \text{ and } nSG \geq 1\}$; Seismic fault displacement, $\mathcal{A}_{SF} = \{\mathbf{a} : \mathbf{a} \in \mathcal{A} \text{ and } nSF \geq 1\}$

Early failure, $\mathcal{A}_E = \mathcal{A}_{EW} \cup \mathcal{A}_{ED}$; Igneous, $\mathcal{A}_I = \mathcal{A}_{II} \cup \mathcal{A}_{IE}$; Seismic, $\mathcal{A}_S = \mathcal{A}_{SG} \cup \mathcal{A}_{SF}$

Scenario Class Probabilities:

$p_A(\mathcal{A}_N)$ = probability of no disruptions of any kind

$p_A(\mathcal{A}_{EW})$ = probability of one or more early WP failures ; $p_A(\mathcal{A}_{ED})$ = probability of one or more early DS failures

$p_A(\mathcal{A}_{II})$ = probability of one or more II events ; $p_A(\mathcal{A}_{IE})$ = probability of one or more IE events

$p_A(\mathcal{A}_{SG})$ = probability of one or more SG motion events; $p_A(\mathcal{A}_{SF})$ = probability of one or more SF displacement events

$p_A(\mathcal{A}_E)$ = probability of one or more early failures ; $p_A(\mathcal{A}_I)$ = probability of one or more igneous events

$p_A(\mathcal{A}_S)$ = probability of one or more seismic events

Although useful conceptually and notationally, the probability space ($\mathcal{A}$, $\mathbb{A}$, p_A) is never explicitly defined in the YM 2008 TSPA. Rather, the characterization of aleatory uncertainty enters the analysis through the definition of probability distributions for the individual elements of **a**. Conceptually, the distributions for the elements of **a** lead to a distribution for **a** and an associated density function $d_A(\mathbf{a})$. The nature of the probability space ($\mathcal{A}$, $\mathbb{A}$, p_A) in the context of the 2008 YM TSPA is summarized in Table I (see Ref. 11, App. J, for additional information).

The second of the three basic mathematical entities that underlie the determination of expected dose is a model that estimates dose to the RMEI. Formally, this model can be represented by the function

$D(\tau|\mathbf{a})$ = dose to RMEI (mrem/yr) at time τ (yr) conditional on the occurrence of the future represented by **a**. (3)

Technically, $D(\tau|\mathbf{a})$ is the committed 50 yr dose to the RMEI that results from radiation exposure incurred in a single year. In the computational implementation of the YM 2008 TSPA, $D(\tau|\mathbf{a})$ is only one of the results calculated with the GoldSim program for the particular analysis configuration defined for the future **a**. In practice, many results are calculated for **a** in addition to dose to the RMEI (see Ref. 11, Table K3-4). Thus, $D(\tau|\mathbf{a})$ is part of a vector containing at least several thousand elements. For notational convenience, this paper presents the analysis for dose to the RMEI $D(\tau|\mathbf{a})$; however, other YM 2008 TSPA results can be handled in exactly the same manner as described for dose. The general nature of $D(\tau|\mathbf{a})$ is described in several following presentations[12-14] and in more detail in Ref. 11.

The third of the three basic mathematical entities that underlie the determination of expected dose is a probabilistic characterization of epistemic uncertainty. Here, epistemic uncertainty refers to a lack of knowledge with respect to the appropriate value to use for a quantity that is assumed to have constant or fixed value in the context of a particular analysis. Specifically, epistemic uncertainty relates to a vector of the form

$$\begin{aligned}\mathbf{e} &= [\mathbf{e}_A, \mathbf{e}_M] \\ &= [e_{A1}, e_{A2}, \ldots, e_{A,nAE}, e_{M1}, e_{M2}, \ldots, e_{M,nME}] \\ &= [e_1, e_2, \ldots, e_{nE}],\ nE = nAE + nME,\end{aligned} \tag{4}$$

where

$$\mathbf{e}_A = [e_{A1}, e_{A2}, \ldots, e_{A,nAE}]$$

is a vector of epistemically uncertain quantities used in the characterization of aleatory uncertainty (e.g., a rate term that defines a Poisson process) and

$$\mathbf{e}_M = [e_{M1}, e_{M2}, \ldots, e_{M,nME}]$$

is a vector of epistemically uncertain quantities used in the determination of dose (e.g., a distribution coefficient).

Epistemic uncertainty results in a set $\mathcal{E}$ of possible values for **e**. In turn, probability is used to characterize the level of likelihood or credence that can be assigned to various subsets of $\mathcal{E}$. In concept, this leads to a probability space ($\mathcal{E}$, $\mathbb{E}$, p_E) for epistemic uncertainty. Like the probability space ($\mathcal{A}$, $\mathbb{A}$, p_A) for aleatory uncertainty, the probability space ($\mathcal{E}$, $\mathbb{E}$, p_E) for epistemic uncertainty is useful conceptually and notationally but is never explicitly defined in the YM 2008 TSPA. Rather, the characterization of epistemic uncertainty enters the analysis through the definition of probability distributions for the individual elements of **e**. These distributions serve as mathematical summaries of all available information with respect to where the appropriate values for individual elements of **e** are located for use in the YM 2008 TSPA. Conceptually, the distributions for the elements of **e** lead to a distribution for **e** and an associated density function $d_E(\mathbf{e})$. The nature of the probability space ($\mathcal{E}$, $\mathbb{E}$, p_E) in the context of the YM 2008 TSPA is indicated in Table II (see Ref. 11, Tables K3-1, K3-2, K3-3, for additional information).

TABLE II. Examples of the nE = 392 Epistemically Uncertain Variables Considered in the YM 2008 TSPA

ASHDENS - Tephra settled density (kg/m^3). *Distribution:* Truncated normal.. *Range:* 300 to 1500. *Mean:* 1000. *Standard Deviation:* 100.
IGRATE - Frequency of intersection of the repository footprint by a volcanic event (yr^{-1}). *Distribution:* Piecewise uniform. *Range:* 0 to 7.76E-07.
INFIL - Pointer variable for determining infiltration conditions: 10th, 30th, 50th or 90th percentile infiltration scenario (dimensionless). *Distribution:* Discrete. *Range:* {1, 2, 3, 4}.
MICPU239 - Groundwater biosphere dose conversion factor (BDCF) for ^{239}Pu in modern interglacial climate ((Sv/year)/(Bq/m^3)). *Distribution:* Discrete. *Range:* 3.49E-07 to 2.93E-06.
SZFISPVO - Flowing interval spacing in fractured volcanic units (m). *Distribution:* Piecewise uniform. *Range:* 1.86 to 80.

IV. EXPECTED DOSE, MEAN DOSE, MEDIAN DOSE

Now that the characterization of epistemic uncertainty has been introduced, the notations used to represent aleatory uncertainty and dose need to be expanded. Because the representation of aleatory uncertainty depends on elements of the vector $\mathbf{e}_A$, each possible value for $\mathbf{e}_A$ could lead to a different probability space ($\mathcal{A}$, $\mathbb{A}$, p_A) for aleatory uncertainty. For notational convenience, this dependence will be indicated by representing the density function associated with aleatory uncertainty by $d_A(\mathbf{a}|\mathbf{e}_A)$. Similarly, the determination of dose depends on elements of the vector $\mathbf{e}_M$, with each possible value for $\mathbf{e}_M$ potentially leading to different dose results. For notational convenience, this dependence will be indicated by representing the dose function by $D(\tau|\mathbf{a}, \mathbf{e}_M)$.

The probability space ($\mathcal{A}$, $\mathbb{A}$, p_A) for aleatory uncertainty characterized by the density function $d_A(\mathbf{a}|\mathbf{e}_A)$, the dose function $D(\tau|\mathbf{a}, \mathbf{e}_M)$, and the probability space ($\mathcal{E}$, $\mathbb{E}$, p_E) for epistemic uncertainty characterized by the density function $d_E(\mathbf{e})$ constitute the three basic parts of the YM 2008 TSPA that come together in the determination of expected dose to the RMEI and the uncertainty in expected dose to the RMEI. Specifically, the expected value for dose at time τ conditional on a specific element $\mathbf{e} = [\mathbf{e}_A, \mathbf{e}_M]$ of $\mathcal{E}$ is given by

$$\begin{aligned}\bar{D}(\tau|\mathbf{e}) &= E_A\left[D(\tau|\mathbf{a}, \mathbf{e}_M)\middle|\mathbf{e}_A\right] \\ &= \int_{\mathcal{A}} D(\tau|\mathbf{a}, \mathbf{e}_M)\, d_A(\mathbf{a}|\mathbf{e}_A)\,\mathrm{d}A,\end{aligned} \tag{5}$$

where $E_A[D(\tau|\mathbf{a}, \mathbf{e}_M)|\mathbf{e}_A]$ denotes expectation over aleatory uncertainty.

In turn, the uncertainty associated with the estimation of $\bar{D}(\tau|\mathbf{e})$ can be determined from the properties of the probability space ($\mathcal{E}$, $\mathbb{E}$, p_E) for epistemic uncertainty. In particular, the cumulative distribution function (CDF) for $\bar{D}(\tau|\mathbf{e})$ and the expected value for $\bar{D}(\tau|\mathbf{e})$ that derive from epistemic uncertainty are given by

$$\begin{aligned}p_E\left[\bar{D}(\tau|\mathbf{e}) \le D\right] &= \int_{\mathcal{E}} \underline{\delta}_D\left[\bar{D}(\tau|\mathbf{e})\right] d_E(\mathbf{e})\,\mathrm{d}E \\ &= \int_{\mathcal{E}} \underline{\delta}_D\left[\int_{\mathcal{A}} D(\tau|\mathbf{a}, \mathbf{e}_M)\, d_A(\mathbf{a}|\mathbf{e}_A)\,\mathrm{d}A\right] d_E(\mathbf{e})\,\mathrm{d}E\end{aligned} \tag{6}$$

and

$$\bar{\bar{D}}(\tau) = E_E\left[\bar{D}(\tau|\mathbf{e})\right] = \int_{\mathcal{E}} \bar{D}(\tau|\mathbf{e})\, d_E(\mathbf{e})\,\mathrm{d}E, \tag{7}$$

respectively, where

$$\underline{\delta}_D\left[\bar{D}(\tau|\mathbf{e})\right] = \begin{cases} 1 & \text{if } \bar{D}(\tau|\mathbf{e}) \le D \\ 0 & \text{if } \bar{D}(\tau|\mathbf{e}) > D \end{cases}$$

and $E_E[\bar{D}(\tau|\mathbf{e})]$ denotes expectation over epistemic uncertainty.

The individual grey curves in Fig. 1 correspond to expected doses $\bar{D}(\tau|\mathbf{e})$ as defined in Eq. (5). The totality of the grey curves provides a display of the uncertainty in $\bar{D}(\tau|\mathbf{e})$ that derives from the uncertainty in $\mathbf{e}$. The red curve in Fig. 1 corresponds to the mean dose $\bar{\bar{D}}(\tau)$ defined in Eq. (7) and used in comparisons with the 10^4 yr standard as specified in Quotes (NRC1) and (NRC2). Specifically, $\bar{\bar{D}}(\tau)$ is the expected value for $\bar{D}(\tau|\mathbf{e})$ over the epistemic uncertainty associated with $\mathbf{e}$.

.

The value of D for which

$$q = p_E\left[\bar{D}(\tau|\mathbf{e}) \le D\right] = \int_{\mathcal{E}} \underline{\delta}_D\left[\bar{D}(\tau|\mathbf{e})\right] d_E(\mathbf{e})\,\mathrm{d}E \tag{8}$$

defines the q quantile (e.g., q = 0.05, 0.5, 0.95) for the distribution of expected dose over epistemically uncertain analysis inputs. For notational purposes, the value of D corresponding to the q quantile of $\bar{D}(\tau|\mathbf{e})$ defined in Eq. (8) will be represented by $Q_{E,q}[\bar{D}(\tau|\mathbf{e})]$. The blue curve in Fig. 1 corresponds to the median dose $Q_{E,0.5}[\bar{D}(\tau|\mathbf{e})]$ defined in Eq. (8) for q = 0.5 and used in comparisons with the proposed post 10^4 yr standard as specified in Quotes (NRC1) and (NRC2).

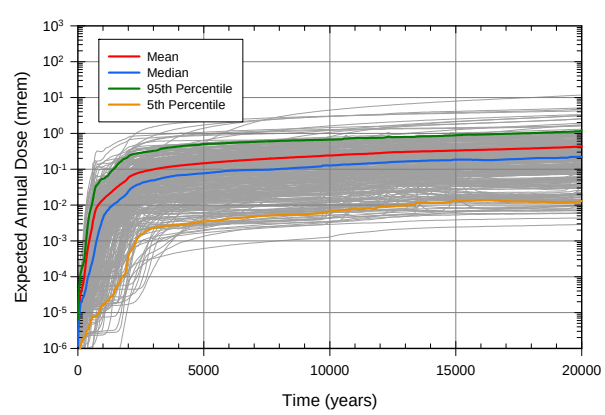

Fig. 1 Expected, mean and median curves for dose to the RMEI

TABLE III. Decomposition of Expected Dose $\bar{D}(\tau \mid \mathbf{e})$ into Expected Incremental Doses $\bar{D}_C(\tau \mid \mathbf{e})$ from Individual Scenario Classes

$$\bar{D}(\tau|\mathbf{e}) = \int_{\mathcal{A}} D(\tau|\mathbf{a}, \mathbf{e}_M)\, d_A(\mathbf{a}|\mathbf{e}_A)\, \mathrm{d}A$$

$$\cong \int_{\mathcal{A}} \left\{ D_N(\tau|\mathbf{a}_N, \mathbf{e}_M) + \sum_{C \in \mathcal{M}C} D_C(\tau|\mathbf{a}, \mathbf{e}_M) \right\} d_A(\mathbf{a}|\mathbf{e}_A)\, \mathrm{d}A \quad \text{with} \begin{cases} D(\tau|\mathbf{a}, \mathbf{e}) \cong D_N(\tau|\mathbf{a}_N, \mathbf{e}_M) + \sum_{C \in \mathcal{M}C} D_C(\tau|\mathbf{a}, \mathbf{e}_M) \\ \mathcal{M}C = \{EW, ED, II, IE, SG, SF\} \end{cases}$$

$$= D_N(\tau|\mathbf{a}_N, \mathbf{e}_M) + \sum_{C \in \mathcal{M}C} \int_{\mathcal{A}} D_C(\tau|\mathbf{a}, \mathbf{e}_M)\, d_A(\mathbf{a}|\mathbf{e}_A)\, \mathrm{d}A$$

$$= D_N(\tau|\mathbf{a}_N, \mathbf{e}_M) + \sum_{C \in \mathcal{M}C} \int_{\mathcal{A}_C} D_C(\tau|\mathbf{a}, \mathbf{e}_M)\, d_A(\mathbf{a}|\mathbf{e}_A)\, \mathrm{d}A$$

$$= D_N(\tau|\mathbf{a}_N, \mathbf{e}_M) + \sum_{C \in \mathcal{M}C} \bar{D}_C(\tau|\mathbf{e})$$

where $\mathbf{a}_N$ corresponds to the single future associated with the nominal scenario class $\mathcal{A}_N$ in which no disruptions of any kind occur, $D_N(\tau \mid \mathbf{a}_N, \mathbf{e}_M)$ is the dose to the RMEI that results solely from processes associated with the nominal scenario class, and $D_C(\tau \mid \mathbf{a}, \mathbf{e}_M)$ is the incremental dose to the RMEI that results solely from the effects of the disruptions that result in the future $\mathbf{a}$ being an element of the scenario class (i.e., set) $\mathcal{A}_C$.

V. COMPUTATIONAL IMPLEMENTATION

Evaluation of expected, mean and median doses as described in the preceding section presents two numerical challenges. First, it is necessary to evaluate integrals over the set $\mathcal{A}$ to obtain expected doses over aleatory uncertainty. Second, it is necessary to evaluate integrals over the set $\mathcal{E}$ to obtain mean and median doses over aleatory and epistemic uncertainty.

Evaluation of integrals over the set $\mathcal{A}$ is considered first. These evaluations are accomplished under the assumption that there are no synergisms between the effects of the disruptions associated with the individual scenario classes that have a significant effect on the expected dose $\bar{D}(\tau \mid \mathbf{e})$. As a result and with the assumption that nominal process releases occur for all scenario classes, $\bar{D}(\tau \mid \mathbf{e})$ can be approximated as indicated in Table III. Example derivations of how the use of disjoint scenario classes to calculate expected dose $\bar{D}(\tau \mid \mathbf{e})$ in combination with the no significant synergisms assumption leads to the relationships Table III are presented in Ref. 16.

Given the decomposition in Table III, $\bar{D}(\tau \mid \mathbf{e})$ can be approximated by (i) approximating $D_N(\tau \mid \mathbf{a}_N, \mathbf{e}_M)$ and individually approximating the integrals defining the expected incremental doses $\bar{D}_C(\tau \mid \mathbf{e})$ as indicated in Table IV (see Ref. 11, App. J, for additional details) and then (ii) adding these approximations to obtain an approximation to $\bar{D}(\tau \mid \mathbf{e})$.

TABLE IV. Integration Procedures Used to Obtain Expected Incremental Dose $\bar{D}_C(\tau \mid \mathbf{e})$ for Individual Scenario Classes in the YM 2008 TSPA

Nominal Conditions: $D_N(\tau|\mathbf{e})$
- Always zero for [0, 2×10^4 yr] in YM 2008 TSPA
- Combined with seismic ground motion for [0, 10^6 yr]

Early WP and DS Failures: $\bar{D}_{EW}(\tau \mid \mathbf{e})$, $\bar{D}_{ED}(\tau \mid \mathbf{e})$
- Summation of probabilistically weighted results for individual failures

Igneous Intrusive Events: $\bar{D}_{II}(\tau \mid \mathbf{e})$
- Quadrature procedure

Igneous Eruptive Events
- Combined Quadrature/Monte Carlo procedure

Seismic Ground Motion Events: $\bar{D}_{SG}(\tau \mid \mathbf{e})$
- Quadrature procedure for [0, 2×10^4 yr]
- Monte Carlo procedure for [0, 10^6 yr]

Seismic Fault Displacement Events: $\bar{D}_{SF}(\tau \mid \mathbf{e})$
- Quadrature procedure

The mean dose $\bar{\bar{D}}(\tau)$ and the median dose $Q_{E,0.5}[\,\bar{D}(\tau\,|\,\mathbf{e})\,]$ are defined by integrals over the set $\mathcal{E}$ of epistemically uncertain analysis inputs as indicated in Eqs. (7) and (8). In the YM 2008 TSPA, these integrals are approximated with use of a Latin hypercube sample (LHS)

$$\mathbf{e}_i = \left[\mathbf{e}_{Ai}, \mathbf{e}_{Mi}\right], i = 1, 2, \ldots, nLHS, \tag{9}$$

of size $nLHS = 300$ generated in consistency with the definition of the probability space ($\mathcal{E}$, $\mathbb{E}$, p_E) (i.e., in consistency with the distributions defined for the individual elements of $\mathbf{e}$). Then, $\bar{\bar{D}}(\tau)$ and $p_E[\,\bar{D}(\tau\,|\,\mathbf{e}) \le D]$ are approximated by

$$\bar{\bar{D}}(\tau) \cong \sum_{i=1}^{nLHS} \bar{D}\left(\tau\middle|\mathbf{e}_i\right)\Big/nLHS \tag{10}$$

and

$$p_E\left[\bar{D}\left(\tau\middle|\mathbf{e}\right) \le D\right] \cong \sum_{i=1}^{nLHS} \delta_D\left[\bar{D}\left(\tau\middle|\mathbf{e}_i\right)\right]\Big/nLHS, \tag{11}$$

respectively. Further, this sample can be used in a numerical determination of the quantiles $Q_{E,q}[\,\bar{D}(\tau\,|\,\mathbf{e})\,]$ for $\bar{D}(\tau\,|\,\mathbf{e})$ defined in Eq. (8). Analogous approximations to mean and median doses over epistemic uncertainty also exist for the individual scenario classes.

VI. DISJOINT AND NONDISJOINT SCENARIO CLASSES

As used in this presentation, a scenario class is any element of the set $\mathbb{A}$ appearing in the formal definition of the probability space ($\mathcal{A}$, $\mathbb{A}$, p_A) for aleatory uncertainty. Specifically, a scenario class is any subset $\mathcal{S}$ of the set $\mathcal{A}$ of possible futures (see Table I) for which a probability $p_A(\mathcal{S})$ can be defined. This definition, which is consistent with the formal development of probability, allows for both disjoint and nondisjoint scenario classes. Consistent with this, both disjoint and nondisjoint scenario classes have significant roles in the YM 2008 TSPA.

As recognized by the NRC in the following statement from the YMRP (Ref. 4, p. 2.2-133), the calculation of expected dose to the RMEI has a conceptual basis that involves the use of disjoint scenario classes: "The occurrence of scenario classes, included in the calculating the annual dose, sum to one." This statement is consistent with the approximation of the expected dose $\bar{D}(\tau\,|\,\mathbf{e})$ defined in Eq. (5) by

$$\bar{D}\left(\tau\middle|\mathbf{e}\right) \cong \sum_{i=1}^{nS} D\left(\tau\middle|\mathbf{a}_i, \mathbf{e}_M\right) p_A\left(\mathcal{S}_i\middle|\mathbf{e}_A\right), \tag{12}$$

where the $\mathcal{S}_i$ are elements of $\mathbb{A}$ (i.e., subsets of $\mathcal{A}$), $\mathcal{S}_i \cap \mathcal{S}_j = \varnothing$ if $i \ne j$, $\cup_i \mathcal{S}_i = \mathcal{A}$, $\mathbf{a}_i \in \mathcal{S}_i$, and $p_A(\mathcal{S}_i|\mathbf{e}_A)$ is the probability of $\mathcal{S}_i$. The preceding approximation to $\bar{D}(\tau\,|\,\mathbf{e})$ corresponds to an expected value calculation in the context of the ordered triplet representation for risk ($\mathcal{S}_i$, pS_i, $\boldsymbol{cS}_i$), i = 1, 2, …, nS, in Eq. (1). Specifically, the sets $\mathcal{S}_i$ are the same, $p_A(\mathcal{S}_i|\mathbf{e}_A)$ corresponds to pS_i, and $D(\tau\,|\,\mathbf{a}_i, \mathbf{e}_M)$ corresponds to $\boldsymbol{cS}_i$.

As indicated in Eq. (12), the calculation of expected dose to the RMEI in the YM 2008 TSPA can be formally based on the consideration of disjoint scenario classes with probabilities that sum to one. However, in computational practice, the number of disjoint scenario classes required for the sum in Eq. (12) to be a reasonable approximation to $\bar{D}(\tau\,|\,\mathbf{e})$ is both large and difficult to determine (e.g., see Ref. 15). For this reason and with described justification (Ref. 11, App. J), the YM 2008 TSPA approximates $\bar{D}(\tau\,|\,\mathbf{e})$ on the basis of the no significant synergisms decomposition indicated in Table III. This decomposition involves the nondisjoint scenario classes $\mathcal{A}_C$, C = *EW*, *ED*, *II*, *IE*, *SG*, *SF*, appearing in Tables I and III. However, the starting integral that defines $\bar{D}(\tau\,|\,\mathbf{e})$ in Eq. (5) is predicated on the concept of disjoint scenario classes. In particular, the correct place to check for conservation of probability in the determination of $\bar{D}(\tau\,|\,\mathbf{e})$ is in the integral definition of $\bar{D}(\tau\,|\,\mathbf{e})$ in Eq. (5) rather than after the no significant synergisms assumption has been implemented at the end of Table III. This decomposition is very beneficial because implementing integrals over the sets $\mathcal{A}_C$ (or modeling cases as they are sometimes called; see Table IV) is much easier that implementing an integral over the set $\mathcal{A}$. This decomposition also facilitates informative uncertainty and sensitivity analyses of the form presented in Refs. 17 and 18 and in more detail in Apps. J and K of Ref. 11.

In addition, when scenario class probabilities are requested, it is likely that the desired probabilities are for the nondisjoint scenario classes $\mathcal{A}_C$, C = *EW*, *ED*, *II*, *IE*, *SG*, *SF*, or possibly some other collection of nondisjoint scenario classes. In particular, it is probabilities for the nondisjoint scenario classes $\mathcal{A}_C$ that are presented in App. J of Ref. 11. For example, if probability of early WP failure is under consideration, then most likely $p_A(\mathcal{A}_{EW}|\mathbf{e}_A)$ rather than $p_A(\{\mathbf{a}|\, nEW > 0, nED = nII = nIE = nSG = nSF = 0\}|\mathbf{e}_A)$ is the probability of interest. Specifically, the $p_A(\mathcal{A}_{EW}|\mathbf{e}_A)$ is the probability that one or more early WP failures occur while $p_A(\{\mathbf{a}|\, nEW > 0, nED = nII =$

$nIE = nSG = nSF = 0\}|\mathbf{e}_A)$ is the probability that one or more early failures occur and also that no other failures of any other type occur; this latter probability is significantly affected by the indicated nonoccurrence assumptions and effectively provides no information on the likelihood of early WP failures.

VII. SUMMARY

As described, the conceptual and computational structure of the YM 2008 TSPA is based on three basic entities: (EN1) a characterization of the uncertainty in the occurrence of future events that could affect the performance of the repository (i.e., a probability space ($\mathcal{A}$, $\mathbb{A}$, p_A) characterizing aleatory uncertainty), (EN2) models for predicting the physical behavior and evolution of the repository system (i.e., a very complex function $D(\tau|\mathbf{a}, \mathbf{e}_M)$ that predicts dose to the RMEI and a large number of additional analysis results), and (EN3) a characterization of the uncertainty associated with analysis inputs that have fixed but imprecisely known values (i.e., a probability space ($\mathcal{E}$, $\mathbb{E}$, p_E) characterizing epistemic uncertainty).

This paper summarizes the first presentation in a special session intended to provide an overview on the YM 2008 TSPA. Following presentations in the session provide summaries of (i) the development and use of the models that collectively constitute the function $D(\tau|\mathbf{a}, \mathbf{e}_M)$,[12-14] (ii) the performance of uncertainty and sensitivity analyses for physical processes based on $D(\tau|\mathbf{a}, \mathbf{e}_M)$ and the characterization of epistemic uncertainty provided by ($\mathcal{E}$, $\mathbb{E}$, p_E),[18] (iii) the performance of uncertainty and sensitivity analyses for expected dose to the RMEI based on the characterization of aleatory uncertainty provided by ($\mathcal{A}$, $\mathbb{A}$, p_A), the function $D(\tau|\mathbf{a}, \mathbf{e}_M)$ and the characterization of epistemic uncertainty provided by ($\mathcal{E}$, $\mathbb{E}$, p_E),[17] and (iv) a summary of the YM 2008 TSPA in the context of the regulatory requirements specified by the NRC in 10 CFR Part 63.[19]

Additional and more detailed information on the YM 2008 PA is available in a detailed analysis report[11] and in the references cited in this report.

ACKNOWLEDGMENTS

Work performed at Sandia National Laboratories (SNL), which is a multiprogram laboratory operated by Sandia Corporation, a Lockheed Martin Company, for the U.S. Department of Energy's (DOE's) National Nuclear Security Administration under Contract No. DE-AC04-94AL85000. The United States Government retains and the publisher, by accepting this article for publication, acknowledges that the United States Government retains a non-exclusive, paid-up, irrevocable, world-wide license to publish or reproduce the published form of this article, or allow others to do so, for United States Government purposes. The views expressed in this article are those of the authors and do not necessarily reflect the views or policies of the DOE or SNL.

REFERENCES

1. PUBLIC LAW 102-486. *Energy Policy Act of 1992*, 1992.
2. U.S. EPA (U.S. ENVIRONMENTAL PROTECTION AGENCY). 40 CFR 197: Public Health and Environmental Radiation Protection Standards for Yucca Mountain, NV; Final Rule. *Federal Register* 2001;66(114):32074-32135.
3. U.S. NRC (U.S. NUCLEAR REGULATORY COMMISSION). 10 CFR Parts 2, 19, 20, etc.: Disposal of High-Level Radioactive Wastes in a Proposed Geologic Repository at Yucca Mountain, Nevada; Final Rule. *Federal Register* 2001;66(213):55732-55816.
4. U.S. NRC (U.S. NUCLEAR REGULATORY COMMISSION). *Yucca Mountain Review Plan, Final Report*.NUREG-1804, Rev. 2.Washington, D.C.: U.S. Nuclear Regulatory Commission 2003.
5. NUCLEAR ENERGY INSTITUTE V. ENVIRONMENTAL PROTECTION AGENCY. 373 F.3d 1 (D.C. Cir. 2004) (NEI) (Docket no. OAR-2005-0083-0080).
6. NRC (NATIONAL RESEARCH COUNCIL). *Technical Bases for Yucca Mountain Standards*. Washington, DC: National Academy Press 1995.
7. U.S. EPA (U.S. ENVIRONMENTAL PROTECTION AGENCY). 40 CFR Part 197: Public Health and Environmental Radiation Protection Standards for Yucca Mountain, Nevada; Proposed Rule. *Federal Register* 2005;10(161):49014-49065.
8. U.S. NRC (U.S. NUCLEAR REGUALTORY COMMISSION). 10 CFR Part 63: Implementation of a Dose Standard after 10,000 Years. *Federal Register* 2005;70(173):53313-53320.
9. KAPLAN S, GARRICK BJ. On the Quantitative Definition of Risk. *Risk Analysis* 1981;1(1):11-27.
10. HELTON JC. Mathematical and Numerical Approaches in Performance Assessment for Radioactive Waste Disposal: Dealing with Uncertainty. In: EM Scott, ed. *Modelling Radioactivity in the Environment*. New York, NY: Elsevier Science, 2003:353-390.
11. SNL (SANDIA NATIONAL LABORATORIES). *Total System Performance Assessment Model/-Analysis for the License Application*.MDL-WIS-PA-000005 Rev 00, AD 01.Las Vegas, NV: U.S.

Department of Energy Office of Civilian Radioactive Waste Management 2008.

12. MACKINNON RJ et al. Yucca Mountain 2008 Performance Assessment: Modeling the Engineered Barrier System. In *Proceedings of the 2008 International High-Level Radioactive Waste Management Conference, September 7-11, 2008*: American Nuclear Society, 2008:this volume.
13. MATTIE PD et al. Yucca Mountain 2008 Performance Assessment: Modeling the Natural System. In *Proceedings of the 2008 International High-Level Radioactive Waste Management Conference, September 7-11, 2008*: American Nuclear Society, 2008:this volume.
14. SEVOUGIAN SD et al. Yucca Mountain 2008 Performance Assessment: Modeling Disruptive Events and Early Failures. In *Proceedings of the 2008 International High-Level Radioactive Waste Management Conference, September 7-11, 2008*: American Nuclear Society, 2008:this volume.
15. HELTON JC, IUZZOLINO HJ. Construction of Complementary Cumulative Distribution Functions for Comparison with the EPA Release Limits for Radioactive Waste Disposal. *Reliability Engineering and System Safety* 1993;40(3):277-293.
16. HELTON JC, SALLABERRY CJ. *Illustration of Sampling-Based Approaches to the Calculation of Expected Dose in Performance Assessments for the Proposed High Level Radioactive Waste Repository at Yucca Mountain, Nevada*.SAND2007-1353. Albuquerque, NM: Sandia National Laboratories 2007.
17. HANSEN CW et al. Yucca Mountain 2008 Performance Assessment: Uncertainty and Sensitivity Analysis for Expected Dose. In *Proceedings of the 2008 International High-Level Radioactive Waste Management Conference, September 7-11, 2008*: American Nuclear Society, 2008:this volume.
18. SALLABERRY CJ et al. Yucca Mountain 2008 Performance Assessment: Uncertainty and Sensitivity Analysis for Physical Processes. In *Proceedings of the 2008 International High-Level Radioactive Waste Management Conference, September 7-11, 2008*: American Nuclear Society, 2008:this volume.
19. SWIFT PN et al. Yucca Mountain 2008 Performance Assessment: Summary. In *Proceedings of the 2008 International High-Level Radioactive Waste Management Conference, September 7-11, 2008*: American Nuclear Society, 2008:this volume.

YUCCA MOUNTAIN 2008 PERFORMANCE ASSESSMENT: UNCERTAINTY AND SENSITIVITY ANALYSIS FOR PHYSICAL PROCESSES

C. J. Sallaberry, A. Aragon , A. Bier, Y. Chen, J.W. Groves, C.W. Hansen, J.C. Helton, S. Mehta, S.P. Miller, J. Min, P. Vo

Sandia National Laboratories, Albuquerque, NM 87185-0776, cnsalla@sandia.gov

The Total System Performance Assessment (TSPA) for the proposed high level radioactive waste repository at Yucca Mountain, Nevada, uses a sampling-based approach to uncertainty and sensitivity analysis. Specifically, Latin hypercube sampling is used to generate a mapping between epistemically uncertain analysis inputs and analysis outcomes of interest. This results in distributions that characterize the uncertainty in analysis outcomes. Further, the resultant mapping can be explored with sensitivity analysis procedures based on (i) examination of scatterplots, (ii) partial rank correlation coefficients, (iii) R^2 values and standardized rank regression coefficients obtained in stepwise rank regression analyses, and (iv) other analysis techniques. The TSPA considers over 300 epistemically uncertain inputs (e.g., corrosion properties, solubilities, retardations, defining parameters for Poisson processes, ….) and over 70 time-dependent analysis outcomes (e.g,, physical properties in waste packages and the engineered barrier system, releases from the engineered barrier system, the unsaturated zone and the saturated zone for individual radionuclides, and annual dose to the reasonably maximally exposed individual (RMEI) from both individual radionuclides and all radionuclides. The obtained uncertainty and sensitivity analysis results play an important role in facilitating understanding of analysis results, supporting analysis verification, establishing risk importance, and enhancing overall analysis credibility. The uncertainty and sensitivity analysis procedures are illustrated and explained with selected results for releases from the engineered barrier system, the unsaturated zone and the saturated zone and also for annual dose to the RMEI.

I. INTRODUCTION

The importance of an appropriate assessment of the uncertainty present in performance assessments (PAs) for the proposed Yucca Mountain (YM) repository for high-level radioactive waste has been strongly emphasized by the U.S. Nuclear Regulatory Commission (NRC) (e.g., Ref. 1, Quotes (NRC4) and (NRC5)). As a result, uncertainty analysis and sensitivity analysis are important parts of the 2008 total system performance assessment (TSPA) for the YM repository, where uncertainty analysis designates the determination of the uncertainty in analysis results that derives from uncertainty in a analysis inputs and sensitivity analysis designates the determination of the contributions of individual uncertain analysis inputs to the uncertainty in analysis results.

As described in a preceding paper[1] and in more detail in an extensive analysis report (Ref. 2, App. J), the conceptual structure and computational organization of the TSPA involves three basic entities: (EN1) a characterization of the uncertainty in the occurrence of future events that could affect the performance of the repository; (EN2) models for predicting the physical behavior and evolution of the repository; and (EN3) a characterization of the uncertainty associated with analysis inputs that have fixed but imprecisely known values. The designators aleatory and epistemic are commonly used for the uncertainties characterized by entities (EN1) and (EN3), respectively. Formally, (EN1) is defined by a probability space $(\mathcal{A}, \mathbb{A}, p_A)$ (Ref. 1, Sect. III); (EN2) corresponds to a very complex function that predicts the time-dependent behavior of many different physical properties associated with the evolution of the YM repository system (Ref. 2, Chap. 6; Refs. 3- 5); and (EN3) is defined by a probability space $(\mathcal{E}, \mathbb{E}, p_E)$ (Ref. 1, Sect. III).

In the context of the preceding entities, uncertainty analysis involves the determination of the uncertainty in predictions by the model that corresponds to (EN2) that derives from the uncertainty in analysis inputs characterized by the probability space $(\mathcal{E}, \mathbb{E}, p_E)$. Further, this determination is made for either (i) results conditional on the occurrence of specific futures contained in the set $\mathcal{A}$ (see Ref. 1, Table I) or (ii) expected results based on the probability space $(\mathcal{A}, \mathbb{A}, p_A)$ and obtained by integrating over the set $\mathcal{A}$ (see Ref. 1, Sect. IV). Similarly, sensitivity analysis involves the determination of the effects of individual variables contained in elements $\mathbf{e}$ of $\mathcal{E}$ (see Ref. 1, Table II) on results of the form just indicated.

The primary emphasis of this paper is on uncertainty and sensitivity analysis for results conditional on the occurrence of specific futures contained in the set $\mathcal{A}$. A

following presentation considers uncertainty and sensitivity analysis for expected results based on the probability space ($\mathcal{A}$, $\mathbb{A}$, p_A) and obtained by integrating over the set $\mathcal{A}$.[6]

II. UNCERTAINTY AND SENSITIVITY ANALYSIS

Conceptually, the component (EN2) of the TSPA can be represented by a function

$$\mathbf{y}(\tau \mid \mathbf{a}, \mathbf{e}) = \mathbf{f}(\tau \mid \mathbf{a}, \mathbf{e}), \tag{1}$$

where

$$\mathbf{a} = [a_1, a_2, ..., a_{nA}] \tag{2}$$

is an element (i.e., future) contained in $\mathcal{A}$ (see Ref. 1, Table I),

$$\mathbf{e} = [e_1, e_2, ..., e_{nE}] \tag{3}$$

is an element of $\mathcal{E}$ (see Ref. 1, Eq. (4) and Table II), and

$$\mathbf{y}(\tau \mid \mathbf{a}, \mathbf{e}) = [y_1(\tau \mid \mathbf{a}, \mathbf{e}), y_2(\tau \mid \mathbf{a}, \mathbf{e}), ..., y_{nY}(\tau \mid \mathbf{a}, \mathbf{e})] \tag{4}$$

is the value of the function $\mathbf{f}(\tau \mid \mathbf{a}, \mathbf{e})$ at time τ (see Ref. 2, Chap. 6, and Refs. 3-5). In general, the dimensions nA and nY of $\mathbf{a}$ and $\mathbf{y}(\tau \mid \mathbf{a}, \mathbf{e})$ can be quite large. Further, the dimension nE of $\mathbf{e}$ in the 2008 TSPA is 392; however, most elements of $\mathbf{y}(\tau \mid \mathbf{a}, \mathbf{e})$ are potentially affected by only a subset of the variables contained in $\mathbf{e}$. The elements of $\mathbf{y}(\tau \mid \mathbf{a}, \mathbf{e})$ include both physical properties of the YM system (e.g., temperature, pH, radionuclide release rates, …) and quantities involving dose to the reasonably maximally exposed individual (RMEI) (e.g., the doses $D_N(\tau \mid \mathbf{a}_N, \mathbf{e})$, $D_C(\tau \mid \mathbf{a}, \mathbf{e})$ and $D(\tau \mid \mathbf{a}, \mathbf{e})$ discussed in Sects. IV and V of Ref. 1 are elements of $\mathbf{y}(\tau \mid \mathbf{a}, \mathbf{e})$).

The uncertainty associated with $\mathbf{e}$ is characterized by a sequence of distributions

$$D_1, D_2, ..., D_{nE}, \tag{5}$$

where D_j is the distribution assigned to the element e_j of $\mathbf{e}$ (i.e., see the variables and distributions indicated in Table II of Ref. 1 and given in full in Tables K3-1, K3-2 and K3-3 of Ref. 2). Correlations and other restrictions are also assumed to exist between some variables. The distributions indicated in Eq. (5) and any associated restrictions characterize epistemic uncertainty and, in effect, define the probability space ($\mathcal{E}$, $\mathbb{E}$, p_E).

Latin hypercube sampling[7,8] is used to propagate the uncertainty characterized by the distributions indicated in Eq. (5) through the 2008 TSPA. Specifically, a Latin hypercube sample (LHS)

$$\mathbf{e}_i = \left[e_{i1}, e_{i2}, \cdots, e_{inE}\right], \quad i = 1, 2, \cdots, n, \tag{6}$$

of size n = 300 is generated from the possible values for $\mathbf{e}$ (i.e., form the set $\mathcal{E}$). Then, the function $\mathbf{f}(\tau \mid \mathbf{a}, \mathbf{e})$ is evaluated for each element $\mathbf{e}_i$ of the LHS indicated in Eq. (6). This creates a mapping

$$\left[\mathbf{e}_i, \mathbf{y}\left(\tau \middle| \mathbf{a}, \mathbf{e}_i\right)\right], \quad i = 1, 2, \cdots, n = 300, \tag{7}$$

from uncertain analysis inputs to uncertain analysis results. In practice, the indicated mapping is generated many times for different values of $\mathbf{a}$ for the calculation of each of the doses $D_C(\tau \mid \mathbf{a}, \mathbf{e})$ indicated in Table III of Ref. 1).

Once generated, the mapping in Eq. (7) provides the basis for both uncertainty analysis and sensitivity analysis. Specifically, each sample element has a weight (i.e., a probability in common but incorrect usage) of $1/n$ = 1/300 that can be used to construct cumulative distribution functions (CDFs) and complementary cumulative distribution functions (CCDFs) that summarize the uncertainty in analysis results. In addition, expected values (i.e., means) and various quantiles can also be obtained and used to summarize the uncertainty in analysis results. Or, most simply, the spread of the results obtained for individual elements of $\mathbf{y}(\tau \mid \mathbf{a}, \mathbf{e})$ can be presented.

Sensitivity analysis results can be obtained by exploring the mapping between analysis inputs and analysis results in Eq. (7) with a variety of procedures. The simplest is to examine scatterplots that graphically show the relationship between an element of $\mathbf{y}(\tau \mid \mathbf{a}, \mathbf{e})$ and individual elements of $\mathbf{e}$ (i.e., plots of points of the form [e_{ij}, $\mathbf{y}_k(\tau \mid \mathbf{a}, \mathbf{e}_i)$], i = 1, 2, …, n, for individual elements e_j and $\mathbf{y}_k(\tau \mid \mathbf{a}, \mathbf{e})$ of $\mathbf{e}$ and $\mathbf{y}(\tau \mid \mathbf{a}, \mathbf{e})$, respectively). More complex analyses involve the use of partial correlation coefficients (PCCs) and stepwise regression analyses to assess the relationships between analysis inputs and analysis results. With stepwise regression analysis, variable importance is indicated by the order of selection in the stepwise process, the incremental increase in R^2 values as variables are added to the regression model, and the standardized regression coefficients (SRCs) in the final regression model. A SRC provides a measure of the fraction of the uncertainty in an

analysis accounted for by a given analysis input; in contrast, a PCC provides a measure of the strength of the linear relationship between an analysis result and a given analysis input after the linear effects of all other analysis inputs have been removed. When nonlinear relationships are present, analyses are often performed with rank transformed data, which results in partial rank correlation coefficients (PRCCs) and standardized rank regression coefficients (SRRCs) rather than PCCs and SRCs.

Additional information on the sampling-based uncertainty and sensitivity analysis procedures used in the TSPA is available in a recent review article.[9]

III. NOMINAL SCENARIO CLASS $\mathcal{A}_N$

A large number of analysis results are considered in the uncertainty and sensitivity analyses for the nominal scenario class $\mathcal{A}_N$ (Table I). The variables indicated in Table I correspond to a subset of the variables $\mathbf{y}_k(\tau \mid \mathbf{a}, \mathbf{e})$ that comprise the elements of $\mathbf{y}(\tau \mid \mathbf{a}, \mathbf{e})$ in Eq. (4). Of these variables, the number of failed commercial spent nuclear fuel waste packages in percolation bin 3 (*NCSFL*) is used as an initial example for illustration (Fig. 1). The element $\mathbf{a}_N$ of $\mathcal{A}$ under consideration corresponds to the future in which no disruptions of any kind take place.

TABLE I. Examples of 11 of the 32 Time-Dependent Results Analyzed for the Nominal Scenario Class (Ref. 2, Table K4.1-1)

BACSFLAD : Average breached area (m^2) on failed CSNF WPs under dripping conditions (Ref. 2, Figures K.4.2-6, K.4.2-7)
DOSTOT: Dose to RMEI (mrem/yr) from all radioactive species (Ref. 2, Figures K4.5-1, K4.5-2, K4.5-3)
DSFLTM : Drip Shield failure time (yr) (Ref. 2, Figure K.4.2-1)
ISCSINAD : Ionic strength (molal) in the invert beneath the WP for CSNF WPs under dripping conditions (Ref. 2, Figures K.4.3-9, K.4.3-11)
NCDFL : Number of failed CDSP WPs (Ref. 2, Figure K.4.2-2)
NCSFL : Number of failed CSNF WPs (Ref. 2, Figures K.2-1, K.4.2-3)
NCSFLAD : Number of failed CSNF WPs under dripping conditions (Ref. 2, Figures K.4.2-4, K.4.2-5)
NCSFLND : Number of failed CSNF WPs under nondripping conditions (Ref. 2, Figures K.4.2-4, K.4.2-5)
PCO2CSIA : Partial pressure of CO_2 (bars) in the invert for CSNF WPs under dripping conditions (Ref. 2, Figures K.4.3-7, K.4.3-8)
PHCSINAD : pH in the invert beneath the WP for CSNF WPs under dripping conditions (Ref. 2, Figures K.4.3-12, K.4.3-13)
RHCDINV : Relative humidity for CDSP WPs in the invert beneath the WP (Ref. 2, Figure K.4.3-6)

The uncertainty in the time dependent values for *NCSFL* is shown by the 300 curves in Fig. 1a, with a single curve resulting for each of the LHS elements $\mathbf{e}_i$ in Eq. (6). Sensitivity analysis results based on PRCCs and stepwise rank regression are presented in Figs. 1b and 1c. In both analyses, the dominant variable with respect to the uncertainty in *NCSFL* is *WDGCA22* (see Table II for variable definitions), with *NCSFL* tending to decrease as *WDGCA22* increases. This effect results because of the role that increasing *WDGCA22* plays in decreasing the rate of general corrosion. The strong effect of *WDGCA22* on *NCSFL* can be seen in the scatterplot in Fig. 1d. After *WDGCA22*, a number of additional variables are identified as having small effects on *NCSFL*.

TABLE II. Variables Appearing in Sensitivity Analyses for *NCSFL* and *DOSTOT* in Figs. 1 and 2 (Ref. 2, Tables K3-1, K3-2, K3-3)

WDGCA22: Temperature dependent slope term of Alloy 22 general corrosion rate (K). *Distribution:* Truncated normal. *Range:* 666 to 7731. *Mean:* 4905. *Standard Deviation:* 1413.
WDZOLID : Deviation from median yield strength range for outer lid (dimensionless). *Distribution:* Truncated normal. *Range:* -3 to 3. *Mean:* 0. *Standard Deviation:* 1.
INFIL : Pointer variable for determining infiltration conditions: 10th, 30th, 50th or 90th percentile infiltration scenario (dimensionless). *Distribution:* Discrete. *Range:* 1 to 4.
THERMCON : Selector variable for one of three host-rock thermal conductivity scenarios (low, mean, and high) (dimensionless). *Distribution:* Discrete. *Range:* 1 to 3.
WDNSCC : Stress corrosion cracking growth rate exponent (repassivation slope) (dimensionless). *Distribution:* Truncated normal. *Range:* 0.935 to 1.395. *Mean:* 1.165. *Standard Deviation:* 0.115.
WDGCUA22: Variable for selecting distribution for general corrosion rate (low, medium, or high) (dimensionless). *Distribution:* Discrete. *Range:* 1 to 3.
SCCTHR : Stress threshold for stress corrosion cracking (MPa). *Distribution:* Uniform. *Range:* 315.9 to 368.55.

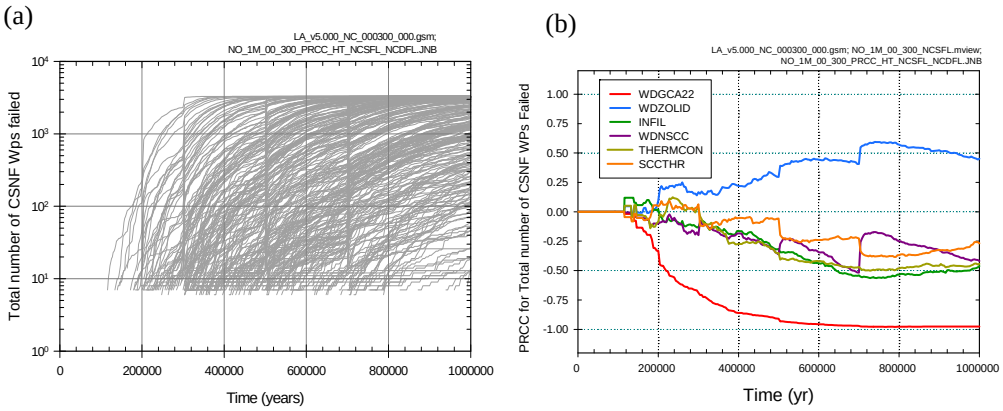

(c)

NCSFL: 1M yr		
Variable[a]	**R^2 [b]**	**SRRC[c]**
WDGCA22	0.91	-0.98
WDZOLID	0.92	0.10
INFIL	0.93	-0.12
THERMCON	0.94	-0.10
WDNSCC	0.95	-0.09
WDGCUA22	0.96	0.09
SCCTHR	0.96	-0.05

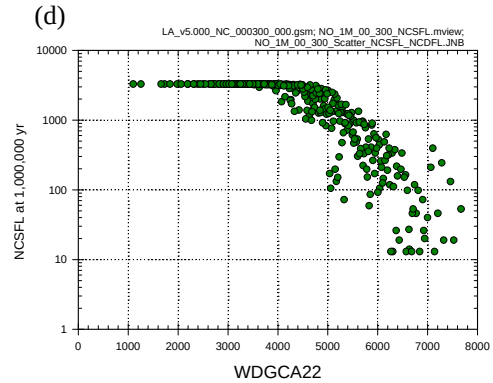

a: Variables listed in order of selection in stepwise regression
b: Cumulative R^2 value with entry of each variable into regression model
c: SRRCs in final regression model

Fig. 1. Uncertainty and sensitivity analysis results for *NCSFL*: (a) *NCSFL* for all (i.e., 300) sample elements, (b) PRCCs for *NCSFL*, (c) stepwise rank regression analysis for *NCSFL* at 10^6 yr, and (d) scatterplot for (*WDGCA22*, *NCSFL*) at 10^6 yr (Ref. 2, Fig. K2-1)

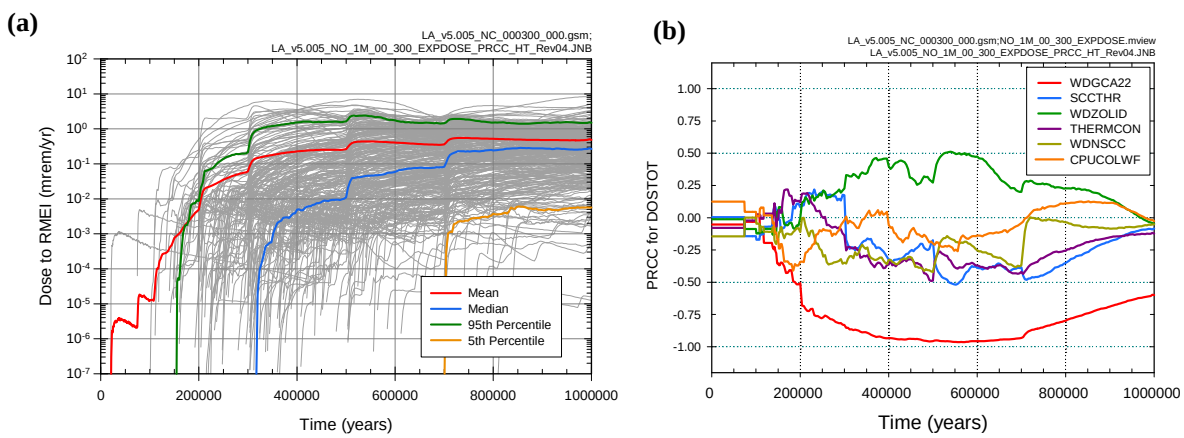

Fig. 2. Uncertainty and sensitivity analysis results for *DOSTOT* (i.e., for $D_N(\tau \mid \mathbf{a}_N, \mathbf{e}_M)$ as defined in Table III of Ref. 1): (a) *DOSTOT* for all (i.e., 300) sample elements, and (b) PRCCs for *DOSTOT* (Ref. 2, Fig. K4.5-1[a]).

As another example, analyses for dose from all radionuclides for the nominal scenario class $\mathcal{A}_N$ (i.e., $D_N(\tau|\mathbf{e}_M)$, or equivalently, *DOSTOT*) are presented in Fig. 2. The uncertainty in the time dependent values for *DOSTOT* is shown by the 300 curves in Fig. 2a, with a single curve resulting for each of the LHS elements $\mathbf{e}_i$ in Eq. (6). Sensitivity analysis results based on PRCCs are presented in Fig. 2b. The dominant variables with respect to the uncertainty in *DOSTOT* are *WDGCA22* and *WDZOLID* (see Table II for variable definitions), with

DOSTOT tending to decrease as *WDGCA22* increases and to increase as *WDZOLID* as increases. These effects result because increasing *WDGCA22* decreases WP failures due to general corrosion (see Fig. 1) and increasing *WDZOLID* increases corrosion-induced failures of welds at the WP lids.

Analyses similar to those presented in Figs. 1 and 2 were carried out for the nominal scenario class for all 32 analysis results indicated in Table I (Ref. 2, Sect. K4).

IV. IGNEOUS INTRUSIVE SCENARIO CLASS $\mathcal{A}_{II}$

As for the nominal scenario class, a large number of analysis results are considered in the uncertainty and sensitivity analyses for the igneous scenario class $\mathcal{A}_{II}$ (Table III). The variables indicated in Table III correspond to a subset of the variables $\mathbf{y}_k(\tau \mid \mathbf{a}, \mathbf{e})$ that comprise the elements of $\mathbf{y}(\tau \mid \mathbf{a}, \mathbf{e})$ in Eq. (4). As examples, this section considers the movement of ^{237}Np through the repository system and the dose to the RMEI that results from this movement. The specific element $\mathbf{a}$ of $\mathcal{A}$ under consideration corresponds to a single igneous intrusive event that occurs at 10 yr after repository closure and damages all waste packages in the repository, and the results selected for use are *ESNP237*, *UZNP237*, *SZNP237* and *DONP237* as defined in Table III.

TABLE III. Examples of 7 of the 49 Time-Dependent Results Analyzed for the Igneous Intrusive Scenario Class (Ref. 2, Table K6.1-1)

DONP237: Dose to RMEI (mrem/yr) from dissolved ^{237}Np (Ref. 2, Figures K.6.6.1-5, K.6.6.1-6, K.6.6.2-3)
ESNP237: Release rate (g/yr) for the movement of dissolved ^{237}Np from the EBS to the UZ (Ref. 2, Figures K.6.3.1-5, K.6.3.1-6, K.6.3.2-3)
ESNP237C : Cumulative release (g) for the movement of dissolved ^{237}Np from the EBS to the UZ (Ref. 2, Figures K.6.3.1-5, K.6.3.1-6, K.6.3.2-3, K.6.4.1-9)
SZNP237: Release rate (g/yr) for the movement of dissolved ^{237}Np across a subsurface plane at the location of the RMEI (Ref. 2, Figures K.6.5.1-7, K.6.5.1-8, K.6.5.2-3)
SZNP237C : Cumulative release (g) for the movement of dissolved ^{237}Np across a subsurface plane at the location of the RMEI (Ref. 2, Figures K.6.5.1-7, K.6.5.1-8, K.6.5.1-9, K.6.5.2-3)
UZNP237: Release rate (g/yr) for the movement of dissolved ^{237}Np from the UZ to the SZ (Ref. 2, Figures K.6.4.1-7, K.6.4.1-8)
UZNP237C : Cumulative release (g) for the movement of dissolved ^{237}Np from the UZ to the SZ (Ref. 2, Figures K.6.4.1-7, K.6.4.1-8, K.6.4.1-9, K.6.5.1-9)

The uncertainty in the time-dependent values for *ESNP237* and *UZNP237* are shown by the 300 curves in Figs. 3a and 3c, with a single curve resulting for each of the LHS elements $\mathbf{e}_i$ in Eq. (6). Sensitivity analysis results for *ESNP237* based on PRCCs are presented in Fig. 3b and indicate (i) positive effects for *EP1NPO2*, *INFIL*, *DELPPCO2* and *EP1LOWAM*, (ii) a negative effect for *PHCSS*, and (iii) a very early positive effect for *THERMCON* (see Table IV for variable definitions). The indicated effects result because (i) increasing *EP1NPO2* and *DELPPCO2* increases the solubility of neptunium, (ii) increasing *INFIL* increases water flow through the EBS, (iii) increasing *EP1LOWAM* increases the solubility of ^{241}Am, which is a parent of ^{237}Np, (iv) increasing *PHCSS* decreases the solubility of neptunium, and (v) increasing *THERMCON* decreases the time required for the repository to reach below-boiling temperatures for water and thereby facilitates early radionclide releases.

TABLE IV. Variables Appearing in Sensitivity Analyses for *ESNP237* and *SZNP237* in Figs. 3 and 4 (Ref. 2, Tables K3-1, K3-2, K3-3)

EP1NPO2: Logarithm of the scale factor used to characterize uncertainty in NpO_2 solubility at an ionic strength below 1 molal (dimensionless). *Distribution:* Truncated normal. *Range:* -1.2 to 1.2. *Mean:* 0. *Standard Deviation:* 0.6.
PHCSS: Pointer variable used to determine pH in CSNF Cell1 under liquid influx conditions (dimensionless). *Distribution:* Uniform. *Range:* 0 to 1.
THERMCON: Selector variable for one of three host-rock thermal conductivity scenarios (low, mean, and high) (dimensionless). *Distribution:* Discrete. *Range:* 1 to 3.
DELPPCO2: Selector variable for partial pressure of CO_2 (dimensionless). *Distribution:* Uniform. *Range:* -1 to 1.
INFIL: Pointer variable for determining infiltration conditions: 10th, 30th, 50th or 90th percentile infiltration scenario (dimensionless). *Distribution:* Discrete. *Range:* 1 to 4.
EP1LOWAM: Logarithm of the scale factor used to characterize uncertainty in americium solubility at an ionic strength below 1 molal (dimensionless). *Distribution:* Truncated normal. *Range:* -2 to 2. *Mean:* 0. *Standard Deviation:* 1.
SZGWSPDM: Logarithm of the scale factor used to characterize uncertainty in groundwater specific discharge (dimensionless). *Distribution:* Piecewise uniform. *Range:* -0.951 to 0.951.
SZFIPOVO: Logarithm of flowing interval porosity in volcanic units (dimensionless). *Distribution:* Piecewise uniform. *Range:* -5 to -1.

The similarity of the scatterplots of cumulative releases for *ESNP237C* and *UZNP237C* at 10^4 yr in Figures 3a and 3c suggest that processes in the unsaturated zone have little effect on the uncertainty in the movement of ^{237}Np. This is confirmed in the scatterplot in Fig. 3d. This means that the PRCCs for *UZNP237* are essentially the same as the PRCCs for *ESNP237*, and would have the same relationships as shown in Fig. 3b for the PRCCs for *ESPN237*

The uncertainty in the time dependent values for *SZNP237* and *DONP237* are shown by the 300 curves in Figs. 4a and 4c. Unlike the unsaturated zone, the saturated zone can have a significant effect on the movement of ^{237}Np to the location of the RMEI (Fig. 5).

Sensitivity analysis results for *ESNP237* based on PRCCs are presented in Fig. 4b and indicate (i) positive effects for *SZGWSDM*, *EP1NPO2* and *INFIL*, (ii) a negative effect for *PHCSS*, and (iii) an early positive effect *THERMCON* and a early negative effect for *SZFIPOVO* (see Table IV for variable definitions). The indicated effects for *EP1NPO2*, *INFIL* and *PHCSS* derive from their previously discussed effects on release from the EBS. The positive effect associated with *SZGWSDM* results from increasing water flow in the SZ, and the early negative effect associated with *SZFIPOVO* results from slowing the initial movement of released radionuclides in the SZ.

The comparison of *SZNP237* and *DONP237* at 10^4 yr in the scatterplot in Fig. 4d shows that the uncertainty in *SZNP237* dominates the uncertainty in *DONP237*. This means that the PRCCs for *DONP237* are essentially the same as the PRCCs for *SZNP237*, and would have the same relationships as shown in Fig. 3b for the PRCCs for *SZPN237*.

Analyses similar to those presented in Figs. 3-5 were carried out for all 49 results for the igneous scenario class indicated in Table III (Ref. 2, Sect. K6).

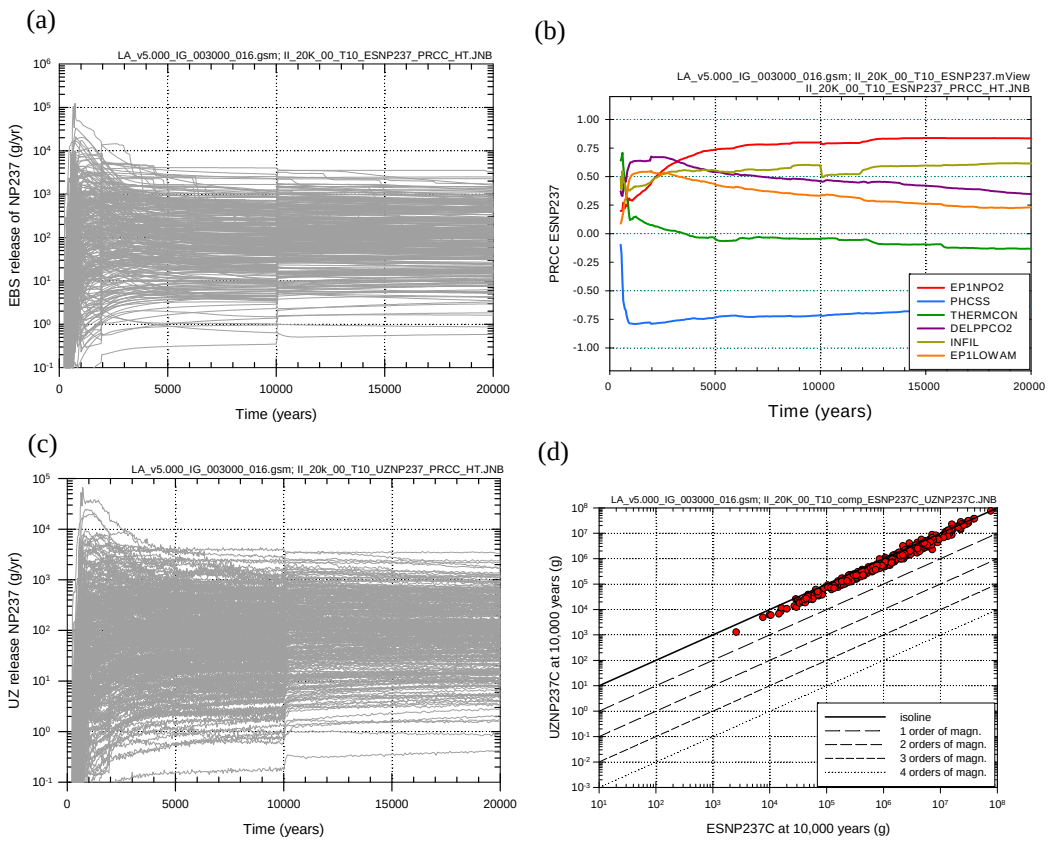

Fig. 3. Uncertainty and sensitivity analysis results for *ESNP237* and *UZNP237*: (a) *ESNP237* for all (i.e., 300) sample elements, (b) PRCCs for *ESNP237*, (c) *UZNP237* for all (i.e., 300) sample elements, and (d) scatterplot for (*ESNP237C*, *UZNP237C*) at 10^4 yr (Ref. 2, Figs. K6.3.1-5, K6.4.1-7, and K6.4.1-9)

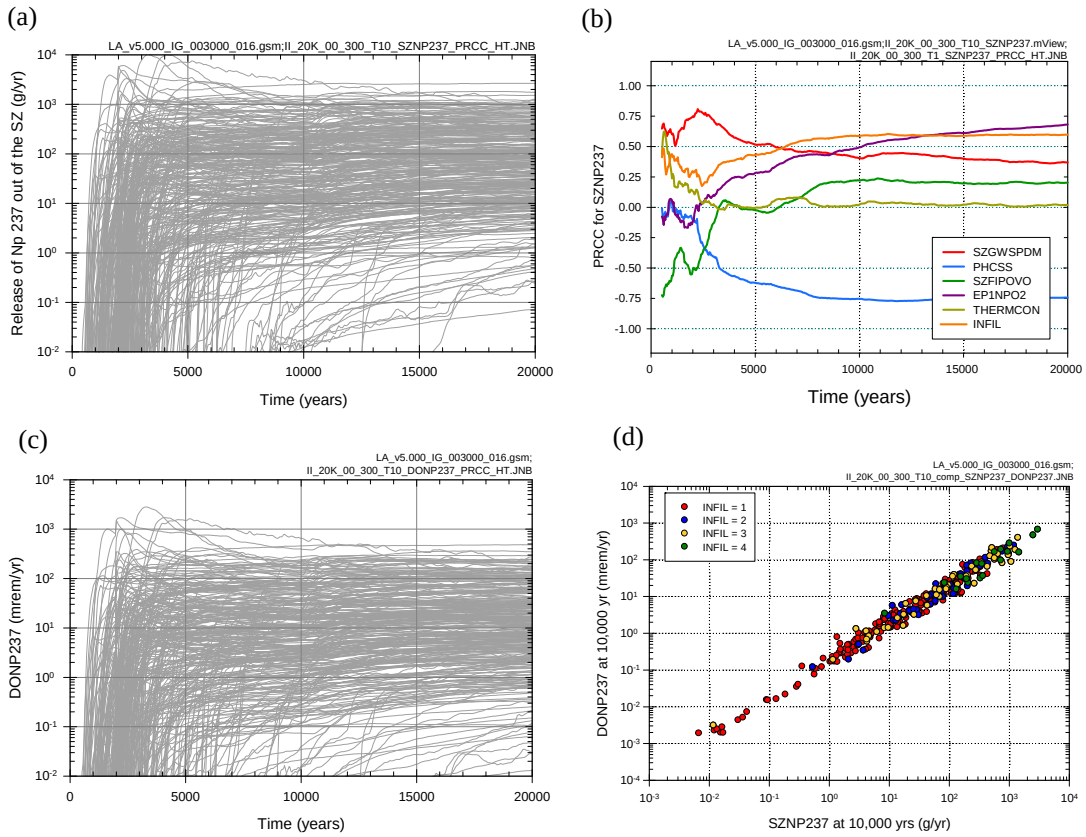

Fig. 4. Uncertainty and sensitivity analysis results for *SZNP237* and *DONP237*: (a) *SZNP237* for all (i.e., 300) sample elements, (b) PRCCs for *SZNP237*, (c) *DONP237* for all (i.e., 300) sample elements, and (d) scatterplot for (*SZNP237*, *DONP237*) at 10^4 yr (Ref. 2, Figs. K6.5.1-7, K6.6.1-5 and K6.6.1-6).

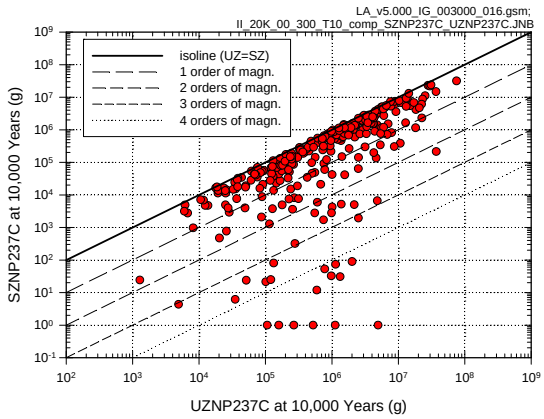

Fig. 5. Scatterplot for (*UZNP237C*, *SZNP237C*) at 10^4 yr (Ref. 2, Fig. K6.5.1-9).

V. ADDITIONAL SCENARIO CLASSES

Example uncertainty and sensitivity analysis results have been presented for the nominal scenario class $\mathcal{A}_N$ and the igneous intrusive scenario class $\mathcal{A}_{II}$. In addition, extensive uncertainty and sensitivity analyses were also carried out as part of the TSPA for the early waste package failure scenario class $\mathcal{A}_{EW}$, the early drip shield failure scenario class $\mathcal{A}_{ED}$, the igneous eruptive scenario class $\mathcal{A}_{IE}$, the seismic ground motion scenario class $\mathcal{A}_{SG}$, and the seismic fault displacement scenario class $\mathcal{A}_{SF}$. In performing these analyses, two different time periods were considered for the definition of the sample space $\mathcal{A}$ for aleatory uncertainty: $[0, 2\times10^4$ yr] and [0, 10^6 yr]. The results of these analyses are given in Apps. J and K of Ref. 2.

VI. SUMMARY

The importance of an appropriate assessment of the uncertainty present in PAs for the proposed YM repository for high-level radioactive waste has been strongly emphasized by the NRC (e.g., see Ref. 1, Quotes (NRC4) and (NRC5)). In response, extensive sampling-based uncertainty and sensitivity analyses have been carried out as part of the 2008 TSPA.

The performance of these uncertainty and sensitivity analyses has a number of benefits, including: (i) permitting analysts to objectively assess the uncertainty present in the models that they developed and/or use, (ii) providing a rigorously derived assessment of the uncertainty present in analysis results, (iii) providing insights into the relationships between uncertainty in individual analysis inputs and the uncertainty in analysis results, (iv) extensively exercising the models in use and thereby contributing to analysis verification, (v) aiding decision makers by explicitly representing the uncertainty in the results that underlie their decisions, and (vi) enhancing the overall credibility of the analysis.

A following paper provides additional uncertainty and sensitivity analysis results involving expected dose to the RMEI.[6] Further, full details of the uncertainty and sensitivity analyses performed as part of the 2008 TSPA are presented in Apps. J and K of Ref. 2.

ACKNOWLEDGMENTS

Work performed at Sandia National Laboratories (SNL), which is a multiprogram laboratory operated by Sandia Corporation, a Lockheed Martin Company, for the U.S. Department of Energy's (DOE's) National Nuclear Security Administration under Contract No. DE-AC04-94AL85000. The United States Government retains and the publisher, by accepting this article for publication, acknowledges that the United States Government retains a non-exclusive, paid-up, irrevocable, world-wide license to publish or reproduce the published form of this article, or allow others to do so, for United States Government purposes. The views expressed in this article are those of the authors and do not necessarily reflect the views or policies of DOE or SNL.

REFERENCES

1. HELTON JC et al. Yucca Mountain 2008 Performance Assessment: Conceptual Structure and Computational Implementation. In *Proceedings of the 2008 International High-Level Radioactive Waste Management Conference, September 7-11, 2008*: American Nuclear Society, 2008:this volume.
2. SANDIA NATIONAL LABORATORIES. *Total System Performance Assessment Model/Analysis for the License Application*.MDL-WIS-PA-000005 REV00, Vols. AD 01.Albuquerque, NM: Sandia National Laboratories 2008.
3. MACKINNON RJ et al. Yucca Mountain 2008 Performance Assessment: Modeling the Engineered Barrier System. In *Proceedings of the 2008 International High-Level Radioactive Waste Management Conference, September 7-11, 2008*: American Nuclear Society, 2008:this volume.
4. MATTIE PD et al. Yucca Mountain 2008 Performance Assessment: Modeling the Natural System. In *Proceedings of the 2008 International High-Level Radioactive Waste Management Conference, September 7-11, 2008*: American Nuclear Society, 2008:this volume.
5. SEVOUGIAN SD et al. Yucca Mountain 2008 Performance Assessment: Modeling Disruptive Events and Early Failures. In *Proceedings of the 2008 International High-Level Radioactive Waste Management Conference, September 7-11, 2008*: American Nuclear Society, 2008:this volume.
6. HANSEN CW et al. Yucca Mountain 2008 Performance Assessment: Uncertainty and Sensitivity Analysis for Expected Dose. In *Proceedings of the 2008 International High-Level Radioactive Waste Management Conference, September 7-11, 2008*: American Nuclear Society, 2008:this volume.
7. HELTON JC, DAVIS FJ. Latin Hypercube Sampling and the Propagation of Uncertainty in Analyses of Complex Systems. *Reliability Engineering and System Safety* 2003;81(1):23-69.
8. MCKAY MD et al. A Comparison of Three Methods for Selecting Values of Input Variables in the Analysis of Output from a Computer Code. *Technometrics* 1979;21(2):239-245.
9. HELTON JC et al. Survey of Sampling-Based Methods for Uncertainty and Sensitivity Analysis. *Reliability Engineering and System Safety* 2006;91(10-11):1175-1209.

YUCCA MOUNTAIN 2008 PERFORMANCE ASSESSMENT: UNCERTAINTY AND SENSITIVITY ANALYSIS FOR EXPECTED DOSE

C.W. Hansen[1], K. Brooks[2], J.W. Groves[3], J.C. Helton[1], K.P. Lee[4], C.J. Sallaberry[1], W. Statham[4], C. Thom[5]
[1]*Sandia National Laboratories, Albuquerque, NM 87185-0776, cwhanse@sandia.gov*
[2]*Sala & Associates, Inc.,* [3]*INTERA,* [4]*Areva Federal Services, LLC,* [5]*Beckman & Associates, Inc*

Uncertainty and sensitivity analyses of the expected dose to the reasonably maximally exposed individual in the Yucca Mountain 2008 total system performance assessment (TSPA) are presented. Uncertainty results are obtained with Latin hypercube sampling of epistemic uncertain inputs, and partial rank correlation coefficients are used to illustrate sensitivity analysis results.

I. INTRODUCTION

A core requirement in 10 CFR Part 63 and the proposed standard for post-10,000 years for the proposed Yucca Mountain (YM) repository for high level radioactive waste is that the mean dose to the reasonably maximally exposed individual (RMEI) is to be less than 15 mrem/yr for the time period [0, 10^4 yr] after repository closure and also that the median dose to the RMEI is to be less than 350 mrem/yr for the time period [10^4, 10^6 yr] after repository closure.[1,2]

In the 2008 total system performance assessment (TSPA) for the proposed YM repository, the indicated mean and median doses are obtained by first calculating a distribution of time-dependent expected doses that result from aleatory uncertainty (i.e., the perceived randomness of future occurrences such as early waste package and drip shield failures, igneous events, seismic events). Then, the desired mean and median doses are obtained from the distribution of time-dependent expected doses.[3]

Specifically, a Latin hypercube sample (LHS) $\mathbf{e}_1$, $\mathbf{e}_2$, …, $\mathbf{e}_{nLHS}$ of size $nLHS$ = 300 was generated from the epistemically uncertain analysis inputs chosen for consideration. Next, a time-dependent expected dose $\bar{D}(\tau \mid \mathbf{e}_i)$ was determined for each of the 300 LHS elements, with each time-dependent expected dose deriving from integration over the possible realizations of aleatory uncertainty (i.e., numbers and properties of early waste package and early drip shield failures, numbers and properties of igneous events, numbers and properties of seismic events). Additionally, the time-dependent dose for nominal conditions (i.e., futures in which no early failures, seismic or igneous events occur) is also computed. Thus, expected doses $\bar{D}_C(\tau \mid \mathbf{e}_i)$ were calculated individually for the following six scenario classes (also termed modeling cases when implemented in the YM 2008 TSPA model): (i) $\bar{D}_{EW}(\tau \mid \mathbf{e}_i)$ with $C = EW$ for the early waste package (WP) failure scenario class $\mathcal{A}_{EW}$, (ii) $\bar{D}_{ED}(\tau \mid \mathbf{e}_i)$ with $C=ED$ for the early drip shield (DS) failure scenario class $\mathcal{A}_{ED}$, (iii) $\bar{D}_{II}(\tau \mid \mathbf{e}_i)$ with $C=II$ for the igneous intrusive scenario class $\mathcal{A}_{II}$, (iv) $\bar{D}_{IE}(\tau \mid \mathbf{e}_i)$ with $C=IE$ for the igneous eruptive scenario class $\mathcal{A}_{IE}$, (v) $\bar{D}_{SG}(\tau \mid \mathbf{e}_i)$ with $C=SG$ for the seismic ground motion scenario class $\mathcal{A}_{SG}$, and (vi) $\bar{D}_{SF}(\tau \mid \mathbf{e}_i)$ with $C=SF$ for the seismic fault displacement scenario class $\mathcal{A}_{SF}$, as well as (vii) $D_N(\tau \mid \mathbf{e}_i)$ with $C=N$ for the nominal scenario class $\mathcal{A}_N$ (see Ref. 3, Table I, for formal definitions of the individual scenario classes). The quantities $\bar{D}_C(\tau \mid \mathbf{e}_i)$ are incremental expected doses that result solely from the effects associated with the corresponding scenario class $\mathcal{A}_C$; thus, summing the preceding seven time-dependent expected doses for corresponding LHS elements produces $\bar{D}(\tau \mid \mathbf{e}_i)$ (see Ref. 3, Sect. V and Table III, for additional discussion).

Finally, the mean dose $\bar{\bar{D}}(\tau)$ was approximated by the point-wise vertical average of the 300 time-dependent expected dose curves $\bar{D}(\tau \mid \mathbf{e}_i)$, and the median dose $Q_{E,0.5}[\,\bar{D}(\tau \mid \mathbf{e})\,]$ was defined analogously as the point-wise median of the expected dose curves. (Ref. 3, Sect. V). Thus, the mean dose curve $\bar{\bar{D}}(\tau)$ is an expectation over the epistemic uncertainty in expected dose, and the median dose curve $Q_{E,0.5}[\,\bar{D}(\tau \mid \mathbf{e})\,]$ is a median over the epistemic uncertainty in expected dose. The mean and median doses are compared against the current and proposed NRC standards for the [0, 10^4 yr] and [10^4, 10^6 yr] time periods, respectively.[1,2]

Uncertainty and sensitivity analysis results for expected dose and associated analysis insights are presented and discussed. Specifically, results are first presented for the individual scenario classes. Then, the outcome of summing the results for the individual scenario classes is presented. Results presented herein are derived from calculations performed separately for the [0,

10^4 yr] and [0, 10^6 yr] time periods with the YM 2008 TSPA model.[4] This presentation provides results for each scenario class (except for the nominal scenario class) for the time period [0, 2×10^4 yr], as well as for the summation over scenario classes for both time periods. For the nominal scenario class, the dose to the RMEI for the time period [0, 2×10^4 yr] is identically zero; results for the time period [0, 10^6 yr] are presented elsewhere.[5] Uncertainty results for scenario classes important in the time period [0, 10^6 yr] are also presented elsewhere.[6,7] Sensitivity analysis techniques employed herein are similar to those employed in analysis of physical processes simulated in the YM 2008 TSPA model.[5]

II. CONCEPTUAL BASIS

As described in a related paper[3] and in more detail in an extensive analysis report[4], the conceptual structure and computational organization of the YM 2008 TSPA involves three basic entities: (EN1) a characterization of the uncertainty in the occurrence of future events that could affect the performance of the repository; (EN2) models for predicting the physical behavior and evolution of the repository; and (EN3) a characterization of the uncertainty associated with analysis inputs that have fixed but imprecisely known values. The designators aleatory and epistemic are commonly used for the uncertainties characterized by entities (EN1) and (EN3), respectively. Formally, (EN1) is defined by a probability space ($\mathcal{A}$, $\mathbb{A}$, p_A) (Ref. 3, Sect. III); (EN2) corresponds to a very complex function that predicts the time-dependent behavior of many different physical properties associated with the evolution of the YM repository system;[4,7,8,9] and (EN3) is defined by a probability space ($\mathcal{E}$, $\mathbb{E}$, p_E) (Ref.3, Sect. III).

In the context of this presentation, (EN2) corresponds to the functions $D(\tau\,|\,\mathbf{a},\mathbf{e})$ and $D_C(\tau\,|\,\mathbf{a},\mathbf{e})$ for C = *EW*, *ED*, *II*, *IE*, *SG* and *SF* that define dose to the RMEI at time τ conditional on elements $\mathbf{a}$ and $\mathbf{e}$ of $\mathcal{A}$ and $\mathcal{E}$, respectively. Specifically, $D(\tau\,|\,\mathbf{a},\mathbf{e})$ is the incremental expected dose to the RMEI at time τ from all disruptions associated with $\mathbf{a}$, and $D_C(\tau\,|\,\mathbf{a},\mathbf{e})$ is the incremental expected dose to the RMEI at time τ that derives only from the disruptions associated with $\mathbf{a}$ that are also associated with the scenario class designated by C.

In turn, $\bar{D}(\tau\,|\,\mathbf{e})$ and $\bar{D}_C(\tau\,|\,\mathbf{e})$ are defined by integrals of $D(\tau\,|\,\mathbf{a},\mathbf{e})$ and $D_C(\tau\,|\,\mathbf{a},\mathbf{e})$ over $\mathcal{A}$ conditional on the element $\mathbf{e}$ of $\mathcal{E}$ (Ref. 3, Sect. IV). Similarly, the mean $\bar{\bar{D}}(\tau)$, the q quantile $Q_{E,q}[\,\bar{D}(\tau\,|\,\mathbf{e})\,]$ (e.g., q = 0.05, 0.5, 0.95) and the median $Q_{E,0.5}[\,\bar{D}(\tau\,|\,\mathbf{e})\,]$ (i.e., q = 0.5) are defined by integrals over $\mathcal{E}$. Corresponding results $\bar{\bar{D}}_C(\tau)$, $Q_{E,q}[\,\bar{D}_C(\tau\,|\,\mathbf{e})\,]$ and $Q_{E,0.5}[\,\bar{D}_C(\tau\,|\,\mathbf{e})\,]$ for individual scenario classes are defined in the same manner.

III. EARLY FAILURE SCENARIO CLASSES

As indicated in Sects. I and II, the YM 2008 TSPA considers two early failure scenario classes: the early drip shield (DS) failure scenario class $\mathcal{A}_{ED}$ and the early waste package (WP) failure scenario class $\mathcal{A}_{EW}$. The occurrence of early DS failures and early WP failures are modeled with binomial probability distributions with defining parameters *PROBDSEF* and *PROBWPEF* (see Table I). The individual DS failure probability *PROBDSEF* applies to all DSs in the repository. Similarly, the individual WP failure probability *PROBWPEF* applies to all WPs in the repository. As modeled, early failures of DSs and WPs occur at repository closure. However, transport of radionuclides from the affected WPs depends on environmental conditions such as the relative humidity in the affected WPs, or the presence of drift seepage.[8]

The time-dependent expected doses to the RMEI from early DS failure, $\bar{D}_{ED}(\tau\,|\,\mathbf{e}_i)$, and from early WP failure, $\bar{D}_{EW}(\tau\,|\,\mathbf{e}_i)$, for the individual LHS elements $\mathbf{e}_i$, i = 1, 2, …, 300, are shown in Figs. 1a and 1c. Fig. 1c shows that expected dose to the RMEI from early-failed WPs begins within the first 2,000 years, followed by increases in $\bar{D}_{EW}(\tau\,|\,\mathbf{e}_i)$ starting at approximately 10^4 yr. These increases correspond to the arrival of radionuclides from early-failed commercial spent nuclear fuel WPs. Because commercial spent nuclear fuel WPs are in general hotter than co-disposed WPs, formation of continuous liquid pathways occurs later,[8] delaying release of radionuclides from commercial spent nuclear fuel WPs.

As shown by the spread of the individual curves, considerable uncertainty exists with respect to the values for $\bar{D}_{ED}(\tau\,|\,\mathbf{e}_i)$ and $\bar{D}_{EW}(\tau\,|\,\mathbf{e}_i)$. Sensitivity analyses for $\bar{D}_{ED}(\tau\,|\,\mathbf{e}_i)$ and $\bar{D}_{EW}(\tau\,|\,\mathbf{e}_i)$ based on partial rank correlation coefficients (PRRCs); (see Ref. 5, Sect. II) are presented in Figs. 1b and 1d (see Table I for definitions of individual variables). The dominant variables with respect to the uncertainty in $\bar{D}_{EW}(\tau\,|\,\mathbf{e})$ and $\bar{D}_{ED}(\tau\,|\,\mathbf{e})$ are *PROBWPEF* and *PROBDSEF*, respectively, with $\bar{D}_{EW}(\tau\,|\,\mathbf{e})$ and $\bar{D}_{ED}(\tau\,|\,\mathbf{e})$ increasing as *PROBWPEF* and *PROBDSEF* increase, because the expected number of early failures increase. After *PROBWPEF* and *PROBDSEF*, the PRCCs indicate smaller effects for a number of additional variables that influence the movement of water through the natural barriers of the repository system.

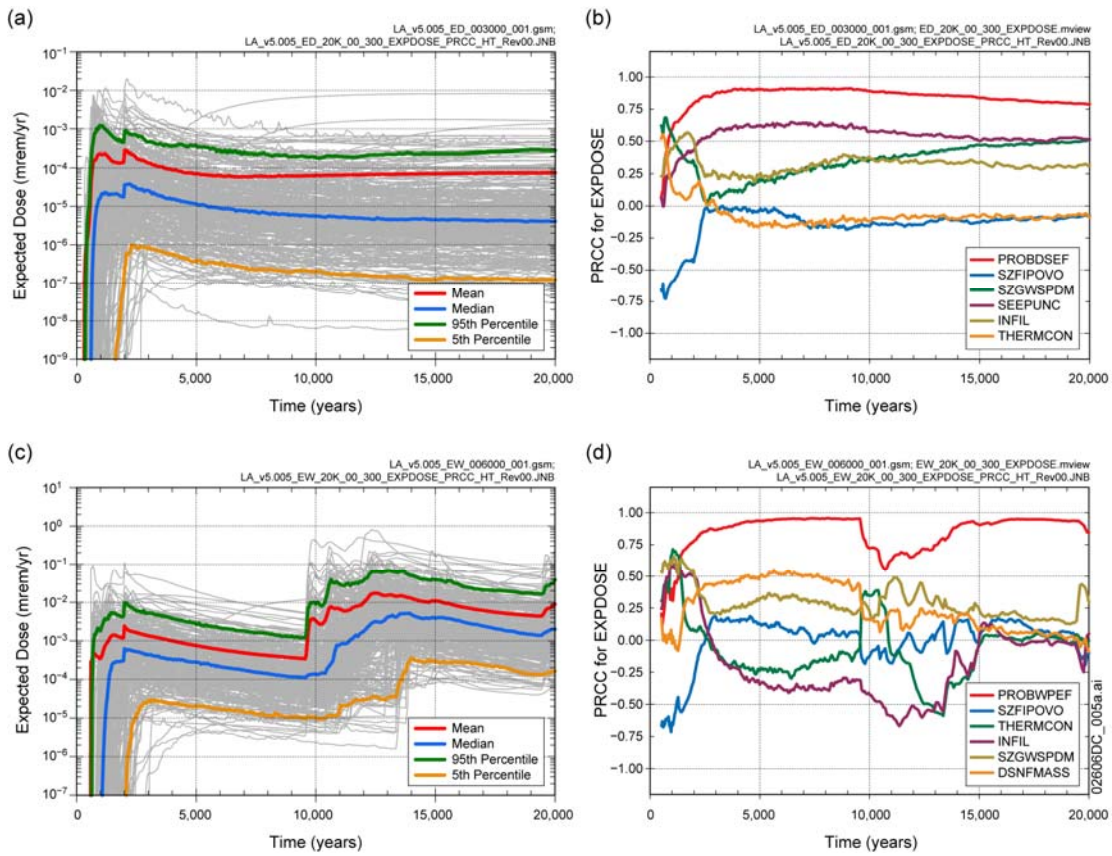

Fig. 1. Expected dose to RMEI (mrem/yr) over $[0, 2\times10^4$ yr] for all radioactive species resulting from early failures: (a, b) $\bar{D}_{ED}(\tau\,|\,\mathbf{e})$ and associated PRCCs for early DS failure (Ref. 3, Fig. K5.7.1-1[a]), and (c, d) $\bar{D}_{EW}(\tau\,|\,\mathbf{e})$ and associated PRCCs for early WP failure (Ref. 4, Fig. K5.7.2-1[a]).

IV. IGNEOUS SCENARIO CLASSES

Two igneous scenario classes are considered in the YM 2008 TSPA: the igneous intrusion scenario class $\mathcal{A}_{II}$ and the igneous eruptive scenario class $\mathcal{A}_{IE}$. The occurrence of igneous intrusion events and igneous eruptive events are modeled by Poisson processes with rates defined by *IGRATE* and *IGERATE* (See Table I). Further, an igneous intrusion event is assumed to destroy all WPs in the repository, and an igneous eruptive event ejects the contents of a small number of WPs into the atmosphere.[7] The time-dependent expected doses to the RMEI from igneous intrusions, $\bar{D}_{II}(\tau\,|\,\mathbf{e}_i)$, and from igneous eruptions, $\bar{D}_{IE}(\tau\,|\,\mathbf{e}_i)$, for the individual LHS elements $\mathbf{e}_i$, i = 1, 2, …, 300, are shown in Figs. 2a and 2c. The smoothness evident in these curves results from the use of quadrature procedures in the evaluation of expected dose.[3] As shown by the spread of the individual curves, considerable uncertainty exists with respect to the values for $\bar{D}_{II}(\tau\,|\,\mathbf{e}_i)$ and $\bar{D}_{IE}(\tau\,|\,\mathbf{e}_i)$. Sensitivity analyses for $\bar{D}_{II}(\tau\,|\,\mathbf{e}_i)$ and $\bar{D}_{IE}(\tau\,|\,\mathbf{e}_i)$ based on PRRCs are presented in Figs. 2b and 2d (see Table I for definitions of individual variables). The dominant variables with respect to the uncertainty in $\bar{D}_{II}(\tau\,|\,\mathbf{e}_i)$ and $\bar{D}_{IE}(\tau\,|\,\mathbf{e}_i)$ are the occurrence rates *IGRATE* and *IGERATE*, respectively, with $\bar{D}_{II}(\tau\,|\,\mathbf{e})$ and $\bar{D}_{IE}(\tau\,|\,\mathbf{e})$ increasing as *IGRATE* and *IGERATE* increase.

The physical processes associated with igneous intrusive events and igneous eruptive events that result in dose to the RMEI are very different.[7] As a result, the variables selected after *IGRATE* and *IGERATE* in Figs. 2b and 2d are very different. Specifically, analysis for $\bar{D}_{II}(\tau\,|\,\mathbf{e})$ in Fig. 2b indicates effects for variables that influence the movement of water through the natural system (*SZGWSPDM*, *INFIL*, *SZFIPOVO* and *SZCOLRAL*) and the contribution of ^{99}Tc to dose to the RMEI (*MICTC99*). The analysis for $\bar{D}_{IE}(\tau\,|\,\mathbf{e})$ in Fig. 2d indicates effects for variables related to the uncertainty in dose to the RMEI by inhalation of contaminated particles (*INHLTPV*), the diffusion of radionuclides downward out of surface soils (*DDIVIDE*), the mass of radionuclides in waste packages (*CSNFMASS*), and the attachment of waste particles to ash particles (*DASHAVG*).

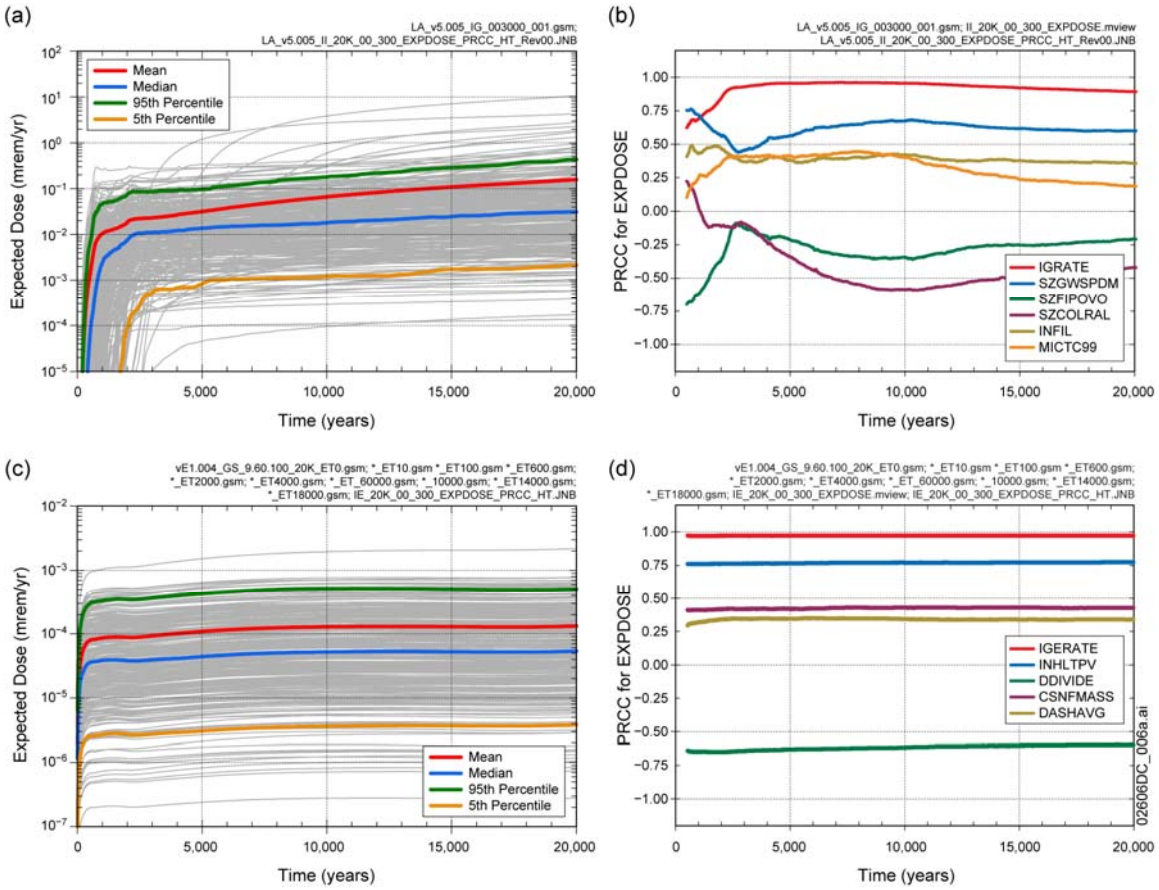

Fig. 2. Expected dose to RMEI (mrem/yr) over $[0, 2\times10^4$ yr] for all radioactive species resulting from igneous events: (a, b) $\bar{D}_{II}(\tau\,|\,\mathbf{e})$ and associated PRCCs for igneous intrusive events (Ref. 3, Fig. K6.7.1-1[a]), and (c, d) $\bar{D}_{IE}(\tau\,|\,\mathbf{e})$ and associated PRCCs for early igneous eruptive events (Ref. 4, Fig. K6.8.1-1).

V. SEISMIC SCENARIO CLASSES

Two seismic scenario classes are considered in the YM 2008 TSPA: the seismic ground motion scenario class $\mathcal{A}_{SG}$ and the seismic fault displacement scenario class $\mathcal{A}_{SF}$. The occurrence of seismic ground motion events and seismic fault displacement events are modeled as Poisson processes defined by underlying hazard curves that define the annual frequencies of seismic ground motion events and seismic fault displacement events of different sizes.[7] A seismic ground motion event that damages WPs is assumed to cause the same damage to all WPs in the repository; in contrast, a seismic fault displacement event damages a relatively small number of WPs.

The time-dependent expected doses to the RMEI from seismic ground motion events, $\bar{D}_{SG}(\tau\,|\,\mathbf{e}_i)$, and from seismic fault displacement events, $\bar{D}_{SF}(\tau\,|\,\mathbf{e}_i)$, for the individual LHS elements $\mathbf{e}_i$, i = 1, 2, …, 300, are shown in Figs. 3a and 3c. The spread of the individual curves shows considerable uncertainty exists with respect to the values for $\bar{D}_{SG}(\tau\,|\,\mathbf{e}_i)$ and $\bar{D}_{SF}(\tau\,|\,\mathbf{e}_i)$. Sensitivity analyses for $\bar{D}_{SG}(\tau\,|\,\mathbf{e})$ and $\bar{D}_{SF}(\tau\,|\,\mathbf{e}_i)$ based on PRRCs are presented in Figs. 3b and 3d (see Table I for definitions of individual variables). The dominant variable with respect to the uncertainty in $\bar{D}_{SG}(\tau\,|\,\mathbf{e})$ is *SCCTHRP*, with $\bar{D}_{SG}(\tau\,|\,\mathbf{e})$ decreasing as *SCCTHRP* increases. The strong effect associated with *SCCTHRP* results because *SCCTHRP* defines the residual stress level at which WPs are considered to be damaged by seismically-induced impacts. The YM 2008 TSPA uses a mean hazard curve to define the annual frequencies of seismic ground motion events of different magnitudes, thus no variable related to the occurrence of seismic events is present in the sensitivity analysis. After *SCCTHRP*, the analyses for $\bar{D}_{SG}(\tau\,|\,\mathbf{e})$ indicates effects for variables that influence movement of water through the natural system (*SZFIPOVO*, *SZGWSPDM*, and

INFIL), the mass of radionuclides in the disposed waste (*DSNFMASS*) and the contribution of ^{99}Tc to dose to the RMEI (*MICTC99*).

For $\bar{D}_{SF}(\tau \mid \mathbf{e}_i)$, effects are indicated for variables related to the movement of water through the natural system (*SZGWSPDM*, *INFIL*, *SEEPUNC*, *SZFIPOVO* and *SEEPPRM*) and the contribution of ^{99}Tc to dose to the RMEI (*MICTC99*). However, unlike the analysis for $\bar{D}_{SG}(\tau \mid \mathbf{e})$, no single variable dominates the uncertainty in $\bar{D}_{SF}(\tau \mid \mathbf{e}_i)$.

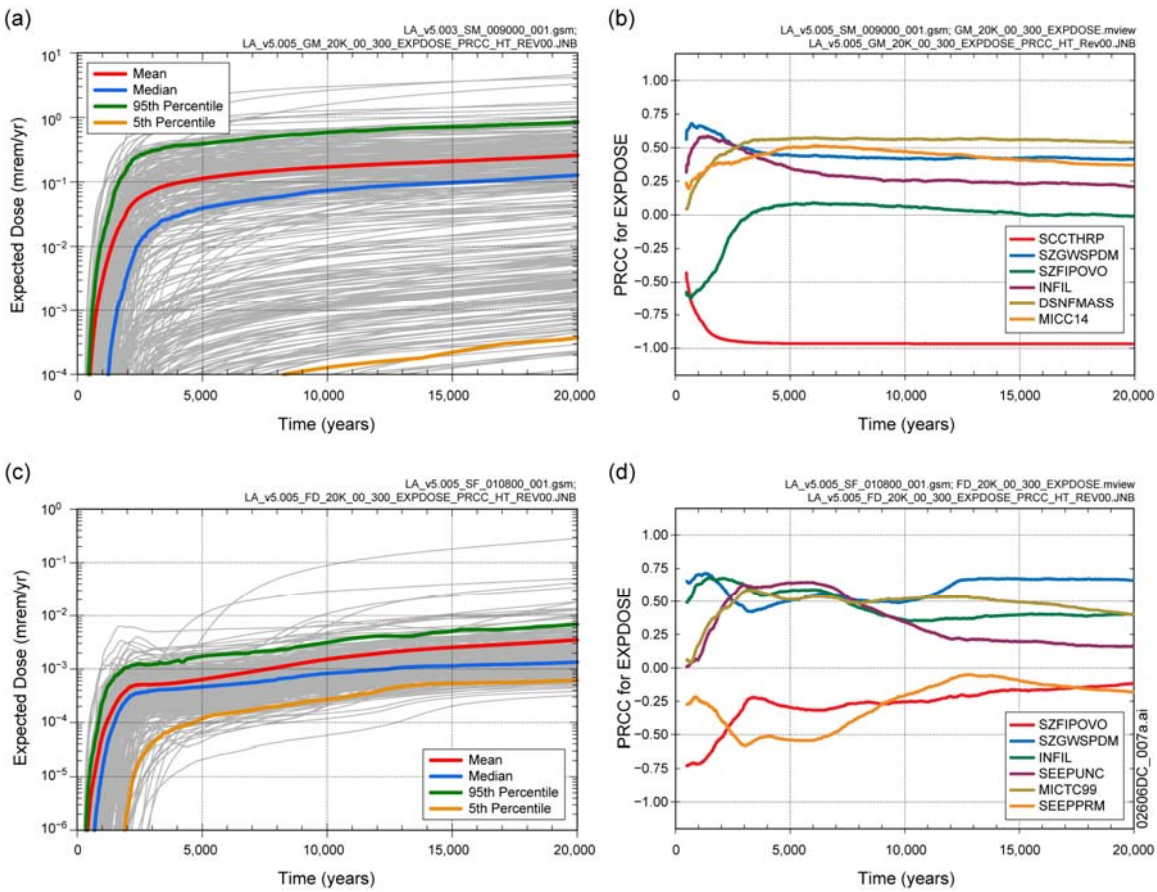

Fig. 3. Expected dose to RMEI (mrem/yr) over $[0, 2\times10^4$ yr] for all radioactive species resulting from seismic events: (a, b) $\bar{D}_{SG}(\tau \mid \mathbf{e}_i)$ and associated PRCCs for seismic ground motion events (Ref. 3, Fig. K7.7.1-1[a]), and (c, d) $\bar{D}_{SF}(\tau \mid \mathbf{e}_i)$ and associated PRCCs for seismic fault displacement events (Ref. 4, Fig. K7.8.1-1[a]).

VI. ALL SCENARIO CLASSES

Expected dose results for individual scenario classes are presented in Sects. III-V. As discussed in Section I, the total expected dose $\bar{D}(\tau \mid \mathbf{e})$ for all scenario classes results from adding the incremental expected doses for the individual scenario classes. Specifically, the total expected doses $\bar{D}(\tau \mid \mathbf{e}_i)$ in Fig. 4a for the time period $[0, 2\times10^4$ yr] result from adding the expected doses in Figs. 1-3 for corresponding LHS elements $\mathbf{e}_i$, i = 1, 2, …, 300. Similarly, the total expected doses $\bar{D}(\tau \mid \mathbf{e}_i)$ in Fig. 4c for the time period [0,10^6 yr] result from adding the expected doses for the individual scenario classes for this time period. Additional detail is provided in an extensive analysis report.[4]

In turn, the total expected doses $\bar{D}(\tau \mid \mathbf{e}_i)$ in Figs. 4a and 4c can be used to estimate mean doses $\bar{\bar{D}}(\tau)$ over aleatory and epistemic uncertainty and quantiles $Q_{Eq}[\bar{D}(\tau \mid \mathbf{e})]$ (e.g., q = 0.05, 0.5, 0.95) for $\bar{D}(\tau \mid \mathbf{e})$ that derive from epistemic uncertainty. Values for $\bar{\bar{D}}(\tau)$ and $Q_{Eq}[\bar{D}(\tau \mid \mathbf{e})]$, q = 0.05, 0.5, 0.95, are shown in Figs. 4a and 4b. The YM 2008 TSPA uses the mean dose $\bar{\bar{D}}(\tau)$ in

comparisons with the 15 mrem/yr dose standard specified by the NRC for the time period $[0,10^4 \text{ yr}]$ [1] and uses the median expected dose $Q_{E,0.5}[\bar{D}(\tau \mid \mathbf{e})]$ in comparisons with the 350 mrem/yr dose standard proposed by the NRC for the time period $[0,10^6 \text{ yr}]$.[2]

The total expected dose $\bar{D}(\tau \mid \mathbf{e})$ for the time period $[0, 2\times10^4 \text{ yr}]$ is primarily determined by the expected dose from seismic ground motion with a secondary contribution from the expected dose from igneous intrusion.[6] All other scenario classes have a marginal contribution to total expected dose. For the time period $[0,10^6 \text{ yr}]$, expected dose from these same scenario classes primarily determine the median expected dose $Q_{E,0.5}[\bar{D}(\tau \mid \mathbf{e})]$.

The smoothness evident in the expected dose results for the time period $[0, 2\times10^4 \text{ yr}]$ results from the quadrature procedure used to evaluate the expected dose from seismic ground motion for this time period.[3] In contrast, the Monte Carlo procedure used to evaluate expected dose from the combination of seismic ground motion and nominal corrosion processes for the time period $[0,10^6 \text{ yr}]$ results in the spikes in total expected dose evident in Fig. 4c. Although these spikes could be smoothed by use of a larger sample size in the calculation, the sample sizes employed are sufficient to yield a stable estimate of the mean dose and median expected dose, as will be shown.

As shown by the spread of the results in Figs. 4a and 4c, a substantial amount of uncertainty is present in the estimation of $\bar{D}(\tau \mid \mathbf{e})$. The sensitivity analyses in Figs. 4b and 4d indicate the variables that are giving rise to the uncertainty in $\bar{D}(\tau \mid \mathbf{e})$. The PRCCs in Fig. 4b indicate that the uncertainty in $\bar{D}(\tau \mid \mathbf{e})$ for the time interval $[0, 2\times10^4 \text{ yr}]$ is dominated by *SCCTHRP* (see Table I for definitions of individual variables), reflecting the dominant contribution to total expected dose from the expected dose from seismic ground motion, and the importance of this variable to the expected dose from seismic ground motion. Smaller effects are evident from the frequency of igneous events (*IGRATE*), from variables that influence movement of water (*SZGWSPDM*, *SZFIPOVO*, and *INFIL*) and from the contribution of ^{14}C to dose to the RMEI (*MICC14*) (the contribution of ^{99}Tc to uncertainty in expected dose is slightly less than the contribution from the variables identified in Fig. 4b).[4] For the time period $[0,10^6 \text{ yr}]$, the PRCCs in Fig. 4d indicate that the three most important variables with respect to the uncertainty in $\bar{D}(\tau \mid \mathbf{e})$ for the time interval are *SCCTHRP*, *IGRATE* and *WDGCA22*. In turn, *SCCTHRP* is the dominant variable affecting the uncertainty in expected dose from seismic ground motion events; *IGRATE* is the dominant variable affecting the uncertainty in expected dose $\bar{D}_{II}(\tau \mid \mathbf{e})$ from igneous intrusive events; and *WDGCA22* is the dominant variable affecting the uncertainty in the dose $D_N(\tau \mid \mathbf{e})$ from nominal processes.[5] In addition, smaller effects are indicated for *SZGWSPDM*, *SZFIPOVO* and for uncertainty in plutonium solubility (*EP1LOWPU*).

The YM 2008 TSPA used a LHS of size 300 to estimate $\bar{D}(\tau \mid \mathbf{e})$ (Ref. 5, Sect V). Given that 392 epistemically uncertain variables are under consideration in the YM 2008 TSPA model (i.e., $\mathbf{e}$ is a vector of length 392), it is reasonable to ask if this is a sufficiently large sample to obtain stable results. To answer this question, the analysis was repeated three times with independently generated LHSs of size 300. As shown in Fig. 5, the values obtained for $\bar{\bar{D}}(\tau)$ and $Q_{Eq}[\bar{D}(\tau \mid \mathbf{e})]$, q = 0.05, 0.5, 0.95, for these three samples are similar. Thus, an LHS of size 300 is adequate to obtain stable results for the propagation of epistemic uncertainty. The reader should note that the stability results summarized in Fig. 5 are from a near-final version of the YM 2008 TSPA model, and hence are slightly different in shape and magnitude from those presented in Fig. 4.

VII. SUMMARY

Uncertainty and sensitivity analysis are important parts of the analysis of expected dose in the TS YM 2008 TSPA. These analyses show that (i) the mean and median for expected dose are below regulatory standards specified by the NRC, (ii) mean and expected doses for all scenario classes are dominated by the doses arising from the seismic ground motion scenario class and the igneous intrusion scenario class for the $[0, 2\times10^4 \text{ yr}]$ time period and by the doses arising from nominal processes, the seismic ground motion scenario class and the igneous intrusion scenario class for the $[0,10^6 \text{ yr}]$ time period, (iii) the uncertainty in the expected dose from disruptive events tends to be dominated by the uncertainty in the rate of occurrence of these events, and (iv) an LHS of size 300 is adequate for the propagation of epistemic uncertainty in the YM 2008 TSPA. In addition, the sampling-based methods used for uncertainty and sensitivity analysis played an important role in analysis verification by allowing a detailed examination of the effects of analysis inputs on analysis results.

Additional extensive uncertainty and sensitivity analyses for dose, expected dose and many other analysis results are available in Apps. J and K of Ref. [4].

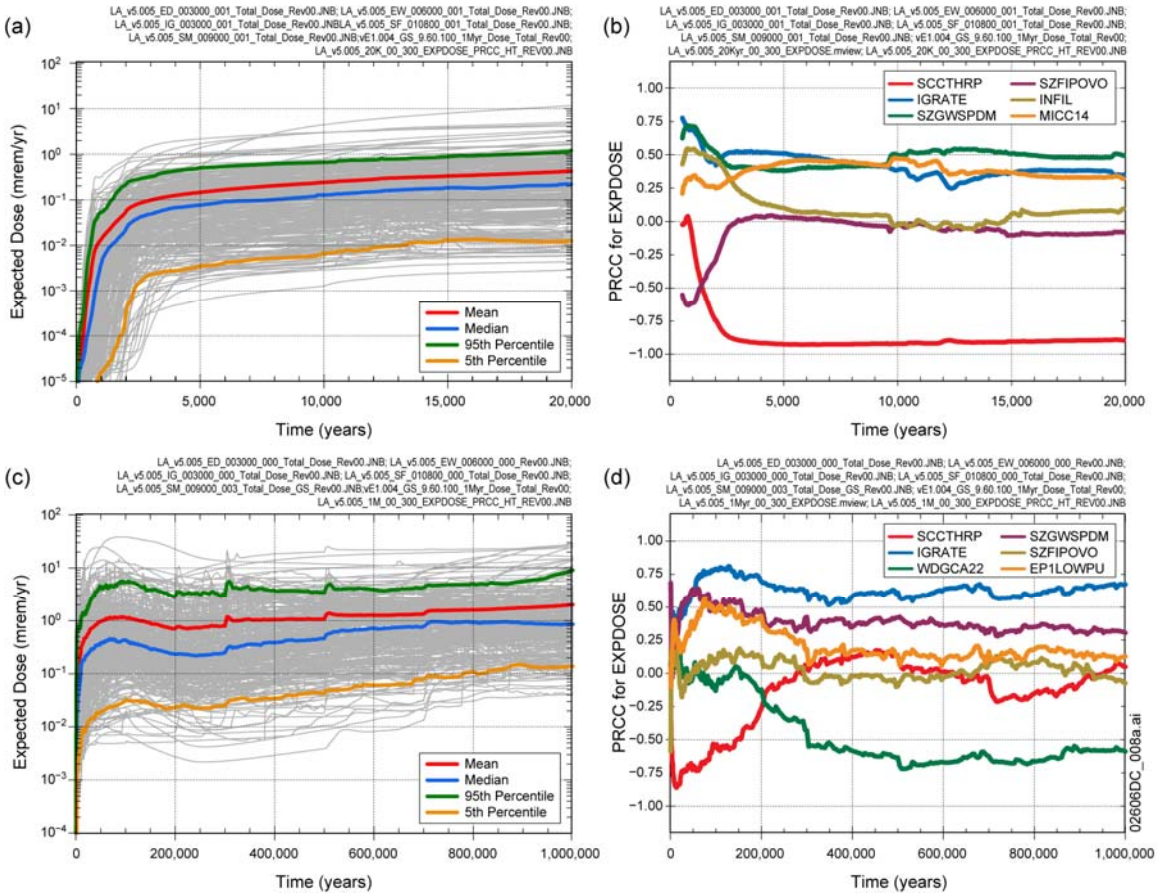

Fig. 4. Expected dose to RMEI (mrem/yr) for all radioactive species and all scenario classes: (a, b) $\bar{D}(\tau \mid \mathbf{e})$ and associated PRCCs for $[0, 2\times10^4$ yr] (Ref. 4, Fig. K8.1-1[a]), and (c, d) $\bar{D}(\tau \mid \mathbf{e})$ and associated PRCCs for $[0,10^6$ yr] (Ref. 4, Fig. K8.2-1[a]).

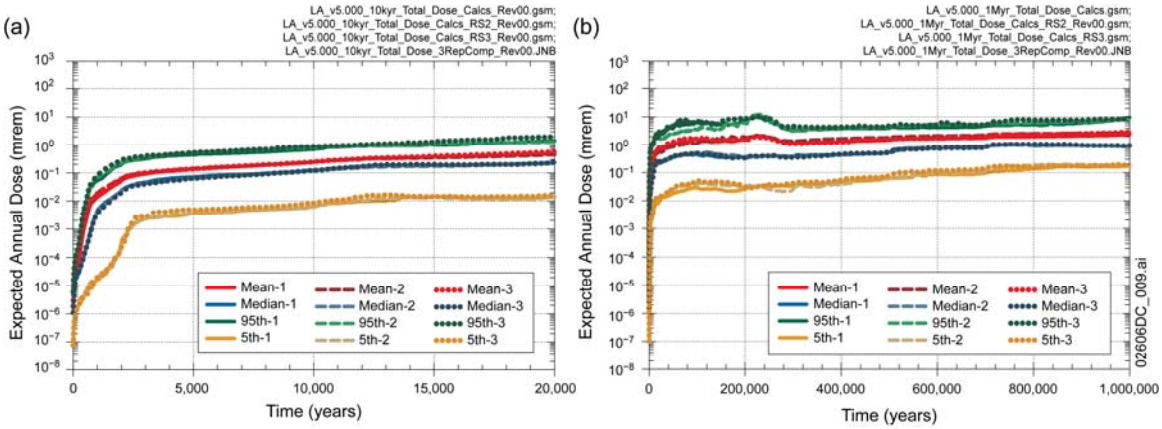

Fig. 5. Stability of estimates of expected dose $\bar{D}(\tau \mid \mathbf{e})$ to RMEI (mrem/yr) for all radioactive species and all scenario classes: (a) $[0, 2\times10^4$ yr] (Ref. 4, Fig. 7.3.1-15a), and (b) $[0,10^6$ yr] (Ref. 4, Fig. 7.3.1-16a).

TABLE I. Variables Appearing in Sensitivity Analyses for *EXPDOSE* in Figs. 1-4.

DASHAVG: Mass median ash particle diameter (cm)
DDIVIDE: Diffusivity of radionuclides in divides of the Fortymile Wash fan (RMEI location) (cm^2/yr).

DSNFMASS: Scale factor used to characterize uncertainty in radionuclide content of DSNF (dimensionless).
EP1LOWPU: Logarithm of the scale factor used to characterize uncertainty in plutonium solubility at an ionic strength below 1 molal (dimensionless).
IGRATE: Frequency of intersection of the repository footprint by a volcanic event (yr^{-1}). *Distribution:* Piecewise uniform.
IGERATE: Frequency of occurrence of volcanic eruptive events (yr^{-1}).
INFIL: Pointer variable for determining infiltration conditions: 10th, 30th, 50th or 90th percentile infiltration scenario (dimensionless).
INHLTPV: Pointer variable for long-term inhalation dose conversion factor for volcanic ash exposure (dimensionless).
MICC14: Groundwater Biosphere Dose Conversion Factor (BDCF) for ^{14}C in modern interglacial climate ((Sv/year)/(Bq/m^3)).
MICTC99: Groundwater Biosphere Dose Conversion Factor (BDCF) for ^{99}Tc in modern interglacial climate ((Sv/year)/(Bq/m^3)).
PROBDSEF: Probability for undetected defects in drip shields (dimensionless).
PROBWPEF: Probability for the undetected defects in waste packages (dimensionless).
SCCTHRP: Residual stress threshold for SCC nucleation of Alloy 22 (as a percentage of yield strength in MPa) (dimensionless).
SEEPPRM: Logarithm of the mean fracture permeability in lithophysal rock units (dimensionless).
SEEPUNC: Uncertainty factor to account for small-scale heterogeneity in fracture permeability (dimensionless).
SZCOLRAL: Logarithm of colloid retardation factor in alluvium (dimensionless).
SZFIPOVO: Logarithm of flowing interval porosity in volcanic units (dimensionless).
SZGWSPDM: Logarithm of the scale factor used to characterize uncertainty in groundwater specific discharge (dimensionless).
THERMCON: Selector variable for one of three host-rock thermal conductivity scenarios (low, mean, and high) (dimensionless).
WDGCA22: Temperature dependent slope term of Alloy 22 general corrosion rate (K).

ACKNOWLEDGMENTS

Sandia is a multi-program laboratory operated by Sandia Corporation, a Lockheed Martin Company, for the United States Department of Energy's National Nuclear Security Administration under contract DE-AC04-94AL85000. The United States Government retains and the publisher, by accepting the article for publication, acknowledges that the United States Government retains a non-exclusive, paid-up, irrevocable, world-wide license to publish or reproduce the published form of this manuscript, or allow others to do so, for United States Government purposes. The views expressed in this article are those of the authors and do not necessarily reflect the views or policies of the United States Department of Energy, Sandia National Laboratories, Sala & Associates, Inc., INTERA, Areva Federal Services, LLC, or Beckman & Associates, Inc.

REFERENCES

1. NRC (US Nuclear Regulatory Commission), *10 Code of Federal Regulations Part 63: Disposal of a High-Level Radioactive Wastes in a Geologic Repository at Yucca Mountain, Nevada* (final rule) (2008).
2. NRC (US Nuclear Regulatory Commission), "Implementation of a Dose Standard After 10,000 Years" (proposed rule), *Federal Register* V. 70, p. 53313 (2005).
3. P. N. SWIFT, M. K. KNOWLES, J. MCNEISH, C. W. HANSEN, R. L. HOWARD, R. MACKINNON, AND S. D. SEVOUGIAN, "Yucca Mountain 2008 Performance Assessment: Summary," *Proceedings of the 2008 International High-Level Radioactive Waste Management Conference*, September 7-11, 2008 (this volume) (2008).
4. J. C. HELTON, C. W. HANSEN, and C. J. SALLABERRY, "Yucca Mountain 2008 Performance Assessment: Conceptual Structure and Computational Organization," *Proceedings of the 2008 International High-Level Radioactive Waste Management Conference*, September 7-11, 2008 (this volume) (2008).
5. SNL (Sandia National Laboratories), *Total System Performance Assessment Model/Analysis for the License Application*, MDL-WIS-PA-000005 Rev 00, AD 01 (2008).
6. C. J. SALLABERRY, A. ARAGON, A. BIER, Y. CHEN, J. GROVES, C. W. HANSEN, J. C. HELTON, S. MEHTA, S. MILLER, J. MIN, and P. VO, "Yucca Mountain 2008 Performance Assessment: Uncertainty and Sensitivity Analyses for Physical Processes," *Proceedings of the 2008 International High-Level Radioactive Waste Management Conference*, September 7-11, 2008 (this volume) (2008).
7. S. D. SEVOUGIAN, A. BEHIE, B. BULLARD, V. CHIPMAN, M. GROSS, and W. STATHAM, "Yucca Mountain 2008 Performance Assessment: Modeling Disruptive Events and Early Failures," *Proceedings of the 2008 International High-Level Radioactive Waste Management Conference*, September 7-11, 2008 (this volume), American Nuclear Society (2008).
8. R. J. MACKINNON, A. BEHIE, V. CHIPMAN, Y. CHEN, J. LEE, K. P. LEE, P. MATTIE, S. MEHTA, K. MON, J. SCHREIBER, S. D. SEVOUGIAN, C. STOCKMAN, and E. ZWAHLEN, "Yucca Mountain 2008 Performance Assessment: Modeling the Engineered Barrier System," *Proceedings of the 2008 International High-Level Radioactive Waste Management Conference*, September 7-11, 2008 (this volume) (2008).
9. P. D. MATTIE, T. HADGU, B. LESTER, A. SMITH, M. WASIOLEK, and E. ZWAHLEN, "Yucca Mountain 2008 Performance Assessment: Modeling the Natural System," *Proceedings of the 2008 International High-Level Radioactive Waste Management Conference*, September 7-11, 2008 (this volume), American Nuclear Society (2008).

This page intentionally left blank

DISTRIBUTION

External Distribution

Prof. Joonhong Ahn
Department of Nucear Engineering
University of California, Berkeley
Berkeley, CA 94720

Prof. J.F. Ahearne
Duke Univ., Sigma Xi
POB 13975, 99 Alexander Dr.
Research Triangle, NC 27709

Prof. G.E. Apostolakis
Department of Nuclear Engineering
Massachusetts Institute of Technology
Cambridge, MA 02139-4307

Prof. Bilal Ayyub
University of Maryland
Center for Technology & Systems Management
Civil & Environmental Engineering
Rm. 0305 Martin Hall
College Park, MD 20742-3021

Prof. Ivo Babuska
TICAM
Mail Code C0200
University of Texas at Austin
Austin, TX 78712-1085

Prof. S. Balachandar
Dept. of Mechanical & Aerospace Engr.
University of Florida
231 MAE-A, PO Box 116250
Gainesville, FL 32611-6205

Prof. Osman Balci
Department of Computer Science
Virginia Tech
Blacksburg, VA 24061

Prof. Bruce Beck
University of Georgia
D.W. Brooks Drive
Athens, GA 30602-2152

Prof. James Berger
Inst. of Statistics and Decision Science
Duke University
Box 90251
Durham, NC 27708-0251

Prof. Daniel Berleant
Department of Information Science
University of Arkansas at Little Rock
ETAS Building, Room 258 D
2801 South University Avenue
Little Rock, Arkansas 72204

Prof. V. M. Bier
Department of Industrial Engineering
University of Wisconsin
Madison, WI 53706

Prof. Mark Brandyberry
Computational Science and Engineering
2264 Digital Computer Lab, MC-278
1304 West Springfield Ave.
University of Illinois .
Urbana, IL 61801

John A. Cafeo
General Motors R&D Center
Mail Code 480-106-256
30500 Mound Road
Box 9055
Warren, MI 48090-9055

Andrew Cary
The Boeing Company
MC S106-7126
P.O. Box 516
St. Louis, MO 63166-0516

James C. Cavendish
General Motors R&D Center
Mail Code 480-106-359
30500 Mound Road
Box 9055
Warren, MI 48090-9055

Prof. Chun-Hung Chen
Department of Systems Engineering &
Operations Research
George Mason University
4400 University Drive, MS 4A6
Fairfax, VA 22030

Prof. Wei Chen
Department of Mechanical Engineering
Northwestern University
2145 Sheridan Road, Tech B224
Evanston, IL 60208-3111

Prof. Hugh Coleman
Department of Mechanical &
Aero. Engineering
University of Alabama/Huntsville
Huntsville, AL 35899

Prof. Roger Cooke
Resources for the Future
1616 P Street NW
Washington, DC 20036

Raymond Cosner
Boeing-Phantom Works
MC S106-7126
P. O. Box 516
St. Louis, MO 63166-0516

Thomas A. Cruse
AFRL Chief Technologist
1981 Monahan Way
Bldg. 12, Room 107
Wright-Patterson AFB, OH 45433-7132

Prof. Alison Cullen
University of Washington
Box 353055
208 Parrington Hall
Seattle, WA 98195-3055

Prof. U. M. Diwekar
Center for Uncertain Systems, Tools for Optimization, and Management
Vishwamitra Research Institute
34 N. Cass Avenue
Westmont, IL 60559

Prof. R. Paul Drake
Center for Radiative Shock Hydrodynamics
2455 Hayward St.
University of Michigan
Ann Arbor, MI 48109-2143

Prof. David Draper
Applied Math & Statistics
147 J. Baskin Engineering Bldg.
University of California
1156 High St.
Santa Cruz, CA 95064

Isaac Elishakoff
Dept. of Mechanical Engineering
Florida Atlantic University
777 Glades Road
Boca Raton, FL 33431-0991

Prof. Ashley Emery
Dept. of Mechanical Engineering
Box 352600
University of Washingtion
Seattle, WA 98195-2600

Prof. Donald Estep
Department of Mathematics
Colorado State University
Fort Collins, CO 80523

Scott Ferson
Applied Biomathematics
100 North Country Road
Setauket, New York 11733-1345

Prof. C. Frey
Department of Civil Engineering
Box 7908, NCSU
Raleigh, NC 27659-7908

B. John Garrick
221 Crescent Bay Dr.
Laguna Beach, CA 92651

Prof. Roger Ghanem
254C Kaprielian Hall
Dept. of Civil Engineering
3620 S. Vermont Ave.
University of Southern California
Los Angles, CA 90089-2531

Prof. James Glimm
Dept. of Applied Math & Statistics
P138A
State University of New York
Stony Brook, NY 11794-3600

Prof. Ramana Grandhi
Dept. of Mechanical and Materials Engineering
3640 Colonel Glenn Hwy.
Dayton, OH 45435-0001

Prof. Raphael Haftka
Dept. of Aerospace and Mechanical
Engineering and Engineering Science
P.O. Box 116250
University of Florida
Gainsville, FL 32611-6250

Prof. Yacov Y. Haimes
Center for Risk Management of Engineering Systems
D111 Thornton Hall
University of Virginia
Charlottesville, VA 22901

Prof. Achintya Haldar
Dept. of Civil Engineering
& Engineering Mechanics
University of Arizona
Tucson, AZ 85721

Tim Hasselman
ACTA
2790 Skypark Dr., Suite 310
Torrance, CA 90505-5345

Prof. Steve Hora
Institute of Business and Economic Studies
University of Hawaii, Hilo
523 W. Lanikaula
Hilo, HI 96720-409 1

R.L. Iman
Southwest Technology Consultants
1065 Tramway Lane, NE
Albuquerque, NM 87122

Prof. George Karniadakis
Division of Applied Mathematics
Brown University
192 George St., Box F
Providence, RI 02912

Prof. W. E. Kastenberg
Department of Nuclear Engineering
University of California, Berkeley
Berkeley, CA 94720

Prof. George Klir
Binghamton University
Thomas J. Watson School of Engineering &
Applied Sciences
Engineering Building, T-8
Binghamton NY 13902-6000

Prof. Vladik Kreinovich
Department of Computer Science
University of Texas at El Paso
500 W. University
El Paso, TX 79968, USA

Averill M. Law
6601 E. Grant Rd.
Suite 110
Tucson, AZ 85715

Prof. Sankaran Mahadevan
Vanderbilt University
Dept. of Civil and Environmental Engineering
Box 6077, Station B
Nashville, TN 37235

Prof. Parviz Moin
Institute for Computational and Mathematical
Engineering and Center for Turbulence Research
Building 500
Stanford University
Stanford, CA 94305

Prof. Max Morris
Department of Statistics
Iowa State University
304A Snedecor-Hall
Ames, IW 50011-1210

Dale Moseley
The Goodyear Tire & Rubber Co
Technical Center D/431A
PO Box 3531
Akron, Ohio 44309-3531

Prof. Robert Moser
Institute for Computational Engineering and Sciences
and Department of Mechanical Engineering
University of Texas at Austin
1 University Station Stop C0200
Austin, TX 78712

Prof. Jayathi Y. Murthy
Director, PRISM: NNSA Center for Prediction of
Reliability, Integrity and Survivability of
Microsystems
Purdue University
585 Purdue Mall
West Lafayette, IN 47907

Prof. Ali Mosleh
Center for Reliability Engineering
University of Maryland
College Park, MD 20714-21 15

Prof. Zissimos P. Mourelatos
Dept. of Mechanical Engineering
School of Engr. and Computer Science
Rochester, MI 48309-4478

Prof. Rafi Muhanna
Regional Engineering Program
Georgia Tech
210 Technology Circle
Savannah, GA 31407-3039

NASA/Ames Research Center (2)
Attn: Unmeel Mehta, MS 229-3
David Thompson, MS 269-1
Moffett Field, CA 94035-1000

NASA/Glenn Research Center (2)
Attn: John Slater, MS 86-7
Chris Steffen, MS 5-11
21000 Brookpark Road
Cleveland, OH 44135

NASA/Langley Research Center (7)
Attn: Dick DeLoach, MS 236
Michael Hemsch, MS 499
Jim Luckring, MS 286
Joe Morrison, MS 128
Ahmed Noor, MS 369
Sharon Padula, MS 159
Thomas Zang, MS 449
Hampton, VA 23681-0001

Thomas J. Nicholson
Office of Nuclear Regulatory Research
Mail Stop T-9C34
U.S. Nuclear Regulatory Commission
Washington, DC 20555

Prof. Efstratios Nikolaidis
MIME Dept.
4035 Nitschke Hall
University of Toledo
Toledo, OH 43606-3390

William L. Oberkampf
2014 Monte Largo Dr. NE
Albuquerque, NM 87112

Prof. Tinsley Oden
TICAM
Mail Code C0200
University of Texas at Austin
Austin, TX 78712-1085

Prof. Michael Ortiz
Mail Code 105-50
Engineering and Applied Sciences Division
California Institute of Technology
Pasadena, CA 91125

Prof. M. Elisabeth Paté-Cornell
Department of Industrial Engineering and Management
Stanford University
Stanford, CA 94305

Prof. Adrian E. Raftery
Department of Statistics
University of Washington
Seattle, WA 98195

Ramesh Rebba
General Motors R&D Center
Mail Code 480-106-256
30500 Mound Road
Box 9055
Warren, MI 48090-9055

Prof. John Renaud
Dept. of Aerospace & Mechanical Engr.
University of Notre Dame
Notre Dame, IN 46556

Patrick J. Roache
1215 Apache Drive
Socorro, NM 87801

Richard Rowberg
Associate Executive Director
Division on Engineering and Physical Sciences
National Research Council
National Academies
500 5th St., NW
Washington, DC 20001

Prof. Tim Ross
Dept. of Civil Engineering
University of New Mexico
Albuquerque, NM 87131

Prof. Chris Roy
Aerospace and Ocean Engineering Dept.
215 Randolph Hall
Virginia Tech
Blacksburg, VA 24061-0203

Prof. J. Sacks
Inst. of Statistics and Decision Science
Duke University
Box 90251
Durham, NC 27708-0251

Len Schwer
Schwer Engineering & Consulting
6122 Aaron Court
Windsor, CA 95492

Prof. Nozer D. Singpurwalla
The George Washington University
Department of Statistics
2140 Pennsylvania Ave. NW
Washington, DC 20052

Prof. C.B. Storlie
Department of Mathematics and Statistics
University of New Mexico
Albuquerque, NM 87131-0001

Southwest Research Institute (3)
Attn: B. Bichon
J. McFarland
B. Thacker
P.O. Drawer 28510
622 Culebra Road
San Antonio, TX 78284

Prof. Raul Tempone
School of Computational Science
400 Dirac Science Library
Florida State University
Tallahassee, FL 32306-4120

Prof. Fulvio Tonon
Department of Civil Engineering
University of Texas at Austin
1 University Station C1792
Austin, TX 78712-0280

Prof. Robert W. Walters
Aerospace and Ocean Engineering
Virginia Tech
215 Randolph Hall, MS 203
Blacksburg, VA 24061-0203

Christopher G. Whipple
Environ
Marketplace Tower
6001 Shellmound St. Suite 700
Emeryville, C.A. 94608

Prof. Karen E. Willcox
Department of Aeronautics & Astronautics
Massachusetts Institute of Technology
77 Massachusetts Ave
Room 37-447
Cambridge, MA 02139

Prof. Alyson Wilson
Department of Statistics
Iowa State University
Ames, IA 50014

Prof. Byeng D. Youn
Department of Mechanical Engineering
0158 Glenn Martin Hall
University of Maryland
College Park, Maryland 20742

Foreign Distribution

Prof. Michael Beer
Dept. of Civil Engineering
National University of Singapore
BLK E1A, #07-03, 1 Engineering Drive 2
SINGAPORE 117576

Prof. D.G. Cacuci
Institute for Nuclear Technology and Reactor Safety
University of Karlsruhe
76131 Karlsruhe
GERMANY

Prof. Yakov Ben-Haim
Department of Mechanical Engineering
Technion-Israel Institute of Technology
Haifa 32000
ISRAEL

Prof. A.P. Bourgeat
UMR 5208 – UCB Lyon1, MCS, Bât. ISTIL
Domaine de la Doua; 15 Bd. Latarjet
69622 Villeurbanne Cedex
FRANCE

CEA Cadarache (2)
Attn: Nicolas Devictor
Bertrand Iooss
DEN/CAD/DER/SESI/CFR
Bat 212
13108 Saint Paul lez Durance cedex
FRANCE

Etienne de Rocquigny
EDF R&D MRI/T56
6 quai Watier
78401 Chatou Cedex
FRANCE

European Commission (5)
Attn: Francesca Campolongo
Mauro Ciechetti
Marco Ratto
Andrea Saltelli
Stefano Tarantola
JRC Ispra, ISIS
2 1020 Ispra
ITALY

Régis Farret
Direction des Risques Accidentels
INERIS
BP2 – 60550 Verneuil en Halatte
FRANCE

Prof. Jim Hall
University of Bristol
Department of Civil Engineering
Queens Building, University Walk
Bristol UK 8581TR

Prof. J.P.C. Kleijnen
Department of Information Systems
Tilburg University
5000 LE Tilburg
THE NETHERLANDS

Prof. Philipp Limbourg
University of Duisburg-Essen,
Bismarckstr. 90, 47057
Duisburg
GERMANY

Prof. A. O'Hagan
Department of Probability and Statistics
University of Sheffield
Hicks Building
Sheffield S3 7RH
UNITED KINGDOM

Prof. G.I. Schuëller
Institute of Engineering Mechanics
Leopold-Franzens University
Technikerstrasse 13
6020 Innsbruck
AUSTRIA

David Watkins
Bldg. 4, AWE Aldermaston
Reading R674PR
United Kingdom

Prof. H.P. Wynn
Department of Statistics
London School of Economics
Houghton Street
London WC2A 2AE
UNITED KINGDOM

Prof. Enrico Zio
Politecnico di Milano
Via Ponzia 3413
20133 Milan
ITALY

Department of Energy Laboratories

Department of Energy (5)
Attn: Njema Frazier, NA-121.2
Robert Hanrahan, NA-121.1
Robert Meisner, NA-121.2
Dimitri Kusnezov NA-121
K. Pao, NA-114
Forrestal Building
1000 Independence Ave., SW
Washington, DC 20585

Idaho National Laboratory (2)
Attn: Dana A. Knoll, MS 3855
Richard R. Schultz, MS 3890
2525 Fremont Ave.
P.O. Box 1625
Idaho Falls, ID 83415

Lawrence Livermore National Laboratory (10)
Attn: Maurice Aufderheide
Scott Brandon
Robert Budnitz
Pieter Dykema
Frank Graziani
Henry Hsieh
Richard Klein
James McEnerney
Joe Sefcik

Charles Tong
7000 East Ave.
P.O. Box 808
Livermore, CA 94550

Los Alamos National Laboratory (38)
Attn: Frank J. Alexander, MS B256
Mark C. Anderson, MS T080
Christine M. Anderson-Cook, MS F600
Jerry S. Brock, MS F663
Gregory A. Brouillette, MS F09
Thomas L. Burr, MS F600
Gregory M. Chavez, MS 609
Scott Doebling, MS T080
Sunil Donald, MS K557
James R. Gattiker, MS F600
William L. Gibson, MS F609
Todd. L. Graves, MS F600
Michael S. Hamada, MS F600
Kriste Henson, MS K488
Don Haynes, MS T086
Francois Hemez, MS F699
David Higdon, MS F600
Joe V. Holland, MS 609
Don R. Hush, MS B265
Aparna V. Huzurbazar, MS F600

David Izraelevitz, MS F609
James Kamm, MS D413
Earl Lawrence, MS F600
Deborah A. Leishman, MS F609
Leslie Moore, MS F600
Kary L. Myers, MS F600
Ralph A. Nelson, MS A113
Richard R. Picard, MS F600
William H. Press, MS F600
Kevin J. Saeger, MS F609
James C. Scovel, MS B265
Kari Sentz, MS F609
George Thompkins, MS F609
Scott A. Vander Wiel, MS F600
Edward Van Eeckhout, MS F609
Timothy C. Wallstrom, MS B213
Joanne Wendelberger, MS F600
Brian Williams, MS F600
Mail Station 5000
P.O. Box 1663
Los Alamos, NM 87545

Pacific Northwest National Laboratory
Attn: Stephen D. Unwin
P.O. Box 999
Mail Stop K6-52
Richland, WA 99354

Sandia Internal Distribution

1	MS 0116	0310	A. L. Camp
1	MS 0829	0415	E. Thomas
1	MS 0321	1400	J. S. Peery
1	MS 0351	1010	J. C. Barbour
1	MS 1415	1110	S. M. Myers
1	MS 1146	1384	P. J. Griffin
1	MS 1316	1400	G. S. Davidson
1	MS 1318	1410	B. A. Hendrickson
1	MS 1318	1411	J. R. Stewart
1	MS 1318	1411	B. Adams
1	MS 1318	1411	M. S. Eldred
1	MS 1318	1411	D. M. Gay
2	MS 1318	1411	L. P. Swiler
1	MS 0370	1411	T. G. Trucano
1	MS 1316	1412	M. D. Rintoul
1	MS 1316	1412	C. F. Diegert
1	MS 1318	1412	W. E. Hart
1	MS 1318	1414	K. F. Alvin
1	MS 1318	1414	B. G. van Bloemen Waanders
1	MS 1318	1414	A. G. Salinger
1	MS 1316	1415	S. A. Mitchell
1	MS 1320	1416	S. S. Collis
1	MS 1316	1416	S. J. Plimpton
1	MS 0376	1421	T. D. Blacker
1	MS 1319	1422	J. A. Ang
1	MS 0822	1424	D. Rogers
1	MS 0378	1431	R. M. Summers
1	MS 0370	1433	J. Strickland
1	MS 0370	1433	G. Backus
1	MS 0370	1433	M. Boslough
1	MS 0370	1433	D. Schoenwald
1	MS 0370	1433	J. Siirola
1	MS 1322	1435	J. B. Aidun
1	MS 0316	1437	J. Castro
1	MS 0316	1437	J. N. Shadid
1	MS 0384	1500	A.C. Ratzel
1	MS 0824	1500	T.Y. Chu
1	MS 0836	1500	M.R. Baer
1	MS 0836	1510	J. S. Lash
1	MS 0346	1514	D. Dobranich
1	MS 0836	1514	R. E. Hogan
1	MS 0825	1515	D. W. Kuntz
1	MS 0825	1515	J. L. Payne
1	MS 0825	1515	W. P. Wolfe
1	MS 0372	1520	J.M. Redmond
1	MS 0847	1520	P. J. Wilson
1	MS 0557	1522	C. C. O'Gorman
1	MS 0346	1523	T. J. Baca
1	MS 0557	1523	T. Simmermacher
1	MS 0372	1524	J. Pott
1	MS 0372	1524	T. D. Hinnerichs
1	MS 0372	1524	K. E. Metzinger
1	MS 1070	1526	C. C. Wong
1	MS 0821	1530	A.L. Thornton
1	MS 1135	1532	S.R. Tieszen
1	MS 1135	1532	T. K. Blanchat
1	MS 0847	1535	J.L. Cherry
1	MS 0833	1536	R. O. Griffith
1	MS 1318	1540	D. E. Womble
1	MS 0382	1541	B. Hassan
1	MS 0382	1541	H. C. Edwards
1	MS 0380	1541	G. D. Sjaardema
1	MS 0380	1542	J. Jung
1	MS 0380	1542	M. W. Heinstein
1	MS 0380	1542	G. M. Reese
1	MS 0382	1543	M. Glass
1	MS 0828	1544	A. A. Giunta
1	MS 0828	1544	A. R. Black
1	MS 0382	1544	K. D. Copps
1	MS 0828	1544	K. J. Dowding
2	MS 0776	1544	J. C. Helton
1	MS 0828	1544	R. G. Hills
1	MS 0557	1544	T. L. Paez
1	MS 0828	1544	J. R. Red-Horse
1	MS 0828	1544	V. J. Romero
1	MS 0847	1544	W. R. Witkowski
1	MS 0382	1545	E. S. Hertel

1	MS 0384	1550	P. Yarrington
1	MS 0828	1551	M. Pilch
1	MS 0457	2010	S. Y. Pickering
1	MS 0457	2011	R. A. Paulsen
1	MS 0479	2134	S. E. Klenke
1	MS 0447	2111	J. F. Lorio
1	MS 0479	2138	J. Arfman
1	MS1452	2552	M. K. Knowles
1	MS 0521	2617	E. A. Boucheron
1	MS 0453	2900	L. S. Walker
1	MS 0374	2991	H. P. Walther
1	MS 1231	5223	S. N. Kempka
1	MS 0529	5350	K. D. Meeks
1	MS 1153	5441	L. C. Sanchez
1	MS 0831	5500	M. O. Vahle
1	MS 0972	5572	S. E. Lott
1	MS 0724	6000	L. E. Shephard
1	MS 1373	6721	S. M. DeLand
1	MS 1138	6322	P. G. Kaplan
1	MS 1137	6323	G. D. Valdez
1	MS 1124	6333	P. S. Veers
1	MS 0757	6414	J. L. Darby
1	MS 0757	6414	G. D. Wyss
1	MS 1002	6470	P. D. Heermann
1	MS 0748	6761	D. G. Robinson
1	MS 1399	6780	E. J. Bonano
1	MS 0778	6780	P. N. Swift
1	MS 0776	6781	R. P. Rechard
1	MS 0776	6782	R. J. MacKinnon
1	MS 1399	6784	J. McNeish
1	MS 0776	6784	C. M. Sallaberry
1	MS 1399	6787	C. W. Hansen
1	MS 0776	6786	J. S. Stein
1	MS 1399	6787	P. Vaughn
1	MS 9007	8205	R. Zurn
1	MS 9404	8240	E. P. Chen
1	MS 9042	8246	M. L. Chiesa
1	MS 9404	8246	J. A. Zimmerman
1	MS 9042	8249	J. J. Dike
1	MS 9042	8249	Carole Le Gall
1	MS 9151	8900	L. M. Napolitano
1	MS 9159	8962	H. R. Ammerlahn
1	MS 9159	8962	P. D. Hough
1	MS 9152	8964	M. F. Hardwick
1	MS 0428	12300	L. A. Schoof
1	MS 0428	12330	T. R. Jones
1	MS 0830	12335	K. V. Diegert
1	MS 0829	12337	J. M. Sjulin
1	MS 0829	12337	B. M. Rutherford
1	MS 0638	12341	D. E. Peercy
1	MS 0405	12346	R. Kreutzfeld
1	MS 0492	12332	T. D. Brown
1	MS 0405	12347	R. D. Waters
1	MS 1030	12870	J. G. Miller
1	MS 0899	9536	Technical Library (electronic copy)

Sandia National Laboratories